Kinetics and mechanism of racemisation reactions of configurationally labile stereogenic centres in drug-like molecules in aqueous solutions; thiohydantoins and related compounds

Hiwa Omer Ahmad

A thesis submitted for the Degree of Doctor of Philosophy

School of Chemistry

Cardiff University

August 2015

DECLARATION

This work has not previously been accepted in substance for any other degree and is not concurrently submitted in candidature for any degree.

Signed …… (Candidate) Date ……

STATEMENT 1

This thesis is being submitted in partial fulfillment of the requirements for the degree of Doctor of philosophy.

Signed …… (Candidate) Date ……

STATEMENT 2

This thesis is the result of my own independent work/investigation, except where otherwise stated.

Other sources are acknowledged by explicit references.

Signed …….. (Candidate) Date ……

STATEMENT 3

I hereby give consent for my thesis, if accepted, to be available for photocopying and for inter-library loan, and for the title and summary to be made available to outside organisations.

Signed …… (Candidate) Date ……

Dedicated to the nations of Kurdistan and their peoples; to the person who declares a free Kurdistan and establishes Justice, safety, equality, for everyone in a country developing its science and economy.

Summary

In this thesis, studies of the kinetic and mechanism of racemisation of several drug-like molecule have been presented. Chapter 1 provides background information on the general mechanisms of racemisation of drugs in general, and hydantoin derivatives. In particular including reviews of the hydrolysis and the mechanism of base-catalysed racemisation of hydantoin derivatives.

The synthesis of different chiral hydantoins, thiohydantoins, thiazolidine-diones, and rhodanines is presented in Chapter 2. Several enantio-enriched 5-substituted 1-acetyl-2-thiohydantoins and two tri-substituted 2-thiohydantoins have been synthesised. Further racemic thiohydantoin derivatives including mono, di, and tri-substituted 2-thiohydantoins have also been prepared.

Chapter 3 focuses on the kinetics and mechanism of hydrolysis of 5-substituted 1-acetyl-2-thiohydantoins in physiological-like buffers. The key reaction involves de-acetylation and this is followed by the hydrolysis of the resulting 5-substituted 2-thiohydantoins. Sodium hydroxide and hydrochloric acid have also been used for the hydrolysis of 1-acetyl-5-phenyl-2-thiohydantoin. Similarly, the hydrolysis of several 5-substituted 2-thiohydantoins has been studied. The rate constants for hydrolysis suggest that the 5-substituted 1-acetyl-2-thiohydantoins hydrolyses faster than the subsequent hydrolysis of 5-substituted 2-thiohydantoins.

Chapter 4 focuses on the racemisation of 5-substituted 1-acetyl-2-thiohydantoins and shows that substituents at N-1 decelerate racemisation. Racemisation of tri-substituted 2-thiohydantoins is fast in comparison with 5-substituted 1-acetyl-2-thiohydantoins. The substituents at the asymmetric carbon affect the rate of racemisation. The solvent kinetic isotope effect on the racemisation were determined for different substituted 2-thiohydantoins and supported the S_E1 mechanism of racemisation.

Chapter 5 concerns further confirmation of the mechanism of racemisation by comparing k_{deu} and k_{rac} and this confirms the S_E1 mechanism for racemisation of 5-substituted 1-acetyl-2-thiohydantoin as k_{deu}/k_{rac} for all compounds approaches 1. For the racemic 5-substituted 2-thiohydantoins the rate constants of deuteration have been obtained using ^{1}H-NMR spectroscopy and showed fast replacement of hydrogen by deuteron. Assuming $k_{deu} = k_{rac}$, we can order the rate constants for racemisation form high to low as rhodanine > thiohydantoin > thiazolidine-2,4-dione > hydantoin.

Acknowledgements

I would like to thank my supervisor, Dr Niek Buurma, for his invaluable teaching, patience, guidance and support. I feel I have developed as a scientist over the last few years, and I am glad I had a chance to work with him.

I would also like to thank Dr. Mazin Othman from Kurdistan to inspire me to come to Cardiff and work in the physical organic chemistry centre. A huge thank you to the POC members who helped me during my earlier work namely Drs. Azzedine, Julia, Mihaela, Jamie, Ismail, and Edward. Special thanks also go to the present and past students in POC especially Ibrahim, Karma, and Ammar, and those who worked with me namely Mesele, Ben, David, Yassine, and Ibrahim Bala.

Huge thanks also to the technical staff at Cardiff University; with particular thanks to Robin Hicks, Simon Waller, and Tom Williams for the mass spectrometry and GC-MS data. Thanks to Steve for repairing the machines which were necessary for my work. I would also like to express my sincere thanks to Dr Rob Jenkins for his help with NMR spectroscopy and keeping those instruments online, and Dr Benson Kariuki for obtaining the crystallographic data.

I would also like to thank Prof. Allemann for allowing me to use the CD machine for my work, and his group for their kind help.

Thanks to the Kurdistan Government / Ministry of Higher Education for funding my scholarship.

More importantly, a very special thanks to my parents for their love and endless support throughout my life. Thank you both for giving me strength to chase my dreams. Nothing I can do would pay off for your hard work, love and sleepless nights that both of you put into helping me get where I am today. My sincere gratitude to my wife Mrs Parishan Hasan for her continuous support, encouragement, quiet patience, and love. There are no words which can express my honour and respect I have for you. I would like to express my deepest gratitude to my children, Sema, Sahand, and Sahen for their patience during my hard work. Thanks also to my brothers, sisters, and my wife's family who helped and contacted us during my study. Last but not least, thanks to everyone who taught and helped me during my life, even by one word.

List of abbreviations

∂	Chemical shifts
°C	Degree Celsius
^{13}C-NMR	Carbon-13 nuclear magnetic resonance
^{1}H-NMR	Proton nuclear magnetic resonance
2-Thiohydantoin	2-Thioxoimidazolidin-4-one
Ac, TH	5-Substituted 1-acetyl-2-thiohydantoins
ACN	Acetonitrile
ACN-D_3	Deuterated acetinitrile
Aq.	Aqueous
Ar	Aryl
B	Base
Benz	Benzyl
calcd	Calculated
CD	Circular dichroism spectroscopy
CD_3CN	Deuterated acetonitrile
$CDCl_3$	Deuterated chloroform
D_2O	Deuterated water
D_3O^+	Hydronium ion
DCM	Dichloromethane
DEP	Diethylpropione
DMAP	4-Dimethylaminopyridine
DMSO	Dimethyl sulfoxide

$DMSO\text{-}d_6$	Deuteriated dimethylsulfoxide
dt	Double triplet
DZ	Diazepam
E	The temperature in °C
e.e.	enantiomeric excess
EI-MS	Electron impact - mass spectrum
ε_r	Dielectric constant
ES	Electrospray - mass spectrum
Et_2O	Diethyl ether
EtOD	Deuterated ethanol
EtOH	Ethanol
f	force constant of the bond
g	Grams
GA	General acid
GB	General base
GC-MS	Gas chromatography-mass spectrometry
H	Hour(s)
h	Planck's constant
H/D exchange	Proton deuterium exchange
H_2SO4	Sulphuric acid
H_3O^+	Hydronium ion
HCl	Hydrochloric acid
HPLC	High pressure liquid chromatography
HRMS	High resolution mass spectrometry
Hydantoin	Imidazolidine-2,4-dione

Hz	Hertz
I	Ionic strength
IPA	Isopropanol
IR	Infra-red
J	Coupling constant
k_0	Rate constant for non-catalysed processes
k_B	the catalytic constant of the reaction catalysed by general base B
k_b	Boltzmann constant
k_{enant}	The rate constant of enantiomerisation
k_H	the second-order rate constant for the reaction catalysed by H_3O^+
$k_{H/D}$ and k_{deut}	Rate constant for H/D exchange
k_{HPO4}^{-2}	Rate constant for racemisation catalysed by the basic component of the phosphate buffer
k_{hyd}	Rate constant for hydrolysis
k_{in}	Rate constant obtained from the intercept
kJ	Kilojoule
k_{obs}	Observed rate constant
k_{OD}	Rate constant for deuteroxide-catalysed processes
k_{OH}	Rate constant for the hydroxide-catalysed reaction
k_{rac}	Rate constant for racemisation
k_θ	Rate constant for loss of ellipticity θ
M	Multiplet
m	The reduced mass of the particles
m/z	Mass over charge ratio
MeCN	Acetonitrile
MeOH	Methanol

mg	Milligram
MHz	Mega hertz
ml	Millilitres
mM	Millimolar
Mp.	Melting point
MS	Mass spectrometry
NH_3	Ammonia
nm	Nanometer
NMR	Nuclear magnetic resonance
NSAIDS	Non-steroidal anti-inflammatory drugs
p-	para
Pd/C	Palladium on carbon
pH	Reading of a pH-meter for an H_2O-based sample at 20 °C
Ph	Phenyl group
pH^*	Reading of a pH-meter for a D_2O-based sample at 20 °C.
pK_a	-log K_a
ppm	Parts per million
Pyr	Pyridine
Q	Quartet
R	Substituents
r.t	Room temperature
rac-	racemic compounds
Rhodanine	2-Thioxothiazolidin-4-one
s	singlet
SE	Electrophilic substitution

SN	Nucleophilic substitution
Su.	Substrate
T	Triplet and the absolute temperature (in *K)*
t	time
TEA	Triethylamine
TFA	Trifluoroacetic acid
TFE	Trifluoroethanol
TH	5-Substituted 2-thiohydantoin
THF	Tetrahydrofuran
Tic	Tetrahydroisoquinoline
TMZ	Temazepam
TRIS	Tris(hydroxymethyl)aminomethane
UV	Ultra-violet
v	The vibrational frequency
vis	Visible
WR	The free energy of formation of reaction complex
α	The Brønsted parameter associated with the reaction catalysed by general bases
β	The Brønsted parameter associated with the reaction catalysed by general bases
$\Delta G^{\ddagger}$	The standard molar free energy of the proton transfer
$\Delta H^{\ddagger}$	Enthalpy of activation for loss of ellipticity
$\Delta S^{\ddagger}$	Entropy of activation for loss of ellipticity
θ	Ellipticity

List of contents

CHAPTER 1

INTRODUCTION

1.1 Racemisation

1.1.1 Enantiomers and racemisation

The geometric property of molecules or drug-like molecules of not being superimposable with their mirror images is called chirality.[1] The two distinct mirror images of chiral isomers are termed enantiomers. Two enantiomers are said to differ in their sense of chirality or handedness in the same way as a right hand differs from a left hand.[2] Optical activity results from the refraction of right and left circularly polarised light to different extents by chiral molecules.[3] Since enantiomers are usually optically active, they turn the plane of polarised light to an equal degree but in opposite directions, which is why enantiomers are also called optical isomers.[2] Some molecules rotate the plane to the right (clockwise), while others rotate the plane to the left (anticlockwise). For example, the two enantiomers (+) and (-) lactic acid (Scheme 1.1) are mirror images of each other. They have identical physical and chemical properties; for example, both have the same melting points in achiral environments. The carbon atom at the centre of lactic acid is attached to four different atoms and is called an asymmetric or stereogenic carbon atom.[4]

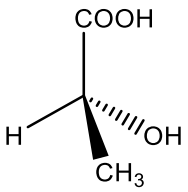

(*S*)-2-hydroxypropanoic acid

L-(+)-lactic acid

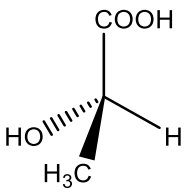

(*R*)-2-hydroxypropanoic acid

D-(-)-Lactic acid

Scheme 1.1: Structures of (+) and (-) lactic acid

1.1.2 Optical rotation

When polarised light passes through (a solution containing) chiral molecules, the medium has indices of refraction for both left and right circularly polarised light. The speed of the left circularly polarised light is not equal to the speed of the right polarised light ($n_L \neq n_R$). The *difference in refractive indices* is expressed by Fresnel's equation 1.1.[3]

$$\varphi = \frac{\pi}{\tau}(n_L - n_R) \qquad \text{Equation 1.1}$$

where φ is the rotation of the plane of polarisation in radians per unit length, τ is the wave length of the incident light, and n_L and n_R are the indices of refraction for both components of polarised light.

1.1.3 Circular dichroism

Optically active compounds have non-zero specific rotation.[3] The angle of rotation (α) can be measured using a polarimeter and the specific rotation is defined as in equation 1.2.[3, 5]

$$[\alpha]_D^E = \frac{\alpha_{obs}}{lc} \qquad \textbf{Equation 1.2}$$

where $[\alpha]_D^E$ is the specific rotation determined at temperature E (in °C) using D-line of sodium light, α_{obs} is the observed plane of polarisation, l is the length of the cell in decimetres, E is the temperature in °C, and c is the concentration of the substance being examined in grams per millilitre of solution.

The *difference in the absorption* of right and left circularly polarised light can be expressed as 'circular dichroism' where the molar absorption coefficient ($\mathcal{E}$) of the R molecule is different from the L molecule.

1.1.4 Racemisation

An equal amount of two enantiomers is called a racemic mixture. Both enantiomers in equal amounts cancel out each other and the mixture is optically inactive.[4] The term racemisation can be described as the total loss of optical activity of a molecule through the irreversible formation of a racemic mixture. The rate of racemisation can be described as the rate of formation of a racemate, which has reversible first-order kinetics (Scheme 1.2).[6, 7]

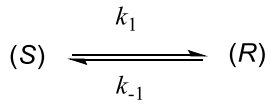

Scheme 1.2: Illustration of enantiomerisation.

The first-order rate law can be written by Equation 1.3

$$-\frac{d[S]}{dt} = k_1[S] - k_{-1}[R] \qquad \textbf{Equation 1.3}$$

where [*S*] and [*R*] are the concentrations of the enantiomers S and R, k_1 and k_{-1} are the interconversion constants for the S and R enantiomer respectively, and *t* is time. Initially, when one of the enantiomers dominates, a chiral medium is present and k_1 may be different from k_{-1}. However, if sufficiently dilute, $k_1 = k_{-1}$ can be assumed.[6]

When racemisation begins with pure S, under first-order conditions, $[S]_0$-$[S]_t = [R]_t$

$$In\left[\frac{[S]_\circ}{2[S]_t - [S]_\circ}\right] = 2kt \qquad \textbf{Equation 1.4}$$

where $[S]_t$ and $[S]_\circ$ are the concentrations of enantiomer S at time *t* and time zero, respectively.

The rate of racemisation can be described as the rate of the formation of a racemate, racemisation is an irreversible first-order reaction, contrary to enantiomerisation (Scheme 1.3).

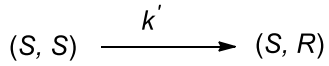

Scheme 1.3: Illustration of racemisation.

When pure enantiomer starts to form a racemate mixture, Equation 1.5 can be used

$$-\frac{d[S]}{dt} = k'[S]_t \qquad \textbf{Equation 1.5}$$

In the case where $[S]_\circ - [S]_t$ is equal to $2[SR]_t$, then Equation 1.5 can be described as

$$In\left[\frac{[S]_\circ}{[S]_t}\right] = In\left[\frac{[S]_\circ}{[S]_\circ - 2[SR]_t}\right] = k' \qquad \textbf{Equation 1.6}$$

where *k*' is the rate constant for racemisation, and [*SR*] is the concentration of the racemate.[6]

Following the racemisation by the loss in optical activity can transform Equation 1.6 into Equation 1.7.[6]

$$In\left[\frac{\alpha_\circ}{\alpha_t}\right] = k't \qquad \textbf{Equation 1.7}$$

where α_t is the optical activity at time *t*, and $\alpha_\circ$ is the optical activity at time zero.

The observed phenomenological pseudo-first-order rate constants for the loss of ellipticity k_θ were obtained by plotting the ellipticity versus time in terms of the first-order-rate equation (Equation 1.8).

$$\theta_t = \theta_{fin} + \Delta\theta * e^{-k_\theta \times t} \qquad \textbf{Equation 1.8}$$

Here, θ_t is the ellipticity at time t, $\theta_{\text{fin}}$is the final ellipticity, $\Delta\theta$ represents the difference between the ellipticity at time zero and θ_{fin}, and k_θ is the observed pseudo-first-order rate constant for loss of ellipticity.

1.1.5 Role of racemisation in optically active drugs

Drug stereoisomerism is recognised as an issue having clinical and regulatory implications in drug development. In the case of optically active drugs, the enantiomers can have different potency, and/or pharmacological activity. If a non-racemising drug is designed to interact with a chiral receptor, then racemic drug mixtures essentially contain 50% of the enantiomer that is pharmaceutically active, the so-called "eutomer".[8, 9] Single enantiomers are therefore expected to have a better effect than racemate drugs on the body because the effective dose of the active drug is higher. The undesired enantiomer may also have undesired effects. In this case, administering a single enantiomer becomes crucial. Finally, even if the target of a drug is not enantioselective, the pharmacokinetics of the enantiomers may still differ as a result of enantioselectivity in the process involved.[10] Even if an enantiopure drug is administered, however, this drug may still racemise. Therefore, it is important to investigate the single enantiomer's configurational stability.[11]

The story of the risk of drug racemisation started with the thalidomide tragedy in the late 1950s. Thalidomide was taken by pregnant women as an anti-nausea treatment between week 5 and 8 after conception. Teratogenic effects were caused by side-effects of the S-thalidomide (Scheme 1.4).[12,13]

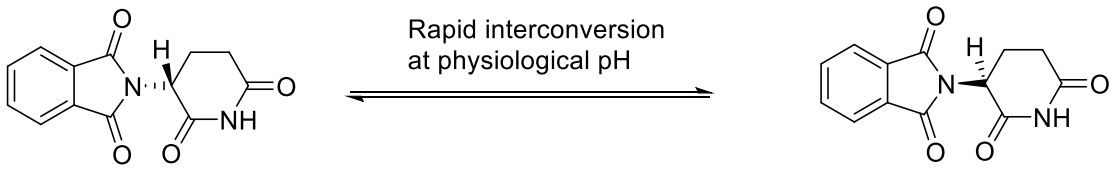

R(+)- Thalidomide

1.1 a

S(-)- Thalidomide

1.1 b

Scheme 1.4: Structures and interconversion of thalidomide enantiomers.

The study of racemic mixtures in drug development is more complicated in pharmacokinetic and biological systems than for single enantiomers. The biological activity of two enantiomers in a racemic mixture is often different. Because many biomacromolecules are chiral and occur as only one enantiomer (*e.g.* proteins and DNA), these interactions are not identical because of diastereomerical binding. For example, if we assume that our target is an R enantiomer, the interactions are (R....R) versus (R.....S).[14] The difference between the Gibbs free energy change involved in the two diastereometrical binding processes is called enantiomer-discrimination.[14] Due to the stronger binding interaction of one enantiomer with a receptor, the difference in Gibbs free energy change upon binding (ΔG^o) is not equal to zero, *i.e.* $\Delta_{RS}\Delta G^o \neq 0$. To calculate the free energy ΔG^o change related to each individual equilibrium constant, the following equation can be used[15,16]

$$\Delta G^o = -2.303\, RT \log K \qquad \textbf{Equation 1. 9}$$

At the physiological condition (T = 310 K), the equilibrium constant can be observed (in kcal mol^{-1}) and ΔG^o is obtained using Equation 1.9 ($\Delta G^o = -1.4 \log K$). A drug binding with a K_d of 10^{-4} M (*i.e.* $K = 10^4$ M^{-1}) at 310 K corresponds to a change in standard molar Gibbs energy of 5.6 kcal mol^{-1} required to dissociate the drug from the receptor.[16]

1.1.6 Configuration instability and selected examples of racemising drugs

It is very important to study drug racemisation because many optically active drugs racemise *in vivo*, which can lead to various side effects.[17] Many articles have been published studying

drug racemisation and also describing factors affecting racemisation such as pH, temperature, solvent and ionic strength. Danel *et al.*[18] studied the racemisation of an N-imidazole derivative (Scheme 1.5) in TRIS buffer pH 7.4 at 30, 50 and 70 °C with the corresponding $t_{1/2}$ of 117.8, 15.4 and 6.6 h, respectively. Chiral inversion could occur through base-induced deprotonation of the labile benzylic proton at the stereogenic carbon, resulting in a planar carbanion. For example, it has been shown that adding TEA increases the rate constant for racemisation of N-imidazole derivatives. The rate constant for racemisation of thiazole-substituted **1.2** (when X = S) has been reported to be twice as fast as that for oxazole (when X = O) (Scheme 1.5).

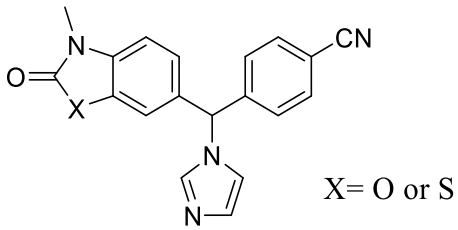

1.2

Scheme 1.5: Structures of N-imidazole derivatives

The racemisation of ketorolac (Scheme 1.6) was studied in aqueous buffer solutions at different pH and temperature. Brandl *et al.*[19] reported that 20% racemisation of ketorolac tromethamine can be achieved after 8 months in 0.04 M of TRIS buffer at pH 7.4 at room temperature (25 °C). The proposed mechanism suggests that racemisation occurs with acid/base through the formation of an enol following protonation on the ketone on one side and transfer of hydrogen on the other.

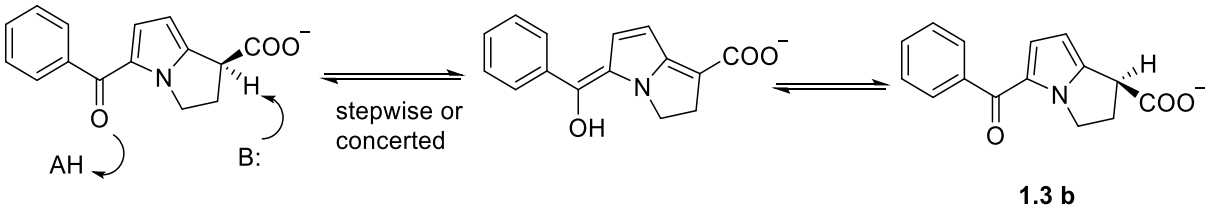

1.3 a **1.3 b**

Scheme 1.6: Proposed mechanism for the racemisation of ketorolac.[19]

Mey *et al.*[20] reported the racemisation of (+)- and (−)-diethylpropion (Scheme 1.7 a) in aqueous solution under physiological conditions. The racemisation was studied with and without cyclodextrins, both in organic solvent and human plasma. In aqueous solution, the racemisation of (+)- and (−)-diethylpropion became faster with increasing pH, temperature and phosphate buffer concentration, while the rate constant decreased with increasing ionic strength. The rate constant of racemisation increased by increasing the polarity of the organic solvent in the case of (−)-DEP. The pseudo-first-order rate constant for (+) - and (−)-DEP was reported to be unaffected by the presence of cyclodextrins and could be slowed down by human plasma. The racemisation of ketoprofen (Scheme 1.7, compound 1.4 b) has been suggested to be very fast and to involve reversible chiral inversion in mice.[21]

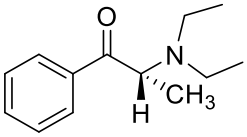

1.4 a

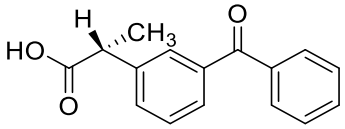

1.4 b

Scheme 1.7: Structures of **1.4** a) (*R*)-diethylpropion, and b) (*R*)-ketoprofen

Chiral stability and degradation, including the sulphonation of adrenalin (Scheme 1.8), were studied by Stepensky *et al.*[22] using chiral HPLC at different pH. It was determined during the storage of metabisulphite stabilised adrenaline injections that the degradation process takes place for the pharmacologically active L-adrenaline isomer involving racemisation oxidation and sulphonation.

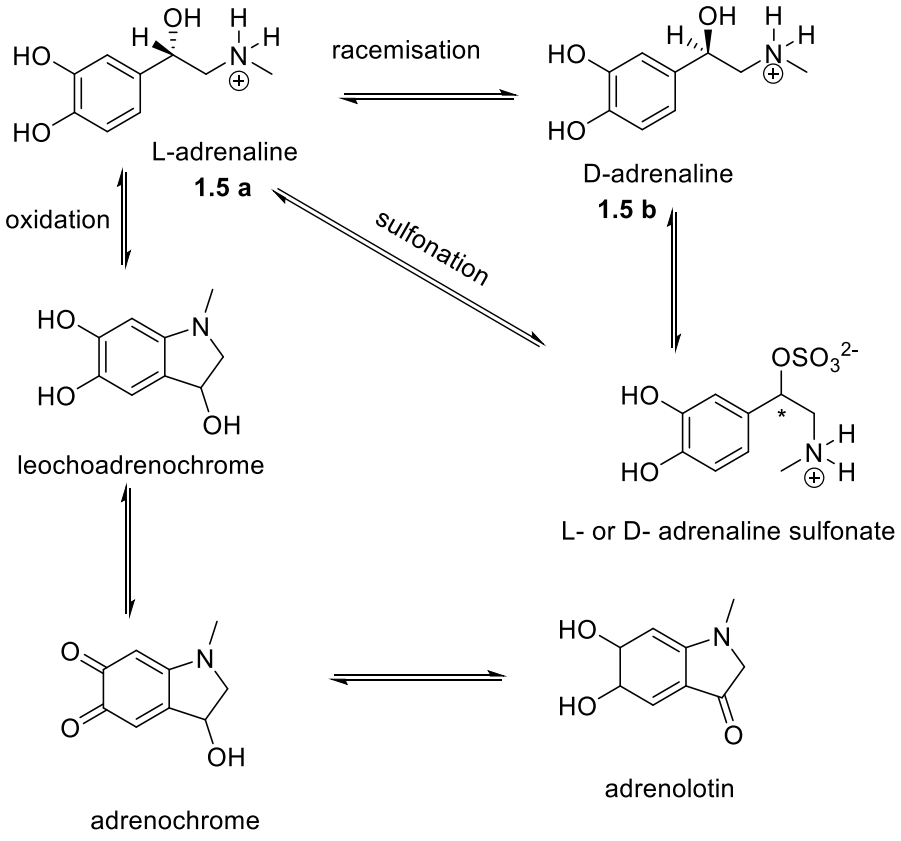

Scheme 1.8: degradation of L-adrenaline.[22]

The base-catalysed racemisation of *R*,*S*-2-(4-isobutylphenyl) propionic acid (ibuprofen) (Scheme 1.9), which is an important example of non-steroidal anti-inflammatory drugs "NSAIDs", has been studied by Xie *et al*.[23] The rate of dynamic equilibrium tautomerism leads to racemisation of the ibuprofen isomers in DMSO-water (4:1, v: v). The racemisation reaction suggested a pseudo-first-order rate constant which depends on the concentration of base catalyst rather than the concentration of the substrate. It has also been reported that using DMSO with base catalyst increases the rate constant of racemisation of ibuprofen while the single enantiomer is highly stable in DMSO without NaOH. The enantiomeric excess (ee) of 75.4% after 6 h racemisation reaction was obtained in DMSO-water mixed medium containing 80% DMSO at 100 °C. The *R*-ibuprofen racemisation has been suggested to involve keto-enol tautomerism, in which the rate determining step is the enolisation of ibuprofen.[23]

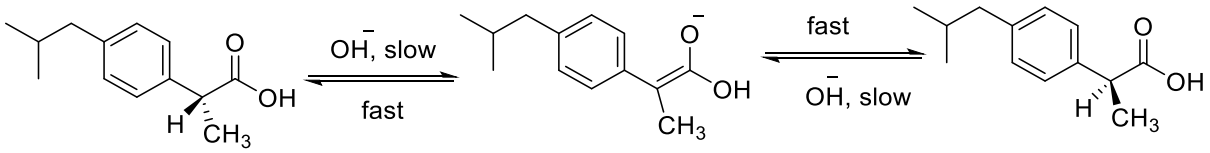

(*R*)-ibuprofen

1.6 a

(*S*)-ibuprofen

1.6 b

Scheme 1.9: Racemisation of ibuprofen enantiomers by keto-enol tautomerism.[23]

Oğuz and Doğan [24] studied the mechanism of the thermal racemisation of 5,5-dimethyl-1-(o-aryl)barbituric and 2-thiobarbituric acid derivatives (Scheme 1.10). The keto-enol tautomerism and variable tautomerism at different positions were suggested as possible mechanisms for the racemisation of the barbituric and 2-thiobarbituric acid derivatives. The lower reported activation energy for the racemisation of the thione derivatives compared to the oxo derivatives was unexpected. Similarly, the racemisation rate constants of thiohydantoin derivatives have been found to be higher than for hydantoin derivatives (*vide infra*). Substituents at the asymmetric carbon greatly influence increases or decreases in activation energy. The ring opening of **1.7** (Scheme 1.10) was also expected to compare with the racemisation of 3-arylthiazoline-2-thione **1.7** and their oxygen analogue, as suggested by Roussel *et al*. (Scheme 1.10).[25]

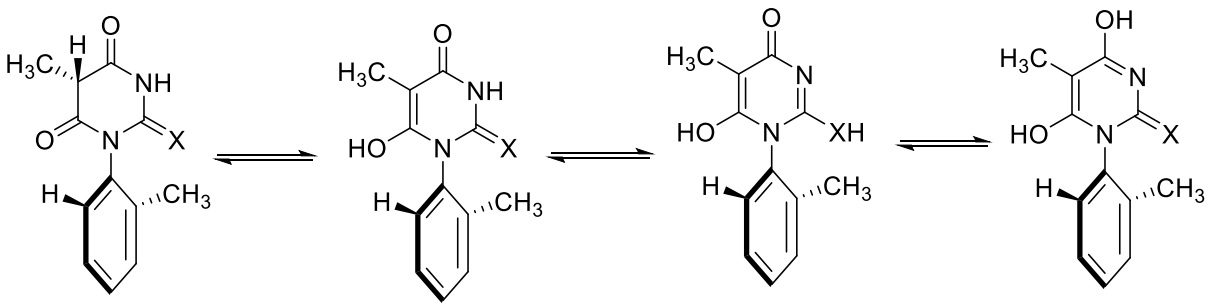

1.7

X = S, or O

Scheme 1.10: Possible tautomers of barbituric and 2-thiobarbituric acid derivatives in ethanol.[24]

Lambert *et al*.[26] reported the cyclisation and racemisation mechanism for ibutilide (Scheme 1.11) at 70 °C to involve an intramolecular substitution reaction. Lambert *et al*. observed

acid- and base-catalysis and also suggested that the rate-determining step for this reaction changes as a function of pH, as suggested by a U-type rate of racemisation as a function of pH. In acidic medium, racemisation takes place by the protonation of the hydroxyl. The racemisation of ibutilide is suggested to occur via a carbocation intermediate. The formation of a cyclic side product resulting from a nucleophilic attack on the intermediate cation by the internal amine is proposed as evidence for the existence of the intermediate carbocation (Scheme 1.11a). However, the S_N1-type mechanism suggested by reference[26] is unlikely to be followed by **1.8** because the carbocation intermediate is likely too high in energy to be a viable reaction intermediate. An alternative mechanism can be drawn as shown in scheme 1.11b.

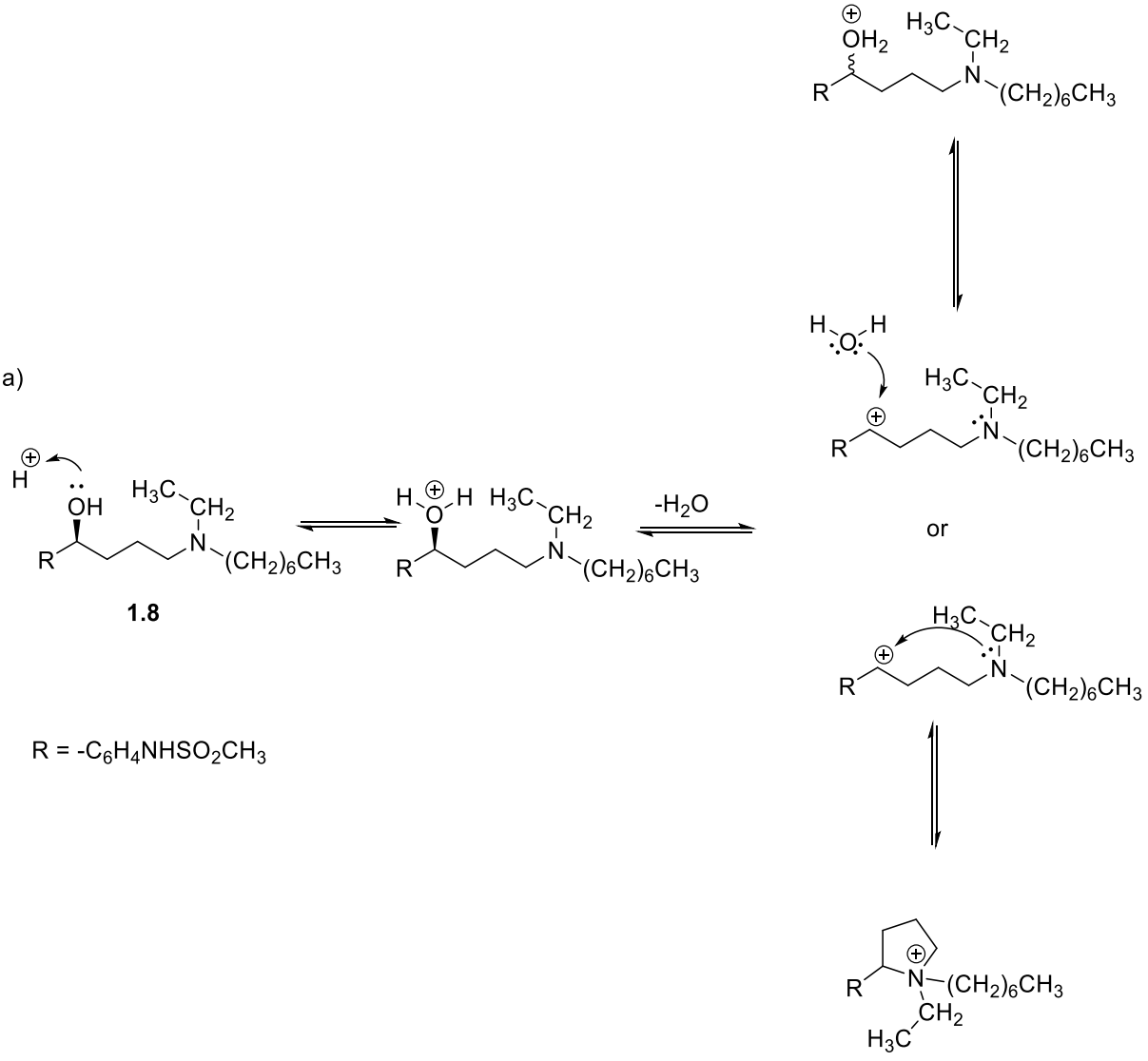

b)

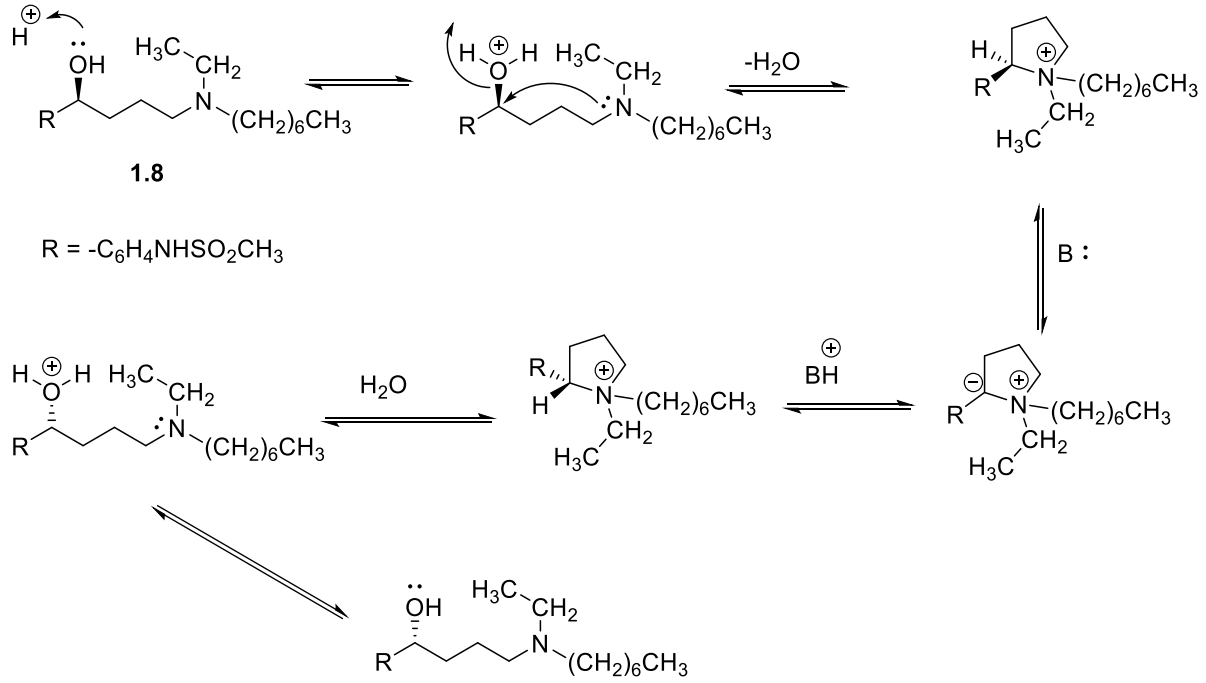

Scheme 1.11: Proposed mechanism for racemisation of ibutilide[26] (a) and an alternative mechanism for inversion via a cyclic intermediate (b).

Yang[27] reported the racemisation of temazepam **1.9** (TMZ) (Scheme 1.12) in acidic methanol and ethanol. The author reported the rate of racemisation observed by CD spectroscopy and the rate of reaction of rac-TMZ to form rac-MeTMZ (or rac-EtTMZ) obtained by ultraviolet-visible spectrophotometry. Ring opening/closing as a possible mechanism for racemisation of *R*-TMZ **1.9a** was reported by Yang in alcoholic solvent. The proposed mechanism involves a hydrogen-bonded intermediate **1.9b** resulting from solvation, which reacts to form **1.9c** by opening the C3-N4 bond of the TMZ ring (Scheme 1.12). The rate constant for acid-catalysed alcoholysis in ethanol ($t_{1/2}$ = 3.0 minutes) was higher than in methanol ($t_{1/2}$ = 4.29 minutes) containing 0.5 M H_2SO_4 at 50 °C. However, MeTMZ was reported to be more easily decomposed than EtTMZ. It was also indicated that the rate for racemisation of the N_4-protonated form of TMZ increases with increasing acid concentration and the rate of racemisation for the un-protonated form of TMZ decreases with increasing acid concentration. Therefore, the N_4-protonated form of TMZ has a lower rate constant for racemisation than the un-protonated form.[27] Using strong base for the racemisation study for TMZ produces 2-(methylamino)-5-chlorobenzophenone due to hydrolysis of TMZ (Scheme 1.12).[28]

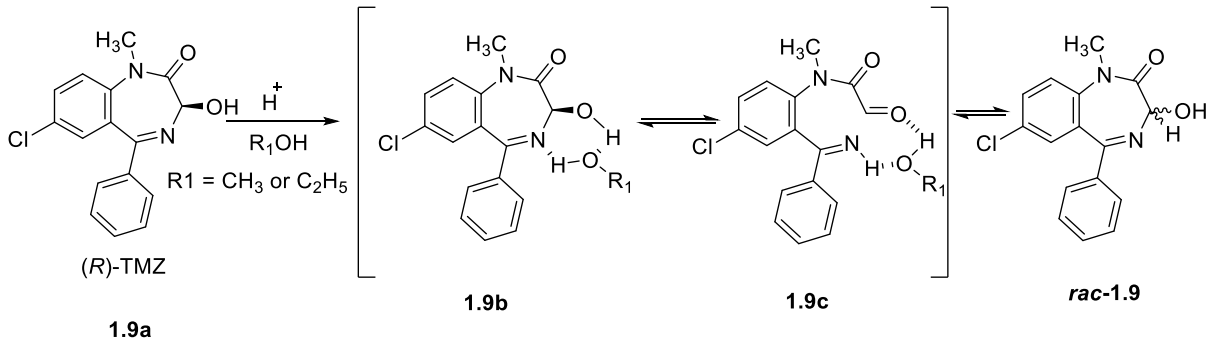

Scheme 1.12: Proposed mechanism of racemisation of (*R*)-7-chloro-3-hydroxy-1-methyl-5-phenyl-1H-benzo[e][1,4]diazepin-2(3H)-one (temazepam TMZ) in alcohol solvent by Yang.[27]

General-base catalysis of the racemisation of amfepramone and cathinone at pH 7.4 was proposed by M. Reist *et al*.[27]

1.1.7 General mechanisms of racemisation

Good leaving groups which detach from stereogenic centres of optically active compounds produce carbocations. The carbocation is achiral because of its planar form and a racemic mixture is formed through recombination of the cation with the anion or solvent (Scheme 1.13).[2]

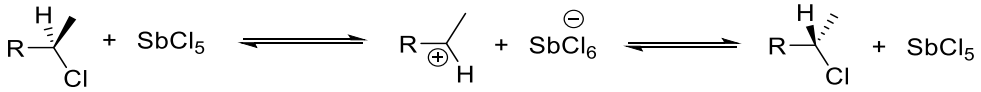

Scheme 1.13: Racemisation mechanism of optically active molecule through formation of a planar carbocation intermediate.

Compounds that can form a carbanion on the stereogenic centre can also racemise because of rapid inversion or planarity of the carbanion. Compounds with a ketone function attached to the stereogenic centre can racemise through keto-enol equilibria (Scheme 1.14). In the case of keto-enol tautomerism, the proton transfer takes place between carbon and oxygen. The interconversion of enantiomers occurs by abstraction of a proton on the stereogenic centre by base, resulting in an enolate intermediate which binds a proton with a pair of electrons on the enolate oxygen to produce an enol-form species.[29]

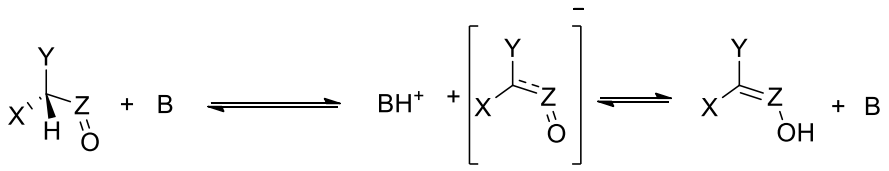

Scheme 1.14: Keto-enol tautomerism mechanism of racemisation.

The carbanion can be formed in suitable solvents in the absence of base when the proton attached to the stereogenic centre is very acidic, for instance in the case of disulphone (Scheme 1.15).[2]

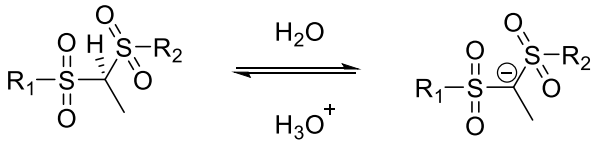

Scheme 1.15: Carbanion formation of optically active disulphone derivative.

Ketones with attached α-hydrogen may racemise in mineral acid through enol intermediates (Scheme 1.16).[2]

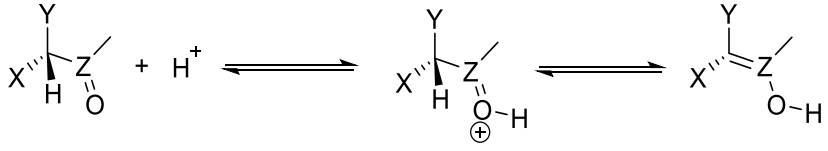

Scheme 1.16: Acid racemisation mechanism of ketone through intermediate formation.

Complete racemisation occurs in the so-called bimolecular S_E1 reaction in which hydrogen attached to the stereogenic centre is removed first in a rate-determining step to give a planar carbanion. Then, an incoming electrophile attaches to either face (Scheme 1.17).[7, 29, 30] Each carbanion is deuterated with equal rate constants from the front and back side in the case of an S_E1 reaction. Therefore, $k_{H/D}/k_{rac}$ approaches unity (See Section 1.3).

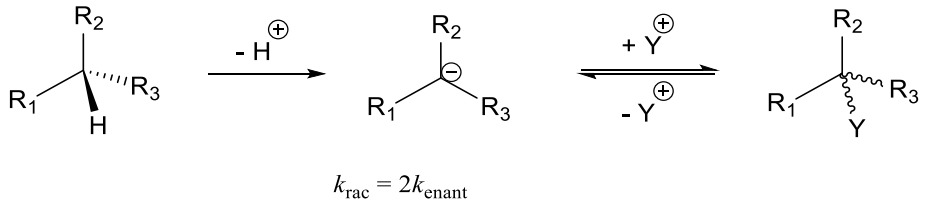

$k_{rac} = 2k_{enant}$

Scheme 1.17: S_E1 mechanism of racemisation.

The 'push-pull' mechanism of racemisation is another possible mechanism for optically active $\underline{R_1R_2R_3H}$ compounds. The termolecular S_E2 mechanism consists of an incoming electrophile (Y^+) initiating the reaction from the back, while simultaneously a proton leaves the molecule from the front, resulting in a chiral inversion of configuration (Scheme 1.18).[2, 7, 29-31] The H/D exchange rate in an S_E2 reaction is half the rate of racemisation and equal to the rate of enantiomerisation. Therefore, $k_{H/D}/k_{rac} = 0.5$ (See also Section 1.3).

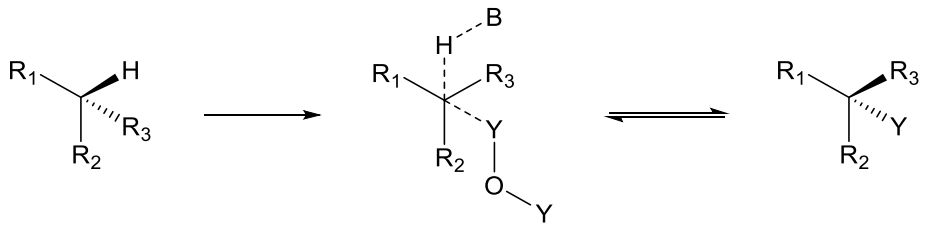

½ $k_{rac} = k_{enant}$

Scheme 1.18: S_E2 mechanism of racemisation.

Two more racemisation mechanisms relying on formation of ion pairs will be discussed in Section 1.3.

1.2 Derivatives of hydantoin and structurally related compounds

Several five-membered heterocyclic rings have been recognised as chiral molecules and their activity studied by the medicinal chemistry community (Scheme 1.19).

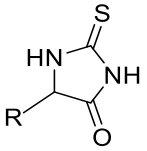

1.10 a

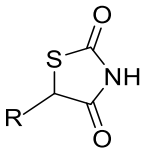

1.10 b

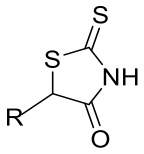

1.10 c

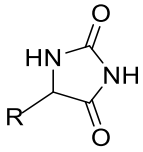

1.10 d

Scheme 1.19: Structures of 1.10 (a) 2-thiohydantoin, (b) thiazolidine-2, 4-dione (c) 2-thioxothiazolidin-4-one and (d) hydantoin

1.2.1 Therapeutic agents

The compounds shown in Scheme 1.19 have the ability to interact with a variety of biological targets and are so-called "frequent hitters" or privileged scaffolds.[32] Substituted five-membered ring heterocyclic molecules have therefore been used widely in the field of therapeutic agents.[33] Using a single enantiomer is essential because drug enantiomers differ in terms of toxicity, and pharmacodynamics.[34] Different hydantoin derivatives have been used in the treatment of epilepsy,[35] as antiarrhythmic agents[36] or anticonvulsants.[37] Thiohydantoin derivatives are known as being hypolipidemic, anticarcinogenic and antimutagenic and have been used in a wide range of applications.[38-40] 2,4-thiazolidinedione derivatives have been marketed as insulin-sensitising agents[41] and also for use in the treatment of different diseases.[42]

1.2.2 Synthesis

It can be difficult to obtain a high optically active drug-like molecules because racemisation can occur during synthesis, particularly if concentrated acid or base conditions and high temperature are required.

The reaction of α-amino acids with isocyanate generally takes place in basic aqueous solution to produce ureido acids. The cyclisation occurs by adding mineral acids to obtain the corresponding hydantoins **1.11** (Scheme 1.20).[43]

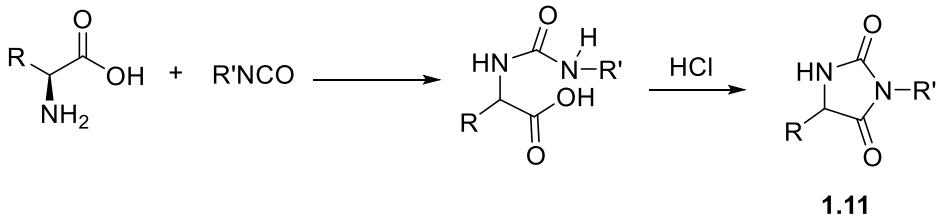

1.11

Scheme 1.20: The condensation of amino acids with isocyanate.

It has also been reported that urea can be used with amino acids to give the corresponding hydantoin **1.12** with a yield of 15-20%.[43] The condensation of urea with amino acids in the absence of solvent needs high temperature. Therefore, the corresponding hydantoin would be a mixture of racemic compounds rather than enantiopure hydantoin (Scheme 1.21).

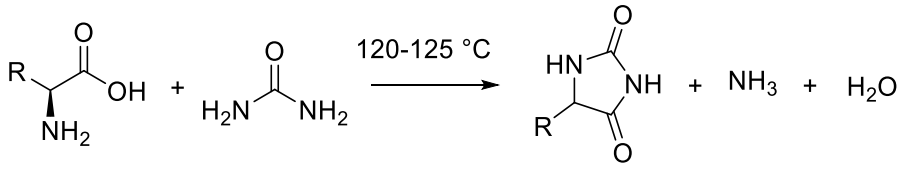

1.12

Scheme 1.21: The condensation of amino acids with urea.

It is also possible to use thiourea instead of urea to prepare the corresponding 2-thiohydantoins (Chapter 2).[38] High temperature during the reaction leads to racemic 5-substituted 2-thiohydantoin rather than an enantioenriched product. Narduolo[31] has used L-amino acid amides with carbonyldiimidazole (CDI) as a coupling agent dissolved in

dichloromethane to prepare (*S*)-5-benzylhydantoin **1.13** (Scheme 1.22). The author reported that (*S*)-5-benzylhydantoin showed a strong negative Cotton effect in CD spectra at 230 nm.

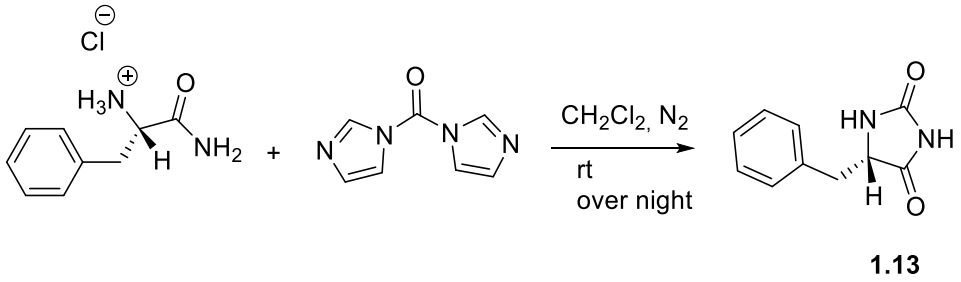

1.13

Scheme 1.22: Synthesis of (*S*)-5-benzylhydantoin as proposed by Narduolo.

The synthesis of 2-thiohydantoin acetylated at the N-1 position has been reported by Johnson[44, 45] by using amino acid with the ammonium thiocyanate in acetic acid and acetic anhydride. This procedure was a successful way to synthesise 5-substituted 1-acetyl-2-thiohydantoin. However, there was no mention of the optical activity of the product. However, in 1932, Csonka and Nicolet[46] reported the synthesis of both racemic and D-1-acetyl-5-methyl-2-thiohydantoin starting from enantiomerically pure D-alanine. The temperature during the reaction was not mentioned by the author. The optically active compound can be prepared by using 5 parts acetic anhydride containing 10% of acetic acid with ammonium thiocyanate. The large excess of acetic anhydride causes the rapid formation of azlactone (**1.14 a**) and produces highly optically active 5-substituted 1-acetyl-2-thiohydantoin (**1.14 b**). In the absence of isothiocyanate, the active azlactone racemises rapidly in half an hour or less. Therefore, sufficient isothiocyanate in the reaction is necessary (Scheme 1.23).[46]

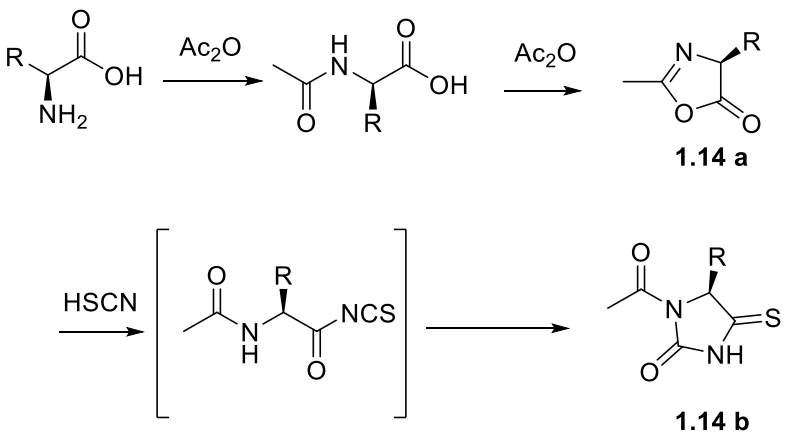

Scheme 1.23: Johnson's suggested mechanism for the formation of 5-substituted 1-acetyl-2-thiohydantoins.[47]

During the reaction, the carboxyl group is activated by the hydrogen of a strong acid used with acetic anhydride. The carboxyl group becomes more liable to be attacked by the nucleophilic isothiocyanate ion in an acid catalysed reaction. Therefore, ammonium thiocyanate is not the best reagent to use without strong acid for the acetylation of thiohydantoin.[48]

Johnson did not report the optical activity of 1-acetyl-2-thioxoimidazolidin-4-one in his publication.

No articles were found to show the synthesis of enantioenriched 5-substituted thiazolidine-2,4-diones and 2-thioxothiazolidin-4-ones.

The condensation of hydantoin with benzaldehyde was first used by Wheeler and Hoffmann in 1911 to prepare 5-benzylidene hydantoin.[49] This method has been applied successfully to achieve the base-catalysed condensation of hydantoin with different aldehydes **1.15 a** (Scheme 1.24).[50,51,31] Similarly, condensation catalysed by bases such as triethylamine or piperidine has been used for the synthesis of thiohydantoins with different substituents **1.15 b** (Scheme 1.24).[52,53]

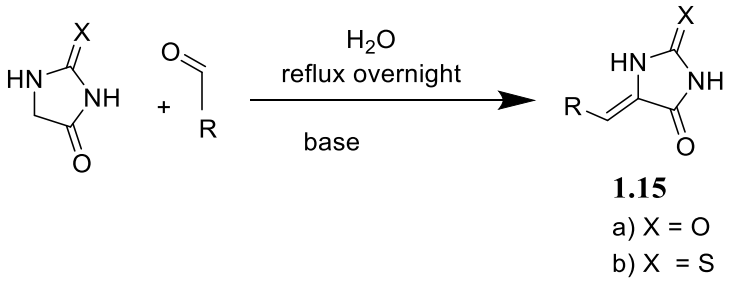

1.15

a) X = O

b) X = S

Scheme 1.24: Synthesis of 5-substituted hydantoins and 2-thiohydantoins

Narduolo used the Knoevenagel condensation of the appropriate aldehydes with hydantoin to prepare 5-arylideneimidazolidine-2,4-dione and suggested that the Z isomer for 5-benzylideneimidazolidine-2,4-dione is formed.[31] Similarly, Waldemar *et al*.[54] suggested the formation of the Z isomer of 5-benzylidene-2-thioxoimidazolidin-4-one when benzylaldehyde reacts with 2-thiohydantoin.

1.2.3 Hydrolysis

Despite the fact that hydantoic acids can cyclise under acidic conditions to produce hydantoin, hydantoin can also hydrolyse under basic conditions.[55] Bergon and Calmon[55] studied the alkaline hydrolysis of 5-aryl and 3-arylimidazolidine-2,4-diones to produce 5- and 3-arylhydantoic acids in aqueous solutions over the pH range 8-14 at 25 °C. The authors showed a straight-line correlation of increasing log*k* versus pH in the pH range from 8 to 12, followed by a plateau at pH >12. The ionisation of the substrate and the formation of the unreactive anion **1.16b** can account for the levelling off of the straight line, resulting in the plateau at high pH.[55] The hydrolysis takes place by attack of OH^- on the unionised substrate **1.16a** to form an intermediate (Scheme 1.25).[56]

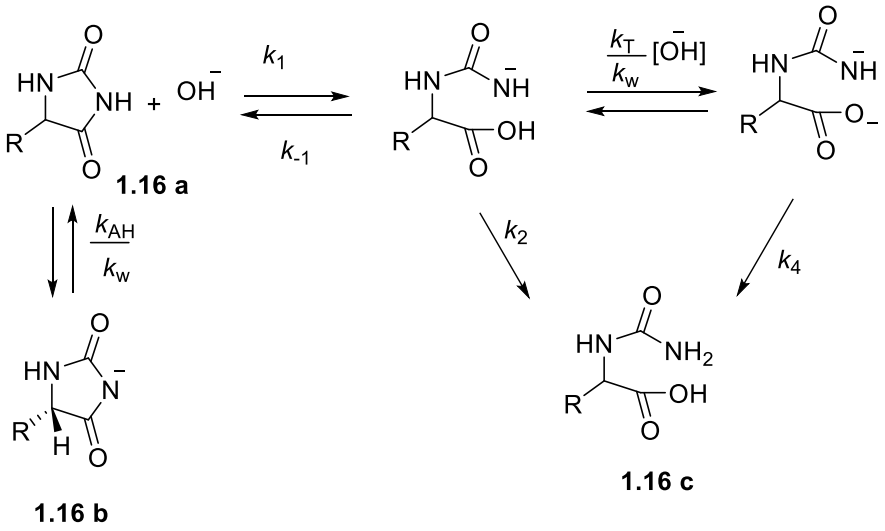

Scheme 1.25: Base-catalysed hydrolysis mechanism of 5-substituted hydantoins, as proposed by Blagoeva *et al*.[56]

Blagoeva *et al*.[56] elucidated the mechanism of alkaline hydrolysis of five ring compounds such as hydantoin **1.17 a** and 3-methylhydantoin **1.17 b,** as well as six-membered rings such as 3-methyldihydrouracil **1.18** (Scheme 1.26). The effect of ring size was examined and it was shown that angle strain in the ring is important. The rate of the addition of hydroxide to the six-membered ring is 2-3 times faster than the rate of the addition to hydantoin and 3-methylhydantoin.[56]

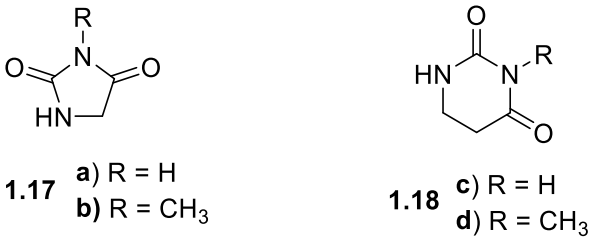

Scheme 1.26: The chemical structures of 1) hydantoin, 2) 5-methylhydantoin, 3) dihydropyrimidine-2,4(1H,3H)-dione (dihydrouracil) and 4) 3-methyldihydrouracil.

At high concentrations of OH^-, breakup of the tetrahedral intermediate can be expected as the rate-determining step. In this case, the reaction is catalysed by OH^- and H_2O, which can be

interpreted as either a specific acid-base catalysed or a general acid-base catalysed mechanism of hydrolysis (section 1.5 and Chapter 3). The same mechanism is expected for the alkaline hydrolysis of dihydropyrimidines.[57]

Congdon and Edward[58] reported the mechanism of base-catalysed hydrolysis of 5-substituted 1-acetyl-2-thiohydantoins (Scheme 1.27). The acyl linkage degradation for thiohydantoin can be related to the base-catalysed deacetylation of polypeptide reported previously. Schlack and Kumpf[59] published an article in 1926 indicating that the acyl group in polypeptide degrades under mild acid or base conditions. 1- acetyl-2-thiohydantoins can ionise as weak acids and have pK_a values of 6.5-7.0, creating a negative charge at the N-3 position (Scheme 1.27).

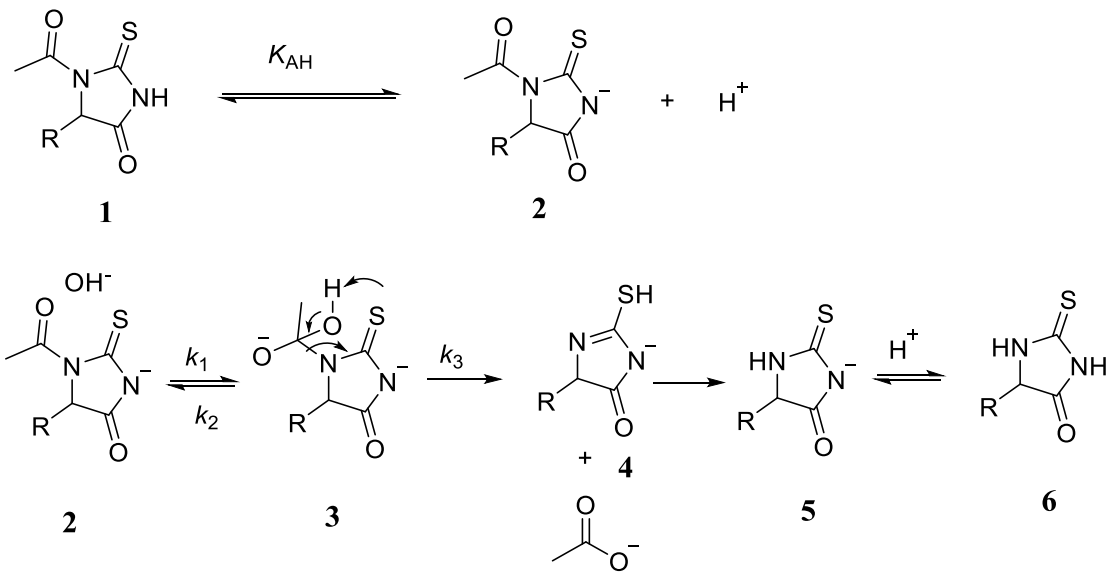

Scheme 1.27: The mechanism of base-catalysed hydrolysis of 5-substituted 1-acetyl-2-thiohydantoins, as proposed by Congdon and Edward.[58]

The effect of substituents at the C-5 position on the acid and base-catalysed hydrolysis of 5-substituted 1-acetyl-2-thiohydantoins has been reported by Congdon and Edward.[58] Substituents at the C-5 position retard the base-catalysed hydrolysis much more than the acid catalysed hydrolysis. The authors also suggested the possibility of the hydrogen bond between the partially negative sulphur and the hydroxyl group as being important in the mechanism (Scheme 1.28).

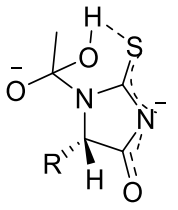

1.19

Scheme 1.28: Hydrogen bond formation between the partially negative sulphur and the hydroxyl group for **1.19**.

The conversion of **2** to **3** (Scheme 1.27) leads to "eclipsing" between the R group at the C-5 position by the solvated O- and R group of the tetrahedral intermediate (Scheme 1.27). As a result, the steric hindrance for the buffer catalysed hydrolysis of 5-substituted 1-benzoyl-2-thiohydantoins has a large effect on the retardation of the rate of hydrolysis (Table 1.1).[60]

Table 1.1: Buffer catalysed hydrolysis of 5-substituted 1-benzoyl-2-thiohydantoins in aqueous phosphate buffer pH 11.2, 0.45 *I*, at 25.3 °C.

1-benzoyl-2-thiohydantoin	$k_{hydrolysis}$ / 10^4 s^{-1}
Unsubstituted	31.40 ± 0.40
5-methyl	12.70 ± 0.21
5-phenyl	10.20 ± 0.66
5-isopropyl	4.77 ± 0.18
5-isobutyl	6.64 ± 0.15
5-sec.butyl	4.65 ± 0. 16
5,5-dimethyl	2.38 ± 0.06

Edward and Nielsen[61] studied the alkaline hydrolysis of 5-substituted 2-thiohydantoin to produce thioureido-acids. Substituents at N-3 speed up hydrolysis because of the lack of ionisation of a more acidic hydrogen.[61]

Benke[62] reported the basic hydrolysis of arylidene-rhodanine **1.20** (Scheme 1.29) supported by recent literature[63] that interpreted rhodanine hydrolysis as being catalysed by base to produce the salt of a thioxo-acid followed by tautomerism to give the thioenolate **1.21** (Scheme 1.29).

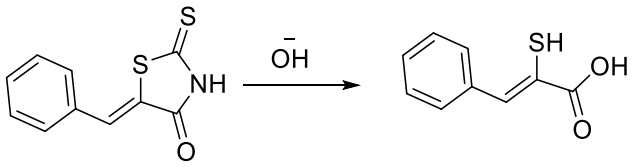

1.20 **1.21**

Scheme 1.29: The hydrolysis product of (Z)-5-benzylidene-2-thioxothiazolidin-4-one.

1.2.4 Racemisation of hydantoin derivatives

Hydantoins and related compounds, including imidazolidine-2,4-dione, 2-thioxoimidazolidin-4-one (2-thiohydantoin), thiazolidine-2,4-dione and 2-thioxothiazolidin-4-one (rhodanine), are subject to racemisation in the presence of a buffer or base. In 1910, Mendel and Dakin[64] published a paper explaining the racemisation of optically active hydantoin in the presence of base. The authors proposed that the proton attached to the stereogenic carbon was transferred by base and produced a planar carbanion, leading to the tautomeric compound forming racemic mixtures.[64] Dudley and Bius[65] reported the mechanism of the interconversion of 5-phenylhydantoin by divalent phosphate *in vivo* without a specific racemase (Scheme 1.30). The change in optical rotation was recorded over time using a spectropolarimeter and the pseudo-first-order rate constants were obtained in pH range 6.0-7.5. It was determined that the rate constant increases linearly with increasing buffer concentration and increasing pH, which suggests general-base catalysis. In this article, it was concluded that the abstraction of a proton at the asymmetric carbon was the rate-determining step. This was also suggested by Dakin.[66] After correcting the kinetic data for the ionisation at the N-3 position at each pH, the authors suggested that the rate constants for racemisation of 5-phenylhydantoin were almost

the same as those for racemisation of 3-methyl-5-phenylhydantoin. The experimentally determined pseudo-first-order rate constant for the racemisation of 5-phenylhydantoin of $(47.20 \pm 1.30).10^3$ /minutes was reported in 0.1 M phosphate buffer (pH 7.5, 0.35 M *I*). After correction, the value was adjusted to $(54.90 \pm 1.30).10^3$/ minutes (Scheme 1.30) .[65]

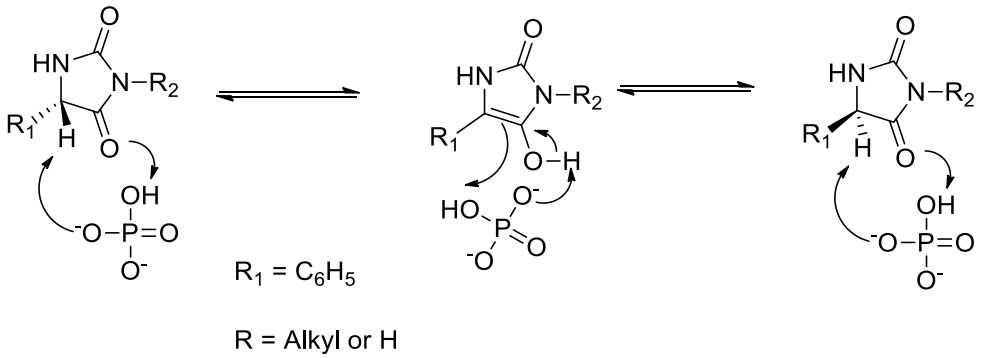

Scheme 1.30: Mechanism of racemisation of optically active 5-phenylhydantoin or 3-methyl-5-phenylhydantoin by di-valent phosphate, as proposed by Dudley and Bius.[65]

Aryl and alkyl groups at the N-1 or N-3 position were suggested by Bovarnic and Clarice[67] to retard the racemisation, and substituents at both positions may even prevent it. Keto-enol tautomerism is essential for hydantoin and thiohydantoin to undergo racemisation. Bovarnic and Clarice proposed two possible bond displacements between the nitrogen at the 1 and 3 positions with the carbonyl at the 2 position and between the hydrogen attached to the asymmetric carbon with the carbonyl at the 4 position (Scheme 1.31).

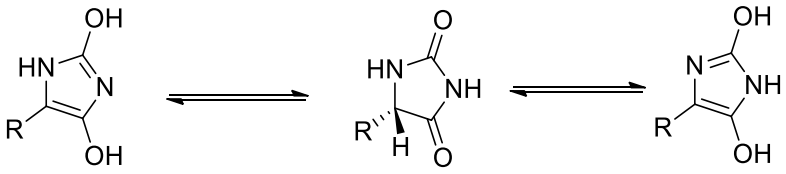

Scheme 1.31: The keto-enol tautomerism and bond displacement of 5-substituted hydantoins, as suggested by Bovarnic and Clarice.[67]

Keto-enol tautomerism has also been detailed for allantoin (5-ureidohydantoin) by Kahn and Tipton[68] and the S_E1 mechanism is expected to be favoured for the base-catalysed racemisation of allantoin (*vide infra*).

Reist *et al*.[69] studied the racemisation of 5-substituted hydantoins (Scheme 1.32) as a model compound in phosphate buffer pH 7.4 at different temperatures. The effect of substituents on the rate constants of racemisation at the C-5 position were also discussed.

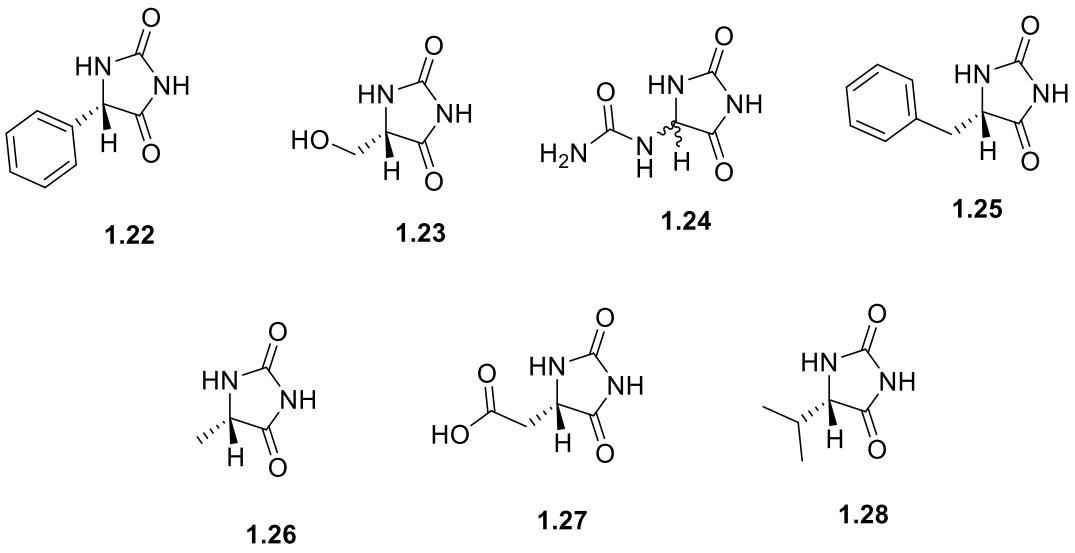

Scheme 1.32: Racemisation of 5-substituted hydantoins studied as a model for chiral drugs by Reist *et al*.[69]

The pseudo-first-order rate constants of racemisation and H/D exchange were determined for compounds **1.22-1.28** and the effect of substituents on the rate constant is quite obvious. A general-base catalysed racemisation was also concluded for the 5-substituted hydantoins racemisation. Narduolo[31] studied the racemisation of hydantoin with different substituents at the C-5 and N-3 positions in aqueous solution (Scheme 1.33) and explained the effect of co-solvents on the rate of racemisation. As can be seen, the methyl group at the N-3 position in compound **1.29** (Scheme 1.33) decreased the rate constant of racemisation compared to compound **1.25** as reported by Narduolo. This retardation in the rate constant of racemisation by the N-3 substituent was also found by Bovarnic and Clarice[67] for hydantoin racemisation.

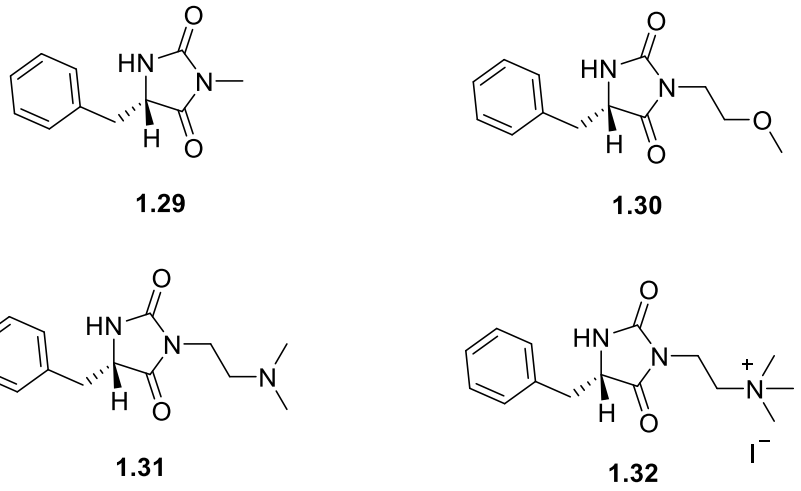

Scheme 1.33: Structures of several 3-substituted hydantoins studied with different 5-substituted hydantoin by Narduolo.

Pseudo-first-order rate constants for racemisation of $(167.3 \pm 1.3).10^{-6}$ s^{-1} and $(114.4 \pm 0.5).10^{-6}$ s^{-1} were reported for compounds **1.25**, and **1.29**, respectively in H_2O phosphate buffers (0.25 M, pH 7.2, 0.5 M *I*, at 60 °C). Similarly, the second-order rate constant for racemisation was shown to be lower for compound **1.29** by approximately 34% by Lazarus[70] in comparison with compound **1.25**. Lazarus studied the racemisation of **1.25** and **1.29** under physiological conditions and proposed general-base catalysed racemisation in which the rate constant of racemisation was increased by increasing the concentration of buffer. Electronegative substituents on the asymmetric carbon or amino group promote the rate constants of racemisation, as suggested previously.[66] Therefore, the rate constants of racemisation for compounds which have electronegative substituents attached to the asymmetric carbon have higher rate constants for racemisation than methyl, isopropyl and benzyl substituted compounds. Cabrera *et al*.[71] studied the enantiomerisation of 5-benzyl-3-phenyl-2-thioxoimidazolidin-4-one **1.33** (Scheme 1.34) using chiral HPLC in methanol-triethylammonium acetate buffer (pH 4.1) (2:98, v/v), 0.8 ml/min at different temperatures. The authors reported the values for the rate constants of enantiomerisation k_1 to be 0.0096, 0.0153 and 0.023 $minute^{-1}$ at 25, 30 and 35 °C, respectively.

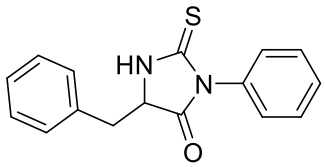

1.33

Scheme 1.34: Racemic 5-benzyl-3-phenyl-2-thioxoimidazolidin-4-one studied by Cabrera *et al.* [34]

Cabordery *et al.*[34] published an important article which reported the mechanism of the racemisation of tetrahydroisoquinoline hydantoin and thiohydantoin (Scheme 1.35) studied using HPLC and capillary electrophoresis. The rate constants, half-lives and energy barrier for racemisation of the different substituted- hydantoin and thiohydantoin compounds were reported. The pseudo-first-order rate constants for racemisation of thiohydantoin **1.34a** and hydantoin **1.34b** in ethanolic-aqueous medium show a linear increase with the concentration of the phosphate buffer and expected temperature dependence.

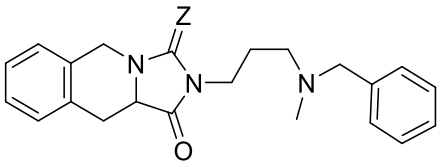

1.34 a) Z = S
b) Z = O

Scheme 1.35: Tetrahydroisoquinoline a) thiohydantoin, and b) hydantoin studied by Cabordery *et al.*[34]

The replacement of the oxygen by sulphur increases the rate constant of racemisation, which also increases the chiral instability of the enantiomers. Cabordery *et al.* reported that the enantiomer of compound **1.34a** needs less than one hour to racemise completely, while the enantiomer of compound **1.34b** requires 270 days for complete racemisation (Scheme 1.35).

1.3 Comparison of racemisation and H/D exchange kinetics

The carbanion intermediate was first studied by Wilson *et al.*[72, 73] who investigated the mechanism of racemisation of l-phenyl-2-methyl-1-butanone by comparing the rate of racemisation with the hydrogen-deuterium exchange rate. Wilson observed equal rates for racemisation and hydrogen-deuterium exchange of optically active 2-methyl-1-phenyl-1-butanone in a solution of dioxane-deuterium oxide-sodium deuterium butanone. It was proposed that a proton was transferred to the base in the rate-determining step, followed by deuteration or protonation of the resulting symmetrical anion on either the oxygen or carbon.[30] The pyramidal inversion of the optically active tetrahedral carbanion $R_2R_1RC^-$ in the racemisation is important to show that both pyramidal configurations are mirror images or enantiomers. The cleavage of the proton from the asymmetric carbon by base to form carbanion is followed by deuterium exchange in the deuterium containing medium.[29, 30] It has previously been shown that a comparison of the rate constants for base-catalysed racemisation and rate constants for hydrogen-isotope exchange of the optically active carbon acids can be used to determine the mechanism of racemisation (Scheme 1.36).[30]

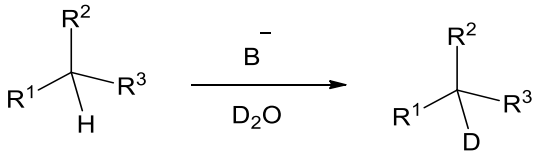

Scheme 1.36: Base-catalysed racemisation and H/D exchange

If a planar carbanion is formed as a result of deprotonation then proton-deuterium exchange occurs with complete racemisation because each carbanion is deuterated with equal rate constants from the front and from the back. Hence, $k_{H/D}/k_{rac}$ approaches unity.[29, 30] Even if the anion is not planar the reprotonation rate of the pyramidal configuration of the carbanion is typically much slower that the rate of inversion of the carbanion, and deuterium exchange will be followed by racemisation. The reaction is therefore expected to follow the S_E1 mechanism if $k_{H/D}$ is equal to k_{rac} (Scheme 1.37).[69]

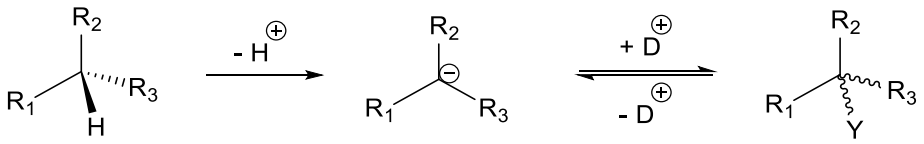

$k_{deut} = k_{rac} = 2k_{enant}$

Scheme 1.37: S_E1 mechanism of racemisation.

In the case of exchange with complete net inversion, on the back side, each carbanion will be captured simultaneously to deprotonation at the front to produce an inverted molecule. Therefore, the exchange rate is half that of racemisation and $k_{H/D}/k_{rac}$ = 0.5 (equal that of enantiomerisation) (Scheme 1.38).[7, 29, 30]

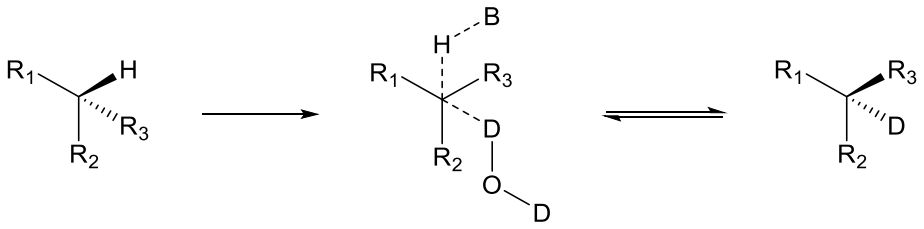

$k_{deut} = ½\ k_{rac} = k_{enant}$

Scheme 1.38: S_E2 mechanism of racemisation.

If racemisation in a deuterated solvent occurs without H/D exchange, then $k_{H/D}$ / k_{rac} approaches 0, also called isoracemisation (Scheme 1.39).[74] Isoracemisation was proposed to occur in two main ways. First, the proton of the asymmetric carbon might be moved from the front side to the backside by external proton donors through intramolecular proton transfer. Second, the proton which was attached to the carbon acid becomes reconnected with the carbanion and produces a racemic molecule without the isotopic exchange because of the absence of sufficiently strong acid to provide protons for the carbanion (Scheme 1.39).[30, 75] For this to occur the carbanion simply rotates 180° while remaining in an ion pair with its counterion, *i.e.* the protonated base (Scheme 1.39). In some cases, moisture can lead to small amounts of deuteration to take place. For example, a value of 0.23 was obtained for $k_{H/D}/k_{rac}$ for 9-deuterio-(or protio)-9-methylfluorene by Cram[76] by heating at 145 °C in dry tetrahydrofuran containing 0.5 M trimethylamine.[30, 77, 78]

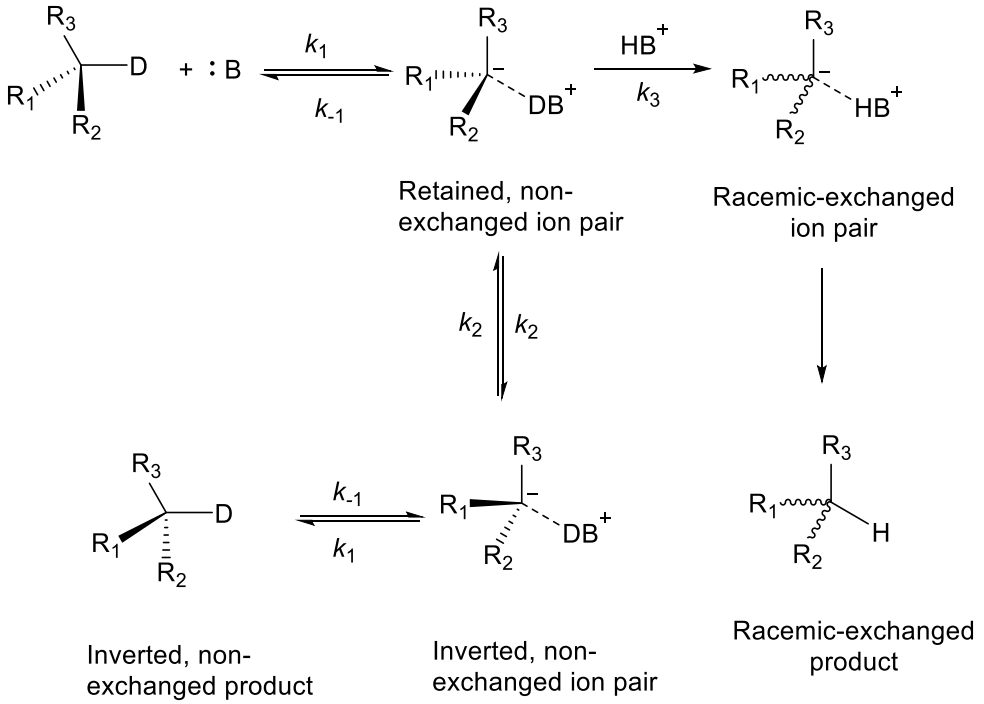

Scheme 1.39: The general mechanism of isoracemisation proposed by Cram.[30]

Cram indicated that isoracemisation takes place only when k_{-1} and $k_2 \geq k_3$.[30] It can be concluded that the reaction medium, including the type of base and solvent used, can change the mechanism of racemisation.[77]

The exchange process occurs with complete retention if the carbanion is pyramidal and protonation is faster than inversion. Complete or predominant retention depends on the relative rate of racemisation.[29] $k_{H/D} / k_{rac}$ approaches infinity for complete retention and $k_{H/D} / k_{rac} > 1$ in the predominant retention of configuration. Using ammonia as a base in the presence of *t*-butyl alcohol with optically active compound **1.35** leads to a high retention of configuration ($k_{H/D} / k_{rac} > 50$ at 200 °C) (Scheme 1.40).[79] The values of $k_{H/D} / k_{rac}$ obtained were equal to 10 or higher in the presence of non-dissociating solvents and potassium oxide bases used as a catalyst for the racemisation of 2-phenylbutane and 2-(N,N-dimethylamido)-9-methylfluorene.[80] Using a high concentration of ammonia in tetrahydrofuran decreases the value of $k_{H/D}/k_{rac}$ for **1.35** because ammonia promotes the reaction rate and ion-pair dissociation. The retention mechanism occurs when k_2 and $k_{-1} > k_3$. The dissociation of the ions becomes faster than ammonium ion rotation if dimethylsulphoxide is used ($k_3 > k_2$). This can form the symmetrical carbanion, with the value of $k_{H/D} / k_{rac}$ going to unity (Scheme 1.40).[30, 79, 80]

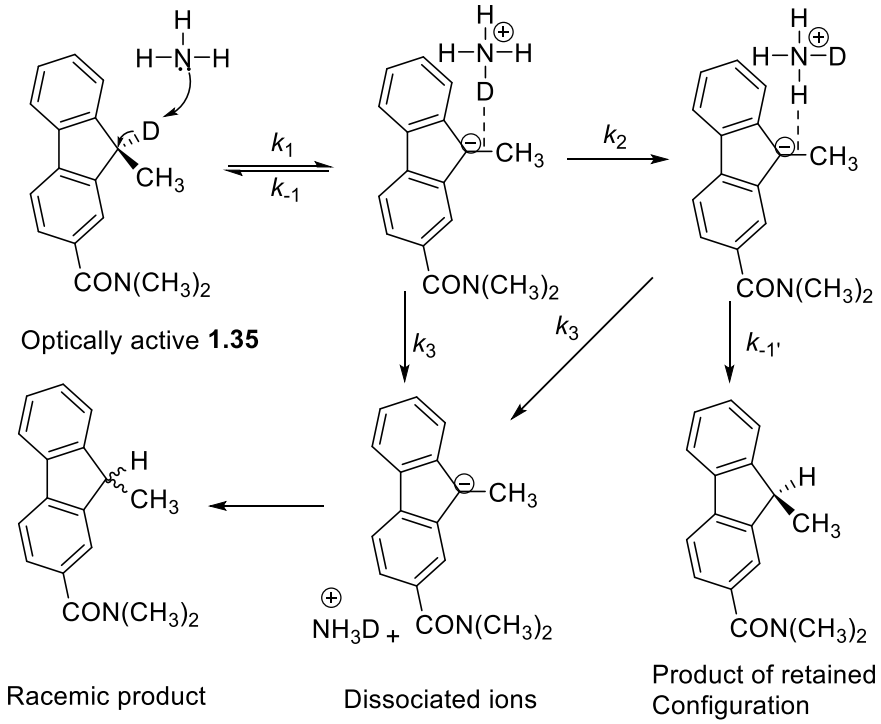

Scheme 1.40: Mechanism of the retention by ammonium ion rotation proposed by Cram[30]

1.4 Kinetic and equilibrium isotope effects

The contribution of rotational, translational and electronic motion to the overall energy of a molecule does not depend significantly on isotopic substitution. On the other hand, the vibrational contribution to the energy depends significantly on the isotopic substitution.[81] Therefore, changing the isotope of an atom can have an effect on equilibrium and rate constants. Primary kinetic isotope effects take place when a bond involving the isotope is broken in the transition state. Secondary kinetic isotope effects occur when the bond involving the isotopic substitution is not broken in the transition state, but breaking of another (adjacent) bond changes the vibrational frequency of the bond involving the isotope substitution. The zero point vibrational energy is given by[29, 82]

$$\varepsilon_{\circ} = \frac{1}{2}\left(h\nu\right) \qquad \textbf{Equation 1. 10}$$

where *h* is Planck's constant and *v* is the vibrational frequency of the bond concerned.

With the vibration frequency *v* given by Equation 1.11

$$\mathrm{v} = \frac{1}{2\pi}\sqrt{\frac{f}{\mu}} \qquad \textbf{Equation 1. 11}$$

where *f* is the force constant of the bond and μ is the reduced mass of the atoms involved in the bond.

The force constants are equal for both isotopes $f_{\mathrm{H}} = f_{\mathrm{D}}$ and μ is the reduced mass given by Equation 1.12.

$$\mu_{HX} = \frac{m_1\, m_2}{(m_1 + m_2)} \qquad \textbf{Equation 1. 12}$$

where m_1, and m_2 are the masses of the atoms linked by the covalent bond.

From Equation 1.11 and Equation 1.12, the reduced mass of the deuterium attached to a much heavier atom becomes 2 and hydrogen attached to a much heavier atom becomes 1. Then the frequency ratio becomes $\sqrt{2}$ (Equation 1.13).

$$\frac{\nu_{HX}}{\nu_{DX}} = \sqrt{\frac{\mu_{\mathrm{DX}}}{\mu_{\mathrm{HX}}}} \approx \sqrt{2} \approx 1.4 \qquad \textbf{Equation 1. 13}$$

The kinetic isotope effect is obtained from the ratio between the rate constants of two reactions that differ in the isotope composition of the reactants (Equation 1.14).[83]

$$\mathrm{KIE} = \frac{k_{\mathrm{light}}}{k_{\mathrm{heavy}}} \qquad \textbf{Equation 1. 14}$$

where k_{light} is the rate constant for the reaction of the light isotope and k_{heavy} is the rate constant for reaction of the heavy isotope.

In the solvent kinetic isotope effect, the vibration frequencies of H_2O and H_3O^+ are different from those of D_2O and D_3O^+. When the solvent is involved in the reaction mechanism, a kinetic isotope effect can arise. The isotope effect can be primary, secondary, normal or inverse depending on the role of the solvent. As a result of D_3O^+ being a stronger acid than H_3O^+, reactants in D_2O solution are protonated more at the same acid concentration (pD) than reactants in H_2O at the same acid concentration (pH). Therefore, a reaction requiring a protonated substrate proceeds faster in D_2O than in H_2O. The ratio $k_{H_2O} / k_{D_2O} < 1$, therefore an inverse solvent kinetic isotope effect is observed. Inverse solvent kinetic isotope effects happen when solvent is not involved as a proton donor in the rate determining step in the reaction. However, the reaction in H_2O will be observed to be faster than D_2O when the proton abstraction is part of the rate determining step and obtain the normal kinetic isotope effect.[84] Normal solvent kinetic isotope effects happens when the proton transfer is part of the rate –determining step and the reaction is faster in H_2O than D_2O.[85]

Proton abstraction from carbon acids in hydantoin and thiohydantoin derivatives has been studied previously. Reist *et al.*[69] observed a small solvent kinetic isotope effect for the racemisation of 5-substituted hydantoins. Solvent kinetic isotope effect values (1.13 ± 0.05) and (1.24 ± 0.08) were observed for the racemisation of (*S*)-5-phenylimidazolidine-2,4-dione (**1.22**) and (*S*)-5-benzylimidazolidine-2,4-dione (**1.25**), respectively, in a 50/50 (v/v) mixture of phosphate buffer and DMSO. A negligible solvent kinetic isotope effect on racemisation was also obtained for **1.22** and **1.25** by Narduolo[31] in D_2O- and H_2O-phosphate buffers (0.25 M, 0.5 M *I*, at 60 °C). Solvent and primary kinetic isotope effects were also determined by Narduolo for the compounds shown in Scheme 1.41.

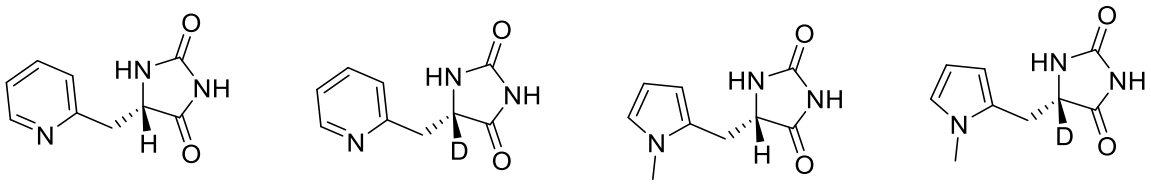

Scheme 1.41: (*S*)-5-H- and (*S*)-5-D- pyridin-2-ylmethyl)imidazolidine-2,4-dione (**1.36**, and **1.37**), and (*S*)-5-H- and (*S*)-5-D- (1-methyl-1H-pyrrol-2-yl)methyl)imidazolidine-2,4-dione (**1.38**, and **1.39**) studied by Narduolo.

Negligible solvent kinetic isotope effects were obtained for compounds **1.36** and **1.38**. Normal primary kinetic isotope effects for racemisation of **1.36** and **1.38** were observed suggesting breaking of the C-H(D) bond in the rate-determining step (Table 1.2).

Table 1.2: Rate constants for racemisation of hydantoins **1.36-1.39** in H_2O- and D_2O-phosphate buffers 0.5 M, 1 M *I*, pH and pH* 7.2, at 60 °C, and related primary kinetic isotope effects studied by Narduolo.

Buffer	k_θ [a] / 10^{-6} s^{-1}		Ratio
	1.36	1.37	
H_2O	494.0 ± 16.0	---------	
D_2O	498.8 ± 6.1	150.5 ± 4.9	3.3 ± 0.1
Buffer	k_θ / 10^{-6} s^{-1}		
	1.38	1.39	
H_2O	208.0 ± 10.0		
D_2O	303.5 ± 5.3	61.9 ± 7.2	4.9 ± 0.6

a) k_θ is the rate constant for the loss of ellipticity determined by CD spectroscopy (See chapter 4).

Cabordery *et al.*[34] obtained the value of the solvent kinetic isotope effect (k_{H_2O} / k_{D_2O}) of 0.78 for 2-(3-(benzyl(methyl)amino)propyl)-3-thioxo-2,3,10,10a-tetrahydroimidazo[1,5-b]isoquinolin-1(5H)-one **1.34a** (Scheme 1.35) in 33 mM of H_2O- and D_2O-phosphate buffer and EtOH and EtOD 75/25 (v/v), pH, and pH* 2.5, and 2.6, respectively, at 15 °C. As mentioned, Narduolo observed the absence of significant solvent kinetic isotope effects for

the general-base catalysed racemisation of substituted hydantoin, which suggests no involvement of the solvent in proton abstraction or donation.

1.5 Acid and base catalysis of reactions involving proton transfer

Acid and base catalysis are important in racemisation and other reactions of drug-like molecules involving proton transfer. There are two major types of acid/base catalysis, namely specific and general catalysis.

1.5.1 Acid catalysis hydrolysis and racemisation

The hydrolysis of 5-substituted 1-acetyl-2-thiohydantoin was studied by Congdon and Edward[86] in sulphuric acid. The acid-catalysed hydrolysis takes place by a mechanism named A_2. Deprotonation may take place for the tetrahedral intermediate to produce the neutral tetrahedral intermediate. There is also another possibility to reprotonate the other oxygen giving a charged intermediate by direct intramolecular proton transfer.[87] This type of mechanism is called specific acid catalysis and is reported for the hydrolysis of ethyl acetate,[87] amide hydrolysis and the cleavage of primary ethers.[82] The observed pseudo-first-order rate constants k_{obs} in specific-acid catalysis has been observed to be linearly dependent upon hydronium ion concentration $[H_3O^+]$ (Equation 1.15).

$$-\frac{d[E]}{dt} = k_{\circ}[E] + k_H\,[H_3O^+][E] \qquad \textbf{Equation 1. 15}$$

which can be rewritten as a first-order rate law (Equation 1.16).

$$-\frac{d[E]}{dt} = k_{obs}[E] \qquad \textbf{Equation 1. 16}$$

The specific-acid catalysed rate constant can then be calculated using Equation 1.17.

$$k_{obs} = k_0 + k_H[H_3O^+] \qquad \textbf{Equation 1. 17}$$

where k_{obs} is the experimental pseudo-first-order rate constant, k_0 is the first-order rate constant for the uncatalysed reaction and k_H is the second-order catalytic rate constant for the reaction catalysed by H_3O^+.

In a general-base catalysed reaction, the reaction is catalysed not only by H_3O^+ but also by any additional weak acid A-H (Equation 1.18).

$$k_{obs} = k_0 + k_H[H_3O^+] + \sum k_{AH} \cdot [AH] \qquad \textbf{Equation 1. 18}$$

where k_{obs} is the experimental pseudo-first-order rate constant, k_0 is the first-order rate constant for the un-catalysed reaction, k_H is the second-order catalytic constant for the reaction catalysed by H_3O^+, k_{AH} is the second-order catalytic constant for the reaction catalysed by the general acid AH, and Σk_{AH} [AH] is the sum over the contributions of all catalytically active acids present.

General-acid catalysis can occur when rate determining proton transfer takes place from acids other than from the solvated proton.[84] Acid-catalysed racemisation of catecholamines **1.40** (Scheme 1.42) was reported by Venter[88] who suggested that racemisation occurs via the formation of a quinoidal intermediate rather than via an S_N1-type reaction. The proposed mechanism involves the loss of the hydroxide group resulting in the formation of a highly stable achiral intermediate and thus loss of optical activity. Stabilisation of the compound may occur by the formation of a quinonoid intermediate.[88]

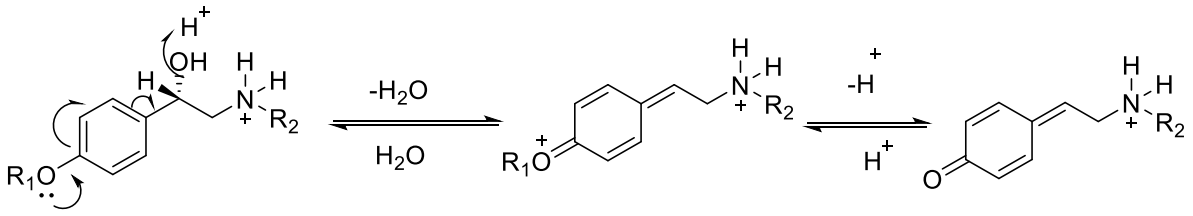

1.40

a) $R_1 = H$, $R_2 = CH_3$

b) $R_1 = CH_3$, $R_2 = CH(CH_3)_2$

Scheme 1.42: Acid-catalysed racemisation mechanism of (S)-2-hydroxy-2-(4-hydroxyphenyl)-N-methylethan-1-aminium (**1.40a**) and (S)-N-(2-hydroxy-2-(4-methoxyphenyl)ethyl)propan-2-aminium (**1.40b**), proposed by Venter.

For comparison, the mechanism shown in Scheme 1.8 was also proposed for the acid-catalysed racemisation of the structurally similar L-adrenaline **1.5** (Scheme 1.8).[88]

1.5.2 Base catalysis in selected hydrolysis and racemisation reactions

The first-order rate constants for a reaction undergoing specific-base catalysis, *i.e.* the reaction is not catalysed by any other bases, vary linearly with [OH^-] according to Equation 1.19.

$$k_{obs} = k_0 + k_{OH}[OH^-] \qquad \textbf{Equation 1.19}$$

where k_{obs} is the experimental pseudo-first-order rate constant, k_0 is the first-order rate constant for the uncatalysed reaction and k_H is the second-order rate constant for the reaction catalysed by OH^-.

Reaction involving fast proton transfer from the molecule to a base, followed by a slow step involving the deprotonated substrate molecule exhibits a specific-base catalysis rate law.[87]

In the general-base catalysis of hydrolysis and racemisation, the reaction is catalysed by OH^- and any base B.[84] The observed rate constant for a reaction undergoing general-base catalysis is given by Equation 1.20.

$$k_{obs} = k_0 + k_{OH}[OH^-] + \sum k_B \cdot [B] \qquad \textbf{Equation 1. 20}$$

where k_{obs} is the experimental pseudo *n*-th order rate constant, k_0 is the rate constant for the uncatalysed reaction, k_{OH} is the catalytic constant of the hydroxide catalysed reaction, k_B is the catalytic constant of the reaction catalysed by general base B, and $\Sigma k_B.[B]$ is the sum over the contributions of all catalytically active bases present.[87] The base-catalysed hydrolysis of the hydantoin and thiohydantoin derivatives have been reported previously.[58, 89, 90] The base-catalysed racemisation of substituted hydantoins and thiohydantoins has also been studied in buffer which catalyses the abstraction of the acidic hydrogen at the asymmetric carbon and buffer therefore racemises the compounds.[31, 34, 69, 70]

1.5.3 Brønsted plots

The proton transfer of the carbon has an important role in racemisation which depends on the acidity of the CH which in turn depends on the polar reaction involving the charge delocalisation, bond formation and cleavage.[91] The enolisation of hydantoin derivatives is subject to general-base catalysis as mentioned by Lazarus[70] and the catalysing power of the base is related to the equilibrium base strength, as expressed by Equation 1.21.

$$\log k_B = \beta \times \mathrm{p}Ka + C \qquad \textbf{Equation 1. 21}$$

where k_B is the second-order catalytic constant for the reaction catalysed by the general base B, β is the Brønsted parameter associated with the reaction catalysed by general-bases which show the sensitivity of the reaction to change in structure of the catalysing base, and pK_a is the dissociation constant of the conjugate acid of the catalytic base B.[92]

The values of α and β in general-acid and base catalysis, respectively, can be determined from the slope of the logarithm of observed rate constant versus pK_a of the conjugated-acid or base. The Brønsted coefficient is typically interpreted as the degree of proton transfer in the transition state, falling between 0 and 1 for most reactions.[82, 84] When the Brønsted coefficient equals 0, it suggests that the transition state is close to the reactant; when it is equal to 1, it suggests a transition state close to the product.[82] As mentioned before, isotope effects also probe proton transfer and can be considered alongside the Brønsted coefficient to show if

proton transfer is involved in the rate-determining step or not. In the solvent kinetic isotope effect, k_{H_2O} / k_{D_2O} can be obtained as normal or inverse based on the mechanism of the proton transfer. In the normal kinetic isotope effect, the proton transfer is part of the rate determining step and rapid equilibrium protonation in the inverse kinetic isotope effect. Lazarus[70] reported a β-value of 0.59 for the base-catalysed racemisation of L-5-benzylhydantoin and 0.51 for L-5-benzyl-3-methylhydantoin. These values suggest that the proton is only half-transferred in the rate determining step. Narduolo[31] obtained a β-value for L-5-benzyl-3-methylhydantoin of 0.57 and 0.59 at 25 and 60 °C, respectively.

The Brønsted coefficient and solvent kinetic isotope effect have been calculated for acetone enolisation at 25 °C.[92] A correlation between β and k_{H_2O}/k_{D_2O} was reported with the largest isotope effects associated with values of β close to 0.5 and the smallest isotope effect correlated with β equal to 0.82.[92]

A general Marcus-type mechanism can be proposed for proton abstraction in aqueous solution in which formation of a hydrogen bond between the acid and base formally preceeds proton transfer. Following proton transfer, the conjugate base of the acid and the protonated base are hydrogen bonded. Reaction is completed by breaking this hydrogen bond (HBC_1 and HBC_2 in Scheme 1.43).[93]

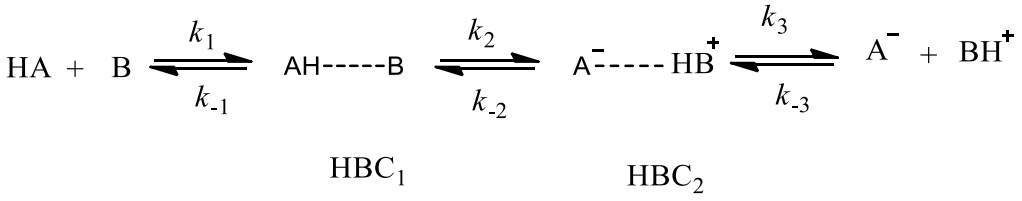

Scheme 1.43: proton transfer mechanism.

The observed rate constant of the proton transfer in Scheme 1.43 from HA to B is given by equation 1.22.[93]

$$k_{\text{obs}} = \frac{k_1 k_2 k_3}{[k_{-1}(k_{-2} + k_3) + k_2 k_3]}$$ **Equation 1. 22**

Assuming the intermediates are present in low concentration, two main mechanisms are possible. First, when $k_2 > k_{-2}$, the formation of H_1 is the rate-determining step and $k_{obs} = k_1$, when $k_2 < k_{-2}$, the k_{obs} for the cleavage of hydrogen bond (HBC_1 and HBC_2 in Scheme 1.43) is $k_{obs} = (k_1/k_{-1})\ (k_2/k_{-2})\ k_3$. In this case, the proton transfer between the HBC_1 and HBC_2 is fast. Second, proton abstraction is the rate-determining step when the interconversion of the complex is slow; then $k_2 < k_{-1}$ and $k_3 > k_{-2}$, and therefore, $k_{obs} = (k_1/k_{-1})\ k_2$ (Scheme 1.44).[93]

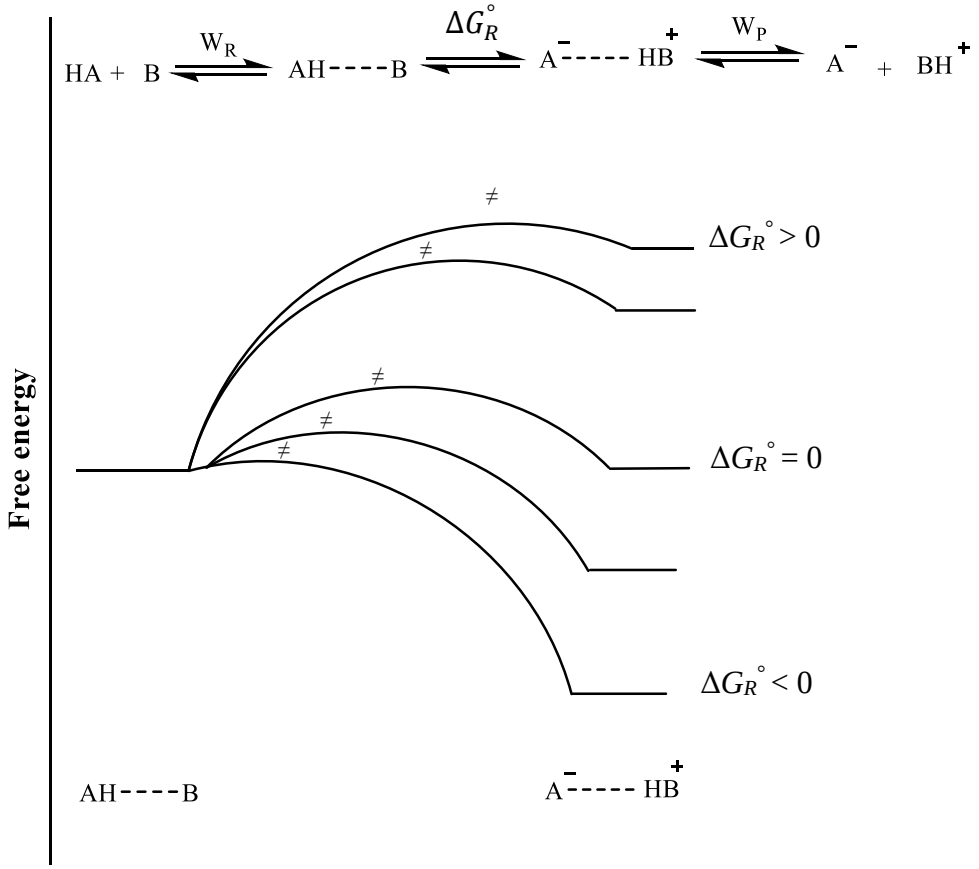

Scheme 1.44: Standard free energy change of proton abstraction reaction and transition state structure differences.[93]

From Schemes 1.43 and 1.44, the reaction becomes exothermic when HA is a much stronger acid than BH^+, and the transition state lies towards the reactant, with $G^{\neq}$ closer to G_R° than to G_p°. Then, the deprotonation reaction will have a Brønsted β of 0. On the other hand, the reaction would be endothermic if HA is a much weaker acid than BH^+ and the transition state lies to the product with $G^{\neq}$ closer to G_p°. In this case the reaction catalysed by A^- will have β = 1.[94]

Since β= 1-α, $\Delta G^{\neq} = G^{\neq} - G_R^{\circ}$ and $\Delta G^{\circ} = G_p^{\circ} - G_R^{\circ}$, the Brønsted coefficient can be expressed as a function of the free energy according to Equations 1.23, 1.24 and 1.25 to obtain 1.26.

$$\delta G^{\neq} = \alpha\, \delta G_p^{\circ} + \beta\, \delta G_R^{\circ} \qquad \textbf{Equation 1. 23}$$

$$\delta G^{\neq} = \alpha\, \delta G_p^{\circ} + \delta G_R^{\circ} - \alpha\, \delta G_R^{\circ} \qquad \textbf{Equation 1. 24}$$

$$\delta G^{\neq} - \delta G_R^{\circ} = \alpha\, (\delta G_p^{\circ} - \delta G_R^{\circ}) \qquad \textbf{Equation 1. 25}$$

$$\alpha \text{ or } \beta = (\delta \Delta G^{\neq})/(\delta \Delta G^{\circ}) \qquad \textbf{Equation 1. 26}$$

where ΔG° is the free energy of the reaction and $\Delta G^{\neq}$ is the free energy of activation.

When the acidity strength of HA and BH^+ is similar, then α and β values will be between 0 and 1. Therefore, changing the strength of B changes ΔG° and ΔG_R°, and according to Equation 1.19, the values of α and β will also change. It can be concluded from Scheme 1.44 that for the symmetrical proton transfer when $\Delta G_R^{\circ} = 0$, the value of β = 0.5, for $\Delta G_R^{\circ} < 0$, the value of β will be less than 0.5, and β will be higher than 0.5 in the case of $\Delta G_R^{\circ} > 0$.[93]

1.5.4 Enzyme catalysed hydrolysis and racemisation of hydantoin derivatives

5-Substituted hydantoins can be considered as amino acids that are cyclised (*vide supra*). Some enzymes can hydrolyse the substituted hydantoins to the carbamoyl amino acid and in some cases produce amino acids.[95, 96] Some bacteria can be used to prepare enantiopure amino acids from racemic 5-substituted hydantoins (Scheme 1.45).[97] The rate constant of racemisation plays an important role in the production of enantiopure L- and D-N-carbamoyl amino acids followed by the formation of L- and D-amino acids. If the rate constant of hydantoin racemisation is quite slow in comparison with the rate constant of the hydrolysis, then the optically active hydrolysed compound can be prepared.[98] On the other hand, the optically active hydrolysed compounds are impossible to prepare when the racemisation process takes place faster than the hydrolysis. Therefore, the substituents at the C-5 position

have an important role in controlling the rate constant of racemisation rather than hydrolysis as discussed for the racemisation and hydrolysis rate constant of thiohydantoin derivatives (Scheme 1.45).

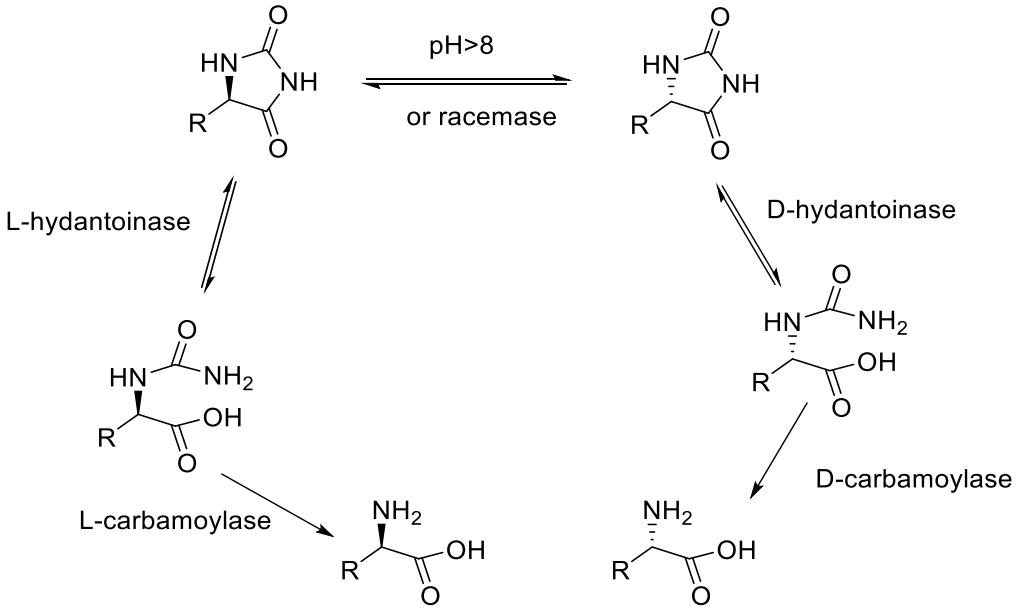

Scheme 1.45: Synthesis of optically active α-amino acids with enantioselective hydantoinase–carbamoylase with *in situ* racemisation, proposed by Servi *et al*.[97]

Lee and Fan[98] studied the enzymatic hydrolysis and racemisation of 5-phenylhydantoin and 5-(p-hydroxyphenyl)hydantoin to produce N-carbamoyl amino acid, as catalysed by hydantoinase. The authors observed an increase in the rate constant for hydrolysis with increasing pH. It has also been observed that the rate constant for racemisation of 5-(p-hydroxyphenyl)hydantoin is higher than the 5-phenylhydantoin racemisation rate constant. The enzymatic synthesis of hydantoin is documented as a well-established process to prepare optically active hydantoin without a toxic chemical compound. The keto-enol tautomerism was also mentioned to be affected by more electronegative hydroxyl substituents at the *para* position which can stabilise the enolate structure and promote the rate constant of the racemisation.

1.6 Mechanistic studies of racemisation reactions

Narduolo[31] reported a k_{rac} / $k_{H/D}$ between 1.2-1.3 for *S*-5-benzylhydantoin which supports the S_E1 rather than the S_E2 mechanism (25 °C using 0.1 and 0.5 M of D_2O-phosphate buffer, pH* 7.2, 1 M *I*). The S_E1 mechanism is illustrated in Scheme 1.46.

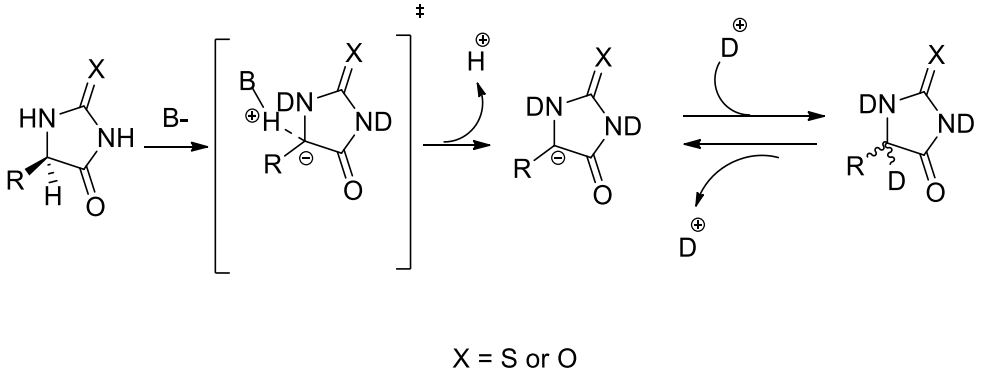

Scheme 1.46: Proposed S_E1 mechanism for hydantoin derivatives.

Cabordery *et al.*[34] proposed the S_E1 mechanism for Tic-hydantoin (**1.34 b**) racemisation in 33 mM, pD 7.3 deuterated-phosphate buffers / EtOD- 75/25 (v/v) at 25 °C which $k_{H/D}$ / k_{rac} ~ 1 and the deuteration occurring with complete racemisation (Scheme 1.35). Similarly, the racemisation of amfepranone and cathinone have been reported to proceed via the S_E1 mechanism in D_2O-phosphate buffer (pD 7.4, 0.43 M *I*).[99]

Reist *et al.*,[69] found $k_{H/D}$ / k_{rac} for 5-benzylhydantoin (**1.25**) (Scheme 1.32) to vary between 0.6 and 0.7 in a mixture of D_2O-phosphate buffer (pD 7.4, 0.1 M, 0.22 M *I*) with 1:1 D_6-DMSO (v:v) between 50 °C to 80 °C. Cabordery *et al.*[34] proposed the S_E2 mechanism for thiohydantoin **1.34 a** (Scheme 1.35) in 33 mM, pD 2.6 deuterated phosphate buffers / EtOD-75/25 (v/v) at 15 °C based on the observation that the rate constant for deuteration was about half the rate constant for racemisation, suggesting that deuteration occurs with an inversion of configuration. The push-pull S_E2 mechanism for thiohydantoin proposed by Reist *et al.* is show in Scheme 1.47 where H or D can be transferred by base or OD on one side and attack by the H or D from the other side, producing the inverted configuration (Scheme 1.47).

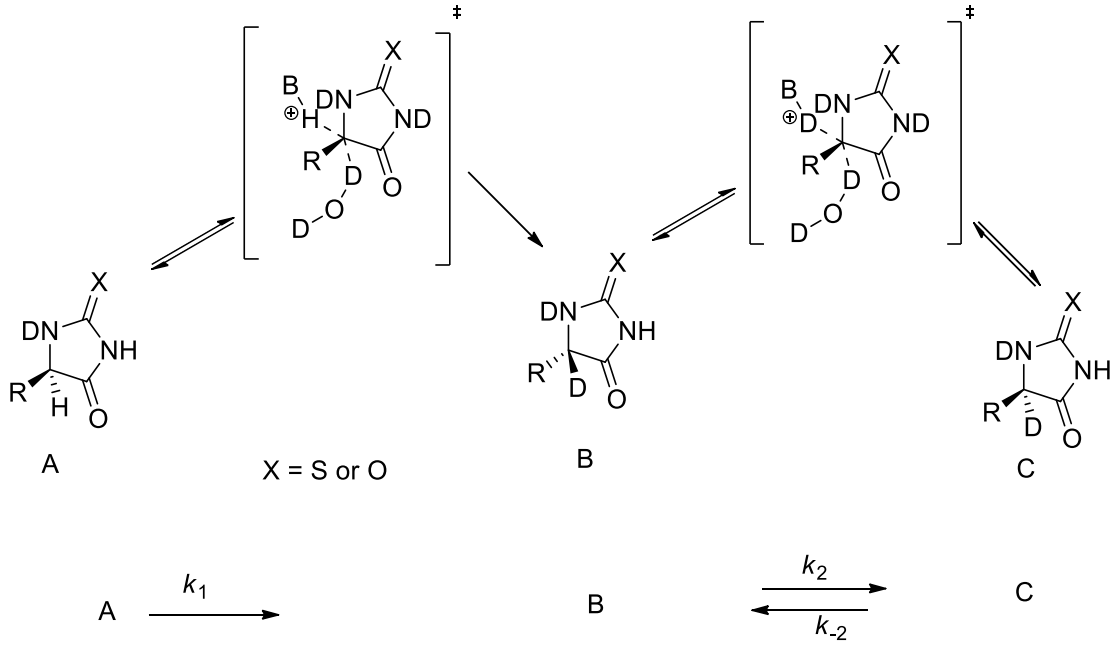

Scheme 1.47: proposed S_E2 mechanism for thiohydantoin and hydantoin derivatives.

The kinetics and mechanism of allantoin racemisation was reported by Kahn and Tipton[68] in D_2O-phosphate buffer at pH between 5.7 and 10 at 22 °C. The authors proposed three possible mechanisms for the racemisation of (*S*)-5-ureido-hydantoin (**1.40**): S_E1, S_E2 and S_N2. The rate constants for H/D exchange ($k_{H/D}$) increase with increasing phosphate buffer concentration. There was no clear explanation to favour the S_E1 mechanism over the S_E2 mechanism or vice versa by Kahn and Tipton for allantoin racemisation. Therefore, only a general S_E mechanism was suggested which could be either S_E1 or S_E2 for the general-base catalysed racemisation of allantoin **1.41** (Scheme 1.48). This was in agreement with the S_E1 mechanism proposed by Narduolo[31] and Cabordery *et al.*[34] and also the S_E2 mechanism suggested by Reist *et al.*[69] for the racemisation of substituted-hydantoin (*vide supra*). Allantoin can racemise via an S_N2-like mechanism, as shown in Scheme 1.48, via the formation of a symmetrical bicyclic intermediate formed between the primary amide and C4. This mechanism is not possible for other 5-substituted hydantoins because of the absence of suitable substituents at the C-5 position of hydantoin.

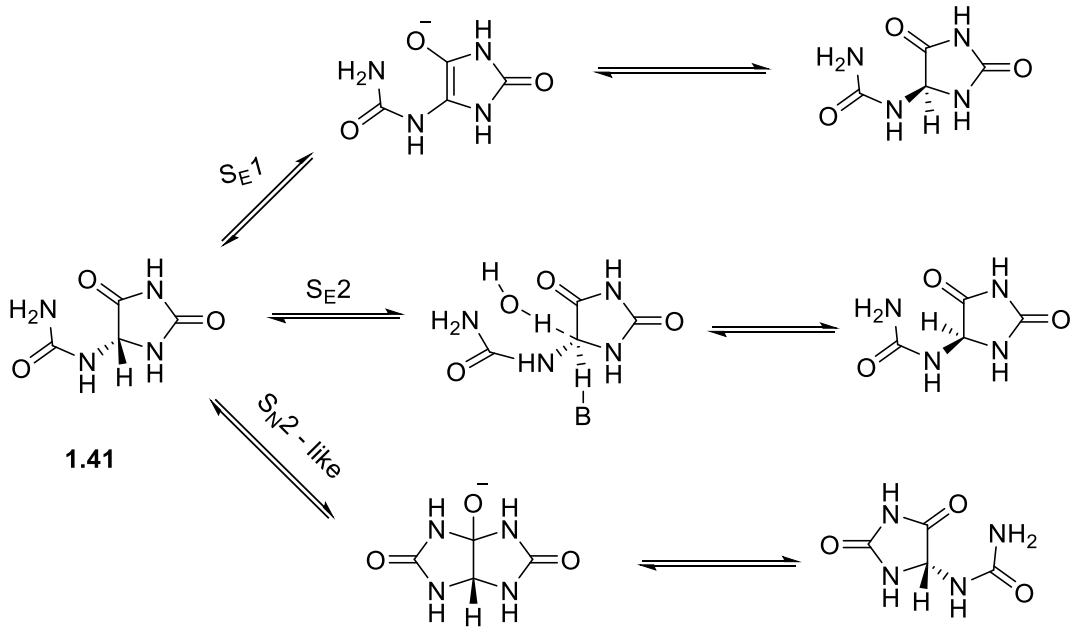

Scheme 1.48: The racemisation mechansim of allantoin, proposed by Kahn and Tipton[68]

There is no practical evidence available to show the mechanism of the racemisation of thiazolidine-2,4-dione (**1.10 b**) and 2-thioxothiazolidin-4-one (**1.10 c**) (Scheme 1.19). Jamali *et al.*[100] reported keto-enol tautomerism, an unsurprising way to convert *R* enantiomers to *S* enantiomers and vice versa for 5-substituted thiazolidine-2,4-dione (Scheme 1.49). Similarly, the keto-enol tautomerism has also been suggested for hydantoin, as mentioned in 1912 by Dakin.[101]

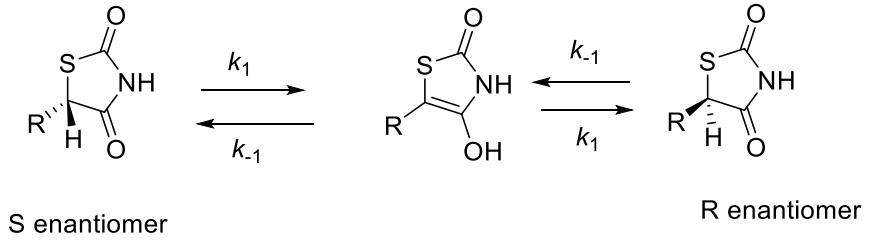

Scheme 1.49: The keto-enol tautomerism of 5-substituted- thiazolidine-2,4-dione.

A theoretical study of the racemisation mechanism and the factors which promote the base-catalysed racemisation of thiazolidine-2,4-dione (**1.10 b**) was conducted by Bharatam and Khanna.[102] The authors suggested that the possibility of keto-enol tautomerism of thiazolidine-2,4-dione is very low in comparison with acetaldehyde. It is known that the

sulphur, phosphorus and electron-withdrawing groups at the α-carbon accelerate H/D exchange and stabilise carbanion formation.[29] Computationally, it has been illustrated that the thiazolidine-2,4-dione ring is liable to be planar and deprotonated at the asymmetric carbon through increased π-delocalisation.[102] The sulphur can be oxidised, which increases the acidity of substituted thiazolidine-2,4-dione. Furthermore, different tautomeric formations of substituted thiazolidine-2,4-dione have been suggested by Bharatam and Khanna which are less favourable in acid-base catalysed racemisation (Scheme 1.50).

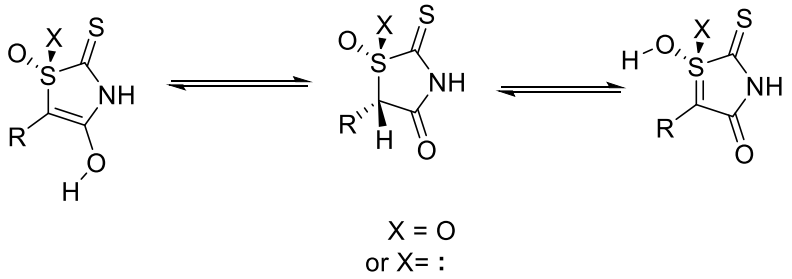

Scheme 1.50: Oxidation and keto-enol tautomerism of substituted-thiazolidine-2,4-dione.

Taxak *et al.*[103] have also suggested that S-oxidation for thiazolidine-2,4-dione increases the acidity of the asymmetric carbon and promotes racemisation. This sulphur-oxidation increases the rate constant of racemisation, which is a major factor for promoting racemisation (Scheme 1.51).

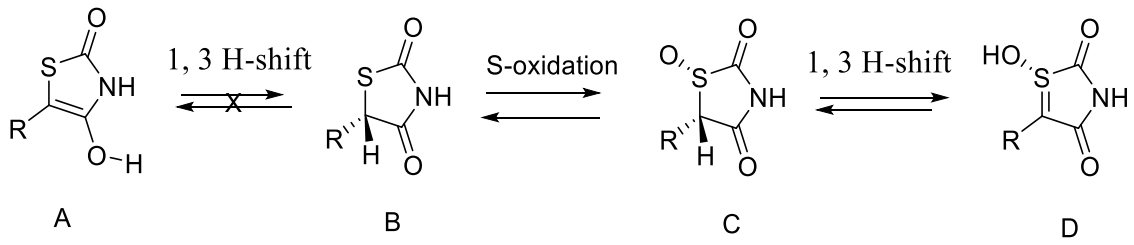

Scheme 1.51: Oxidation and keto-enol tautomerism proposed by Taxak *et al*.

Scheme 1.51 illustrates that direct keto-enol tautomerism from C to D is more likely to take place for the racemisation of 5-substituted thiazolidine-2,4-dione than B to A as expected by Taxak *et al*. No H/D exchange rate constant studies have been carried out for 5-substituted thiazolidine-2,4-diones and 2-thioxothiazolidin-4-ones to compare with the rate constants of racemisation. Hence, it has been thus far impossible to assign a mechanism for these reactions similar to Narduolo's[31] work on hydantoin and Reist *et al*.[69] Jamali *et al*.[100] studied the racemisation of the enantiomers of pioglitazone **1.42** and rosiglitazone **1.43** in 25 mM phosphate buffer (pH 2.5, 7.4, and 9.3 at 37 °C). Full racemisation was observed for **1.42** and **1.43** within 48 hours at pH 7.4 and 24 hours at pH 9.3 (Scheme 1.52).

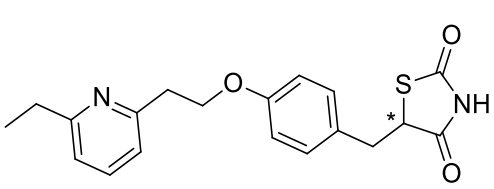

1.42

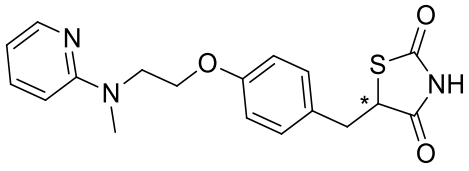

1.43

Scheme 1.52: Structures of pioglitazone and rosiglitazone studied by Jamali *et al*.[100]

Welch *et al*.[104] studied the racemisation of 5-arylthiazolidine-2,4-dione (Scheme 1.53) in different solvents and observed fast racemisation of compound **1.44** in various media including dog plasma**.**

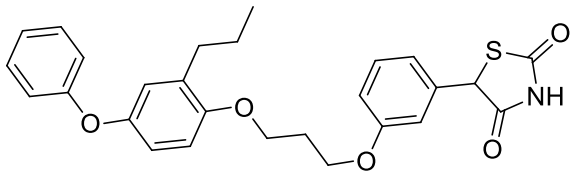

1.44

Scheme 1.53: 5-Arylthiazolidine-2,4-dione studied by Welch *et al*.[104]

The racemisation half-life, $t_{1/2}$, of **1.44** in ethanol at 10-14 hours showed rapid racemisation to reach 50% ee. Using 0.2 eq of trimethylamine caused **1.44** to racemise in a few minutes. However, using 0.2 eq. of acetic acid increases the half-life $t_{1/2} > 20$ h, and in chloroform the compound needs more than a week to racemise. The racemisation of **1.44** has also been studied in a mixture of ethanol and pH 9 buffer, where **1.44** can be racemised in less than 2 h.

1.7 Aims and Objectives

The main goal of this work is to measure the racemisation rate constants for 2-thioxoimidazolidin-4-ones (thiohydantoins), 2-thioxoimidazolidin-4-ones, and 2-thioxothiazolidin-4-ones (rhodanines) as drug-like molecules under physiological conditions. The hydrolysis of these molecules is one of the possible side reactions which may affect the observed kinetics and it is therefore important to study and compare the hydrolysis with the racemisation reaction. There are many factors influencing the rate of racemisation and hydrolysis that should be studied, such as temperature, pH, and the presence of acids and bases. The effect of various substituents at the asymmetric carbon and different position of the molecules on the rate of racemisation and hydrolysis will be investigated. The H/D exchange reaction of the molecules will be studied. The observed rate constants for H/D exchange can be divided by the corresponding rate constants for racemisation. Together with solvent kinetic isotope effects, the kinetic data will allow us to propose a mechanism for the racemisation of chiral substituted 2-thioxoimidazolidin-4-ones (thiohydantoins), 2-thioxoimidazolidin-4-ones, and 2-thioxothiazolidin-4-ones (rhodanines).

1.8 References

1. J. McConathy and M. J. Owens, *Primary care companion to the Journal of clinical psychiatry*, 2003, 5, 70.
2. D. Nasipuri, *Stereochemistry of organic compounds: principles and applications*, New Age International, 1994.
3. I. Ali, U. Kulsum, K. Saleem and A. Hussain, *Chiral Pollutants*, Wiley Online Library, 2004.
4. G. Arora, *Stereochemistry In Organic Compounds*, Anmol Publications Pvt. Ltd, 1997.
5. G. Snatzke and P. Badoz, *Optical Rotatory Dispersion and Circular Dichroism in Organic Chemistry: Including Applications from Inorganic Chemistry and Biochemistry: Proceedings of NATO Summer School Held at Bonn, 24 September-1 October 1965*, Heyden, 1967.
6. E. J. Ebbers, G. J. Ariaans, J. P. Houbiers, A. Bruggink and B. Zwanenburg, *Tetrahedron*, 1997, 53, 9417-9476.
7. A. Ballard, *Kinetics and mechanism of HD exchange reactions and racemisation in aqueous solutions: configurational stability of ester and amide arylglycine derivatives*, Cardiff University, 2011.
8. K. Cabrera, M. Jung, M. Fluck and V. Schurig, *Journal of Chromatography A*, 1996, 731, 315-321.
9. E. J. Ariëns, *Trends in Pharmacological Sciences*, 1986, 7, 200-205.
10. A. G. Leach, E. A. Pilling, A. A. Rabow, S. Tomasi, N. Asaad, N. J. Buurma, A. Ballard and S. Narduolo, *MedChemComm*, 2012, 3, 528-540.
11. B. Jamali, I. Bjørnsdottir, O. Nordfang and S. H. Hansen, *Journal of pharmaceutical and biomedical analysis*, 2008, 46, 82-87.
12. A. Dally, *The Lancet*, 1998, 351, 1197-1199.
13. M. E. Franks, G. R. Macpherson and W. D. Figg, *The Lancet*, 2004, 363, 1802-1811.
14. Z. J. Li and D. J. W. Grant, *Journal of Pharmaceutical Sciences*, 1997, 86, 1073-1078.
15. A. R. Fassihi, *International Journal of Pharmaceutics*, 1993, 92, 1-14.
16. P. Andrews, *Trends in Pharmacological Sciences*, 1986, 7, 148-151.
17. I. Ali, V. K. Gupta, H. Y. Aboul-Enein, P. Singh and B. Sharma, *Chirality*, 2007, 19, 453-463.
18. C. Danel, C. Foulon, J.-F. Goossens, J.-P. Bonte and C. Vaccher, *Tetrahedron: Asymmetry*, 2006, 17, 2317-2321.
19. M. Brandl, D. Conley, D. Johnson and D. Johnson, *J Pharm Sci*, 1995, 84, 1045-1048.
20. B. Mey, H. Paulus, E. Lamparter and G. Blaschke, *Chirality*, 1998, 10, 307-315.
21. F. Jamali, R. Lovlin and G. Aberg, *Chirality*, 1997, 9, 29-31.
22. D. Stepensky, M. Chorny, Z. Dabour and I. Schumacher, *J Pharm Sci*, 2004, 93, 969-980.
23. X. Yuchun, L. Huizhou and C. Jiayong, *International Journal of Pharmaceutics*, 2000, 196, 21-26.
24. S. F. Oğuz and İ. Doğan, *Tetrahedron: Asymmetry*, 2003, 14, 1857-1864.
25. C. Roussel, M. Adjimi, A. Chemlal and A. Djafri, *The Journal of Organic Chemistry*, 1988, 53, 5076-5080.
26. W. J. Lambert, P. G. Timmer, R. R. Walters and C.-Y. L. Hsu, *Journal of Pharmaceutical Sciences*, 1992, 81, 1028-1031.
27. S. K. Yang, *Chirality*, 1999, 11, 179-186.
28. S. K. Yang, R. Tang, T. J. Yang, Q.-L. Pu and Z. Bao, *Journal of Pharmaceutical Sciences*, 1996, 85, 745-748.
29. E. Buncel, *Carbanions: Mechanistic And Isotopic Aspects*, Elsevier Scientific Publishing Company, 1975.

30. D. J. Cram, *Fundamentals of carbanion chemistry*, Academic Press, 1965.
31. S. Narduolo, Thesis (Ph D) - Cardiff University, 2011.
32. T. Mendgen, C. Steuer and C. D. Klein, *Journal of Medicinal Chemistry*, 2012, 55, 743-753.
33. Y.-D. Gong and T. Lee, *Journal of Combinatorial Chemistry*, 2010, 12, 393-409.
34. A.-C. Cabordery, M. Toussaint, N. Azaroual, J.-P. Bonte, P. Melnyk, C. Vaccher and C. Foulon, *Tetrahedron: Asymmetry*, 2011, 22, 125-133.
35. T. Miura, Y. Mikano and M. Murakami, *Organic Letters*, 2011, 13, 3560-3563.
36. J. Marton, J. Enisz, S. Hosztafi and T. Timar, *Journal of Agricultural and Food Chemistry*, 1993, 41, 148-152.
37. L. Konnert, B. Reneaud, R. M. de Figueiredo, J.-M. Campagne, F. Lamaty, J. Martinez and E. Colacino, *The Journal of Organic Chemistry*, 2014, 79, 10132-10142.
38. Z. D. Wang, S. O. Sheikh and Y. Zhang, *Molecules*, 2006, 11, 739-750.
39. H. A. El Hady, *Der Pharma Chemica*, 2012, 4.
40. M. M. Sim and A. Ganesan, *Journal of Organic Chemistry*, 1997, 62, 3230-3235.
41. D. Rakowitz, R. Maccari, R. Ottana and M. G. Vigorita, *Bioorg Med Chem*, 2006, 14, 567-574.
42. G.-Q. Lin and X.-W. Sun, in *Chiral Drugs*, John Wiley & Sons, Inc., 2011, DOI: 10.1002/9781118075647.ch2, pp. 29-76.
43. E. Ware, *Chemical Reviews*, 1950, 46, 403-470.
44. T. B. Johnson and W. M. Scott, *Journal of the American Chemical Society*, 1913, 35, 1130-1136.
45. T. B. Johnson and B. H. Nicolet, *Journal of the American Chemical Society*, 1911, 33, 1973-1978.
46. F. A. Csonka and B. H. Nicolet, *Journal of Biological Chemistry*, 1932, 99, 213-216.
47. T. B. Johnson and W. M. Scott, *Journal of the American Chemical Society*, 1913, 35, 1136-1143.
48. A. S. Inglis, M. W. Duncan, P. Adams and A. Tseng, *Journal of Biochemical and Biophysical Methods*, 1992, 25, 163-171.
49. T. B. Johnson and J. S. Bates, *Journal of the American Chemical Society*, 1915, 37, 383-385.
50. J. He, G. Ouyang, Z. Yuan, R. Tong, J. Shi and L. Ouyang, *Molecules*, 2013, 18, 5142-5154.
51. J. C. Thenmozhiyal, P. T. H. Wong and W. K. Chui, *Journal of Medicinal Chemistry*, 2004, 47, 1527-1535.
52. H. A. El Hady, *Der Pharma Chemica*, 2012, 4, 2202-2207.
53. M. E. Garst, L. J. Dolby, S. Esdandiari, A. A. Avey, K. V. R. Mac and D. C. Muchmore, Google Patents, 2007.
54. W. Książek, K. Kieć-Kononowicz and J. Karolak-Wojciechowska, *Journal of Molecular Structure*, 2009, 921, 109-113.
55. M. Bergon and J. P. Calmon, *Journal of the Chemical Society-Perkin Transactions 2*, 1978, DOI: 10.1039/p29780000493, 493-497.
56. I. B. Blagoeva, I. G. Pojarlieff and V. S. Dimitrov, *Journal of the Chemical Society-Perkin Transactions 2*, 1978, DOI: 10.1039/p29780000887, 887-892.
57. E. G. Sander, *Journal of the American Chemical Society*, 1969, 91, 3629-3634.
58. W. I. Congdon and J. T. Edward, *Canadian Journal of Chemistry*, 1972, 50, 3780-3788.
59. P. Schlack and W. Kampf, *Hoppe-Seyler´ s Zeitschrift für physiologische Chemie*, 1926, 154, 125-172.
60. W. I. Congdon, Thesis (PhD) - McGill University, 1970.
61. J. Edward and S. Nielsen, *Journal of the Chemical Society*, 1957, 5080-5083.
62. F. D. Benke, Thesis (phD)-Durham University, 1983.

63. J. Brem, S. S. van Berkel, W. Aik, A. M. Rydzik, M. B. Avison, I. Pettinati, K.-D. Umland, A. Kawamura, J. Spencer, T. D. W. Claridge, M. A. McDonough and C. J. Schofield, *Nature Chemistry*, 2014, 6, 1084-1090.
64. L. B. Mendel and H. D. Dakin, *Journal of Biological Chemistry*, 1910, 7, 153-156.
65. K. H. Dudley and D. L. Bius, *Drug Metabolism and Disposition*, 1976, 4, 340-348.
66. G. G. Smith and T. Sivakua, *The Journal of Organic Chemistry*, 1983, 48, 627-634.
67. M. Bovarnick and H. Clarke, *Journal of the American Chemical Society*, 1938, 60, 2426-2430.
68. K. Kahn and P. A. Tipton, *Bioorganic Chemistry*, 2000, 28, 62-72.
69. M. Reist, P.-A. Carrupt, B. Testa, S. Lehmann and J. J. Hansen, *Helvetica Chimica Acta*, 1996, 79, 767-778.
70. R. A. Lazarus, *The Journal of Organic Chemistry*, 1990, 55, 4755-4757.
71. K. Cabrera, M. Jung, M. Fluck and V. Schurig, *Journal of Chromatography A*, 1996, 731, 315-321.
72. S. Hsü, C. Ingold and C. Wilson, *J. chem. Soc.[London]*, 1938, 78.
73. D. J. Cram, B. Rickborn, C. A. Kingsbury and P. Haberfield, *Journal of the American Chemical Society*, 1961, 83, 3678-3687.
74. W. D. Kollmeyer and D. J. Cram, *Journal of the American Chemical Society*, 1968, 90, 1779-1784.
75. D. J. Cram, W. T. Ford and L. Gosser, *Journal of the American Chemical Society*, 1968, 90, 2598-2606.
76. D. J. Cram, *Fundamentals Of Carbanion Chemistry*, Academic Press, 1965.
77. D. J. Cram and L. Gosser, *Journal of the American Chemical Society*, 1964, 86, 5457-5465.
78. D. J. Cram and L. Gosser, *Journal of the American Chemical Society*, 1964, 86, 5445-5457.
79. D. J. Cram and L. Gosser, *Journal of the American Chemical Society*, 1963, 85, 3890-3891.
80. D. J. Cram and R. T. Uyeda, *Journal of the American Chemical Society*, 1964, 86, 5466-5477.
81. M. I. Page and A. Williams, *Organic And Bio-Organic Mechanisms*, Longman, 1997.
82. N. S. Isaacs, *Physical Organic Chemistry*, Longman Scientific & Technical, 1987.
83. D. Roston, Z. Islam and A. Kohen, *Archives of Biochemistry and Biophysics*, 2014, 544, 96-104.
84. F. A. Carey and R. J. Sundberg, *Advanced Organic Chemistry: Part A: Structure and Mechanisms*, Springer, 2007.
85. F. A. Carey and R. J. Sundberg, *Advanced Organic Chemistry. Part A, Structure And Mechanisms*, Springer, New York, 5th edn., 2007.
86. W. I. Congdon and J. T. Edward, *Canadian Journal of Chemistry*, 1972, 50, 3767-3779.
87. H. Maskill, *The physical basis of organic chemistry*, Oxford University Press, Incorporated, 1985.
88. D. P. Venter, *Tetrahedron*, 1991, 47, 5019-5024.
89. I. B. Blagoeva, I. G. Pojarlieff and V. S. Dimitrov, *Journal of the Chemical Society, Perkin Transactions 2*, 1978, DOI: 10.1039/P29780000887, 887-892.
90. J. T. Edward and J. K. Liu, *Canadian Journal of Chemistry*, 1968, 46, 71-73.
91. B. J. Dodd, Thesis (phD)-Durham University, 2004.
92. M. D. Waddington and J. E. Meany, *Journal of Chemical Education*, 1978, 55, 60.
93. C. Bamford, C. Tipper and R. Compton, *Proton Transfer. Comprehensive Chemical Kinetics*, Elsevier Science & Technology, 1977.
94. K. P. Shelly, *General Acid and General Base Catalysis of the Enolization of Acetone: An Extensive Study*, University of British Columbia, 1988.

95. A. Yamashiro, K. Kubota and K. Yokozeki, *Agricultural and biological chemistry*, 1988, 52, 2857-2863.
96. R. G. Murray, Thesis (phD)- University of St Andrews, 2008.
97. S. Servi, D. Tessaro and G. Pedrocchi-Fantoni, *Coordination Chemistry Reviews*, 2008, 252, 715-726.
98. C.-K. Lee and C.-H. Fan, *Enzyme and microbial technology*, 1999, 24, 659-666.
99. M. Reist, L. H. Christiansen, P. Christoffersen, P.-A. Carrupt and B. Testa, *Chirality*, 1995, 7, 469-473.
100. B. Jamali, I. Bjørnsdottir, O. Nordfang and S. H. Hansen, *Journal of Pharmaceutical and Biomedical Analysis*, 2008, 46, 82-87.
101. L. B. Mendel and H. Dakin, *Journal of Biological Chemistry*, 1910, 7, 153-156.
102. P. V. Bharatam and S. Khanna, *The Journal of Physical Chemistry A*, 2004, 108, 3784-3788.
103. N. Taxak, V. Parmar, D. S. Patel, A. Kotasthane and P. V. Bharatam, *The Journal of Physical Chemistry A*, 2011, 115, 891-898.
104. C. J. Welch, M. H. Kress, M. Beconi and D. J. Mathre, *Chirality*, 2003, 15, 143-147.

Chapter 2

Synthesis of substituted 2-thiohydantoins and related compounds

2.1 Introduction

2.1.1 Five-membered heterocyclic rings in medicine

Five-membered multi-heterocyclic rings play important roles in medicinal chemistry and many have biological activity.[1,2,3] Drugs based on five-membered heterocycles include hydantoins, 2-thiohydantoins, thiazolidine-2,4-dione and thioxothiazolidin-4-one, and these motifs are widely used in drug discovery (Scheme 2.1).[3]

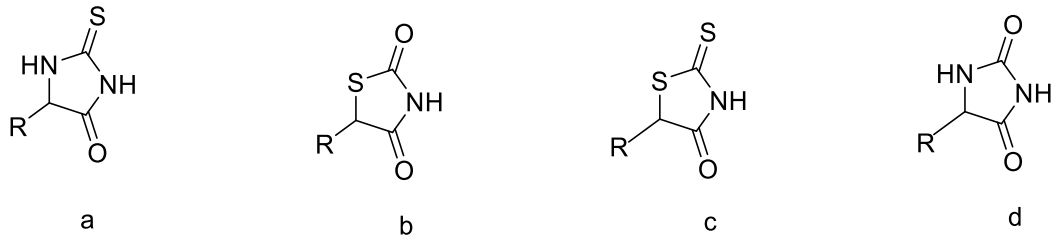

Scheme 2.1: Structures of (a) 2-thiohydantoin[1a)] (2-thioxoimidazolidin-4-one), (b) thiazolidine-2, 4-dione[1b)] (c) 2-thioxothiazolidin-4-one[1c)] (rhodanine), and (d) hydantoin[1d)] (imidazolidine-2,4-dione).

For many drugs, it is known that their biological activity is related to their chirality. Therefore, both the synthesis and configurational stability of single enantiomers of drugs are important for investigation in research studies.[4,5]

---

1) In this thesis, various nomenclatures for the studied compounds have been used, viz. the common and IUPAC names as follows:

a) 2-Thioxoimidazolidin-4-one is the same as 2-thiohydantoin.

b) 2-Thioxothiazolidin-4-one is the same as rhodanine.

c) Thiazolidine-2,4-dione is always mentioned called as such.

d) Hydantoin is the same as imidazolidine-2,4-dione.

2.1.2 Synthesis of thiohydantoins

The simplest preparation of thiohydantoin involves heating the hydrochloride salt of ethyl amino acetate with potassium thiocyanate at 140-150 °C and was reported by Peter Klason in 1890.[6] The resulting product is a basic thiohydantoin which has been used as a starting material in reactions with different aldehydes to prepare 5-arylidene-2-thiohydantoins (Scheme 2.2).[7]

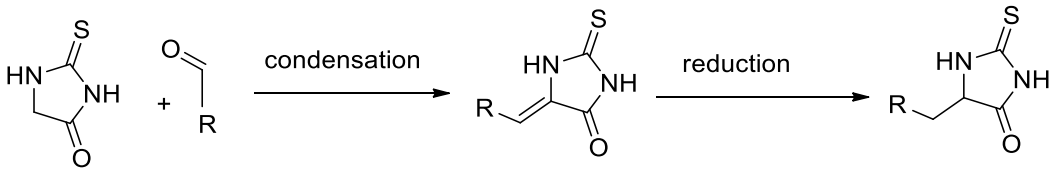

Scheme 2.2: Condensation and reduction process of 2-thiohydantoin.

Different aromatic aldehydes have been condensed with thiohydantoin in the presence of triethylamine or triethanolamine to prepare arylidene derivatives.[8,7] The reduction of such arylidene thiohydantoin derivatives (Scheme 2.2) has been carried out using Pd / C dissolved in THF. However, for thiohydantoins, this reaction typically produces poor yields, in contrast to hydantoin derivatives. Instead, using zinc dust in acetic acid to reduce the double bond has been successful in the preparation of a wide range of racemic 5-substituted 2-thiohydantoins with good yields, as reported by Garst.[9] Furthermore, 5-substituted 2-thiohydantoins have been synthesised, including with alkyl substituents at the 5-position by mixing various amino acids with thiourea and melting together at 180 °C in a solvent-free process.[10] Using high temperatures to melt the reactants led to formation of non-optically active products.

The acetylation of 2-thiohydantoin at the N-1 position was developed by Johnson in 1911.[11] Johnson *et al*. published an initial article showing the preparation of 1-acetyl-2-thiohydantoin using the amino acid glycine and ammonium thiocyanate in the presence of acetic acid, and acetic anhydride produces 1-acetyl-2-thiohydantoins (Scheme 2.3). Further amino acids were used to prepare 1-acetyl-2-thiohydantoin subsequently.[12,13,14, 15]

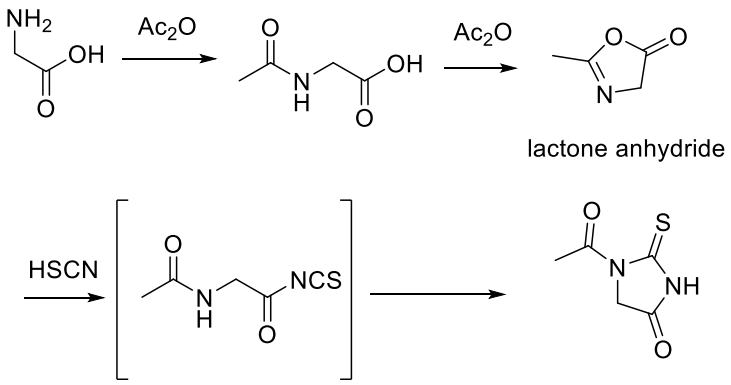

Scheme 2.3: Johnson's suggested mechanism for the formation of 1-acetyl-2-thiohydantoin

The reaction between amino acids and acetic anhydride produces acetyl amino acids, as suggested by Johnson[13]. These are transformed directly during the reaction to the corresponding lactone-anhydrides by reacting with extra acetic anhydride (Scheme 2.3). The corresponding lactone-anhydride then reacts with the thiocyanic acid which is formed from ammonium thiocyanate by the action of acidic anhydride to produce the corresponding acyl isothiocyanate. Finally, 1-acetyl-2-thiohydantoin is obtained by the intramolecular rearrangement of unstable acyl isothiocyanate (Scheme 2.3).[13, 15, 16] On the other hand, Johnson did not mention the optical activity of his compounds which is important for the research described in this thesis. Csonka and Nicolet[17] prepared an optically active 1-acetyl-5-methyl-2-thioxoimidazolidin-4-one by following Johnson's method, using acetic anhydride and acetic acid. Furthermore, racemic 3,5-disubstituted 1-acetyl-2-thiohydantoins can also be prepared followed LeTiran's method,[18] as confirmed by Reyes and Burgess.[14]

The cyclisation process is one of the most interesting ways to prepare a library of hydantoins or thiohydantoins substituted at all three sites. A range of aromatic aldehydes in the presence of phenyl isothiocyanate and methyl esters of various amino acids together with triethylamine and tri-acetoxyborohydride were used to obtain the corresponding substituted 2-thiohydantoins with substituents at the 1,3, and 5 positions.[19] This method has been reported for the preparation of a library of 1,3,5 trisubstituted 2-thiohydantoins by cyclative cleavage in solid phase synthesis.[19,20]

The condensation reaction between different aromatic aldehydes with thiazolidine-2,4-dione and 2-thioxothiazolidin-4-one was performed by the Knoevenagel condensation.[21] Commercially available thiazolidine-2,4-dione and 2-thioxothiazolidin-4-one were condensed

with aldehydes in ethanol, containing piperidine, to prepare several 5-arylidenethiazolidine-2,4-diones and 5-arylidene-2-thioxothiazolidin-4-ones.[22]

The reductions of 5-arylidenethiazolidine-2,4-diones were carried out using zinc dust in acetic acid.[9] Garst *et al*.[9] prepared 5-benzyl-2-thioxoimidazolidin-4-one from 5-benzylidene-2-thioxoimidazolidin-4-one. Lithium borohydride in THF in the presence of pyridine was also used to reduce (Z)-5-arylidenethiazolidine-2,4-dione to prepare the corresponding chiral compounds.[23,24]

2.2 Results and discussion

2.2.1 Synthesis of 5-substituted derivatives of 2-thioxoimidazolidin-4-one

5-Benzylidine-2-thiohydantoin was synthesised following the methods previously used for 5-benzylidinehydantoin by using commercially available hydantoin dissolved in ethanol in the presence of benzaldehyde and triethylamine (this was done following the success of a test reaction).[25, 8] The same procedure was used to prepare different substituted thiohydantoins at the 5-position by using different aldehydes (Scheme 2.4).[9]

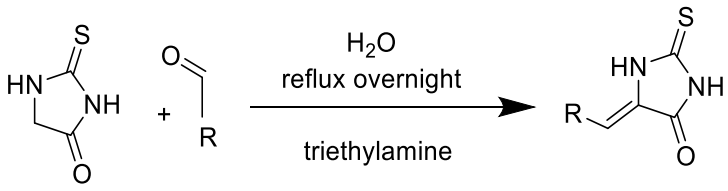

Scheme 2.4: Synthesis of 5-substituted 2-thiohydantoins

Several aromatic aldehydes were used with commercially available 2-thiohydantoin and the procedure was employed to prepare unsaturated 5-substituted 2-thiohydantoin (see experimental section).

2.2.2 Synthesis of 5-substituted derivatives thiazolidine-2,4-dione and 2-thioxothiazolidin-4-one

The Knoevenagel condensation was also used for the condensation of aldehydes with thiazolidine-2,4-dione[26,21] in ethanol in the presence of piperidine to prepare (Z)-5-benzylidenethiazolidine-2,4-dione, (Z)-5-(pyridin-2-ylmethylene)thiazolidine-2,4-dione and (Z)-5-(4-methoxybenzylidene)thiazolidine-2,4-dione (Scheme 2.5, X=O). Likewise, the Knoevenagel condensation was successfully applied to commercially available thioxothiazolidin-4-one with benzaldehyde and 2-pyridine-carboxaldehyde to synthesise the corresponding 5-substituted- 2-thioxothiazolidin-4-ones (X=S) (Scheme 2.5).

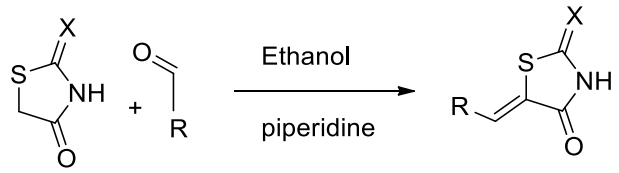

Scheme 2.5: Knoevenagel condensation reaction of aromatic aldehydes with thiazolidine-2,4-dione and 2-thioxothiazolidin-4-one

The Z isomer of 5-(pyridin-2-ylmethylene)-2-thioxothiazolidin-4-one was obtained through a Knoevenagel condensation reaction in the present work. The 3D structure of representative 5-(pyridin-2-ylmethylene)-2-thioxothiazolidin-4-one was determined using X-ray crystal structure analysis (Figure 2.1).

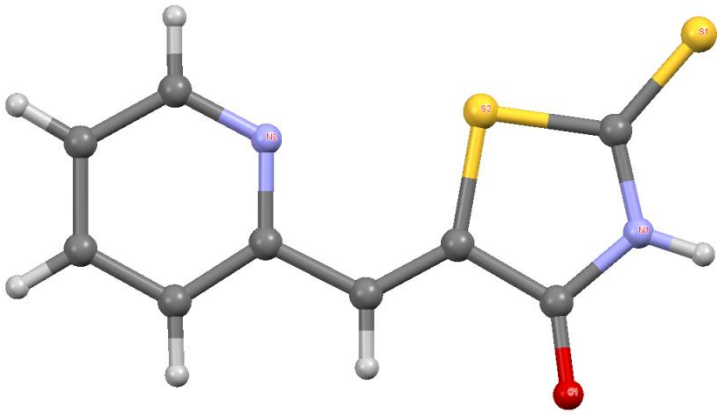

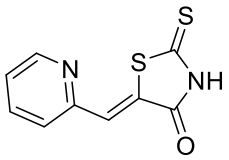

18

Figure 2.1: The molecular structure of compound **18** determined by X-ray crystallography**.**

Many derivatives of 2-thioxoimidazolidin-4-one, thiazolidine-2,4-dione and 2-thioxothiazolidin-4-one with substituents at the 5-position were prepared. ^{1}H-NMR spectra for all compounds showed a typical signal for the hydrogen on the double bond (CH=C) in the range of 5.6-7.6 ppm for thioxoimidazolidin-4-one, and in the range of 7.75-7.9 ppm for thiazolidine-2,4-dione and 2-thioxothiazolidin-4-one. No overlaps were seen in ^{1}H-NMR spectra between a typical signal for the hydrogen on the double bond and aromatic ring signals for thiazolidine-2,4-dione and 2-thioxothiazolidin-4-one.

2.2.3 The reduction reaction of 5-substituted derivatives of 2-thiohydantoin, thiazolidine-2,4-dione and 2-thioxothiazolidin-4-one

The reduction of the double bond in (Z)-5-benzylidene-2-thioxoimidazolidin-4-one was carried out using Pd/C as a catalyst and THF as a solvent.[8] The product was obtained, but in poor yield. The use of Zn dust with acetic acid was previously used just for (Z)-5-benzylidene-2-thioxoimidazolidin-4-one.[9] Using this procedure, we were able to reduce not only compound **1** but also all other unsaturated 2-thioxoimidazolidin-4-ones, except compound **7** (Scheme 2.6).

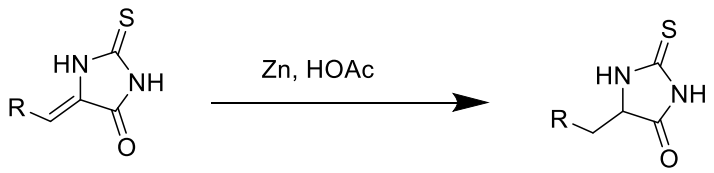

Scheme 2.6: Synthesis of racemic 5-substituted 2-thiohydantoins.

The reduction procedure in Scheme 2.6 was used for compound 7; however, we obtained an unknown product. The reduction procedure by zinc and acetic acid was repeated using a longer reaction time to reduce compound 7. Despite this, no clear result was obtained (Scheme 2.7).

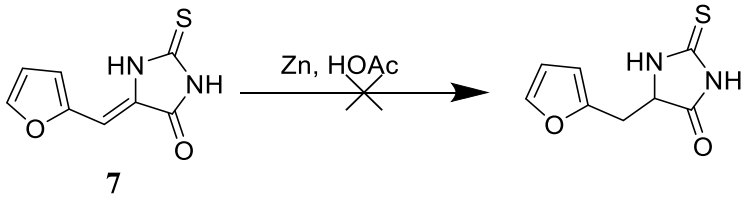

7

Scheme 2.7: Attempted synthesis of compound **7**.

Fortunately, the adjacent hydrogen on the stereogenic centre and diastereotopic protons on the CH_2 for all compounds, except compound **7**, were clearly visible in ^{1}H-NMR spectra, confirming the reduction process, and thus generation of the stereogenic centre.

Similarly, the catalysed reduction using zinc dust was also tried for 5-substituted thiazolidine-2,4-diones. However, its success depends on the types of substituents involved. The reduction process by zinc dust was not accomplished for 5-benzylidenethiazolidine-2,4-dione **12** in the attempted synthesis of **13** (Scheme 2.8).

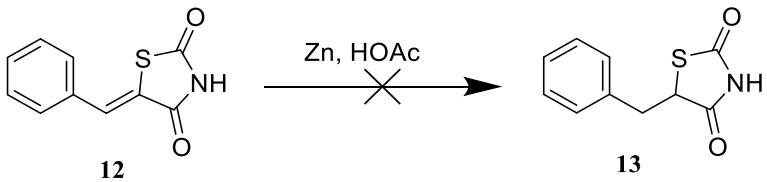

12 **13**

Scheme 2.8: Attempted synthesis of compound **13**.

The reduction process by zinc and acetic acid was successful for 5-(pyridin-2-ylmethylene) thiazolidine-2, 4-dione **14** and pure **15** was obtained in good yield. The zinc acid catalysed reduction also worked for **16** and **18** to produce compounds **17** and **19**, respectively (Scheme 2.9).

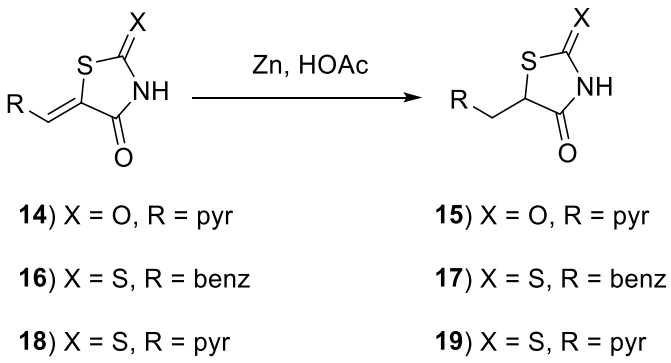

14) X = O, R = pyr

15) X = O, R = pyr

16) X = S, R = benz

17) X = S, R = benz

18) X = S, R = pyr

19) X = S, R = pyr

Scheme 2.9: Reduction of compounds **14**, **16** and **18**.

As an alternative, reduction using $LiBH_4$ in THF was tried for (Z)-5-benzylidenethiazolidine-2,4-dione **12**. The reduction of the double bond at room temperature and purification by column chromatography produced the desired 5-benzylthiazolidine-2, 4-dione **13** (Scheme 2.10).

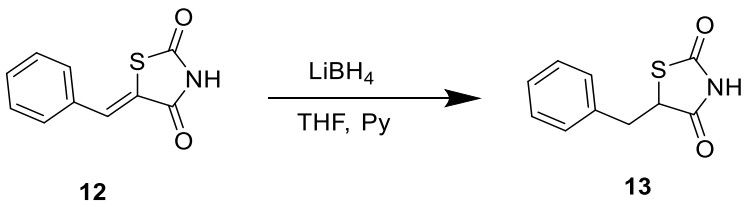

12 **13**

Scheme 2.10: Reduction of 5-benzylidenethiazolidin-2,4-dione.

Finally, microwave heating (300 W, 120 °C, max pressure 300 psi) was also used to synthesise 5-benzylthiazolidine-2,4-dione using the $LiBH_4$ procedure, as previously reported,[23] and this procedure was successful.

2.2.4 Synthesis of 5-substituted 2-thiohydantoin under solvent free conditions

The condensation of thiourea with different amino acids serves as an excellent starting point in the preparation of 5-substituted 2-thiohydantoins.[27,10] We have used several amino acids with thiourea to synthesise the corresponding 5-substituted 2-thioxoimidazolidin-4-ones under solvent free conditions. Compounds **20**-**25** were synthesised using thermal heating between 180-200 °C, i.e. in liquid thiourea. The required reaction time ranged from 15 to 25 min, with 14.0- 42.0 % yields obtained (Scheme 2.11).

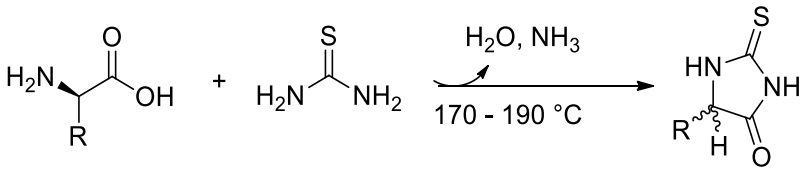

Scheme 2.11: Conditions proposed by Wang and co-workers for the synthesis of racemic 5-substituted 2-thiohydantoins[10]

The use of high temperature during the reaction resulted in all products being non-optically active compounds, i.e. racemic mixtures. We tried quenching the products in organic solvent without adding water, followed by washing with water at room temperature and evaporation of the organic solvent. Our efforts failed to produce enantioenriched compounds, although the literature suggested this should be possible[10] by the condensation of thiourea with enantiopure amino acids under solvent free conditions. The authors reported that this procedure is safe to prepare, even for enantiopure 5-substituted 2-thiohydantoins, but this was reported without the confirmation of optical activity. Unfortunately, all products prepared were non-optically active compounds, as confirmed by either polarimetry or CD spectroscopy. All 5-substituted 2-thiohydantoins were characterised by ^{1}H-NMR, ^{13}C-NMR and MS.

2.2.5 Synthesis of 5-substituted 1-acetyl-2-thiohydantoin

We started the synthesis of 5-substituted 1-acetyl-2-thiohydantoin from different amino acids and ammonium thiocyanate with acetic acid and acidic anhydride, as previously reported (Scheme 2.12, and see section 2.1.2).[9,7]

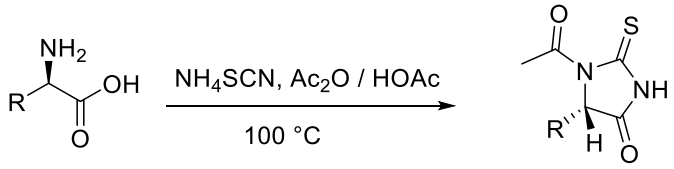

Scheme 2.12: Synthesis of 5-substituted 1-acetyl-2-thiohydantoins by the reaction of amino acid derivatives with ammonium thiocyanate including acetic acid and acetic anhydride.

We follow the post-1907 nomenclature for 2-thiohydantoins according to which the acetyl group in Scheme 2.12 is substituted at the N-1 position. The same compound, 1-acetyl-2-thioxoimidazolidin-4-one, has also been named 3-acetyl-2-thioxoimidazolidin-4-one by Davis *et al*.[28] who used the same synthetic procedure as Johnson. 2-D COSY NMR spectroscopy confirmed that the acetyl group was substituted at the NH-1 rather than the NH-3. Unfortunately, the change in nomenclature has affected several publications where an incorrect nomenclature is used.[9, 28]

We followed the procedure of Csonka and Nicolet[17] for the synthesis of optically active 5-substituted 1-acetyl-2-thioxoimidazolidin-4-ones, with various changes (see Chapter 1). However, the temperature of the reaction was not indicated by the authors. Generally, the same amount of acetic anhydride and acetic acid was used to prepare several 5-substituted 1-acetyl-2-thiohydantoins by using the corresponding enantiopure amino acids and different reaction times. Essentially, the temperature and the reaction time were decreased to synthesise as much as possible of the high optically active compounds (Scheme 2.13).

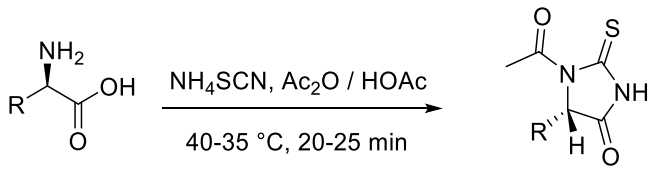

Scheme 2.13: Synthesis of optically active 5-substituted 1-acetyl-2-thioxoimidazolidin-4-ones.

L-phenyl alanine, L-valine, L-tryptophan and L-methionine were reacted gently with ammonium thiocyanate, acetic anhydride and acetic acid to produce the corresponding optically active 5-substituted 1-acetyl-2-thioxoimidazolidin-4-ones (See experimental section). Using L-phenyl glycine produces racemic 1-acetyl-5-phenyl-2-thioxoimidazolidin-4-one. All reactions involving amino acids as starting material were successful in producing products, although as the racemates. The reaction involving histidine failed to produce the required product altogether. The preparation of thiohydantoin from histidine was unsuccessful, despite trying different temperatures and concentrations of ammonium thiocyanate, acetic anhydride and acetic acid. This procedure was previously tried by Swan[29] in 1952, who used histidine and N-acetyl histidine and warming with acetic anhydride and ammonium thiocyanate to produce an unstable compound. At the end, the unstable products are converted by dilute acetic acid into a mono-acetyl compound, such as 5-(1-acetyl-4-iminazolyimethyl)-2-thiohydantoin, rather than 1-acetyl compounds.[11] Using an excess of acetic anhydride causes racemisation and produces racemic compounds,[30] and the formation of lactone anhydride (azlactone) destroys the second mole of acetic anhydride (see Scheme 2.3). Therefore, active intermediate azlactone might prevent the racemisation if formed rapidly.[17] Column chromatography was performed over silica gel using hexane and diethyl ether as eluents to purify the compounds. The structures of all compounds prepared by my own procedure and those of Johnson were confirmed by ^{1}H-NMR, ^{13}C-NMR, FTIR and MS. Furthermore, for further verification, the GC-MS was recorded. The spectra obtained showed products to be pure with the correct molecular structures.

The deacylation process was done for compound **27** by dissolving in 12 M HCl and heating for 1 hour at 60 °C. Pure **2** was collected (Scheme 2.14).[31]

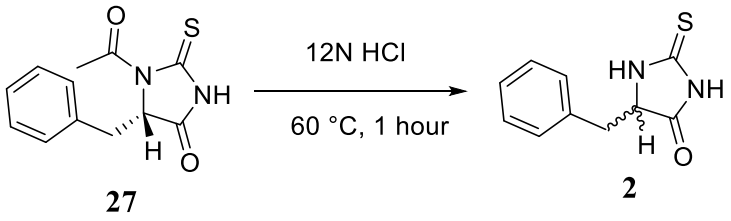

27 **2**

Scheme 2.14: The deacetylation of compound **27** to prepare compound **2**.

The product was extracted by ethyl acetate and then dried. There was no acetyl peak observed in ^{1}H-NMR and ^{13}C-NMR spectra and the yield was 73.5% 5-benzyl-2-thiohydantoin.

2.2.6 The enantiomeric excess and intensity of enantioenriched compounds

The specific rotations of **27-32** were recorded using a polarimeter and were found to be different from one another. During the synthesis of 5-substituted 1-acetyl-2-thiohydantoins from the corresponding amino acids, acetic acid and acetic anhydride with ammonium isothiocyanate was used. Csonka and Nicolet[17] reported the high specific rotation of compound **29** ($[\alpha]_D^{20}$ = 118.5°) in 1% alcohol solution for white light filtered through 2 cm by using a similar procedure to the one we used with some modification. However, the specific rotation we found was lower ($[\alpha]_D^{20}$ = + 83.9°), recorded in 0.3% acetonitrile solution. However, it should be noted that Csonka and Nicolet used a higher concentration of **29** in their measurements. The specific rotations of **27-32** at different concentrations are shown in Table 2.1.

Table 2.1: Specific rotation of **27-32** in different solvents and at different concentrations determined by polarimetry.

Substrate	$[\alpha]_D^{20}$	Concentration
27	+94.5°	0.25 g / l00 ml (Acetonitrile)
29	+83.9°	0.29 g / l00 ml (Acetonitrile)
30	+116.8°	0.40 g / l00 ml (Acetone)
31	+94.5°	0.4 g / l00 ml (Acetone)
32	+118.6°	0.40 g / l00 ml (Acetone)

Reetz *et al*.[32] described how to determine enantiomeric excess (ee %) by using the anisotropy factor obtained by dividing the ellipticity by absorbance (Equation 2.1).

$$g = \frac{\theta}{A}$$ **Equation 2. 1**

where g is the anisotropy factor, θ is the ellipticity and A is the UV absorbance.[33]

By using Equation 2.1, the anisotropy factor was calculated for **27-32** by using the maximum ellipticity and absorbance in 10 % water and 90 % of 0.2 M phosphate buffer (0.9 M *I*, pH 7.4) and 37 °C (Table 2.2).

Table 2.2: The specific rotation of **27-32** in different solvents and at different concentrations determined by polarimetry. The compounds were dissolved in 10 % water and 90 % 0.2 M phosphate buffer (0.9 M *I*, pH 7.4) at 37 °C.

Substrate	Con./ mM	Maximum Ellipticity	Absorbance	g/ factors
27	0.081	-15.722 (265 nm)	1.013 (291 nm)	-15.528
29	0.017	-7.216 (262 nm)	0.925 (288 nm)	-7.800
30	0.025	-9.910 (266 nm)	0.758 (288 nm)	-13.067
31	0.012	-5.590 (260 nm)	0.716 (287 nm)	-7.696
32	0.011	-4.953 (263 nm)	0.855 (290 nm)	-5.796

The enantiomeric excess of **27-32** (Table 2.2) is unknown and pure enantiomers were not identified by either HPLC or GC-MS. Therefore, it is impossible to determine the enantiomeric excess for **27-32**.

2.2.7 Synthesis of racemic 5-substituted 3-phenyl-2-thiohydantoin

For studies of the effect of substituents at the N-3 position of 2-thiohydantoin, several di-substituted 2-thiohydantoins were required. These have been prepared from the corresponding amino acids esters. The substituent at the 3-position originating from the use of phenyl isothiocyanate or allyl isothiocyanate with phenylalanine methyl ester HCl using the procedure was previously reported for the synthesis of 3-benzyl-5-methyl-2-thioxoimidazolidin-4-one.[14] The reaction between hydrochloride salts of amino acid methyl ester and phenyl or alkyl isocyanate / isothiocyanate (X = O or S) in the presence of triethylamine or pyridine proceeds in two steps. The first step is a condensation process which produces 3-substituted (thio) ureido-phenyl acetic acid. The following step is the cyclisation of the acid derivative upon refluxing in basic medium (Scheme 2.15).[34]

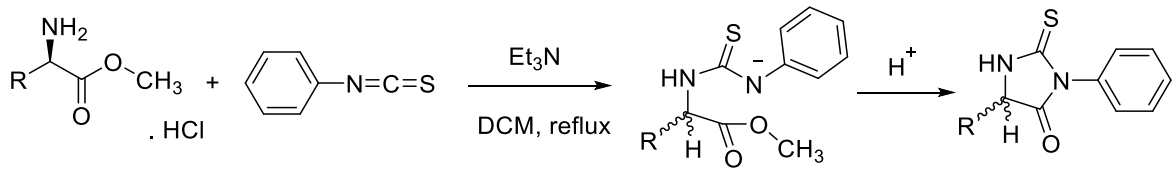

Scheme 2.15: Synthesis of racemic 5-substituted 3-phenyl-2-thioxoimidazolidin-4-ones by the reaction of amino acid methyl ester HCl derivatives with phenyl isothiocyanate in basic medium.

This procedure was used to synthesise the 3,5-disubstituted 2-thiohydantoins **33-36** in this project in good yields. All these thiohydantoin derivatives were optically inactive products if prepared under basic conditions. It is difficult to dissolve amino acid methyl ester HCl in DCM, but by adding triethylamine the mixture becomes completely soluble. To address this, acidified water was used to remove the excess of trimethylamine and amino acid methyl ester HCl, while hexane is a very good solvent to remove the remaining phenyl isothiocyanate from the solution.

Very good yields of 84.0- 96.8% were obtained for compounds **33-35** and a yield of 46.3% was obtained for **36** using this procedure. Clear analytical NMR, MS and FTIR data was obtained.

2.2.8 Synthesis of tri-substituted 2-thiohydantoin

2.2.8.1 Synthesis of rac-tri-substituted 2-thiohydantoin

Sim and Ganesan[35] prepared a library of trisubstituted 2-thiohydantoins from α-amino ester, aromatic aldehydes and phenyl isothiocyanate, which was followed in the present work to prepare compounds **37-41.** The reductive amination reaction of amino esters with aromatic aldehydes in the presence of sodium triacetoxyborohydride containing triethylamine was done in the first step. After one hour stirring, the cyclisation was carried out by adding isothiocyanate and extra triethylamine for another hour under stirring. The product was purified by column chromatography (Scheme 2.16).

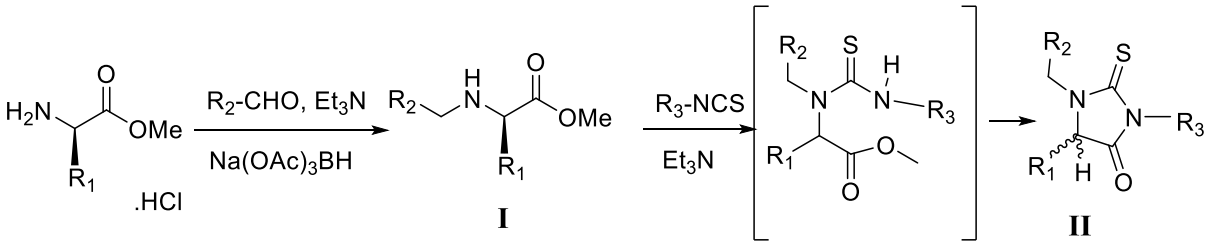

Scheme 2.16: Synthesis of racemic trisubstituted 2-thiohydantoin[19]

The α-amino acid ester reacts with the aromatic aldehyde to produce an iminium ion followed by reduction using sodium triacetoxyborohydride (Scheme 2.17). The electron-withdrawing capacity and steric effects of the three acetoxy groups stabilise the boron-hydrogen bond and both properties are responsible for the reduction process.[36] Compound **I** reacts with isothiocyanate to form compound **II** in the presence of base (Scheme 2.16) after the reductive amination process (Scheme 2.17).

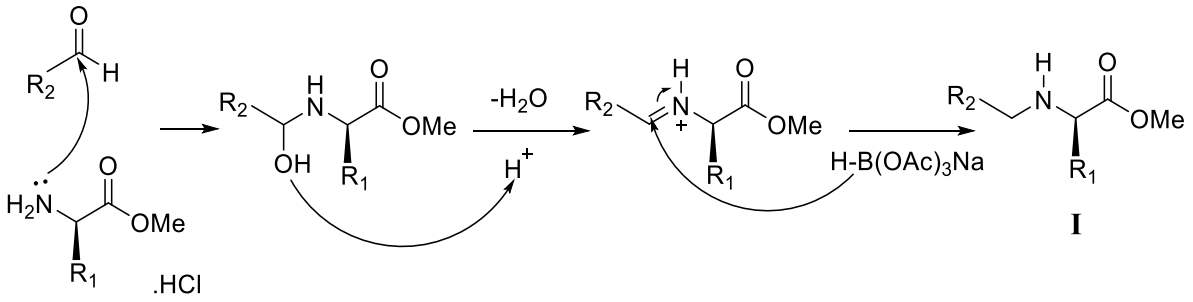

Scheme 2.17: The reduction process of imine to form the corresponding amine.

Several compounds were prepared by this procedure showing clear analytical data by using different aromatic aldehydes. There was no obvious product from the reaction using DL-serine methyl ester HCl with 4(5)-imidazolecarboxaldehyde in the attempt to synthesis cyclised trisubstituted 2-thiohydantoin. Unfortunately, all thiohydantoin derivatives were optically inactive under these conditions. Adding extra triethylamine resulted in the product being optically inactive without finding a critical time to end cyclisation. An alternative way to synthesise optically active trisubstituted 2-thiohydantoin is presented in the next section.

2.2.8.2 Synthesis of enantiomerically-enriched trisubstituted 2-thiohydantoin

(*S*)-5-isopropyl-3-phenyl-1-(pyridin-2-ylmethyl)-2-thioxoimidazolidin-4-one **38** was synthesised following Sim and Ganesan's procedure[35] by slightly changing the amount of reagents and reaction time. A mixture of products **38** and **34** was detected by GC-MS spectroscopy. The products were separated using column chromatography (Scheme 2.18).

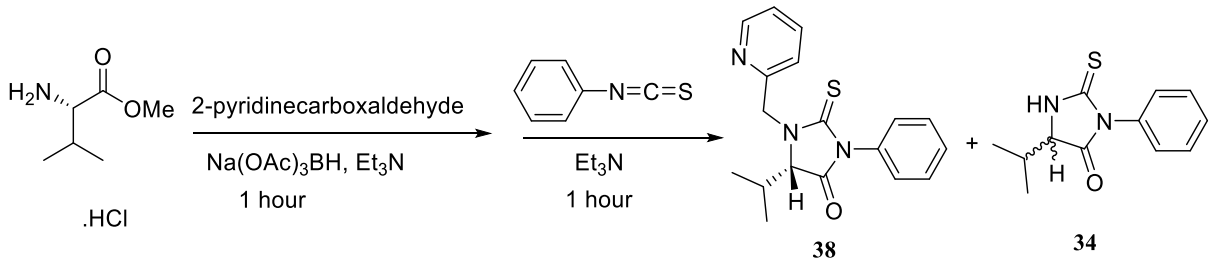

Scheme 2.18: Synthesis of enantiomerically-enriched **38** and racemic **34**

The mixture of **38** and **34** was separated using column chromatography. Compounds **38** and **34** were collected separately after purification with yields of 60.4 and 18.1 %, respectively. Unfortunately, thiohydantoin **34** is completely optically inactive. On the other hand, compound **38** is optically active and has been used for kinetic studies. The formation of **34** in this procedure shows that the reaction between α-amino ester derivatives **I** with isothiocynate (Scheme 2.15) occurs on the same timescale as the cyclisation of intermediate **I** (Scheme 2.16). The ring closed compounds **34** and **38** racemise much faster in the presence of triethylamine than the compounds before cyclisation.

Similarly, (*R*)-5-benzyl-3-phenyl-1-(pyridin-2-ylmethyl)-2-thioxoimidazolidin-4-one **37** (Scheme 2.19) has been prepared by a variation of the method of Sim and Ganesan[35] by decreasing the reaction time and amount of triethylamine. It was found that adding triethylamine, which causes the product to be racemic, is not essential in both steps. However, triethylamine was just added in the first step, and instead of stirring for two hours in both steps, the solution was stirred for 35 minutes. TLC showed that the reaction had finished (Scheme 2.19).

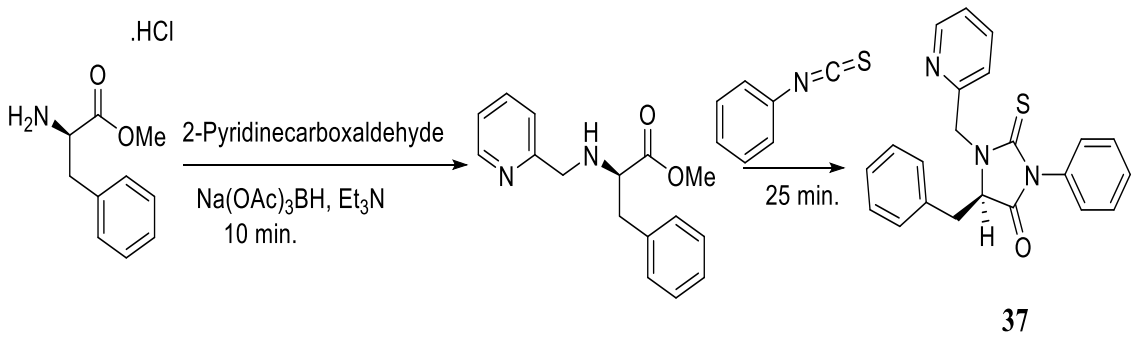

Scheme 2.19: Combination synthesis of enantiomerically-enriched compound **37**

GC-MS showed that **37** was pure. In comparison, the NMR and MS data for racemic **37**, which had been prepared previously (Scheme 2.16), and enantioenriched thiohydantoin were similar (for CD data for enantioenriched **37,** see Chapter 4).

2.3 Conclusions

2-Thioxoimidazolidin-4-ones derivatives with substituents at the 1, 3 and 5 positions have been prepared as racemic and enantioenriched compounds by different procedures (Chapter 2). Knoevenagel condensation worked successfully to react different aldehydes with 2-thioxoimidazolidin-4-ones to prepare the corresponding unsaturated 5-substituted-2-thioxoimidazolidin-4-ones derivatives. Knoevenagel condensation was also successful in preparing unsaturated 5-substituted thiazolidine-2,4-diones and 5-substituted 2-thioxothiazolidin-4-one derivatives. To prepare saturated 5-substituted 2-thioxoimidazolidin-4-ones, zinc and acetic acid were used to reduce the double bond to a single bond and prepare racemic 5-substituted 2-thioxoimidazolidin-4-ones. The reduction process worked well for all unsaturated 2-thioxoimidazolidin-4-ones prepared, except for (Z)-5-(furan-2-ylmethylene)-2-thioxoimidazolidin-4-one **7**, which produced an unknown product. Zn/acetic acid were also successful in reducing (Z)-5-(pyridin-2-ylmethylene)thiazolidine-2,4-dione **14**, but not (Z)-5-benzylidenethiazolidine-2,4-dione **12,** the reason being unclear. As an alternative, $LiBH_4$ in the presence of pyridine, for catalytic reduction in THF, was tried for (Z)-5-benzylidenethiazolidine-2,4-dione **12** and found to be successful. The reduction process was successful in preparing racemic 5-substituted 2-thioxothiazolidin-4-one by using zinc/acetic acid on one hand, and $LiBH_4$ with pyridine as a catalytic reduction in THF on the other. Our attempts to prepare enantioenriched 5-substituted 2-thioxoimidazolidin-4-ones derivatives starting from enantiopure amino acids with thiourea failed because of the high reaction

temperature. However, several enantioenriched 5-substituted 1-acetyl-2-thioxoimidazolidin-4-one derivatives were synthesised using the corresponding amino acids with ammonium thiocyanate, including acetic acid and acetic anhydride. Several racemic tri-substituted 2-thioxoimidazolidin-4-ones were prepared using the pure enantiomer of amino acid methyl ester HCl. Using the same procedure for racemic tri-substituted 2-thioxoimidazolidin-4-ones with various changes to reaction time and amount of base, two enantioenriched tri-substituted 2-thioxoimidazolidin-4-ones were prepared. In this way, N-acetyl substituted 2-thioxoimidazolidin-4-ones could be obtained with some enantiomeric excess.

2.4 Experimental section

Chemicals

All reagents were purchased from Fisher Scientific, Sigma-Aldrich, Alfa Aesar, Fluorochem, Acros Organic, Applichem, BDH, and Lancaster Synthesis and used without purification.

2.5 Experimental techniques

Infra-Red spectra (IR)

Infrared spectra were recorded in the range 4000-600 cm^{-1} using a SHIMADZU CORP series FTIR instrument. Samples were either thin films or powders. All absorptions are quoted in cm^{-1}.

Nuclear Magnetic Resonance (NMR)

^{1}H-NMR and ^{13}C-NMR spectra were recorded on a Bruker DPX 400 (400 MHz) or DPX 500 (500 MHz) spectrometer. Chemical shifts are expressed in parts per million downfield from tetramethylsilane as an internal standard. NMR spectra were recorded in solutions in deuterated-dimethylsulfoxide (DMSO-d_6) or chloroform ($CDCl_3$). HMBC and HSQC experiments were used on the same spectrometers to confirm assignments when necessary.

Melting Point

Melting points were recorded using a Gallenkamp Melting Point Apparatus.

Mass spectrometry

LCMS experiments were performed using a Waters 2790 liquid chromatography system and a Waters ZQ mass spectrometer. Samples were loaded using a Gilson 232XL auto-sampler. Low-resolution mass spectrometric data were determined using a Fisons VG Platform II quadrupole instrument using electrospray ionisation (ES), unless otherwise stated. High-resolution mass spectrometric data were obtained in electrospray (ES) mode unless otherwise reported, on a Waters Q-TOF micro-mass spectrometer.

Polarimetry

Optical rotations were measured with a Schmidt-Haensch Polartronic I in a 5.00 cm path length cell. The solvent and concentration (expressed in g/100 ml) of the solutions used for the measurements are reported in the individual sections.

X-ray crystallography

A Bruker CCD diffractometer with graphite-mono-chromatised Mo-K radiation (λ =0.71073 Å) was used for X-Ray crystallographic studies, carried out at by the X-Ray Crystallography Service. The structures were solved by direct methods and refined using the SHELXTL software package.

2.6 Methods

All compounds were prepared according to one of the following general methods.

Method 1

Commercially available 2-thiohydantoin was placed with the required aldehydes in a round bottom flask equipped with a magnetic stirrer and reflux condenser under a nitrogen atmosphere in triethylamine and water. The mixture was stirred overnight at room temperature and the pH was adjusted to 3 by adding 3 M HCl. The solid product was filtered off and washed with diethyl ether and water. The pure compounds were collected and dried.

Method 2

Thiazolidine-2, 4-dione or 2-thioxothiazolidin-4-one and the appropriate aldehydes were added to 20 ml ethanol containing piperidine. The mixture was refluxed under nitrogen for 3 h. The precipitate was filtered off, washed with ethanol and dried.

Method 3

The compounds used in method **2** were dissolved in 10 ml anhydrous THF containing 10 ml pyridine at room temperature. Lithium borohydride was slowly added to the mixture causing bubbles to form during the addition. The stirred mixture was refluxed for 4 days. When the reaction was finished, the mixture was cooled on an ice bath to 5 ˚C and 8 ml of 12 N hydrochloric acid and 50 ml of deionised water were added. The mixture was refluxed again for 1 h. The residue formed after evaporation of the solvent was dissolved in chloroform, washed with 3 x 150 ml of water and dried over MgSO4.

Method 4

The condensation products prepared according method **1** and **2** were dissolved in acetic acid in a round bottom flask under nitrogen atmosphere, stirrer and refluxed. Zinc dust was added to the solution and the mixture was heated for 3 hours at 130 °C under reflux. The mixture

was then allowed to cool down to 50 °C and 50 ml of methanol was added to the solution. The temperature was then returned to 115 °C for about 5 minutes. The mixture was allowed to cool to 63 °C and filtered. The liquid was concentrated under reduced pressure. The resulting paste was mixed with 3:7 isopropanol DCM and filtered again. The solution was washed with 100 ml of water and 50 ml of brine. The combined organic layer was filtered through filter paper and the solvent was evaporated under reduced pressure. The product was dried under high vacuum.

Method 5_a

Acetylated 2-thiohydantoins were synthesised by reacting ammonium thiocyanate with several amino acids. The amino acids were mixed with ammonium isothiocyanate and dissolved in 9:1 acetic anhydride / acetic acid at 100 °C under nitrogen atmosphere and refluxed for 30 minutes. The solution was poured into 20 ml of an ice/water mixture and stored in a fridge overnight. The solid was filtered and dried using a freeze dryer. Racemic products were obtained.

Method 5_b

Enantioenriched 5-substituted 1-acetyl-2-thiohydantoins were synthesised by the method described above (method 5a) with the slight variation of dissolving the mixture at 70 °C in a sonication bath for 5 -10 minutes and reducing the temperature to 35 °C. The mixture was heated at 35 °C for a further 25 minutes. The mixture was cooled down, washed with 50 ml of water and mixed with ethyl acetate. The reaction mixtures were washed twice with brine. All compounds were purified by column chromatography over silica using 50:50 diethyl ether and hexane. Significant optical activity was found for the resulting products.

Method 6

In a round bottom flask, 1:2 amino acid and thiourea was mixed together under reflux and nitrogen atmosphere at 180 °C using an oil bath. When the mixture started to melt, the temperature was increased to 190 °C and a yellow vapour was observed inside the condenser. The mixture was allowed to heat under reflux at the same temperature for 25 minutes. Water

was then added to the mixture after reducing the temperature to about 80 °C. The mixture was then put in a refrigerator for the product to precipitate.

Method 7

Different α-amino acid methyl esters HCl were dissolved in a mixture of CH_2Cl_2 and triethylamine. Phenyl isothiocyanate was slowly added to the solution and stirred for 1 hour at 25 °C. The temperature was then raised to 40 °C under reflux and continued to be stirred for another hour. The solution was cooled down to room temperature and evaporated under reduced pressure. The residue was redissolved in CH_2Cl_2 and washed twice with acidified water (pH 3.0) to remove triethylamine and amino acid methyl ester HCl. The solution was then washed with brine and dried over Na_2SO_4. The solid product was triturated with hexane until an excess of phenyl isothiocyanate was removed.

Method 8

Different amino acid methyl ester hydrochlorides were dissolved in a mixture of CH_2Cl_2 (10 ml) and triethylamine. Aldehyde and sodium triacetoxyborohydride were added to the solutions and stirred at room temperature (*ca*. 20 °C). Phenyl isothiocyanate or allylisothiocyanate were added to the mixture and stirred for another hour. The solution was treated with glycine solution and extracted with CH_2Cl_2. The organic solvent was evaporated and an oily compound was obtained. All compounds were purified by column chromatography over silica.

Synthesis of 5-benzilidine-2-thiohydantoin (1)

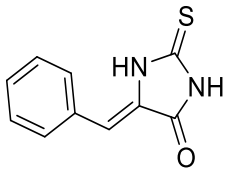

1

Utilising method **1**, thiohydantoin (2.0 g, 17.2 mmol), trimethylamine (4.9 ml, 37 mmol) and benzaldehyde (1.9 ml, 19 mmol) were added to 50 ml of water.

Yield= 69.9 %, Mp 270-272 °C, HRMS calculated for $C_{10}H_8N_2OS$ m/z $[M+H]^+$ 204.0358; found 204.0358; ^{1}H-NMR (400 MHz, DMSO-d_6): δ 12.41 (s, H, N**H)**, δ 12.19 (s, H, N**H)**, δ 7.74 (d, *J* = 7.4 Hz, 2H, phen), δ 7.45-7.37 (m, 3H, phenyl), δ 6.49 (s, H, C**H=C**).^{13}C-NMR (101 MHz, d_6-DMSO): δ 177.3 (**C**=S), δ 164.0 (**C**O), δ 130.5 (**C**=CH), δ 128.6 (2x**C**H), δ 127.3 (**C**), δ 127.0 (2x**C**H), δ 126.0 (**C**H), δ 109.7 (**C**H=C). IR (neat): vmax= 3225 cm^{-1} (NH), 1723 cm^{-1} (C=O), 1475 cm^{-1} (C=S), 1643 cm^{-1} (C=C). (File reference: NMR: 400_HA_exp 1A DFA).

Synthesis of 5-benzyl-2-thiohydantoin (2)

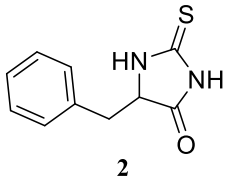

2

Utilising method **4**, 5-benzilidine-2-thiohydantoin (1.5 g, 7.4 mmol) was dissolved in acetic acid (10 ml, 175 mmol) and zinc dust (1.18 g, 18 mmol) was added.

Yield= 29.5 %, Mp 168-170 °C, HRMS calculated for $C_{10}H_{10}N_2OS$ m/z $[M+H]^+$ 206.0517; found 206.0517; ^{1}H-NMR (400 MHz-d6-DMSO): δ 11.45 (s, 1H, N**H**), δ 10.10 (s, 1H, N**H**), δ 7.34 – 7.16 (m, 5H, phenyl), δ 4.56 (apparent t, *J* = 5.3 Hz, 1H, C**H**), δ 2.99 (m, 2H, C**H**$_2$).^{13}C NMR (101 MHz, DMSO): δ 182.5 (**C**=S), δ 176.1 (**C**O), δ 135.39 (**C**), δ 130.3 (2X**C**), δ 128.5 (2x**C**), δ 127.2 (CH), δ 61.7 (**C**HCH2), δ 36.0 (CHCH2). IR (neat): vmax = 1738 cm^{-1} (C=O), 1543 cm^{-1} (C=S). (File reference: NMR: 400_HA_exp 1B DFA).

Synthesis of (Z)-5-(pyridin-2-ylmethylene)-2-thioxoimidazolidin-4-one (3)

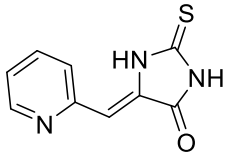

3

Utilising method **1**, thiohydantoin (2.0 g, 17.2 mmol), triethylamine (4.8 ml, 37 mmol) and 2-pyridinecarboxyaldehyde (1.8 ml, 22 mmol) were added to 50 ml of water.

Yield= 86.7 %, M.p. 262-263 °C, HRMS calculated for $C_9H_7N_3OS$ m/z $[M+H]^+$ 205.0310; found 205.0311; ^{1}H-NMR (400 MHz, DMSO): δ 8.74 (d, *J* = 3.8 Hz, 1H, C**H**N), δ 7.89 (td, *J* = 7.7, 1.8 Hz, 1H, C**H**CHCHN), δ 7.72 (d, *J* = 7.9 Hz, 1H, C**H**CN), δ 7.38 (dd, *J* = 7.6, 4.9 Hz, 1H, C**H**CHCHN), δ 6.61 (C**H**=). ^{13}C-NMR (101 MHz, d_6-DMSO): δ 179.2 (**C**=S), δ 165.8 (**C**O), δ 153.6 (**C**N), δ 150.2 (**C**HN), δ 137.7 (**C**=CH), δ 131.4 (**C**HCHCN), δ 126.3 (**C**HCN), δ 123.9 (**C**HCHN), δ 107.5 (**C**H=C).IR (neat): vmax=1719 cm^{-1} (C=O), 1660 cm^{-1} (C=C), 1489 cm^{-1} (C=S). File reference: ^{1}H-NMR: 400_hiwa-5PT-333.^{13}C-NMR: 400_HA_exp 3A DFA 1).

Synthesis of 5-(pyridin-2-ylmethyl)-2-thioxoimidazolidin-4-one (4)

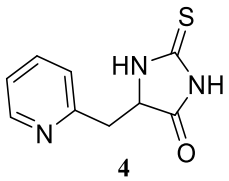

4

Utilising method **4**, (Z)-5-(pyridin-2-ylmethylene)-2-thioxoimidazolidin-4-one (1.5 g, 7.3 mmol) was dissolved in 30 ml of methanol and acetic acid (12 ml, 210 mmol) and zinc dust (1.0 g, 15.3 mmol) were added (the product was recrystallised using ethanol).

Yield= 30.5 %, M.p. 211-213 °C, HRMS calculated for $C_9H_9N_3OS$ m/z $[M+H]^+$ 207.0466; found 207.0463; ^{1}H-NMR (400 MHz DMSO): δ 11.62 (s, 1H, N**H**), δ 9.96 (b, 1H, N**H**), δ 8.49 (d, *J* = 4.3 Hz, 1H, C**H**N), δ 7.77 (td, *J* = 7.7, 1.8 Hz, 1H, C**H**CHCHN), δ 7.30 (dd, *J* = 11.2, 6.4 Hz, 2H, C**H**CN and C**H**CHN), δ 4.66 (apparent t, *J* = 5.4 Hz, 1H, C**H**CH_2CN), δ 3.20 (qd, *J* = 14.9, 5.8 Hz, 2H, CHC$\mathbf{H}_A$C$\mathbf{H}_B$CN). ^{13}C-NMR (101 MHz, d_6-DMSO): δ 183.0

(**C**=S), δ 176.7 (**C**O), δ 156.0 (**C**N), δ 149.4 (**C**HN), δ 136.9 (**C**HCHCHN), δ 124.6 (**C**HCN), δ 122.4 (**C**HCHN), δ 60.4 (**C**HCH$_2$), δ 38.2 (CH**C**H$_2$). IR (neat): vmax=1711 cm^{-1} (C=O), 1519 cm^{-1} (C=S). File reference: ^{1}H-NMR: 400_HA_exp 3B_5pt_FDA.^{13}C-NMR: 400_hiwa-5PT-444).

Synthesis of (Z)-5-(1-methyl-1H-pyrrol-2-yl) methylene)-2-thioxoimidazolidin-4-one (5)

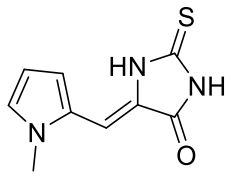

5

Utilising method **1**, thiohydantoin (2.3 g, 19.8 mmol), triethylamine (5.9 ml, 42.3 mmol) and 1-methyl pyrrole-2-carboxaldehyde (2.0 ml, 18.6 mmol) were added to 50 ml of water.

Yield = 64.3 %, M.p. 263-265 °C, HRMS calculated for $C_9H_9N_3OS$ m/z $[M+H]^+$ 207.0466; found 207.0463; ^{1}H-NMR (400 MHz, DMSO): δ 7.24 (dd, *J*=4.03, 1.28 Hz, 1H, C**H**N), δ 7.08 (t, *J* = 2.2 Hz, 1H, C**H**CHN), δ 6.43 (s, 1H, C**H**=C), δ 6.20 (dd, *J* = 3.9, 2.6 Hz, 1H, C**H**CN), δ 3.71 (s, 3H, **H**$_3$CN).^{13}C-NMR (126 MHz, d$_6$-DMSO): δ 177.3 (**C**=S), δ 165.92 (**C**O), δ 128.5 (**C**CH**C**NCH$_3$), δ 125.8 (**C**NCH$_3$), δ 122.9 (**C**HNCH$_3$), δ 115.3 (**C**HCNCH$_3$), δ 110.1 (**C**H=), δ 101.7 (**C**HCHNCH$_3$), δ 33.4 (**C**H$_3$N). IR (neat): vmax=1712 cm^{-1} (C=O), 1633 cm^{-1} (C=C), 1431cm^{-1} (C=S). File reference: ^{1}H-NMR: 400_hiwa-5MPT-555.^{13}C-NMR: 500_HA_ exp 4 A C13).

Synthesis of 5-((1-methyl-1H-pyrrol-2-yl) methyl)-2-thioxoimidazolidin-4-one (6)

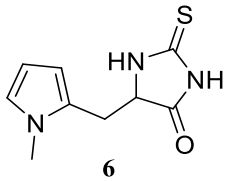

6

Utilising method **4**, 5-((1-methyl-1H-pyrrol-2-yl) methyl)-2-thioxoimidazolidin-4-one (2.0 g, 7.3 mmol) was dissolved in 75 ml of methanol, acetic acid (30 ml, 524 mmol) and Zn dust (1.2 g, 18.4 mmol) was added.

Yield= 27.3 %, M.p. 203-205 °C, HRMS calculated for $C_9H_9N_3OS$ m/z $[M+H]^+$ 209.0623; found 209.0622; ^{1}H-NMR (500 MHz DMSO): δ 10.01 (b, 1H, N**H**) δ 6.59 (t, *J* = 2.2 Hz, 1H, C**H**NCH$_3$), δ 5.84 (t, *J* = 3.1 Hz, 1H, C**H**CNCH$_3$), δ 5.77 (m, 1H, C**H**CN), δ 4.66 (apparent t, *J* = 4.9, Hz, 1H, C**H**CH$_2$CN), δ 2.97 (d, *J* = 4.9 Hz, 1H, CHC**H**$_A$C**H**$_B$CN).^{13}C-NMR (126 MHz, d$_6$-DMSO): δ 182.2 (**C**=S), δ 175.3 (**C**O), δ 125.8 (**C**NCH$_3$), δ 121.9 (**C**HN), δ 107.5 (**C**HCHNCH$_3$), δ 106.3 (**C**HCNCH$_3$), δ 60.7 (**C**HCH$_2$), δ 33.3 (**C**H$_3$N), δ 26.3 (**C**H$_2$CH). IR (neat): vmax=1737 cm^{-1} (C=O), 1548 cm^{-1} (C=S). File reference: ^{1}H-NMR: 500_HA_exp 4 B.^{13}C-NMR: 500_HA_ exp 4B C13F).

Synthesis of (Z)-5-(furan-2-ylmethylene)-2-thioxoimidazolidin-4-one (7)

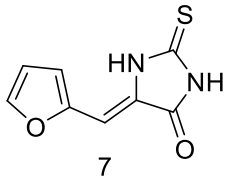

7

Utilising method **1**, thiohydantoin (2.0 g, 17.2 mmol), triethylamine (5.7 ml, 40.9 mmol) and furan-2-carbaldehyde (1.8 ml, 21.7 mmol) were added to 25 ml of water.

Yield= 92.9 %, M.p. 223-225 °C, HRMS calculated for $C_8H_6N_2O_2S$ m/z $[M+H]^+$ 194.0150; found 194.0150; ^{1}H-NMR (400 MHz DMSO): δ 7.85 (d, *J* = 1.5 Hz, 1H, C**H**O), δ 7.12 (d, *J*= 3.51 Hz, 1H, C**H**CO), δ 6.76 (dd, *J* = 3.5, 1.8 Hz, 1H, C**H**CHO), δ 6.76 (s, 1H, C**H**=C). ^{13}C-NMR (101 MHz, d$_6$-DMSO): δ 178.4 (**C**=S), δ 165.7 (**C**O), δ 149.2 (CH**C**O), δ 146.2 (**C**=CH), δ 125.8 (CH**C**HO), δ 115.9 (**C**HCHO), δ 113.6 (**C**HCO), δ 99.4 (**C**H=). IR (neat):

vmax=1722 cm^{-1} (C=O), 1651 cm^{-1} (C=C), 1592 cm^{-1} (C=S). File reference: ^{1}H-NMR: 400_HA_exp 5A_DF.^{13}C-NMR: 400_hiwa-5-furT-7777).

Synthesis of (Z)-5-(4-methoxybenzylidene)-2-thioxoimidazolidin-4-one (8)

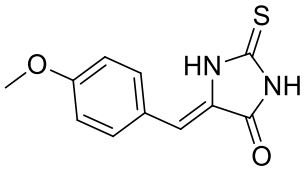

8

Utilising method **1**, thiohydantoin (2.0 g, 17.2 mmol), triethylamine (6.0 ml, 43.0 mmol), and 4-methoxybenzaldehyde (2.6 ml, 21.3 mmol) were added to 25 ml of water.

Yield= 52.73 %, M.p. 267- 269 °C, HRMS calculated for $C_{11}H_{10}N_2O_2S$ m/z $[M+H]^+$ 234.0463; found 234.0467; ^{1}H-NMR (400 MHz, DMSO): δ 7.73 (2 x C**H**, d, *J* = 8.7 Hz, 2H, C**H**COC**H**, δ 6.99 (2x C**H**, d, *J* = 8.7 Hz, 2H, C**H**CC**H**), δ 6.47 (s, 1H, C**H=**C**),** δ 3.81 (s, 3H, C**H$_3$)** .^{13}C-NMR (101 MHz, d_6-DMSO): δ 179.1 (**C**=S), δ 165.9 (**C**O), δ 160.7 (H_3C**C**O), δ 132.2 (2xC, **C**HCO**C**H), δ 125.9 (**C**=CH), δ 124.9 (CH**C**CH), δ 114.4 (**C**HC**C**H), δ 112.2 (**C**H=C), δ 55.4 (O**C**H_3). IR (neat): vmax=1723 cm^{-1} (C=O), 1645 cm^{-1} (C=C), 1596 cm^{-1} (C=S). File reference: NMR: 400_hiwa-anis-BT-999).

Synthesis of 5-(4-methoxybenzyl)-2-thioxoimidazolidin-4-one (9)

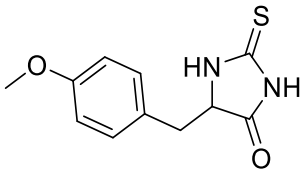

9

Utilising method **4**, (Z)-5-(4-methoxybenzylidene)-2-thioxoimidazolidin-4-one (1.5 g, 6.4 mmol) was dissolved in 50 ml of methanol, and acetic acid (23 ml, 401.8 mmol) and Zn dust (1.0 g, 15.3 mmol) were added.

Yield= 37.7%, M.p. 192-194 °C, HRMS calculated for $C_{11}H_{12}N_2O_2S$ m/z [M+H]+ 236.0619; found 236.0617;^{1}H-NMR (400 MHz DMSO): δ 11.43 (s, 1H, N**H**), δ 10.07 (s, 1H, N**H**), δ 7.086 (2x C**H**, d, *J* = 8.8 Hz, 2H, C**H**COC**H**), δ 6.82 (2 x C**H**, d, *J* = 8.5 Hz, 2H, C**H**CC**H**), δ 4.49 (apparent t, *J* = 4.6 Hz, 1H, C**H**CH_2C), δ 3.60 (s, 3H, OC**H**$_3$), δ 2.92 (d, *J* = 4.7 Hz, 2H, C$\mathbf{H}_A$C$\mathbf{H}_B$CH). ^{13}C-NMR (101 MHz, d_6-DMSO): δ 182.7 (**C**=S), δ 176.3 (**C**O), δ 158.4 (H_3C**C**O), δ 131.3 (2 x **C**HCO), δ 127.1 (**C**CH_2CH), δ 113.9 (2 x **C**HC), δ 62.0 (**C**HCH_2), δ 55.5 (O**C**H_3), δ 34.8 (CH**C**H_2). IR (neat): vmax=1727 cm^{-1} (C=O), 1523 cm^{-1} (C=S). File reference: ^{1}H-NMR: 400_HA_exp 6B DFA1.^{13}C-NMR: 400_hiwa-5-anis-BT-101010).

Synthesis of (Z)-5-((tetrahydrofuran-3-yl) methylene)-2-thioxoimidazolidin-4-one (10)

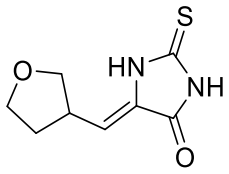

10

Utilising method **1**, thiohydantoin (3.0 g, 25.9 mmol), triethylamine (5.5 ml, 39.5 mmol) and tetrahydrofuran-3-carbaldehyde (4.0 ml, 42.4 mmol) were added to 25 ml of water.

Yield= 39.1%, M.p. 223-225 °C, HRMS calculated for $C_8H_{10}N_2O_2S$ m/z $[M+H]^+$ 198.0463; found 198.0466;^{1}H-NMR (400 MHz DMSO): δ 5.61 (d, *J* = 10.2 Hz, 1H, C**H**=), δ 3.86 - 3.79 (m, 2H, CHC$\mathbf{H}_A$$H_B$O + CH_2C$\mathbf{H}_A$$H_B$O), δ 3.72 (dd, *J* = 14.9, 7.6 Hz, 1H, C**H**C$H_A$$H_B$O), δ 3.41-3.26 (m, 2H, CHC$H_A$$\mathbf{H}_B$O+$CH_2CH_A$$\mathbf{H}_B$O), δ 2.16-2.08 (m, 1H, CHC$\mathbf{H}_A$$H_B$$CH_2$), δ 1.77 (m, 1H, CHC$H_A$$\mathbf{H}_B$$CH_2$). ^{13}C-NMR (101 MHz, d_6-DMSO): δ 178.6 (**C**=S), δ 164.7 (**C**O), δ 131.5 (**C**=CH), δ 116.9 (**C**H=C), δ 72.2 (**C**H_2O), δ 67.8 (**C**H_2O), δ 37.2 (**C**H_2CH), δ 32.9 (CH_2**C**H). IR (neat): vmax = 1725cm^{-1} (C=O), 1672 cm^{-1} (C=C), 1534 cm^{-1} (C=S). File reference: ^{1}H-NMR: 400_hiwa-5-hydro-fur-yl-2-thiohydamntoin.^{13}C-NMR: 400_hiwa-hydro-f-111111).

Synthesis of 5-((tetrahydrofuran-3-yl) methyl)-2-thioxoimidazolidin-4-one (11)

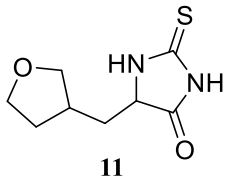

11

Utilising method **4**, (Z)-5-((tetrahydrofuran-3-yl)methylene)-2-thioxoimidazolidin-4-one (2.0 g, 10.0 mmol) was dissolved in 50 ml methanol, and acetic acid (10 ml, 174.6 mmol) and zinc dust (1.0 g, 15.3 mmol) were added.

Yield= 24.8 %, M.p. 166-168 °C, HRMS calculated for $C_8H_{12}N_2O_2S$ m/z $[M+H]^+$ 200.0619; found 200.0621; ^{1}H-NMR (400 MHz, DMSO-d_6): δ 11.74 (s, 2x1H, N**H**), δ 10.11, 10.07 (2 x s, 2 x 1H, N**H**), δ 4.26-4.21 (m, 2 x 1H, COC**H**CH_2), δ 3.77- 3.67 (m, 2 x 2H, CHC**H**$_A$H$_B$O + CH_2C**H**$_A$H$_B$O), δ 3.63-3.57 (m, 2 x 1H, CH_2CH_A**H**$_B$O), δ 3.25 (t, *J* = 7.8 Hz) and 3.18 (t, *J* = 7.8 Hz) ($CHCH_A$**H**$_B$O), δ 2.30-2.20 (m, 2 x 1H, CH_2C**H**CH_2O), δ 2.01-1.94 (m, 2 x 1H, CH_2C**H**$_A$H$_B$CH), δ 1.74-1.63 (m, 2 x 2H, CHC**H**$_A$**H**$_B$CH), δ 1.52-1.41 (m, 2 x 1H, CH_2CH_A**H**$_B$CH).^{13}C-NMR (126 MHz, d_6-DMSO): δ 182.2 (2 x **C**=S), δ 176.3, 176.2 (2 x **C**O), δ 72.0, 71.7 (2 x O**C**H_2CH), δ 66.7, 66.5 (O**C**H_2CH_2), δ 59.7 (br, 2 x CO**C**HCH_2), δ 34.8, 34.7 (2 x CH_2**C**HCH_2), δ 33.8, 33.6 (2 x CH**C**H_2CH), δ 31.9, 31.2 (2 x CH_2**C**H_2CH). R_f = 1.5 (ethyl acetate: dichloromethane 2:1); FTIR vmax = 1747 cm^{-1} (C=O), 1531 cm^{-1} (C=S). File reference: ^{1}H-NMR: 400_HA_exp 14 DFA.^{13}C-NMR: 500_hiwa 5 THf M 2 thiohydantoin 500).

Synthesis (Z)-5-benzylidenethiazolidine-2, 4-dione (12)

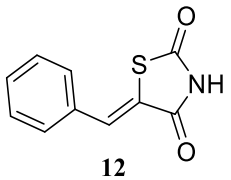

12

Utilising method **2**, benzaldehyde (0.95 ml, 9.35 mmol) and thiazolidine-2, 4-dione (1.0 g, 8.53 mmol) were together suspended in ethanol (20 ml). Piperidine (0.2 ml, 2.02 mmol) was then added.

Yield= 74.5 %, M.p. 195-197°C, HRMS calculated for $C_{10}H_7NO_2S$ m/z $[EI]^+$ 205.0198; found 2045.0196; ^{1}H-NMR (500 MHz DMSO): δ 7.79 (s, 1H, **H**C=C**)**, δ 7.60 (d, *J* = 7.5 Hz, 2H, C**H**CC**H**), δ 7.53 (t, *J* = 7.5 Hz, 2H, C**H**CHC**H**), δ 7.48 (t, *J* = 7.1 Hz, 1H, CHC**H**CH).^{13}C-NMR (126 MHz, d_6-DMSO): δ 167.8 (S**C**=O), δ 167.3 (C**C**O), δ 133.0 (C=**C**H), δ 133.0 (C=CH**C**), δ 130.4 (**C**H), δ 130.0 (2 x **C**H), δ 127.0 (2 x **C**H), δ 129.3 (CH=**C**). IR (neat): vmax=1750 cm^{-1} (C=O), 1700 cm^{-1} (C=O), 1608 cm^{-1} (C=C). File reference: NMR: 500_EXP1 BT_DOBbond).

Synthesis 5-benzylthiazolidine-2,4-dione (13)

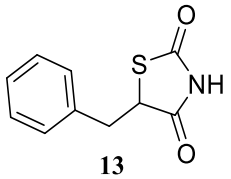

13

Utilising method **3**, (Z)-5-benzylidinethiazolidine-2, 4-dione (0.65 g, 3.17 mmol) was dissolved in the mixture of 10 ml of pyridine and 10 ml of anhydrous tetrahydrofuran (THF) at room temperature. Lithium borohydride (0.154 g, 6.98 mmol) was slowly added to a stirred solution.

Yield= 55.0 %, M.p. 98-100 °C, HRMS calculated for $C_{10}H_9NO_2S$ m/z $[EI]^+$ 207.0354; found 207.0353; ^{1}H NMR (400 MHz, $CDCl_3$); δ 7.26 – 7.11 (m, 5H, phenyl), δ 4.43 (dd, *J* = 9.9, 3.9 Hz, 1H, C**H**), δ 3.44 (dd, *J* = 14.0, 3.8 Hz, 1H, CHC$\mathbf{H}_A$CH_B), δ 3.03 (dd, *J* = 14.0, 9.9 Hz, 1H, CHCH_AC$\mathbf{H}_B$).^{13}C NMR (101 MHz, $CDCl_3$), δ 172.9 (**C**O), δ 169.2 (**C**O), δ 134.7 (**C**), δ 128.1 (2 X **C**), δ 127.9 (2 x **C**), δ 126.7 (**C**H), δ 52.4 (**C**HCH_2), δ 37.6 (CH**C**H_2). IR (neat): IR (neat): vmax=1745 cm^{-1} (C=O), 1682 cm^{-1} (C=O). File reference: ^{1}H-NMR: 400_BT1.^{13}C-NMR: 400_BT c13).

Synthesis (Z)-5-(pyridin-2-ylmethylene) thiazolidine-2,4-dione (14)

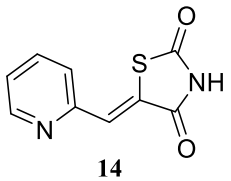

14

Utilising method **2**, 2-pyridine carboxaldehyde (1.9 ml, 19.97 mmol) and thiazolidine-2, 4-dione (2.0 g, 17.07 mmol) were together suspended in ethanol (40ml). Piperidine (0.3 ml, 3.03 mmol) was added to the mixture.

Yield= 64.0 %, M.p. 258-260 °C, HRMS calculated for $C_9H_6N_2O_2S$ m/z $[EI]^+$ 206.0150; found 206.0155; ^{1}H-NMR (500 MHz DMSO): δ 8.76 (d, *J* = 4.4 Hz, 1H, C**H**N), δ 7.94 (td, *J* = 7.7, 1.8 Hz, 1H, C**H**CHCHN), δ 7.85 (d, *J* = 7.8 Hz, 1H, C**H**CN), δ 7.82 (s, 1H, C**H**=), δ 7.42 (ddd, *J* = 7.6, 4.8, 1.1 Hz, 1H, C**H**CHN).^{13}C-NMR (126 MHz, d_6-DMSO): δ 171.9 (**C**O), δ 167.4 (**C**O), δ 151.3 (**C**N), δ 149.3 (**C**HN), δ 137.5 (C=**C**H), δ 128.0 (**C**HCHCN), δ 27.8 (**C**HCN), δ 127.7 (**C**HCHN), δ 123.9 (**C**H=C). IR (neat): vmax = 1740 cm^{-1} (C=O), 1680 cm^{-1} (C=O), 1620 cm^{-1} (C=C). File reference: ^{1}H-NMR: 500_HA exp108pythi.^{13}C-NMR: 500_HA-exp 106 C13).

Synthesis 5-(pyridin-2-ylmethyl) thiazolidine-2,4-dione (15)

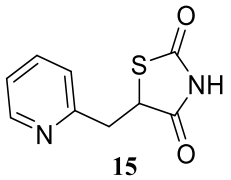

15

Utilising method **4**, (Z)-5-(pyridin-2-ylmethylene) thiazolidine-2, 4-dione (1.25 g, 60.07 mmol) was dissolved in 50 ml of acetic acid under nitrogen atmosphere. Zinc dust (1.5 g, 22.94 mmol) was added to the mixture at 130 ˚C.

Yield= 72.1 %, M.p. 98-100 °C, HRMS calculated for $C_9H_8N_2O_2S$ m/z $[EI]^+$ 208.0306; found 208.0309; ^{1}H-NMR (500 MHz DMSO): δ 12.10 (s, 1H, N**H**), δ 8.54 (d, *J* = 4.2 Hz, 1H, C**H**N), δ 7.81 (td, *J* = 7.7, 1.8 Hz, 1H, C**H**CHCHN), δ 7.39 (d, *J* = 7.8 Hz, 1H, C**H**CN), δ 7.33 (dd, *J* = 7.1, 5.2 Hz, 1H, C**H**CHN), δ 4.99 (dd, *J* = 10.1, 3.9 Hz, 1H, CH), δ 3.69 (dd, *J* = 16.0, 3.9 Hz, 1H, CHC**H**$_A$CH$_B$), δ 3.44 (dd, *J* = 16.0, 10.1 Hz, 1H, CHCH$_A$C**H**$_B$).^{13}C-NMR (126 MHz, d_6-DMSO): δ 176.5 (**C**O), δ 172.8 (**C**O), δ 156.7 (**C**N), δ 148.8 (**C**HN), δ 136.7 (**C**HCHCN), δ 123.6 (**C**HCN), δ 122.0 (**C**HCHN), δ 49.7 (**C**HCH$_2$), δ 21.1 (CH**C**H$_2$). IR (neat): vmax = 3010 cm^{-1} (NH), 1689 cm^{-1} (C=O), 1668 cm^{-1} (C=O). File reference: ^{1}H-NMR: 500_ha-EXP 108 hmbc.^{13}C-NMR: 500_HA_exp 108 CH2).

Synthesis (Z)-5-benzylidene-2-thioxothiazolidin-4-one (16)

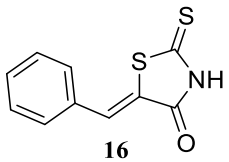

16

Utilising method **2**, benzaldehyde (3.82 ml, 37.61 mmol) and 2-thioxothiazolidin-4-one (5.0 g, 37.60 mmol) were suspended in ethanol (100 ml). Piperidine (1.0 ml, 10.12 mmol) was added to the mixture.

Yield= 90.0 %, Mp: 190-192°C, HRMS calculated for $C_{10}H_7NOS_2$ m/z [EI]+ 220.9969; found 220.9969; ^{1}H-NMR (500 MHz, DMSO): δ 7.64 (s, 1H, **H**C=C**)**, δ 7.61-7.48 (m, 5H, phenyl). ^{13}C-NMR (126 MHz, d_6-DMSO): δ 195.6 (**C**=S), δ 169.4 (**C**O), δ 132.9 (C=**C**H), δ 131.6 (C=CH**C**), δ 130.7 (**C**H), δ 130.4 (2 x **C**H), δ 129.4 (2 x **C**H), δ 125.5 (CH=**C**). IR (neat): vmax = 1699 cm^{-1} (C=O), 1660 cm^{-1} (C=S), 1587 cm^{-1} (C=C). File reference: NMR: 500_ EXP1 BR_DOUBLEBOND).

Synthesis 5-benzyl-2-thioxothiazolidin-4-one (17)

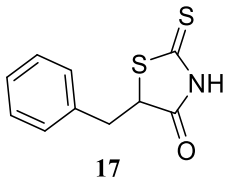

17

Utilising method **4**, (Z)-5-benzylidene-2-thioxothiazolidin-4-one (0.5 g, 2.22 mmol) was dissolved in 50 ml of acetic acid under nitrogen atmosphere. Zinc dust (1.5 g, 22.94 mmol) was added to the mixture at 130 ˚C.

Yield= 60.0 %, HRMS calculated for $C_{10}H_9NOS_2$ m/z $[ES]^-$ 222.0047; found 222.0043; ^{1}H NMR (400 MHz, $CDCl_3$); δ 7.30-7.14 (m, 5H, phenyl), δ 4.54 (dd, *J* = 10.1, 4.0 Hz, 1H, C**H**), δ 3.48 (dd, *J* = 14.1, 4.0 Hz, 1H, CHC**H**$_A$CH$_B$), δ 3.09 (dd, *J* = 14.1, 10.1 Hz, 1H, CHCH$_A$C**H**$_B$).^{13}C NMR (101 MHz, $CDCl_3$): δ 199.2 (**C**S), δ 175.7 (**C**O), δ 134.6 (**C**), δ 128.0 (2 X **C**), δ 128.2 (2 x **C**), δ 126.8 (**C**H), δ 55.7 (**C**HCH$_2$), δ 37.3 (CH**C**H$_2$). IR (neat): vmax = 1745 cm^{-1} (C=O), 1682 cm^{-1} (C=S). File reference: NMR: 400_HA_benzylrhodanine_ZN).

Synthesis (Z)-5-(pyridin-2-ylmethylene)-2-thioxothiazolidin-4-one (18)

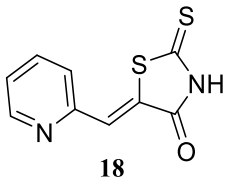

18

Utilising method **2**, 2-pyridinecarboxaldehyde (1.5 ml, 15.76 mmol) and 2-thioxothiazolidin-4-one (2.0 g, 15.04 mmol) were together suspended in ethanol (60 ml). Piperidine (0.2 ml, 2.02 mmol) was added to the mixture.

Yield= 85.0 %, M.p. 258-261 °C, HRMS calculated for $C_9H_6N_2OS_2$ m/z $[MS\ EI]^+$ 221.9922; found 221.9920; ^{1}H-NMR (500 MHz, DMSO): δ 13.68 (s, 1H, N**H**), δ 8.78 (d, *J* = 4.6 Hz, 1H, C**H**N), δ 7.94 (td, *J* = 7.6, 1.7 Hz, 1H, C**H**CHCHN), δ 7.88 (d, *J* = 7.8 Hz, 1H, C**H**CN), δ

7.66 (s, 1H, C**H**=), δ 7.43 (ddd, *J* = 7.5, 4.8, 1.2 Hz, 1H, C**H**CHN).^{13}C-NMR (126 MHz, d_6-DMSO): δ 201.9 (**C**S), δ 169.3 (**C**O), δ 151.0 (**C**N), δ 149.5 (**C**HN), δ 137.6 (C=**C**H), δ 129.7 (**C**HCHCN), δ 128.1 (**C**HCN), δ 127.4 (**C**HCHN), δ 124.0 (**C**H=C). IR (neat): vmax = 1720 cm^{-1} (C=O), 1610 cm^{-1} (C=S), 1579 cm^{-1} (C=C). NMR: 500_EXP1 PYR_DouBond)

Synthesis 5-(pyridin-2-ylmethyl)-2-thioxothiazolidin-4-one (19)

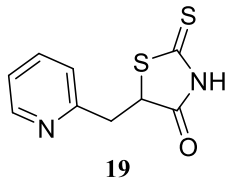

19

Utilising method **4**, (Z)-5-(pyridin-2-ylmethylene)-2-thioxothiazolidin-4-one (0.5 g, 2.25 mmol) was dissolved in 50 ml of acetic acid under nitrogen atmosphere. Zinc dust (0.8 g, 12.23 mmol) was added to the mixture at 130 ˚C.

Yield= 68.0 %, M.p. 100-102 °C, HRMS calculated for $C_9H_8N_2OS_2$ m/z [MS ES]$^-$ 223.0002; found 223.0000; ^{1}H-NMR (500 MHz $CDCl_3$): δ 8.46 (dd, *J* = 5.7, 1.5 Hz, 1H, C**H**N), δ 7.58 (tt, *J* = 4.5, 2.3 Hz, 1H, C**H**CHCHN), δ 7.13 (dd, *J* = 7.6, 4.5 Hz, 2H, C**H**CN + C**H**CHN), δ 4.85 (dd, *J* = 10.5, 3.9 Hz, 1H, CH), δ 3.73 (dd, *J* = 16.1, 3.9 Hz, 1H, CHC$\mathbf{H}_A$CH_B), δ 3.38 (dd, *J* = 16.1, 10.5 Hz, 1H, CHCH_AC$\mathbf{H}_B$).^{13}C-NMR (126 MHz, d_6-DMSO): δ 205.0 (**C**S), δ 178.6 (**C**O), δ 156.4 (**C**N), δ 148.7 (**C**HN), δ 136.8 (**C**HCHCN), δ 123.5 (**C**HCN), δ 122.2 (**C**HCHN), δ 52.5 (**C**HCH_2), δ 38.2 (CH**C**H_2). IR (neat): vmax = 1699 cm^{-1} (C=O), 1593 cm^{-1} (C=S). File reference: ^{1}H-NMR: 500_HA_IBRpyrrhod.^{13}C-NMR: 500_HA_IBRpyrrhod_DMSO).

Synthesis of 5-methyl-2-thioxoimidazolidin-4-one (20)

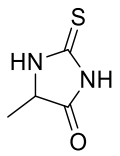

20

Utilising method **6**, 1:3 L-alanine (1.0 g, 11.22 mmol) and thiourea (2.56 g, 33.67 mmol) were mixed together and heated under stirring.

Yield= 30.0%, M.p. 138-140 °C, HRMS calculated for $C_4H_6N_2OS$ m/z $[EI]^+$ 130.0201; found 130.0199; ^{1}H-NMR (400 MHz DMSO): δ 10.02 (s, 1H, N**H**), δ 4.24 (q, *J* = 7.0 Hz, 1H, C**H**), δ 1.24 (d, *J* = 7.0 Hz, 3H,C**H**$_3$). ^{13}C-NMR (101 MHz, d_6-DMSO): δ 182.5 (**C**=S), δ 177.9 (**C**O), δ 56.8 (**C**HCH$_3$), δ 16.27 (CH**C**H$_3$). IR (neat): vmax = 1740 cm^{-1} (C=O), 1544 cm^{-1} (C=S). (File reference: ^{1}H-NMR: 400_HA-exp 42_16-9 long.^{13}C-NMR: 400_ha_EXP 42 _12_9).

Synthesis of 5-isopropyl-2-thioxoimidazolidin-4-one (21)

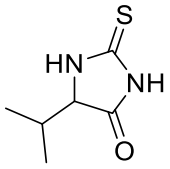

21

Utilising method **6**, 1:3 L-valine (1.0 g, 8.53 mmol) and thiourea (1.95 g, 25.60 mmol) were mixed together and heated under stirring.

Yield= 14.0 %, M.p. 122-123 °C, HRMS calculated for $C_6H_{10}N_2OS$m/z $[EI]^+$ 158.0507; found 158.0514; ^{1}H-NMR (400 MHz DMSO): δ 11.76 (s, 1H, N**H**), δ 10.07 (s, 1H, N**H**), δ 4.12 (dd, *J* = 3.6, 1.1 Hz, 1H, C**H**), δ 2.10 (m, 1H, H$_3$CC**H**CH$_3$), δ 0.96 (d, *J* = 7.0 Hz, 3H, C**H**$_3$), δ 0.81 (d, *J* = 6.8 Hz, 3H,C**H**$_3$).^{13}C-NMR (101 MHz, d_6-DMSO): δ 183.3 (**C**=S), δ 176.3 (**C**=O), δ

66.0 (NH**C**HCH), δ 30.4 (H_3C**C**HCH_3), δ 18.4 (H_3**C**$CHCH_3$), δ 16.6 (H_3CCH**C**H_3). IR (neat): vmax=1723 cm^{-1} (C=O), 1524 cm^{-1} (C=S). (File reference: NMR: 400_EXp52FD)

Synthesis of 5-((1H-indol-3-yl) methyl)-2-thioxoimidazolidin-4-one (22)

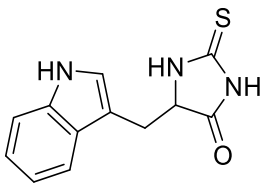

22

Utilising method **6**, L-tryptophan (1.0 g, 4.89 mmol) and thiourea (1.11 g, 14.58 mmol) were mixed together and heated under stirring.

Yield= 26.7 %, M.p. 112-113°C, HRMS calculated for $C_{12}H_{11}N_3OSm/z$ $[ES]^-$ 244.05465; found 244.0540; ^{1}H-NMR (400 MHz DMSO): δ 11.28 (s, 1H, N**H**), δ 10.93 (s, 1H, HCN**H**), δ 10.08 (s, 1H, N**H**), δ 7.54 (d, *J* = 7.9 Hz, 1H, C**H**CC), δ 7.32 (d, *J* = 8.1 Hz, 1H, C**H**CNH), δ 7.10 (d, *J* = 2.4 Hz, 1H, C**H**N), δ 7.05 (t, *J* = 7.0 Hz, 1H, C**H**CHCNH), δ 6.97 (t, *J* = 6.9 Hz, 1H, C**H**CHCC), δ 4.53 (apparent t, *J* = 4.7 Hz, 1H,C**H**CH_2), δ 3.12 (qd, *J* = 15.1, 4.7 Hz, 2H, C$\mathbf{H}_A$C$\mathbf{H}_B$CH).^{13}C-NMR (101 MHz, d_6-DMSO): δ 182.4 (**C**=S), δ 176.3 (**C**O), δ 135.6 (**C**NH), δ 127.6 (**C**CNH), δ 124.0 (**C**HNH), δ 121.0 (**C**HCHCNH), δ 118.5 (**C**HCHCC), δ 111.3 (**C**HCC), δ 109.4 (**C**HCNH), δ 107.4 (**C**CHNH), δ 61.8 (**C**HCH_2), δ 27.4 (CH**C**H_2). IR (neat): vmax = 1744 cm^{-1} (C=O), 1524 cm^{-1} (C=S). (File reference: ^{1}H-NMR: 400_ha_EXP 54df2.^{13}C-NMR: 400_HA_exp 54).

Synthesis of 3-thioxohexahydro-1H-pyrrolo [1, 2-c] imidazol-1-one (23)

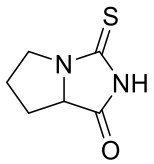

23

Utilising method **6**, 1:3 L-proline (1.4 g, 12.16 mmol) and thiourea (2.8 g, 36.48 mmol) were mixed together and heated under stirring.

Yield = 42.2 %, M.p. 133-135 °C, HRMS calculated for $C_6H_8N_2OS$ m/z [MS EI]$^+$ 156.0357; found 156.0361, ^{1}H-NMR (500 MHz DMSO): δ 4.39 (dd, *J* = 10.01, 6.3 Hz, 1H, NC**H**CH_2), δ 3.74-3.65 (m, 1H, C**H**$_A$N), δ 3.43 (ddd, *J* = 11.4, 8.2, 2.9 Hz, 1H, C**H**$_B$N), δ 2.18-2.02 (m, 3H, C**H**$_A$C**H**$_B$$CH_2$N + C**H**$_A$$CH_B$CH), δ 1.72-1.57 (m, 1H, CH_AC**H**$_B$CH).^{13}C-NMR (126 MHz, d_6-DMSO): δ 186.30 (**C**=S), δ 175.58 (**C**O), δ 66.55 (N**C**HCH_2), δ 47.59 (**C**H_2N), δ 27.02 (**C**H_2CH_2N), δ 26.16 (**C**H_2CHN). IR (neat): vmax = 1750 cm^{-1} (C=O), 1554 cm^{-1} (C=S). (File reference: NMR: 500_hiwa_proline 2thio last).

Synthesis of 5-(2-(methylthio) ethyl)-2-thioxoimidazolidin-4-one (24)

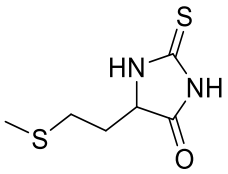

24

Utilising method **6**, 1:3 L-methionine (1.4 g, 12.16 mmol) and thiourea (2.8 g, 36.48 mmol) were mixed together and heated under stirring.

Yield= 25.0 %, M.p. 81-82°C, HRMS calculated for $C_6H_{10}N_2OS_2$ m/z [MS EI]$^+$ 190.0235; found 190.02235;^{1}H-NMR (500 MHz DMSO): δ 11.70 (s, 1H, N**H**), δ 10.80 (s, 1H, N**H**), δ 4.30 (dd, *J* = 7.5, 4.9 Hz, 1H,C**H**CH_2), δ 2.56 – 2.52 (m, 2H, C**H**$_2$S), δ 2.03 (s, 3H, C**H**$_3$S), δ

1.99 (m, 1H, C**H**$_A$CH$_B$CH), δ 1.96 (m, 1H, CH$_A$C**H**$_B$CH).^{13}C-NMR (126 MHz, d$_6$-DMSO): δ 183.0 (**C**=S), δ 176.4 (**C**O), δ 59.5 (**C**HCH$_2$), δ 30.2 (**C**H$_2$CH$_2$S), δ 28.5 (CH$_2$**C**H$_2$S), δ 14.40 (S**C**H$_3$). IR (neat): vmax= 1738 cm^{-1} (C=O), 1541 cm^{-1} (C=S). (File reference: NMR: 500_HA_exp 58 _C13).

Synthesis of 5-((1H-imidazol-4-yl) methyl)-2-thioxoimidazolidin-4-one (25)

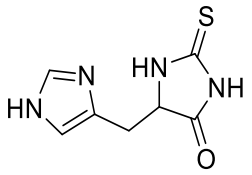

25

Utilising method **6**, D-histidine (0.5 g, 3.22 mmol) and thiourea (1.0 g, 13.13 mmol) were mixed together and heated under stirring.

Yield= 16.0 %, HRMS calculated for $C_7H_8N_4OS$ m/z [MS EI]$^+$ 196.0419; found 196.0413; ^{1}H-NMR (500 MHz DMSO): δ 11.57 (s, 1H, SCN**H**), δ 9.92 (s, 1H, HCN**H**), δ 7.71 (s, 1H, NHC**H**N), δ 6.87 (s, 1H, NHC**H**C), δ 4.45 (apparent t, *J* = 5.5 Hz, 1H, C**H**CH$_2$C), δ 2.98 (dd, *J* = 15.2, 5.0, 1H, CHC**H**$_A$ CH$_B$C), δ 2.89 (dd, *J* = 15.2, 6.0, 1H, CHCH$_A$ C**H**$_B$C). ^{13}C-NMR (126 MHz, d$_6$-DMSO): δ 182.8 (**C**=S), δ 176.2 (**C**O), δ 134.8 (NH**C**HN), δ 131.5 (CHCH$_2$**C**), δ 116.3 (NH**C**HC), δ 60.6 (**C**HCH$_2$C), δ 28.20 (CH**C**H$_2$C). (File reference: ^{1}H-NMR: 500_hiwa histidin dilute_2.^{13}C-NMR: 500_hiwa_histidin 2 thio 0005).

Synthesis of 1-acetyl-2-thioxoimidazolidin-4-one (26)

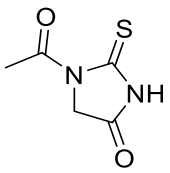

26

Utilising method **5a**, glycine (1.0 g, 13.3 mmol) and NH_4SCN (1.038 g, 13.3 mmol) were ground together. A mixture of 9 ml acetic anhydride and 1 ml of acetic acid was added.

Yield= 73.28 %, M.p. 170-172°C, HRMS calculated for $C_5H_6N_2O_2S$ m/z [MS EI]$^+$ 158.0150; found 158.0150; ^{1}H-NMR (400 MHz DMSO): δ 4.40 (s, 2H, C**H**$_2$), δ 2.68 (s, 3H, C**H**$_3$). ^{13}C-NMR (101 MHz, d$_6$-DMSO): δ 181.9 (**C**=S), δ 170.0 (**C**O), δ 168.9 (H$_3$C**C**O), δ 51.7 (**C**H$_2$), δ 26.1 (H$_3$**C**CO). IR (neat): vmax = 1755 cm^{-1}, 1661 cm^{-1} (C=O), 1645 cm^{-1} (C=S). (File reference: NMR: 400_HA_exp 16 DFA).

Synthesis of (S)-1-acetyl-5-benzyl-2-thioxoimidazolidin-4-one (27)

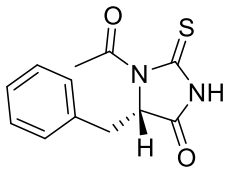

27

Utilising method **5b**, L-phenyl alanine (1.0 g, 6.0 mmol) and NH_4SCN (1.0 g, 13.2 mmol) were ground together. A mixture of 4.5 ml of acetic anhydride and 0.5 ml of acetic acid was added.

Yield= 35.9 %, M.p. 124-125 °C, $[\alpha]_D^{20}$ = +94.5° (0.25 g/l00 ml in acetonitrile), HRMS calculated for $C_{12}H_{12}N_2O_2S$ m/z [M+H]+ 248.0619; found 248.0624; ^{1}H-NMR (500 MHz DMSO): δ 7.30-7.23 (m, 3H, phen), δ 6.99 - 6.97 (m, 2H, phen), δ 4.99 (dd, *J* = 5.9, 2.57 Hz, 1H, C**H**), δ 3.41-3.37 (dd, *J* = 13.9, 5.8 Hz, 1H, C**H**$_A$CH$_B$CH), δ 3.14-3.11 (dd, *J* = 13.9, 2.57 Hz, 1H, CH$_A$C**H$_B$**CH), δ 2.69 (s, 1H, C**H**$_3$).^{13}C-NMR (126 MHz, d$_6$-DMSO): δ 182.1 (**C**=S), δ 172.3 (**C**O), δ 169.8 (H$_3$C**C**O), δ 134.2 (**C**CH$_2$), δ 129.0 (2X**C**HCH), δ 128.2 (2 x **C**HC), δ 127.05 (**C**H), δ 63.30 (**C**HCH$_2$), δ 34.3 (CH**C**H$_2$), δ 27.0 (H$_3$**C**CO). IR (neat): vmax = 1761 cm^{-1}, 1699 cm^{-1} (C=O), 1456 cm^{-1} (C=S). (File reference: ^{1}H-NMR: 500_hiwa_acetyl_5_benzyl_2_thiohydantoin. ^{13}C-NMR: 500_hiwa_acetyl_5BT1001).

Synthesis of (S)-1-acetyl-5-phenyl-2-thioxoimidazolidin-4-one (28)

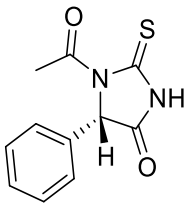

28

Utilising method **5b**, L-phenyl glycine (1.0 g, 6.0 mmol) and NH_4SCN (1.0 g, 13.2 mmol) were ground together. A mixture of 4.5 ml of acetic anhydride and 0.5 ml of acetic acid was added.

Yield= 64.0%, $[\alpha]_D^{20}$ = +14.0° (0.43 g/l00 ml in methanol), HRMS calculated for $C_{11}H_{10}N_2O_2S$ m/z $[EI]^+$ 234.0463; found 234.0463; ^{1}H-NMR (400 MHz DMSO): δ 7.44-7.33 (m, 3H, phen), δ 7.26 (d, *J* = 7.3 Hz, 2H, phen), δ 5.71 (s, 1H, C**H**), δ 2.72 (s, 1H, C**H**$_3$). ^{13}C-NMR (101 MHz, d_6-DMSO): δ 183.0 (**C**=S), δ 171.7 (**C**O), δ 169.5 (H_3C**C**O), δ 134.8 (**C**CH), δ 129.3 (2 x **C**HCH), δ 128.8 (2 x **C**HC), δ 126.7 (**C**H), δ 66.4 (**C**HCH_2), δ 27.6 (H_3**C**CO). IR (neat): vmax = 1761 cm^{-1}, 1699 cm^{-1} (C=O), 1456 cm^{-1} (C=S). (File reference: ^{1}H-NMR: 400_HA_exp49 last in DMSO.^{13}C-NMR: 400_HA_exp 49).

Synthesis of (S)-1-acetyl-5-methyl-2-thioxoimidazolidin-4-one (29)

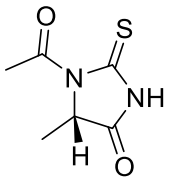

29

Utilising method **5b**, L-alanine (1.0 g, 11.2 mmol) and NH_4SCN (1.0 g, 13.2 mmol) were ground together. A mixture of 4.5 ml of acetic anhydride and 0.5 ml of acetic acid was added.

Yield= 14.6 %, M.p. 161-162 °C, $[\alpha]_D^{20}$ = +83.9° (0.29 g/l00 ml in acetonitrile), HRMS calculated for $C_6H_8N_2O_2S$ m/z [M+H] + 171.0228; found 171.0223, ^{1}H-NMR (500 MHz, d_6-

DMSO): δ 12.62 (s, 1H, N**H**), δ 4.69 (q, *J* = 6.8 Hz, 1H,C**H**CH_3), δ 2.72 (S, 1H, COC**H**$_3$), δ 1.44 (d, *J* = 6.9 Hz, 1H,CHC**H**$_3$).^{13}C-NMR (126 MHz, d_6-DMSO): δ 182.5 (**C**=S), δ 174.2 (**C**O), δ 169.7 (H_3C**C**O), δ 58.9 (**C**HCH_3), δ 27.3 (H_3**C**CO), δ 15.9 (CH**C**H_3). (File reference: ^{1}H-NMR: 500_HA_exp 46 DFD.^{13}C-NMR: 500_HA_exp 46 CDF3).

Synthesis of (S)-1-acetyl-5-isopropyl-2-thioxoimidazolidin-4-one (30)

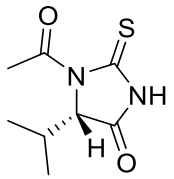

30

Utilising method **5b**, L-valine (1.0 g, 8.5 mmol) and NH_4SCN (1.0 g, 13.2 mmol) were ground together. A mixture of 4.5 ml of acetic anhydride and 0.5 ml of acetic acid was added.

Yield= 35.0%, M.p. 96-97°C, $[\alpha]_D^{20}$ = +116.8° (0.40 g/l00 ml in acetone), HRMS calculated for $C_8H_{12}N_2O_2S$ m/z [AP]$^-$ 199.0535; found 199.0541; ^{1}H-NMR (400 MHz, d_6-DMSO): δ 12.64 (s, 1H, NH), δ 4.57 (d, *J* = 3.4 Hz, 1H,C**H**), δ 2.71 (s, 3H, **H$_3$**CCO), δ 2.45-2.39 (m, 1H, H_3CC**H**CH_3), δ 1.08 (d, *J* = 7.1 Hz, 3H, C**H$_3$**), δ 0.75 (d, *J* = 6.9 Hz, 3H, C**H$_3$**).^{13}C-NMR (101 MHz, d_6-DMSO): δ 182.6 (**C**=S), δ 171.9 (**C**O), δ 169.5 (H_3C**C**O), δ 66.3 (**C**HCH_2), δ 28.7 (H_3C**C**HCH_3), δ 27.6 (H_3**C**CO), δ 17.2 (H_3**C**CHCH_3), δ 15.2 (H_3CCH**C**H_3). IR (neat): vmax = 1757 cm^{-1} (C=O), 1703 cm^{-1} (C=O), 1460 cm^{-1} (C=S). (File reference: NMR: 400_HA_exp 47 DFM).

Synthesis of 5-((1H-indol-3-yl) methyl)-1-acetyl-2-thioxoimidazolidin-4-one (31)

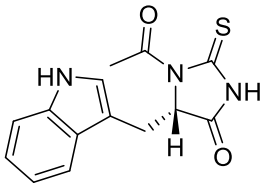

31

Utilising method **5b**, L-tryptophan (0.5 g, 2.4 mmol) and NH_4SCN (0.5 g, 6.6 mmol) were ground together. A mixture of 2250 µl of acetic anhydride and 250 µl of acetic acid was added.

Yield= 42.0 %, M.p. 153-154 °C, $[\alpha]_D^{20}$ = +94.5° (0.4 g/l00 ml in acetone), HRMS calculated for $C_{14}H_{13}N_3O_2S$ m/z $[ES]^-$ 286.0650; found 286.0640; ^{1}H-NMR (400 MHz, d_6-DMSO): δ 12.29 (s, 1H, N**H**), δ 10.95 (s,1H, HCN**H**), δ 7.35 (d, *J* = 7.9 Hz, 1H, C**H**CC), δ 7.31 (d, *J* = 8.1 Hz, 1H, C**H**CNH), δ 7.07-7.031 (t, *J* = 7.5 Hz, 1H, C**H**CHCNH), δ 6.98 (m, 2H, C**H**CHCC + C**H**NH), δ 4.99 (dd, *J* = 5.5, 2.6 Hz, 1H, C**H**CH_2), δ 3.57-3.52 (dd, *J* = 14.6, 5.6 Hz, 1H, C**H**$_A$CH_BCH), δ 3.29 (dd, *J* = 14.8, 3.8 Hz, 1H, CH_AC**H**$_B$CH), δ 2.68 (s, 3H, **H**$_3$CCO).^{13}C-NMR (101 MHz, d_6-DMSO): δ 181.3 (**C**=S), δ 171.8 (**C**O), δ 169.0 (H_3C**C**O), δ 134.6 (**C**NH), δ 126.0 (**C**CNH), δ 122.8 (**C**HNH), δ 120.0 (**C**HCHCNH), δ 117.5 (**C**HCHCC), δ 117.9 (**C**HCC), δ 110.2 (**C**HCNH), δ 104.9 (**C**CHNH), δ 63.6 (**C**HCH_2), δ 27.3 (CH**C**H_2), δ 24.6 (H_3**C**CO). IR (neat): vmax = 1750 cm^{-1} (C=O), 1688 cm^{-1} (C=O), 1456 cm^{-1} (C=S). (File reference: NMR: 400_HA_exp 53 DFM).

Synthesis of (*S*)-1-acetyl-5-((methylthio) methyl)-2-thioxoimidazolidin-4-one (32)

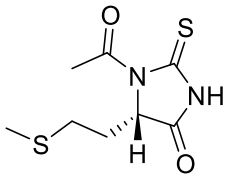

32

Utilising method **5b**, L-methionine (0.5 g, 3.4mmol) and NH_4SCN (0.5 g, 6.6 mmol) were ground together. A mixture of 2250 µl of acetic anhydride and 250 µl of acetic acid was added.

Yield= 38.0 %, M.p. 81-82°C, $[\alpha]_D^{20}$ = +118.6° (0.40 g/l00 ml in acetone), HRMS calculated for $C_8H_{12}N_2O_2S_2$ m/z [MS ES]$^-$ 231.0262; found 231.0266; ^{1}H-NMR (400 MHz, d_6-DMSO): δ 12.69 (s, 1H, N**H**), δ 4.76 (dd, *J* = 7.1, 3.2 Hz, 1H, C**H**CH_2), δ 2.68 (s, 3H, OCC**H$_3$**), δ 2.51 – 2.41 (m, 1H, overlapped with DMSO, C**H$_A$**CH_BS), δ 2.34 (m, 1H, CH_AC**H$_B$**S), δ 2.24 – 2.06 (m, 2H, C**H**$_2$CH), δ 1.96 (s, 3H, SC**H$_3$**).^{13}C-NMR (101MHz, d_6-DMSO): δ 183.3 (**C**=S), δ 173.5 (**C**O), δ 170.3 (H_3C**C**O), δ 61.8 (**C**HCH_2), δ 28.4 (**C**H_2S), δ 27.9 (CH_2**C**H_2CH), δ 27.81 (**C**H_3CO), δ 14.80 (S**C**H_3). IR (neat): vmax = 1761 cm^{-1} (C=O), 1704 cm^{-1} (C=O), 1446 cm^{-1} (C=S). (File reference: ^{1}H-NMR: 400_HA_exp 57 after CC_01.^{13}C-NMR: 400_HA_exp 57 DFCH).

Synthesis of 5-benzyl-3-phenyl-2-thioxoimidazolidin-4-one (33)

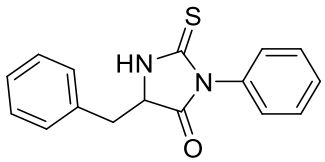

33

Utilising method **7**, to a mixture of L-phenyl alanine methyl ester hydrochloride salt (1.0 g, 4.35 mmol) and Et_3N (1.5 ml, 10.76 mmol) in 25 ml of CH_2Cl_2, phenylisothiocyanate (1.5 ml, 12.56 mmol) was slowly added.

Yield= 84.0 %, M.p. 178-179°C, HRMS calculated for $C_{16}H_{14}N_2OS$ m/z $[EI]^+$ 282.0827; found 282.0825; ^{1}H-NMR (500 MHz, d_6-DMSO): δ 10.62 (s, 1H, N**H**), δ 7.42-6.76 (m, 10H, phenyl), δ 4.78 (apparent t, *J* = 4.5, 1H, C**H**), δ 3.13 (d, *J* = 4.5 Hz, 2H, C$\mathbf{H}_A$C$\mathbf{H}_B$CH). ^{13}C-NMR (126 MHz, d_6-DMSO): δ 181.9 (**C**=S), δ 173.3 (**C**O), δ 134.0 (**C**N), δ 132.8 (**C**CH_2), δ 129.4 (2 x **C**H), δ 128.6 (2 x **C**H), δ 128.5 (**C**H), δ 128.0 (2 x **C**H), δ 127.7 (2 x **C**H), δ 126.6 (**C**HCHCHC), δ 59.7 (**C**HCH_2), δ 35.7 (CH**C**H_2). IR (neat): vmax = 1746 cm^{-1} (C=O), 1494 cm^{-1} (C=S). (File reference: NMR: 500_hiwa_5benz3phe2thio).

Synthesis of 5-isopropyl-3-phenyl-2-thioxoimidazolidin-4-one (34)

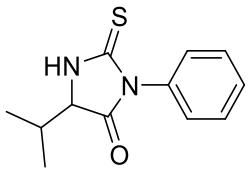

34

Utilising method **7**, to a mixture of L-valine methyl ester hydrochloride salt (1.0 g, 5.96 mmol) and Et_3N (1.5 ml, 10.76 mmol) in 25 ml of CH_2Cl_2, phenylisothiocyanate (1.5 ml, 12.56 mmol) was slowly added.

Yield= 90.5 %, M.p. 159-161 °C, HRMS calculated for $C_{12}H_{14}N_2OS$ m/z $[EI]^+$ 234.0827; found 234.0832; ^{1}H-NMR (400 MHz, d_6-DMSO): δ 10.59 (s, 1H, N**H**), δ 7.52-7.22 (m, 5H, phenyl), δ 4.33 (d, *J* = 3.6 Hz, 1H, C**H**), δ 2.19 (m, 1H, H_3CC**H**CH_3), δ 1.05 (d, *J* = 6.9 Hz, 3H, C$\mathbf{H_3}$), δ 0.92 (d, *J* = 6.6 Hz, 3H, C$\mathbf{H_3}$).^{13}C-NMR (126 MHz, d_6-DMSO): δ 182.6 (**C**=S), δ 173.4 (**C**O), δ 133.1 (**C**N), δ 129.6 (2 x **C**H), δ 128.5 (2 x **C**H), δ 129.1 (**C**H), δ 64.1 (**C**HCH_2), δ 30.3 (H_3C**C**HCH_3), δ 17.9 (H_3**C**CHCH_3), δ 15.9 (H_3CCH**C**H_3). IR (neat): vmax = 1756 cm^{-1} (C=O), 1514 cm^{-1} (C=S). (File reference: NMR: 500_hiwa_5 valin 3 phenyl 2 thio).

Synthesis of 5-methyl-3-phenyl-2-thioxoimidazolidin-4-one (35)

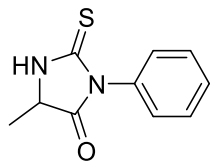

35

Utilising method **2**, to a mixture of L-alanine methyl ester hydrochloride salt (1.0 g, 7.16 mmol) and Et_3N (1.4 ml, 10.04 mmol) in 25 ml of CH_2Cl_2, phenylisothiocyanate (1.5 ml, 12.56 mmol) was slowly added.

Yield= 96.8%, M.p. 154- 156 °C, HRMS calculated for $C_{10}H_{10}N_2OS$ m/z [MS EI]$^+$ 206.0514; found 206.0518; ^{1}H-NMR (400 MHz, d_6-DMSO): δ 10.53 (s, 1H, N**H**), δ 7.54-7.25 (m, 5H, phenyl), δ 4.47 (q, *J* = 6.7 Hz, 1H, C**H**CH_3), δ 1.40 (d, *J* = 6.8 Hz, 3H, CHC**H$_3$**).^{13}C-NMR (101 MHz, d_6-DMSO): δ 182.0 (**C**=S), δ 174.9 (**C**O), δ 133.5 (**C**N), δ 128.8 (2 x **C**H), δ 128.6 (2 x **C**H), δ 128.4 (**C**H), δ 55.0 (**C**HCH_3), δ 16.1 (CH**C**H_3). IR (neat): vmax= 1750 cm^{-1} (C=O), 1498 cm^{-1} (C=S). (File reference: ^{1}H-NMR: 400_HA_exp 25 C13).

Synthesis of 3-allyl-5-benzyl-2-thioxoimidazolidin-4-one (36)

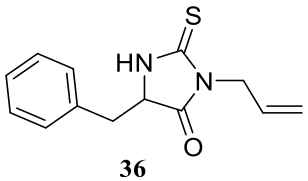

36

Utilising method **7**, to a mixture of L-alanine methyl ester hydrochloride salt (0.2 g, 0.87 mmol) and Et_3N (0.2 ml, 1.44 mmol) in 5 ml of CH_2Cl_2, phenylisothiocyanate (0.2 ml, 2.0 mmol) was slowly added.

Yield= 46.3 %, M.p. 107-108 °C, HRMS calculated for $C_{13}H_{14}N_2OS$ m/z [MS EI]$^+$ 245.0749; found 245.0742; ^{1}H-NMR (400 MHz, d_6-DMSO): δ 10.45 (s, 1H, N**H**), δ 7.31-7.09 (m, 5H,

phenyl), δ 5.50 – 5.37 (m, 1H, C**H**=CH_ACH_B), δ 4.85 (dd, *J* = 10.4, 1.3, 1H, CH=C**H**$_ACH_B$), δ 4.65 (dd, *J* = 4.8, 3.7 Hz, 1H, C**H**CH_2), δ 4.48 (dd, *J* = 17.3, 1.3, 1H, CH= CH_AC**H**$_B$), δ 4.08 (m, 2H, C**H**$_2$CH= CH_ACH_B), δ 3.04 (d, *J* = 4.8 Hz, 2H, C**H**$_2$CH). ^{13}C-NMR (101 MHz, d_6-DMSO): δ 182.5 (**C**=S), δ 174.0 (**C**O), δ 135.0 (**C**CH_2CH), δ 131.6 (**C**H=CH_ACH_B), δ 130.2 (2 x **C**H), δ 128.6 (2 x **C**H), δ 127.3 (**C**H), δ 116.4 (CH=**C**H_2), δ 59.9 (CCH_2**C**H), δ 45.9 (N**C**H_2CH=CH_2), δ 36.0 (CH**C**H_2). IR (neat): vmax = 1739cm^{-1} (C=O), 1495 cm^{-1} (C=S). (File reference: ^{1}H-NMR: 400_HA_exp 200 dry HV.^{13}C-NMR: 400_HA_exp 200_13C1).

Synthesis of (R)-5-benzyl-3-phenyl-1-(pyridin-2-ylmethyl)-2-thioxoimidazolidin-4-one (37)

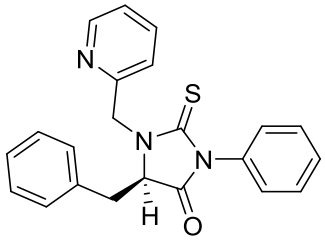

37

Utilising method **8**, D-phenylalanine methyl ester hydrochloride salt (0.25 g, 1.16 mmol) was dissolved in dichloromethane (5 ml) in the presence of triethylamine (0.08 ml, 0.57 mmol). 2-pyridinecarboxaldehyde (0.15 ml, 1.6 mmol) and sodium triacetoxyborohydride (0.40 g, 1.89 mmol) were added and the mixture allowed to stir for 10 minutes at room temperature. Phenyl isothiocyanate (0.15 ml, 1.26 mmol) was added to the mixture and stirred for another 25 minutes. The solution was washed with acidic water 3 times to remove the base and amino acid methyl ester. The organic phase was evaporated under reduced pressure and 3x10 ml of hexane was added to the solid to extract all impurities. The product was dried by high vacuum and NMR spectra were recorded.

Yield= 46.2%, Mp. 104-105 °C, $[\alpha]_D^{20}$ = +55.0° (0.41 g/l00 ml in acetone), HRMS calculated for $C_{22}H_{19}N_3OS$ m/z $[EI]^+$ 374.1327; found 374.1320; ^{1}H-NMR (500 MHz, $CDCl_3$): δ 8.52 (d, *J* = 4.0 Hz, 1H, C**H**N), δ 7.7 (t, *J* = 7.6 Hz, 1H, C**H**CHN), δ 7.5 (d, *J* = 7.8 Hz, 1H, C**H**CN), δ 7.31-7.18 (m, 7H, phenyl+ pyridine), δ 7.07 (m, 2H, phenyl), δ 6.71 (m, 2H, phenyl), δ 5.81 (d, *J* = 15.1 Hz, 1H, C**H**$_ACH_BN$), δ 4.75 (apparent t, *J* = 4.3 Hz, 1H, C**H**CH_2), δ 4.63 (d, *J* = 15.1 Hz, 1H, CH_AC**H**$_BN$), δ 3.42 (dd, *J* = 14.5, 4.4 Hz, 1H, C**H**$_ACH_BCH$), δ 3.25 (dd, *J* = 14.5, 4.1 Hz, 1H, CH_AC**H**$_BCH$). ^{13}C-NMR (126 MHz, $CDCl_3$): δ 182.4 (**C**=S), δ 173.1 (**C**O),

δ 155.4 (CH_2**C**N), δ 149.8 (**C**HN), δ 137.4 (**C**NCS), δ 134.5 (**C**HCHCN), δ 133.8 (**C**CH_2CH), δ 130.0 (2 x **C**H), δ 129.3 (2 x **C**H), δ 128.9 (4 x **C**H), δ 127.5 (**C**H), δ 123.3 (**C**HCN), δ 122.9 (**C**HCHN), δ 63.9 (**C**HCH_2), δ 49.6 (N**C**H_2), δ 34.4 (CH**C**H_2). IR (neat): vmax = 1746 cm^{-1} (C=O), 1593 cm^{-1} (C=S). (File reference: NMR: 500_hiwa_exp 33 CC 002).

Synthesis of (S)-5-isopropyl-3-phenyl-1-(pyridine -2-ylmethyl)-2-thioxoimidazolidin-4-one (38)

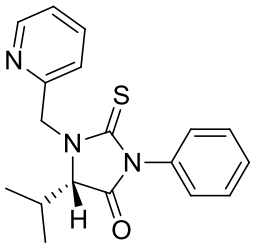

38

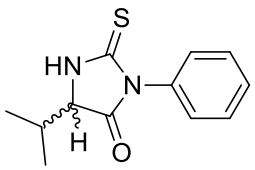

34

Utilising method **8**, L-valine methyl ester hydrochloride salt (1.00 g, 5.97 mmol) was dissolved in dichloromethane (40 ml) in the presence of triethylamine (0.91 ml, 6.52 mmol). 2-pyridinecarboxaldehyde (0.62 ml, 6.56 mmol) and sodium triacetoxyborohydride (1.9 g, 8.96 mmol) were added to the mixture, allowing stirring for 1 hour at room temperature. Phenyl isothiocyanate (0.97 ml, 6.56 mmol) and triethylamine (0.83 ml, 5.97 mmol) were added to the mixture and allowed to stir for another hour. The yellow oily product was washed with ethanol (4 x 10 ml) and subjected to column chromatography (40% acetone: 60% hexane). The mixture of compounds **34** (R_f = 1.8) and **38** (R_f= 1.3) was collected and characterised by GC-MS. The mixture was again subjected to column chromatography (90% diethyl ether: 10% hexane). The pure compounds of **34** and **38** were collected separately with yields of 18.1 % and 60.4 %, respectively.

Yield= 60.4%, M.p. 88- 89°C, $[\alpha]_D^{20}$ = -27.0° (0.37 g/l00 ml in acetone), HRMS calculated for $C_{18}H_{19}N_3OS$ m/z $[ES]^-$ 324.1171; found 324.1164; ^{1}H-NMR (400 MHz, $CDCl_3$): δ 8.49 (d, *J* = 4.8 Hz, 1H, C**H**N), δ 7.6 (dd, *J* = 7.7, 5.9 Hz, 1H, C**H**CHN), δ 7.4-7.10 (m, 7H, phenyl+ pyridine), δ 5.69 (d, *J* = 15.4 Hz, 1H, C$\mathbf{H}_A$CH_BN), δ 4.60 (d, *J* = 15.4 Hz, 1H, CH_AC$\mathbf{H}_B$N), δ 4.2 (d, *J* = 3.4 Hz, 1H, C**H**CHCH_3), δ 2.45 (m, 1H, CH_3C**H**CH_3), δ 1.17 (d, *J* = 7.0 Hz, 1H,

$CH_3CHC\mathbf{H_3}$), δ 0.86 (d, *J* = 6.9 Hz, 1H, $C\mathbf{H_3}CHCH_3$). ^{13}C-NMR (101 MHz, $CDCl_3$): δ 183.0 (**C**=S), δ 172.0 (**C**O), δ 155.1 ($CH_2\mathbf{C}N$), δ 150.2 (**C**HN), δ 137.0 (**C**NCS), δ 133.8 (**C**HCHCN), δ 129.8 (2 x **C**H), δ 129.0 (**C**H), δ 128.5 (2 x **C**H), δ 123.1 (CH**C**HCN), δ 122.9 (**C**HCHN), δ 67.6 (**C**HCHCH$_3$), δ 50.1 (CH**C**HCH$_3$), δ 28.8 (N**C**H$_2$), δ 17.6 (**C**H$_3$CHCH$_3$), δ 15.8 (CH$_3$CH**C**H$_3$). IR (neat): vmax = 1750 cm^{-1} (C=O), 1618 cm^{-1} (C=S).

Yield= 18.1 %; ^{1}H-NMR (400 MHz, $CDCl_3$): δ 7.47-7.37 (m, 3H, phenyl), δ 7.25-7.20 (m, 2H, phenyl), δ 4.11 (d, *J* = 3.7, 1.1 Hz, 1H, C**H**), δ 2.32 (m, 1H, H$_3$CC**H**CH$_3$), δ 1.08 (d, *J* = 7.0 Hz, 3H, $C\mathbf{H_3}$), δ 0.98 (d, *J* = 6.8 Hz, 3H, $C\mathbf{H_3}$).^{13}C-NMR (101 MHz, $CDCl_3$): δ 184.7 (**C**=S), δ 173.5 (**C**O), δ 133.0 (**C**N), δ 129.8 (2 x **C**H), δ 129.7 (2 x **C**H), δ 128.6 (**C**H), δ 65.3 (**C**HCH$_2$), δ 31.6 (H$_3$C**C**HCH$_3$), δ 19.3 (H$_3$**C**CHCH$_3$), δ 16.6 (H$_3$CCH**C**H$_3$). File reference: NMR: 400_HA_exp 51A spot 1).

Synthesis 1-(furan-2-ylmethyl)-5-isopropyl-3-phenyl-2-thioxoimidazolidin-4-one (39)

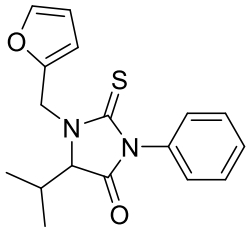

39

Utilising method **8**, L-valine methyl ester hydrochloride salt (1.00 g, 5.97 mmol) was dissolved in dichloromethane (30 ml) in the presence of triethylamine (0.62 ml, 4.44 mmol). 2-furancarboxaldehyde (0.51 g, 5.3 mmol) and sodium triacetoxyborohydride (1.9 g, 8.96 mmol) were added to the mixture, allowing stirring for 1 hour at room temperature. Phenyl isothiocyanate (0.83 ml, 6.94 mmol) and triethylamine (0.80 ml, 5.73 mmol) were added and the mixture was stirred for another hour.

Yield= 53.0 %, M.p. 90-92°C, HRMS calculated for $C_{17}H_{18}N_2O_2S$ m/z [ES]$^-$ 313.1011; found 313.1015; ^{1}H-NMR (400 MHz, $CDCl_3$): δ 7.46 –7.31 (m, 4H, phenyl + CHO furan), δ 7.22-7.15 (m, 2H, phen), δ 6.38 (d, *J* = 3.1 Hz, 1H, C**H**CHO), δ 6.31 (dd, *J* = 3.2, 1.9 Hz, 1H,C**H**CO), δ 5.65 (d, *J* = 15.7 Hz, 1H, NC$\mathbf{H_A}CH_BCO$), δ 4.46 (d, *J* = 15.7 Hz, 1H,

$NCH_AC\mathbf{H}_BCO$), δ 3.97 (d, *J* = 3.4 Hz, 1H, C**H**$CHCH_3$), δ 2.45 (m, 1H, $CH_3C\mathbf{H}CH_3$), δ 1.17 (d, *J* = 7.0 Hz, 3H, $CH_3CHC\mathbf{H_3}$), δ 0.91 (d, *J* = 6.9 Hz, 3H, $C\mathbf{H_3}CHCH_3$). ^{13}C-NMR (101 MHz, $CDCl_3$): δ 183.0 (**C**=S), δ 172.3 (**C**O), δ 148.7 (CH**C**O), δ 143.4 (**C**HO), δ 133.8 (**C**N), δ 129.7 (**C**HCHCHCN), δ 129.6 (2 x **C**H), δ 128.9 (2 x **C**H), δ 111.2 (**C**HCO), δ 110.6 (**C**HCHO), δ 66.7 (**C**$HCHCH_3$), δ 41.8 (**C**H_2N), δ 29.8 ($CH_3\mathbf{C}HCH_3$), δ 17.8 (**C**H_3CHCH_3), δ 16.1 ($CH_3CH\mathbf{C}H_3$). IR (neat): vmax = 1749 cm^{-1} (C=O), 1499 cm^{-1} (C=S). (File reference: NMR: 400_HA_exp 51 D).

Synthesis 1-benzyl-5-isopropyl-3-phenyl-2-thioxoimidazolidin-4-one (40)

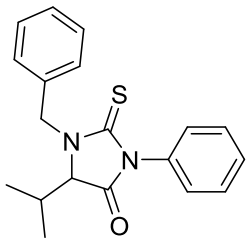

40

Utilising method **8**, L-valine methyl ester hydrochloride salt (1.00 g, 5.97 mmol) was dissolved in dichloromethane (40 ml) in the presence of triethylamine (0.91 ml, 6.52 mmol). Benzaldehyde (0.67 ml, 6.56 mmol) and sodium triacetoxyborohydride (1.9 g, 8.96 mmol) were added and the mixture was allowed to stir for 1 hour at room temperature. Phenyl isothiocyanate (0.97 ml, 6.95 mmol) and triethylamine (0.83 ml, 5.97 mmol) were added and the mixture was stirred for another hour.

Yield= 71.7%, M.p. 124-125 °C, HRMS calculated for $C_{19}H_{20}N_2OS$ m/z $[ES]^-$; found; ^{1}H-NMR (400 MHz, $CDCl_3$): δ 7.50 –7.22 (m, 10H, phenyl), δ 5.89 (d, *J* = 15.1 Hz, 1H, $NC\mathbf{H}_ACH_BCCH$), δ 4.33 (d, *J* = 15.1 Hz, 1H, $NCH_AC\mathbf{H}_BCCH$), δ 3.84 (d, *J* = 3.4 Hz, 1H, C**H**$CHCH_3$), δ 2.40-2.30 (m, 1H, $CH_3C\mathbf{H}CH_3$), δ 1.12 (d, *J* = 7.1 Hz, 3H, $CH_3CHC\mathbf{H_3}$), δ 0.92 (d, *J* = 6.9 Hz, 3H, $C\mathbf{H_3}CHCH_3$). ^{13}C-NMR (101 MHz, $CDCl_3$): δ 183.6 (**C**=S), δ 172.4 (**C**O), δ 135.3 (**C**NCS), δ 133.9 (**C**NCH_2N), δ 129.6 (**C**H), δ 129.6 (2 x **C**H), δ 129.5 (2 x **C**H), δ 128.9 (2 x **C**H), δ 128.8 (**C**H), δ 128.7 (2 x **C**H), δ 65.9 (**CH**$CHCH_3$), δ 48.9 (**C**H_2), δ 29.7 (CH**C**HCH_3), δ 17.8 ($H_3\mathbf{C}CHCH_3$), δ 16.3 ($H_3CCH\mathbf{C}H_3$). IR (neat): vmax = 1748 cm^{-1}

(C=O), 1501 cm^{-1} (C=S). (File reference: ^{1}H-NMR: 400_HA_exp 51B.^{13}C-NMR: 400_HA_exp 51B _C13).

Synthesis 3-(3, 5-bis(trifluoromethyl)phenyl)-5-methyl-1-((1-methyl-1H-pyrrol-2-yl)methyl)-2-thioxoimidazolidin-4-one (41)

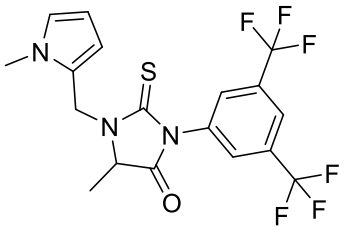

41

Utilising method **8**, L-alanine methyl ester hydrochloride salt (1.00 g, 7.16 mmol) was dissolved in dichloromethane (16 ml) in the presence of triethylamine (0.93 ml, 6.3 mmol). 1-methyl-1H-pyrrole-2-carbaldehyde (0.80 ml, 7.40 mmol) and sodium triacetoxyborohydride (2.1 g, 9.91 mmol) were added and the mixture, allowing stirring over night at room temperature. 1-isothiocyanato-3,5-bis (trifluoromethyl) benzene (2.60 ml, 14.23 mmol) and triethylamine (0.20 ml, 1.43 mmol) were added and the mixture was stirred for another hour.

Yield= 64.0 %, M.p. 173-174°C, HRMS calculated for $C_{17}H_{12}F_6N_3OS$ m/z $[EI]^+$ 435.0840; found 435.0840; ^{1}H-NMR (500 MHz, $CDCl_3$): δ 7.86 (s, 1H, C**H**CF_3), δ 7.79 (s, 2H, C**H**CC**H**), δ 6.61 (t, *J* = 3.2 Hz, 1H, C**H**NCH_3), δ 6.16 (dd, *J* = 3.5, 1.7 Hz, 1H, C**H**CHNCH_3), δ 6.04 (t, *J* = 3.2 Hz, 1H, C**H**CNCH_3), δ 5.69 (d, *J* = 15.6 Hz, 1H, C**H**$_A$$CH_B$N), δ 4.49 (d, *J* = 15.6 Hz, 1H, CH_AC**H**$_B$N), δ 3.98 (q, *J* = 7.2 Hz, 1H, C**H**CH_3), δ 3.60 (s, 3H, NC**H**$_3$), δ 1.51 (d, *J* = 7.2 Hz, 3H, CHC**H**$_3$), ^{13}C-NMR (126 MHz, $CDCl_3$): δ 179.3 (**C**=S), δ 172.5 (**C**O), δ 134.3 (**C**NCH_3), δ 132.2 (**C**HN), δ 124.3 (2x**C**HN), δ 124.2 (**C**HCCF_3), δ 122.7 (**C**HCHN), δ 121.7 (**C**HCN), δ 111.3 (2 x **C**CF_3), δ 107.7 (2 x **C**F_3), δ 57.2 (**C**HCH_3), δ 40.8 (N**C**H_3), δ 34.8 (**C**H_2NCH_3), δ 15.5 (CHC**H**$_3$). IR (neat): vmax = 1756 cm^{-1} (C=O), 1480 cm^{-1} (C=S). ^{1}H-NMR: 500_hiwa_exp 34 13C.^{13}C-NMR: 500_HIWA_EXP 34 003).

Acknowledgements

I would like to thank Ben Davies for the synthesis of compounds **38** and **40**, and David Tucker for preparing compound **39**. I thank Ibrahim Bala for the preparation of **12**, **13** and **16-19**. Dr Benson Kariuki is acknowledged for the determination of the X-ray structure of **18**. I gratefully acknowledge Dr Rob Jenkins for his invaluable help in conducting NMR experiments. I am grateful to Mr Robin Hicks, Mr Simon Waller and Mr Tom Williams for recording mass and GC-mass spectra.

2.7 References

1. O. A. Attanasi, S. Bartoccini, G. Favi, G. Giorgi, F. R. Perrulli and S. Santeusanio, *The Journal of Organic Chemistry*, 2011, 77, 1161-1167.
2. T. Miura, Y. Mikano and M. Murakami, *Organic Letters*, 2011, 13, 3560-3563.
3. T. Mendgen, C. Steuer and C. D. Klein, *Journal of Medicinal Chemistry*, 2012, 55, 743-753.
4. K. Cabrera, M. Jung, M. Fluck and V. Schurig, *Journal of Chromatography A*, 1996, 731, 315-321.
5. R. Crossley, *Tetrahedron*, 1992, 48, 8155-8178.
6. R. L. Datta, *Journal of the American Chemical Society*, 1913, 35, 780-784.
7. J. Marton, J. Enisz, S. Hosztafi and T. Timar, *Journal of Agricultural and Food Chemistry*, 1993, 41, 148-152.
8. S. Narduolo, Thesis (Ph D) - Cardiff University, 2011.
9. M. E. Garst, L. J. Dolby, S. Esdandiari, A. A. Avey, K. V. R. Mac and D. C. Muchmore, Google Patents, 2007.
10. Z. D. Wang, S. O. Sheikh and Y. Zhang, *Molecules*, 2006, 11, 739-750.
11. T. B. Johnson and B. H. Nicolet, *Journal of the American Chemical Society*, 1911, 33, 1973-1978.
12. T. B. Johnson and W. M. Scott, *Journal of the American Chemical Society*, 1913, 35, 1130-1136.
13. T. B. Johnson and W. M. Scott, *Journal of the American Chemical Society*, 1913, 35, 1136-1143.
14. S. Reyes and K. Burgess, *Journal of Organic Chemistry*, 2006, 71, 2507-2509.
15. E. Ware, *Chemical Reviews*, 1950, 46, 403-470.
16. S. O. J. Reyes, T. A and M. University, *Expanding Beta-turn Analogs for Mimicking Protein-protein Hot Spots*, Texas A&M University, 2006.
17. F. A. Csonka and B. H. Nicolet, *Journal of Biological Chemistry*, 1932, 99, 213-216.
18. A. LeTiran, J. P. Stables and H. Kohn, *Bioorganic & Medicinal Chemistry*, 2001, 9, 2693-2708.
19. M. M. Sim and A. Ganesan, *The Journal of Organic Chemistry*, 1997, 62, 3230-3235.
20. Y. Lu and W. Zhang, *Molecular Diversity*, 2005, 9, 91-98.
21. S. Heng, W. Tieu, S. Hautmann, K. Kuan, D. S. Pedersen, M. Pietsch, M. Gütschow and A. D. Abell, *Bioorganic & Medicinal Chemistry*, 2011, 19, 7453-7463.

22. O. Zvarec, S. W. Polyak, W. Tieu, K. Kuan, H. Dai, D. S. Pedersen, R. Morona, L. Zhang, G. W. Booker and A. D. Abell, *Bioorganic & Medicinal Chemistry Letters*, 2012, 22, 2720-2722.
23. D. Rakowitz, R. Maccari, R. Ottanà and M. G. Vigorita, *Bioorganic & Medicinal Chemistry*, 2006, 14, 567-574.
24. R. G. Giles, N. J. Lewis, J. K. Quick, M. J. Sasse, M. W. J. Urquhart and L. Youssef, *Tetrahedron*, 2000, 56, 4531-4537.
25. J. C. Thenmozhiyal, P. T. H. Wong and W. K. Chui, *Journal of Medicinal Chemistry*, 2004, 47, 1527-1535.
26. D. A. Heerding, L. T. Christmann, T. J. Clark, D. J. Holmes, S. F. Rittenhouse, D. T. Takata and J. W. Venslavsky, *Bioorganic & Medicinal Chemistry Letters*, 2003, 13, 3771-3773.
27. H. B. Lewis, *Journal of Biological Chemistry*, 1913, 14, 245-256.
28. R. A. Davis, W. Aalbersberg, S. Meo, R. M. d. Rocha and C. M. Ireland, *Tetrahedron*, 2002, 58, 3263-3269.
29. J. Swan, *Australian Journal of Chemistry*, 1952, 5, 711-720.
30. A. Neuberger, *Biochemical Journal*, 1938, 32, 1452.
31. J. M. Bailey and J. E. Shively, *Biochemistry*, 1990, 29, 3145-3156.
32. M. T. Reetz, K. M. Kühling, H. Hinrichs and A. Deege, *Chirality*, 2000, 12, 479-482.
33. A. Ballard, Thesis (Ph D) - Cardiff University, 2011.
34. G. G. Muccioli, N. Fazio, G. K. Scriba, W. Poppitz, F. Cannata, J. H. Poupaert, J. Wouters and D. M. Lambert, *Journal of Medicinal Chemistry*, 2006, 49, 417-425.
35. M. M. Sim and A. Ganesan, *Journal of Organic Chemistry*, 1997, 62, 3230-3235.
36. A. F. Abdel-Magid, K. G. Carson, B. D. Harris, C. A. Maryanoff and R. D. Shah, *The Journal of Organic Chemistry*, 1996, 61, 3849-3862.

Chapter 3

Hydrolysis of substituted 2-thiohydantoins and related compounds

3.1 Introduction

3.1.1 Hydrolysis of hydantoins

Hydantoin derivatives decompose either by base-catalysed or acid-catalysed hydrolysis to the urido-acid. Enzyme catalysis is another way to hydrolyse hydantoin in particular, and other drugs more generally, in the body (Scheme 3.1).[1]

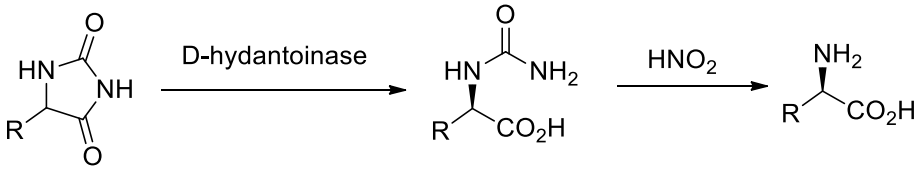

Scheme 3.1: Enzyme hydrolysis of hydantoin derivatives.[2]

3.1.2 Hydrolysis of 1-acetyl 2-thiohydantoins

5-Substituted 1-acetyl-2-thiohydantoins are hydrolysed by acid- or base-catalysed processes. De-acetylation is the first step to produce 5-substituted 2-thiohydantoins by acid [3,4] or base.[5] Cleavage of 5-substituted 1-acetyl-2-thiohydantoins was originally reported by Schlack and Kumpf, followed by Nicolet[6] in connection with the degradation of peptides and proteins under basic conditions. Congdon and Edward[5] reported that 1-acetyl-5-methyl-2-thiohydantoin starts to be hydrolysed under alkaline conditions and the negative charge on the 3-position N^- is not delocalised over the 1-acetyl-carbonyl group, allowing hydrolysis to take place (Scheme 3.2). Similarly, Kjaer and Eriksen[7] reported the hydrolysis of 1-acetyl-2-thiohydantoin and 1-benzoyl-2-thiohydantoin by using dilute base which was deacetyled rapidly to form 2-thiohydantoin.

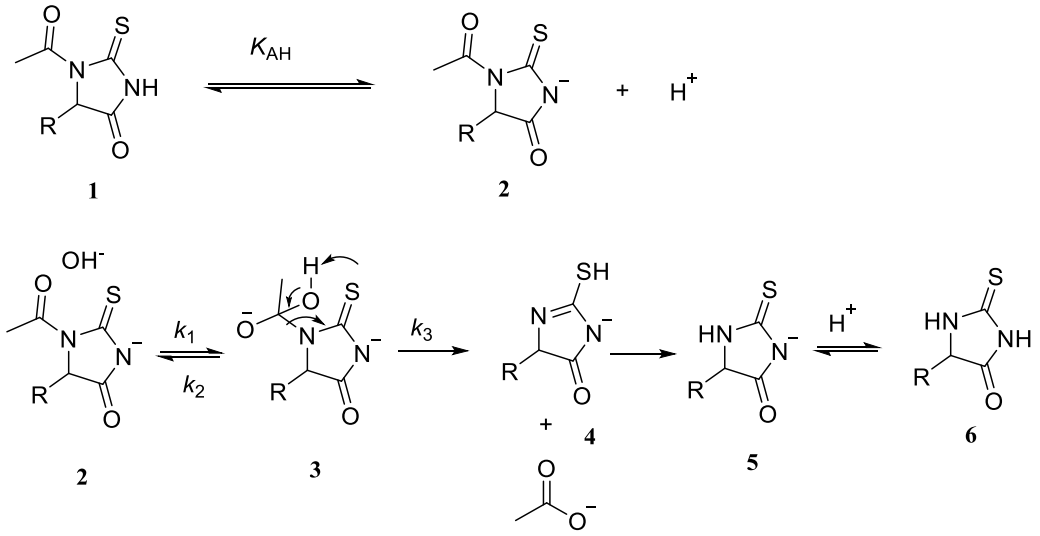

Scheme 3.2: Mechanism of base-catalysed hydrolysis of 5-substituted 1-acetyl-2-thiohydantoins, as suggested by Congdon[8]

The negative charge at N-3 position (2) (Scheme 3.2) can reduce the reactivity of 5-substituted 1-acetyl-2-thiohydantoin because the hydrolysis must proceed by the attack of the hydroxide ion on anion. Congdon[8] reported the hydrolysis of some 1-acetyl-2-thiohydantoins and 1-benzoyl-2-thiohydantoins which were slowly hydrolysed at low pH and rapidly hydrolysed at high pH. It has been explained that the benzoyl on the N-1 position is lost as a result of hydrolysis more quickly than acetyl because of the co-planarity effect of acetyl. The acyl carbonyl and the thiocarbonyl groups can be in a coplanar conformation, but will be separated as much as possible (the parallel coplanar conformation involves strong dipolar repulsion). On the contrary, to avoid the dipolar repulsion in 1-benzoyl-2-thiohydantoin, the benzene ring twists about 90° out of the plane of the acyl group. Congdon and Edward[5] reported the pseudo-first-order rate constant of 1-benzoyl-2-thiohydantoins with C-5 substituent in phosphate buffer (pH 11.2, 0.45 M *I*, at 25 °C). The authors reported the pseudo-first-order rate constants for different 1-benzoyl-2-thiohydantoins and the effect of C-5 substituents on the hydrolysis in the order un-substituted>5-methyl>5-phenyl>5-isobutyl>5-isopropyl.[5]

3.1.3 Hydrolysis of 2-thiohydantoin

The following step after the deacetylation process of 1-acetyl-2-thiohydantoin involves converting 5-substituted 2-thiohydantoin to thioureido-acids[9] which are finally hydrolysed to amino acids.[10] The base-catalysed hydrolysis of peptides proceeds to form substituted 2-thioureidopropanoic acid, reducing the yield of C-terminal thiohydantoin derivatives (Scheme 3.3).[11] Edward and Nielsen[12] suggested the mechanism for the base-catalysed hydrolysis of 5-substituted 2-thiohydantoins to produce thioureido-acids.

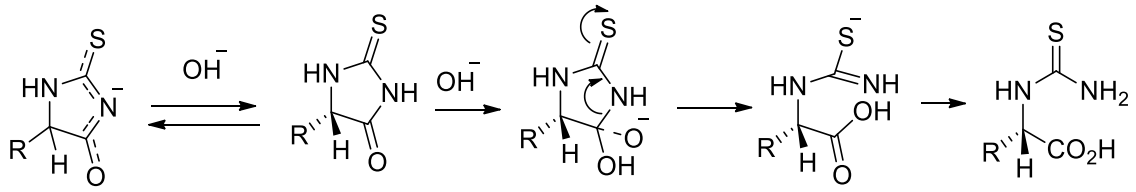

Scheme 3.3: Mechanism of base-catalysed hydrolysis of 5-substituted 2-thiohydantoins proposed by Edward and Nielsen.[12]

3.2 Results and discussion

3.2.1 Kinetics and mechanism of base-catalysed hydrolysis of 5-substituted 1-acetyl-2-thiohydantoins

3.2.1.1 UV-visible spectroscopy

Several acetylated 2-thiohydantoins were selected to study their kinetics and mechanism of hydrolysis (Scheme 3.4).

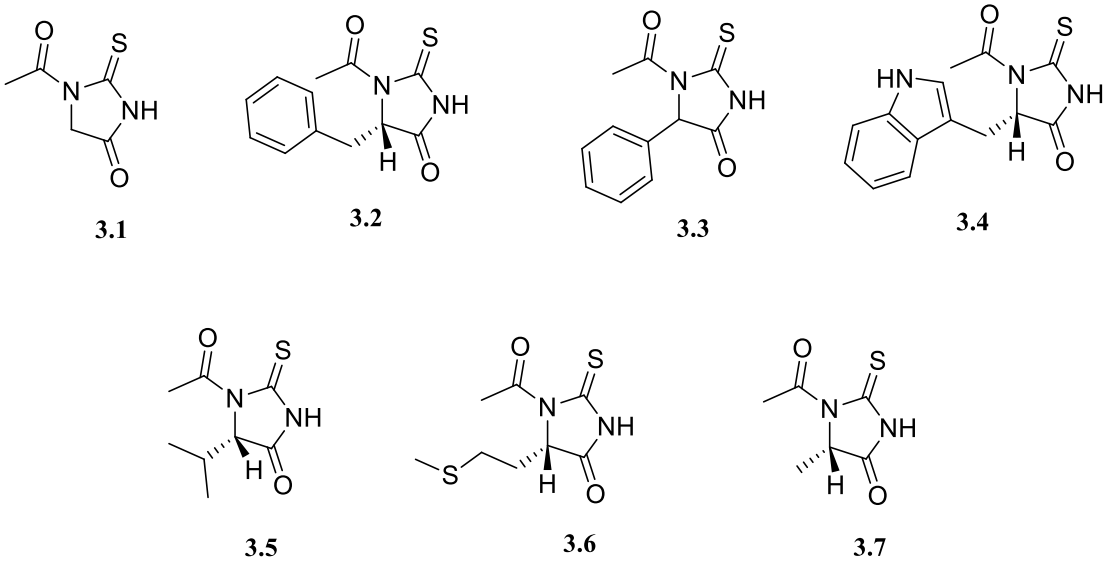

Scheme 3.4: The chemical structure of compounds **3.1**-**3.7**

To study the hydrolysis of 5-substituted 1-acetyl-2-thiohydantoins, different concentrations of phosphate buffer were used (pH 7.4, 0.9 M *I* at 37 °C). The kinetics of hydrolysis for all compounds was studied in aqueous solution without the use of a co-solvent. The acetyl group at the N-1 position is deacetyled to form 5-substituted 2-thiohydantoin and acetic acid. The UV-visible spectrum of 5-substituted 1-acetyl-2-thiohydantoins **3.1**-**3.7** exhibits a strong absorption band at around 287-291 nm. In the presence of different concentrations of buffer, the absorption spectrum of the compounds decrease as a function of time and the new absorption spectrum increases in intensity (Figure 3.1).

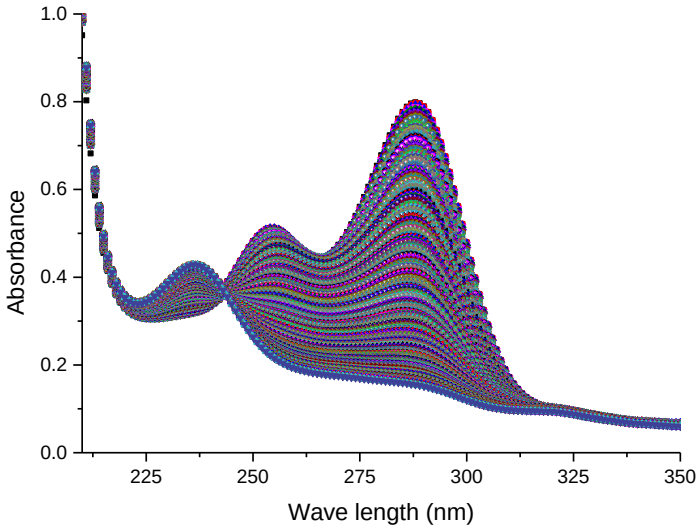

Figure 3.1: Typical UV–visible spectra of (S)-1-acetyl-5-methyl-2-thioxoimidazolidin-4-one **3.7** at 37 °C, recorded during a kinetic run in non-deuterated phosphate buffer, pH 7.4, 0.27 M, 0.9 M *I*.

Figure 3.1 shows that the absorbance at 255 and 290 nm of **3.7** decreases as a function of time in non-deuterated buffer solution (pH 7.4, 0.27 M, 0.9 M *I)*. There is no clear isosbestic point between the peaks at 190 nm and 255 nm, suggesting that more than one hydrolysis process has taken place (*vide infra*). Nevertheless, the largest absorbance band at 290 nm decreases in intensity in a process following a first-order rate law. We therefore attribute this absorbance to 1-acetyl-2-thiohydantoins with negligible contributions from potential downstream reaction intermediates and products. This assignment is in agreement with the UV-visible spectra observed for the deacetylated compounds (see section 3.2.2). The absorbance spectra of **3.7** in different phosphate buffers (0.045, 0.09, 0.18, 0.27 and 0.36, pH 7.4, 0.9 M *I*, at 37 °C) were plotted versus time to obtain the pseudo-first-order rate constants for hydrolysis (Figure 3.2). Similarly, the absorbance spectra of **3.1**-**3.6** were plotted versus time (see appendix).

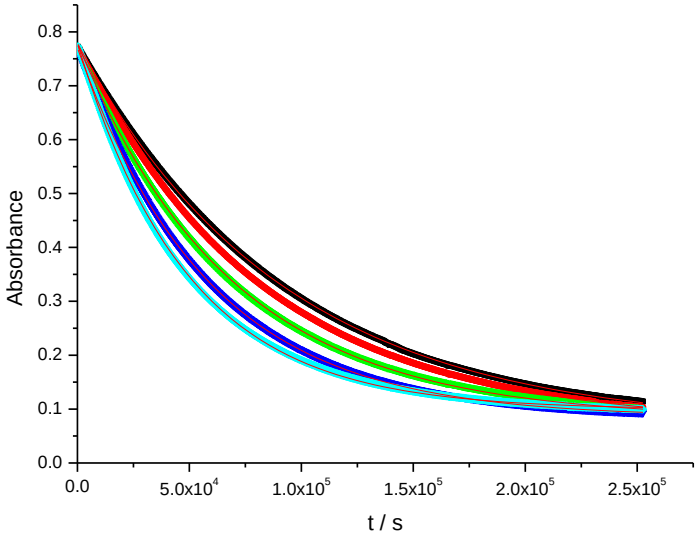

Figure 3.2: Fits of experimental data from hydrolysis experiments of (*S*)-1-acetyl-5-methyl-2-thioxoimidazolidin-4-one **3.7** hydrolysis at 290 nm in (■) 0.045 M, (●) 0.09 M, (▲) 0.18 M, (▼) 0.27 M, and (♦) 0.36 M, non-deuterated phosphate buffer (pH 7.4, 0.9 M *I*, at 37 °C).

Figure 3.2 shows the hydrolysis of **3.7** in 0.045, 0.09, 0.18, 0.27 and 0.36 M phosphate buffer (pH 7.4, 0.9 M *I* at 37 °C) and a fit of the data with a pseudo-first-order kinetic rate law. Similarly, the same conditions were used for compounds **3.1**-**3.6,** with a decrease in absorbance as a function of time also observed.

The decrease of absorbance with time at the selected wavelengths was reproduced well by the pseudo-first-order kinetic rate law (Equation 3.1).[13]

$$A_{\mathrm{t}} = A_{\mathrm{fin}} + \Delta A \mathrm{e}^{-k_{obs}t} \qquad \textbf{Equation 3. 1}$$

Here A_{t} is the absorbance at time *t*, A_{fin} is the final absorbance, ΔA represents the difference between the absorbance at time zero and A_{fin}, and k_{obs} is the observed pseudo-first-order rate constant for hydrolysis.

Equation 3.1 was used to obtain pseudo-first-order rate constants for hydrolysis of **3.1**-**3.7** at every single concentration of buffer. The data for **3.1**-**3.7** were reproduced very well by the pseudo-first-order rate law (see appendix).

The rate constants for hydrolysis of **3.1**-**3.7** were plotted versus the concentration of the basic component of phosphate buffer in different total concentrations of phosphate buffer (pH 7.4, 0.9 M *I*, at 37 °C) (Figure 3.3)

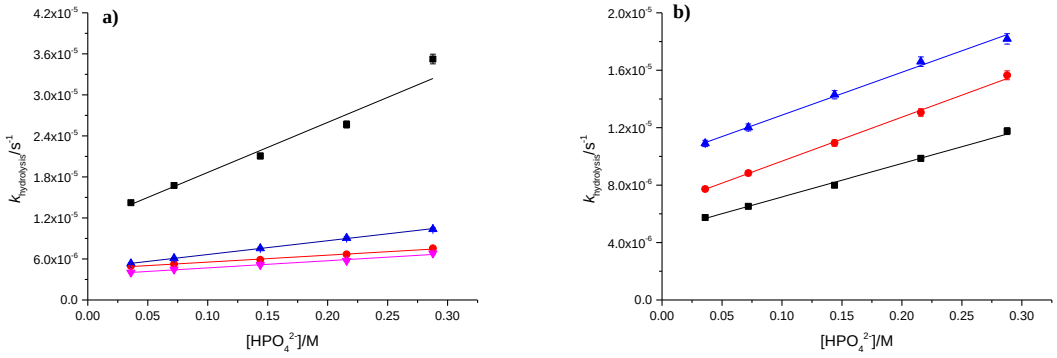

Figure 3.3: Observed rate constants of hydrolysis of a) (■) **3.1**, (●) **3.2**, (▲) **3.3**, (▼) **3.4** and b) (▲) **3.5**, (●) **3.6**, (■) **3.7** as a function of the concentration of the basic component of H_2O-based phosphate buffer (37 °C, 0.9 M *I*, pH 7.4) with total phosphate concentration of 0.45 M, 0.36 M, 0.27 M, 0.18 M and 0.09 M.

Figure 3.3 shows a linear increase in the first-order rate constants for hydrolysis of **3.1**-**3.7** as a function of the concentration of the basic component of the buffer, i.e. HPO_4^{2-}, at pH 7.4. The data show that not only is the concentration of base important, but also that the linear increase suggests that the hydrolysis reaction is subject to general-base catalysis by the phosphate dianion. The experimentally observed rate constants follow the rate law given by Equation 3.2.

$$k_{obs} = k_{\circ} + k_{\mathrm{OH^-}}[OH^-] + k_{\mathrm{H3O^+}}[H_3O^+] + k_{\mathrm{buffer}}[HPO_4{}^{2-}] \qquad \textbf{Equation 3. 2}$$

where k_0 is the rate constant of the non-catalysed reaction, k_{OH^-} and k_{H3O+} are the rate constants for the catalysed reaction by hydroxide and hydronium ion, respectively, obtained together from the intercept (k_{in}), k_{buffer} is the second-order rate constant for buffer catalysed hydrolysis obtained from the slope, and k_{obs} is the observed rate constant for hydrolysis.

The observed second-order rate constants for the HPO_4^{2-}-catalysed hydrolysis of **3.1**-**3.7** k_{hyd} and the observed rate constant k_{in} obtained from the slope and intercept, respectively, are shown in Table 3.1.

Table 3.1: Second-order rate constants for hydrolysis k_{hyd} of **3.1**-**3.7** in H_2O-phosphate buffer at 0.36 M, 0.27 M, 0.18 M, 0.09 M and 0.045 M total phosphate buffer, and 0.29 M, 0.22 M, 0.14 M, 0.072 M and 0.036 M HPO_4^{2-}, respectively, with ionic strength of 0.9 M *I*, pH 7.4 at 37 °C.

Substrate	R	k_{hyd} / 10^{-6} s^{-1} M^{-1}	k_{in} / 10^{-6} s^{-1}
3.1	H	73.2 ± 7.1	11.3 ± 0.9
3.2	Bz	10.2 ± 0.5	4.5 ± 0.07
3.3	Ph	20.2 ± 0.3	4.6 ± 0.04
3.4	3-Met-indole	10.5 ± 0.6	3.7 ± 0.09
3.5	*i*-Pr	23.3 ± 0.08	4.8 ± 0.1
3.6	$CH_2CH_2SCH_3$	30.7 ± 0.7	6.6 ± 0.09
3.7	Me	29.9 ± 1.0	9.9 ± 0.2

Table 3.1 shows the differences in the second-order rate constants k_{hyd} for **3.1**-**3.7**. The presence of substituents on C-5 was found to affect the rate of hydrolysis and decrease the reactivity.[12] The substituents might impede the change from trigonal **2** to tetrahedral **3** by a non-bonded interaction (Scheme 3.2). Compound **3.1,** which is non-substituted at position 5, is hydrolysed faster than the other C-5 substituted 1-acetyl-2-thiohydantoins **3.2**-**3.7**. The rate constants in Table 3.1 thus show the steric hindrance for attack on the acetyl group at the N-1 position exerted by different groups at the C-5 position.[5]

The order of decreasing rate constants for base-catalysed hydrolysis, and thus increasing stability in Table 3.1 is **3.1**, **3.6**, **3.7**, **3.5**, **3.3**, **3.4** and **3.2**. The highest rate constant is found for **3.1**, which does not carry any group substituents on the 5-position, as a result of the absence of steric effects compared with the 5-substituted 1-acetyl-2-thiohydantoins (Table 3.1).

The reaction proceeds by attack of OH^- on the acetyl moiety and the hydrolysis rate is decreased due to an increase of the steric strain for the tetrahedral intermediate in combination with a hindered approach of the nucleophile. The comparison between aromatic substituents on the 5-position and aliphatic substituents is obvious. The linear aliphatic substituents on the 5-position of 1-acetyl-2-thiohydantoins **3.6** and **3.7** display the highest rate constants for hydrolysis after the non-substituted compound, showing the effect of substituent size and steric hindrance. The branched isopropyl group in **3.5** leads to a slower reaction than observed for **3.6** and **3.7** with unbranched the aliphatic substituents. The phenyl group in **3.3** appears to have a similar effect as the isopropyl group in **3.5** which is not unreasonable considering the similar "branching" and the fact that the reaction centre is not in direct conjugation with the aromatic ring. When larger groups are attached to the C-5 position it becomes more difficult for the nucleophile to reach the carbonyl carbon to produce the tetrahedral intermediate.[14] Compounds **3.2** and **3.4** are therefore hydrolysed more slowly than the other compounds. An additional effect of substituents may affect the acidity of the reactant. It has been shown that 1-acetyl-2-thiohydantoin is able to ionise to produce compound **2** (Scheme 3.2), with pK_a values of 6.5-7.0.[5] The rate constant of hydrolysis will be different when base-catalysed attack takes place on the un-ionised compound (**1**) and ionised compound (**2**) (Scheme 3.2). The rate constant of hydrolysis is faster by factor 10^3 when the base attacks the unionised compound (**1**) rather than the ionised compound (**2**), as previously reported.[8] pK_a values of 7.03 and 6.95 for **3.1** and **3.7** have been reported in water, respectively. *N*-1-acetylated thiohydantoins compounds **3.1** and **3.7** are thus slightly stronger acids than the corresponding non-acetylated hydantoins.[8, 15] Similarly, the pK_a of 2-thiohydantoin is 8.5, making it a slightly stronger acid than corresponding hydantoin (pK_a = 9.0).[15, 16]

3.2.1.2 Determination of the rate constant for hydrolysis of 1-acetyl-5-isopropyl-2-thiohydantoin by NMR spectroscopy

The absence of an isosbestic point in the overlay spectra for hydrolysis (Figure 3.1) suggests that multiple reactions are occurring. To explore this behaviour further, we plotted the absorbance at 260 nm as a function of time (Figure 3.4).

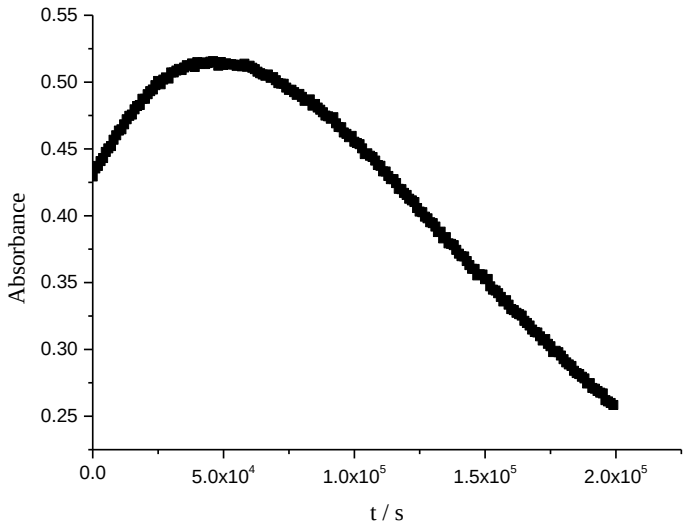

Figure 3.4: Absorbance of **3.5** as a function of time at 260 nm in deuterated-phosphate buffer (pH* 7.4, 0.36 M, 0.9 M *I*).

Figure 3.4 shows that at 260 nm, the absorbance increased and subsequently decreases. This suggests that two reactions occur.

To confirm if the process followed in Section 3.2.1.1 corresponds to a loss of acetate, the hydrolysis of compound **3.5** was also studied using ^{1}H-NMR spectroscopy in 0.36 M phosphate buffer (0.9 M ionic strength at 37 °C). It was noticed during ^{1}H-NMR studies that one of the hydrolysis products of **3.5** is not soluble in aqueous solution and precipitates. In order to observe the peak of **3.5** in ^{1}H-NMR, a higher concentration of compound compared to that used in the UV-visible studies was used. Therefore, the precipitation was noticed during the hydrolysis process. The hydrolysis of **3.5** is slow and the area of all peaks relative to methyl and CH in **3.5** decreases during the hydrolysis. Therefore, tetramethylammonium bromide was used as an internal reference with the peak at 3.02 ppm (Figure 3.5).

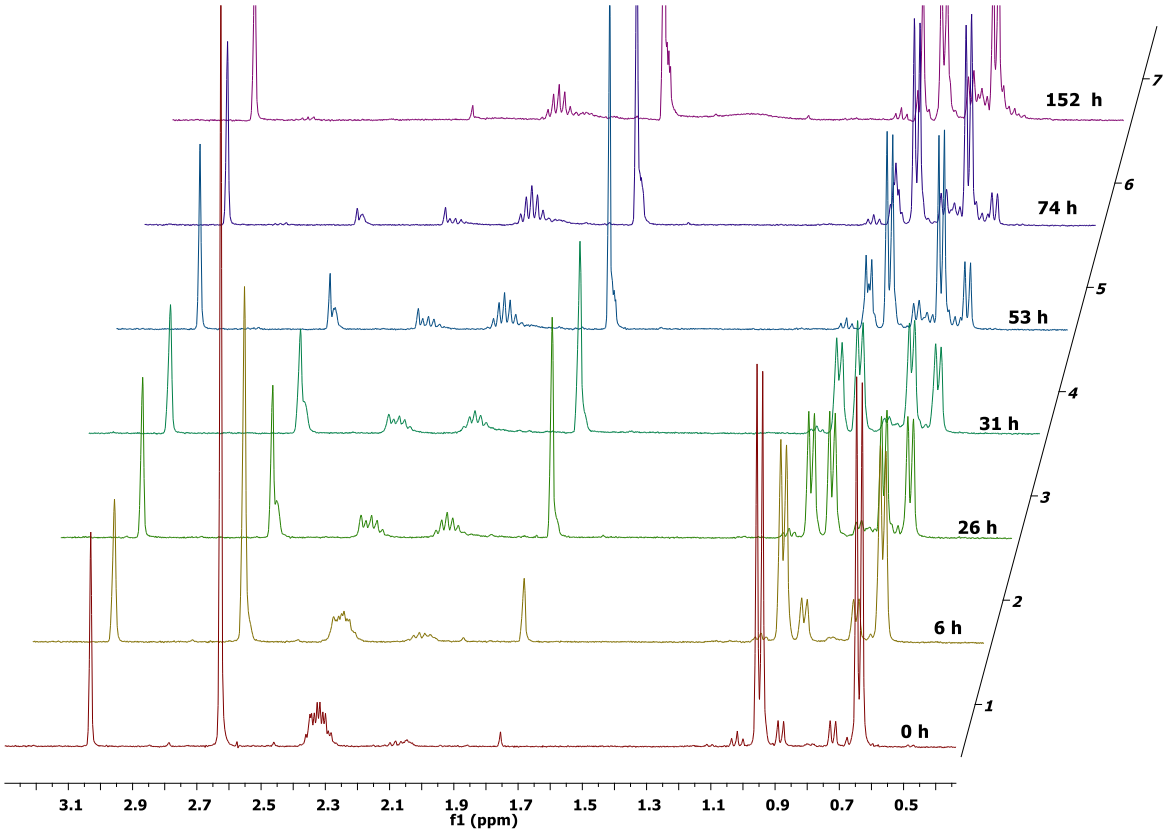

Figure 3.5: Time resolved ^{1}H-NMR spectra of **3.5** by using 0.36 M of total D_2O-phosphate buffer (0.9 M *I*, pH 7.4 at 37 °C with no d_3-acetonitrile).

Figure 3.5 shows the disappearance of peaks for **3.5** and the appearance of new peaks for new compounds. It is clear that the acetyl peak has decreased over time and a new peak of acetate is observed at 1.75 ppm. To confirm that the new peak belongs to acetate, sodium acetate was added to the solution after the hydrolysis reaction had taken place. The ^{1}H-NMR spectrum of the resulting solution confirmed that the new peak corresponded to acetate. The relative area of the peak for the methyl group in the acetylated thiohydantoin at 2.65 ppm decreases and the relative area of the peak for the methyl at 1.75 ppm increases. Both peaks are referenced against tetramethylammonium bromide. The relative peak areas were plotted as a function of time and suggest pseudo-first-order behaviour of hydrolysis of **3.5** (Figure 3.6).

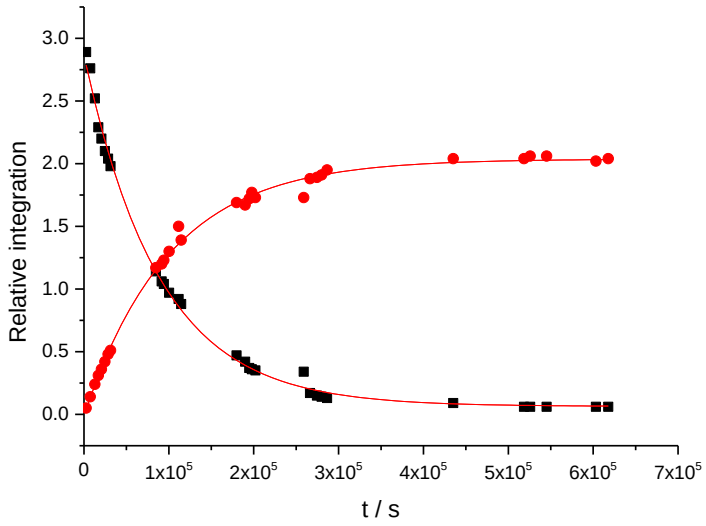

Figure 3.6: The hydrolysis process of **3.5** in 0.36 M D_2O-phosphate buffer (0.9 M *I*, pH 7.4 at 37 °C). a) (■) the relative area 3H of **H**$_3$CCO decreases over time, and (●) the relative area of 3H of **H**$_3$CCO (one hydrogen disappears with integration) increases over time.

Figure 3.6 shows the plot for the relative integration of decreasing acetyl CH3 at the N-1 position of 3.5 at 2.65 ppm and increasing the acetate CH3 at 1.75 ppm as a function of time. Both peaks were fitted to the pseudo-first-order rate constant and the rate constant of hydrolysis obtained by using Equation 3.1. It is important to note that the integration of three hydrogens has appeared at 2.65 ppm from 0 hour in 1H-NMR (Figure 3.6). However, the peak of CH3 of acetate after hydrolysis at 152 hours at 1.75 ppm shows just two hydrogens which might be because of the precipitation of acetate or evaporation of acetic acid. An alternative reason for the reduced relative signal observed for acetate formed in the hydrolysis reaction might be an additional H/D exchange process on the acetyl methyl group. This H/D exchange process, if occurring, would presumably take place before hydrolysis because the negative charge on the acetate anion would strongly inhibit the H/D exchange process after hydrolysis. The pseudo-first-order rate constants for the hydrolysis of **3.5** by ^{1}H-NMR are shown in Table 3.2 by the relative area of the disappearance and appearance of the methyl group during the deacetylation process.

Table 3.2: Pseudo-first-order rate constants for hydrolysis k_{hyd} of (*S*)-1-acetyl-5-isopropyl-2-thioxoimidazolidin-4-one (**3.5**) in D_2O-phosphate buffer at 0.36 M total phosphate buffer with ionic strength of 0.9 M *I*, pH 7.4 at 37 °C (No d_3-acetonitrile), and using 80% of 0.01 M of total phosphate buffer, 0.9 M *I*, pH 7.4 at 37 °C, with 20% of d_3-acetonitrile, determined by ^{1}H-NMR spectroscopy.

Con./M	k_{hyd} (D_2O) / 10^{-6} s^{-1} (■)	k_{hyd} (D_2O) / 10^{-6} s^{-1} (●)
0.36	11.3 ± 0.4	9.9 ± 0.3
0.008	0.5 ± 0.03	0.5 ± 0.03

Table 3.2 shows the pseudo-first-order rate constants for hydrolysis k_{hyd} in aqueous 0.36 M total phosphate buffer with precipitation. In order to solve the precipitation problem, a solution of 20 % d_3-acetonitrile with 80% 0.01 M D_2O-phosphate buffer pH 7.4, 1 M *I*, was used (Table 3.2) (see appendix). Interestingly, though the amount of precipitation decreased, solid particles were still observed indicating that the hydrolysis product of **3.5** has limited solubility in aqueous solution. The isopropyl and methyl substituents at the C-5 position of 1-acetyl-2-thiohydantoin have higher solubility than other substituents such as benzyl and phenyl. Therefore, experiments with further compounds were not attempted.

3.2.1.3 Brønsted plot for hydrolysis of (*S*)-1-acetyl-5-methyl-2-thioxoimidazolidin-4-one

The hydrolysis of **3.7** was studied in aqueous solution in a series buffers with different pK_a. Pseudo-first-order rate constants for hydrolysis were determined as before (Section 3.2.1.1). The hydrolysis was studied using acetate, phosphate, TRIS, borate and methylamine buffers over the pH range 5.0-9.7 at 37 °C. The second-order rate constants for hydrolysis in the different buffers were determined by plotting the pseudo-first-order rate constants of hydrolysis versus the concentration of the basic component of each buffer (Figure 3.7).

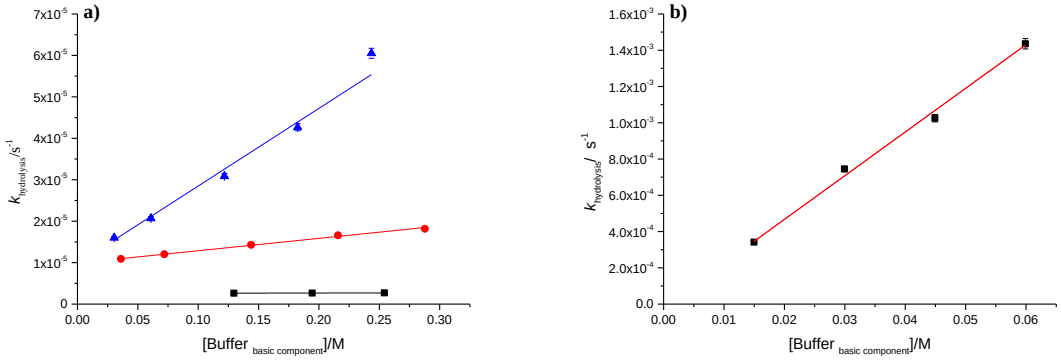

Figure 3.7: Observed pseudo-first-order rate constants for the hydrolysis of **3.7** in 0.45 M, 0.36 M, 0.27 M, 0.18 M and 0.09 M of total acetate, phosphate, TRIS and methyl amine, 0.9 M *I* of a) (■) acetate buffer pH 5.0 (●), phosphate buffer pH 7.4 (▲) TRIS buffer pH 8.2 and b) (■) methyl amine pH 9.7, all buffers are H_2O-based and experiments were carried out at 37 °C; data are plotted as a function of the concentration of the basic buffer component.

A good linear correlation between k_{hyd} with the basic component of the buffer is observed. This linear correlation suggests general base catalysis of hydrolysis. The second-order rate constants for hydrolysis were obtained using Equation 3.2 for every buffer at constant ionic strength from Figure 3.6 a, and b and these are reported in Table 3.3.

Table 3.3: The pK_a and the second-order rate constants for hydrolysis k_{hyd} of **3.7** in acetate, phosphate, TRIS, and methyl amine buffers at 0.9 M *I*, pH 5.0, 7.4, 8.2 and 9.7, respectively, at 37 °C.

Buffers	pK_a	pH	k_{hyd} / 10^{-6} s^{-1} M^{-1}	k_{in} / 10^{-6} s^{-1}
Acetate	4.59[a]	5.0	0.4 ± 0.1	2.6 ± 0.02
phosphate	6.8[b]	7.4	29.9 ± 1.0	9.9 ± 0.2
TRIS	7.88[a]	8.2	187 ± 14	9.8 ± 1.2
Methyl amine	10.4[a]	9.7	24100 ± 1140	-14.9 ± 28.1

a) pK_a at 37 °C.[17,18]

b) The value reported previously at 37 °C.[19, 20]

Table 3.3 shows that the second-order rate constants for hydrolysis increase with increasing buffer pK_a, as expected for general-base catalysis.

To measure the sensitivity of the reaction to the basicity of the catalytic base, the following equation was used:[21]

$$\log k_{obs} = \beta * pKa + C \qquad \textbf{Equation 3. 3}$$

where, logk_{obs} is the logarithm of the observed second-order rate constant k_{hyd} in different buffers determined using UV-visible spectroscopy, pK_a is the dissociation constant of the acidic component of every buffer for the given ionic strength at 37 °C and β is the measure of the sensitivity of the hydrolysis reaction to change in the strength of the base.

The logarithm of second-order rate constants for the hydrolysis of **3.7** in acetate, phosphate, TRIS and methylamine was plotted versus the pK_a of acetate, phosphate, TRIS and methyl amine buffers (Figure 3.8).

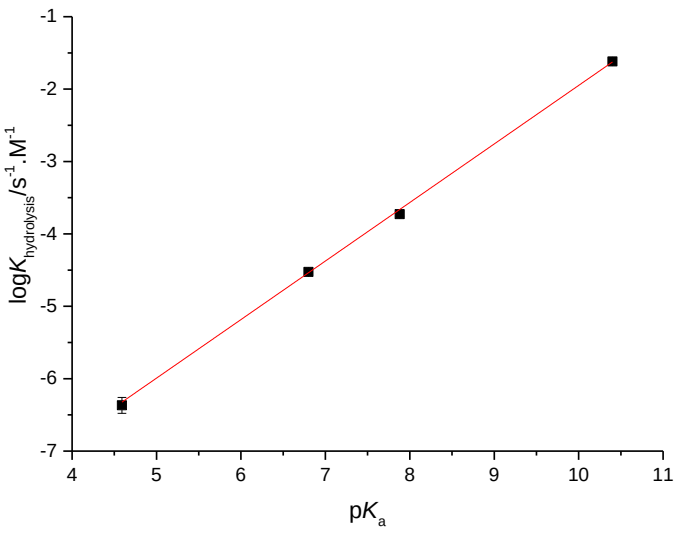

Figure 3.8: Brønsted plot for the base-catalysed hydrolysis of **3.7** (data from Table 3.3).

The least-squares-calculated values of the intercept (C) and the Brønsted slope (β) were found to be -10.03 ± 0.091 and 0.81 ± 0.011, respectively. The intercept (C) has no physical significance beyond an intrinsic reactivity, which is not relevant here. The slope in Figure 3.7 corresponds to β [14] and is close to unity, which suggests that the proton is almost fully transferred in the transition state.[22] Unless the reaction takes place by nucleophilic catalysis,

at least one water molecule is involved in the transition state in general-base catalysed hydrolysis reactions (Scheme 3.5).[23]

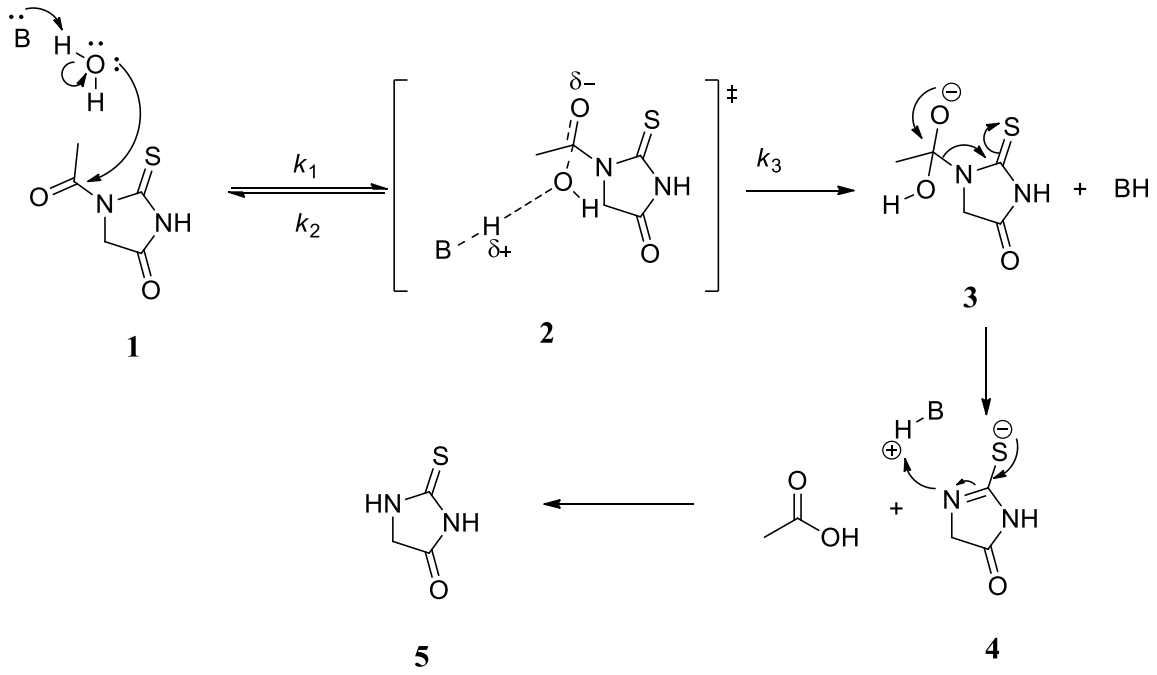

Scheme 3.5: Proton transfer mechanism for general-base catalysis of hydrolysis of 1-acetyl-2-thioxoimidazolidin-4-one **3.7**

The high value of Brønsted β of 0.81 ± 0.011 suggests that proton-transfer in the rate-determining step of hydrolysis of **3.7** is almost complete. From the mechanism in Scheme 3.5 it can be surmised that the tetrahedral intermediate is formed by the general-base catalysed nucleophilic attack of a water molecule on **3.7**. The unstable intermediate (**3**) breaks down to the product (**5**) (Scheme 3.5).

3.2.1.4 Kinetics of acid- and base-catalysed hydrolysis of 1-acetyl-5-phenyl-2-thioxoimidazolidin-4-one

The deacetylation process discussed in Chapter 2 was done using 12 M HCl to remove the acetyl group and obtain 5-substituted 2-thioxoimidazolidin-4-ones. To study in more detail

the acid and base catalysis of hydrolysis of **3.3**, acyl cleavage was followed spectrophotometrically at different concentrations of HCl and NaOH at 37 °C (Figure 3.9).

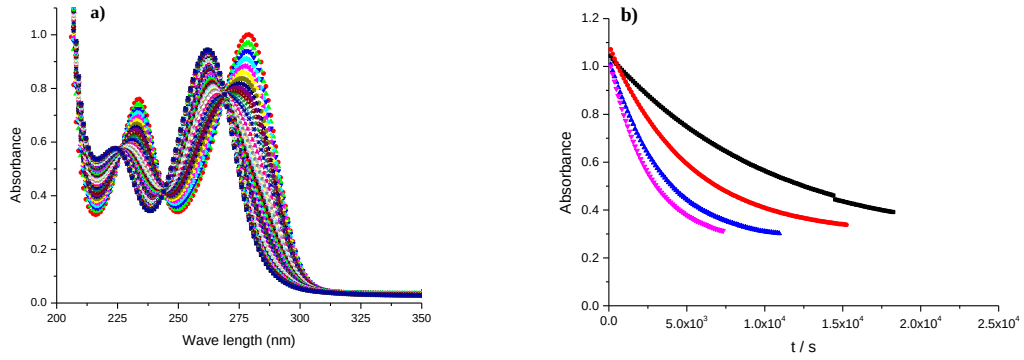

Figure 3.9: a) UV–visible spectra of 1-acetyl-5-phenyl-2-thioxoimidazolidin-4-one **3.3** recorded in 0.9576 M HCl at 37 °C and b) fits of the first-order rate law to experimental data from hydrolysis experiments of 1-acetyl-5-phenyl-2-thioxoimidazolidin-4-one at 37 °C in (■) 0.24 M, (●) 0.48 M, (▲) 0.72 M and (▼) 0.96 M HCl.

Figure 3.8 shows a clear drop in the intensity of the band at 279 nm and the formation of a new band at 260 nm. The presence of isosbestic points suggests that only one reaction is taking place and this reaction is expected to produce 5-phenyl-2-thioxoimidazolidin-4-one. For comparison, in base-catalysed hydrolysis using buffer (*vide supra*) and sodium hydroxide (*vide infra*), an increase in absorbance at 260 nm followed by a decrease was observed, indicating that (at least) two reactions were taking place. The apparent rate constant for hydrolysis of **3.3** was determined by taking the maximum absorbance at 279 nm and plotting it as a function of time. The pseudo-first-order rate constant of hydrolysis was determined by fitting Equation 3.1 to the data, as shown in Table 3.4.

Table 3.4: Pseudo-first-order rate constants for hydrolysis k_{hyd} determined using UV-visible spectroscopy for 1-acetyl-5-phenyl-2-thioxoimidazolidin-4-one (**3.3**) in 0.96 M, 0.72 M, 0.48 M and 0.24 M HCl at 37 °C.

Acid concentrations /M	k_{hyd} / 10^{-6} s^{-1}
0.24	89.7 ± 1.8 (± 0.6)[a]
0.48	197.0 ± 3.9 (± 0.2)[a]
0.72	296.5 ± 5.9 (± 0.7)[a]
0.96	395.9 ± 7.9 (± 0.8)[a]

a) Where the error from the data fit is reported to be less than 2% of the rate constant, an error of 2% was assumed. The values in brackets are the errors from the data fit, which are less than 2%.

Table 3.4 shows that the pseudo-first-order rate constants for hydrolysis increase with increasing concentration of hydrochloric acid, suggesting acid catalysis. The second-order rate constant for hydrolysis was obtained by plotting the pseudo-first-order rate constants against the concentrations of hydrochloric acid (Figure 3.10).

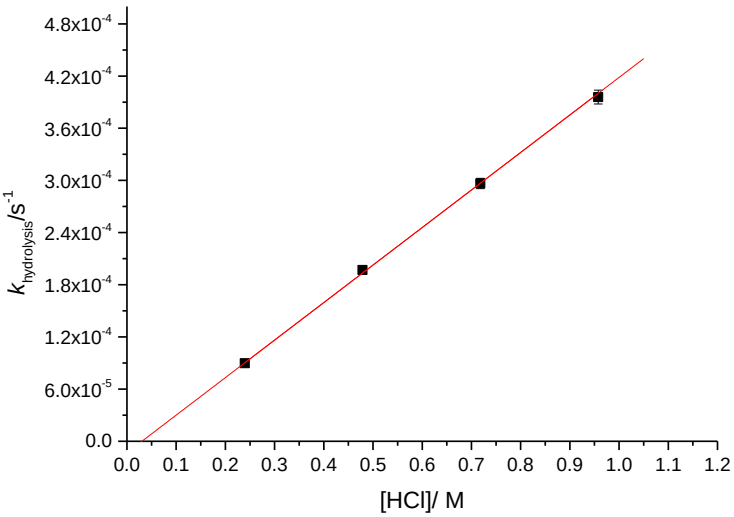

Figure 3.10: Observed pseudo-first-order rate constants for hydrolysis of **3.3** in acid versus hydrochloric acid concentration at 37 °C.

The straight line in Figure 3.10 suggests acid catalysis for the hydrolysis of **3.3** with HCl. The observed second-order rate constant for hydrolysis was determined from the slope of the straight line fit in Figure 3.10 using Equation 3.4.

$$k_{obs} = k_{\circ} + k_{\mathrm{hyd,H}}[HCl] \qquad \textbf{Equation 3.4}$$

Where k_{H} is the rate constant for the hydrogen ion catalysed reaction and $k_{\circ}$ is the uncatalysed rate constant of hydrolysis.

The second-order rate constant for the hydrolysis of **3.3** is shown in Table 3.5 at 37 °C.

Table 3.5: Second-order rate constant of the acid catalysed hydrolysis $k_{\mathrm{hyd,\,H}}$ of **3.3** in different concentrations of HCl at 37 °C.

Substrate	$k_{\mathrm{hyd,\,H}}$ HCl / 10^{-6} s^{-1} M^{-1}	k_{in} / 10^{-6} s^{-1}
3.3	431.5 ± 6.3	-13.1 ± 2.4

The rate constant for the uncatalysed reaction k_{in} of **3.3** is a negative value, which is impossible. We assume that an apparently significant negative value has been obtained due to underestimating the margin of error margin for the first-order rate constants (Figure 3.10).

To study the differences between acid catalysis and base-catalysed hydrolysis of **3.3**, different concentrations of sodium hydroxide were used (Figure 3.11).

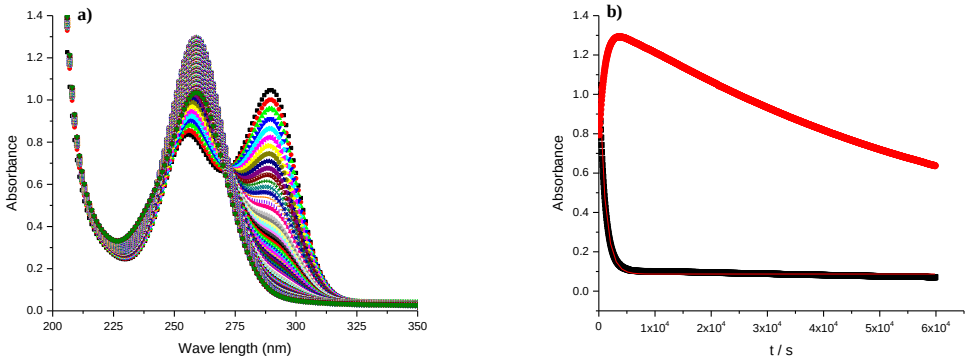

Figure 3.11: a) Typical UV–visible spectra of 1-acetyl-5-phenyl-2-thioxoimidazolidin-4-one **3.3** recorded during a kinetic run in 0.0025 M NaOH at 37 °C, and b) the absorbance of a solution of **3.3** as a function of time at (■) 290 and (●) 260 nm in 0.0025 M of NaOH at 37 °C.

Figure 3.11 shows that the absorbance of **3.3** decreases as a function of time at 290 nm and initially increases at 260 nm. This suggests deacetylation in the first step to produce 5-phenyl-2-thioxoimidazolidin-4-one. There is a second decrease at 260 nm after the initial de-acetylation process which indicates that the base has further hydrolysed the 5-phenyl-2-thioxoimidazolidin-4-one. Similarly, the increase and decrease of the peak at 260 nm is also seen when using phosphate buffer (*vide supra*), suggesting two reactions take place during the hydrolysis reaction.

The absorbance at 290 nm corresponding to the deacylation process for different concentrations of NaOH was plotted versus time (Figure 3.12).

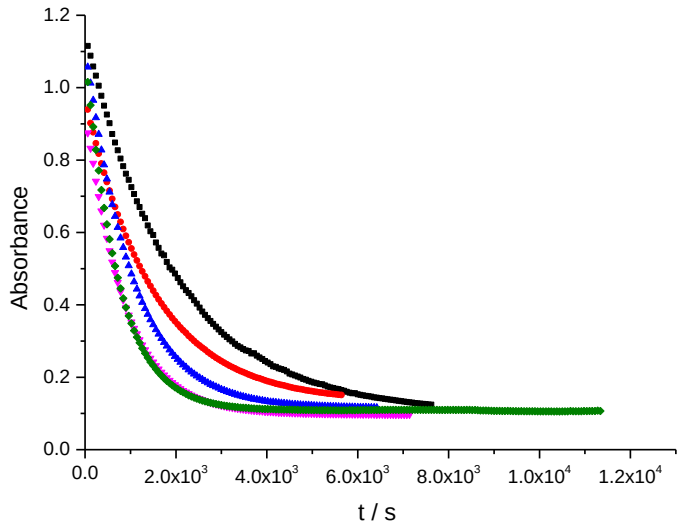

Figure 3.12: Fits of experimental data from hydrolysis experiments of 1-acetyl-5-phenyl-2-thioxoimidazolidin-4-one **3.3** at 37 °C in (■) 0.0017 M, (●) 0.0025 M, (▲) 0.0033 M, (▼) 0.0042 M and (♦) 0.005 M NaOH at 290 nm.

Figure 3.12 shows that the plots for all concentrations are reproduced well by the pseudo-first-order rate law. The pseudo-first-order rate constants for the hydrolysis of **3.3** were obtained using Equation 3.1 (Table 3.6).

Table 3.6: Rate constants for hydrolysis k_{hyd} of 1-acetyl-5-phenyl-2-thioxoimidazolidin-4-one (**3.3**) in 0.005 M, 0.0042 M, 0.0033 M, 0.0025 M and 0.0017 M sodium hydroxide at 37 °C, determined by UV-visible spectroscopy.

Base concentration/ M	k_{hyd} / 10^{-6} s^{-1}
0.0017	514 ± 10 (± 1.2)[a]
0.0025	669 ± 13 (± 0.5)[a]
0.0033	983 ± 20 (± 1.4)[a]
0.0042	1176 ± 24 (± 2.3)[a]
0.0050	1390 ± 28 (± 2.2)[a]

a) Where the error from the data fit is reported to be less than 2% of the rate constant, an error of 2% was assumed. The values in brackets are the errors from the data fit which are less than 2%.

As can be seen from Table 3.6, upon increasing the concentration of sodium hydroxide, the rate constants of hydrolysis increase. This agrees with both base catalysis and direct nucleophilic attack by OH^-. The second-order rate constant for basic hydrolysis was determined by plotting the observed pseudo-first-order rate constants for hydrolysis versus the concentration of sodium hydroxide (Figure 3.13).

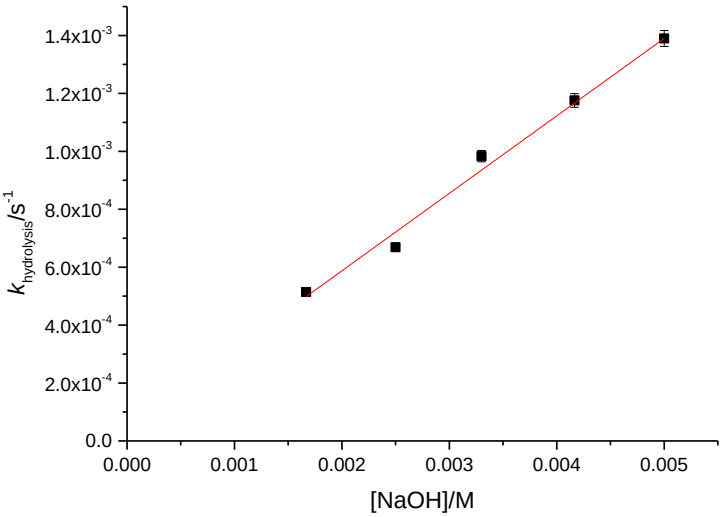

Figure 3.13: Observed pseudo-first-order rate constants of hydrolysis of **3.3** in sodium hydroxide obtained from Table 3.6 at 37 °C versus the concentrations of sodium hydroxide.

The second-order rate constant of hydrolysis for compound **3.3** was expressed using the following equation:

$$k_{\text{obs}} = k_{\text{H}}[\text{H}^+] + k_{\circ} + k_{\text{hyd,OH}}[\text{OH}^-] \qquad \textbf{Equation 3. 5}$$

where k_{H} is the rate constant for the hydronium ion catalysed reaction, $k_{\circ}$ is the rate constant for uncatalysed hydrolysis and k_{OH} is the rate constant for the hydroxide catalysed reaction.

The second-order rate constant for the base-catalysed hydrolysis k_{hyd} was determined from the slope and the combined rate constant for hydronium catalysed hydrolysis and uncatalysed hydrolysis of **3.3** k_{in} was obtained from the intercept (Table 3.7).

Table 3.7: Second-order rate constants of the hydrolysis k_{hyd} of **3.3** in different concentrations of sodium hydroxide at 37 °C.

Substrate	$k_{hyd, OH}$ / 10^{-6} s^{-1} M^{-1}	k_{in} / 10^{-6} s^{-1}
3.3	267471 ± 9295	53 ± 53

Table 3.7 shows that the second-order rate constant for base-catalysed hydrolysis of **3.3** is significantly higher than the rate constant for acid catalysed hydrolysis. As the intercept is zero within error, in the presence of base, deacetylation will be catalysed by base and depends on the strength of the base or acid.

3.2.2 Kinetics and mechanism of base-catalysed hydrolysis of 5-substituted 2-thioxoimidazolidin-4-ones

To study the continued hydrolysis of the non-acetylated 2-thioxoimidazolidin-4-one, different 5-substituted 2-thioxoimidazolidin-4-ones (Scheme 3.6) have been prepared (Chapter 2).

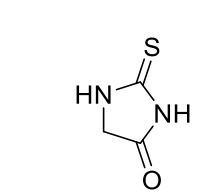

3.8

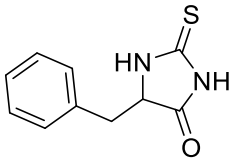

3.9

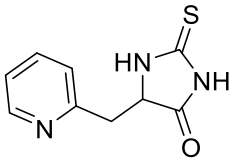

3.10

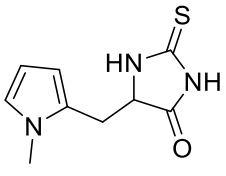

3.11

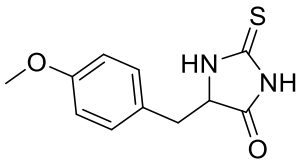

3.12

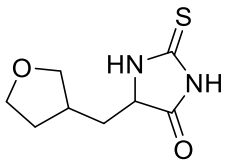

3.13

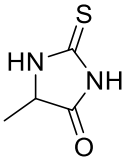

3.14

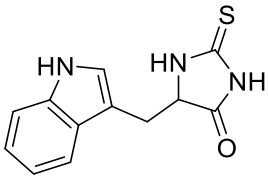

3.15

Scheme 3.6: Structures of compounds **3.8**-**3.15**

Scheme 3.6 shows the structures of the different 5-substitituted 2-thioxoimidazolidin-4-ones which allow us to analyse the effect of the groups attached to C-5 on the base-catalysed hydrolysis of **3.8**-**3.15**. In alkaline solution, 5-substituted thioxoimidazolidin-4-ones act as weak acids and ionise. The 5-substituted 2-thioxoimidazolidin-4-ones are also quite slowly hydrolysed to produce the salt of thioureido-acids.[12, 24, 25] The change in absorption spectrum was used to determine the rate constant of hydrolysis (Figure 3.14).

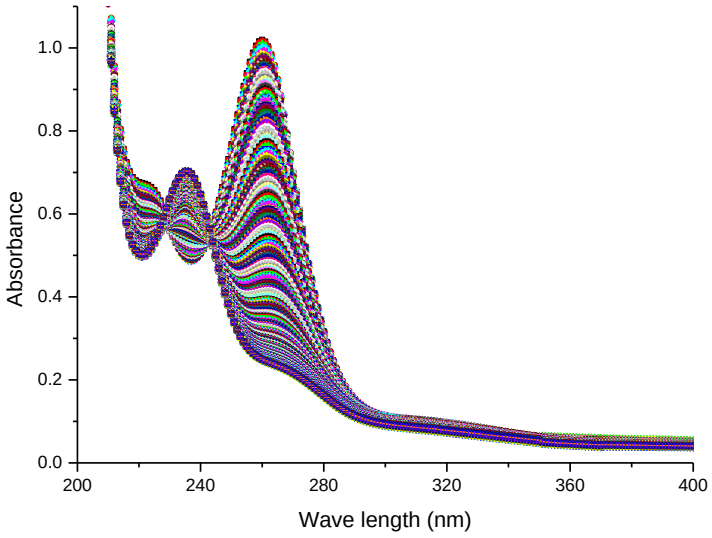

Figure 3.14: UV-visible spectra recorded for a solution of (*S*)-5-methyl-2-thioxoimidazolidin-4-one **3.14** at 37 °C in non-deuterated-phosphate buffer (pH 7.4, 0.36 M, 0.9 M *I*).

Figure 3.14 shows a decrease at 260 and an increase at 235 nm in the absorbance of compound **3.14** over time. The obvious presence of isosbestic points for the hydrolysis is in contrast to the base-catalysed hydrolysis of 5-substituted 1-acetyl-2-thioxoimidazolidin-4-ones which did not show any (Figure 3.1). For example, for compound **3.7** (Figure 3.1), the band at 260 nm first increases and then decreases at 260 nm while the band at 235 nm increases. The spectra here confirm that compound **3.7** has hydrolysed quite fast to produce **3.14** and that the hydrolysis has continued to produce thioureido-acids.

The absorbances at 260 nm for the hydrolysis of **3.14** in the presence of different concentrations of phosphate buffer (pH 7.4, 1 M *I*) were plotted versus time (Figure 3.15). Similarly, the absorbances of **3.8**, **3.9**, **3.10**, **3.11**, **3.12**, **3.13**, and **3.15** at various wavelengths were plotted as a function of time in different concentrations of phosphate buffer (pH 7.4, 1 M *I*) (see appendix).

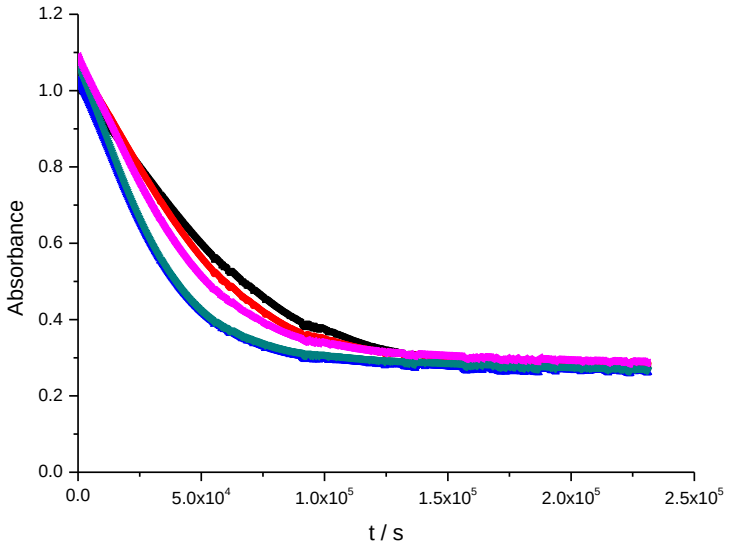

Figure 3.15: Fits of a first-order rate law to the experimental data from hydrolysis k_{hyd} experiments of (*S*)-5-methyl-2-thioxoimidazolidin-4-one **3.14** at 37 °C in non-deuterated phosphate buffer, pH 7.4, (■) 0.045, (●) 0.09, (▲) 0.18, (▼) 0.27, and (◀) 0.36 M total phosphate concentration (0.9 M *I*) at 264 nm.

The first-order rate constants for the hydrolysis of **3.14** in Figure 3.15 were determined using Equation 3.1. The values of pseudo-first-order rate constants for the hydrolysis of **3.8**-**3.15** are summarised in the appendix. The second-order rate constants for the hydrolysis of **3.8**-**3.15** were determined by plotting the pseudo-first-order rate constants for hydrolysis against the concentration of the basic component of the phosphate buffer according to Equation 3.2 (Figure 3.16).

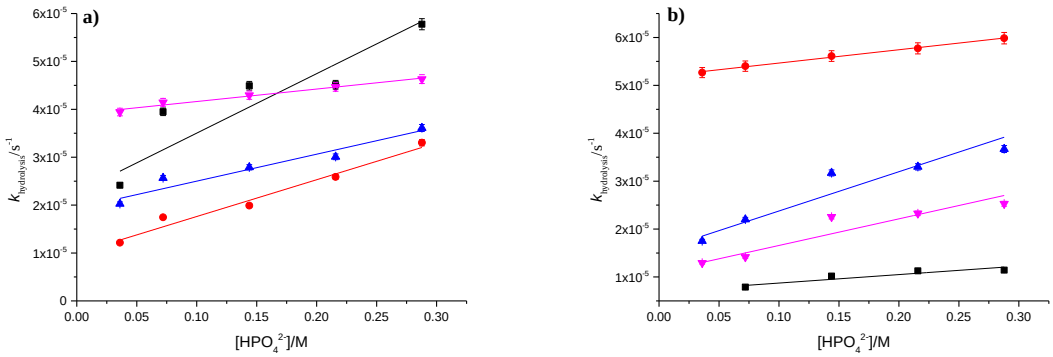

Figure 3.16: Observed rate constants for hydrolysis k_{hyd} of a) (■) **3.8**, (●) **3.9**, (▲) **3.10**, and (▼) **3.11**, and b) (■) **3.12**, (●) **3.13**,(▲) **3.14**, and (▼) **3.15** versus the concentration of the basic components of H_2O-based phosphate buffer at 37 °C, 0.9 M *I*, pH 7.4 (0.45 M,0.36 M, 0.27 M, 0.18 M, and 0.09 M total phosphate concentration).

Equation 3.2 was used to determine the second-order rate constants for the HPO_4^{2-}-catalysed hydrolysis k_{hyd} of **3.8**-**3.15** from the slope and $k_0 + k_{OH^-}[OH^-] + k_{H_3O^+}[H_3O^+]$ from the intercept (Table 3.8). The linear correlation of pseudo-first-order rate constants and the concentration of the basic component of the buffer for compounds **3.8**-**3.15** are not as a good as the linear correlation observed for the deacetylation of compounds **3.1**-**3.7.**

Table 3.8: Second-order rate constants for hydrolysis k_{hyd} of **3.8**-**3.15** in H_2O-phosphate buffer at 0.36 M, 0.27 M, 0.18 M, 0.09 M and 0.045 M total phosphate buffer and 0.29, 0.22, 0.14, 0.072 and 0.036 M of HPO_4^{2-}, respectively, with ionic strength of 0.9 M *I*, pH 7.4 at 37 °C.

Substrate	k_{hyd} / 10^{-6} s^{-1} M^{-1}	k_{in} / 10^{-6} s^{-1}
3.8	124 ± 31	22.6 ± 4.1
3.9	76.8 ± 8.7	9.9 ± 1.1
3.10	36.0 ± 13.0	10.6 ± 1.9
3.11	26.0 ± 2.4	39.0 ± 0.4
3.12	17.7 ± 4.5	7.0 ± 0.8
3.13	27.8 ± 1.1	51.9 ± 0.2
3.14	82.0 ± 12.8	15.6 ± 1.7
3.15	65.3 ± 9.2	10.6 ± 1.2

Table 3.8 shows that substituted 2-thioxoimidazolidin-4-ones undergo base-catalysed hydrolysis more slowly than the parent compound **3.8**. Table 3.8 shows that 2-thioxoimidazolidin-4-ones with aliphatic substituents on the C-5 have higher second-order rate constants k_{hyd} for HPO_4^{2-}-catalysed hydrolysis than k_{hyd} for 2-thioxoimidazolidin-4-ones with aromatic substituents on the 5-position. It has previously been mentioned that substitution, particularly in the 5-position of 5-membered ring compounds, such as hydantoins, and thiohydantoins, leads to decreased reactivity.[26] The substituents in the 5-position impede the change from a trigonal to tetrahedral configuration at the C-4 of thiohydantoin by non-bonded interactions.[27] The effect of steric hindrance and size attached substituents at the C-5 position as observed for hydrolysis leading to deacetylation of **3.1**-**3.7**, also plays a role in the hydrolysis of compounds **3.8**-**3.15**. Some factors should be taken into consideration for the hydrolysis of hydantoins, dihydrouracils and open-chain acylurea including the configuration of the open chain derivative and angle strain in the ring systems.[28] In the case of hydantoin and thiohydantoin, as explained before, N-3 can be deprotonated forming an anion because it is more acidic than N-1.[15, 29] There is another possibility to deprotonate both hydrogens on O-H in the tetrahedral intermediate, as mentioned previously for the base-catalysed hydrolysis of allantoin (Chapter 1).[28, 30] For this mechanism, the plot of

the rate constant of hydrolysis of hydantoin and allantoin has been reported to display a plateau in the intermediate region.

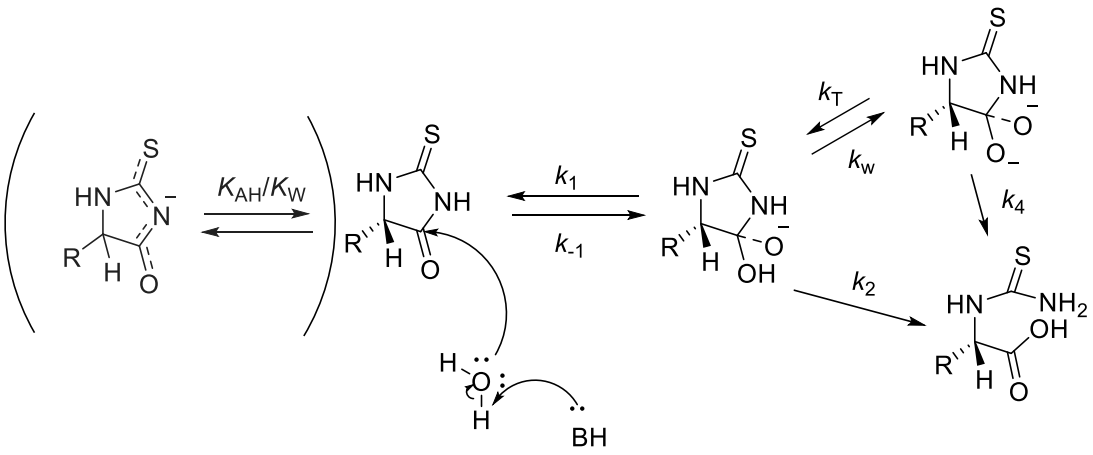

Scheme 3.7: Mechanism for base-catalysed hydrolysis of 5-substituted 2-thiohydantoin mechanism based on the slow breakdown of the tetrahedral intermediate as a mono and di-anion to the product.

3.2.3 Kinetics and mechanism of base-catalysed hydrolysis of 3,5-di-substituted 2-thiohydantoins

To avoid complications resulting from deprotonation at N-3, the rate constants for hydrolysis of **3.16** were also studied using UV-visible spectroscopy (Scheme 3.8).

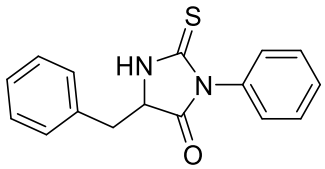

3.16

Scheme 3.8: The chemical structure of **3.16**

Because the H/D exchange of compound **3.16** was extremely fast by ^{1}H-NMR spectroscopy (See chapter 5) in comparison with compounds **3.1**-**3.5**, low concentrations of buffers were

used in the studies of the hydrolysis of **3.16** so that the data also serve to compare with the H/D exchange process. The absorbance of **3.16** decreases over time at different concentrations of phosphate buffer (pH 7.4, 0.9 M *I*) (Figure 3.17).

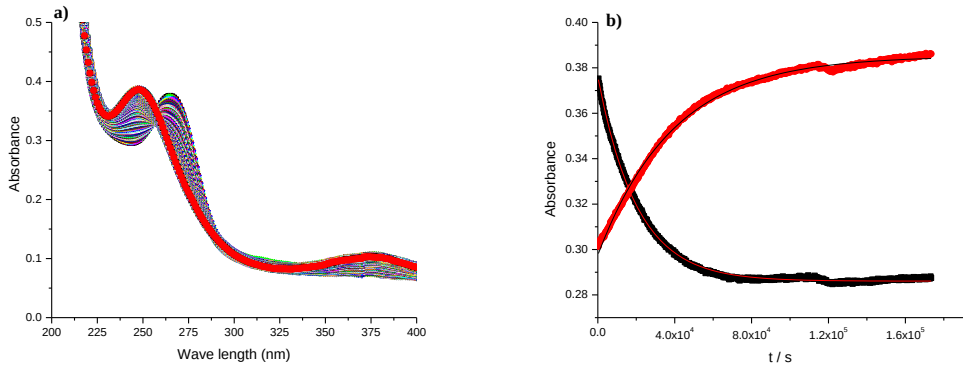

Figure 3.17: Typical UV–visible spectra of **3.16** in non-deuterated phosphate buffer, pH 7.4, 0.009 M total phosphate buffer, 0.9 M *I* at 37 °C, and b) the absorbance of **3.16** as a function of time at (■) 265 and (●) 248 nm in non-deuterated phosphate buffer (pH* 7.4, 0.009 M, 0.9 M *I*, 37 °C).

As can be seen from Figure 3.17, the absorbance of **3.16** gradually decreases at 265 nm over time and simultaneously increases at 248 and 375 nm. The absorbance increase at 375 nm is a new observation which has not been seen for compounds **3.1-3.15**. The decrease in absorbance for the hydrolysis of **3.16** at 265 nm has been plotted versus time at different concentrations of phosphate buffers (pH 7.4, 1 M *I*) (Figure 3.18).

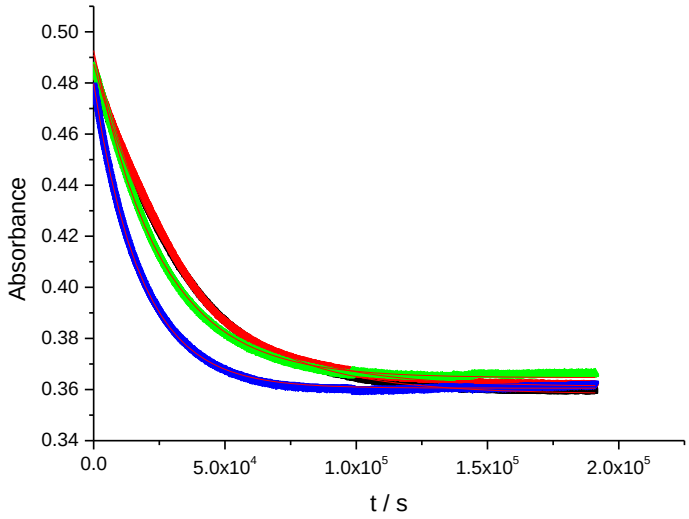

Figure 3.18: Fits of the first-order rate law to experimental data for hydrolysis of 5-benzyl-3-phenyl-2-thioxoimidazolidin-4-one **3.16** at 37 °C in non-deuterated phosphate buffer in pH 7.4, (■) 0.009 M, (●) 0.018 M, (▲) 0.027 M, and (▼) 0.036 M total phosphate buffer (0.9 M *I*) at 265 nm.

The pseudo-first-order rate law was fitted to the data in Figure 3.17 and as can be seen, the rate constants increase with increasing concentration of phosphate buffer. The observed pseudo-first-order rate constants of hydrolysis were plotted versus the concentration of the basic component of the phosphate buffer (Figure 3.19). From the slope, the second-order rate constant for the HPO_4^{2-}-catalysed hydrolysis of **3.16** was observed and $k_0 + k_{OH^-}\left[OH^-\right] + k_{H_3O^+}\left[H_3O^+\right]$ was obtained from the intercept using Equation 3.2, as done previously (Figure 3.19).

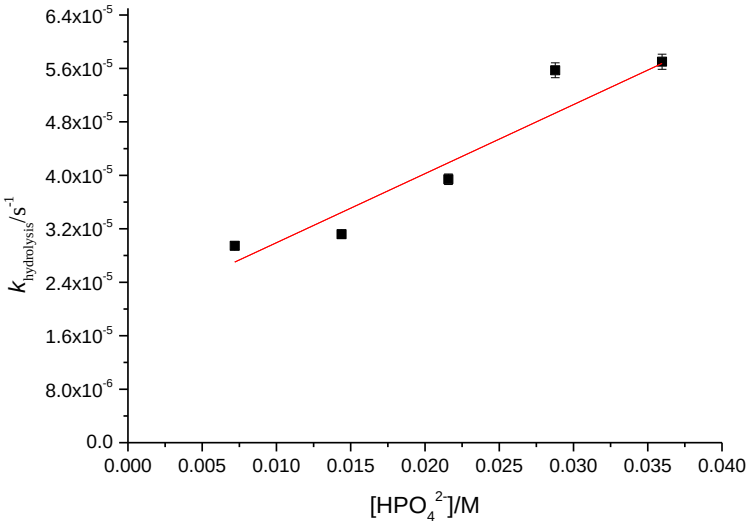

Figure 3.19: Observed rate constants for hydrolysis of **3.16** as a function of the concentration of H_2O-based phosphate buffer at 37 °C, 0.9 M *I*, pH 7.4, basic phosphate concentrations correspond to (0.045 M, 0.036 M, 0.027 M, 0.018 M, and 0.009 M total phosphate).

The observed rate constants are (19.6 ± 3.8). 10^{-6} s^{-1} for k_{in} and (1030.0 ± 202). 10^{-6} $M^{-1}s^{-1}$ for the second-order rate constant for HPO_4^{2-} catalysed hydrolysis.

The second-order rate constant for the hydrolysis of 5-benzyl-3-phenyl-2-thioxoimidazolidin-4-one **3.16** is approximately 14 times higher than the rate constant for the hydrolysis of 5-benzyl-2-thioxoimidazolidin-4-one **3.9**. The substituents on 2-thioxoimidazolidin-4-ones clearly have an effect on the reactivity of the neutral molecule possibly through eliminating ionisation leading to a change in the rate of hydrolysis.[12] The alkaline hydrolysis of 2-thioxoimidazolidin-4-ones substituted at the N-3 position might be comparable with the hydrolysis of dihydropyrimidines[31] substituted at the 3-position to form a tetrahedral intermediate and breakdown to the product (Scheme 3.9).

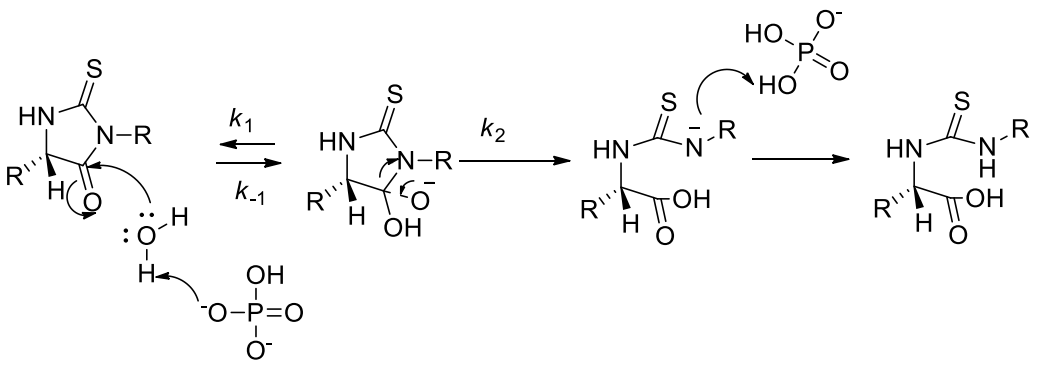

Scheme 3.9: Mechanism of base-catalysed hydrolysis of 3,5-di-substituted 2-thiohydantoin.

The methyl group on N-3 alone decreases the rate constant of hydrolysis in five-membered rings such as hydantoin but increases the rate constant of hydrolysis in six-membered rings such as 3-methyldihydrouracil.[28] Steric hindrance is expected to affect the rate of hydrolysis. Furthermore, the endocyclic bond angles of the tetrahedral intermediate become smaller, leading to the methyl group being shifted away from the neighbouring oxygen.[28] The second-order rate constants for hydrolysis of 3,5-di-substituted 2-thiohydantoin were found to be higher than 5-substituted 2-thiohydantoin. Despite the substitution at N-3 stabilising the neutral molecule, the lack of ionisation at N-3 leads to an increase in the hydrolysis of 3-substituted 2-thiohydantoin.[12]

3.3 Conclusions

The kinetics of hydrolysis of compounds **3.1**-**3.16** with different substituents at C-5, N-1, and N-3 with mono-, and di- substitution were studied in buffers mimicking physiological conditions. The pseudo-first-order and second-order rate constants of hydrolysis were obtained. From these results and comparison with different substituted 2-thiohydantoins, the following conclusions can be made.

First, the acetyl substituent on the N-1 position can be removed by acid or base rapidly. Two processes were identified to have taken place during the hydrolysis of **3.1**-**3.7** using buffer: deacetylation to form 5-substituted 2-thiohydantoins followed by further hydrolysis.

Second, the various substitutions on the C-5 of 2-thiohydantoin also have a strong influence on the rate constant of hydrolysis. The rate constant of hydrolysis is lower in comparison to

the C-5 of un-substituted 2-thiohydantoin. C-5 substituents impede the conversion from trigonal to tetrahedral configuration by non-bonded interaction at C-4.

Third, the second-order rate constants for hydrolysis of **3.3** are significantly higher when using sodium hydroxide compared to hydrochloric acid.

Fourth, compound **3.16** was hydrolysed more rapidly than **3.9** and **3.7**. This shows the effect of the phenyl at the N-3 position on the rate constant of hydrolysis. This result shows that rate constants of hydrolysis can be increased by phenyl substituents at the N-3 position.

3.4 Experimental

General Experimental

Materials

All chemicals and reagents were purchased from commercial sources and used without further purification. Sodium dihydrogen orthophosphate and sodium hydroxide were purchased from Fisher Scientific. Sodium hydroxide was purchased from BDH and anhydrous sodium acetate was purchased from CALBIOCHEM. Tris-(hydroxymethyl)-aminomethane (molecular biology grade, >99.9%) was purchased from Melford. CAPS buffer was purchased from Sigma Aldrich. Methyl amine 40 wt. % in H_2O was purchased from Sigma Aldrich. Water used for the preparation of buffers and solutions was demineralised by means of a PureLab Option water purification system from Elga.

Buffer preparation

H_2O-phosphate buffers (pH 7.4) were prepared by dissolving the appropriate amounts of sodium di-hydrogen ortho-phosphate dihydrate and sodium chloride in water followed by adjusting the pH to 7.4 by adding sodium hydroxide. Sodium acetate tri-hydrate was dissolved to prepare acetate buffers (pH 5.0) with 1 M *I* and acetic acid used to adjust the pH. Tris-(hydroxymethyl)-amino methane was used to prepare TRIS buffer (pH 8.2, 1 M *I*), the pH was adjusted to the desired value by the addition of hydrochloric acid. To prepare borate buffers (pH 9.3, 1 M *I*), the appropriate amount of sodium tetraborate-decahydrate was dissolved and hydrochloric acid was added to adjust the pH. The CAPS buffer (pH 9.7, 1 M *I*) was prepared by dissolving N-cyclohexyl-3-aminopropanesulphonic acid in water and sodium hydroxide was added to adjust to the desired pH. A 40% methyl amine solution in water was

used to prepare methyl amine buffer (pH 9.7, 1 M *I*) and the pH was adjusted to the desired value by adding HCl. Sodium chloride was used for all buffer solutions to adjust the ionic strength. The basic and acidic component of buffers were calculated by using the Henderson–Hasselbalch equation.

General kinetic measurements

Hydrolysis experiments were carried out by preparing stock solutions of compounds **3.1**-**3.15** in water. All compounds had enough absorbance in water to allow UV-visible spectroscopy to be used for the kinetic studies, except compound **3.16,** which has low absorbance and is difficult to dissolve in water. An ultrasonic bath sonicator was used to speed up dissolution of all compounds in water. The stock solutions were transferred to plastic Eppendorfs and centrifuged for 7 minutes two times at 13.3 rpm on a Jencons-pls Spectrafuge 24.D centrifuge. The clear supernatant was transferred to a new vial and diluted to appropriate absorbance for UV-visible spectroscopy. The stock solution of thiohydantoins was then mixed with the concentration of buffer in a 10%-90% (v-v) ratio. Experiments were carried out in 1 cm path length quartz cuvettes containing 3.4 ml of the aqueous solution of interest. The hydrolysis reactions were followed at 286, 289, 291, 283, 288, 290 and 290 nm for **3.1**-**3.7**, and at 264, 263, 264, 262, 264, 262,260, 263 and 265 nm for **3.8**-**3.16**, respectively, at 37 °C. For ^{1}H-NMR studies, a stock solution of compound **3.5** in D_2O was prepared by dissolving 0.0106 g of **3.5** in 100 µl D_2O and 900 µl of deuterated-phosphate buffer (0.4 M, 1 M *I*, pH* 7.55). The solution was transferred to the ultrasound sonicator bath to dissolve and was centrifuged for 7 minutes two times to avoid precipitation during the kinetic experiments. The solution was placed in an NMR tube and kept at 37 °C in a Fisher Scientific circulating water bath. ^{1}H-NMR spectra were recorded over time.

Instruments

Hydrolysis reactions were monitored by parallel kinetic measurements using a JASCO V650 UV-visible spectrophotometer with an Auto Peltier thermostatting unit with six-position cell changer PAC-743R. A JASCO V630 UV-visible spectrophotometer was also used for some experiments. Materials were weighed on an analytical balance Fisher Brand PS-100 (Max 100 g, d=0.1 mg). Volumes of solutions were measured by means of Gilson or Eppendorf

Research micropipettes. pH measurements were carried out at room temperature using a Hanna Instruments pH 210 pH meter. The pH meter was calibrated before each measurement with certified traceable NIST buffers at pH 7.00+0.01 (at 25 °C) (from Fisher), pH 10.01+0.02 (at 25 °C) (from Fisher) and pH 4.00+0.01 (at 25 °C) (from Fisher). A thermostatic water bath Julabo MB-5 Heating Circulator (temperature stability ± 0.2 °C) was used to control the temperature of solutions if not kept in thermostated cell holders in the NMR machine.

3.5 References

1. M. O'Neill, B. Hauer, N. Schneider and N. J. Turner, *ACS Catalysis*, 2011, 1, 1014-1016.
2. D. Ager, *Handbook Of Chiral Chemicals*, CRC Press, 2005.
3. S. Reyes and K. Burgess, *The Journal of Organic Chemistry*, 2006, 71, 2507-2509.
4. W. I. Congdon and J. T. Edward, *Canadian Journal of Chemistry*, 1972, 50, 3767-3779.
5. W. I. Congdon and J. T. Edward, *Canadian Journal of Chemistry*, 1972, 50, 3780-3788.
6. B. H. Nicolet, *Journal of Biological Chemistry*, 1930, 88, 403-407.
7. a. A. Kjaer and p. Eriksen, *Acta chemica Scandinavica*, 1952, 6, 448.
8. W. I. Congdon, Thesis (PhD) - McGill University, 1970.
9. N. Kharasch, *Organic Sulfur Compounds*, Elsevier, 2013.
10. J. Swan, *Australian Journal of Chemistry*, 1952, 5, 711-720.
11. T. E. Hugli and Protein Society. Annual meeting, *Techniques In Protein Chemistry*, Academic Press, San Diego ; London, 1989.
12. J. Edward and S. Nielsen, *Journal of the Chemical Society (Resumed)*, 1957, 5080-5083.
13. L. Onel and N. J. Buurma, *The Journal of Physical Chemistry B*, 2011, 115, 13199-13211.
14. E. V. Anslyn and D. A. Dougherty, *Modern Physical Organic Chemistry*, University Science Books, Sausalito, Calif., 2006.
15. Z. S. Safi, *European Journal of Chemistry*, 2012, 3, 348-355.
16. M. Puszyńska-Tuszkanow, M. Daszkiewicz, G. Maciejewska, A. Adach and M. Cieślak-Golonka, *Structural Chemistry*, 2010, 21, 315-321.
17. http://www.biomol.net/en/tools/buffercalculator.htm
18. http://www.liv.ac.uk/buffers/buffercalc.html
19. R. A. Lazarus, *Journal of Organic Chemistry*, 1990, 55, 4755-4757.
20. H. Fukada and K. Takahashi, *Proteins*, 1998, 33, 159-166.
21. K. P. Shelly, *General Acid and General Base Catalysis of the Enolization of Acetone: An Extensive Study*, University of British Columbia, 1988.
22. W. H. Ahmad, Y.-L. Sim and M. Niyaz Khan, *Monatshefte für Chemie - Chemical Monthly*, 2013, 144, 1299-1305.
23. T. H. Fife, R. Singh and R. Bembi, *The Journal of Organic Chemistry*, 2002, 67, 3179-3183.
24. E. Ware, *Chemical Reviews*, 1950, 46, 403-470.
25. M. L. Bender and R. D. Ginger, *Journal of the American Chemical Society*, 1955, 77, 348-351.

26. C. K. Ingold, S. Sako and J. F. Thorpe, *Journal of the Chemical Society, Transactions*, 1922, 121, 1177-1198.
27. H. C. Brown, J. H. Brewster and H. Shechter, *Journal of the American Chemical Society*, 1954, 76, 467-474.
28. I. B. Blagoeva, I. G. Pojarlieff and V. S. Dimitrov, *Journal of the Chemical Society, Perkin Transactions 2*, 1978, DOI: 10.1039/P29780000887, 887-892.
29. F. Cristiani, F. A. Devillanova, A. Diaz, F. Isaia and G. Verani, *Spectrochimica Acta Part A: Molecular Spectroscopy*, 1985, 41, 487-490.
30. G. D. Vogels, F. E. de Windt and W. Bassie, *Recueil des Travaux Chimiques des Pays-Bas*, 1969, 88, 940-950.
31. E. G. Sander, *Journal of the American Chemical Society*, 1969, 91, 3629-3634.

Chapter 4

Kinetics and mechanism for racemisation of substituted 2-thiohydantoins

4.1 Introduction

Enantiomers of drugs may exhibit different pharmacological profiles and toxicity, e.g. one enantiomer may be active while the other is inactive or even toxic.[1,2-4] Single enantiomer drugs improve the clinical effect and decrease drug toxicity. Indeed, in 1997, 54 % of the world's best-selling drugs were single enantiomers.[5] For chiral drugs the potential for racemisation should be studied in order to determine if enantiomers are configurationally stable under physiological conditions.[6] Substituted hydantoins, thiohydantoins, thiazolidines and rhodanines are molecules of pharmaceutical interest which are characterised by the presence of a stereogenic centre at the C-5 position. Reist *et al.*[7] and Narduolo[8] have studied the kinetics and mechanism of racemisation of 5-substituted hydantoin under physiological-like conditions. Cabordery *et al.*[6] studied the kinetics and mechanism of racemisation of Tic-hydantoins, including Tic-thiohydantoin, while Cabera *et al.*[9] determined the enantiomerisation barrier of 3-phenyl-5-benzyl-2-thiohydantoin. Typically, substituents at the stereogenic carbon in the chiral molecule have a strong effect on the reactivity in racemisation reactions. Previous authors reported that the chemical racemisation of hydantoin proceeds via keto-enol tautomerism[10, 11] by forming a planar enolate intermediate (Scheme 4.1).

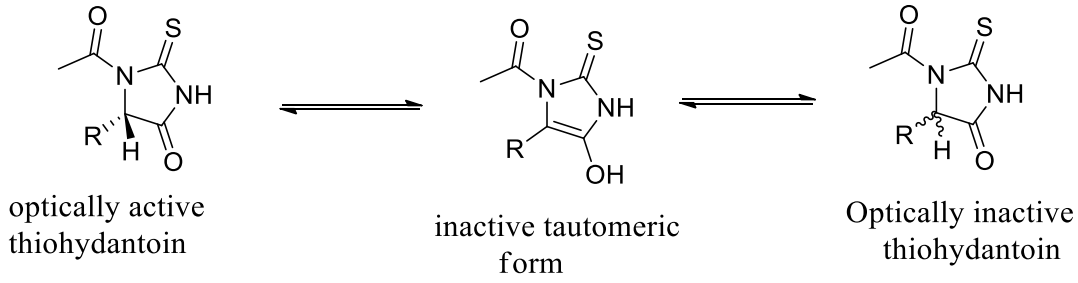

Scheme 4.1: Proposed keto-enol tautomerism of 5-subsituted 2-thiohydantoin.[12]

Mendil and Dakin[12] proposed keto-enol tautomerism as the mechanism for hydantoin racemisation forming optically inactive hydantoin (see Chapter 1). During the keto-enol tautomerism, the labelled hydrogen on the α-carbon is lost to form an inactive tautomeric-enolate salt which is reprotonated to produce racemised products.[13] Tian *et al.*[14] reported the role of water to facilitate proton transfer and act as a catalyst to reduce the enantiomerisation barrier by ≈ 30 kcal mol^{-1}.

Divalent phosphate catalysis as reported by Dudley and Bius[15] (Chapter 1) for the mechanism of racemisation of 5-phenylhydantoin is also a possibility for racemisation of thiohydantoin derivatives *in vivo* without a specific racemase (Scheme 4.2).

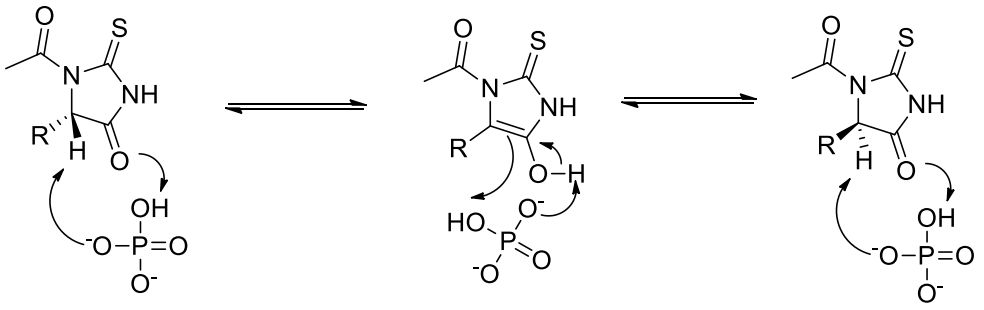

Scheme 4.2: Possible mechanism for the racemisation of 5-substituted 1-acetyl-2-thiohydantoins by divalent phosphate for hydantoin based on the mechanism proposed by Dudley and Bius[15] for 5-phenylhydantoin.

4.2 Results and discussion

4.2.1 Racemisation of 5-substituted 1-acetyl-2-thiohydantoins

4.2.1.1 Determination of rate constants for loss of ellipticity

In order to study the racemisation of chiral thiohydantoins, enantioenriched 5-substituted 1-acetyl-2-thiohydantoins were synthesised from the corresponding amino acids (Chapter 2). The loss of optical activity, as quantified by the loss of ellipticity of compounds **4.1**-**4.5** (Scheme 4.3), was monitored using circular dichroism spectroscopy in aqueous systems under mimicked physiological conditions using different concentrations of buffer at pH 7.4.

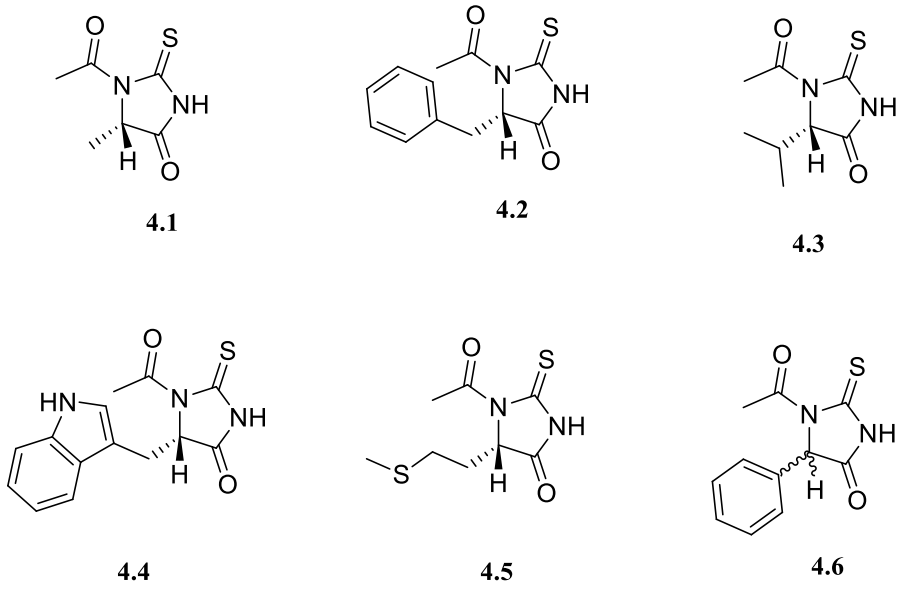

Scheme 4.3: The chemical structures of compounds **4.1**-**4.6**

As Scheme 4.3 shows, compounds **4.1**-**4.6** have different substituents at the stereogenic centre and an acetyl group at the N-1 position. Each compound was dissolved in water or D_2O and the resulting solution mixed with phosphate buffer and centrifuged two times to avoid precipitation. Kinetic studies of the loss of ellipticity for all enantioenriched compounds **4.1**-**4.5** was carried out in different concentrations of both non-deuterated and deuterated phosphate buffers using CD spectroscopy at pH 7.4 and 0.9 M *I* at 37 °C. Changes in ellipticity as a function of time for **4.1**-**4.5** in 0.27 M non-deuterated-phosphate buffer (pH 7.4, 0.9 M *I* at 37 °C) are shown in Figure 4.1. For all further experiments of **4.1**-**4.5** in H_2O- and D_2O-phosphate buffers pH 7.4[a)] and pH* 7.4[a)] and 0.9 M *I* at 37 °C, see the Appendix.

[a)] Buffers pH 7.4: A series of concentrations of phosphate buffer in H_2O were prepared by adjusting $pH^{20°C}$ to 7.4. Buffers pH* 7.55: the H_2O-phosphate buffers were evaporated three times and D_2O subsequently added to prepare deuterated-phosphate buffers with $pH^{20°C}$ 7.55. This procedure ensures that the buffer ratio is the same in our H_2O based and D_2O based buffers.

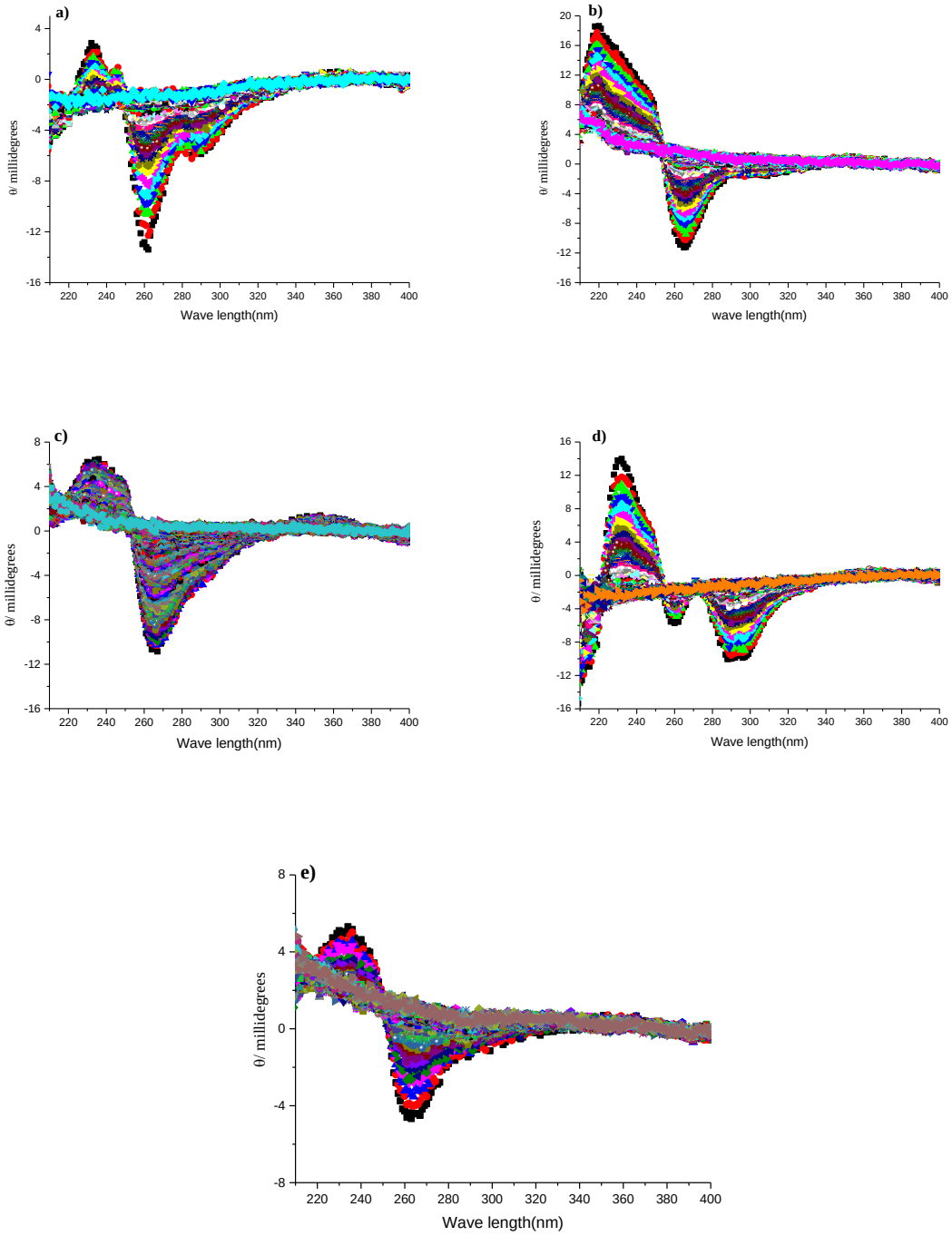

Figure 4.1: Change in ellipticity over time for solutions of a) **4.1**, b) **4.2**, c) **4.3**, d) **4.4**, and c) **4.5** at 37 °C. For every experiment, 10 vol% of a stock solution of each compound in water was mixed with 90 vol% of a 0.3 M non-deuterated-phosphate buffer (pH 7.4, 1 M *I*).

Figure 4.1 shows that the ellipticity of solutions of compounds **4.1**-**4.5** decreased as a function of time. The ellipticities at the wavelength of maximum ellipticity of compounds **4.1**-**4.5** in 0.27 M of phosphate buffer (pH 7.4, 1 M *I* at 37 °C) were plotted versus time (Figure 4.2). For kinetic traces at other buffer concentrations, see Appendix.

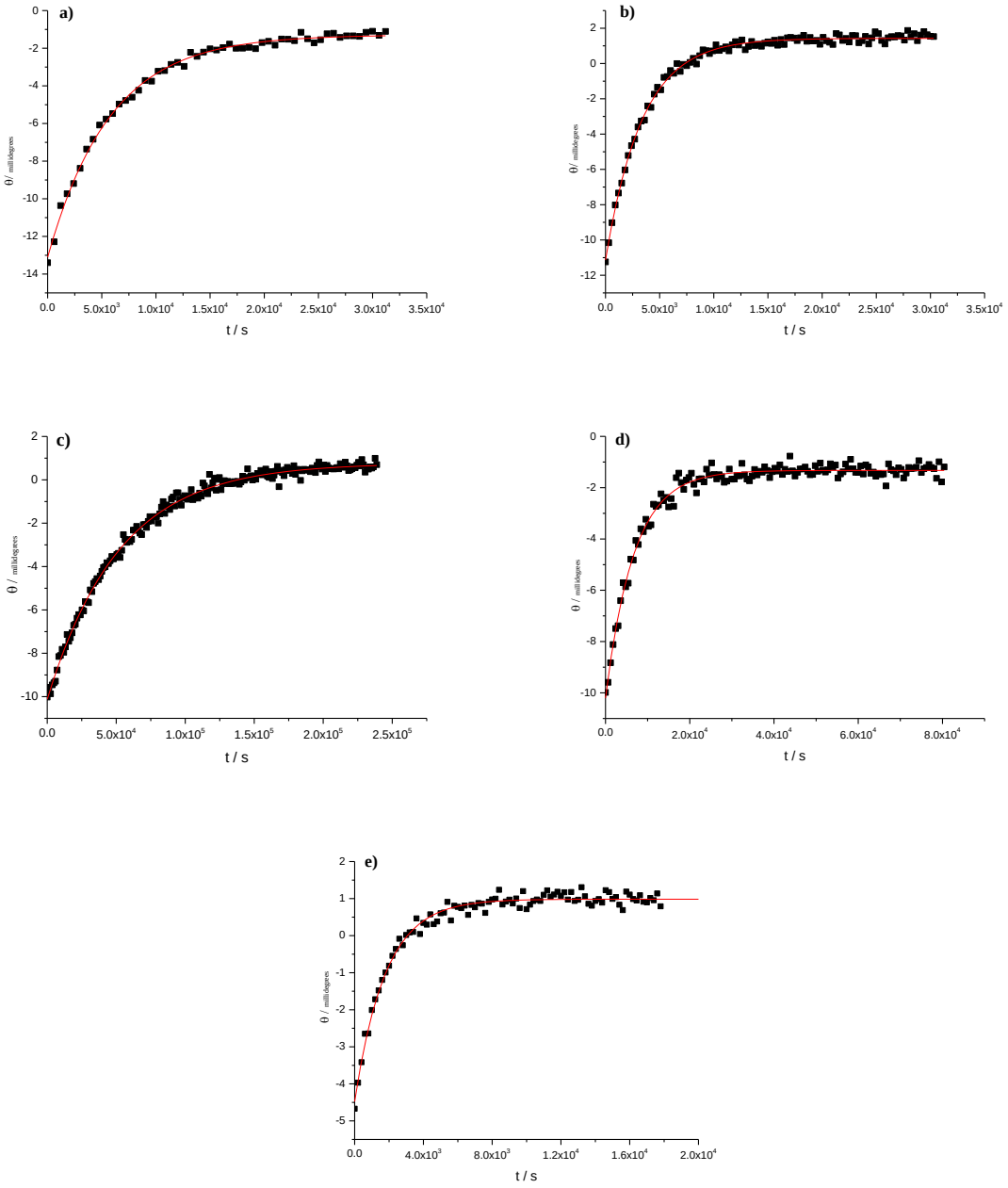

Figure 4.2: The ellipticities of a) **4.1** at 262 nm, b) **4.2** at 265 nm, c) **4.3** at 268 nm, d) **4.4** at 290 nm and e) **4.5** at 263 nm versus time. Solid lines are fits in terms of the first-order rate law.

Figure 4.2 shows that the first-order rate law reproduces the data for all compounds well. The observed phenomenological pseudo-first-order rate constants for loss of ellipticity k_θ were obtained by plotting the ellipticity versus time in terms of the first-order-rate equation (Equation 4.1).

$$\theta_t = \theta_{fin} + \Delta\theta * e^{-k_\theta t} \qquad \textbf{Equation 4.1}$$

Here θ_t is the ellipticity at time t, $\theta_{\text{fin}}$is the final ellipticity, $\Delta\theta$ represents the difference between the ellipticity at time zero and θ_{fin}, and k_θ is the observed pseudo-first-order rate constant for loss of ellipticity.

Using Equation 4.1, the pseudo-first-order rate constants k_θ for loss of ellipticity of compounds **4.1**-**4.5** in aqueous solution were determined and these are listed in the Appendix. By using different concentrations of buffer (pH 7.4, 0.9 M *I*), it was found that by increasing the concentration of buffer the rate constant k_θ also increases. Therefore, the racemisation proceeds via a general-base catalysed pathway (Equation 4.2).

$$k_{obs} = k_0 + k_{OH^-}\left[OH^-\right] + k_{H_3O^+}\left[H_3O^+\right] + k_{buffer}[\text{buffer}] \qquad \textbf{Equation 4.2}$$

where k_0 is the rate constant for the non-catalysed reaction, k_{OH^-} and k_{H3O^+} are the rate constants for the catalysed reaction by base and hydronium, respectively, which is obtained from the intercept (k_{in}), while k_{buffer} is the second-order rate constant for the buffer catalysed loss of ellipticity, which is obtained from the slope, and k_{obs} is the rate constant for the observed reaction.

4.2.1.2 Relation between base-catalysed hydrolysis and racemisation

The rate constants for the loss of ellipticity of acetylated 2-thiohydantoins were determined by CD spectroscopy in phosphate buffer. The acetyl group on the N-1 position is liable to be hydrolysed even in mild acid and base medium. During the racemisation process, it was noticed that the absorbance of enantioenriched compounds **4.1**-**4.5** in CD spectroscopy decreases over time (Figure 4.3). Therefore, it was important to study the hydrolysis under the same conditions as those used for the racemisation studies (Chapter 3).

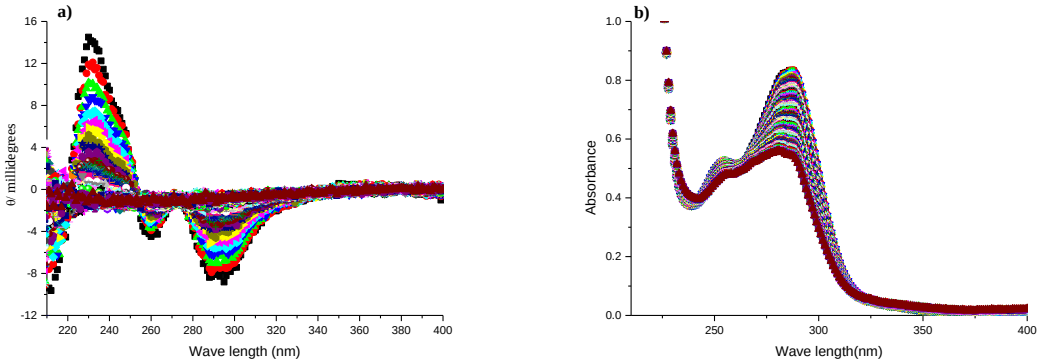

Figure 4.3: Time-resolved a) ellipticity and b) absorbance of **4.4**.

From Figure 4.3 it is clear that the loss of ellipticity is complete before the hydrolysis process is completed. Furthermore, the rate constant for loss of ellipticity is higher than the rate constant for hydrolysis of **4.1**, **4.2**, **4.4** and **4.5**. However, the loss of ellipticity of **4.3** is quite slow, though still faster than its hydrolysis. Scheme 4.4 illustrates the relation between the racemisation and hydrolysis processes.

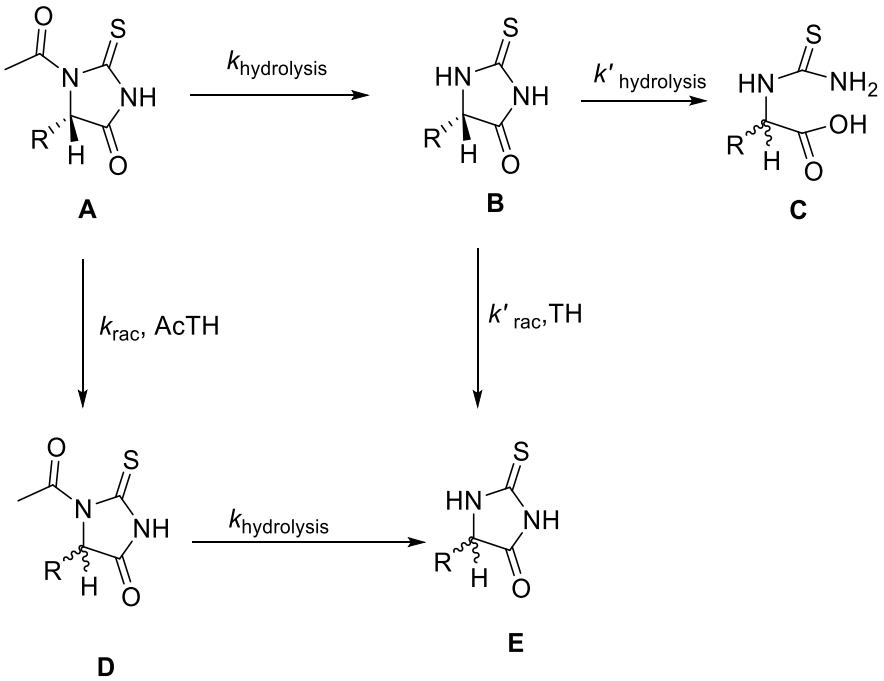

Scheme 4.4: Competition between hydrolysis and racemisation.

From Chapter 3, it has been explained that compounds **4.1**-**4.6** undergo base-catalysed hydrolysis to produce 5-substituted 2-thiohydantoin (**B**) and these continue to undergo

hydrolysis to obtain a ring-opened compound (**C**) (Scheme 4.4). In fact, the rate constants of racemisation of 5-substituted 2-thiohydantoins (**B**) are much faster than those of the 5-substituted 1-acetyl-2-thiohydantoins (**A**) $k_{rac\ (TH)} >> k_{rac\ (AcTH)}$.[16] To identify the real rate constants of racemisation of each 5-substituted 1-acetyl-2-thiohydantoin, the rate constants for the loss of ellipticity, which have been obtained by CD spectroscopy, have to be corrected for the effect of the hydrolysis process. For $k_{rac\ (TH)} >> k_{rac\ (AcTH)}$, k_{θ} is the sum of the rate constants of racemisation and the rate constants of hydrolysis (Equation 4.3).

$$k_{\theta} = k_{rac} + k_{hyd} \qquad \textbf{Equation 4. 3}$$

From Equation 4.3

$$k_{\mathrm{rac}} = k_{\theta} - k_{\mathrm{hyd}} \qquad \textbf{Equation 4. 4}$$

Where k_{θ} is the rate constant for the loss of ellipticity, corresponding to racemisation and hydrolysis together, k_{rac} is the rate constant for racemisation and k_{hyd} is the rate constant for hydrolysis.

Using Equation 4.1, the pseudo-first-order rate constants for loss of ellipticity in different concentrations of phosphate buffer k_{θ} and the rate constant of hydrolysis k_{hyd} at the same conditions were determined. Equation 4.4 was subsequently used to calculate k_{rac} for every single concentration of phosphate buffer by calculating the margin of error. k_{rac} for **4.1**-**4.5** were then plotted versus the concentration of the basic component of the H_2O-phosphate buffer to determine the slope and intercept by fitting a straight line to the data (Figure 4.4).

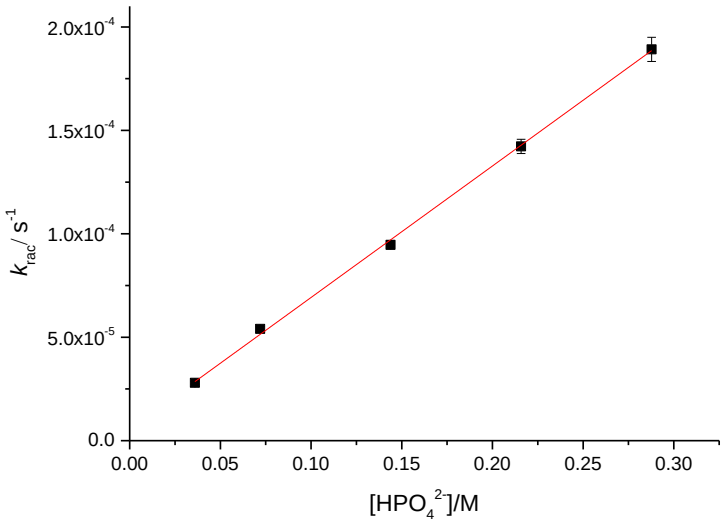

Figure 4.4: Observed pseudo-first-order rate constants for racemisation of **4.4** calculated by Equation 4.4 for every single concentration of buffer, and plotted versus the concentration of the basic component of H_2O-phosphate buffer (0.9 M *I*, pH 7.4 at 37 °C)**.**

The pseudo-first-order rate constants k_{θ}, k_{rac} and k_{hyd} for **4.1** were plotted versus the basic component of phosphate (Figure 4.5). In the previous section the k_{θ} in H_2O and D_2O-phosphate buffers were plotted, therefore here the k_{θ} in D_2O is not included. However, Figure 4.5 shows that k_{rac} is determined by k_{θ} for **4.1**. The same is true for **4.2**-**4.5**.

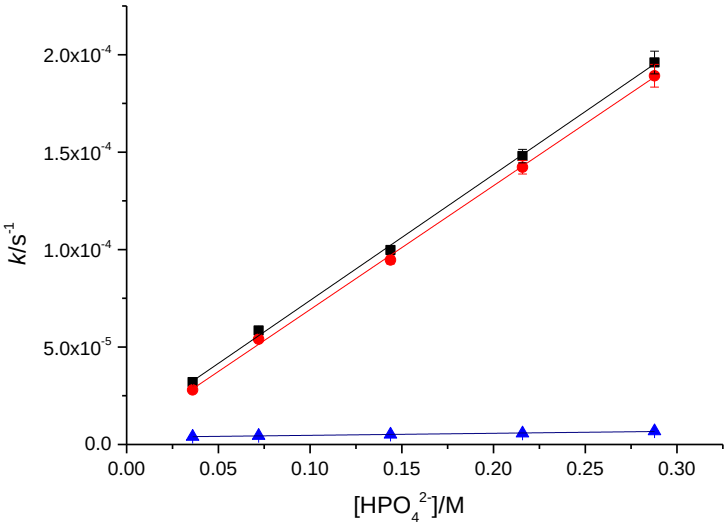

Figure 4.5: The relation between rate constants of (■) k_{θ}, (●) k_{rac} and (▲) k_{hyd} for buffer catalysed racemisation of **4.1** in H_2O phosphate buffers (0.9 M *I*, pH 7.4 at 37 °C).

Figures 4.4 and 4.5 show that the rate constants for the loss of ellipticity k_{Θ}, racemisation k_{rac} and hydrolysis k_{hyd} increase linearly versus the concentration of the basic component of phosphate buffer (0.9 M *I*, pH 7.4 at 37 °C). The hydrolysis process discussed in Chapter 3 for **4.1**, **4.2**, **4.4** and **4.5** are slow in comparison with the racemisation. This is obvious from Figure 4.5 in that k_{rac} is slightly less than k_{Θ} for **4.1** and the same is true for **4.2**, **4.4** and **4.5**. On the other hand, the rate constants for racemisation, k_{rac}, of **4.3** is quite low in comparison with the rest of the 5-substituted 1-acetyl-2-thiohydantoins, and the difference between the rate constants for hydrolysis and racemisation is less. The second-order rate constants k_{Θ}, k_{hyd} and $k_{rac}(=k_{obs}-k_{hyd})$, which were determined from the slopes for **4.1**-**4.5**, and k_{in} from the intercept of k_{rac}, are shown in Table 4.1.

Table 4.1: Second-order rate constants k_{Θ}, k_{hyd} and k_{rac} for buffer HPO_4^{2-} catalysed loss of ellipticity, hydrolysis and racemisation, respectively, and the combined uncatalysed, deuteroxide catalysed and hydronium catalysed k_{in} for **4.1**-**4.5** in H_2O-phosphate buffers (0.9 M *I*, pH 7.4 at 37 °C).

Substrate	$k_{\Theta\ (H2O)}$ / 10^{-6} s^{-1} M^{-1}	$k_{hyd,\ H2O}$ / 10^{-6} s^{-1} M^{-1}	$k_{rac,\ H2O}$ / 10^{-6} s^{-1} M^{-1}	$k_{in\ (rac.)}$ / 10^{-6} s^{-1}
4.1	763 ± 29	29.9 ± 1.0	735 ± 30 [a]	6.5 ± 2.5
4.2	1356 ± 86	10.2 ± 0.5	1347 ± 86 [a]	9.3 ± 6.7
4.3	61.3 ± 9.4	23.3 ± 0.08	45.0 ± 9.0 [a]	0.4 ± 1.7
4.4	646 ± 19.4	10.5 ± 0.6	636 ± 19 [a]	5.7 ± 1.4
4.5	2495 ± 131	30.7 ± 0.7	2465 ± 131 [a]	35.0 ± 9.0

[a]) Standard errors calculated according to Equation 4.8

From Table 4.1, the hydrolysis processes are being affected by substituents at the C-5 position which is explained in terms of the effect of steric hindrance on the hydrolysis.[17] There is a big difference between the rate constants for base-catalysed hydrolysis and base-catalysed racemisation of **4.1**-**4.5**, as can be seen in Table 4.1. Generally, because the rate constants for loss of ellipticity are much higher than the rate constants for hydrolysis, the rate constants for racemisation similarly increase or decrease depending on substituents. The order of the rate constants for racemisation k_{rac} is **4.5**>**4.2**>**4.1**>**4.4**>**4.3**. For comparison, the order of the rate constants for hydrolysis is **4.1>4.5>4.4>4.3>4.2**.

Because the acetyl group at the N-1 position is present on all compounds, the effect of acetyl on the racemisation for all compounds is similar. However, the variable substituents on the stereogenic centre have an effect on the rate constant for loss of ellipticity, as can be clearly seen in Table 4.2. The rate constants for racemisation is also dependent on the bulkiness and electronic effect of substituents at the stereogenic centre. The combined effects of substituents are analogous to the effects on the rate constants for the racemisation of amino acids which follow the order Ala>Leu>Ile>Val.[18]

Compounds **4.1** and **4.3** with methyl and isopropyl substituents at the C-5 position, respectively, display rate constants for racemisation **4.1** > **4.3**, which is similar to the order for corresponding amino acids Ala > Val. The compoundracemising fastest is **4.5**, which is also substituted with an aliphatic substituent with the presence of a sulphur atom. It is clear that the sulphur atom promotes the racemisation of compound **4.5** during the proton transfer reaction in the presence of base. The sulphur will accelerate the deprotonation because of its inductive electronegative contribution.[19] Likewise, sulphur can promote C-H acidity, as reported by Barber and Jones[20] for base-catalysed racemisation of methionine. The authors also explained the reason for the increase in racemisation by sulphur in methionine by proposing that the π orbital of the delocalised enolate overlaps with the d orbital of sulphur.[19, 20]

Benzyl-substituted thiohydantoin **4.2** racemises two times faster than **4.4**. The aryl group, substituted at the 5-position, can act as an electron sink to stabilise the developing carbanion in the transition state, reducing $\Delta H^{\neq}$.[21] Unfortunately, compound **4.6** racemised during the preparation, confirming how the different substituent groups affect the racemisation. The phenyl group on the asymmetric α-carbon accelerates the racemisation because of resonance processes which stabilise the carbanion.[22]

The H/D exchange process for compound **4.6** was studied using ^{1}H-NMR spectroscopy and was shown to be much faster than for other compounds (*vide infra*). Reist *et al*.[7] reported the rate constants for racemisation of 5-phenylhydantoin in deuterated-phosphate buffer to be 188, 342 and 1883 times faster than 5-benzyl-, 5-methyl- and 5-isopropylhydantoin, respectively. The k_{in} for **4.1**, **4.2**, **4.4** and **4.5** are zero within the margin of error in deuterated-phosphate buffer pH* 7.4. **4.3** racemises too slowly and k_{in} is not so different from the values found for the other compounds in the series. Therefore, specific base catalysis can be discounted in deuterated phosphate buffer pH* 7.4. However, the k_{in} is significant within the margin of error in the non-deuterated phosphate buffer pH 7.4 and higher than in the deuterated phosphate buffer pH* 7.4.

4.2.1.3 Solvent kinetic isotope effects on the racemisation of 5-substituted 1-acetyl-2-thiohydantoins

The solvent kinetic isotope effect for the racemisation of hydantoins has been reported previously.[7, 8] The rate constants for loss of ellipticity of compounds **4.1**-**4.5** were determined using CD spectroscopy in different concentrations of phosphate buffer at pH 7.4 in both H_2O and D_2O. The pseudo-first-order rate constants for loss of ellipticity were obtained using varying concentrations of buffer. Upon increasing the concentration of buffer, the rate constant k_θ increased, confirming general-base catalysis for loss of ellipticity. The solvent kinetic isotope effect can be estimated by dividing the second-order rate constants for loss of ellipticity in non-deuterated phosphate buffer ($k_{\theta\,(H_2O)}$) by the second-order rate constants for loss of ellipticity in deuterated phosphate buffer ($k_{\theta\,(D_2O)}$), for compounds where $k_{hyd} << k_\theta$.

Therefore, the second-order rate constants for loss of ellipticity were obtained by plotting the observed rate constants of racemisation versus the concentration of the basic component of phosphate buffer in H_2O and D_2O based buffers (Figure 4.6).

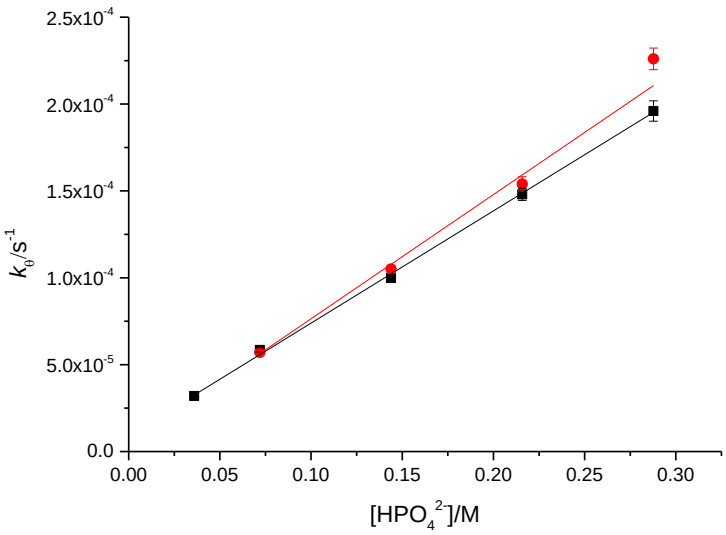

Figure 4.6: Second-order rate constants for the buffer catalysed loss of ellipticity for **4.4** in (■) H_2O and (●) D_2O phosphate buffers (0.9 M *I*, pH and pH* 7.4 at 37 °C).

Figure 4.6 shows the linear increases of pseudo-first-order rate constants k_θ for **4.4** against the concentration of basic component of phosphate buffer. The slopes in Figure 4.7 for compound

4.4 and the rest of the compounds in H_2O and D_2O phosphate buffer represent the second-order rate constants k_θ (figures shown in Appendix of Chapter 4). The intercept gives the sum of the contribution of $k_{in} = k_0 + k_{OH^-}[OH^-] + k_{H_3O^+}[H_3O^+]$ which represent the uncatalysed, specific-base-catalysed, and specific-acid-catalysed rate constants for the loss of optical activity. The comparison of rate constants in non-deuterated and deuterated medium illustrates the solvent kinetic isotope effect on racemisation of **4.1**-**4.5**, as shown in Table 4.2. For the results of the solvent kinetic isotope effect, we used the phenomenological rate constants k_θ to approximate the mechanistic rate constants k_{rac}.

Table 4.2: Second-order rate constants for buffer catalysed loss of ellipticity for the combined uncatalysed, deuteroxide catalysed and hydronium catalysed racemisation of **4.1**-**4.5** in H_2O and D_2O phosphate buffers (0.9 M *I*, pH and pH* 7.4 at 37 °C).

Subs.	k_θ H_2O / 10^{-6} s^{-1} M^{-1}	k_{in} H_2O / 10^{-6} s^{-1}	k_θ D_2O / 10^{-6} s^{-1} M^{-1}	k_{in} D_2O / 10^{-6} s^{-1}	$k_{\theta,\ H_2O}$/ $k_{\theta,\ D_2O}$
4.1	763 ± 29	16.5 ± 2.3	811.44± 66.37	8.86 ± 8.38	0.94 ± 0.03[a]
4.2	1356 ± 86	14.0 ± 6.7	1579 ±78	-10.2 ± 9.2	0.86 ± 0.02[a]
4.3	61.3 ± 9.4	6.6 ± 1.5	53.5 ± 4.0	3.4 ± 0.8	1.15 ± 0.20[a]
4.4	646 ± 19	9.3 ± 1.4	715 ± 43	4.9 ± 4.9	0.90 ± 0.03[a]
4.5	2495 ± 131	41.7 ± 9.0	3007 ± 19	-2.4 ± 2.0	0.83 ± 0.04[a]

[a]) Standard errors calculated using Equation 4.7

Table 4.2 shows small inverse solvent kinetic isotope effects for compounds **4.1**, **4.2**, **4.4** and **4.5** and a small normal kinetic isotope effect for **4.3** with a bigger margin of error than for the rest of the compounds. The solvent kinetic isotope effect describes the involvement of the solvent in the rate determining step of the reaction. The rate constants of racemisation in deuterated phosphate buffer and non-deuterated phosphate buffer had been determined for 5-substituted hydantoin previously.[23, 8, 7]

Narduolo[8] has reported the pseudo-first-order rate constants for racemisation of 5-benzylhydantoin in non-deuterated and deuterated phosphate buffer pH and pH* 7.2 (Table 4.3). The phenomenological rate constants k_θ for hydantoins can be assumed to be equal to the mechanistic rate constants k_{rac} for racemisation of substituted hydantoin because no hydrolysis

process has been identified during the racemisation of substituted hydantoin, as reported by Reist *et al*. and Narduolo.

Table 4.3: Rate constants of racemisation of (*S*)-5-benzylhydantoin in D_2O and H_2O phosphate buffers pH and pH* 7.2, respectively (0.25 M, 0.5 M *I*, at 60 °C).[8]

Hydantoin C(5) Substituent	k_{racH} / 10^{-6} s^{-1}	k_{racD} / 10^{-6} s^{-1}	k_H/k_D
$PhCH_2$	167.3 ± 1.3	175.0 ± 0.2	0.96 ± 0.01

Table **4.2** and **4.3** show small differences for the rate constants of thiohydantoin and hydantoin in non-deuterated and deuterated phosphate buffers. Reist *et al*.[7] reported the solvent kinetic isotope effect (k_{H_2O} / k_{D_2O}) to be 1.13 ± 0.05 and 1.24 ± 0.08 for (*S*)-5-phenylhydantoin and *(S)*-5-benzylhydantoin, respectively, in a 50/50 (v/v) mixture of phosphate buffer and DMSO. The inverse solvent kinetic isotope effects for **4.1**-**4.5** in Table 4.2 indicate no involvement of solvent as a proton donor in the rate determining step in the reaction, indicating that the S_E2 mechanism is unlikely.

4.2.1.4 Brønsted plot for proton transfer

The proton transfer from the chiral carbon of thiohydantoin to the base and the effect of buffer strength on the rate constants for racemisation of **4.1** were studied. The racemisation was studied using acetate, phosphate, TRIS, borate and methyl amine buffer over the pH 5.0-9.7 at 37 °C. Furthermore, racemisation was studied in the same conditions as those used to study hydrolysis for **4.1** (Chapter 3). Pseudo-first-order rate constants for racemisation were determined in the same conditions as those used for non-deuterated phosphate buffer (0.9 M *I*, pH 7.4 at 37 °C). The second-order rate constants for loss of optical activity were obtained using Equation 4.2. Equation 4.4 was used to determine the rate constants for racemisation corrected for hydrolysis (Chapter 3) in acetate pH 5.0, phosphate pH 7.4, TRIS buffer pH 8.2 and methyl amine pH 9.7. Pseudo-first-order rate constants of racemisation, obtained by Equation 4.1, were plotted versus the concentration of basic component of acetate, phosphate, TRIS and methyl amine buffers (Figure 4.7).

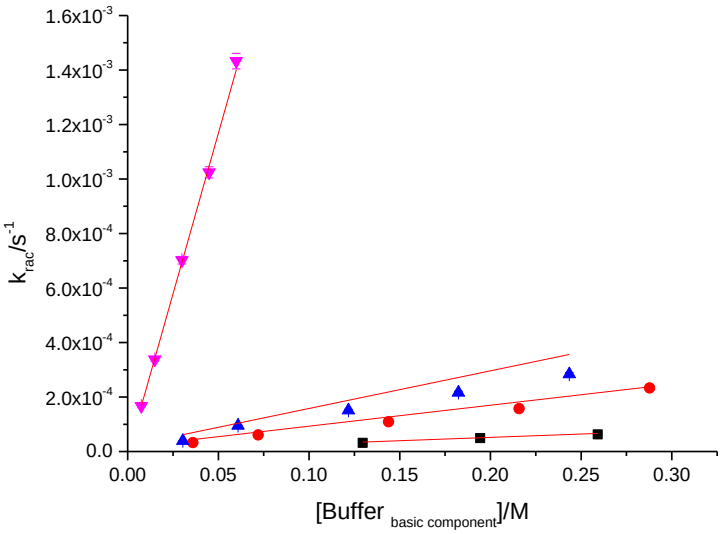

Figure 4.7: Dependence of the apparent first-order rate constants of **4.1** on the concentration of the basic component of **(■)** acetate (pH 5.0), **(●)** phosphate (pH 7.4) **(▲)** TRIS (pH 8.2) and **(▼)** methyl amine (pH 9.7) buffers.

Figure 4.7 shows that the pseudo-first-order rate constants for the racemisation of **4.1** plotted versus the concentration of the basic component of acetate, phosphate, TRIS and methylamine buffers increase linearly with straight line fits passing through the origin. This indicates that general-base catalysis of racemisation occurs in all four buffers. The second-order rate constants for racemisation k_{rac} were determined for acetate, phosphate and TRIS buffer from the slope of the linear plot using Equation 4.2 (Table 4.4). Equation 4.4 could not be used to determine k_{rac} in methyl amine buffer (pH 9.7) because k_{hyd} was slightly higher than k_{o}.

Table 4.4: The pK_a and second-order rate constants for racemisation **4.1** in acetate, phosphate, TRIS and methyl amine buffers (0.9 M *I*) at, pH 5.0, 7.4, 8.2 and 9.7, respectively

Buffers Con./ mM	pK_a	$k_{rac\ (H_2O)}$ / 10^{-6} s^{-1} M^{-1}	k_{in} / 10^{-6} s^{-1}
Acetate	4.59[a]	253.5 ± 13.0	-0.9 ± 2.3
phosphate	6.8[b]	735± 30	6.5 ± 2.5
TRIS	7.88[a]	1248 ± 139	10.2 ± 9.3

a) pK_a at 1 M ionic strength at 37 °C.[24, 25]

b) As reported previously.[11, 26]

To quantify the sensitivity of the general-base catalysis to changing the strength of the catalytic base, the Brønsted equation (Equation 4.5) was used.

$$\log k_{obs} = \beta \times pKa + C \qquad \textbf{Equation 4.5}$$

where logk_{obs} is the logarithm of the observed second-order rate constant in different buffers determined using CD spectroscopy, pK_a is the dissociation constant of every buffer at ionic strength 0.9 M, according to Table 4.4 at 37 °C, and β is the measure of the sensitivity of the racemisation reaction to change in the strength of the base. Therefore, the logarithm of the second-order rate constants for racemisation of **4.1** in acetate, phosphate, TRIS and methylamine were plotted versus the dissociation constants of **4.1** in these same buffers (Figure 4.9).

The second-order rate constants for ellipticity loss of **4.1** and for hydrolysis in acetate, phosphate, TRIS and methyl amine buffers were plotted versus the dissociation constant of the buffers (Figure 4.8).

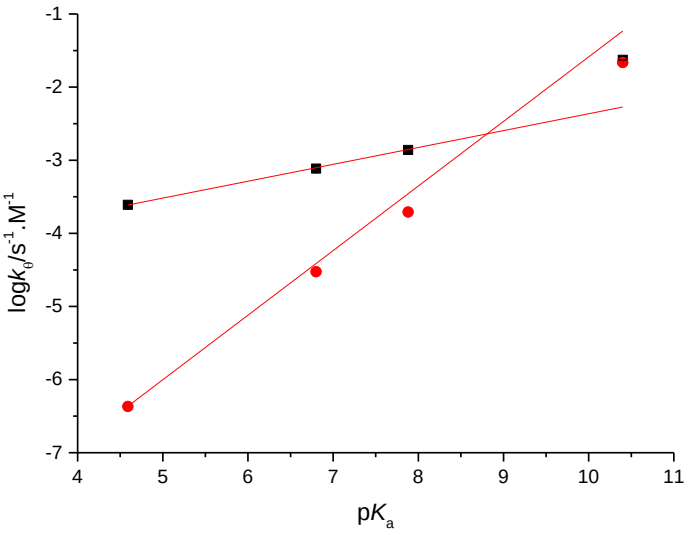

Figure 4.8: Brønsted plot for base catalysis for (■) loss of ellipticity and (●) hydrolysis of **4.1** (0.9 M *I*, 37 °C).

Figure 4.8 shows overlapping of the second-order rate constants for ellipticity loss and the second-order rate constant of hydrolysis at pH 9.7 in trimethylamine buffer. Therefore, Equation 4.4 gives negative results for the determination of the second-order rate constant of racemisation in methyl amine buffer. The logarithm of the second-order rate constants of racemisation of **4.1** in acetate, phosphate and TRIS were plotted versus the dissociation constants of acetate, phosphate and TRIS buffers (Figure 4.9).

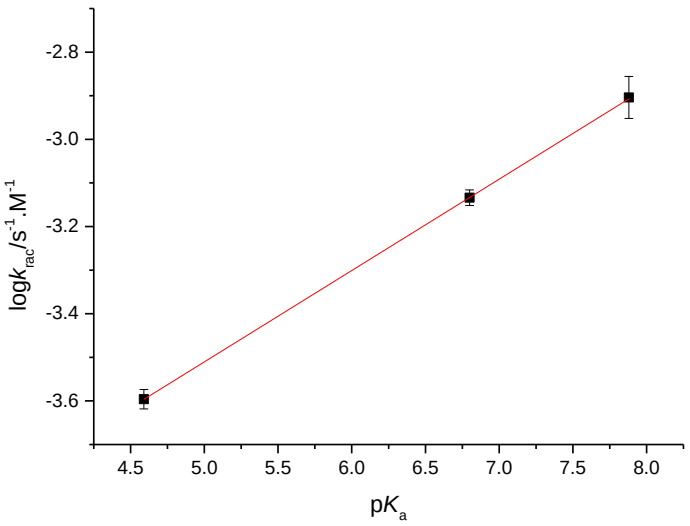

Figure 4.9: Brønsted plot for base-catalysed racemisation of **4.1**.

Figure 4.9 shows an increase in second-order rate constants for racemisation with increasing pK_a. A Brønsted β of 0.21 ± 0.0008 was determined from the slope of the second-order rate constants for racemisation versus pK_a of buffers. A β-value of 0.21 ± 0.0008 indicates an early transition state. Lazarus[11] reported a β-value of 0.59 for the base-catalysed racemisation of L-5-benzylhydantoin and 0.51 for L-5-benzyl-3-methylhydantoin. Narduolo obtained β-values for L-5-benzyl-3-methylhydantoin of 0.57 and 0.59 at 25 and 60 °C, respectively. Our value is thus significantly lower, which we attribute to deprotonation of thiohydantoin at the N-3 position. The β-value for neutral **4.1** will be calculated in the next section according to the dissociation constant of **4.1**.

Different concentrations of borate buffer were used and the rate constants for racemisation of **4.1** were determined. The pseudo-first-order rate constant for loss of ellipticity were plotted versus the concentration of the basic component of borate buffer (Figure 4.10).

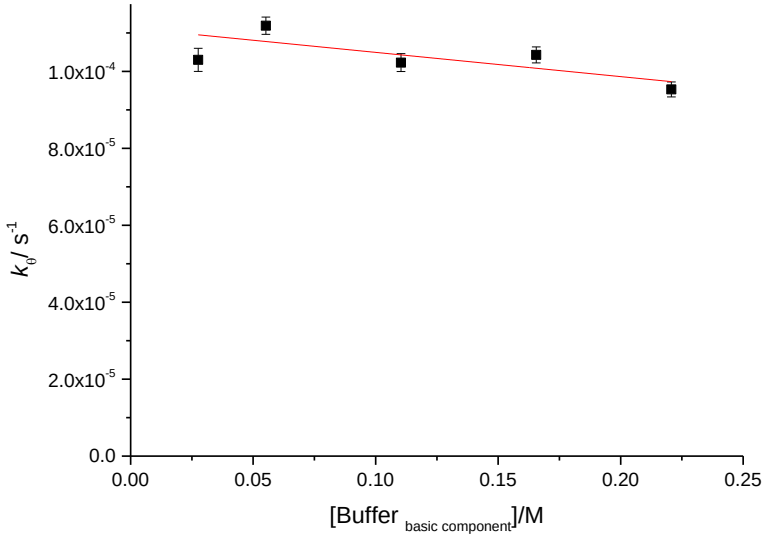

Figure 4.10: First-order rate constants for racemisation against the basic component of borate buffer for **4.1** in H_2O-phosphate buffers (0.9 M *I*, pH 9.3 at 37 °C).

Figure 4.10 shows that the racemisation is apparently not catalysed by the basic components of borate buffer; in fact we obtained a slope of (-6.301 ± 2.972) x 10^{-5} s^{-1} M^{-1}. In contrast, general-base catalysis was observed for substituted hydantoin by Narduolo[8] in borate buffer.

4.2.1.5 The effect of ionisation at the N-3 position on the rate constant of racemisation

The reason for the low Brønsted β for the racemisation of **4.1** may be due to the acidity of the N-3 of thiohydantoin, leading to the possibility of ionisation (Scheme 4.5). Lazarus[27] has described the kinetic equivalence of general-base catalysis of the neutral form and rate determining protonation of the anionic form of 5-benzylhydantoin, which must be taken into consideration.[11]

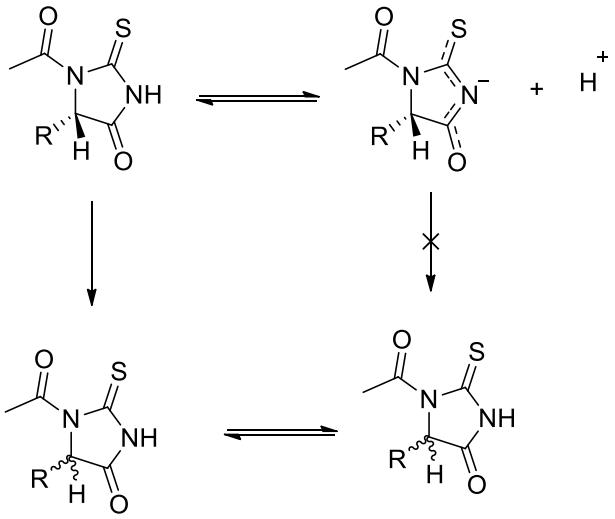

Scheme 4.5: Ionisation of 5-substituted 1-acetyl-2-thiohydantoins at the N-3 position.

In Scheme 4.5, the negative charge at N-3 impedes racemisation compared to the protonated compound and the acidity of the proton at the stereogenic centre decreases because of the presence of the negative charge.[17] All second-order rate constants of racemisation in acetate, phosphate, TRIS and methyl amine were determined without taking deprotonation into account. The dissociation constant pK_a^{NH} of 6.95 has been previously reported for **4.1** in water, which was used in the present work.[17] This value was used to correct k_{rac} for the deprotonation of thiohydantoin (Table 4.5).

Table 4.5: The pK_a and second-order rate constants for racemisation of total and protonated **4.1** in acetate, phosphate, TRIS and methyl amine buffers (0.9 M *I*) at pH 5.0, 7.4, 8.2 and 9.7, respectively.

Buffer pK_a	pH	k_{rac} / 10^{-6} s^{-1} M^{-1}	Fraction protonated	$k_{rac,\ corrected}$ / 10^{-6} s^{-1} M^{-1}
4.59[a]	5.0	253.5 [c] ± 13.0 [d]	98.9%	256.3 ± 13.2
6.8[b]	7.4	734.8 [c] ± 30.1[d]	26.2%	2806 ± 115
7.88[a]	8.2	1248[c] ± 139[d]	5.3%	23400 ± 2600

a) pK_a at 1 M ionic strength at 37 °C.[31, 32]

b) The value reported previously.[11, 26]

c) Values obtained using Equation 4.4.

d) Standard errors according to Equation 4.8.

The methyl amine buffer was not used in Table 4.5 because Equation 4.4 cannot be applied when the second-order rate constant of hydrolysis is higher than the rate constant of loss of ellipticity. Therefore, the logarithm of the corrected second-order rate constants for racemisation of neutral **4.1** were plotted as a function of buffer p*K*a for acetate, phosphate and TRIS only (Figure 4.11).

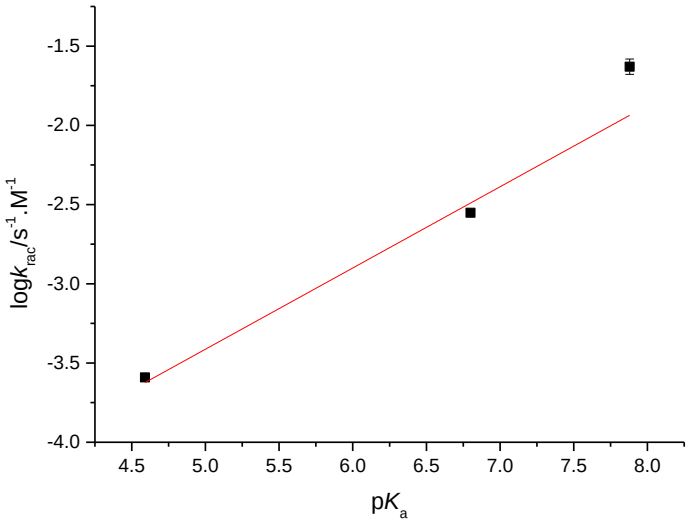

Figure 4.11: Brønsted plot for base-catalysed racemisation of protonated **4.1**.

The Brønsted β for racemisation of the protonated form of **4.1** was found to be 0.51 ± 0.085, in agreement with general-base catalysis of racemisation and suggests that the proton at the 5-position is half way between thiohydantoin and the buffer in the transition state (Scheme 4.6).

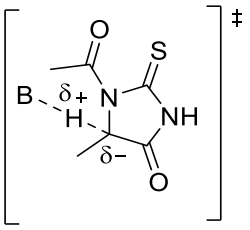

Scheme 4.6: Transition state of general-base catalysis of **4.1** based on the Brønsted β-value from Figure 4.11.

4.2.2 Racemisation of tri-substituted 2-thiohydantoins

In order to show the effects of the different substituents on the three positions of thiohydantoin on the rate constants for racemisation, different substituted 2-thiohydantoins were prepared (Chapter 2). The previous literature reported that the N_3-H group on hydantoin and thiohydantoin is more acidic than N1-H.[28, 29] Therefore, the substituents on the N-3 or N-1 or both change the pK_a and the observed rate constants of racemisation. The solvent kinetic isotope effect of tri-susbtituuted 2-thiohydantoin was also studied.

4.2.2.1 Determination of the rate constant for racemisation

Two enantioenriched trisubstituted thiohydantoin derivatives were prepared to study the rate of racemisation in deuterated and non-deuterated buffer (Scheme 4.7).

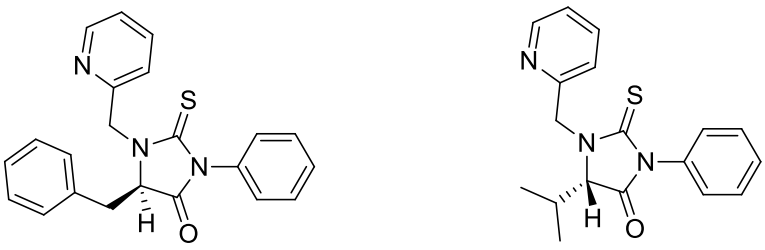

4.7 **4.8**

Scheme 4.7: The chemical structures of compounds **4.7**-**4.8**

To deal with the lack of solubility of both thiohydantoins **4.7** and **4.8**, 10 vol-% acetonitrile and acetonitrile-d_3 were used to be able to observe sufficient signals in CD spectroscopy. The kinetics for the loss of ellipticity for **4.7** and **4.8** were followed using a physiological buffer at pH and pH* 7.4 (0.9 M ionic strength at 37 °C). Low concentrations of total phosphate buffer were used because if the same conditions were used as those for compounds **4.1**-**4.5**, **4.7** and **4.8** would racemise extremely fast. The kinetic study of all enantioenriched compounds was carried out in non-deuterated and deuterated phosphate buffer in mixtures consisting of 90 vol-% phosphate buffer (0.01M, 0.02 M, 0.03 M, 0.04 M, and 0.05 M total phosphate buffer, pH and pH* 7.4) or 10 vol-% of acetonitrile or acetonitrile-d_3. Reactions were monitored at 37 °C using CD spectroscopy (Figure 4.12).

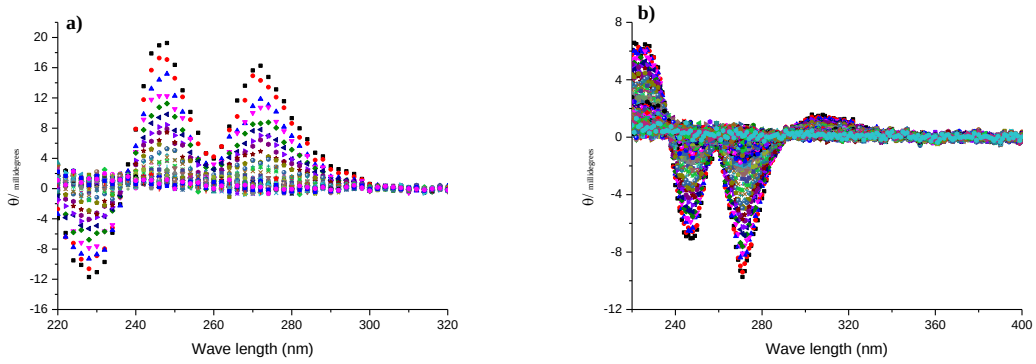

Figure 4.12: CD spectra observed for racemisation of a) **4.7** and b) **4.8**. A stock solution of each compound in acetonitrile and 0.01 M non-deuterated phosphate buffer (10 vol-% and 90 vol-% ratio, respectively; pH 7.4, 1 M *I*) were mixed and the ellipticity was followed at 37 °C as a function of time.

Figure 4.12 shows that ellipticity decreases over time. The ellipticity at 248 and 272 nm for compound **4.7** and at 247 and 271 nm for **4.8** were plotted versus time for every buffer concentration according to Equation 4.1 (Figure 4.13 and Appendix 3).

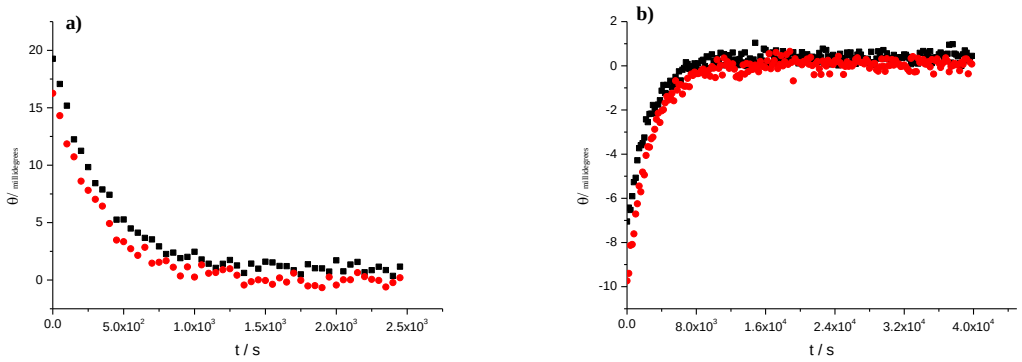

Figure 4.13: Ellipticity as a function of time for compounds a) **4.7** at (■) 248 and (●) 272 nm and b) **4.8** at (■) 247 and (●) 271 nm by using 10 % acetonitrile and 90 % 0.01 M non-deuterated phosphate buffer (pH 7.4, 1 M *I*, at 37 °C).

Figure 4.13 shows that the ellipticity at 248 and 272 nm of compound **4.7** decreases over time. For compound **4.8**, the ellipticity at 247 and 271 nm increases with time. Pseudo-first-order rate constants k_o were determined for the five different concentrations of 0.009 M, 0.018 M, 0.027 M, 0.036 M and 0.045 M total phosphate buffer (0.9 M *I*, pH and pH* 7.4 of non-deuterated and deuterated phosphate buffer). The second-order rate constants were determined by plotting the pseudo-first-order rate constants versus the basic component of the phosphate buffers, as discussed below.

4.2.2.2 Solvent kinetic isotope effect of racemisation

The kinetics of racemisation of compounds **4.7** and **4.8** were studied in non-deuterated and deuterated phosphate buffer to study the mechanism of proton transfer. The racemisation took place rapidly in comparison with compounds **4.1**-**4.5** if the same phosphate buffer concentrations were used (pH 7.4, 09 M *I*, at 37 °C). Therefore, lower concentrations of phosphate buffer were used with constant ionic strength at 37 °C. The pseudo-first-order rate constants for racemisation in non-deuterated and deuterated phosphate buffer pH and pH* 7.4,

(0.9 M *I* at 37 °C) were obtained according to Equation 4.1 (Section 4.2.2.1). The second-order rate constants of racemisation were determined by plotting the observed rate constants for loss of ellipticity in non-deuterated and deuterated phosphate buffer versus the concentration of the basic component of the phosphate buffers (Figure 4.14).

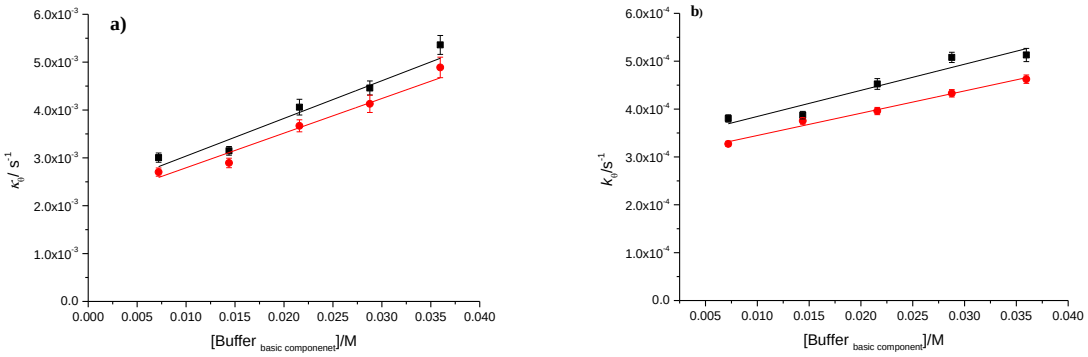

Figure 4.14: Pseudo first-order rate constants for loss of ellipticity for a) **4.7** and b) **4.8** in (■) H_2O and (●) D_2O phosphate buffers (0.9 M *I*, pH and pH* 7.4 at 37 °C).

Figure 4.14 shows a linear correlation of the observed pseudo-first order rate constants for racemisation of **4.7** and **4.8** with the concentration of the basic component of phosphate buffer, suggesting general-base catalysis of racemisation. The solvent kinetic isotope effect was obtained by dividing the second-order rate constants for racemisation in deuterated and non-deuterated phosphate buffer (Table 4.6).

Table 4.6: Second-order rate constants for buffer-catalysed loss of ellipticity k_θ of **4.7** and **4.8** at 272 and 271 nm, respectively, in H_2O and D_2O phosphate buffers (0.9 M *I*, pH and pH* 7.4 at 37 °C) and the solvent kinetic isotope effect.

Substrate	k_θ H_2O / 10^{-6} s^{-1} M^{-1}	k_θ D_2O / 10^{-6} s^{-1} M^{-1}	k_H/k_D
4.7	78700 ± 12700	72400 ± 9800	1.09 ± 0.23[a]
4.8	60 ± 980	4650 ± 320	1.17 ± 0.22[a]

a) Standard errors calculated using Equation 4.7

Table 4.6 shows significant second-order rate constants for loss of ellipticity for **4.7** and **4.8** which are drastically higher than the corresponding rate constants for **4.1**-**4.5**. The high rate constants indicate the effect of substituents at the N-3 position, which is free of substituents in **4.1**-**4.6**. It is also interesting to note that the isopropyl substituent at the C-5 position of **4.8** has a strong rate-retarding effect in comparison with the benzyl substituent of **4.7**. This stronger rate-retarding effect of isopropyl over benzyl was also observed for the rate constant of loss of ellipticity for **4.2 (**1356 ± 86). 10^{-6} s^{-1} M^{-1}, which was much higher than the rate constant for **4.3** ((61.3 ± 9.4). 10^{-6} s^{-1} M^{-1}) (Table 4.1). Compound **4.7,** with an additional substituent at the 3-position loses ellipticity 58 times faster than di-substituted **4.2**. Compound **4.8** loses ellipticity 89 times faster than **4.3**. Bovarnick and Clarke[30] suggested the possibility of conjugation influencing the ease of racemisation.[30]

The solvent kinetic isotope effects for racemisation of **4.7** and **4.8** are 1.09 ± 0.2 and 1.2 ± 0.2, respectively, both are within error from 1. As shown before, the solvent kinetic isotope effects on the racemisation of compounds **4.1**, **4.2**, **4.4** and **4.5** were inverse kinetic isotope effects due to (de) protonation at N-3. The main difference between compounds **4.1**-**4.5** on the one hand and **4.7**-**4.8** on the other hand is that the more acidic position N-H is free of the substituent for **4.1**-**4.6**, while in compound **4.7** and **4.8** the N-H position is substituted by a phenyl group. The partial deprotonation of **4.1**-**4.5** causes the rate of racemisation in H_2O phosphate buffer to be slower and shows an inverse solvent kinetic isotope effect. Similarly, Cabordery *et al.*[23] reported a solvent kinetic isotope effect of 0.77 for 2-(3-(benzyl(methyl)amino)propyl)-3-thioxo-2,3,10,10a-tetrahydroimidazo[1,5-b]isoquinolin-1(5H)-one in 75/25 phosphate buffer pH 2.5 and pD 2.6 and ethanol at 15 °C. There is no depronation at the N-3 position in **4.7** and **4.8** in H_2O-phosphate buffer, therefore, no inverse solvent kinetic isotope effects were observed. In an attempt to explore the significance of the kinetic isotope effect even further, the weighted average of the second-order rate constant for loss of ellipticity as studied at 248 and 271 nm for compound **4.7** and as studied at 247 and 271 for compound **4.8** were calculated. The weighted average of the second-order rate constants k_Θ in H_2O and D_2O phosphate buffer at 248 and 272 nm for **4.7** are (83800 ± 8900). 10^{-6} s^{-1} $M^{-1}$and (70700± 7700). 10^{-6} s^{-1} M^{-1}, respectively. The solvent kinetic isotope effect for loss of ellipticity then become 1.18 ± 0.18 *i.e.* within error margin of 1. This observation suggests no involvement of a proton transfer from water or from the buffer to the substrate in the rate determining step.

From previous literature, the rate constants for racemisation of hydantoin have been reported at both different pH and temperature. It is interesting to compare the rate constants of

substituted 2-thiohydantoin racemisation in the present work with substituted hydantoin rate constants of racemisation from previous work. It has been reported that the sulphur atom in thiohydantoin increases the chiral instability of the enantiomer.[23] Narduolo[8] reported the rate constants of racemisation for various substituted hydantoins in D_2O phosphate buffer (pH 7.2 at 60 °C) (Scheme 4.8).

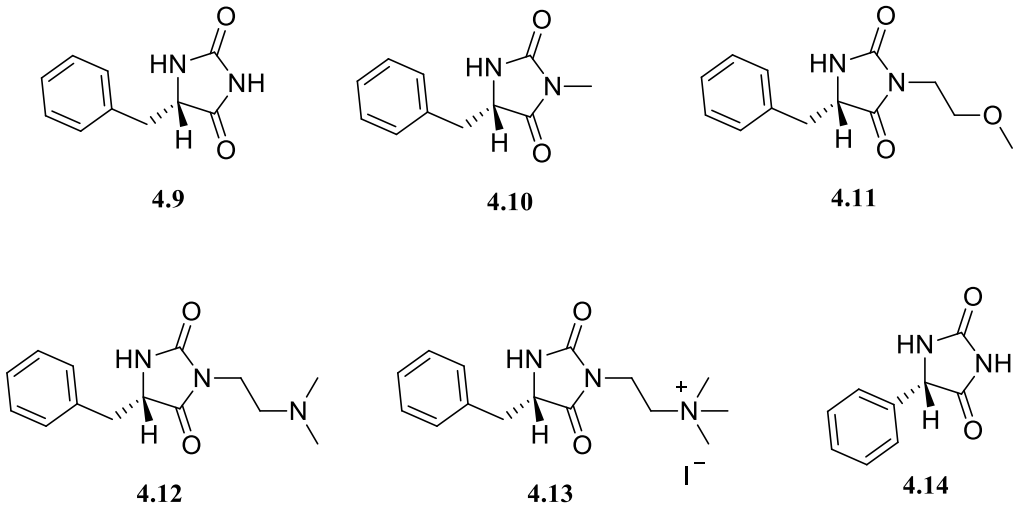

Scheme 4.8: Substituted hydantoin studied by Narduolo.

The racemisation of **4.9** was also studied by Reist *et al*.[7] Narduolo reported the second- order rate constants for racemisation of **4.9**-**4.13** in deuterated phosphate buffer (pH 7.2, 1 M *I*, at 60 °C) (Table 4.7).

Table 4.7: Rate constants for buffer catalysed and for the combined uncatalysed and deuteroxide catalysed racemisation of substituted hydantoins **4.9**-**4.13** in D_2O phosphate buffer (pH 7.2, 1 M *I*, at 60 °C).

Substrate	k_{Θ} D_2O / 10^{-6} s^{-1} M^{-1}	k_{in} / 10^{-6} s^{-1}
4.9	542.2 ± 2.5	17.7 ± 0.5
4.10	342.6 ± 0.9	15.1 ± 0.1
4.11	231.2 ± 1.7	8.6 ± 0.5
4.12	2127.0 ± 9.0	51.1 ± 0.8
4.13	1106.0 ± 19.0	58.3 ± 2.8

From Table 4.7, it is clear that the methyl group substituted at the N-3 position of hydantoin in **4.10** retards racemisation in comparison with unsubstituted hydantoin **4.9**. Similarly, the hydrogen replacement of N-3 by (2-methoxyethyl) (**4.11**) and (2-(dimethylamino) ethyl) (**4.12**) also reduces the rate of racemisation. The phenyl substituent on the N-3 position enhances the rate of racemisation of hydantoin, as previously reported.[30]

Reist *et al.*[7] also determined the pseudo-first-order rate constants for racemisation of compounds **4.9** and **4.14** in H_2O and D_2O phosphate buffer with 50% DMSO (Table 4.8).

Table 4.8: Pseudo-first-order rate constants for buffer catalysed racemisation of **4.9** and **4.14** in 50 % H_2O and D_2O phosphate buffers (0.1 M, 0.22 M *I*, pH and pH* 7.4 and 50% of dimethyl-sulphoxide at 50 °C).

	$k_{rac\ (bffer)}$ H_2O / h^{-1}	$k_{rac\ (bffer)}$ D_2O / h^{-1}	k_H/k_D
4.9	0.12 ± 0.006	0.09 ± 0.02	1.27 ± 1.26
4.14	23.7 ± 3.0	21.1 ± 1.4	1.12 ± 1.12

It is obvious that **4.14** (with phenyl substituent) racemises 199 times faster than **4.9,** showing the differences between the benzyl and phenyl group on the asymmetric carbon. There is also no solvent kinetic isotope effect within the margin of error for **4.9** and **4.14**.

4.2.2.3 Relation between base-catalysed hydrolysis and racemisation

For compounds 4.1-**4.6**, rate constants for racemisation were determined from the rate constants for loss of ellipticity by correcting for the effect of hydrolysis. For compound **4.7**, the absorbance was not noted to decrease during the kinetic experiments because the decrease of ellipticity over time was extremely fast. However, the ellipticity of compound **4.8** decreases more slowly in the buffer at 37 °C, and therefore, the decrease of absorbance in the CD measurements was noted (Figure 4.15). The rate constants for hydrolysis have therefore also been measured by UV-visible spectroscopy under the same conditions as those used for racemisation.

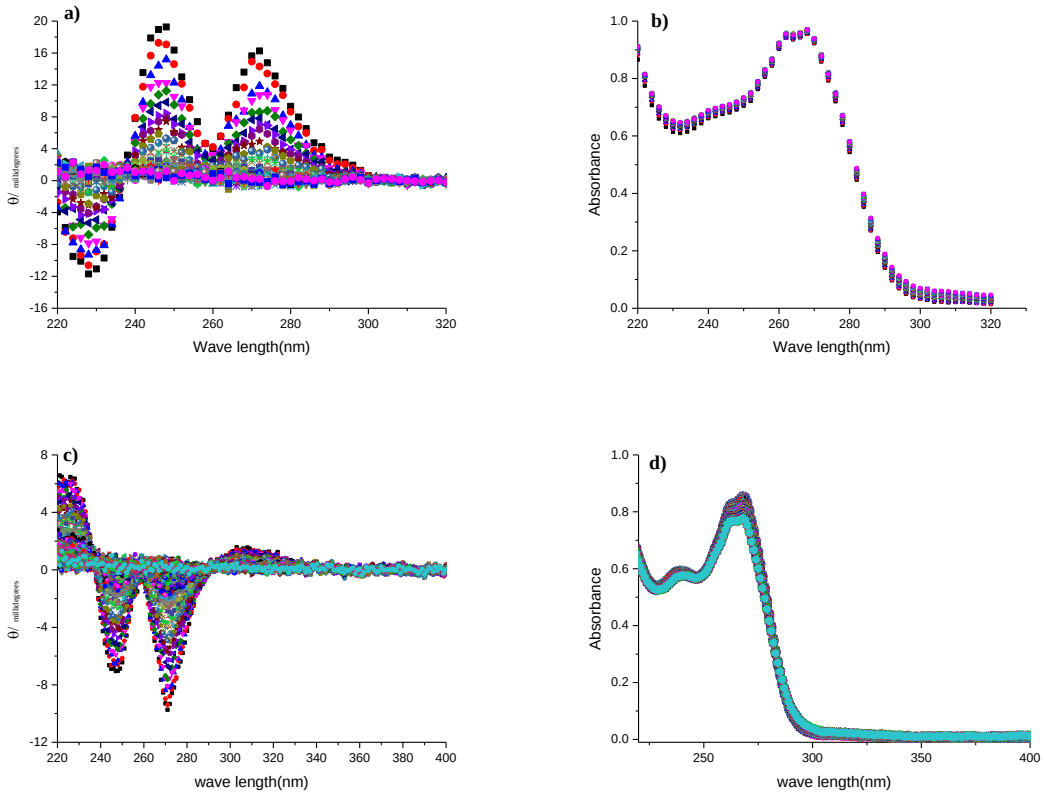

Figure 4.15: CD observation for loss of ellipticity of **4.7** (a) and **4.8** (c) and absorbance of **4.7** (b), and **4.8** (d) as a function of time. A solution of each compound in 10 % acetonitrile was mixed with 90% 0.01 M phosphate buffer (pH 7.4, 1 M *I* at 37 °C) over time.

Figure 4.15 shows very slow hydrolysis for compounds **4.7** and **4.8** during the loss of ellipticity in phosphate buffer **(**pH 7.4, 0.9 M *I* at 37 °C). The rate constants of hydrolysis

were determined for compounds **4.7** and **4.8** by following the reaction using UV-visible spectroscopy under the same conditions as those used in CD measurements.

The rate constants for the loss of ellipticity k_{rac} were plotted for **4.7** and **4.8** versus the concentration of the basic component of phosphate buffer to determine the slope and intercept by fitting the straight line (Figure 4.16).

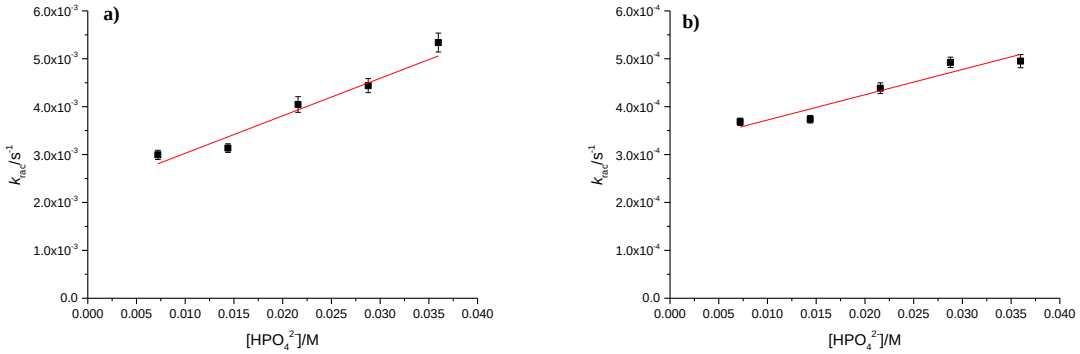

Figure 4.16: Pseudo-first-order rate constant k_{rac} determined by Equation 4.4 for a) **4.7** and b) **4.8** without the effect of hydrolysis and in H_2O phosphate buffers (0.9 M *I*, pH 7.4 at 37 °C).

Compounds **4.7** and **4.8** lose optical activity drastically fast in comparison with compound **4.1**-**4.5** in phosphate buffer (pH 7.4, 0.9 M *I*, at 37 °C) and with only slight hydrolysis during the process (Table 4.9). The second-order rate constants for loss of ellipticity k_{θ} and second-order rate constants for hydrolysis k_{hyd} are compared in Table 4.9.

Table 4.9: Second-order rate constants k_{θ} and k_{hyd} for **4.7** and **4.8** in H_2O phosphate buffers (0.9 M *I*, pH and pH 7.4 at 37 °C).

	k_{θ} / 10^{-6} s^{-1} M^{-1}	k_{hyd} / 10^{-6} s^{-1} M^{-1}
4.7	78700 ± 12700	372 ± 63
4.8	5460 ± 970	167 ± 25

Table 4.9 suggests that the hydrolysis has a negligible effect on the rate constant for the loss of ellipticity.

4.2.2.4 Activation parameters for the racemisation of (*R*)-5-benzyl-3-phenyl-1-(pyridin-2-ylmethyl)-2-thioxoimidazolidin-4-one

The kinetic study of compound **4.7** was carried out at different temperatures in phosphate buffer (pH 7.4, 0.9 M *I*) and the activation parameters for racemisation were determined using the Eyring equation. [31]

$$\ln\left(\frac{k_{\mathrm{rac}}.h}{k_{\mathrm{B}}.T}\right) = -\frac{\Delta H^{\ddagger \ominus}}{R.T} + \frac{\Delta S^{\ddagger \ominus}}{R} \qquad \textbf{Equation 4.6}$$

where k_{rac} is the second-order rate constant for racemisation which is assumed to be equal to the second-order rate constant for loss of ellipticity $k_{\ominus}$ (in s^{-1} M^{-1}), h is Planck's constant, k_b is the Boltzmann constant, R is the gas constant and T is the absolute temperature (in *K).*

The pseudo-first-order rate constants $k_{\ominus}$ were determined in different non-deuterated phosphate buffer concentration (pH 7.4) at 15, 20, 25, 30 and 37 °C, while the second-order rate constants were calculated according to Equation 4.2. The rate constants for the loss of ellipticity were observed to increase with increasing temperature. The pseudo-first-order rate constants for the loss of ellipticity were observed by CD spectroscopy at 15, 20, 25, 30 and 37 °C and plotted versus the basic component of phosphate buffer (pH 7.4, 0.9 M *I*) (Figure 4.17).

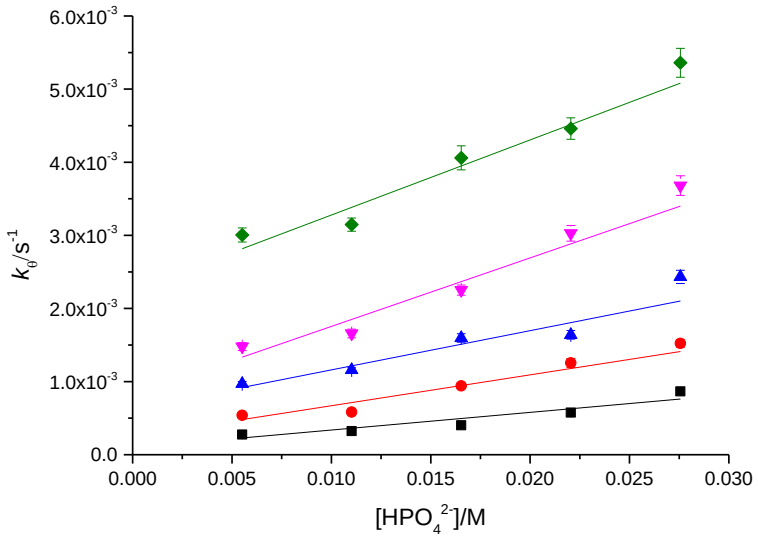

Figure 4.17: Pseudo-first-order rate constants for buffer catalysed racemisation for **4.7** versus basic component of H_2O phosphate buffers (pH 7.4, 0.9 M *I*) at (■) 15, (●) 20, (▲) 25, (▼) 30 and (♦) 37 °C.

Figure 4.17 shows that the loss of ellipticity for **4.7** is highly temperature dependent; the second-order rate constants are reported in the Appendix of Chapter 4. The second-order rate constants for loss of ellipticity were calculated by the weighted average value at 272 and 248 nm by using Equation 4.9 and 4.10. The activation parameters were then determined by plotting In $\left(\frac{k_{rac}.h}{k_B.T}\right)$ versus 1/T using Equation 4.6 to determine the standard enthalpy change for activation $\Delta H^{\ddagger}$ and standard entropy for activation $\Delta S^{\ddagger\ominus}$ (Figure 4.18).

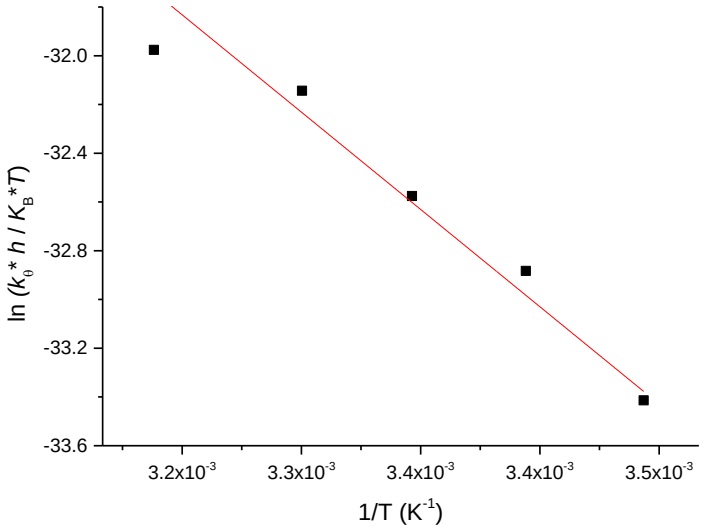

Figure 4.18: Eyring plot for racemisation of **4.7** in H_2O phosphate buffer (0.9 M *I*, pH 7.4) at 15, 20, 25, 30 and 37 °C.

From the slope and intercept of Figure 4.18, the enthalpy ($\Delta H^{\ddagger\ominus}$) and entropy of activation ($\Delta S^{\ddagger\ominus}$) for general-base catalysed racemisation in H_2O phosphate buffer pH 7.4 were calculated using Equation 4.6 (Table 4.10).

Table 4.10: Standard activation parameters for racemisation of **4.7** in H_2O-phosphate buffers (0.9 M *I*, pH 7.4).

	$\Delta H^{\ddagger\ominus}$ / kJ mol^{-1}	$\Delta S^{\ddagger\ominus}$ / J K^{-1} mol^{-1}	$\Delta G^{\ddagger\ominus}$ /kJ mol^{-1}
4.7	47.6 ± 6.2	-112 ± 21	82 ± 22

The relatively low value of $\Delta H^{\ddagger\ominus}$ suggests simultaneous breaking and forming of bonds in the activated complex.[32] The large negative value for the entropy of activation, $\Delta S^{\ddagger\ominus}$, for racemisation of **4.7** indicates significant loss of translational, vibrational, and/or rotational degrees of freedom and is in line with a bimolecular reaction. In comparison with the racemisation of amino acids, aliphatic amino acids have higher enthalpies of activation than aromatic amino acids. However, for entropy, this trend is the opposite, as can be seen in the

previous literature.[18] It is attractive to compare the activation parameters of the present study with those for the deuteration of 5-substituted hydantoins, reported previously by Testa *et al*. (Table 4.11).[7]

Table 4.11: **A**ctivation parameters for deuteration of 5-monosubstituted hydantoins from Reist *et al*.[7]

Hydantoin	$\Delta H^{\ddagger\ominus}$ / kJ mol^{-1}	$\Delta S^{\ddagger\ominus}$ / J K^{-1} mol^{-1}	$\Delta G^{\ddagger\ominus}$ / kJ mol^{-1}
-Ph	72.3 ± 4.0	-68.2 ± 5.0	94.6 ± 11.7
-CH_2OH	76.7 ± 2.8	-86.6 ± 4.6	105.0 ± 9.6
-$NHONH_2$	94.1 ± 2.1	-39.3 ± 1.3	106.7 ± 5.4
-CH_2Ph	94.3 ± 2.5	-43.1 ± 1.7	108.4 ± 6.7
-CH_3	85.3 ± 2.1	-77.0 ± 2.9	110.0 ± 6.7
-CH_2COOH	98.4 ± 3.2	-42.3 ± 2.1	112.1 ± 11.7
-$CH(CH_3)_2$	80.7 ± 3.0	-105.4 ± 6.7	114.6 ± 11.7

Table 4.11 shows that the enthalpy of activation is between 72.3 ± 4.0 and 98.4 ± 3.2 kJ mol^{-1} and the entropy for activation is between -39.3 ± 1.3 and -105.4 ± 6.7 J K^{-1} mol^{-1} for 5-substituted hydantoin. Unfortunately, Reist *et al*. used the pseudo-first-order rate constant for deuteration to calculate activation parameters rather than second-order rate constants which are used in the present work, so we can only compare $\Delta H^{\ddagger\ominus}$ rather than $\Delta S^{\ddagger\ominus}$. It should be noted that the values in Table 4.11 were observed by Reist *et al*. for 5–substituted hydantoins by using DMSO and phosphate buffer in a 1:1 proportion. Reist *et al*. indicated the partial responsibility of inductive and resonance effects on the transition state, which is reflected in the change of $\Delta H^{\ddagger\ominus}$.[33] In particular, the entropy of activation affects the rate of racemisation and deuteration strongly which prevented the author from deriving a general rule to anticipate the effect of substituents on the chiral stability of 5-subsituted hydantoins. Table 4.11 shows a large negative $\Delta S^{\ddagger}$ for 5-isopropylhydantoin, which might indicate the effect of steric hindrance on racemisation. It is also important to mention that racemisation of **4.3** is quite slow in comparison with compounds **4.1**, **4.2**, **4.4** and **4.5** because of the steric effect (Table

4.1). Using 50% DMSO to obtain the rate of deuteration at different temperatures has also an effect on the entropy of activation.

Narduolo[8] reported the values of activation parameter for base-catalysed racemisation of hydantoins with different groups at the N-3 position of hydantoin (Table 4.12).

Table 4.12: Activation parameters for base-catalysed racemisation of **4.10**, **4.11** and **4.13** in D_2O phosphate buffer (pH 7.2, 1 M *I*) from Narduolo.[8]

Hydantoin *N*- Substituent	$\Delta H^{\ddagger\ominus}$ / kJ mol^{-1}	$\Delta S^{\ddagger\ominus}$ / J K^{-1} mol^{-1}
4.10	83.7 ± 0.8	-55.2 ± 2.9
4.11	87.9 ± 2.9	-44.8 ± 10.0
4.13	93.7 ± 2.1	-13.4 ± 6.7

From Table 4.12, it is clear that the type of substituent at the N-3 position changing the activation parameter is important as it can be seen comparing 5-benzylhydantoin **4.9** and 3-methyl-5-benzylhydantoin **4.10**. The rate constant of racemisation decreased for compounds **4.10** and **4.11** in comparison with 5-benzylhydantoin **4.9** and the enthalpy of activation is also reduced. It has been argued that there is no simple relationship between the effects of substituents and the enthalpies of activation.[18]

For compound **4.7**, we found a higher negative value for the entropy of activation and a lower enthalpy of activation with bigger margins of error than those reported for 5-substituted hydantoins[7] or even disubstituted hydantoins.[8] The highly negative activation entropy for racemisation of **4.7** suggests the loss of translational and rotational degrees of freedom associated with the highly ordered transition state[32] which can be interpreted as bulkiness of the substituents at the C-5, N-1 and N-3 positions. $\Delta H^{\ddagger\ominus}$ for thiohydantoin is lower than for hydantoin while $\Delta S^{\ddagger\ominus}$ is more negative for thiohydantoin than for hydantoin.

4.2.2.5 Effect of co-solvents on the kinetics of racemisation

Compounds **4.1**-**4.5** are sufficiently soluble to be able to see their peaks using CD spectroscopy. To study the effect of added co-solvent on the rate constants for racemisation of

4.2 and **4.3** the second-order rate constants for loss of ellipticity were also obtained in aqueous solution in the presence and absence of 10 vol-% acetonitrile. Solutions were prepared mixing 10 vol-% H_2O or D_2O containing either **4.2** or **4.3** with 90 vol-% H_2O and D_2O-phosphate buffers. On the other hand, solutions were also prepared in 10 vol-% acetonitrile or acetonitrile-d_3 and mixed with 90 vol-% H_2O and D_2O-phosphate buffers (Table 4.13).

Table 4.13: Pseudo first-order rate constants for loss of ellipticity of **4.2** and **4.4** in the absence and presence of 10 vol-% acetonitrile and acetonitrile-D_3.

Su.	k_Θ ACN[a] / 10^{-6} s^{-1}	k_Θ ACN-d_3[a] / 10^{-6} s^{-1}	SKIE	k_Θ H_2O [b] / 10^{-6} s^{-1}	k_Θ D_2O[b] / 10^{-6} s^{-1}	SKIE
4.2	96.0 ± 1.9	96.7 ± 1.9	0.99 ±0.03	105.6 ±2.1	105.3 ± 2.1	1.00 ±0.03
4.4	50.7 ± 1.3	48.7± 1.0	1.04 ±0.03	58.5 ±1.2	57.1 ±1.2	1.02 ±0.03

a) A solution of each compound contains 10 vol-% H_2O or 10 vol-% D_2O with 90% 0.1 M phosphate buffer (pH or pH^* 7.4, 1 M *I* at 37 °C).

b) A solution of each compound contains 10 vol-% acetonitrile or 10 vol-% acetonitrile-D_3 with 90% 0.1 M phosphate buffer (pH or pH^* 7.4, 1 M *I* at 37 °C).

As can be seen in Table 4.13, the rate constant for the loss of ellipticity k_Θ in 100 % H_2O phosphate buffer is approximately 1.1 and 1.15 times faster than k_Θ in 10% acetonitrile and 90% H_2O phosphate for **4.2** and **4.4**, respectively. As mentioned before, water may catalyse and enhance proton transfer, reducing the enantiomerisation barrier by approximately 30 kcal mol^{-1}.[14] Tian et al.[14] also suggested that the hydroxide ion can further reduce the energy barrier to about 24 kcal mol^{-1} under basic conditions by accelerating the proton transfer. The literature also reports how water can catalyse the interconversion of thalidomide by promoting the proton transfer where a one-dimentional water chain can act as a water bridge through the Grotthuss mechanism[34] for the proton transfer.[14] These mechanisms may also play a role in the (small) rate retardation observed here.

The kinetic studies of racemisation for **4.7** and **4.8** were undertaken by dissolving the compound in acetonitrile or acetonitrile-d_3 and subsequently mixing with H_2O and D_2O phosphate buffer. To investigate the effect of different co-solvents on the rate of racemisation,

other co-solvents were also used to compare with the effect of 90% acetonitrile 0.01 M phosphate buffer (pH 7.4, 1 M I at 37 °C). The pseudo-first-order rate constants k_θ in buffers with 10 vol-% of MeCN, DMSO, EtOH, MeOH, IPA and TFE were obtained under otherwise identical conditions (Figure 4.19).

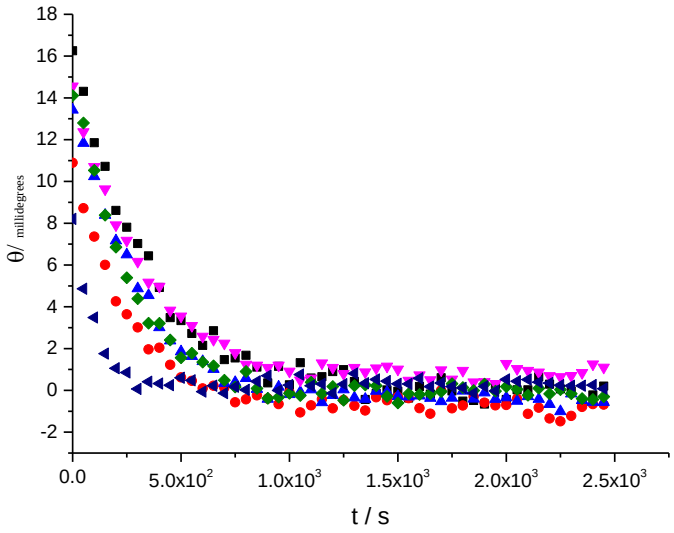

Figure 4.19: CD observation as a function of time at 272 nm for racemisation of **4.7**. 10 vol-% of compound **4.7** in acetonitrile (■), DMSO (●), ethanol (▲), isopropanol (▼), methanol (♦) trifluoroethanol (◄) was mixed with 90 vol-% 0.01 M phosphate buffer (pH 7.4, 1 M *I* at 37 °C).

The pseudo-first-order rate constants for loss of ellipticity k_θ were determined according to Equation 4.1. All pseudo-first-order rate constants k_θ were plotted versus co-solvent to show the effect of co-solvent on the rate constant for ellipticity loss. There is no pseudo-first-order rate constant k_θ in aqueous solution without added co-solvents because compound **4.7** does not dissolve in water (Figure 4.20).

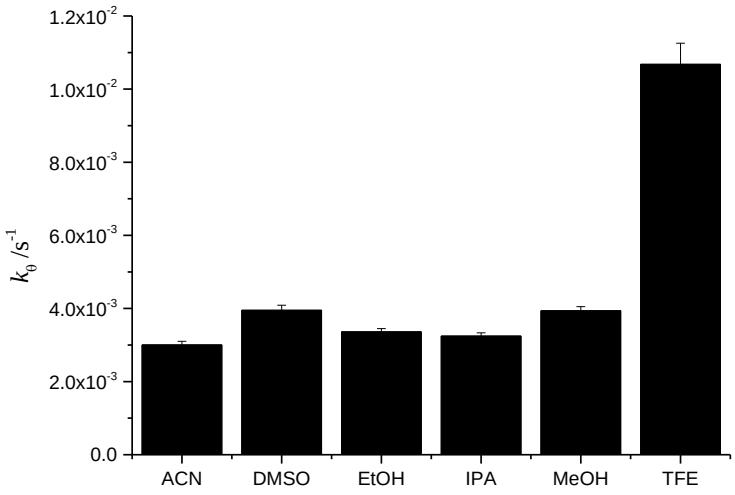

Figure 4.20: Comparison of pseudo-first-order rate constants for ellipticity loss of **4.7** in a solution of 10 vol-% MeCN, DMSO, EtOH, IPA, MeOH and TFE, mixed with 90 vol-% 0.01 M phosphate buffer (pH 7.4, 1 M *I* at 37 °C).

From Figure 4.20, the rate constants in the presence of different co-solvents are higher than those in the presence of acetonitrile. The highest rate constant k_θ was obtained using 10 % trifluoroethanol with 90 vol-% buffer (3.55 times higher than acetonitrile). DMSO and methanol increase the rate k_θ by about 1.35 and 1.30 times, respectively. Ethanol and isopropanol have less effect on racemisation, with rate constants which are higher than those in the presence of acetonitrile by approximately 1.1 and 1.08 times when using ethanol and isopropanol, respectively (Table 4.14).

Table 4.14: Pseudo-first-order rate constants for racemisation of **4.7**. 10 vol-% of a solution of each compound in acetonitrile, DMSO, ethanol, isopropanol, methanol and tri-fluoroethanol was mixed with 90 vol-% 0.01 M phosphate buffer (pH 7.4, 1 M *I* at 37 °C).

k_{θ} (ACN) / 10^{-6} s^{-1}	k_{θ} (DMSO) / 10^{-6} s^{-1}	k_{θ} (EtOH) / 10^{-6} s^{-1}
3005 ± 96	3951 ± 137	3363 ± 88
k_{θ} (MeOH) / 10^{-6} s^{-1}	k_{θ} (IPA) / 10^{-6} s^{-1}	k_{θ} (TFE) / 10^{-6} s^{-1}
3936 ± 116	3246 ± 87	10680 ± 575

The effect of DMSO on the racemisation of different optically active compounds has been reported previously;[35,8, 36] DMSO typically accelerates racemisation. The rate of racemisation increases by increasing the volume of DMSO, which is attributed to the reduced efficiency of the solvation of the dianion in DMSO containing buffers.[37] The anions in aprotic polar solvents are partially blocked and strong solvation deactivates the role of anions as basic catalyst in the racemisation process.[38]

It is interesting to compare the effect of co-solvent on racemisation of thiohydantoin with that on racemisation of hydantoin. Narduolo[8] has used different co-solvents with non-deuterated and deuterated phosphate buffers for **4.9**-**4.11** and **4.13** (Table 4.15).

Table 4.15: Rate constants for racemisation of hydantoins **4.9-4.11** and **4.13**, at 60 °C, in mixtures composed of 50 volume-% H_2O and D_2O phosphate buffers 0.5 M, 1 M / and 50 volume-% of H_2O or mixtures 1:1 (v:v) of H_2O non-deuterated co-solvent and D_2O or mixtures 1:1 (v:v) of D_2O-deuterated co-solvent, respectively, to give a total concentration of co-solvent of 25 volume-% (v:v).[8]

H_2O buffer $pH^{25\,°C}$ 7.2				
hydantoin	k_Θ / 10^{-6} s^{-1}			
	no co-solvent	2-propanol	TFE	dioxane
4.9	167.3 ± 1.3	129.9 ± 1.0	208.0 ± 1.8	134.8 ± 1.5
4.10	114.5 ± 0.5	76.3 ± 0.7	128.7 ± 1.0	89.3 ± 0.4
4.11	78.4 ± 0.6	48.8 ± 0.2	95.5 ± 0.3	57.6 ± 0.2
4.13	524.1 ± 13.4	808.5 ± 14.7	676.2 ± 30.1	947.8 ± 29.6
D_2O buffer (pH* 7.3)				
hydantoin	k_Θ / 10^{-6} s^{-1}			
	no co-solvent	2-propanol	TFE	dioxane
4.9	175.0 ± 1.5	134.8 ± 1.9	191.4 ± 2.4	140.5 ± 1.2
4.10	112.8 ± 0.4	77.4 ± 0.4	107.3 ± 0.6	86.7 ± 0.6
4.11	77.0 ± 0.3	46.7 ± 0.1	82.5 ± 0.3	56.1 ± 0.3
4.13	539.7 ± 15.1	896.9 ± 15.5	615.4 ± 17.0	968.8 ± 21.6

It is obvious from Table 4.15 that trifluoroethanol accelerates and isopropanol decelerates the rate of ellipticity loss both in deuterated and non-deuterated phosphate buffer. The effect of trifluoroethanol on increasing the rate of racemisation was also found for compound **4.7** in H_2O phosphate buffer (pH 7.4). Narduolo[8] also reported that the pH of the phosphate buffer appeared to be higher by using 25 vol-% co-solvent increasing from 7.24 to 7.78 (IPA), 7.91 (dioxane) and 8.28 (DMSO). Furthermore, adding 25 % TFE with 75% phosphate buffer increased the pH of phosphate buffer from 7.24 to just 7.32.

4.2.3 Racemisation of 5-substituted 2-thiohydantoins

As described in Chapter 2, we were not able to synthesise enantioenriched 5-substituted 2-thiohydantoin. Even pure enantiomers of amino acids have been tried as starting material. Several racemic 5-substituted 2-thiohydantoins have been synthesised from the corresponding amino acids and aldehydes. The chirobiotic T column was tried in chiral HPLC for enantioseparation for several 5-substituted 2-thiohydantoins in different conditions (see

Chapter 2). The enantiomers of the two compounds were collected by chiral column HPLC (Scheme 4.9).

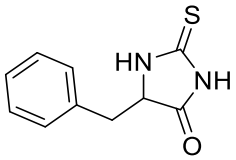

4.15

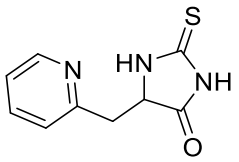

4.16

Scheme 4.9: The chemical structure of 5-benzyl-2-thioxoimidazolidin-4-one (**4.15**) and 5-(pyridin-2-ylmethyl)-2-thioxoimidazolidin-4-one (**4.16**)

We collected multiple enantioenriched fractions of **4.15** and **4.16** to have enough absorbance and ellipticity to be measurable in CD spectroscopy. To confirm separation of the enantiomers, we recorded CD spectra to confirm the inverse peaks for both enantiomers. Both enantiomers of **4.16** were observed by CD spectroscopy which showed opposite CD spectra for both enantiomers with low intensity. Unfortunately, it was found that **4.15** and **4.16** racemised completely during the process of HPLC sample collection and subsequent solvent evaporation. Bovarnick and Clarke[30] have explained that the replacement of hydrogen at the N-1 position of hydantoin by substituents will decrease the rate constants of racemisation. It is notable that the acetyl group on the N-1 retards the rate of ellipticity loss for **4.1-4.5**.

4.3 Conclusion

The kinetics of racemisation of thiohydantoins were studied in physiological like buffer to obtain the rate constants of racemisation. Firstly, it was observed that the acetyl group substituted at the N-1 position has a rate retarding effect on racemisation. It is known that during racemisation, the cleavage of the acetyl bond occurs which influences the observed rate constant for ellipticity loss. Therefore, the rate constant for ellipticity loss determined using CD spectroscopy is higher than the rate constant for racemisation. Secondly, the solvent kinetic isotope effect was also studied and suggested negligible solvent kinetic isotope effect for the racemisation of **4.1**-**4.5**, **4.7** and **4.8**. Thirdly, the corresponding amino acid substituents on the asymmetric C-5 carbon influenced the rate of racemisation of thiohydantoin, which varied between increasing and decreasing the rate of **4.1**-**4.5**. Finally,

our data suggest the S_E1 mechanism for the racemisation of thiohydantoin rather than the S_E2 mechanism.

4.4 Experimental

4.4.1 General Experimental

4.4.1.1 Apparatus

All solvents used were HPLC grade and purchased from Fischer Scientific or Sigma Aldrich. All materials used were weighed out on an analytical Fisher Brand PS-100 balance (Max 100 g, d=0.1 mg). For every buffer concentration, the required buffer was mixed with a freshly prepared stock solution of thiohydantoin. The volumes for all stock solutions were measured by Gilson or Eppendorf Research micropipettes. The stock solutions of thiohydantoin were centrifuged three times to avoid precipitation inside the stock solution. The pH measurements for all concentrations of buffer in non-deuterated and deuterated buffer were carried out at 20 °C using a Hanna Instruments pH 210 pH meter. The pH meter was calibrated before each measurement with certified traceable NIST buffers at pH 10.01+0.02 (at 20 °C) (from Fisher) and pH 4.00+0.01 (at 20 °C) (from Reagecon). Kinetic experiments of racemisation were carried out on a Chirascan CD spectrometer equipped with a temperature controlled sample holder for circular dichroism (temperature stability: ± 0.02 °C) in 1.00 cm path length quartz cuvettes, unless otherwise stated.

4.4.1.2 Preparation of solutions

All non-deuterated buffers were prepared by the procedures described in Chapter 3. Deuterated phosphate buffers were prepared by evaporating the different concentrations of H_2O phosphate buffer (pH* 7.4, 1 M *I*) by freeze dryer and adding D_2O three times to guarantee the exchange of deuteron. The measurement of pH of the above described solutions gave values of $pH^{*20°C}$ (D_2O) = 7.55 and $pH^{20°C}$ (H_2O) = 7.44. For the stock solutions, 5-substituted 1-acetyl-2-thiohydantoins were dissolved in H_2O and D_2O and placed in an ultrasonic bath sonicator for approximately 5 minutes. The solutions were subsequently put in plastic Eppendorfs and centrifuged for 8 minutes at 13.3 rpm on a Jencons-pls Spectrafuge 24.D centrifuge. Every buffer concentration was mixed with a freshly prepared stock solution

of thiohydantoin. The supernatants were transferred to new Eppendorfs and centrifuged 2 times. The supernatants were collected and measured in a UV-visible spectrophotometer to confirm appropriate absorbance even with the dilution.

4.4.1.3 Error calculation

Error propagation in the present work was calculated in different ways. For the pseudo-first and second-order rate constants, the errors were obtained using the Origin 9.0 program. For the slope and intercept, the errors appeared in origin without having to calculate manually. However, the errors of solvent kinetic isotope effect (k_{H_2O}/k_{D_2O}) on racemisation and rate constants in deuterated phosphate buffer divided by hydrogen-deuterium exchange process (k_{D2O}/k_{HD}) were calculated using the following equation[39, 40]

$$Errork_H/k_D = \sqrt{(\frac{1}{k_\theta^D})^2.(erroronk_\theta^H)^2 + [\frac{k_\theta^H}{(k_\theta^D)^2}]^2.(errorink_\theta^D)^2} \qquad \textbf{Equation 4.7}$$

$k_{\theta H}$ and $k_{\theta D}$ were determined using CD spectroscopy in different concentrations of non-deuterated and deuterated phosphate buffer. The error in $k_{\theta H}$ and $k_{\theta D}$ were obtained in Origin 9.0.

The error margins for $k_\theta - k_{hyd}$ were calculated using the following equation[40]

$$Error(k_\theta - k_{\mathrm{hyd}}) = \sqrt{(1)^2(error\ in\ k_\theta)^2 + (-1)^2(error\ in\ k_{hyd})^2} \qquad \textbf{Equation 4.8}$$

The errors in the k_θ and k_{hyd} were obtained using Origin 9.0.

Weighted averaged data were used to calculate the rate constant for loss of ellipticity at different wavelengths for **4.7** (see Section 4.2.2.2). Two rate constants for racemisation of **4.7** were observed at different wave length. To calculate the weighted average of two rate constants, the following equation was used[40]

$$\text{Weight Average rate} = \frac{\left(\frac{1}{(\text{error } k_1)^2} * \text{k}_1\right) + \left(\frac{1}{(\text{error } k_2)^2} * \text{k}_2\right)}{\left(\frac{1}{(\text{error k}_1)^2} + \frac{1}{(\text{error k}_2)^2}\right)} \qquad \textbf{Equation 4.9}$$

Here, all rate constants were obtained using either CD spectroscopy, with the exception of k_{HD} for H/D exchange which was obtained using ^{1}H-NMR spectroscopy. The error margins for individual *k* in the equation were obtained using Origin 9.0.

To calculate the error margin of the weight average, the following equation was used[40]

$$\text{Error of weight average rate constant} = \sqrt{\frac{1}{\frac{1}{(error k_1)^2} + \frac{1}{(error k_2)^2}}} \qquad \textbf{Equation 4.10}$$

Here, all errors for the rate constants were obtained in Origin 9.0**.**

The error propagation equation has been used for the data in the Eyring plots to obtain the error margins on activation enthalpy and entropy.[40,41]

4.4.1.4 Standard state

The usual choice of 1 mol dm^{-3} has been used as the reference state for concentration.

Acknowledgment

I would like to thank Professor Rudolf Allemann for access to CD spectroscopy and his group for their kind help. I also thank Dr Rob Jenkins and Mr Robin Hicks for their kind help with NMR studies.

4.5 References

1. G. Gübitz and M. G. Schmid, *Journal of Chromatography A*, 2008, 1204, 140-156.
2. C. Danel, N. Azaroual, A. Brunel, D. Lannoy, P. Odou, B. Décaudin, G. Vermeersch, J.-P. Bonte and C. Vaccher, *Tetrahedron: Asymmetry*, 2009, 20, 1125-1131.
3. J. Haginaka, *Journal of Pharmaceutical and Biomedical Analysis*, 2002, 27, 357-372.
4. A. G. Leach, E. A. Pilling, A. A. Rabow, S. Tomasi, N. Asaad, N. J. Buurma, A. Ballard and S. Narduolo, *MedChemComm*, 2012, 3, 528-540.
5. N. G. Anderson, in *Practical Process Research & Development*, ed. N. G. Anderson, Academic Press, San Diego, 2000, DOI: http://dx.doi.org/10.1016/B978-012059475-7/50019-3, pp. 329-344.
6. A. C. Cabordery, M. Toussaint, N. Azaroual, J. P. Bonte, P. Melnyk, C. Vaccher and C. Foulon, *Tetrahedron Asymmetry*, 2011, 22, 125-133.
7. M. Reist, P.-A. Carrupt, B. Testa, S. Lehmann and J. J. Hansen, *Helvetica Chimica Acta*, 1996, 79, 767-778.
8. S. Narduolo, Thesis (Ph D) - Cardiff University, 2011.
9. K. Cabrera, M. Jung, M. Fluck and V. Schurig, *Journal of Chromatography A*, 1996, 731, 315-321.
10. L. Onel and N. J. Buurma, *The Journal of Physical Chemistry B*, 2011, 115, 13199-13211.
11. R. A. Lazarus, *Journal of Organic Chemistry*, 1990, 55, 4755-4757.
12. L. B. Mendel and H. D. Dakin, *Journal of Biological Chemistry*, 1910, 7, 153-156.
13. H. D. Dakin, *Journal of Biological Chemistry*, 1912, 13, 357-362.
14. C. Tian, P. Xiu, Y. Meng, W. Zhao, Z. Wang and R. Zhou, *Chemistry – A European Journal*, 2012, 18, 14305-14313.
15. K. H. Dudley and D. L. Bius, *Drug Metabolism and Disposition*, 1976, 4, 340-348.
16. Chiral HPLC has been used to separate both enantiomers for 5-benzyl-2-thiohydantoin and 5-pyridinemethyl-2-thiohydantoin.We have been able to separate both enantiomers but unfortunately, after the solvent evaporation process, those compounds were racemised.
17. W. I. Congdon, Thesis (PhD) - McGill University, 1970.
18. G. G. Smith and T. Sivakua, *The Journal of Organic Chemistry*, 1983, 48, 627-634.
19. M. J. O. Anteunis, F. Borremans, D. Wante and R. Schrooten, *Tetrahedron Letters*, 1981, 22, 3101-3104.
20. M. Barber, J. H. Jones and M. J. Witty, *Journal of the Chemical Society, Perkin Transactions 1*, 1979, DOI: 10.1039/P19790002425, 2425-2428.
21. G. G. Smith and T. Sivakua, *Journal of Organic Chemistry*, 1983, 48, 627-634.
22. S. Martínez-Rodríguez, F. Javier Las Heras-Vázquez, L. Mingorance-Cazorla, J. M. Clemente-Jiménez and F. Rodríguez-Vico, *Applied and Environmental Microbiology*, 2004, 70, 625-630.
23. A.-C. Cabordery, M. Toussaint, N. Azaroual, J.-P. Bonte, P. Melnyk, C. Vaccher and C. Foulon, *Tetrahedron: Asymmetry*, 2011, 22, 125-133.
24. http://www.biomol.net/en/tools/buffercalculator.htm
25. http://www.liv.ac.uk/buffers/buffercalc.html
26. H. Fukada and K. Takahashi, *Proteins*, 1998, 33, 159-166.
27. R. A. Lazarus, *The Journal of Organic Chemistry*, 1990, 55, 4755-4757.
28. Z. S. Safi, *2012*, 2012, 3.
29. M. Puszyńska-Tuszkanow, M. Daszkiewicz, G. Maciejewska, A. Adach and M. Cieślak-Golonka, *Structural Chemistry*, 2010, 21, 315-321.
30. M. Bovarnick and H. T. Clarke, *Journal of the American Chemical Society*, 1938, 60, 2426-2430.

31. H. Maskill, *The physical basis of organic chemistry*, Oxford University Press, Incorporated, 1985.
32. F. A. Carey and R. J. Sundberg, *Advanced Organic Chemistry. Part A, Structure And Mechanisms*, Springer, New York, 5th edn., 2007.
33. M. F. Eichelbaum, B. Testa and A. Somogyi, *Stereochemical aspects of drug action and disposition*, Springer Science & Business Media, 2012.
34. N. Agmon, *Chemical Physics Letters*, 1995, 244, 456-462.
35. Y.-C. Xie, H.-Z. Liu and J.-Y. Chen, *Biotechnology Letters*, 1998, 20, 455-458.
36. D. K. Jaiswal, J. R. Jones and R. Fuchs, *Journal of the Chemical Society, Perkin Transactions 2*, 1976, DOI: 10.1039/P29760000102, 102-104.
37. E. J. Ebbers, G. J. A. Ariaans, J. P. M. Houbiers, A. Bruggink and B. Zwanenburg, *Tetrahedron*, 1997, 53, 9417-9476.
38. F. N. Gonawan, L. Sie Yon, A. H. Kamaruddin and M. H. Uzir, *Industrial & Engineering Chemistry Research*, 2013, 53, 635-642.
39. P. R. Bevington and D. K. Robinson, *Data Reduction And Error Analysis For The Physical Sciences*, McGraw-Hill, Boston, 3rd edn., 2003.
40. J. R. Taylor, *An Introduction To Error Analysis: The Study Of Uncertainties In Physical Measurements*, University Science Books, 1997.
41. http://laffers.net/blog/2010/11/15/error-propagation-calculator/

Chapter 5

Kinetics of H/D exchange and racemisation for substituted 2-thiohydantoins and related compounds

5.1 Introduction

The mechanism of racemisation can be studied by comparing the rate constant of racemisation k_{rac} with the rate constant of hydrogen-deuterium exchange k_{deut}. Wilson *et al.*[1] proposed the mechanism of racemisation of optically active 2-methyl-1-phenyl-1-butanone in this way. If k_{deu}/k_{rac} approaches unity, the exchange occurs with complete racemisation.[2] S_E1 and S_E2 mechanisms have been suggested for the racemisation of 5-substituted hydantoins by Narduolo[3] and Reist *et al.*[4] Narduolo[3] reported k_{rac} / $k_{H/D}$ to be between 1.2 and 1.3 for S-5-benzylhydantoin (25 °C using 0.1 and 0.5 M of D_2O-phosphate buffer, pH^* 7.2, 1 M *I*), which is close to unity, therefore indicating S_E1 rather than S_E2. This was further supported by a wealth of additional data. The racemisation of amfepranone and cathinone have also been reported to proceed via the S_E1 mechanism in D_2O-phosphate buffer (pH^* 7.4, 0.43 M *I*).[5] However, Reist *et al*. suggested the S_E2 mechanism for the racemisation of 5-substituted hydantoins in 50% DMSO and 50% buffer with rate constants of deuteration half those of racemisation, and k_{deut} / k_{rac} approaching 0.5. Cabordery *et al.*[6] proposed the S_E2 mechanism for the racemisation of thiohydantoin (33 mM, pD 2.6 deuterated phosphate buffers / EtOD-75/25 (v/v) at 15 °C), where the rate constant for deuteration was about half that for racemisation, suggesting that deuteration occurs with inversion of configuration. Both S_E1 and S_E2 mechanisms were suggested for the racemisation of 5-substituted hydantoin by Narduolo and Reist *et al.*, respectively, as shown in Scheme 5.1.

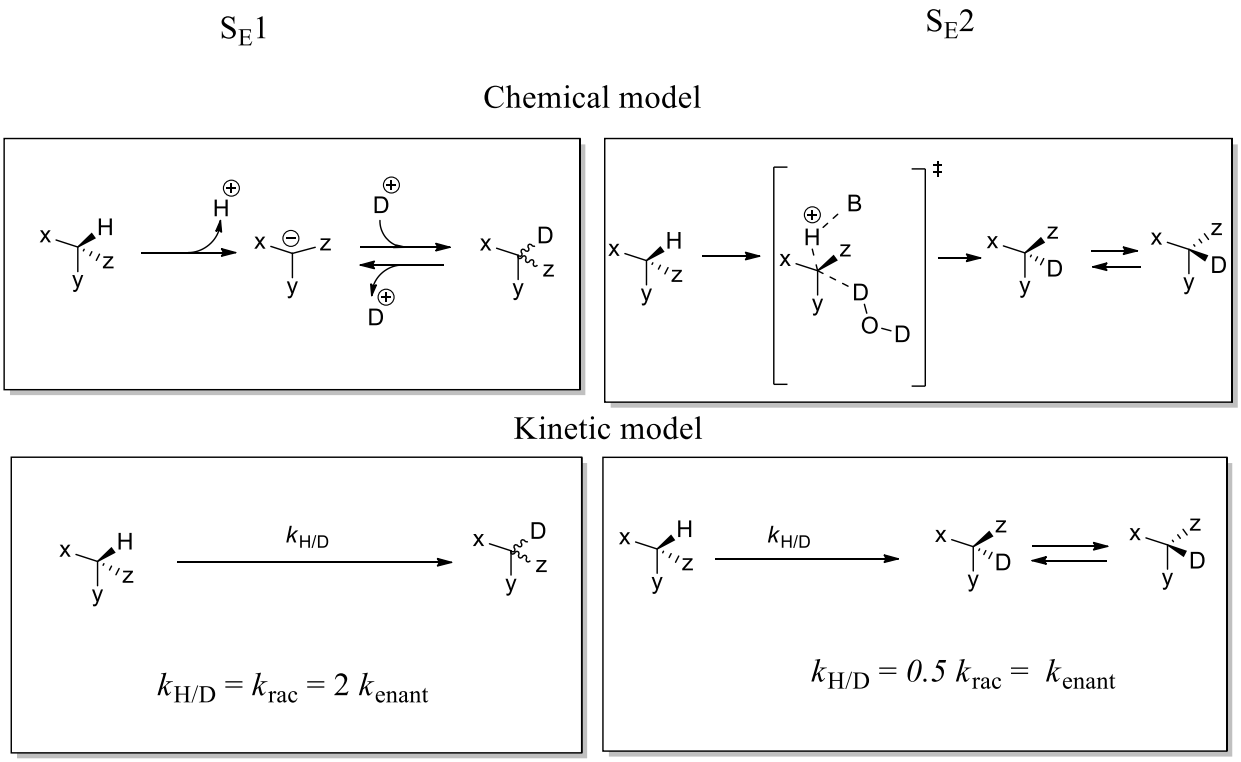

Scheme 5.1: S_E1 and S_E2 mechanisms of racemisation

The S_E2 mechanism was suggested for thiohydantoin racemisation by Cabordery *et al.*[6] because the isotopic exchange occurring with k_{deut}/ k_{rac} is equal to 0.68 at pH 2.6 with complete net inversion of configuration (Scheme 5.2).[2]

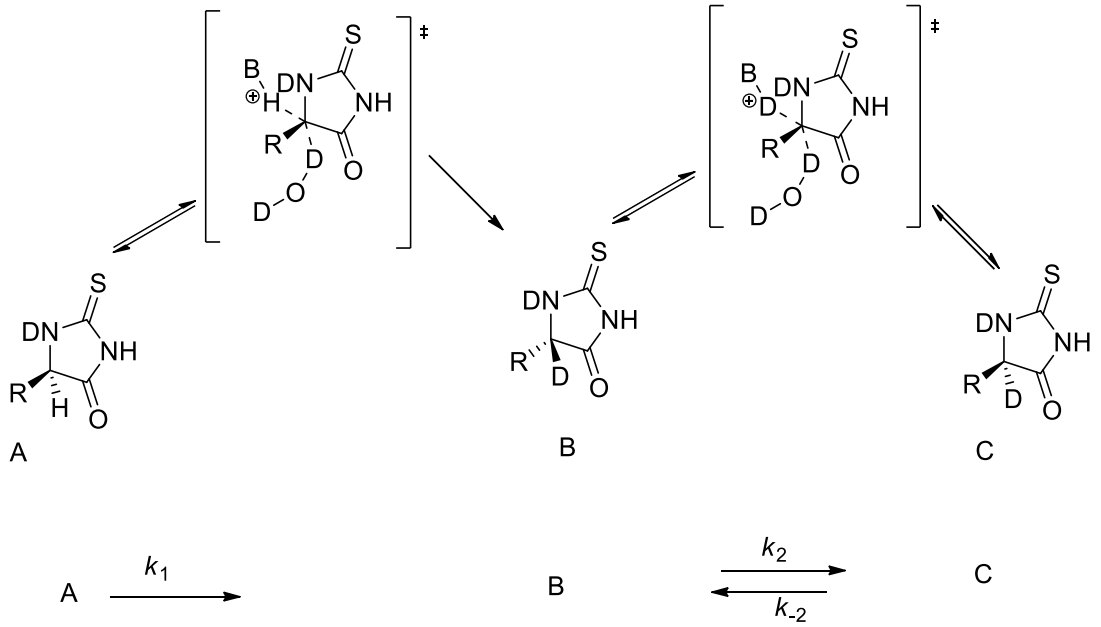

Scheme 5.2: S_E2 mechanism for thiohydantoin racemisation proposed by Cabordery *et al*.[6]

5.2 Results and discussion

5.2.1 The hydrogen/deuterium exchange of 5-substituted 1-acetyl-2-thiohydantoin

5.2.1.1 Determination of hydrogen/deuterium exchange of 5-substituted 1-acetyl-2-thiohydantoin

To study the mechanism of racemisation, ^{1}H-NMR experiments in D_2O-phosphate buffers (pH* 7.4, 0.9 M *I*, at 37 °C) were performed for the deuteration of labile hydrogen at the chiral centre of compounds **5.1**-**5.5** (Scheme 5.3) to complement the racemisation experiments described in Chapter 4.

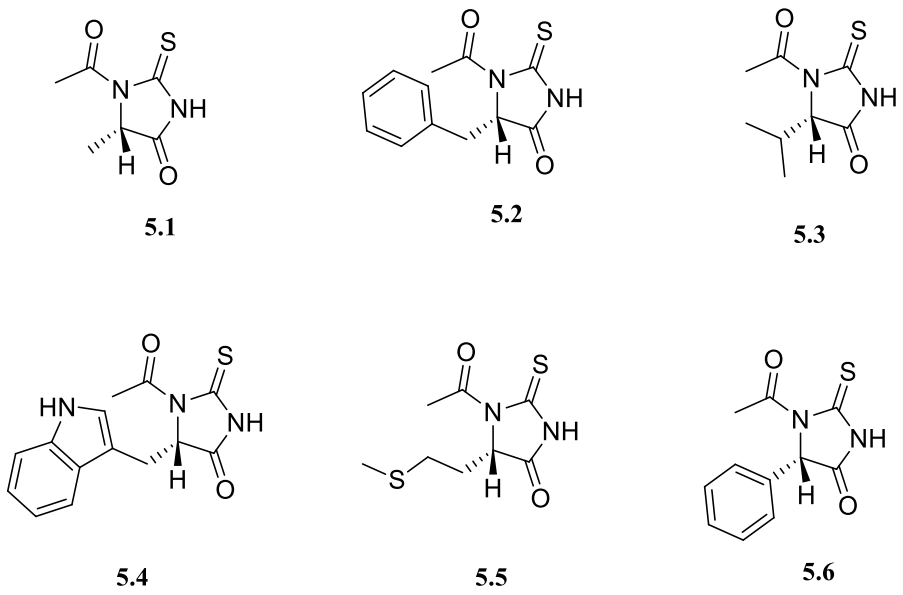

Scheme 5.3: The chemical structures of compounds **5.1**-**5.6**

Scheme 5.3 shows different groups attached at the C-5 position with acetyl substituted at N-1. Their racemisation was discussed in Chapter 4 in non-deuterated and deuterated phosphate buffer pH (pH* 7.4, 0.9 M *I*, at 37 °C). Compounds **5.1** and **5.3** had sufficient solubility in aqueous buffers for peaks in their ^{1}H-NMR spectra to be observed. Different concentrations of D_2O-phosphate buffer were used for **5.1** and **5.3** and ^{1}H-NMR spectra were recorded as a function of time (Figure 5.1). Because of the lack of solubility in aqueous solution of compounds **5.2**, **5.4** and **5.5**, 10 vol-% of d_3-acetonitrile was used to dissolve sufficient quantities of these compounds.

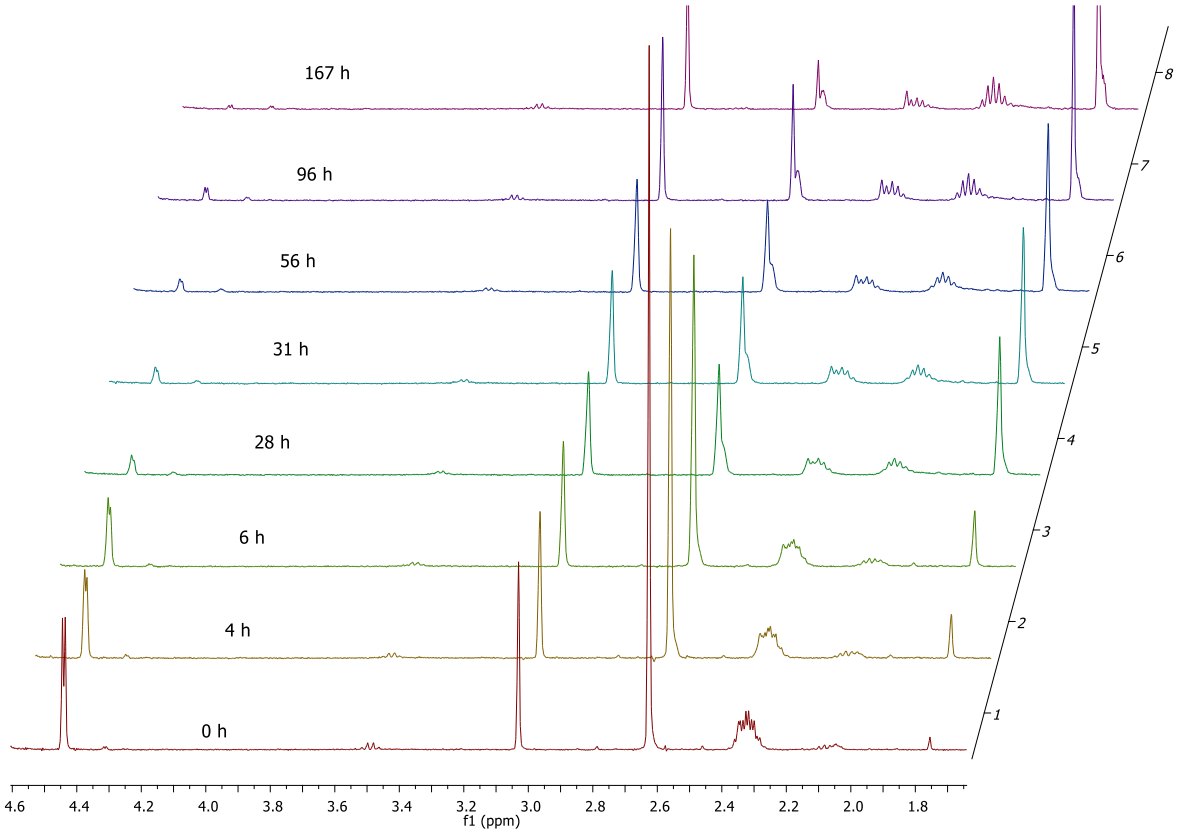

Figure 5.1: ^{1}H-NMR spectra of **5.3** between 0 and 167 h in 0.36 M D_2O-phosphate buffer (pH* 7.4, 0.9 M *I*, at 37 °C).

Figure 5.1 shows hydrolysis and a decrease in the signal for the labile hydrogen at the stereogenic centre for compound **5.3**. This is in agreement with the observation for the loss of ellipticty of **5.1-5.5** in Chapter 4. We discussed how the rate constants for the loss of ellipticity are not equal to the rate constants for racemisation because hydrolysis occurs during the reaction. Therefore, to determine k_{rac}, the equation k_{θ}-k_{hyd} = k_{rac} was used to obtain the rate constants of racemisation of **5.1-5.5** (*vide supra*) in H_2O and D_2O-phosphate buffer. Similarly, the rate constant observed from the decrease of the relative integration of the hydrogen at the stereogenic centre over time does not represent the rate constants for H/D exchange because of the hydrolysis of **5.1-5.5**, as can be seen in Figure 5.1. As a result, the equation $k_{H,\,obs}$ - k_{hyd} = $k_{H/D}$ can be used to obtain the rate constants for H/D exchange $k_{H/D}$. However, we have not carried out hydrolysis experiments for **5.1-5.5** in D_2O-phosphate buffer using UV-visible spectroscopy (as we did to determine k_{hyd} in H_2O-phosphate buffer, Chapter 4). Therefore, $k_{H/D}$ cannot be compared with k_{rac} but can be compared with k_{θ}. Nevertheless, $k_{H,\,obs}$ is represented as $k_{H/D}$ in this chapter, *i.e.* $k_{H,\,obs} \approx k_{H/D}$.

^{1}H-NMR spectroscopy, using tetramethylammonium bromide as a reference, indicates that the signal for the labile hydrogen on the stereogenic centre decreases for **5.3** in deuterated-phosphate buffer (pH* 7.4) (Figure 5.1). The reason for using tetramethylammonium bromide as a reference is because the $k_{H,\,obs}$ of **5.3** is low, approximately twice k_{hyd}.

In contrast, the $k_{H,\,obs}$ are much higher than k_{hyd} for the rest of compounds **5.1**, **5.2**, **5.4** and **5.5** (*vide infra*). The reaction was followed using ^{1}H-NMR spectroscopy in D_2O-phosphate buffer pH* 7.4 for compounds **5.1**, **5.2**, **5.4**, **5.5** and **5.6**. The integrated peak areas, relative to a reference signal, for the hydrogens at the stereogenic centres were calculated over time (see appendix).

For these compounds, integrations were normalised relative to a signal for non-exchanging protons in the compounds themselves. The relative integration areas of the hydrogen signal were plotted versus time for **5.1**-**5.6** to determine the pseudo-first-order rate constants of H/D exchange (Figure 5.2 and Appendix).

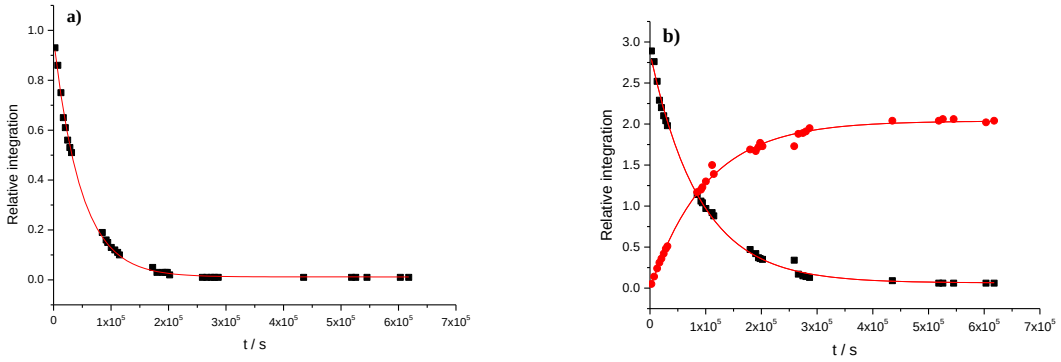

Figure 5.2: a) The relative area of labile hydrogen on the stereogenic centre of **5.3** over time in 0.36 M D_2O-phosphate buffer (pH* 7.4, 0.9 M *I*, at 37 °C), and b) the relative integration area (●) increasing and (■) decreasing of the acetyl methyl group over time in 0.36 M D_2O-phosphate buffer (pH* 7.4, 0.9 M *I*, at 37 °C). Solid lines are fits in terms of the first order rate law.

The pseudo-first-order rate constant for H/D exchange, $k_{H/D}$, of **5.3** (21.1 ± 0.5). 10^{-6} s^{-1} (Figure **5.2** a) is higher than k_{hyd} for **5.3** as quantified by both the rate constant for loss of the N-acetyl-CH_3 of (11.3 ± 0.4).10^{-6} s^{-1} and the rate constant observed for formation of the acetate-CH_3 of (9.9 ± 0.3). 10^{-6} s^{-1} (Figure 5.2 b). Rate constants for hydrolysis in D_2O-phosphate buffer were not determined for every compound by UV-visible spectroscopy (only H_2O-phosphate buffers were used in Chapter 3). There are two possibilities for the signal of the proton at the stereogenic centre in the hydrolysed product:1) it overlaps with the signal of

the starting material or 2) it is found elsewhere. However, considering that H/D exchange for the deacetylated compound is much faster than for the acetylated compound, the signal is unlikely to contribute significantly to the relative integral for the proton on the stereogenic centre in **5.3**. Therefore, the rate constant of H/D exchange here also contains the rate constant for hydrolysis. The highest rate constant of hydrolysis of **5.3** was observed by ^{1}H-NMR spectroscopy in D_2O-phosphate buffer, which is approximately half of the rate constant of H/D exchange (Figure 5.2 b). This value can be considered reasonable because in the case of the racemisation in H_2O-phosphate buffer, k_{hyd} also approaches half of the rate constant for the racemisation (see appendix).

The pseudo-first-order rate constants for H/D exchange were determined for **5.1** and **5.3** by using Equation 5.1 (Experimental Section) in different concentrations of D_2O-phosphate buffer (pH* 7.4 at 37 °C) without using co-solvent. However, 10% d_3-ACN was used with the D_2O–phosphate buffer for compounds **5.2**, **5.4**, **5.5** and **5.6** to record ^{1}H-NMR data. From Figure 5.2a for **5.3**, the data is reproduced well by the pseudo-first-order rate law. Similarly, the pseudo-first-order rate law was fit to the data for the H/D exchange of the rest of the compounds, as illustrated in the Appendix. To show the effect of the basic component of the buffer on the hydrogen-deuterium replacement, different concentrations of D_2O-phosphate buffer were used for **5.1** and **5.3**. The second-order rate constants for H/D exchange were obtained by plotting the pseudo-first-order rate constant versus the concentration of the basic component of the phosphate buffers (Figure 5.3).

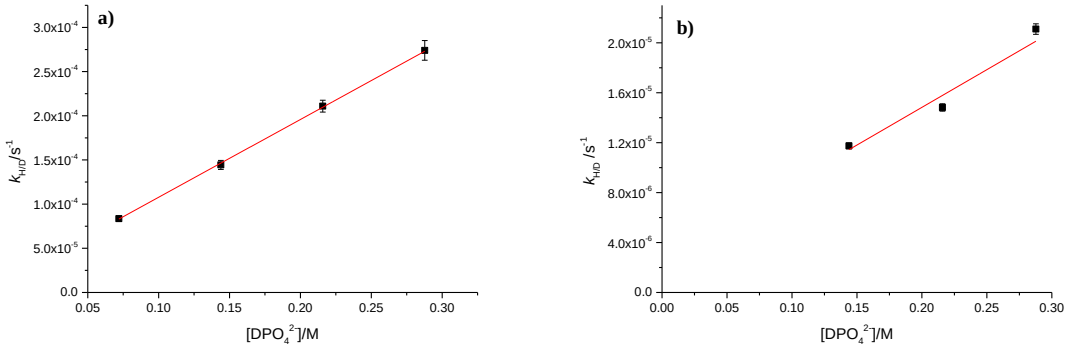

Figure 5.3: First-order rate constants for buffer catalysed H/D exchange of a) **5.1** and b) **5.3** in D_2O-phosphate buffers (0.9 M *I*, pH* 7.4 at 37 °C).

Figure 5.3 shows a good linear correlation, confirming general-base catalysis for H/D exchange. The rate constants of racemisation for **5.1**-**5.6** also increased by increasing the

buffer concentration (Chapter 4). The second-order rate constants for **5.1** and **5.3**, observed in D_2O-phosphate buffer (pH* 7.4 at 37 °C), are shown in Table 5.1.

Table 5.1: Second-order rate constants of H/D exchange $k_{H/D}$ of **5.1** and **5.3** in D_2O-phosphate buffer measured by ^{1}H-NMR spectroscopy at 0.36, 0.27, 0.18 and 0.09 M total phosphate and 0.2877, 0.2158, 0.1438, 0.0719 and 0.0360 M basic phosphate, respectively (0.9 M *I*, pH* 7.4 at 37 °C).

Substrate	$k_{H/D}$ / 10^{-6} s^{-1} M^{-1}	k_{in} / 10^{-6} s^{-1}
5.1	880 ± 12	19.8 ± 1.7
5.3	60.4 ± 13.3	2.8 ± 2.6

Moreover, it is obvious that the substituents at the chiral centre have an influence on the rate of racemisation. It should also be noted from Table 5.1 that the substituents at the C-5 position affect the H/D exchange in a similar way to racemisation. It was reported that the aliphatic and aromatic groups at the C-5 also increase or decrease the acidity of C-H because of the inductive effect, which is not the only effect but indeed can be considered important.[7]

5.2.1.2 Comparison of the rate constant of racemisation and H/D exchange

The hydrogen-deuterium exchange process can be considered a useful probe in the investigation of carbanions.[8] Comparison between the rate constant of H/D exchange and that of racemisation can support a proposed mechanism of racemisation. The S_E1 mechanism for hydantoin racemisation was previously suggested.[3, 6] The S_E1 mechanism occurs in the racemisation when k_{deu} / k_{rac} approaches unity and deuteration takes place with complete racemisation.[6] The base-catalysed hydrogen exchange reaction of 5-substituted 1-*N*-acetyl-2-thiohydantoin is proposed to proceed via the S_E1 mechanism, as shown in Scheme 5.4.

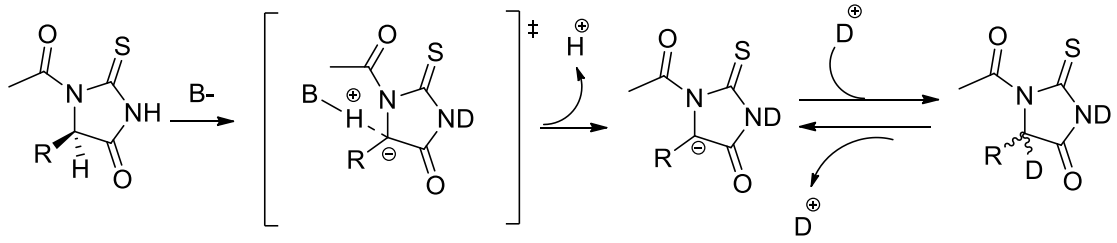

Scheme 5.4: The proposed S_E1 mechanism for thiohydantoin racemisation.

The rate constants for the loss of optical activity k_θ were obtained using CD spectroscopy in different concentrations of deuterated-phosphate buffer, as mentioned in Chapter 4. Under the same conditions, the pseudo-first-order rate constants for H/D exchange of **5.1** and **5.3** were determined from ^{1}H-NMR spectroscopic data in various concentrations of phosphate buffer (Equation 5.1). The second-order rate constants of H/D exchange were determined at pH* 7.4 at 37 °C (Equation 5.2) (Table 5.2).

Table 5.2: Second-order rate constants for H/D exchange $k_{H/D}$ of **5.1** and **5.3** in D_2O phosphate buffer measured by ^{1}H-NMR spectroscopy (ionic strength 0.9 M *I*, pH* 7.4 at 37 °C).

Compound	k_θ (D_2O) / 10^{-6} s^{-1} M^{-1}	$k_{H/D}$ / 10^{-6} s^{-1} M^{-1}	$k_{\theta\ D2O}/k_{H/D}$
5.1	811 ± 66	880 ± 12	0.92 ± 0.08
5.3	53.5 ± 4.0	60.4 ± 13.3	0.89 ± 0.21

From Table 5.2, the second-order rate constant for the loss of ellipticity of both **5.1** and **5.3** in D_2O-phosphate buffer divided by the second-order rate constant for H/D exchange are approximately equal to unity. For compound **5.1** and **5.3,** the value of k_{rac}/k_{deut} is approximately equal to unity within the margin of error, confirming S_E1 rather than S_E2 is the mechanism for thiohydantoin racemisation.

Compounds **5.1**, **5.2**, **5.4**, and **5.6** were studied in 0.09 M phosphate buffer without and with 10 vol-% d_3-acetonitrile, respectively while compounds **5.3** and **5.5** were studied in 0.36 M phosphate buffer with and without 10 vol-% d_3-acetonitrile, respectively. The presence of d_3-

acetonitrile increased the solubility of the sample allowing us to obtain the pseudo-first-order rate constants for H/D exchange (Table 5.3).

Table 5.3: Pseudo-first-order rate constants for the loss of ellipticity k_θ for solutions of **5.1**, **5.2** and **5.4** and for H/D exchange $k_{H/D}$ of **5.2**, **5.4** and **5.6** in D_2O-phosphate buffer measured by ^{1}H-NMR spectroscopy at 0.09 M total phosphate (0.072 M basic phosphate), and k_θ and $k_{H/D}$ at 0.36 M total phosphate (0.29 M basic phosphate) for **5.3** and **5.5** (ionic strength of 0.9 M *I*, pH* 7.4 at 37 °C).

Compound	k_θ (D_2O) / 10^{-6} s^{-1}	$k_{H/D}$ /10^{-6} s^{-1}	$k_{\theta\,(D2O)}/k_{H/D}$
5.1	68.5 ± 1.4 [a]	83.5 ± 3.2[a]	0.82 ± 0.04
5.2	96.7 ± 1.2[b]	111.9 ± 3.6[b]	0.86 ± 0.03
5.4	48.7 ± 1.0 [b]	45.3 ± 1.5 [b]	1.08 ± 0.04
5.6	----------	521 ± 13[b]	----------
5.3	19.0 ± 0.4[a]	21.1 ± 0.4 [a]	0.90 ± 0.03
5.5	870 ± 28 [a]	866 ± 30 [b]	0.97 ± 0.05

a) No d_3-acetonitrile used.

b) 10% acetonitrile used.

It is clear that the ratios of the rate constants of racemisation with the rate constants of H/D exchange are closer to unity than to 0.5 or 2 for 5-substituted 1-acetyl-2-thiohydantoins. The value of k_{rac} / k_{HD} approaching unity confirms S_E1 rather than S_E2, with the proposed mechanism illustrated in Scheme 5.2.

The rate constant for H/D exchange of the racemic compound **5.6** (Table 5.3) is the highest measured. This suggests a high rate constant for racemisation as well. Therefore, during the preparation, the compound racemised; this was not noticed for the other enantioenriched 5-substituted 1-acetyl-2-thiohydantoins. Similarly, it was reported that 5-phenylhydantoin racemised significantly faster ($t_{1/2}$: 0.3 h) than 5-benzylhydantoin ($t_{1/2}$: 5 h), and 5-isopropylhydantoin ($t_{1/2}$: 56 h).[9] The highest rate constant for racemisation and H/D exchange for **5.6** is in agreement with the results of Reist *et al*.[4] and Narduolo,[3] which showed high rate constants for H/D exchange of 5-phenylhydantoin compared with other substituted

hydantoins. The phenyl group on the stereogenic centre of thiohydantoin and hydantoin stabilise the intermediate carbanion by resonance.[10]

5.2.2 The H/D exchange process of 5-substituted 2-thiohydantoins

As mentioned before, the separation of enantiomers of **5.8** and **5.12** was attempted using chiral HPLC. However, before kinetic studies could be carried out, **5.8** and **5.12** had already racemised during solvent evaporation. We also attempted to study the racemisation of 5-(pyridin-2-ylmethyl)-2-thioxoimidazolidin-4-one **5.12**, after the separation of both enantiomers by chiral HPLC without evaporating the eluent used in the HPLC separation and observed that racemisation was quite fast in comparison with compounds **5.1**-**5.5**. Similarly, compounds **5.7**-**5.14** (Scheme 5.5) could not be obtained in enantioenriched form. As mentioned in the last section, there is a strong relationship between the racemisation and H/D exchange process, with k_{rac} approximately equal to $k_{H/D}$ for substituted 1-acetyl-2-thiohydantoins. We therefore decided to use ^{1}H-NMR spectroscopy as an alternative way to obtain rate constants related to the rate constants for racemisation.

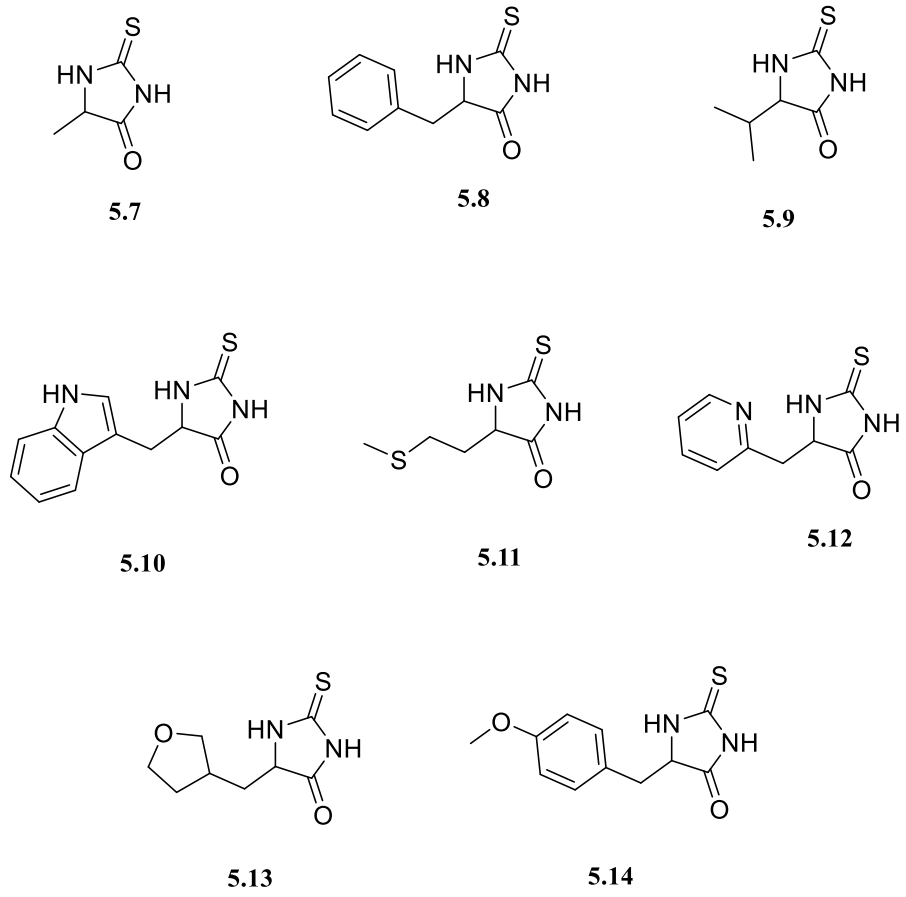

Scheme 5.5: The chemical structures of compounds **5.7**-**5.14**

Such rapid racemisation indicates that the hydrogen attached to the stereogenic centre of 5-substituted 2-thiohydantoins is replaced by deuterium more rapidly than in the case of hydantoin, as reported previously.[3, 4]

When the concentrations of buffer used in ^{1}H-NMR spectroscopic experiments were as used for compounds **5.1**-**5.6**, there were not enough data points obtained for **5.7**-**5.14** to plot the relative area versus time and obtain a rate constant. Use of lower concentrations of buffer was essential to obtain enough data points to plot relative integration areas of hydrogen on the stereogenic carbon versus time. ^{1}H-NMR spectroscopy was used to obtain the H/D exchange rate constants of **5.7**-**5.14** in 10% d_3-ACN and 90% 0.01 M D_2O-phosphate buffer (pH* 7.4, 1 M *I*, at 37 °C).

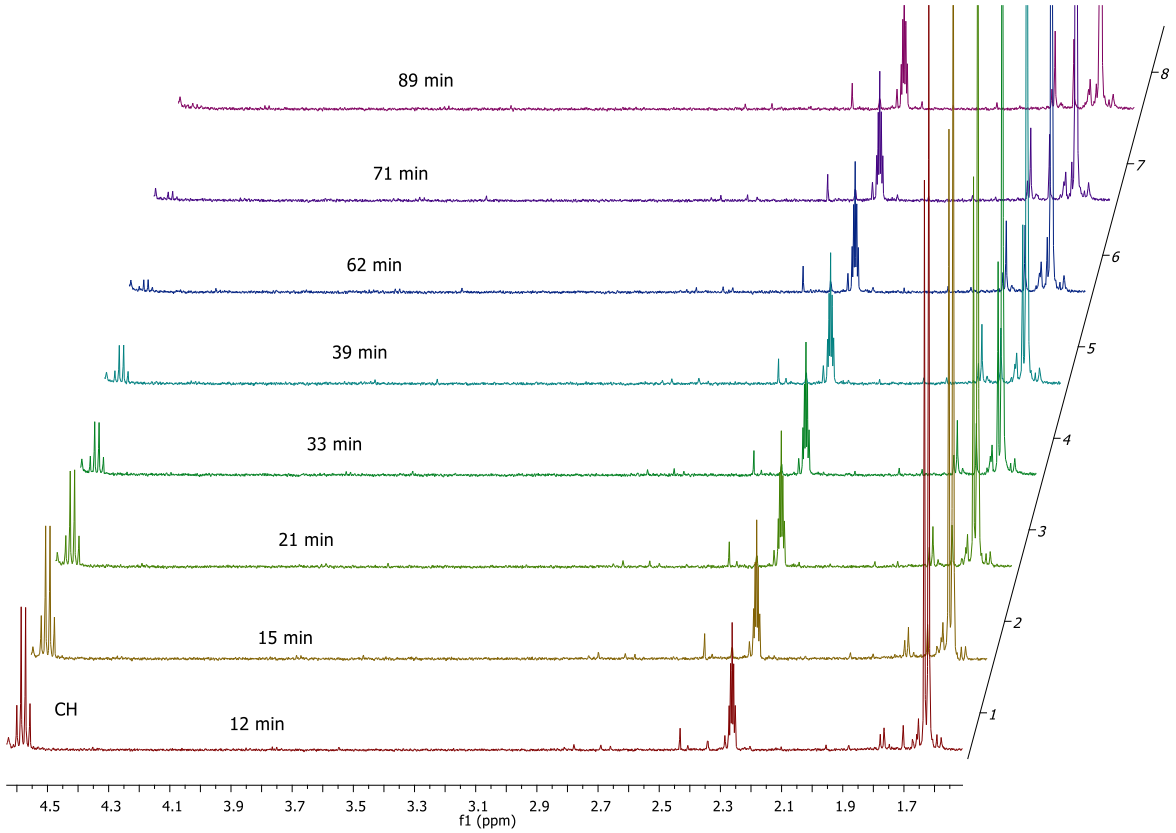

Figure 5.4: ^{1}H-NMR spectra for **5.7** from 12 to 89 min in 10 % d_3-acetonitrile and 90% 0.01 M D_2O-phosphate buffer (pH* 7.4, 1 M *I*, at 37 °C).

From Figure 5.4, it is clear that the signal for the hydrogen on the stereogenic carbon (at 4.6 ppm) decreases over time and the relative integration areas of the hydrogen were plotted versus time to determine the pseudo-first-order rate constants for H/D exchange (Figure 5.5). Unfortunately, the peaks for the hydrogen at the asymmetric carbons for several of the compounds synthesised (Chapter 2) overlapped with the water peak of the solvent. Therefore, the H/D exchange process could not be measured for several of the 5-substituted 2-thiohydantoins reported in Chapter 2.

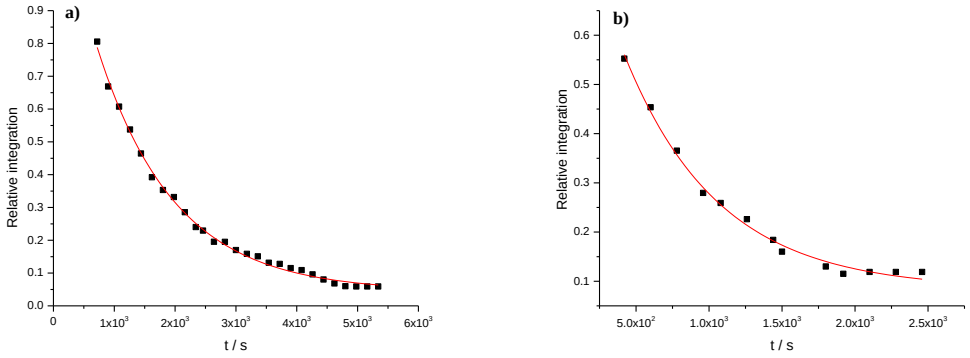

Figure 5.5: Relative integrals for the proton on the stereogenic centre of a) **5.7** and b) **5.8** in 10% d_3-acetonitrile and 90% 0.01 M D_2O-phosphate buffer (pH^* 7.4, 1 M *I*, at 37 °C). Solid lines are fits to the first order rate law.

Figure 5.5 shows the pseudo-first-order rate law fit to the data for the H/D exchange process in 10% d_3-ACN with 90% D_2O-phosphate buffer (pH^* 7.4, 0.01 M, 1 M *I*, at 37 °C). Fortunately, there was no precipitation while mixing the co-solvents (10%) such as d_3-ACN and d_6-DMSO with the deuterated-phosphate buffer (90%) (pH^* 7.4, 0.01 M, 1 M *I*, at 37 °C) for 5-substituted 2-thiohydantoins. The temperature of the NMR machine was set to 37 °C and the number of scans decreased to reduce the measurement time and obtain a higher number of points. It is also important to note that the time between zero minutes and the first integration is long in comparison with the other points because it was impossible to shorten the time required for the shimming of the NMR machine at the beginning. The other figures for the compounds shown in Scheme 5.6 are illustrated in the Appendix. The pseudo-first-order rate constants were obtained by using Equation 5.1 for compound **5.7**-**5.14** and these are summarised in Table 5.4.

Table 5.4: Pseudo-first-order rate constants for H/D exchange, $k_{H/D}$, determined using ^{1}H-NMR spectroscopy of **5.7**-**5.14** in D_2O-phosphate buffer at 0.009 M total phosphate (ionic strength of 0.9 M *I*, pH* 7.4 at 37 °C).

Substrate	Total phosphate /M	Basic phosphate / M	$k_{H/D}$ (D_2O) / 10^{-6} s^{-1}
5.7	0.009	0.0072	789 ± 23[a]
5.8	0.009	0.0072	1550 ± 103 [a]
5.9	0.009	0.0072	202.9 ± 2.4[b]
5.10	0.009	0.0072	705 ± 24[b]
5.11	0.009	0.0072	2880 ± 230[b]
5.12	0.009	0.0072	3010 ± 220[b]
5.13	0.009	0.0072	3020 ± 250[b]
5.14	0.009	0.0072	1312 ± 90[a]

[a] 10% d_3-acetonitrile and 90% 0.01 M D_2O-phosphate buffer (pH* 7.4, 1 M *I*, at 37 °C).

[b]10% d_6-DMSO and 90 % 0.01 M D_2O-phosphate buffer (pH* 7.4, 1 M *I*, at 37 °C).

The rate constants for H/D exchange of **5.7**-**5.14** in Table 5.4 strongly depend on the substituent at the 5-position, as shown also by the rate constants of racemisation for these compounds (*vide supra*). As explained before, steric hindrance has a significant effect on the promotion or retardation of racemisation. Compound **5.9**, with an isopropyl substituent at C-5, has the slowest rate constant for H/D exchange, analogous to the low rate constant for racemisation of 1-acetyl-5-isopropyl-2-thiohydantoin. The presence of a benzyl group in **5.8** increases the acidity of the hydrogen on the asymmetric carbon. The highest rate constants of H/D exchange were obtained for compounds **5.11**-**5.13** which contain oxygen, sulphur and nitrogen in the substituent at the asymmetric carbon. The protonation of the pyridine substituent of compound **5.12** makes the compound much more electron-withdrawing in comparison with **5.8** and increases the rate constant for racemisation and H/D exchange.

The rate constant for H/D exchange has previously been studied for 5-substituted hydantoins at different concentrations of buffer and at different temperatures. Reist *et al*.[4] reported the rate constants for H/D exchange for various 5-substituted hydantoins at 50 °C, while the rate constants of H/D exchange for 5-phenylhydantoin and 5-benzylhydantoin have been reported at different temperatures. The buffer concentrations and temperatures in these studies are not

similar to the present work, making it difficult to compare the thiohydantoin and hydantoin derivatives (Table 5.5).

Table 5.5: Comparison of the pseudo-first-order rate constants of H/D exchange $k_{H/D}$ of 5-substituted hydantoin determined by Testa *et al.*[4] and the 5-subsituted 2-thiohydantoin in the present work.

	$k_{H/D}$[a] / 10^{-6} s^{-1}	R group	$k_{H/D}$[b] / 10^{-6} s^{-1}	
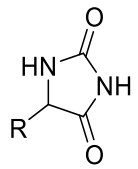	3140 ± 530	Ph	------	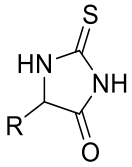
	16.7 ± 1.1	CH_2Ph	1550 ± 103	
	77.8 ± 15.3	CH_2OH	-------	
	32.8 ± 1.7	$NH_2(O)NH$	-------	
(**1**)	9.2 ± 0.3	CH_3	789 ± 23	(**2**)
	4.7 ± 0.3	CH_2COOH	-------	
	1.7 ± 0.2	$CH(CH_3)_2$	202.9 ± 2.4	

[a] determined in a mixture of D_2O phosphate buffer (pD 7.4, 0.1 M, I = 0.22) and d_6-DMSO in a 1:1 (*v*/*v*) proportion at 50 °C.

[b] determined in a mixture of phosphate buffer (pH* 7.4, 0.01 M, 1 M I) and d_6-DMSO and d_3-ACN in a 9:1 (*v*/*v*) proportion at 37 °C.

Table 5.5 shows that the pseudo-first-order rate constants for H/D exchange of 5-substituted hydantoin in the higher concentration of buffer, lower ionic strength and higher temperature are lower than the $k_{H/D}$ of the corresponding 5-substituted-2-thiohydantoin. Unfortunately, there are no exact conditions that have been reported previously for hydantoin to compare with the present conditions used for thiohydantoin. This indicates that the role of the sulphur atom in the increase in the rate of racemisation and H/D exchange occurs through increasing the stability of the carbanion.[6]

5.2.3 The H/D exchange process of 3-phenyl-5-benzyl-2-thiohydantoin

As mentioned in Chapter 3, the presence of substituents at the N-3 position increased the rate constant for hydrolysis. However, it has been reported that replacing one of the hydrogen atoms at the N-3 or N-1 position may retard racemisation. Furthermore it has been reported that replacement of both hydrogens should prevent a decrease in the rate of racemisation.[11] For compounds **5.16** and **5.17**, the pseudo-first-order rate constants for H/D exchange were reported by Narduolo[3] who showed the effect of substituents at the N-3 position. Narduolo[3] and Lazarus[12] reported that when the N-3 hydrogen of hydantoin was replaced by a methyl group, H/D exchange became slower (Scheme 5.6).

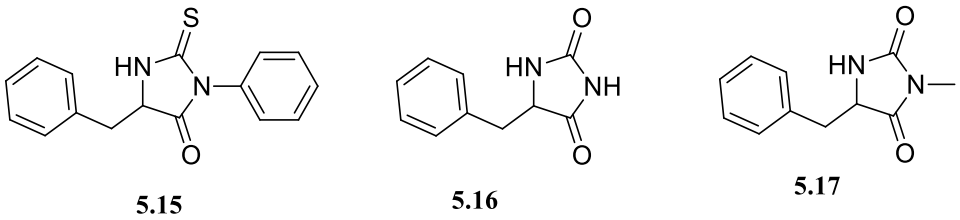

Scheme 5.6: The chemical structures of compounds **5.15**-**5.17**

Using 10 % d_3-ACN or d_6-DMSO caused the precipitation of **5.15** with 90 % phosphate buffer (pH* 7.4, 0.01 M, 1 M *I*). Sufficient concentrations of compound **5.18** were required to observe the peak in ^{1}H-NMR spectra. Therefore, 20 % d_3-ACN was used with 80 % D_2O-phosphate buffer to avoid precipitation from taking place. The relative areas of the signal for the hydrogen at the stereogenic carbon was followed over time to determine the pseudo-first-order rate constant for H/D exchange of **5.15** (Figure 5.6).

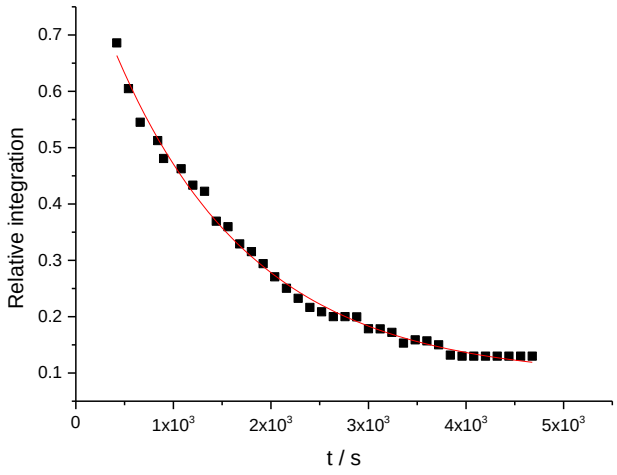

Figure 5.6: Relative integrals for the proton on the stereogenic centre for **5.15** in 20% d_3-acetonitrile and 80% 0.01 M D_2O-phosphate buffer (pH* 7.4, 1 M *I*, at 37 °C).

The line in Figure 5.6 is a fit of the pseudo-first-order law to the data for H/D exchange. Equation 5.1 was used to observe the rate constant $k_{H/D}$. It is interesting to compare the rate constant for H/D exchange, $k_{H/D}$, for **5.15** (containing a 3-*N*-phenyl substituent) with $k_{H/D}$ for **5.8** (which is unsubstituted on N-3) to show the effect of a substituent at the N-3 position on the racemisation process (Table 5.6).

Table 5.6: Comparison of the pseudo-first-order rate constants of H/D exchange $k_{H/D}$ of 5-benzyl-3-phenylimidazolidine-2,4-dione and 5-benzylimidazolidine-2,4-dione determined by Narduolo[3], and 5-benzyl-3-phenyl-2-thioxoimidazolidin-4-one and 5-benzyl-2-thioxoimidazolidin-4-one in the present work.

Substrate	$k_{H/D}$ / 10^{-6} s^{-1}	Substrate	$k_{H/D}$ / 10^{-6} s^{-1}
5.15	707 ± 28[a]	**5.8**	1550 ± 103 [a]
5.17	3.4 ± 0.1[b]	**5.16**	5.4 ± 0.4 [b]

[a] determined in D_2O-phosphate buffer (0.5 M, 1 M *I*, kept constant with KC1, pH* 7.2, at 25 °C).

[b] determined in a mixture of phosphate buffer (pH* 7.4, 0.01 M, 1 M *I*) and d_6-DMSO or d_3-ACN in a 9:1 (*v*/*v*) proportion at 37 °C.

Table 5.6 shows that the introduction of substituents at N-3 retards H/D exchange for both hydantoins and 2-thiohydantoins. The results in Table 5.6 are in agreement with the suggestion of Bovarnic and Clarice that the substituent at the N-3 position decreases the rate constant for racemisation k_{rac}. The k_{rac} was found to be similar to $k_{H/D}$ in the previous section for **5.1**-**5.4** (indicating an S_E1 mechanism). Therefore, the substituent at the N-3 position retards the rate constant $k_{H/D}$ in a similar way to the racemisation as expected by Bovarnic. Unfortunately, there has been no data for H/D exchange reported for hydantoin derivatives under similar conditions to compare with the thiohydantoins in the present work.

5.2.4 The H/D exchange process of 5-substituted thiazolidine-2,4-diones

The racemisation of the three glitazones (also called thiazolidine-2,4-dione) balaglitazone, pioglitazone and rosiglitazone (Scheme 5.7) were reported previously.[13]

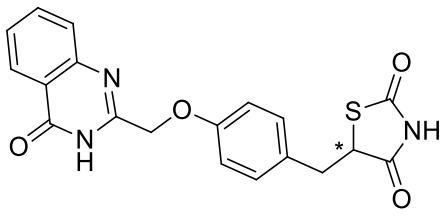

5.18

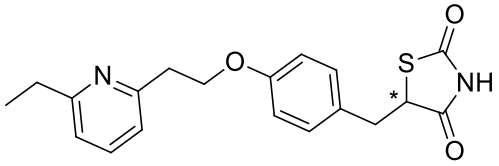

5.19

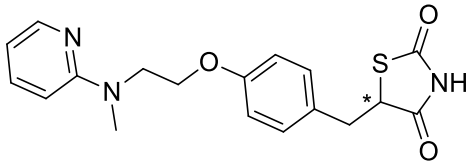

5.20

Scheme 5.7: Structure of the three glitazones: (**5.18**) balaglitazone, (**5.19**) pioglitazone and (**5.20**) rosiglitazone. The marked carbon atom with the star (*) shows the chiral centre.[13]

The C-5 stereogenic centre is anticipated to be relatively acidic because deprotonation induces sp^2 character to C-5 and increases π -delocalisation. Therefore, base-catalysed ionisation of thiazolidine-2,4-dione is anticipated to play an important role in the racemisation process.[14] Jamali *et al.*[15] reported that keto-enol tautomerism is the expected pathway to convert the R

enantiomer to its S enantiomer (and vice versa) for 5-substituted thiazolidine-2,4-dione, as explained also in Chapter 1 (Scheme 5.8).

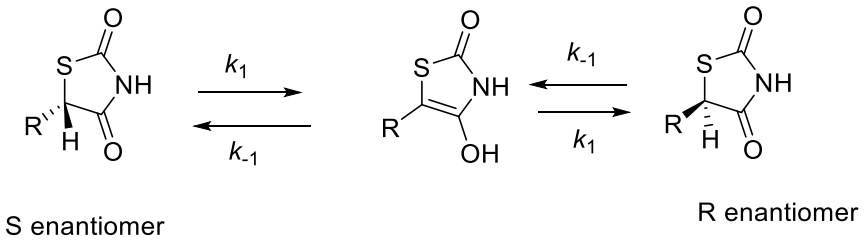

Scheme 5.8: The keto-enol tautomerism of 5-substituted- thiazolidine-2,4-dione

5-Substituted thiazolidine-2,4-dione derivatives have also been prepared as racemic compounds. There is a close relation between the rate constants for H/D exchange ($k_{H/D}$) and racemisation processes (k_{rac}) (*vide supra*). No optically active 5-substituted thiazolidine-2,4-diones could be prepared to study the kinetics of racemisation using CD spectroscopy. Therefore, the H/D exchange process was studied as an alternative to obtaining the rate constants for racemisation (Scheme 5.9).

Scheme 5.9: The chemical structures of compounds **5.21** and **5.22**

Similar conditions as those used for kinetic studies of compounds **5.1**-**5.5** were used for **5.21** and **5.22** because 5-substituted thiazolidine-2,4-dione racemised more slowly than 5-substituted 2-thioxothiazolidin-4-one (thiohydantoin). The relative area of the ^{1}H-NMR signal for hydrogen at C-5 was followed over time in D_2O-phosphate buffer (0.09, 0.18 and 0.27 M total phosphate buffer, 0.9 M *I*, pH* 7.4, at 37 °C). The integrated areas were plotted against time to determine the pseudo-first-order rate constant for H/D exchange $k_{H/D}$ (Figure 5.7).

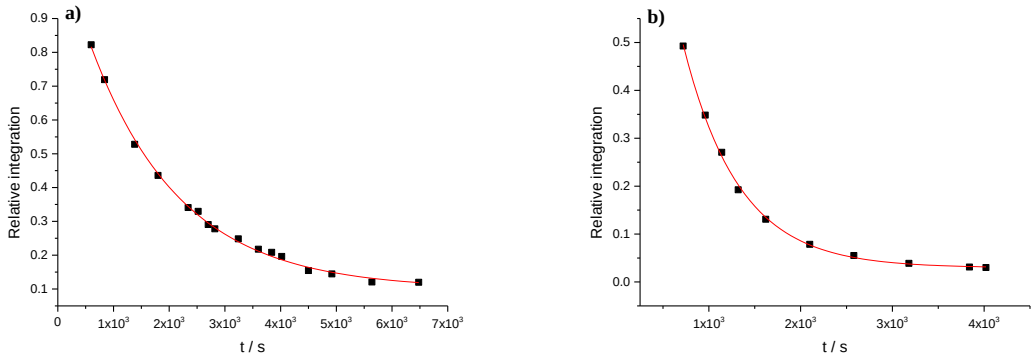

Figure 5.7: Relative integrals for the proton on the stereogenic centre of **5.24** and **5.25** in 10 vol-% d_3-acetonitrile and 90 vol-% (0.2 M D_2O-phosphate buffer pH* 7.4, 1 M *I*, at 37 °C).

In Figure 5.7, the lines are fits of the pseudo-first-order rate law to the rate constant for H/D exchange $k_{H/D}$. The pseudo-first-order rate constants $k_{H/D}$ at 0.27 M, 0.18 M, and 0.09 M of total D_2O-phosphate (0.9 M *I*, pH* 7.4 and 37 °C) are shown in Table 5.7.

Table 5.7: Pseudo-first-order rate constants $k_{H/D}$ determined using ^{1}H-NMR spectroscopy of 5-benzylthiazolidine-2,4-dione (**5.21**) and 5-(pyridin-2-ylmethyl)thiazolidine-2,4-dione (**5.22**) in D_2O-phosphate buffer at 0.27, 0.18, and 0.09 M total phosphate and 0.22, 0.14, and 0.072 M HPO_4^{2-}, respectively (0.9 M *I*, pH* 7.4 and 37 °C) using 10% d_3-ACN.

	5.21	**5.22**
Total Buffer / M	$k_{H/D}$ (D_2O)[a] /10^{-6} s^{-1}	$k_{H/D}$ (D_2O)[a] /10^{-6} s^{-1}
0.09	411± 16	1269 ± 25
0.18	619 ± 19	1651 ± 49
0.27	800 ± 40	1918 ± 98

[a] The data were collected by Ibrahim Bala[16]

The $k_{H/D}$ for **5.21** and **5.22** increased by increasing the concentration of D_2O-phosphate buffer. The pseudo-first-order rate constants for H/D exchange of **5.24** and **5.25** were plotted against the concentration of the basic component of deuterated-phosphate buffer (pH* 7.4, 0.9 M *I*, at 37 °C) (Figure 5.8).

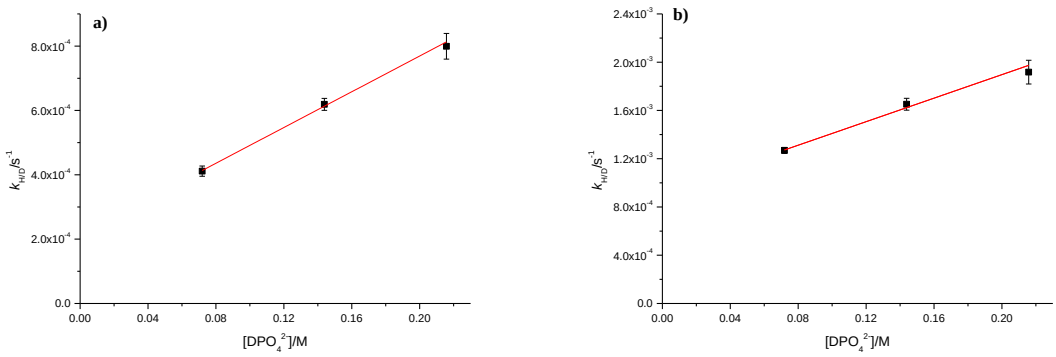

Figure 5.8: First-order rate constants for buffer-catalysed H/D exchange followed using ^{1}H-NMR spectroscopy of a) **5.21** and b) **5.22** in D_2O-phosphate buffer (0.9 M *I*, pH* 7.4 at 37 °C).

Figure 5.8 shows a linear correlation between the first-order rate constants and the basic component of the phosphate buffer. Equation 5.2 was used to obtain the second-order rate constant $k_{H/D}$ for **5.21** and **5.22**. The uncatalysed, specific acid and base-catalysed rate constants are combined in the intercept and the bimolecular rate constant $k_{H/D}$ is obtained from the slope in Figure 5.8. The values are listed in Table 5.8.

Table 5.8: Second-order rate constants for H/D exchange $k_{H/D}$ of **5.21** and **5.22** in D_2O-phosphate buffer determined using ^{1}H-NMR spectroscopy at 0.27, 0.18, and 0.09 M total phosphate and 0.22, 0.14, and 0.072 M basic phosphate, respectively, (0.9 M *I*, pH* 7.4 at 37 °C) using 10 % d_3-ACN.

Substrate	$k_{H/D}$ / 10^{-6} s^{-1} M^{-1}	k_{in} / 10^{-6} s^{-1}
5.21	2780 ± 250	214 ± 30
5.22	4880 ± 450	922 ± 45

It is obvious from Table 5.8 that the compound with the 5-(pyridin-2-ylmethyl) substituent at the C-5 position has a higher rate constant $k_{H/D}$ than its homologue with benzyl substituents, as also observed for the thiohydantoin derivatives.

5.2.5 The H/D exchange process of 2-thioxothiazolidin-4-one

No previous studies are available for the racemisation or H/D exchange process of 2-thioxothiazolidin-4-ones. The H/D exchange process of racemic 5-substituted 2-thioxothiazolidin-4-ones **5.23** and **5.24** (Scheme 5.10) were compared with imidazolidine-2,4-dione, 2-thioxoimidazolidin-4-one and thiazolidine-2,4-dione.

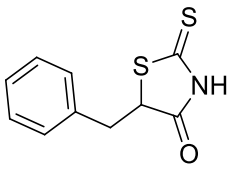

5.23

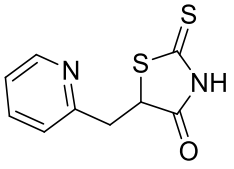

5.24

Scheme 5.10: The chemical structures of compounds **5.23** and **5.24**

It can be expected that the 2-thioxothiazolidin-4-one derivative also racemises by keto-enol tautomerism similar to imidazolidine-2,4-dione, 2-thioxoimidazolidin-4-one and thiazolidine-2,4-dione (Scheme 5.8). The presence of the sulphur atom next to the asymmetric carbon is similar for 2-thioxothiazolidin-4-one and thiazolidine-2,4-dione and might accelerate the enolisation. We tried to study the H/D exchange for compounds **5.23** and **5.24** but during the shim of the NMR, *i.e.* 5-10 minutes, the reaction has finished (D_2O-phosphate buffer at 0.09 M total phosphate with ionic strength of 0.9 M *I*, pH^* 7.4 and 37 °C, using 10 vol-% of d_3-CAN as a cosolvent). Therefore, we could not collect any points to construct a plot between relative integration area and time. It can be concluded from the fast deuteration that the sulphur atom attached to the asymmetric carbon not only accelerates the racemisation and deuteration. The thiocarbonyl is also important because 2-thioxoimidazolidin-4-one (thiohydantoin) with thiocarbonyl and a nitrogen atom at the 1-position racemises faster than 2- thiazolidine-2,4-dione with carbonyl and sulphur at the 1-position. Therefore, thioxoimidazolidin-4-ones (compounds **5.23** and **5.24**) containing both thiocarbonyl and sulphur have higher rate constants for deuteration and racemisation than compounds **5.1**-**5.22**.

5.3 Conclusions

Racemisation and H/D exchange were studied. The k_{deut} / k_{rac} values of approximately 1 in the present work for compounds **5.1**-**5.5** indicates the S_E1 mechanism for racemisation rather than the S_E2 mechanism. The H/D exchange of compound **5.6** with a phenyl substituent at the C-5 position was determined with its $k_{H/D}$ value found to be higher than the $k_{H/D}$ values for **5.1**-**5.5**. This is because of the resonance stabilisation of the anion in **5.6**.

The rate constants for H/D exchange were obtained by using ^{1}H-NMR for racemic 5-substituted 2-thiohydantoins **5.7**-**5.14**. The values of $k_{H/D}$ depend on the substituents at the C-5 position, which have a major influence on the rate constant of racemisation and H/D exchange.

The phenyl substituent at the N-3 position in **5.15** decreases the rate constant for H/D exchange in comparison with 5-substituted 2-thiohydantoins.

The H/D exchange for the 5-substituted thiazolidine-2,4-diones (**5.21** and **5.22**) was also studied and the rate constants for H/D exchange $k_{H/D}$ were determined. The 2-thiohydantoins, with thiocarbonyl at the 2-position and nitrogen at the 1-position, have higher rate constants $k_{H/D}$ than thiazolidine-2,4-dione, with carbonyl at the 2-position and sulphur at the 1-position.

For 2-thioxothiazolidin-4-ones, with thiocarbonyl at the 2-position and sulphur at the 1-position, it was impossible to collect even one data point because the H/D exchange reactions for **5.23** and **5.24** were found to finish in less than 10 minutes.

From the present study it can be concluded that the rate constants of racemisation and H/D exchange increase by increasing the sulphur atoms either with thiocarbonyl or bound to the asymmetric carbon.

The comparison of the present work with previous studies suggests decreasing rate constants in the order 2-thioxothiazolidin-4-one (rhodanine) > 2-thioxoimidazolidin-4-one (2-thiohydantoin) > thiazolidine-2,4-dione > imidazolidine-2,4-dione (hydantoin).

5.4 Experimental

General Experimental

Buffer preparation

The preparation of all H_2O and D_2O phosphate buffers used in this chapter were explained in Chapter 4. The concentrations of the acid and basic components were calculated using the Henderson-Hasselbalch equation, taking into account the effect of ionic strength and temperature (37 °C) on the pK_a. Stock solutions of 0.09-0.1 M of studied compounds were used containing 10% d_3-ACN and 90 vol-% D_2O-phosphate buffer for the H/D exchange process for compound **5.2**, **5.4**, **5.5** and **5.6.** No overlap between the hydrogen attached to the stereogenic centre and water in ^{1}H-NMR spectroscopy was found.

General methods

All non-deuterated solvents were HPLC grade obtained from commercial supplies and used without further purification. Deuterated ACN and DMSO were purchased from Fluorochem or Sigma Aldrich. Materials used were weighed on an analytical Fisher Brand PS-100 balance (Max 100 g, d = 0.1 mg). Volumes for preparing stock solutions were measured by Gilson research micropipettes. Aqueous stock solutions were centrifuged three times to avoid precipitation inside the stock solution. pH measurements for all concentrations of buffers in non-deuterated and deuterated-buffer conditions were carried out at 20 °C using a Hanna Instruments pH 210 pH meter. The pH meter was calibrated before each measurement with certified (traceable to NIST) buffers at pH 10.01+ 0.02 (at 20 °C) (from Fisher) and pH 4.00 + 0.01 (at 20 °C) (from Reagecon). Kinetic experiments of racemisation were carried out on a Chirascan CD spectrometer equipped with a temperature-controlled sample holder for circular dichroism (temperature stability: ± 0.02 °C) in 1.00 cm path length quartz cuvettes, unless otherwise stated. Kinetic experiments of H/D exchange were carried out on a Bruker Avance 400 and a Bruker Avance 500 NMR spectroscopy. Origin pro 9.0 and Mestrenova were used for data analysis.

4.4.1.5 Preparation of solutions

Stock solutions of 0.05-0.06 M of **5.1** and **5.3** were prepared by dissolving the thiohydantoin in 10 % D_2O and 90 % deuterated phosphate buffer. An ultrasonic bath sonicator was used to accelerate the dissolution process. Aqueous solutions of **5.1** and **5.3** were put in plastic Eppendorfs and centrifuged for 8 minutes at 13.3 rpm on a Jencons-pls Spectrafuge 24.D centrifuge. The remaining compounds were dissolved in d_3-ACN or d_6-DMSO and mixed with 90% D_2O- phosphate buffer.

4.4.1.6 Kinetic studies

The temperature of **5.1**-**5.4** samples during kinetic experiments of H/D exchange was controlled in a water bath because the reaction was slow in comparison with the other compounds. However, the temperature of the NMR holder for the other compounds was set at 37 °C because the reaction was fast.

4.4.1.7 Data analysis

^{1}H-NMR data were analysed for all compounds by the Mestrenova NMR program and the areas were integrated. The relative areas for the asymmetric hydrogens for all compounds were plotted versus time and the pseudo-first-order rate constant of H/D exchange determined using Origin pro 9.0.

Kinetic equations

To calculate the pseudo-first-order rate constants for H/D exchange of the studied compounds, the following equation was used:

$$R_t = R_{fin} + \Delta R\, e^{-k \times t} \qquad \textbf{Equation 5. 1}$$

Here, R_t is the relative area at time t, R_{fin} is the final relative area, ΔR represents the difference between the relative area at time zero and R_{fin}, and k is the observed pseudo-first-order rate constant of the hydrogen-deuterium exchange.

To calculate the second-order rate constants for H/D exchange, the following equation was used:

$$k_{obs} = k_0 + k_{OD^-}\left[OD^-\right] + k_{D_3O^+}\left[D_3O^+\right] + k_{buffer}[\text{buffer}] \qquad \textbf{Equation 5. 2}$$

where k_0 is the rate constant for the non-catalysed reaction, k_{OD^-} and k_{D3O+} are the specific base and acid catalysed rate constants for H/D exchange, respectively, which can be obtained from the intercept (k_{in}), k_{buffer} is the second-order rate constant for the buffer catalysis of H/D exchange, which is determined from the slope, and k_{obs} is the observed rate constant of the reaction.

4.4.1.8 Error calculation

The errors of pseudo-first-order and second-order rate constants were provided by non-linear and linear equations in Origin Pro 9.0. The errors of k_{rac}/k_{deut} were calculated by using Equation 4.9 in Chapter 4 (*vide supra*). The weighted average and its error equation (for equations, see Chapter 4) were used for compound **5.5** after obtaining two non-linear graphs, which were corrected with and without the base line in ^{1}H-NMR spectroscopy by the Mestrenova program.

4.4.1.9 Acknowledgment

I would like to thank Dr Rob Jenkins and Robin Hicks for their kind help with NMR experiments. I also thank Ibrahim Bala who obtained rate constants for the H/D exchange of compounds **5.21** and **5.22**.

5.5 References

1. D. J. Cram, B. Rickborn, C. A. Kingsbury and P. Haberfield, *Journal of the American Chemical Society*, 1961, 83, 3678-3687.
2. D. J. Cram, *Fundamentals of carbanion chemistry*, Academic Press, 1965.
3. S. Narduolo, Thesis (Ph D) - Cardiff University, 2011.
4. M. Reist, P.-A. Carrupt, B. Testa, S. Lehmann and J. J. Hansen, *Helvetica Chimica Acta*, 1996, 79, 767-778.
5. M. Reist, L. H. Christiansen, P. Christoffersen, P.-A. Carrupt and B. Testa, *Chirality*, 1995, 7, 469-473.
6. A. C. Cabordery, M. Toussaint, N. Azaroual, J. P. Bonte, P. Melnyk, C. Vaccher and C. Foulon, *Tetrahedron Asymmetry*, 2011, 22, 125-133.
7. P. G. Gassman and F. V. Zalar, *Journal of the American Chemical Society*, 1966, 88, 3070-3074.
8. E. Buncel, *Carbanions: Mechanistic and Isotopic Aspects*, Elsevier Scientific Publishing Company, 1975.
9. A. S. Bommarius, M. Schwarm and K. Drauz, *Journal of Molecular Catalysis B: Enzymatic*, 1998, 5, 1-11.
10. S. Martínez-Rodríguez, F. J. Las Heras-Vázquez, L. Mingorance-Cazorla, J. M. Clemente-Jiménez and F. Rodríguez-Vico, *Applied and Environmental Microbiology*, 2004, 70, 625-630.
11. M. Bovarnick and H. T. Clarke, *Journal of the American Chemical Society*, 1938, 60, 2426-2430.
12. R. A. Lazarus, *The Journal of Organic Chemistry*, 1990, 55, 4755-4757.
13. B. Jamali, G. C. Theill and L.-L. Sørensen, *Journal of Chromatography A*, 2004, 1049, 183-187.
14. P. V. Bharatam and S. Khanna, *The Journal of Physical Chemistry A*, 2004, 108, 3784-3788.
15. B. Jamali, I. Bjørnsdottir, O. Nordfang and S. H. Hansen, *Journal of pharmaceutical and biomedical analysis*, 2008, 46, 82-87.
16. I. A. Bala, Thesis (MSc)- Cardiff University, 2014.

Chapter 6

Epilogue

6.1 General conclusions

In the present work, the kinetics and mechanism of racemisation and H/D exchange of substituted 2-thiohydantoins (2-thioxoimidazolidin-4-ones), thiazolidine-2,4-diones and rhodanines (2-thioxothiazolidin-4-ones) have been studied under conditions mimicking physiological conditions. From the present work, the following conclusion can be drawn.

First, 2-thioxoimidazolidin-4-one derivatives with substituents at the 1, 3 and/or 5-positions have been prepared as racemic and enantioenriched compounds (Chapter 2). Knoevenagel condensation worked successfully in reactions involving different aldehydes with the parent 2-thioxoimidazolidin-4-ones to prepare the corresponding unsaturated 2-thioxoimidazolidin-4-ones. Knoevenagel condensation also worked in the preparation of unsaturated 5-substituted thiazolidine-2,4-diones and 5-substituted 2-thioxothiazolidin-4-one derivatives. To prepare saturated 5-substituted 2-thioxoimidazolidin-4-ones, zinc and acetic acid were used to reduce the double bond to a single bond and prepare racemic 5-substituted 2-thioxoimidazolidin-4-ones. The reduction process worked well for all unsaturated 2-thioxoimidazolidin-4-ones prepared, except for (Z)-5-(furan-2-ylmethylene)-2-thioxoimidazolidin-4-one which produces an unknown product. Zn/acetic acid was also a good agent to reduce (Z)-5-(pyridin-2-ylmethylene)thiazolidine-2,4-dione but not (Z)-5-benzylidenethiazolidine-2,4-dione; the reason for this difference was unclear. As an alternative, $LiBH_4$ in the presence of pyridine for catalytic reduction in THF was tried for (Z)-5-benzylidenethiazolidine-2,4-dione and was found to be successful. Our attempts to prepare enantioenriched 5-substituted 2-thioxoimidazolidin-4-ones derivatives starting from enantiopure amino acids with thiourea failed because of the high temperature required for the reaction. Chiral HPLC was used for the separation of 5-(pyridin-2-ylmethyl)-2-thioxoimidazolidin-4-one *R*- and *S*- enantiomers.

Several enantioenriched 5-substituted 1-acetyl-2-thioxoimidazolidin-4-one derivatives were synthesised from the corresponding amino acids with ammonium thiocyanate in the presence of acetic acid and acetic anhydride. N-acetyl substituted 2-thioxoimidazolidin-4-ones could be obtained with some enantiomeric excess.

Second, during racemisation studies (Chapter 4) the buffer-catalysed hydrolysis of 2-thioxoimidazolidin-4-one was observed. Kinetic studies of this process were described in Chapter 3. The acetyl substituent on the N-1 position of 5-substituted 1-acetyl-2-thioxoimidazolidin-4-ones can be rapidly removed by acid or base. It was concluded that by using a base, such as sodium hydroxide and a buffer, the hydrolysis of 5-substituted 1-acetyl-2-thioxoimidazolidin-4-ones produces 5-substituted 2-thioxoimidazolidin-4-ones and the

subsequent continued hydrolysis produces substituted 2-thioureidopropanoic acids. On the other hand, using acids, such as hydrochloric acid, produces 5-substituted 2-thioxoimidazolidin-4-ones without continued hydrolysis. The substituents at the C-5 position change the rate constants for hydrolysis, depending on steric hindrance. It is also interesting to note that a phenyl substituent at the N-3 position increases the rate constant for the hydrolysis of 2-thioxoimidazolidin-4-ones derivatives.

Third, in Chapter 4 the rate constants for the loss of the optical activity k_{θ} were determined directly using CD spectroscopy. The substituents at C-5 influenced the rate constants through steric hindrance and the presence of highly electronegative atoms and electron-withdrawing groups on the substituent. The k_{θ} were observed at different concentrations of buffer and were found to increase linearly with increasing concentration of buffers, suggesting general-base catalysed of racemisation. The comparison of k_{θ} in H_2O- and D_2O-phosphate buffer showed negligible solvent kinetic isotope effect, with the rate constants within the margin of error. The rate constants for racemisation, k_{rac}, were determined by subtracting the rate constant of hydrolysis k_{hyd} from the rate constants for the loss of optical activity k_{θ}. The sensitivity of the proton transfer for the nature of the buffer was studied using different buffers (acetate, phosphate and TRIS) and observing the rate constants k_{θ} and k_{rac}. The β-value of 0.21 ± 0.0008 for **4.1** was obtained from the Brønsted plot, which suggests an early transition state. However, it was noted that the ionisation of the most acidic hydrogen at N-3 affects the value of β. Therefore, by using the pK_a of the substituted 2-thioxoimidazolidin-4-ones, together with the pH, the rate constants of racemisation for the protonated (*S*)-1-acetyl-5-methyl-2-thioxoimidazolidin-4-one were calculated and plotted versus the pK_a of buffers. The resulting β-value of 0.51 ± 0.09 for the protonated (*S*)-1-acetyl-5-methyl-2-thioxoimidazolidin-4-one confirmed general-base catalysis of racemisation and suggests the proton is approximately halfway between the reactant and product in the transition state. The rate constants k_{θ} and k_{rac} in different concentrations of H_2O- and D_2O based phosphate buffers were also determined for the trisubstituted 2-thioxoimidazolidin-4-ones. Similar to the 5-substituted 1-acetyl-2-thioxoimidazolidin-4-one derivatives, a negligible solvent kinetic isotope effect on the racemisation was found. The rate constants for racemisation of trisubstituted 2-thioxoimidazolidin-4-ones were quite high in comparison with the rate constants for racemisation of 5-substituted 1-acetyl- tri-substituted 2-thioxoimidazolidin-4-ones. From the temperature dependence, the racemisation reaction of (*R*)-5-benzyl-3-phenyl-1-(pyridin-2-ylmethyl)-2-thioxoimidazolidin-4-one, a positive enthalpy value and negative entropy value of activation was found for the loss of optical activity. Addition of 10 vol-% of a co-solvent

with phosphate buffer changed the rate constant k_θ in comparison with 100% aqueous solution. DMSO, TFE and methanol increase the rate constant of racemisation k_θ to **4.7**. It was found that 5-substituted 2-thioxoimidazolidin-4-ones racemise fast, not only in buffer, but also in water and organic solvents.

Fourth, the mechanism of racemisation for 5-substituted 1-acetyl-2-thioxoimidazolidin-4-ones was described in Chapter 5 by comparing $k_{H/D}$ (determined using ^{1}H-NMR spectroscopy) and k_θ (obtained using CD spectroscopy) in D_2O based phosphate buffer. We found that $k_{H/D}/k_{rac}$ is close to unity, which confirms the S_E1 mechanism rather than the S_E2 mechanism for the racemisation of 5-substituted 1-acetyl-2-thioxoimidazolidin-4-ones. Therefore, as an alternative to studying the racemisation process, H/D exchange was studied for racemic 5-substituted 2-thioxoimidazolidin-4-one derivatives assuming $k_{H/D} = k_{rac}$. The H/D exchange process was studied for a variety of compounds with different substituents at the asymmetric carbon using ^{1}H-NMR spectroscopy. Similar to our observations for racemisation, substituents at C-5 have a significant effect on the rate constants for H/D exchange. The rate constants $k_{H/D}$ for 5-substituted 2-thioxoimidazolidin-4-ones were high in comparison with the $k_{H/D}$ for 5-substituted 1-acetyl-2-thioxoimidazolidin-4-ones. The rate constant for H/D exchange of 5-((tetrahydrofuran-3-yl)methyl)-2-thioxoimidazolidin-4-one was the highest, with the lowest rate constant for H/D exchange found for 5-isopropyl-2-thioxoimidazolidin-4-one. The phenyl substituent at the N-3 position slows down H/D exchange of 5-benzyl-3-phenyl-2-thioxoimidazolidin-4-one in comparison with 5-benzyl-2-thioxoimidazolidin-4-one. Our reported data showed that $k_{H/D}$ was lower for 5-benzylthiazolidine-2,4-dione and 5-(pyridin-2-ylmethyl)thiazolidine-2,4-dione than for the corresponding 5-substituted 2-thioxoimidazolidin-4-ones (thiohydantoin). It can be concluded from comparison with previous reports such as those by Narduolo[1], Reist *et al*.[2] and Lazarus[3] that the $k_{H/D}$ and k_{rac} of imidazolidine-2,4-dione (hydantoin) derivatives are lower than for thiazolidine-2,4-dione derivative (Scheme 6.1).

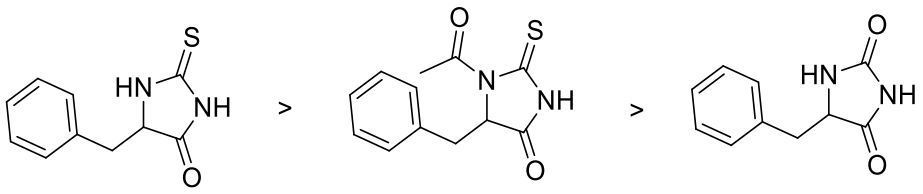

Scheme 6.1: Comparison of the rate constants for H/D exchange for 5-benzyl-2-thioxoimidazolidin-4-one, 1-acetyl-5-benzyl-2-thioxoimidazolidin-4-one and 5-benzylimidazolidine-2,4-dione

The H/D exchange process was studied for 5-benzyl-2-thioxothiazolidin-4-one and 5-(pyridin-2-ylmethyl)-2-thioxothiazolidin-4-one and loss of the hydrogen at the asymmetric carbon in less than 10 minutes was observed, corresponding to the fastest exchange measured in this study. The $k_{H/D}$ or k_{rac} can thus be ordered imidazolidine-2,4-dione (hydantoin) < thiazolidine-2,4-dione < 2-thioxoimidazolidin-4-one (thiohydantoin) < 2-thioxothiazolidin-4-one (rhodanine) derivatives.

6.2 Future work

In order to complete the studies on 2-thioxoimidazolidin-4-ones (thiohydantoin), it would be interesting to synthesise enantioenriched 5-substituted 2-thioxoimidazolidin-4-ones by carrying out the reaction at low temperature. Alternatively, using chiral columns such as CHIRALPAK® or CHIRALCEL® to separate racemic 5-substituted 2-thioxoimidazolidin-4-one and keeping the sample at very low temperature to avoid racemisation could also be attempted. We have already tried the Astec Chirobiotic T chiral column without success for the separation of several racemic 5-substituted 2-thioxoimidazolidin-4-ones, with the exception of 5-benzyl-2-thioxoimidazolidin-4-one and 5-(pyridin-2-ylmethyl)-2-thioxoimidazolidin-4-one. The further preparation of enantioenriched tri-susbtituted 2-thioxoimidazolidin-4-one might be carried out by the same procedure described in Chapter 2. Alternatively, enantioenriched N-acetylated 2-thiohydantoins could be prepared by hydrolysis under acidic conditions. The acidic solutions could be mixed rapidly, for example in a stopped-flow apparatus. Solvent kinetic isotope effects for the hydrolysis of substituted 2-thiohydantoin could be carried out in H_2O- and D_2O based phosphate buffer. The effect of electron-donating and electron-withdrawing groups on the phenyl group attached to the

stereogenic centre of 2-thiohydantoin on racemisation and hydrolysis could be studied by constructing a Hammett plot.

It might well be possible to determine racemisation rate constants for compounds such as those in Scheme 6.2 without need for optical resolution.

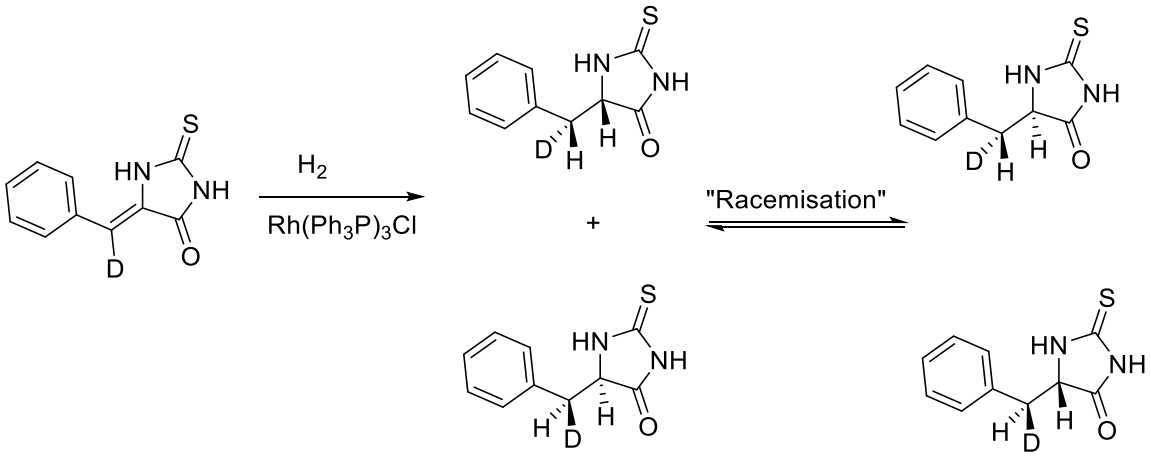

Scheme 6.2: Synthesis and racemisation of (S)-5-((R)-phenylmethyl-d)-2-thioxoimidazolidin-4-one

The "racemisation" could then be followed through the different vicinal J_{HH} for the different diastereoisomers.

Lower concentrations of buffer would be useful to observe the rate constant of the H/D exchange of thioxothiazolidin-4-one (rhodanine) derivatives. It would also be possible to study the hydrolysis of imidazolidine-2,4-dione (hydantoin), thiazolidine-2,4-dione, 2-thioxoimidazolidin-4-one (thiohydantoin) and 2-thioxothiazolidin-4-one (rhodanine) derivatives using 2D-NMR spectroscopy to confirm the exact structure of the hydrolysed product. Kinetic studies of racemisation of other 5-ring compounds similar to hydantoin derivatives would also be interesting, e.g. 2-thioxooxazolidin-4-ones and oxazolidine-2,4-diones.

Future work might involve a study of the binding between our synthesised product and DNA or protein. It would also be fascinating to study metal complexes formed between the synthesised compounds using by X-ray crystallography. Studying the enzyme catalysed racemisation process and comparing with the present results would also be of interest.

6.3 References

1. S. Narduolo, Thesis (Ph D) - Cardiff University, 2011.
2. M. Reist, P.-A. Carrupt, B. Testa, S. Lehmann and J. J. Hansen, *Helvetica Chimica Acta*, 1996, 79, 767-778.
3. R. A. Lazarus, *The Journal of Organic Chemistry*, 1990, 55, 4755-4757.

Appendices

for

Kinetics and mechanism of racemisation reactions of configurationally labile stereogenic centre in drug-like molecules in aqueous solutions; thiohydantoins and related compounds

Hiwa Omer Ahmad

A thesis submitted for the Degree of Doctor of Philosophy

School of Chemistry

Cardiff University

August 2015

Appendix 1

for Chapter 2

Synthesis of substituted 2-thiohydantoins and related compounds

X-ray for compound **18**

Table 1. Crystal data and structure refinement for compound **18**

Identification code	shelx	
Empirical formula	$C_9 H_6 N_2 O S_2$	
Formula weight	222.28	
Temperature	150 (2) K	
Wavelength	1.54184 Å	
Crystal system	Triclinic	
Space group	P $^{-1}$	
Unit cell dimensions	a = 3.8308 (2) Å	a= 76.754(5) °.
	b = 11.0036 (7) Å	b= 88.094(5) °.
	c = 11.3316 (7) Å	g = 82.962(5) °.
Volume	461.44(5) Å^3	
Z	2	
Density (calculated)	1.600 Mg/m^3	
Absorption coefficient	4.942 mm-1	
F(000)	228	
Crystal size	0.333 x 0.046 x 0.042 mm^3	
Theta range for data collection	4.008 to 73.763°.	
Index ranges	-4<=h<=4, -13<=k<=13, -14<=l<=13	
Reflections collected	2747	
Independent reflections	1778 [R (int) = 0.0222]	
Completeness to theta = 67.684°	98.5 %	
Refinement method	Full-matrix least-squares on F^2	
Data / restraints / parameters	1778 / 0 / 127	
Goodness-of-fit on F2	1.042	
Final R indices [I>2sigma (I)]	R1 = 0.0336, wR2 = 0.0881	
R indices (all data)	R1 = 0.0355, wR2 = 0.0917	
Extinction coefficient	n/a	
Largest diff. peak and hole	0.330 and -0.322 e.Å^{-3}	

Table 2. Atomic coordinates (x 104) and equivalent isotropic displacement parameters ($Å^2$x 10^3)

For compound **18**. U (eq) is defined as one third of the trace of the orthogonalized Uij tensor.

	X	y	z	U(eq)
C(1)	3327(4)	3388(2)	6536(2)	23(1)
C(2)	6463(4)	1994(2)	5485(2)	22(1)
C(3)	5249(4)	1111(2)	6568(2)	21(1)
C(4)	6048(4)	-141(2)	6727(2)	22(1)
C(5)	5084(4)	-1067(2)	7789(2)	23(1)
C(6)	6049(5)	-2349(2)	7870(2)	28(1)
C(7)	5165(5)	-3195(2)	8913(2)	33(1)
C(8)	3375(5)	-2738(2)	9835(2)	32(1)
C(9)	2494(5)	-1444(2)	9672(2)	29(1)
N(1)	5197(4)	3219(1)	5536(1)	24(1)
N(2)	3305(4)	-614(1)	8670(1)	25(1)
O(1)	8324(3)	1738(1)	4667(1)	29(1)
S(1)	1704(1)	4750(1)	6822(1)	28(1)
S(2)	2849(1)	1944(1)	7532(1)	22(1)

Table 3. Bond lengths [Å] and angles [°] for compound **18**

C(1)-N(1)	1.357(2)
C(1)-S(1)	1.6482(17)
C(1)-S(2)	1.7510(17)
C(2)-O(1)	1.214(2)
C(2)-N(1)	1.389(2)
C(2)-C(3)	1.481(2)
C(3)-C(4)	1.345(2)
C(3)-S(2)	1.7508(17)
C(4)-C(5)	1.457(2)
C(4)-H(4)	0.9500
C(5)-N(2)	1.344(2)
C(5)-C(6)	1.397(2)
C(6)-C(7)	1.387(3)
C(6)-H(6)	0.9500
C(7)-C(8)	1.386(3)
C(7)-H(7)	0.9500
C(8)-C(9)	1.394(3)
C(8)-H(8)	0.9500
C(9)-N(2)	1.338(2)
C(9)-H(9)	0.9500
N(1)-H(1)	0.8800
N(1)-C(1)-S(1)	126.08(13)
N(1)-C(1)-S(2)	110.97(12)
S(1)-C(1)-S(2)	122.95(11)
O(1)-C(2)-N(1)	122.98(15)
O(1)-C(2)-C(3)	127.50(15)
N(1)-C(2)-C(3)	109.50(14)
C(4)-C(3)-C(2)	121.54(15)
C(4)-C(3)-S(2)	128.27(13)
C(2)-C(3)-S(2)	110.18(12)
C(3)-C(4)-C(5)	124.83(16)
C(3)-C(4)-H(4)	117.6
C(5)-C(4)-H(4)	117.6
N(2)-C(5)-C(6)	123.07(16)
N(2)-C(5)-C(4)	116.47(15)
C(6)-C(5)-C(4)	120.45(16)
C(7)-C(6)-C(5)	118.51(17)

C(7)-C(6)-H(6)	120.7
C(5)-C(6)-H(6)	120.7
C(8)-C(7)-C(6)	118.92(17)
C(8)-C(7)-H(7)	120.5
C(6)-C(7)-H(7)	120.5
C(7)-C(8)-C(9)	118.68(16)
C(7)-C(8)-H(8)	120.7
C(9)-C(8)-H(8)	120.7
N(2)-C(9)-C(8)	123.25(17)
N(2)-C(9)-H(9)	118.4
C(8)-C(9)-H(9)	118.4
C(1)-N(1)-C(2)	117.41(14)
C(1)-N(1)-H(1)	121.3
C(2)-N(1)-H(1)	121.3
C(9)-N(2)-C(5)	117.56(15)
C(3)-S(2)-C(1)	91.87(8)

Symmetry transformations used to generate equivalent atoms:

Table 4. Anisotropic displacement parameters ($Å^2 x\ 10^3$) for compound **18**. The anisotropic displacement factor exponent takes the form: $-2p^2[\ h^2 a^{*2} U^{11} + ... + 2\ h\ k\ a^*\ b^*\ U^{12}\ ]$

	U^{11}	U^{22}	U^{33}	U^{23}	U^{13}	U^{12}
C(1)	24(1)	22(1)	23(1)	-6(1)	3(1)	-2(1)
C(2)	26(1)	21(1)	20(1)	-6(1)	2(1)	-3(1)
C(3)	23(1)	21(1)	21(1)	-6(1)	3(1)	-3(1)
C(4)	25(1)	21(1)	21(1)	-7(1)	4(1)	-2(1)
C(5)	25(1)	21(1)	23(1)	-6(1)	0(1)	-3(1)
C(6)	34(1)	23(1)	26(1)	-7(1)	3(1)	-2(1)
C(7)	42(1)	20(1)	35(1)	-4(1)	-1(1)	-3(1)
C(8)	39(1)	29(1)	26(1)	0(1)	3(1)	-9(1)
C(9)	35(1)	29(1)	22(1)	-5(1)	6(1)	-6(1)
N(1)	30(1)	18(1)	23(1)	-4(1)	6(1)	-3(1)
N(2)	28(1)	22(1)	24(1)	-5(1)	4(1)	-3(1)
O(1)	38(1)	24(1)	25(1)	-7(1)	10(1)	-2(1)
S(1)	34(1)	19(1)	32(1)	-9(1)	10(1)	-1(1)
S(2)	25(1)	19(1)	21(1)	-6(1)	6(1)	-3(1)

Table 5. Hydrogen coordinates ($x\ 10^4$) and isotropic displacement parameters ($Å^2 x\ 10^3$) for compound **18**.

	x	y	z	U(eq)
H(4)	7335	-444	6101	27
H(6)	7282	-2636	7225	33
H(7)	5777	-4074	8995	39
H(8)	2761	-3296	10562	38
H(9)	1256	-1135	10304	35
H(1)	5593	3860	4943	29

Appendix 2

for Chapter 3

Hydrolysis of substituted 2-thiohydantoins and related compounds

A.3.1 Kinetics and mechanism of base-catalysed hydrolysis of 5-substituted 1-acetyl-2-thiohydantoins

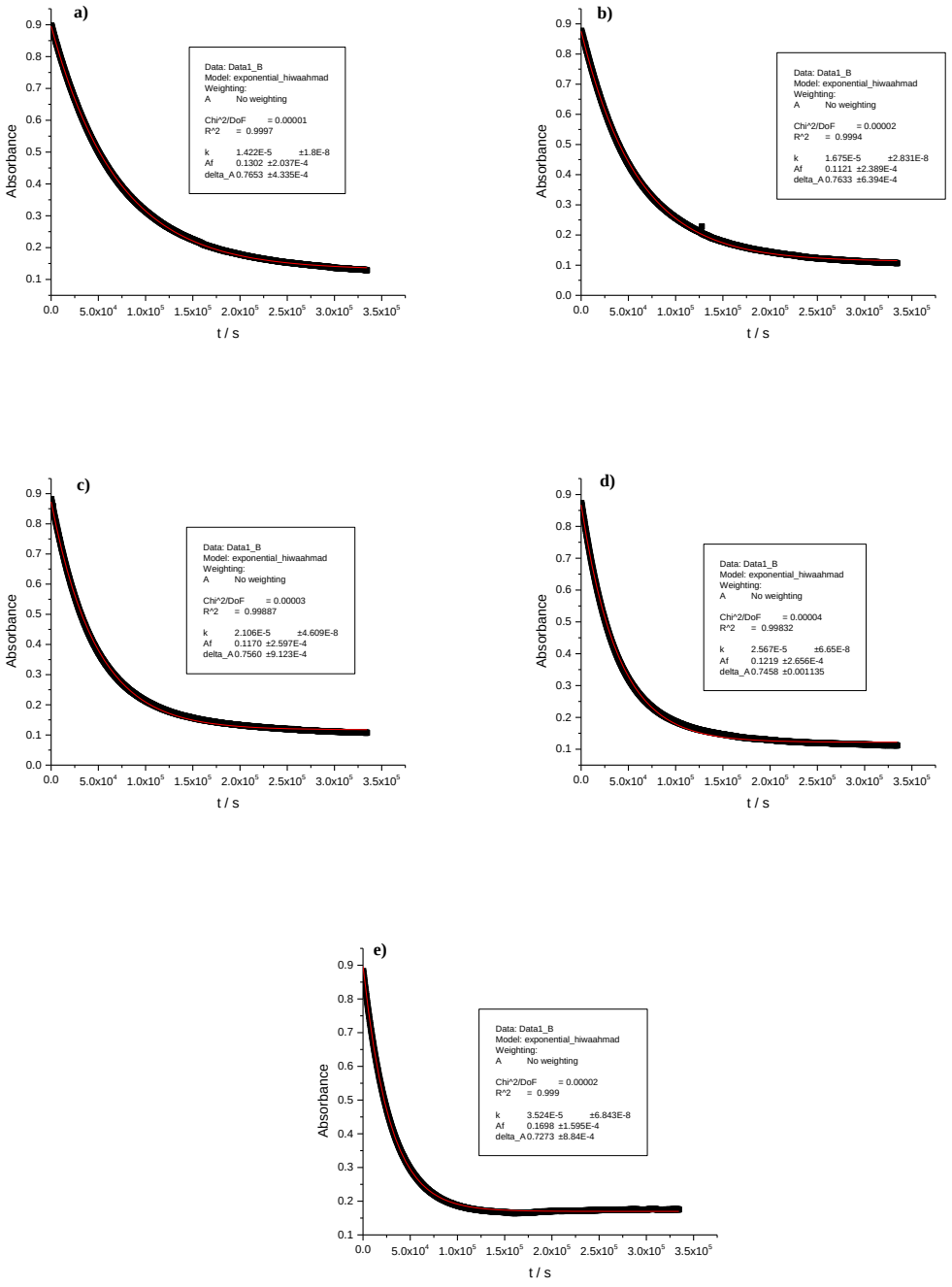

Figure a3.1: Hydrolysis of **3.1** at 286 nm in H_2O-phosphate buffer at a) 0.045 M, b) 0.09 M, c) 0.18 M, d) 0.27 M and e) 0.36 M total phosphate with ionic strength of 0.9 M *I*, pH 7.4 at 37 °C. The squares (■) are the experimental points, and the red solid lines are the fits to pseudo-first-order kinetics.

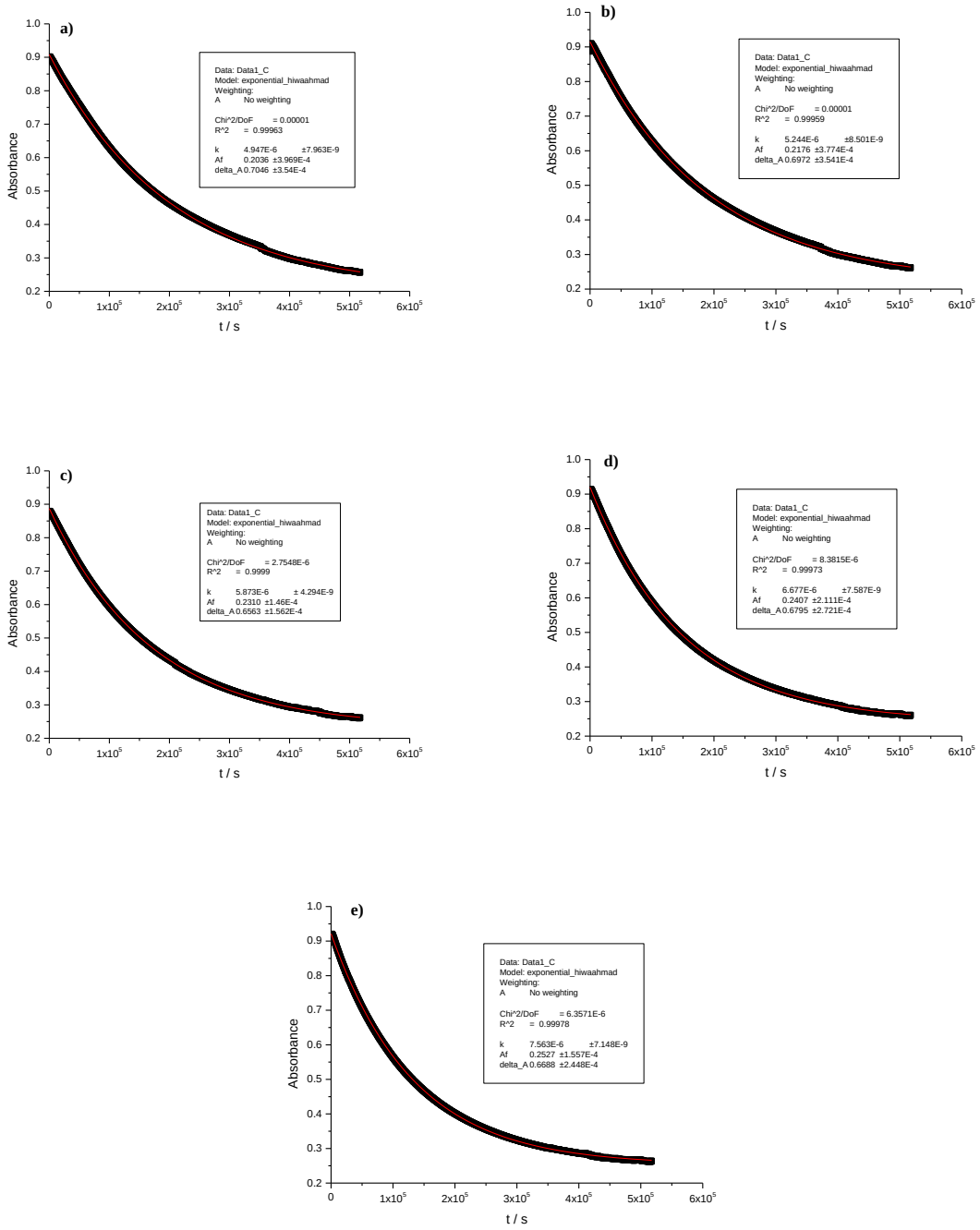

Figure a3.2: Hydrolysis of **3.2** at 289 nm in H_2O-phosphate buffer at a) 0.045 M, b) 0.09 M, c) 0.18 M, d) 0.27 M and e) 0.36 M total phosphate with ionic strength of 0.9 M *I*, pH 7.4 at 37 °C. The squares (■) are the experimental points, and the red solid lines are the fits to pseudo-first-order kinetics.

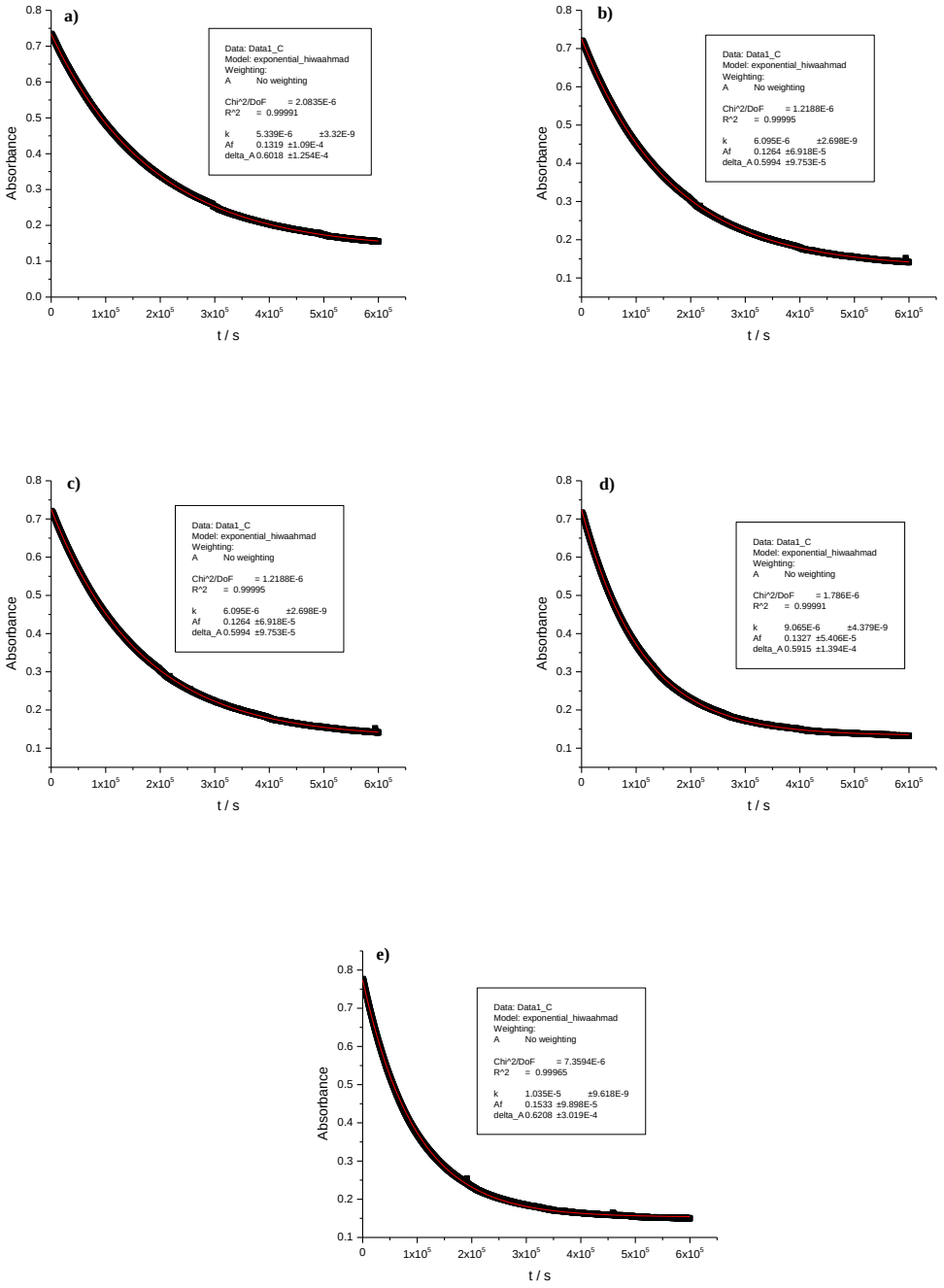

Figure a3.3: Hydrolysis of **3.3** at 291 nm in H_2O-phosphate buffer at a) 0.045 M, b) 0.09 M, c) 0.18 M, d) 0.27 M and e) 0.36 M total phosphate with ionic strength of 0.9 M *I*, pH 7.4 at 37 °C. The squares (■) are the experimental points, and the red solid lines are the fits to pseudo-first-order kinetics.

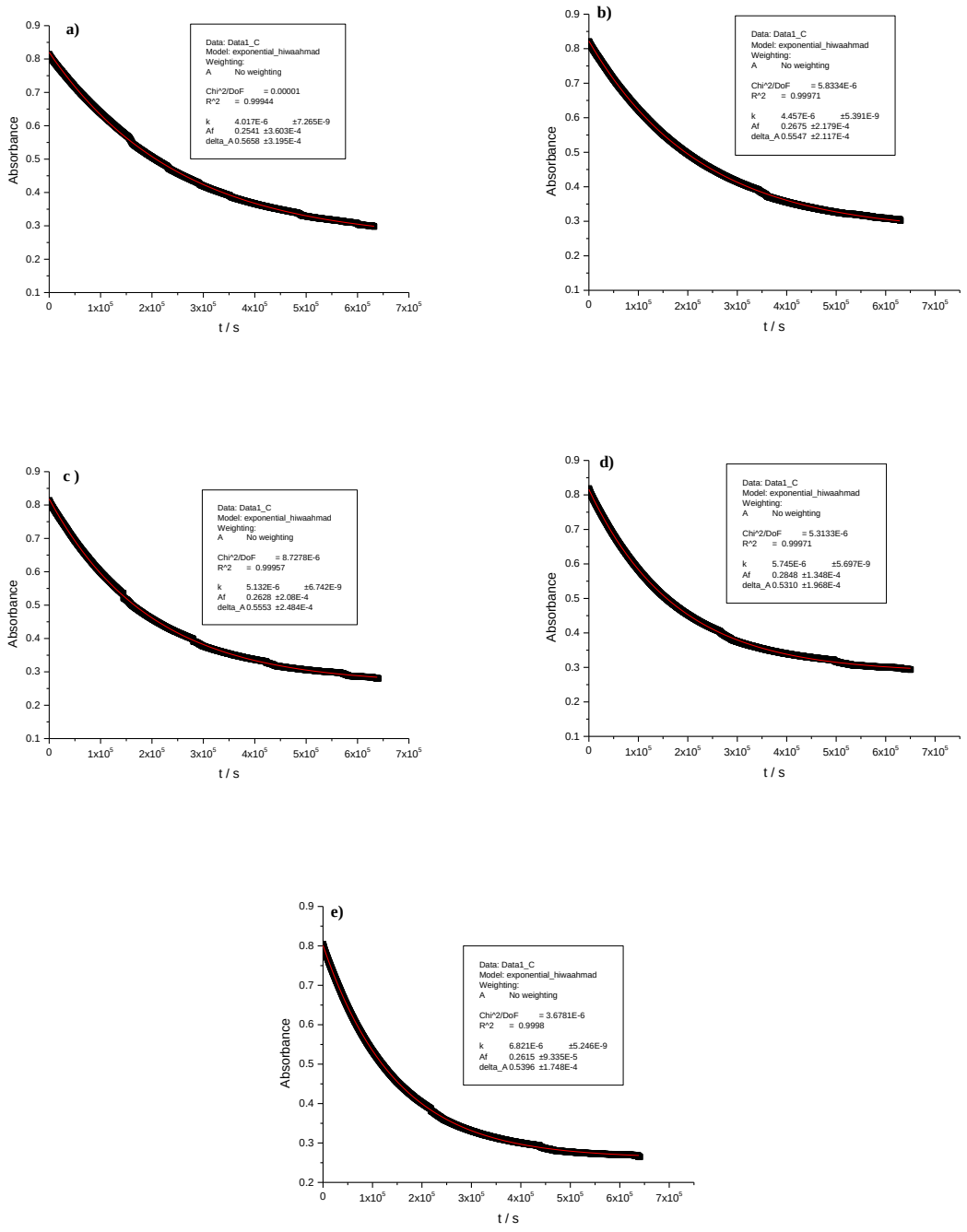

Figure a3.4: Hydrolysis of **3.4** at 283 nm in H_2O-phosphate buffer at a) 0.045 M, b) 0.09 M, c) 0.18 M, d) 0.27 M and e) 0.36 M total phosphate with ionic strength of 0.9 M *I*, pH 7.4 at 37 °C. The squares (■) are the experimental points, and the red solid lines are the fits to pseudo-first-order kinetics.

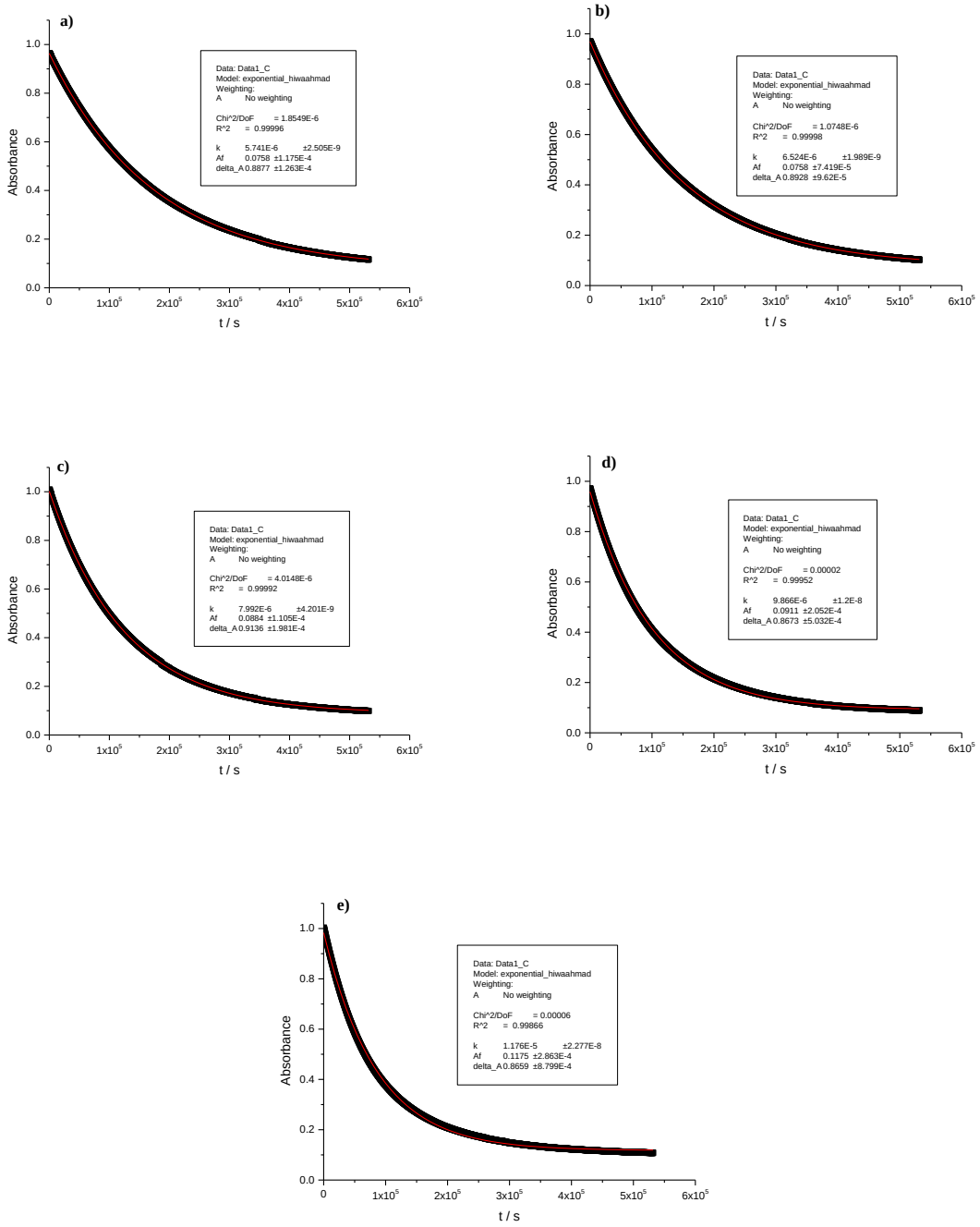

Figure a3.5: Hydrolysis of **3.5** at 288 nm in H_2O-phosphate buffer in a) 0.045 M, b) 0.09 M, c) 0.18 M, d) 0.27 M and e) 0.36 M total phosphate with ionic strength of 0.9 M *I*, pH 7.4 at 37 °C. The squares (■) are the experimental points, and the red solid lines are the fits to pseudo first-order kinetics.

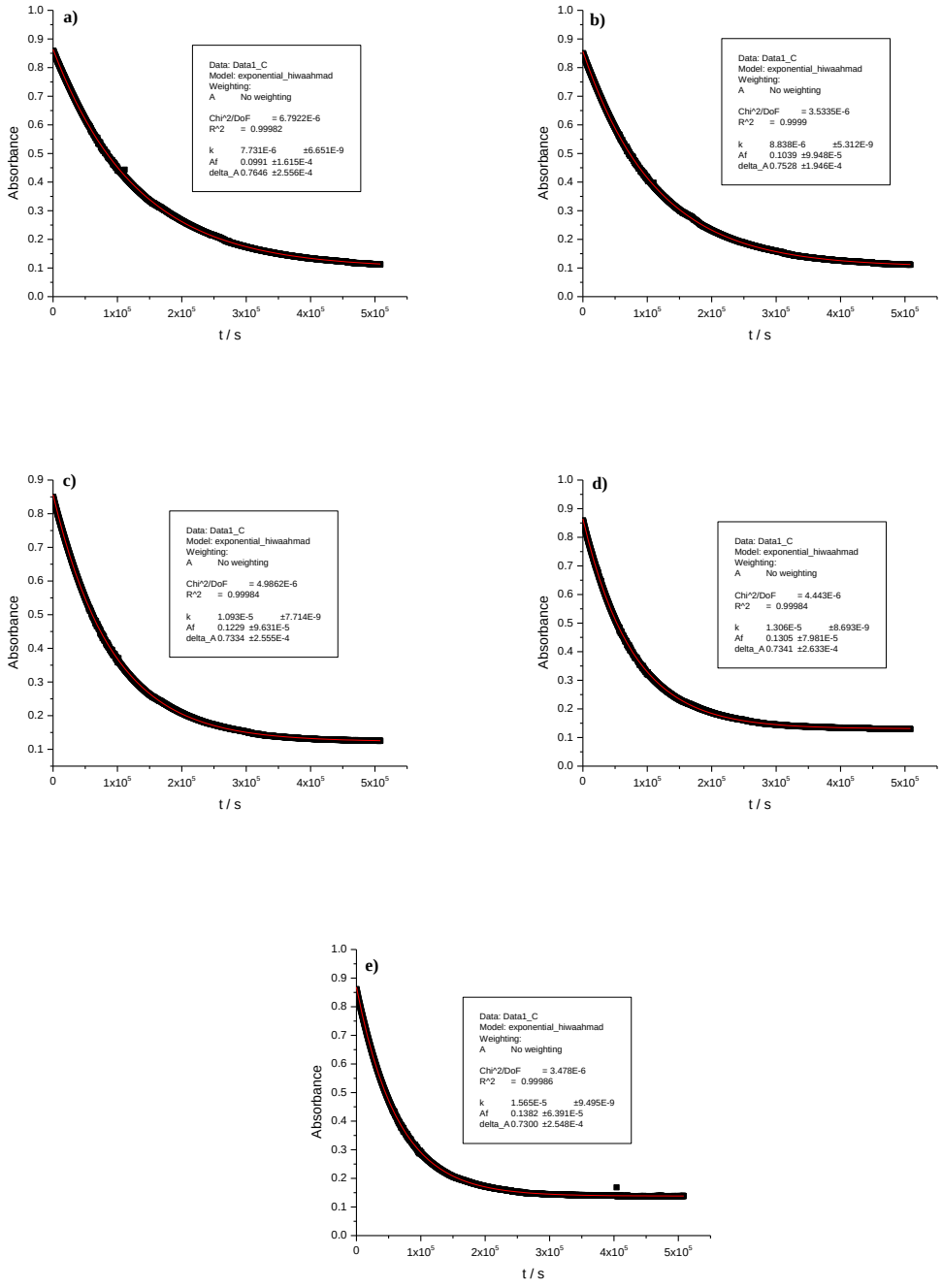

Figure a3.6: Hydrolysis of **3.6** at 290 nm in H_2O-phosphate buffer in a) 0.045 M, b) 0.09 M, c) 0.18 M, d) 0.27M and e) 0.36 M total phosphate with ionic strength of 0.9 M *I*, pH 7.4 at 37 °C. The squares (■) are the experimental points, and the red solid lines are the fits to pseudo-first-order kinetics.

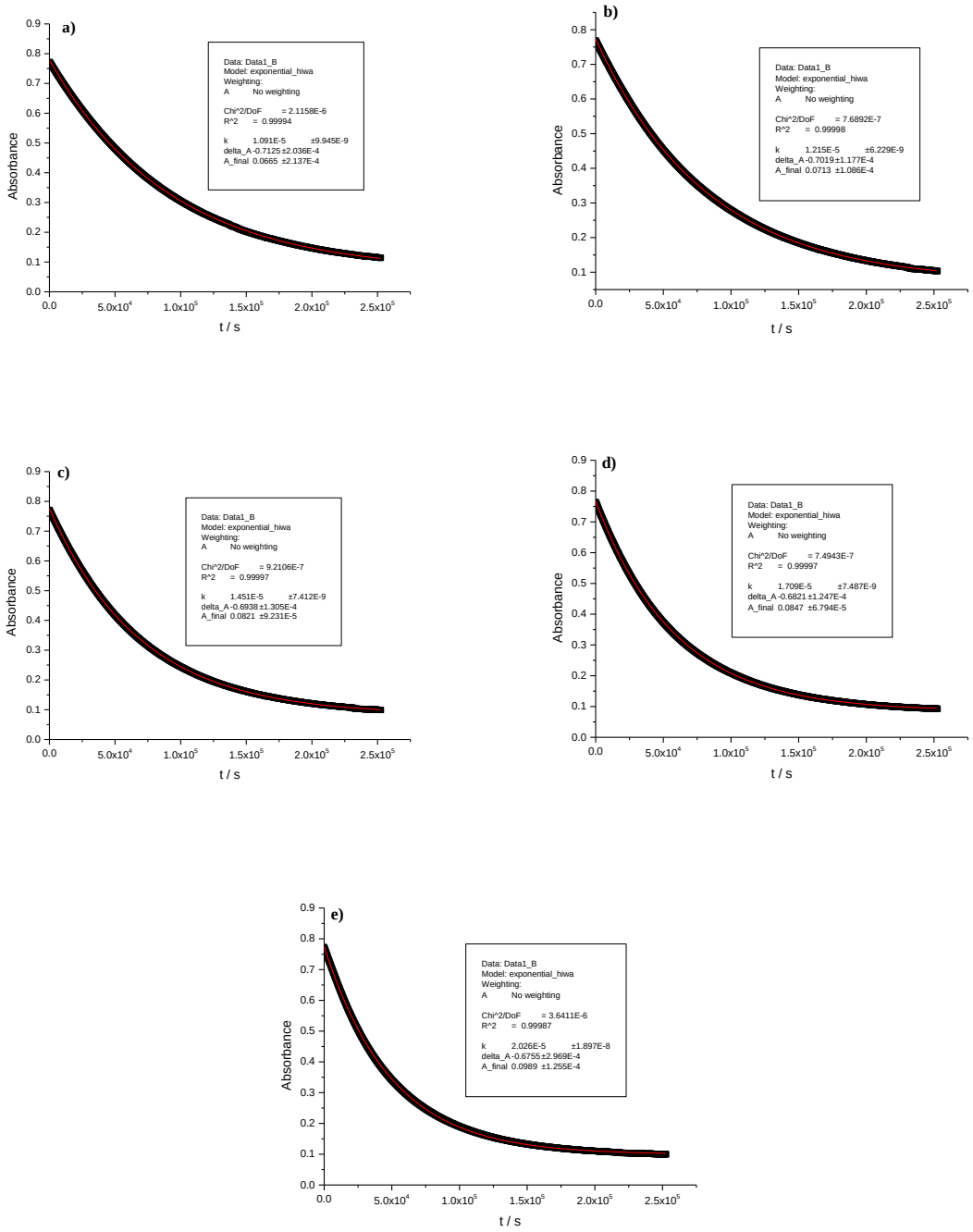

Figure a3.7: Hydrolysis of **3.7** at 290 nm in H_2O-phosphate buffer in a) 0.045 M, b) 0.09 M, c) 0.18 M, d) 0.27 M and e) 0.36 M total phosphate with ionic strength of 0.9 M *I*, pH 7.4 at 37 °C. The squares (■) are the experimental points, and the red solid lines are the fits to pseudo-first-order kinetics.

Table a3.1: Pseudo-first-order rate constants of hydrolysis k_{hyd} determined by UV-visible spectroscopy of 1-acetyl-2-thioxoimidazolidin-4-one (**3.1**) in H_2O-phosphate buffer at 0.36 M, 0.27 M, 0.18 M, 0.09 M and 0.045 M total phosphate with ionic strength of 0.9 M *I*, pH 7.4 at 37 °C.

Buffer conc./M	Basic phosphate	k_{hyd} H_2O/ 10^{-6} s^{-1}
0.045	0.036	14.2 ± 0.3 (± 0.02)[a]
0.09	0.072	16.8 ± 0.3 (± 0.03)[a]
0.18	0.14	21.1 ± 0.4 (± 0.05)[a]
0.27	0.22	25.7 ± 0.5 (± 0.07)[a]
0.36	0.29	35.2 ± 0.7 (± 0.07)[a]

b) Where the error from the data fit is reported as less than 2% of the rate constant, an error of 2% was assumed. Values in brackets are the errors from the data fit which are less than 2%.

Table a3.2: Pseudo-first-order rate constants of hydrolysis k_{hyd} determined by UV-visible spectroscopy of (S)-1-acetyl-5-benzyl-2-thioxoimidazolidin-4-one (**3.2**) in H_2O-phosphate buffer at 0.36 M, 0.27 M, 0.18 M, 0.09 M and 0.045 M total phosphate with ionic strength of 0.9 M *I*, pH 7.4 at 37 °C.

Buffer conc./M	Basic phosphate buffer	k_{hyd} H_2O/ 10^{-6} s^{-1}
0.045	0.036	5.0 ± 0.1 (± 0.008)[a]
0.09	0.072	5.2 ± 0.1 (± 0.008)[a]
0.18	0.14	5.9 ± 0.1 (± 0.004)[a]
0.27	0.22	6.7 ± 0.1 (± 0.008)[a]
0.36	0.29	7.6 ± 0.2 (± 0.007)[a]

a) Where the error from the data fit is reported as less than 2% of the rate constant, an error of 2% was assumed. Values in brackets are the errors from the data fit which are less than 2%.

Table a3.3: Pseudo-first-order rate constants of hydrolysis k_{hyd} determined by UV-visible spectroscopy of 1-acetyl-5-phenyl-2-thioxoimidazolidin-4-one (**3.3**) in H_2O-phosphate buffer at 0.36 M, 0.27 M, 0.18 M, 0.09 M and 0.045 M total phosphate with ionic strength of 0.9 M *I*, pH 7.4 and 37 °C.

Buffer conc./M	Basic phosphate buffer	k_{hyd} H_2O/ 10^{-6} s^{-1}
0.045	0.036	5.3 ± 0.1 (± 0.003)[a]
0.09	0.072	6.1 ± 0.1 (± 0.003)[a]
0.18	0.14	7.6 ± 0.2 (± 0.003)[a]
0.27	0.22	9.1 ± 0.2 (± 0.004)[a]
0.36	0.29	10.4 ± 0.2 (± 0.01)[a]

a) Where the error from the data fit is reported as less than 2% of the rate constant, an error of 2% was assumed. Values in brackets are the errors from the data fit which are less than 2%.

Table a3.4: Pseudo-first-order rate constants of hydrolysis k_{hyd} determined by UV-visible spectroscopy of (S)-5-((1H-indol-3-yl)methyl)-1-acetyl-2-thioxoimidazolidin-4-one (**3.4**) in H_2O-phosphate buffer at 0.36 M, 0.27 M, 0.18 M, 0.09 M and 0.045 M total phosphate with ionic strength of 0.9 M *I*, pH 7.4 at 37 °C.

Buffer conc./M	Basic phosphate buffer	k_{hyd} H_2O/ 10^{-6} s^{-1}
0.045	0.036	4.0 ± 0.08 (± 0.007)[a]
0.09	0.072	4.5 ± 0.09 (± 0.005)[a]
0.18	0.14	5.1 ± 0.1 (± 0.007)[a]
0.27	0.22	5.8 ± 0.1 (± 0.006)[a]
0.36	0.29	6.8 ± 0.1 (± 0.005)[a]

a) Where the error from the data fit is reported as less than 2% of the rate constant, an error of 2% was assumed. Values in brackets are the errors from the data fit which are less than 2%.

Table a3.5: Pseudo-first-order rate constants of hydrolysis k_{hyd} determined by UV-visible spectroscopy of (S)-1-acetyl-5-isopropyl-2-thioxoimidazolidin-4-one (**3.5**) in H_2O- phosphate buffer at 0.36 M, 0.27 M, 0.18 M, 0.09 M and 0.045 M total phosphate with ionic strength of 0.9 M *I*, pH 7.4 at 37 °C.

Buffer conc./M	Basic phosphate buffer	k_{hyd} H_2O/ 10^{-6} s^{-1}
0.045	0.036	5.7 ± 0.1 (± 0.003)[a]
0.09	0.072	6.5 ± 0.1 (± 0.002)[a]
0.18	0.14	8.0 ± 0.2 (± 0.004)[a]
0.27	0.22	9.9 ± 0.2 (± 0.010)[a]
0.36	0.29	11.8 ± 0.2 (± 0.020)[a]

a) Where the error from the data fit is reported as less than 2% of the rate constant, an error of 2% was assumed. Values in brackets are the errors from the data fit which are less than 2%.

Table a3.6: Pseudo-first-order rate constants of hydrolysis k_{hyd} determined by UV-visible spectroscopy of (S)-1-acetyl-5-(2-(methylthio)ethyl)-2-thioxoimidazolidin-4-one (**3.6**) in H_2O-phosphate buffer at 0.36 M, 0.27 M, 0.18 M, 0.09 M and 0.045 M total phosphate with ionic strength of 0.9 M *I*, pH 7.4 at 37 °C.

Buffer conc./M	Basic phosphate buffer	k_{hyd} H_2O/ 10^{-6} s^{-1}
0.045	0.036	7.7 ± 0.2 (± 0.007)[a]
0.09	0.072	8.8 ± 0.2 (± 0.005)[a]
0.18	0.14	10.9 ± 0.2 (± 0.008)[a]
0.27	0.22	13.1 ± 0.3 (± 0.009)[a]
0.36	0.29	15.7 ± 0.3 (± 0.010)[a]

a) Where the error from the data fit is reported as less than 2% of the rate constant, an error of 2% was assumed. Values in brackets are the errors from the data fit which are less than 2%.

Table a3.7: Pseudo-first-order rate constants of hydrolysis k_{hyd} determined by UV-visible spectroscopy of (S)-1-acetyl-5-methyl-2-thioxoimidazolidin-4-one (**3.7**) in H_2O-phosphate buffer at 0.36 M, 0.27 M, 0.18 M, 0.09 M and 0.045 M total phosphate with ionic strength of 0.9 M *I*, pH 7.4 at 37 °C.

Buffer conc./M	Basic phosphate buffer	k_{hyd} H_2O/ 10^{-6} s^{-1}
0.045	0.036	10.9 ± 0.2 (± 0.010)[a]
0.09	0.072	12.2 ± 0.2 (± 0.006)[a]
0.18	0.14	14.5 ± 0.3 (± 0.007)[a]
0.27	0.22	17.1 ± 0.3 (± 0.008)[a]
0.36	0.29	20.3 ± 0.4 (± 0.020)[a]

a) Where the error from the data fit is reported as less than 2% of the rate constant, an error of 2% was assumed. Values in brackets are the errors from the data fit which are less than 2%.

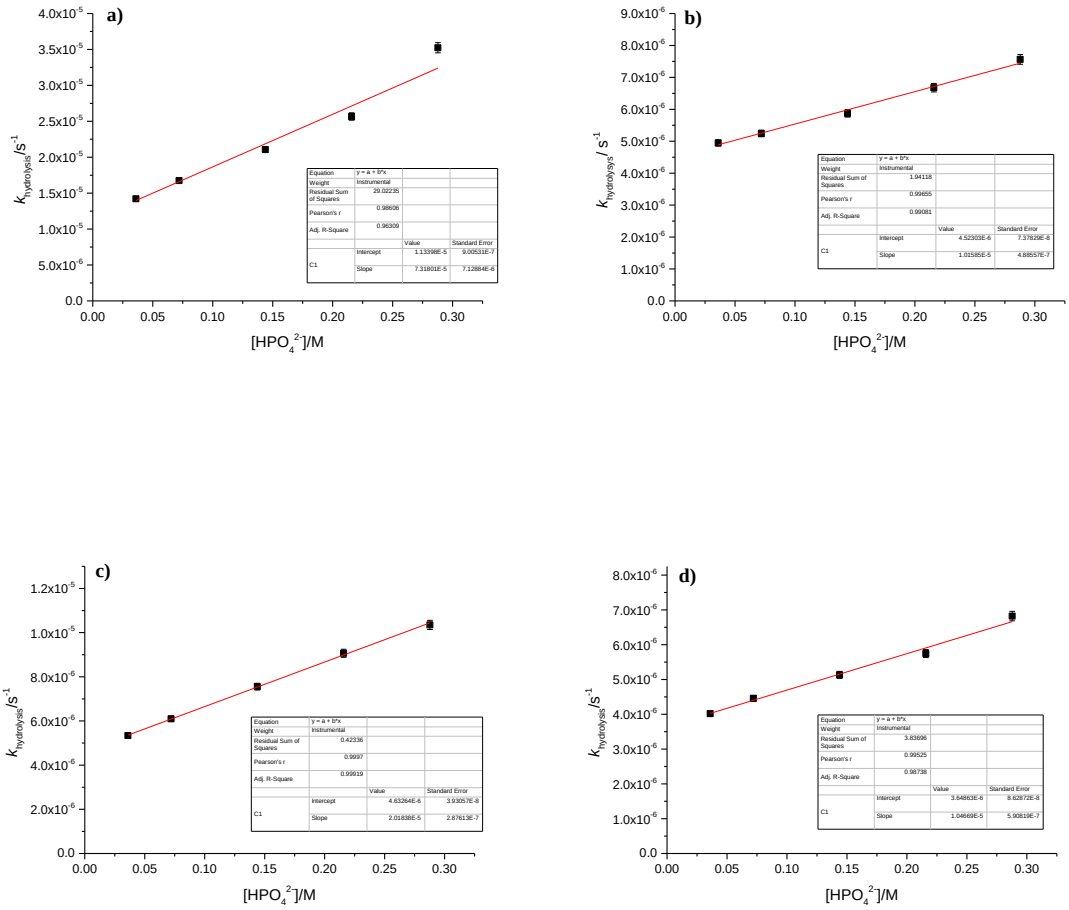

Figure a3.8: Observed rate constants of hydrolysis of a) **3.1**, b) **3.2**, c) **3.3**, and d) **3.4** as a function of the concentration of the basic components of (H_2O-based phosphate buffer at 37 °C, 0.9 M *I*, pH 7.4, 0.36 M, 0.27 M, 0.18 M, 0.09, and 0.045 M.

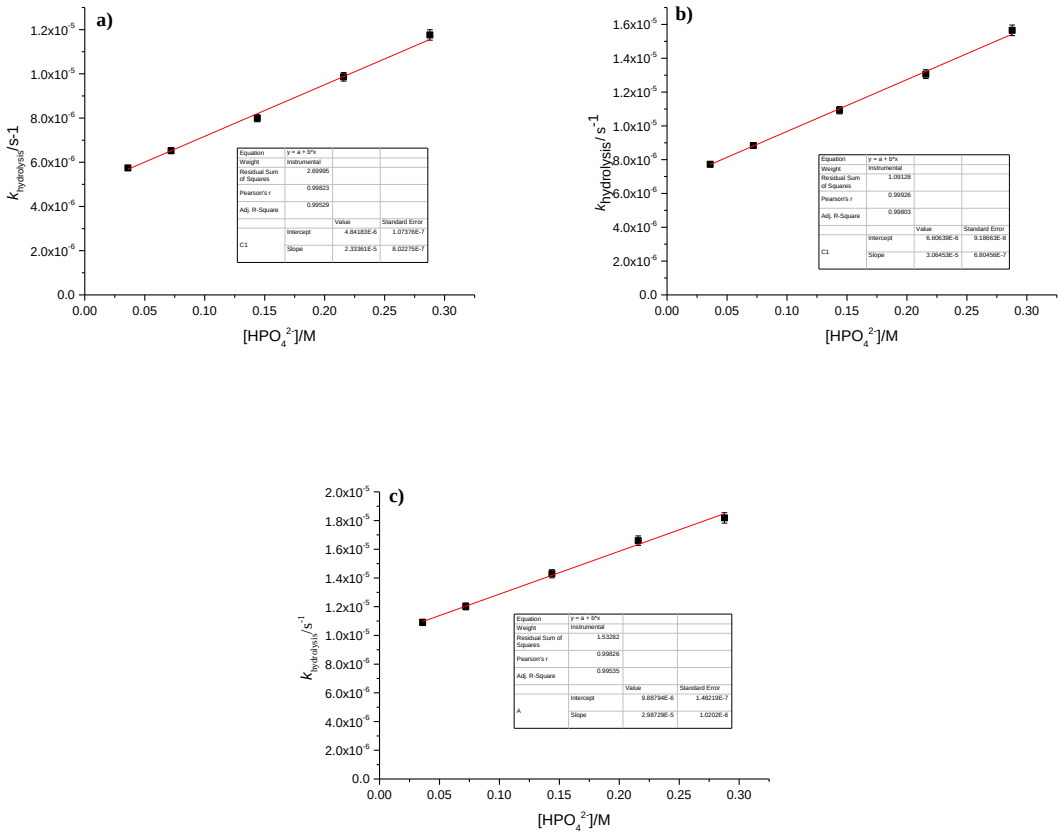

Figure a3.9: Observed rate constants of hydrolysis of a) **3.5**, b) **3.6**, and c) **3.7** as a function of the concentration of the basic components of (H_2O-based phosphate buffer at 37 °C, 0.9 M *I*, pH 7.4, 0.36 M, 0.27 M, 0.18 M, 0.09 and 0.045 M.

A.3.2 Determination of the rate constant for hydrolysis of 1-acetyl-5-isopropyl-2-thiohydantoin by NMR spectroscopy

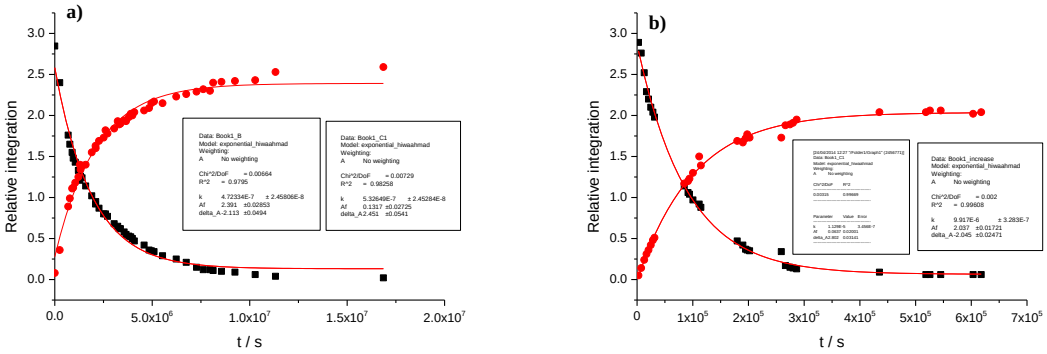

Figure a3.10: The hydrolysis process of **3.5** by using a) 0.008 M of D_2O-phosphate buffer, 0.8 M *I*, pH 7.4 at 37 °C (using 80% of 0.01 M of D_2O-phosphate buffer, 1 M *I*, pH 7.4 at 37 °C, with 20% of d_3-acetonitrile), and b) 0.36 M of D_2O-phosphate buffer, 0.9 M *I*, pH 7.4 at 37 °C (No d_3-acetonitrile). (■) the relative area 3H of **H**$_3$CCO decreased over time, and (●) the relative area of 3H of **H**$_3$CCO (one hydrogen disappeared in regards with the integration) increased over time. The squares (●) and (■) are the experimental points, and the red solid

A.3.3. Brønsted plot for hydrolysis of (*S*)-1-acetyl-5-methyl-2-thioxoimidazolidin-4-one

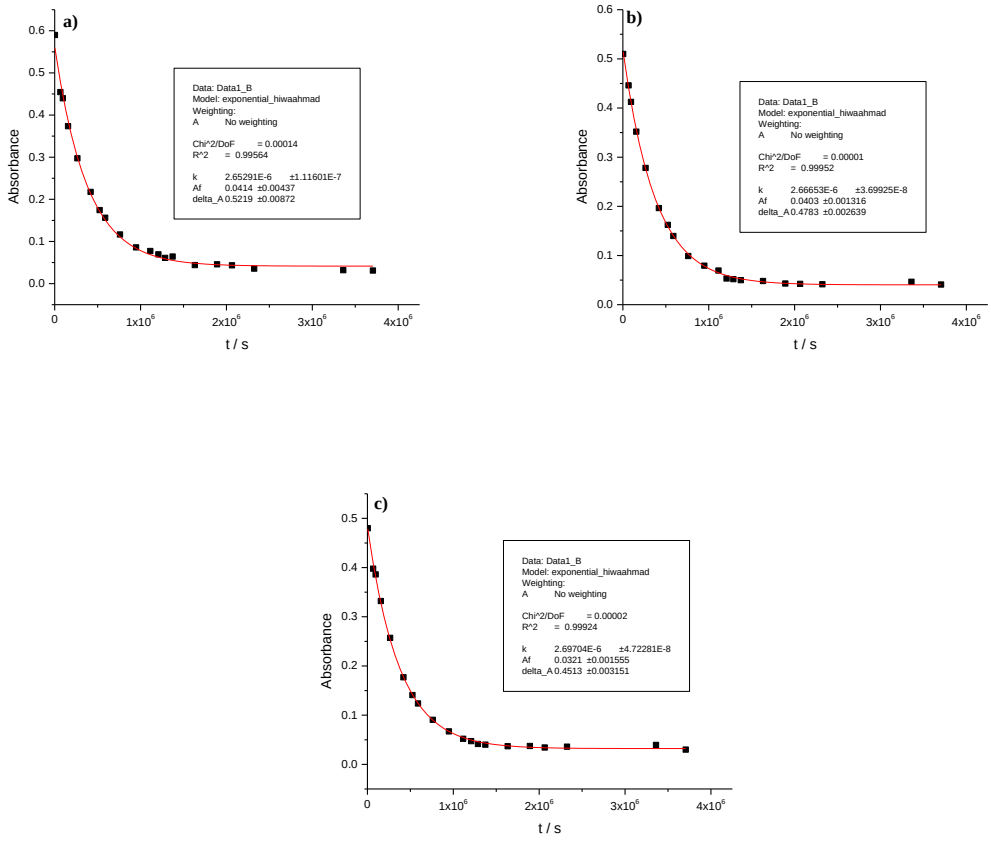

Figure a3.11: Hydrolysis of **3.7** at 290 nm in H_2O acetate buffer in a) 0.18 M, b) 0.27M and c) 0.36 M total acetate buffer with ionic strength of 0.9 M *I*, pH 7.4 at 37 °C. The squares (■) are the experimental points, and the red solid lines are the fits to pseudo-first-order kinetics.

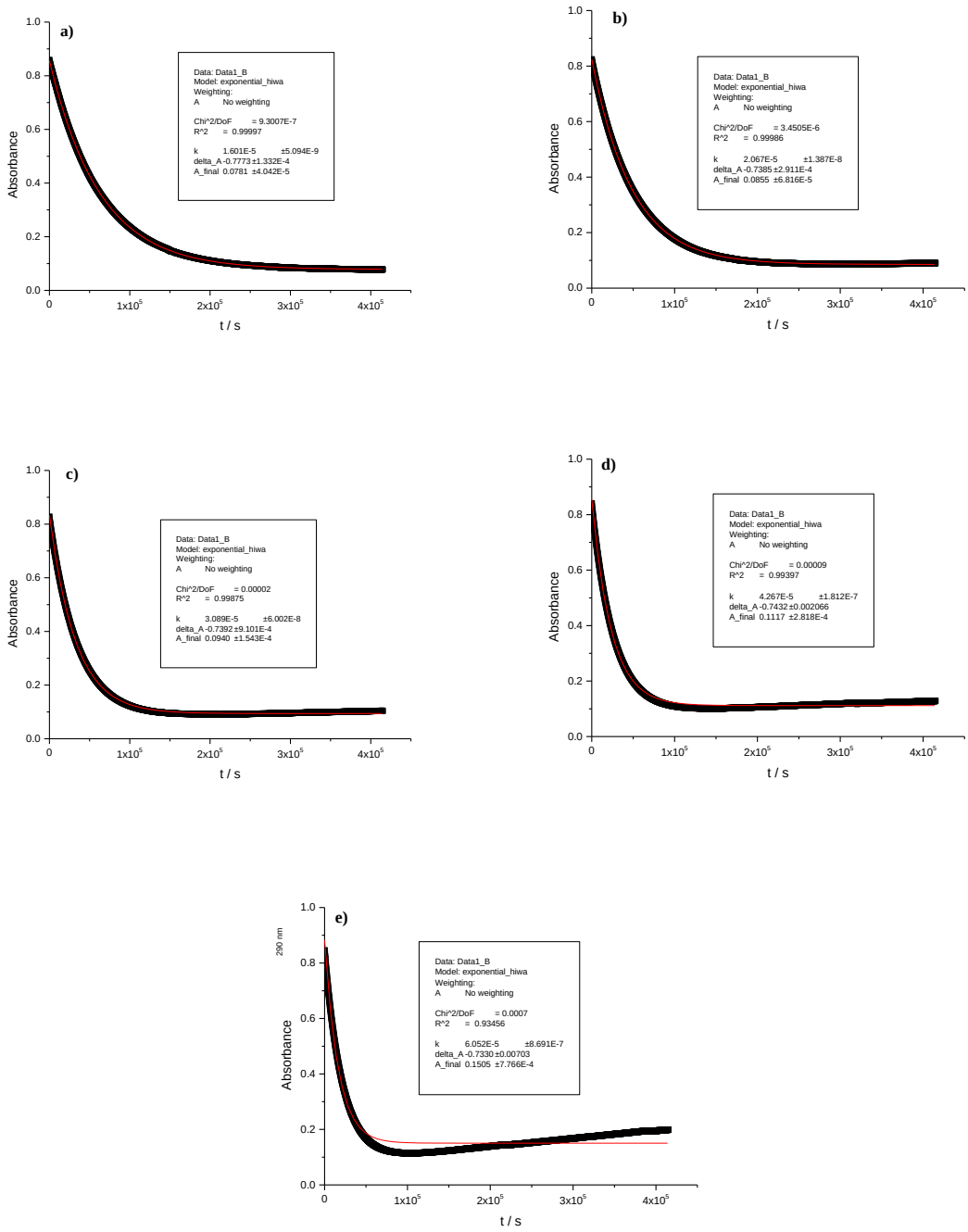

Figure a3.12: Hydrolysis of **3.7** at 290 nm in H_2O TRIS buffer in a) 0.045 M, b) 0.09 M, c) 0.18 M, d) 0.27M and e) 0.36 M total TRIS with ionic strength of 0.9 M *I*, pH 8.2 at 37 °C. The squares (■) are the experimental points, and the red solid lines are the fits to pseudo-first-order kinetics.

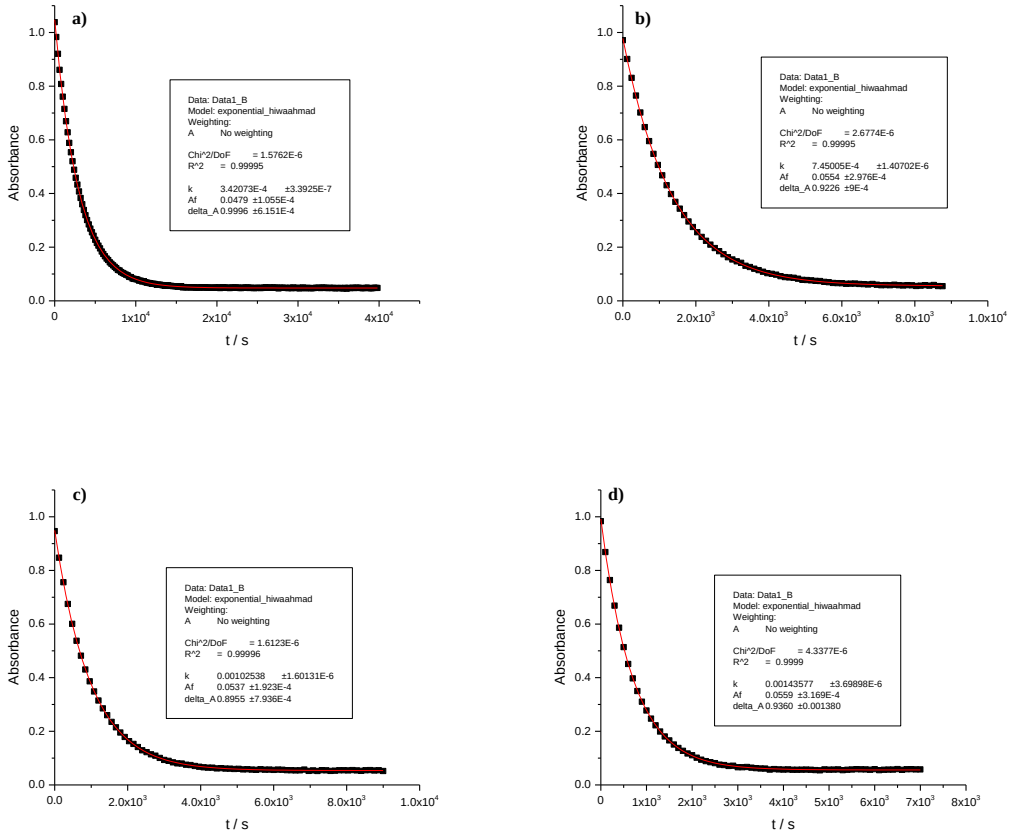

Figure a3.13: Hydrolysis of **3.7** at 290 nm in H_2O methyl amine buffer in, a) 0.09 M, b) 0.18 M, c) 0.27 M and d) 0.36 M total methyl amine with ionic strength of 0.9 M *I*, pH 9.7 at 37 °C. The squares (■) are the experimental points, and the red solid lines are the fits to pseudo-first-order kinetics.

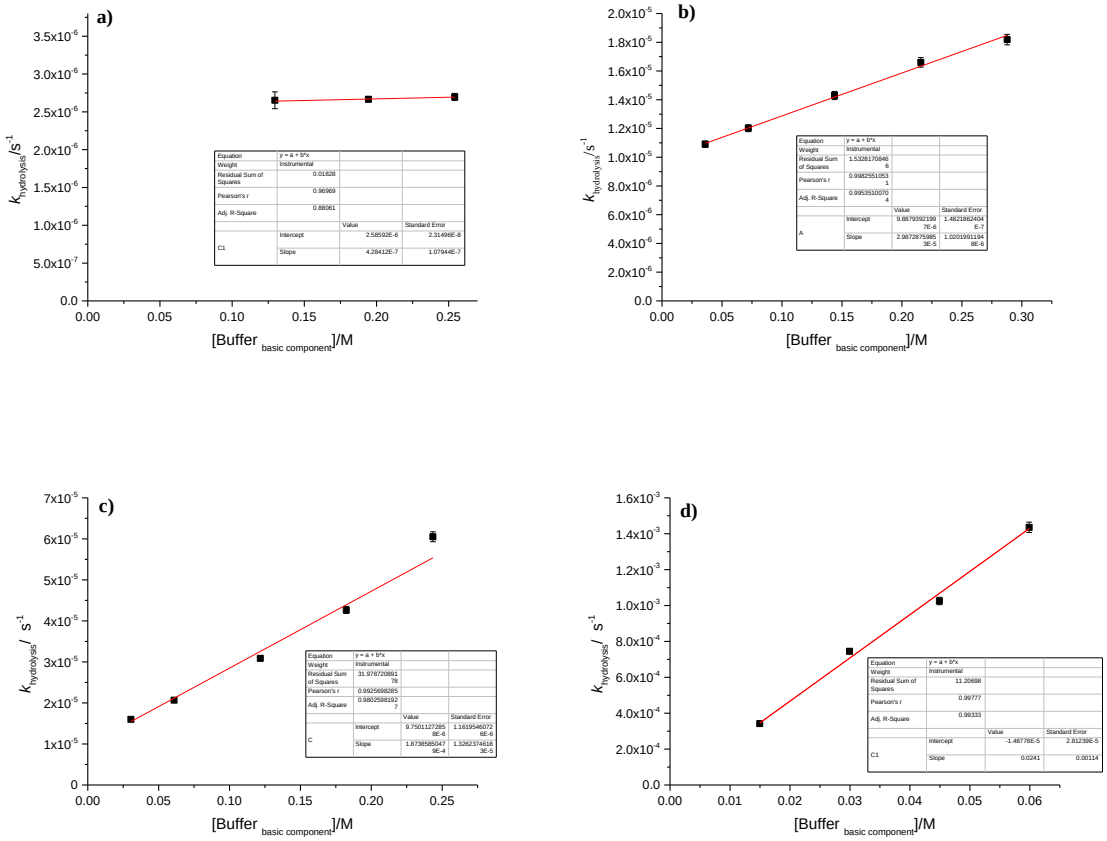

Figure a3.14: rate constants of hydrolysis of **3.7**, in H_2O a) acetate buffers, pH^{25} 5.0 b) phosphate buffer pH^{25} 7.4, c) TRIS buffer pH^{25} 8.2, and d) methyl amine buffer pH^{25} 9.7 at 37 °C plotted as a function of the concentration of basic buffer components considering values of pK_a of a) 4.59 b) 6.8 c) 7.88 , and d) 10.4

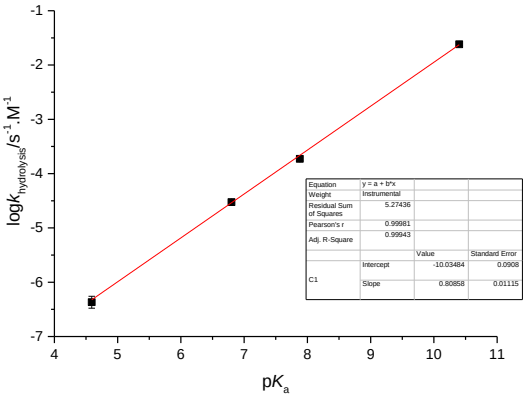

Figure a3.**15**: Bronsted plot for the base-catalysed hydrolysis of **3.7**.

A.3.4. Kinetics of acid and base-catalysed hydrolysis of 1-acetyl-5-phenyl-2-thioxoimidazolidin-4-one

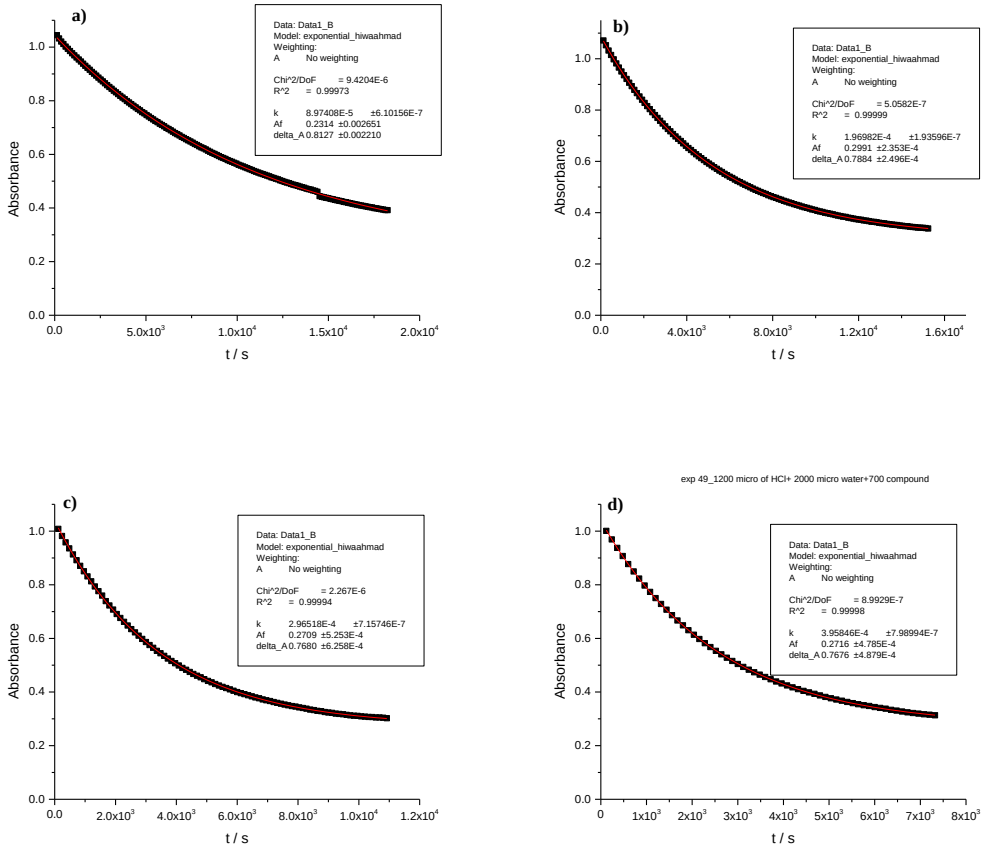

Figure a3.16: Hydrolysis of **3.3** at 279 nm in a) 0.24 M, b) 0.48 M, c) 0.72 M, and d) 0.96 M of HCl at 37 °C. The squares (■) are the experimental points, and the red solid lines are the fits to pseudo-first-order kinetics.

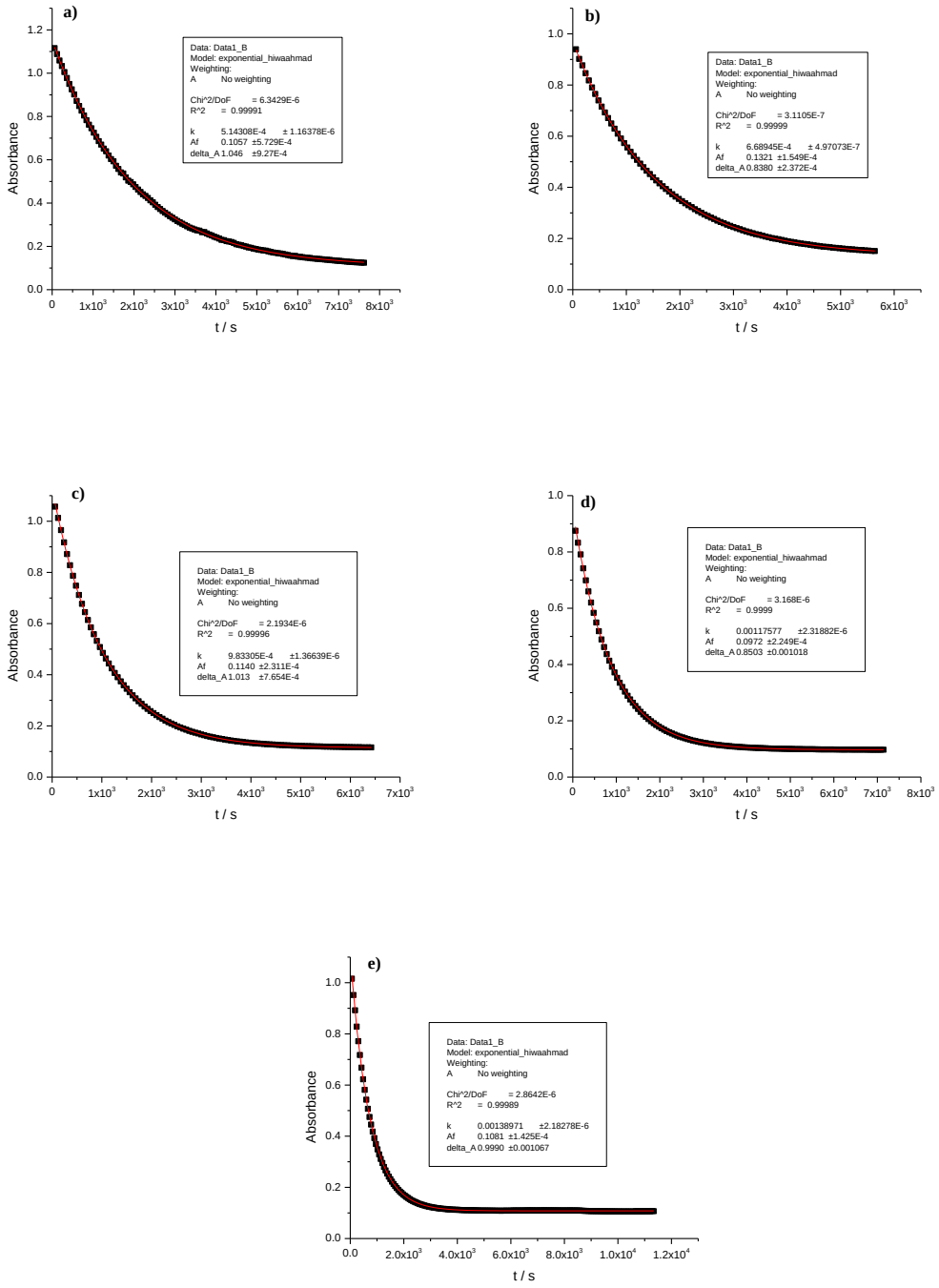

Figure a3.17: Hydrolysis of **3.3** at 290 nm in a) 0.0017 M, b) 0.0025 M, c) 0.0033 M, d) 0.0042 M, and e) 0.005 M of NaOH at 37 °C. The squares (■) are the experimental points, and the red solid lines are the fits to pseudo-first-order kinetics.

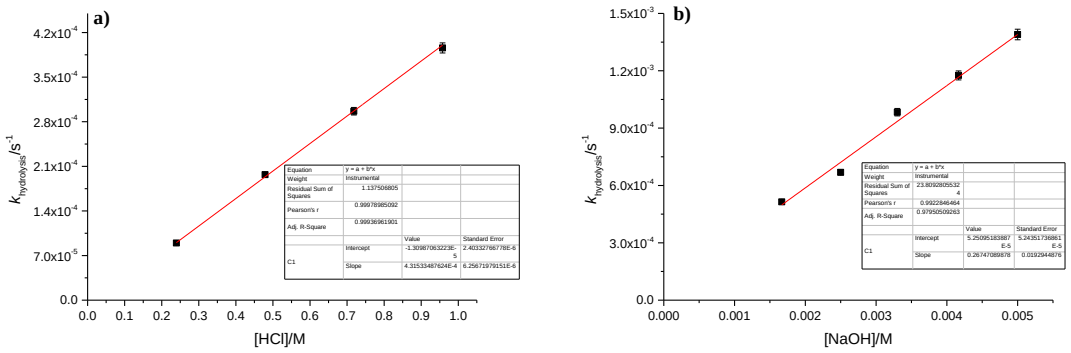

Figure a3.18: Rate constants of hydrolysis of **3.7**, in a) HCl, and b) NaOH plotted as a function of the concentration of HCl and NaOH, respectively at 37 °C.

A.3.5. Kinetics and mechanism of base-catalysed hydrolysis of 5-substituted 2-thioxoimidazolidin-4-ones

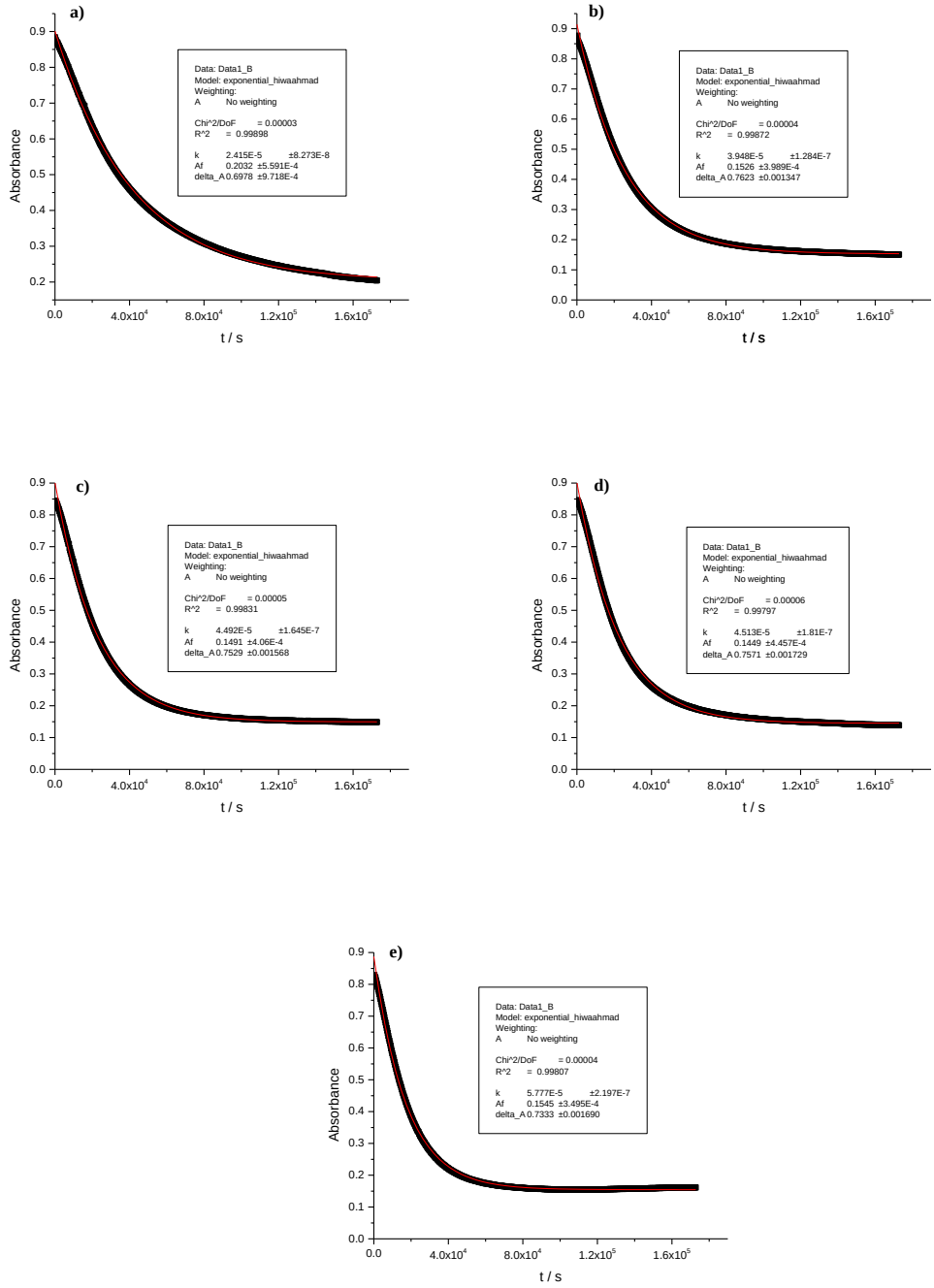

Figure a3.19: Hydrolysis of **3.8** at 259 nm in H_2O-phosphate buffer at a) 0.045 M, b) 0.09 M, c) 0.18 M, d) 0.27 M and e) 0.36 M total phosphate with ionic strength of 0.9 M *I*, pH 7.4 at 37 °C. The squares (■) are the experimental points, and the red solid lines are the fits to pseudo-first-order kinetics.

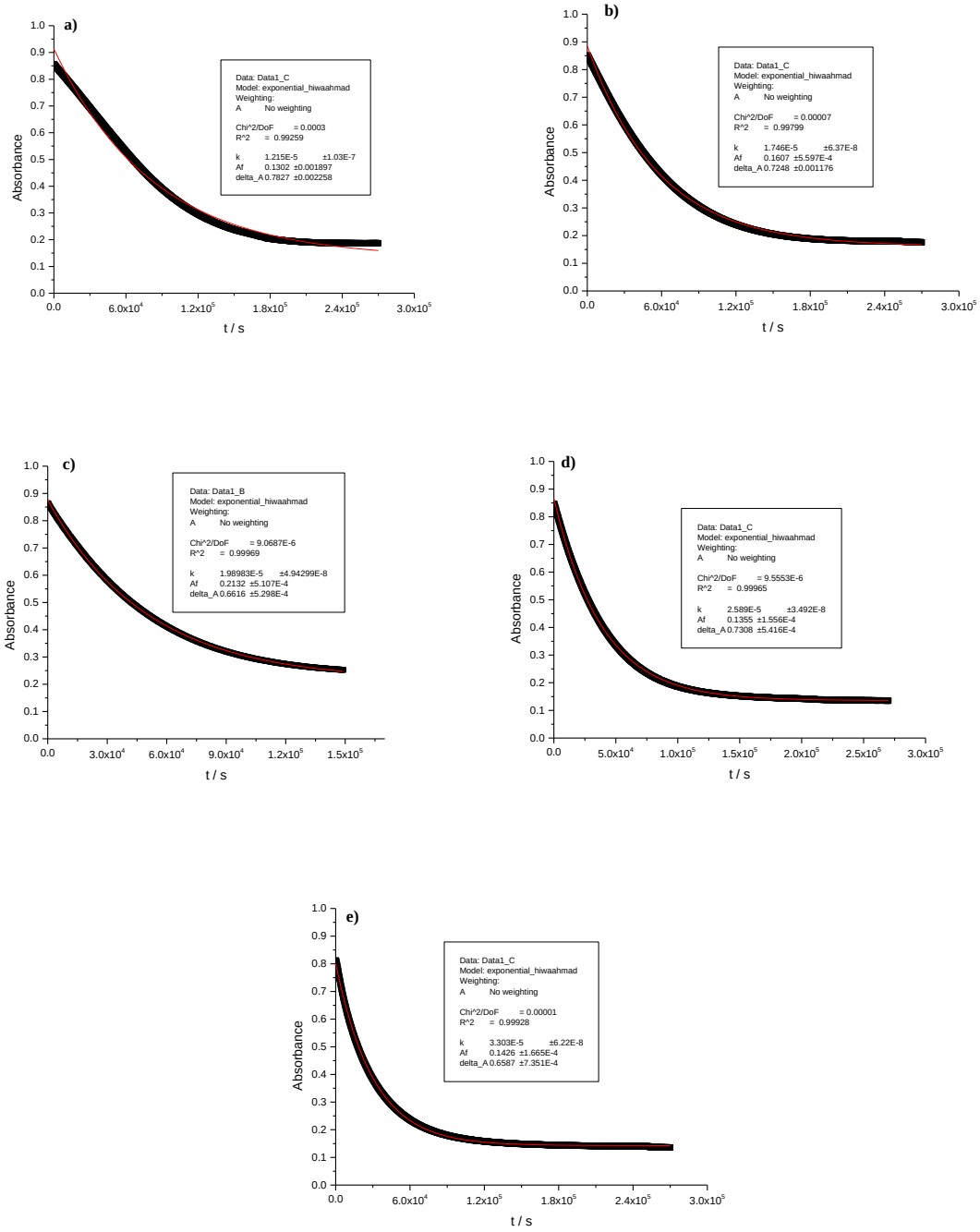

Figure a3.20: Hydrolysis of **3.9** at 262 nm in H_2O-phosphate buffer at a) 0.045 M, b) 0.09 M, c) 0.18 M, d) 0.27 M and e) 0.36 M total phosphate with ionic strength of 0.9 M *I*, pH 7.4 at 37 °C. The squares (■) are the experimental points, and the red solid lines are the fits to pseudo-first-order kinetics.

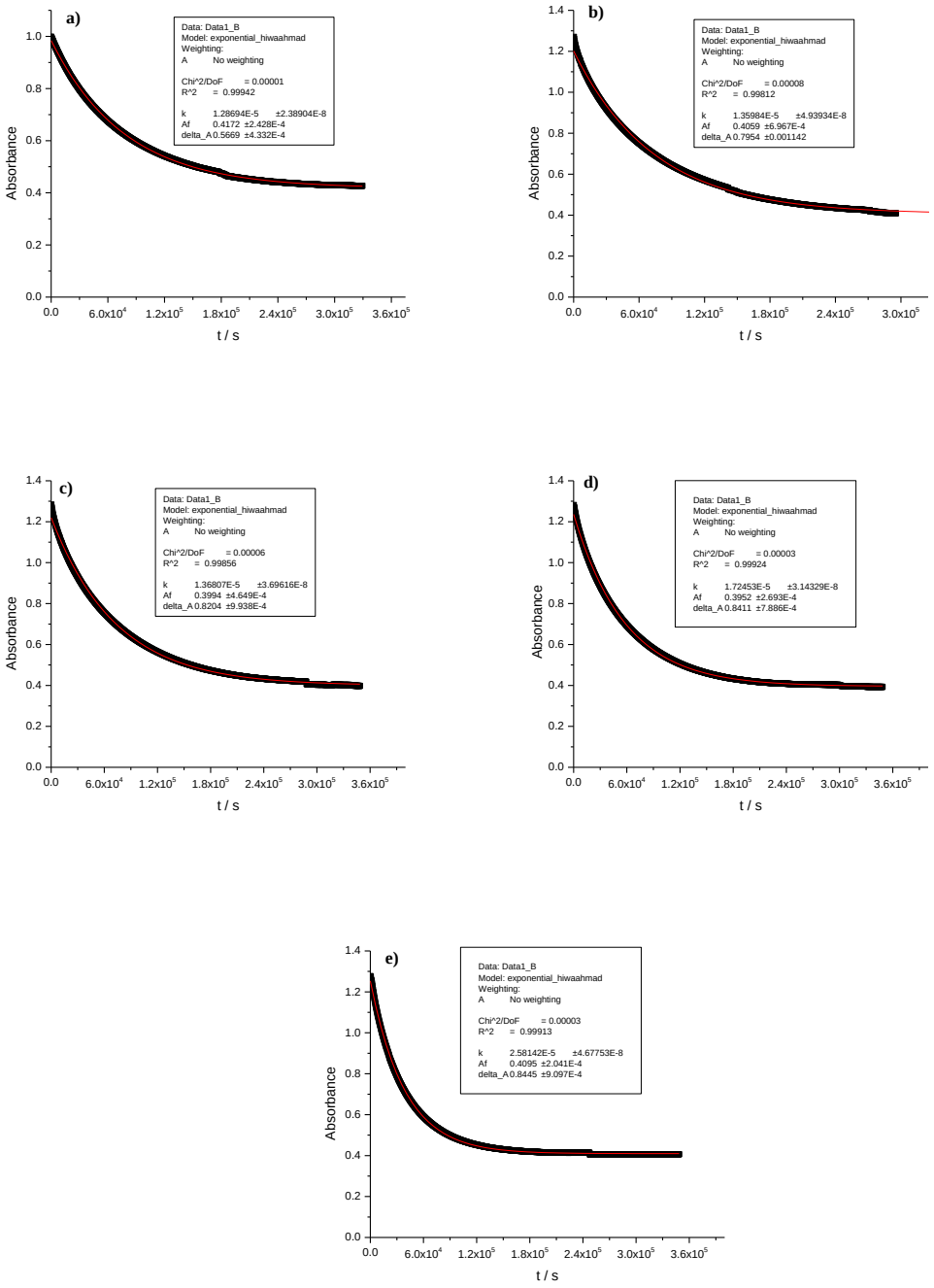

Figure a3.21: Hydrolysis of **3.10** at 262 nm in H_2O phosphate buffer at a) 0.045 M, b) 0.09 M, c) 0.18 M, d) 0.27 M and e) 0.36 M total phosphate with ionic strength of 0.9 M *I*, pH 7.4 at 37 °C. The squares (■) are the experimental points, and the red solid lines are the fits to pseudo-first-order kinetics.

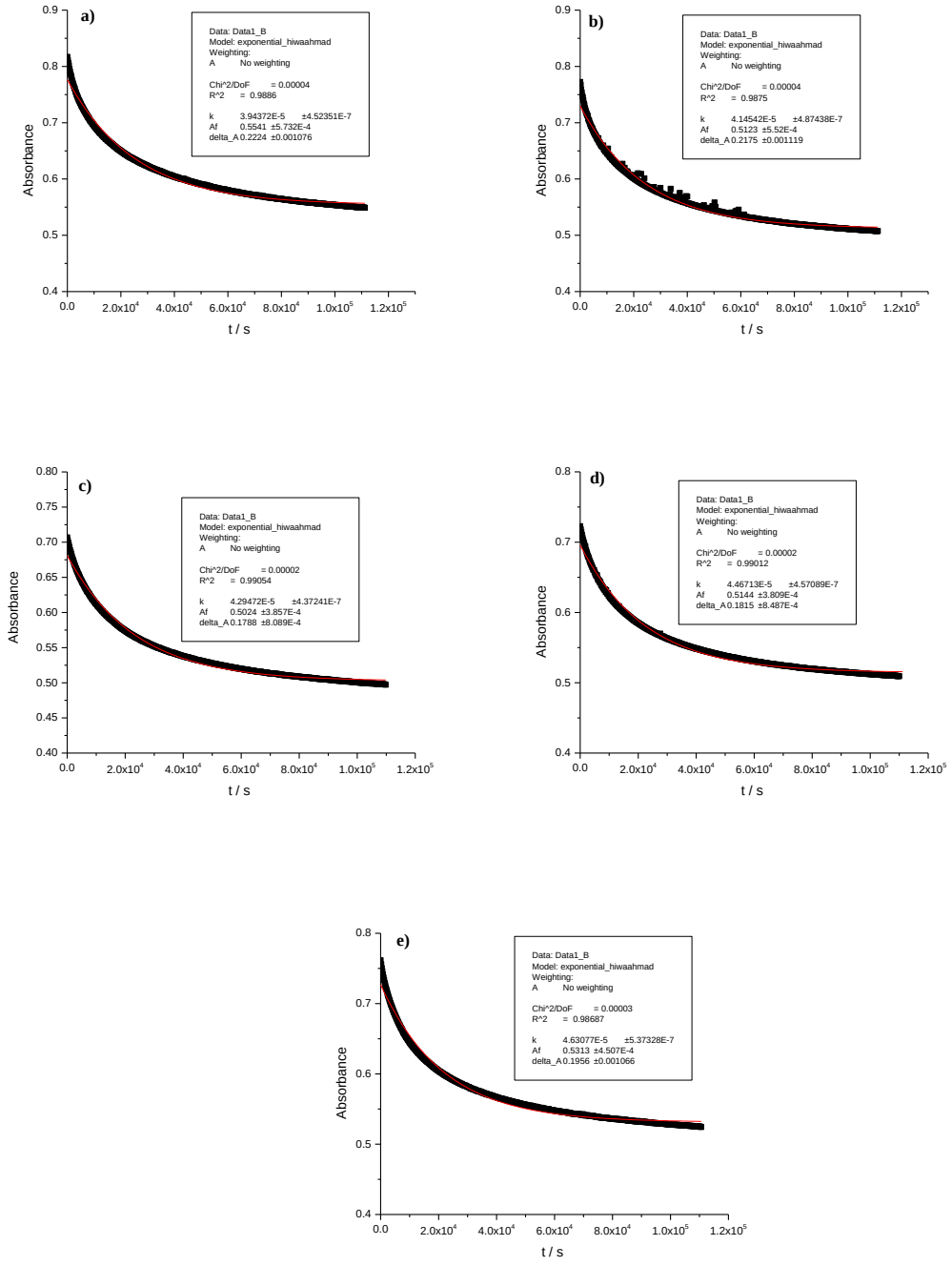

Figure a3.22: Hydrolysis of **3.11** at 262 nm in H_2O-phosphate buffer at a) 0.045 M, b) 0.09 M, c) 0.18 M, d) 0.27 M and e) 0.36 M total phosphate with ionic strength of 0.9 M *I*, pH 7.4 at 37 °C. The squares (■) are the experimental points, and the red solid lines are the fits to pseudo-first-order kinetics.

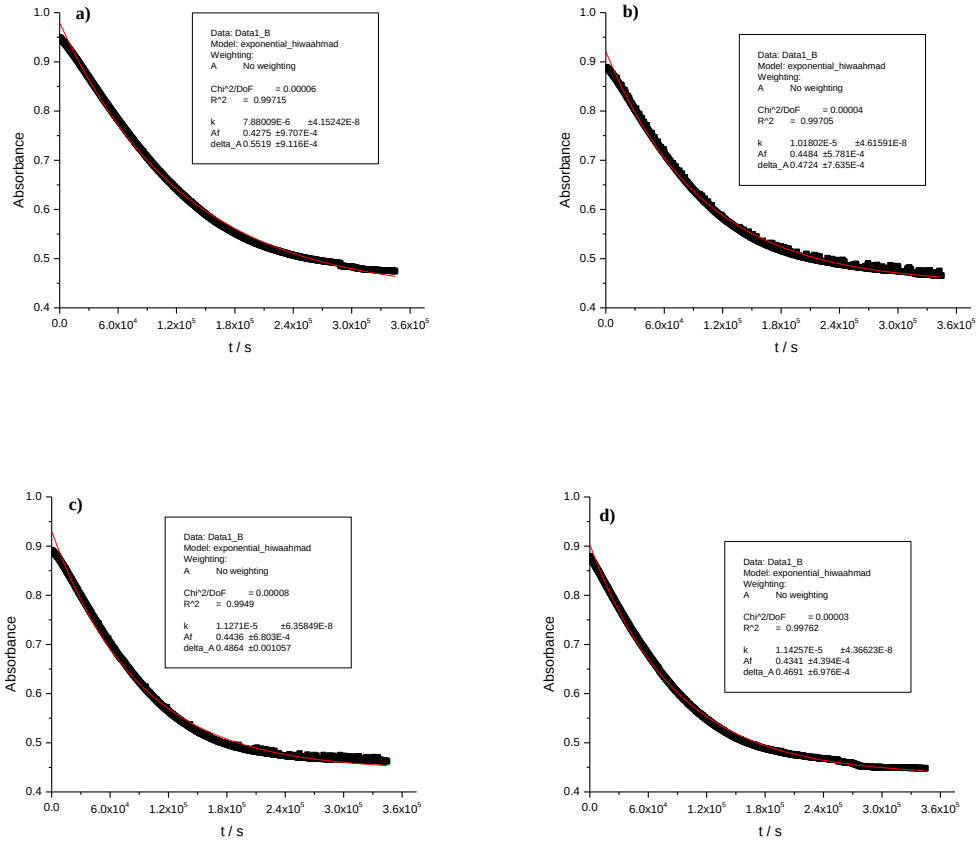

Figure a3.23: Hydrolysis of **3.12** at 264 nm in H_2O-phosphate buffer at a) 0.09 M, b) 0.18 M, c) 0.27 M and d) 0.36 M total phosphate with ionic strength of 0.9 M *I*, pH 7.4 at 37 °C. The squares (■) are the experimental points, and the red solid lines are the fits to pseudo-first-order kinetics.

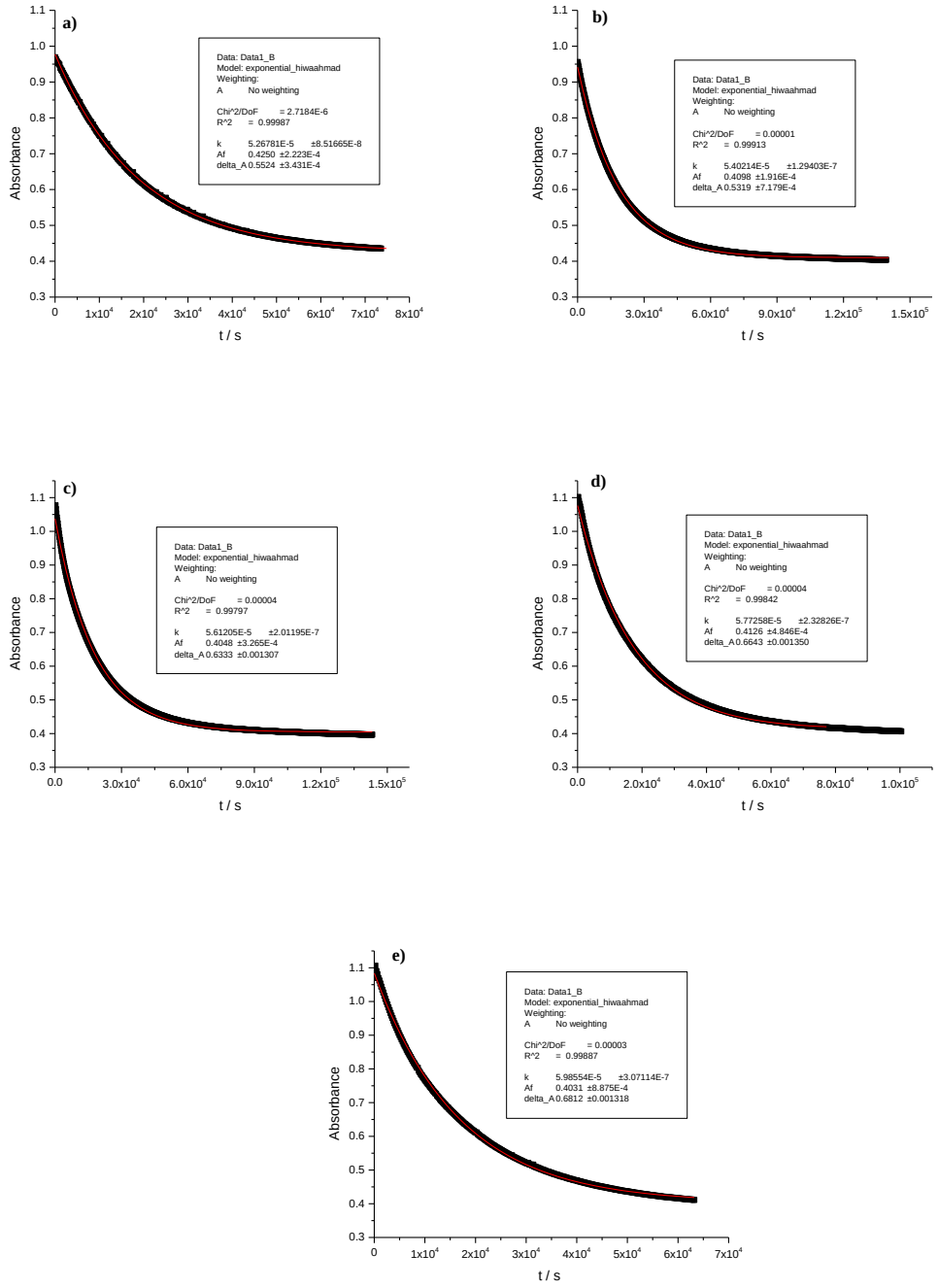

Figure a3.24: Hydrolysis of **3.13** at 264 nm in H_2O-phosphate buffer at a) 0.045 M, b) 0.09 M, c) 0.18 M, d) 0.27 M and e) 0.36 M total phosphate with ionic strength of 0.9 M *I*, pH 7.4 at 37 °C. The squares (■) are the experimental points, and the red solid lines are the fits to pseudo-first-order kinetics.

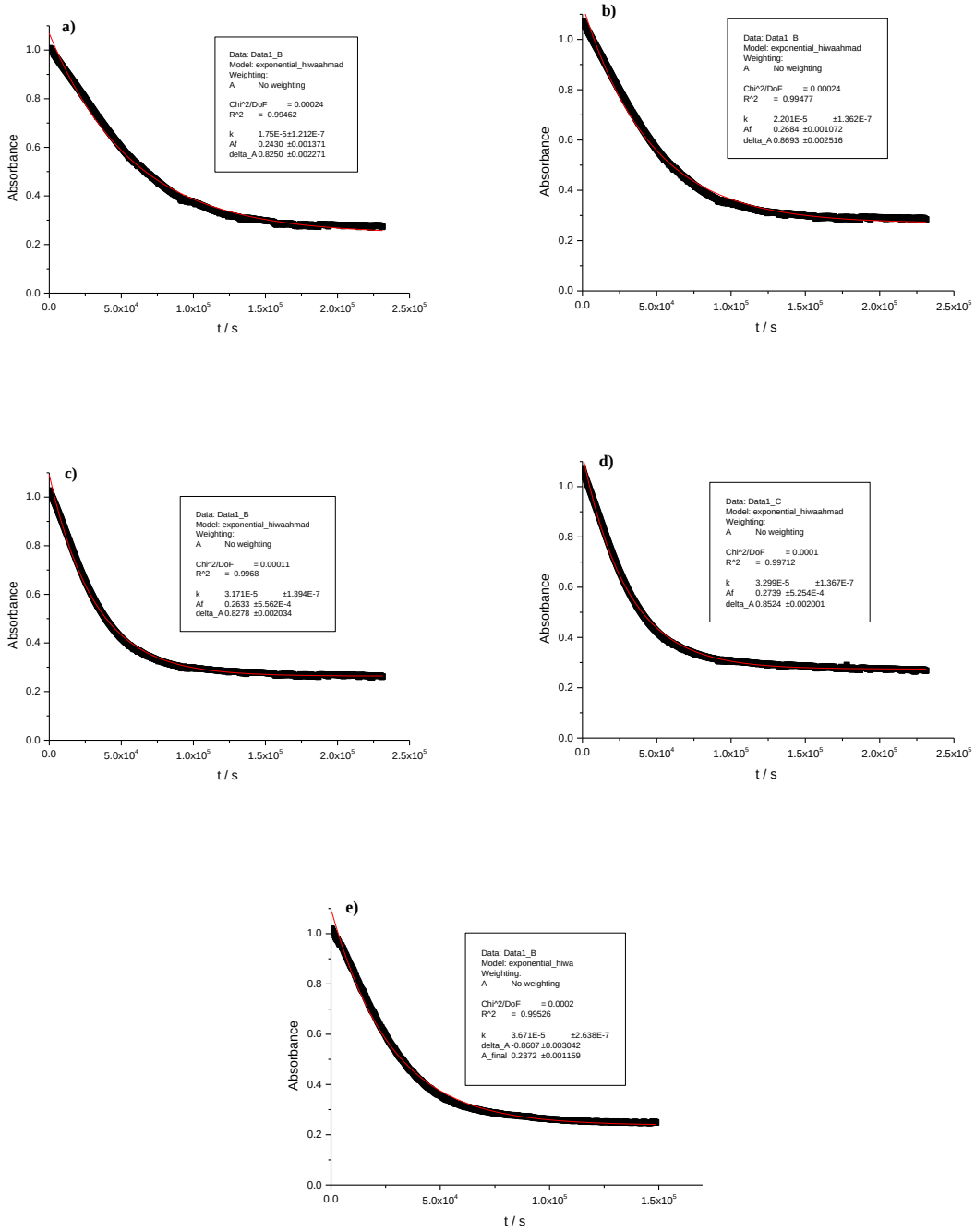

Figure a3.25: Hydrolysis of **3.14** at 264 nm in H_2O-phosphate buffer at a) 0.045 M, b) 0.09 M, c) 0.18 M, d) 0.27 M and e) 0.36 M total phosphate with ionic strength of 0.9 M *I*, pH 7.4 at 37 °C. The squares (■) are the experimental points, and the red solid lines are the fits to pseudo-first-order kinetics.

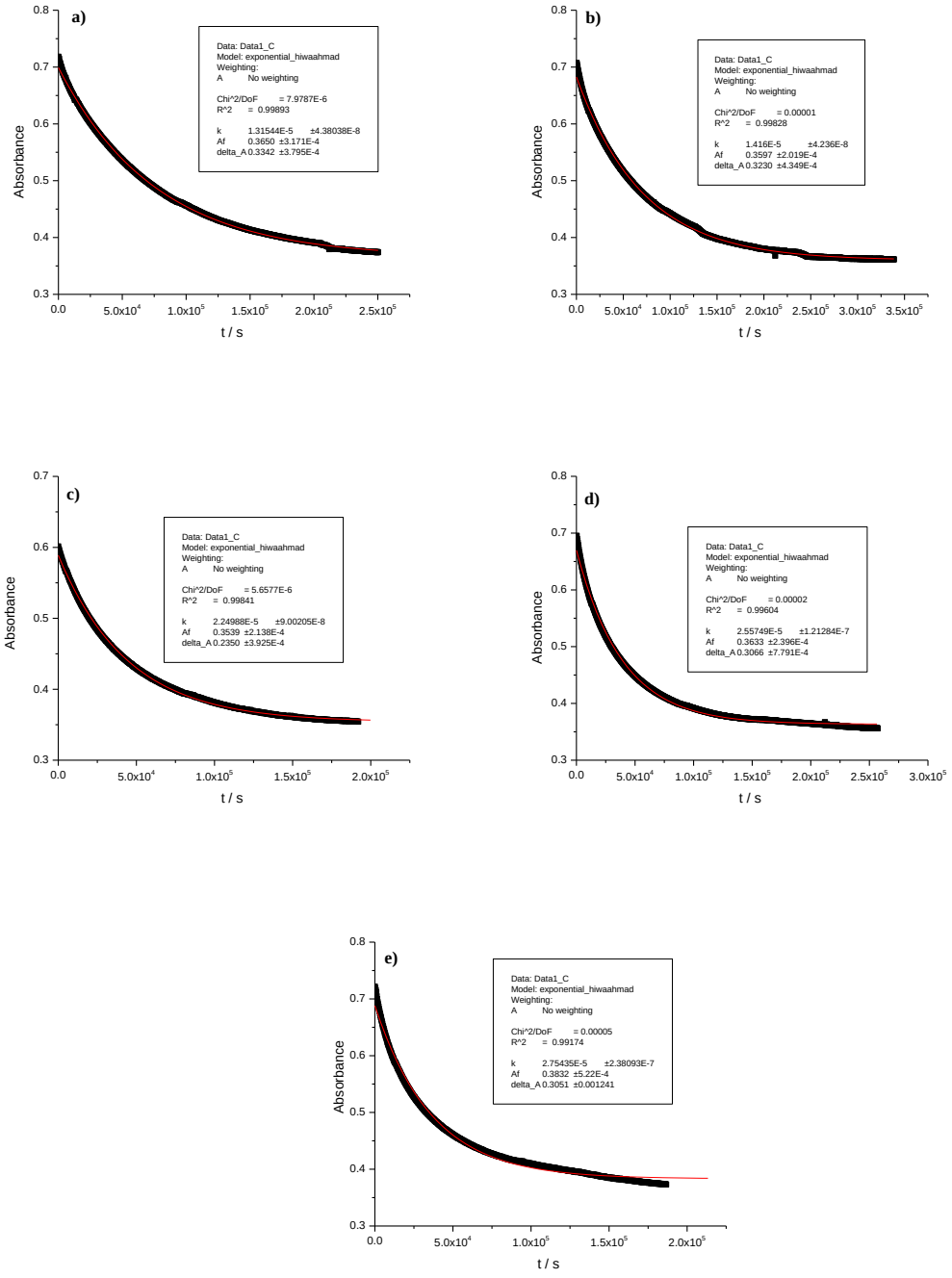

Figure a3.26: Hydrolysis of **3.15** at 262 nm in H_2O-phosphate buffer at a) 0.045 M, b) 0.09 M, c) 0.18 M, d) 0.27 M and e) 0.36 M total phosphate with ionic strength of 0.9 M *I*, pH 7.4 at 37 °C. The squares (■) are the experimental points, and the red solid lines are the fits to pseudo-first-order kinetics.

Table a3.8: Pseudo-first-order rate constants od hydrolysis k_{hydro} determined by UV-visible spectroscopy for 2-thioxoimidazolidin-4-one (**3.8**) in H_2O-phosphate buffer at 0.36 M, 0.27 M, 0.18 M, 0.09 M and 0.045 M total phosphate with ionic strength of 0.9 M *I*, pH 7.4 and 37 °C.

Buffer conc./M	Basic phosphate buffer/M	k_{hyd} H_2O/ 10^{-6} s^{-1}
0.045	0.036	24.2 ± 0.5 (± 0.08)[a]
0.09	0.072	39.5 ± 0.8 (± 0.1)[a]
0.18	0.14	44.9 ± 0.9 (± 0.2)[a]
0.27	0.22	45.1 ± 0.9 (± 0.2)[a]
0.36	0.29	57.8 ± 1.2 (± 0.2)[a]

a) Where the error from the data fit is reported as less than 2% of the rate constant, an error of 2% was assumed. Values in brackets are the errors from the data fit which are less than 2%.

Table a3.9: Pseudo-first-order rate constants od hydrolysis k_{hydro} determined by UV-visible spectroscopy for 5-benzyl-2-thioxoimidazolidin-4-one (**3.9**) in H_2O-phosphate buffer at 0.36 M, 0.27 M, 0.18 M, 0.09 M and 0.045 M total phosphate with ionic strength of 0.9 M *I*, pH 7.4 and 37 °C.

Buffer conc./M	Basic phosphate buffer/M	k_{hyd} H_2O/ 10^{-6} s^{-1}
0.045	0.036	12.2 ± 0.2 (± 0.1)[a]
0.09	0.072	17.5 ± 0.4 (± 0.06)[a]
0.18	0.14	19.9 ± 0.4 (± 0.05)[a]
0.27	0.22	25.9 ± 0.5 (± 0.04)[a]
0.36	0.29	33.0 ± 0.7 (± 0.06)[a]

a) Where the error from the data fit is reported as less than 2% of the rate constant, an error of 2% was assumed. Values in brackets are the errors from the data fit which are less than 2%.

Table a3.10: Pseudo-first-order rate constants od hydrolysis k_{hyd} determined by UV-visible spectroscopy for 5-(pyridin-2-ylmethyl)-2-thioxoimidazolidin-4-one (**3.10**) in H_2O phosphate buffer at 0.36 M, 0.27 M, 0.18 M, 0.09 M and 0.045 M total phosphate with ionic strength of 0.9 M *I*, pH 7.4 and 37 °C.

Buffer conc./M	Basic phosphate buffer/M	k_{hyd} H_2O/ 10^{-6} s^{-1}
0.045	0.036	12.9 ± 0.3 (± 0.02)[a]
0.09	0.072	13.6 ± 0.3 (± 0.05)[a]
0.18	0.14	13.7 ± 0.3 (± 0.04)[a]
0.27	0.22	17.2 ± 0.4 (± 0.03)[a]
0.36	0.29	25.8 ± 0.5 (± 0.05)[a]

a) Where the error from the data fit is reported as less than 2% of the rate constant, an error of 2% was assumed. Values in brackets are the errors from the data fit which are less than 2%.

Table a3.11: Pseudo-first-order rate constants od hydrolysis k_{hyd} determined by UV-visible spectroscopy for 5-((1-methyl-1H-pyrrol-2-yl)methyl)-2-thioxoimidazolidin-4-one (**3.11**) in H_2O phosphate buffer at 0.36 M, 0.27 M, 0.18 M, 0.09 M total phosphate with ionic strength of 0.9 M *I*, pH 7.4 and 37 °C.

Buffer conc./M	Basic phosphate buffer/M	k_{hyd} H_2O/ 10^{-6} s^{-1}
0.045	0.036	39.4 ± 0.8 (± 0.5)[a]
0.09	0.072	41.5 ± 0.8 (± 0.5)[a]
0.18	0.14	43.0 ± 0.9 (± 0.4)[a]
0.27	0.22	44.7 ± 0.9 (± 0.5)[a]
0.36	0.29	46.3 ± 0.9 (± 0.5)[a]

a) Where the error from the data fit is reported as less than 2% of the rate constant, an error of 2% was assumed. Values in brackets are the errors from the data fit which are less than 2%.

Table a3.12: Pseudo-first-order rate constants od hydrolysis k_{hyd} determined by UV-visible spectroscopy for 5-(4-methoxybenzyl)-2-thioxoimidazolidin-4-one (**3.12**) in H_2O phosphate buffer at 0.36 M, 0.27 M, 0.18 M, and 0.09 M total phosphate with ionic strength of 0.9 M *I*, pH 7.4 and 37 °C.

Buffer conc./M	Basic phosphate buffer / M	k_{hyd} H_2O/ 10^{-6} s^{-1}
0.045	0.036	
0.09	0.072	7.9 ± 0.2 (± 0.04)[a]
0.18	0.14	10.2 ± 0.2 (± 0.05)[a]
0.27	0.22	11.3 ± 0.2 (± 0.06)[a]
0.36	0.29	11.4 ± 0.2 (± 0.04)[a]

a) Where the error from the data fit is reported as less than 2% of the rate constant, an error of 2% was assumed. Values in brackets are the errors from the data fit which are less than 2%.

Table a3.13: Pseudo-first-order rate constants od hydrolysis k_{hyd} determined by UV-visible for 5-((tetrahydrofuran-3-yl)methyl)-2-thioxoimidazolidin-4-one (**3.13**) in H_2O phosphate buffer at 0.36 M, 0.27 M, 0.18 M, 0.09 M and 0.045 M total with ionic strength of 0.9 M *I*, pH 7.4 and 37 °C.

Buffer conc./M	Basic phosphate buffer/M	k_{hydro} H_2O/ 10^{-6} s^{-1}
0.045	0.036	52.7 ± 1.1 (± 0.09)[a]
0.09	0.072	54.0 ± 1.1 (± 0.1)[a]
0.18	0.14	56.1 ± 1.1 (± 0.2)[a]
0.27	0.22	57.7 ± 1.2 (± 0.2)[a]
0.36	0.29	59.9 ± 1.2 (± 0.3)[a]

a) Where the error from the data fit is reported as less than 2% of the rate constant, an error of 2% was assumed. Values in brackets are the errors from the data fit which are less than 2%.

Table a3.14: Pseudo-first-order rate constants od hydrolysis k_{hyd} determined by UV-visible for 5-methyl-2-thioxoimidazolidin-4-one (**3.14**) in H_2O phosphate buffer at 0.36 M, 0.27 M, 0.18 M, 0.09 M and 0.045 M total phosphate with ionic strength of 0.9 M *I*, pH 7.4 at 37 °C.

Buffer conc./M	Basic phosphate buffer/M	k_{hydro} H_2O/ 10^{-6} s^{-1}
0.045	0.036	17.5 ± 0.4 (± 0.1)[a]
0.09	0.072	22.0 ± 0.4 (± 0.1)[a]
0.18	0.14	31.7 ± 0.6 (± 0.1)[a]
0.27	0.22	33.0 ± 0.7 (± 0.1)[a]
0.36	0.29	36.7 ± 0.7 (± 0.3)[a]

a) Where the error from the data fit is reported as less than 2% of the rate constant, an error of 2% was assumed. Values in brackets are the errors from the data fit which are less than 2%.

Table a3.15: Pseudo-first-order rate constants od hydrolysis k_{hyd} determined by UV-visible for 5-((1H-indol-3-yl)methyl)-2-thioxoimidazolidin-4-one (**3.15**) in H_2O phosphate buffer at 0.36, 0.27, 0.18, 0.09 and 0.045 M total phosphate with ionic strength of 0.9 M *I*, pH 7.4 at 37 °C.

Buffer conc./M	Basic phosphate buffer	k_{hyd} H_2O/ 10^{-6} s^{-1} M^{-1}
0.045	0.036	13.2 ± 0.3 (± 0.04)[a]
0.09	0.072	14.2 ± 0.3 (± 0.04)[a]
0.18	0.14	22.5 ± 0.5 (± 0.09)[a]
0.27	0.22	25.6 ± 0.5 (± 0.1)[a]
0.36	0.29	27.5 ± 0.6 (± 0.2)[a]

a) Where the error from the data fit is reported as less than 2% of the rate constant, an error of 2% was assumed. Values in brackets are the errors from the data fit which are less than 2%.

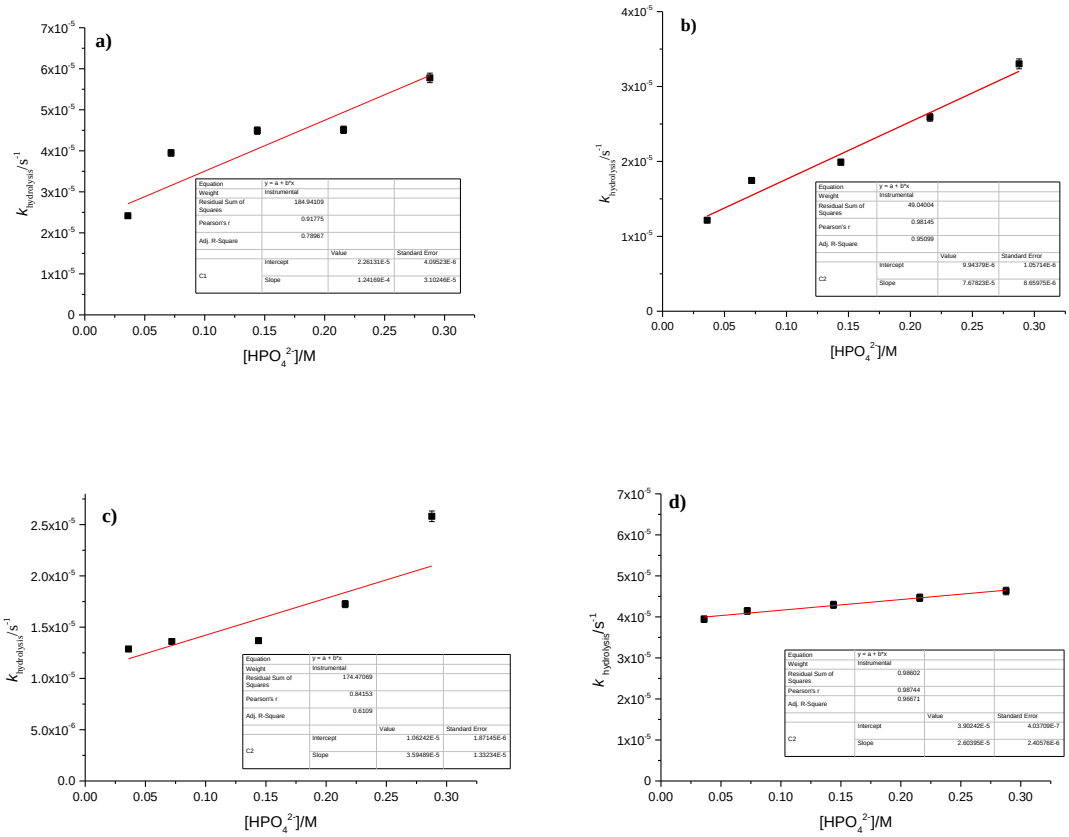

Figure a3.27: Observed rate constants of hydrolysis of a) **3.8**, b) **3.9**, c) **3.10**, and d) **3.11** as a function of the concentration of the basic components of (H_2O-based phosphate buffer at 37 °C, 0.9 M *I*, pH 7.4, 0.36 M, 0.27 M, 0.18 M, 0.09, and 0.045 M.

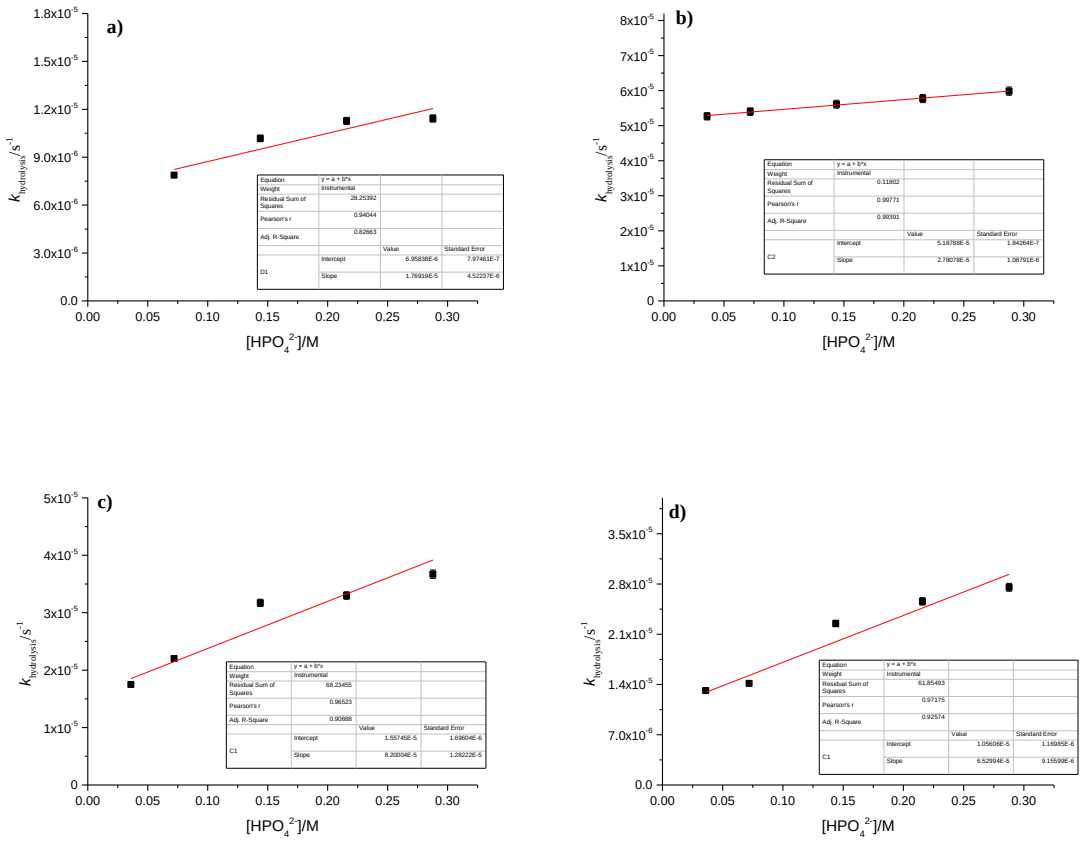

Figure a3.28: Observed rate constants of hydrolysis of a) **3.12**, b) **3.13**, c) **3.14**, and d) **3.15** as a function of the concentration of the basic components of (H_2O-based phosphate buffer at 37 °C, 0.9 M *I*, pH 7.4, 0.36 M, 0.27 M, 0.18 M, 0.09, and 0.045 M.

A.3.6. Kinetics and mechanism of base-catalysed hydrolysis of 3,5-di-substituted 2-thiohydantoins

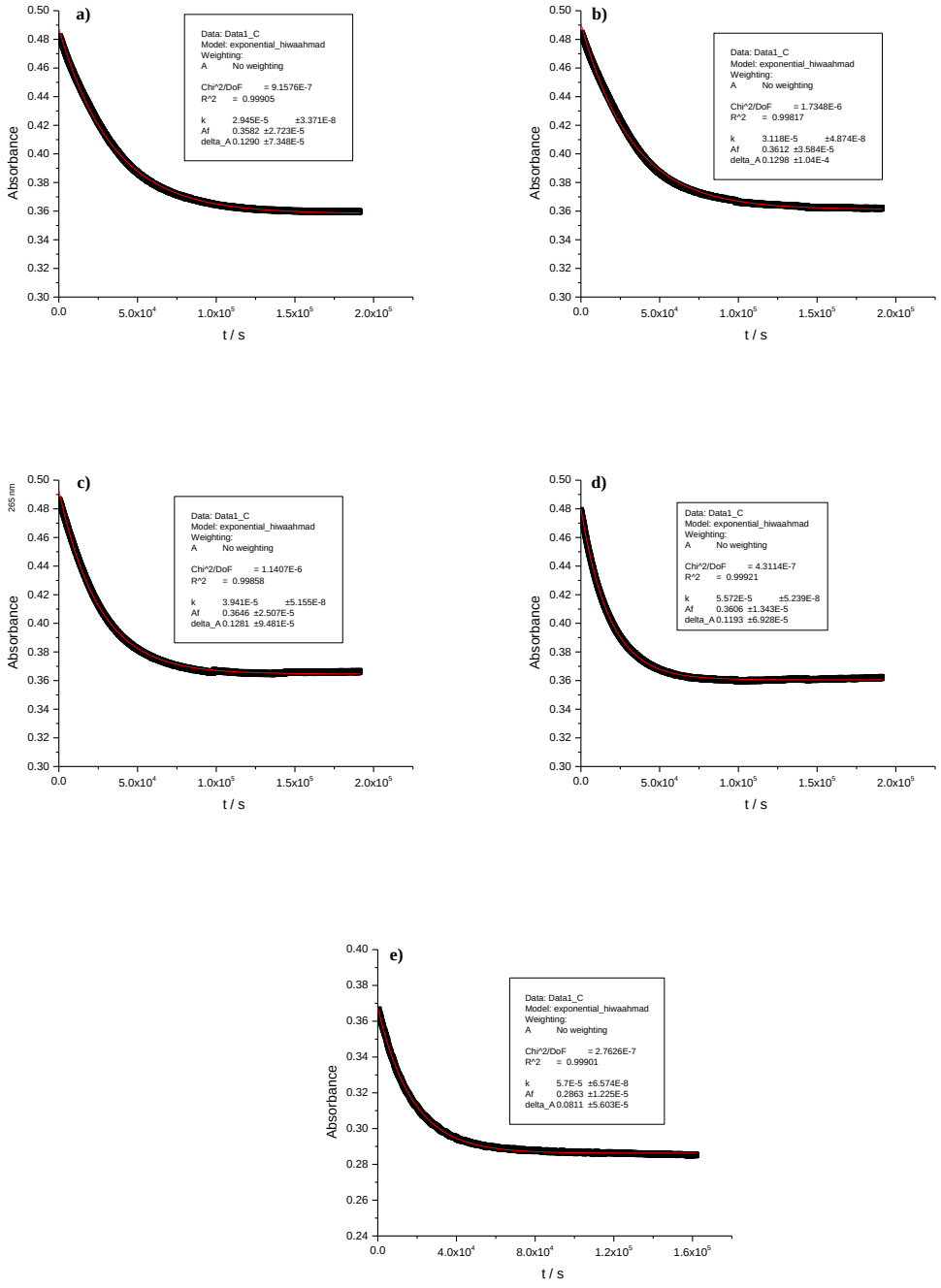

Figure a3.29: Hydrolysis of **3.16** at 265 nm in H_2O-phosphate buffer at a) 0.009 M, b) 0.018 M, c) 0.027 M and d) 0.036 M, and e) 0.045 M total phosphate with ionic strength of 0.9 M *I*, pH 7.4 at 37 °C. The squares (■) are the experimental points, and the red solid lines are the fits to pseudo-first-order kinetics.

Table a3.16: Pseudo-first-order rate constants od hydrolysis k_{hyd} determined by UV-visible spectroscopy for 5-benzyl-3-phenyl-2-thioxoimidazolidin-4-one (**3.16**) in H_2O-phosphate buffer at 0.009 M, 0.018 M, 0.027 M , 0.036 M and 0.045 M total phosphate and 0.0072 M, 0.014 M, 0.021 M, 0.028 M and 0.035 M phosphate basic, respectively with ionic strength of 0.9 M *I*, pH 7.4 and 37 °C.

Buffer conc./M	Basic phosphate buffer	k_{hydro} H_2O/ 10^{-6} s^{-1}
0.009	0.0072	29.5 ± 0.6 (0.03)[a]
0.018	0.014	31.2 ± 0.6 (0.05)[a]
0.027	0.022	39.4 ± 0.8 (0.05)[a]
0.036	0.029	55.7 ± 1.1 (0.05)[a]
0.045	0.036	57.0 ± 1.1 (0.07)[a]

a) Where the error from the data fit is less than 2% of the error of the rate constants have been set to 2%. Values in brackets are the errors from the data fit which are less than 2%.

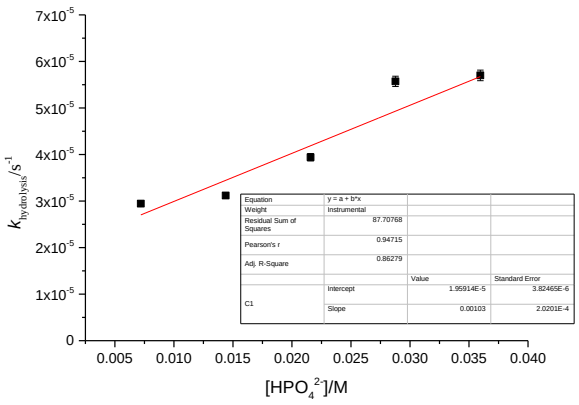

Figure a3.30: Observed rate constants of hydrolysis of **3.16** as a function of the concentration of the basic components of (H_2O-based phosphate buffer at 37 °C, 0.9 M *I*, pH 7.4 at 37 °C.

Appendix 3

for Chapter 4

Kinetics and mechanism for racemisation of substituted 2-thiohydantoins

A4.1 Racemisation of 5-substituted 1-acetyl-2-thiohydantoins

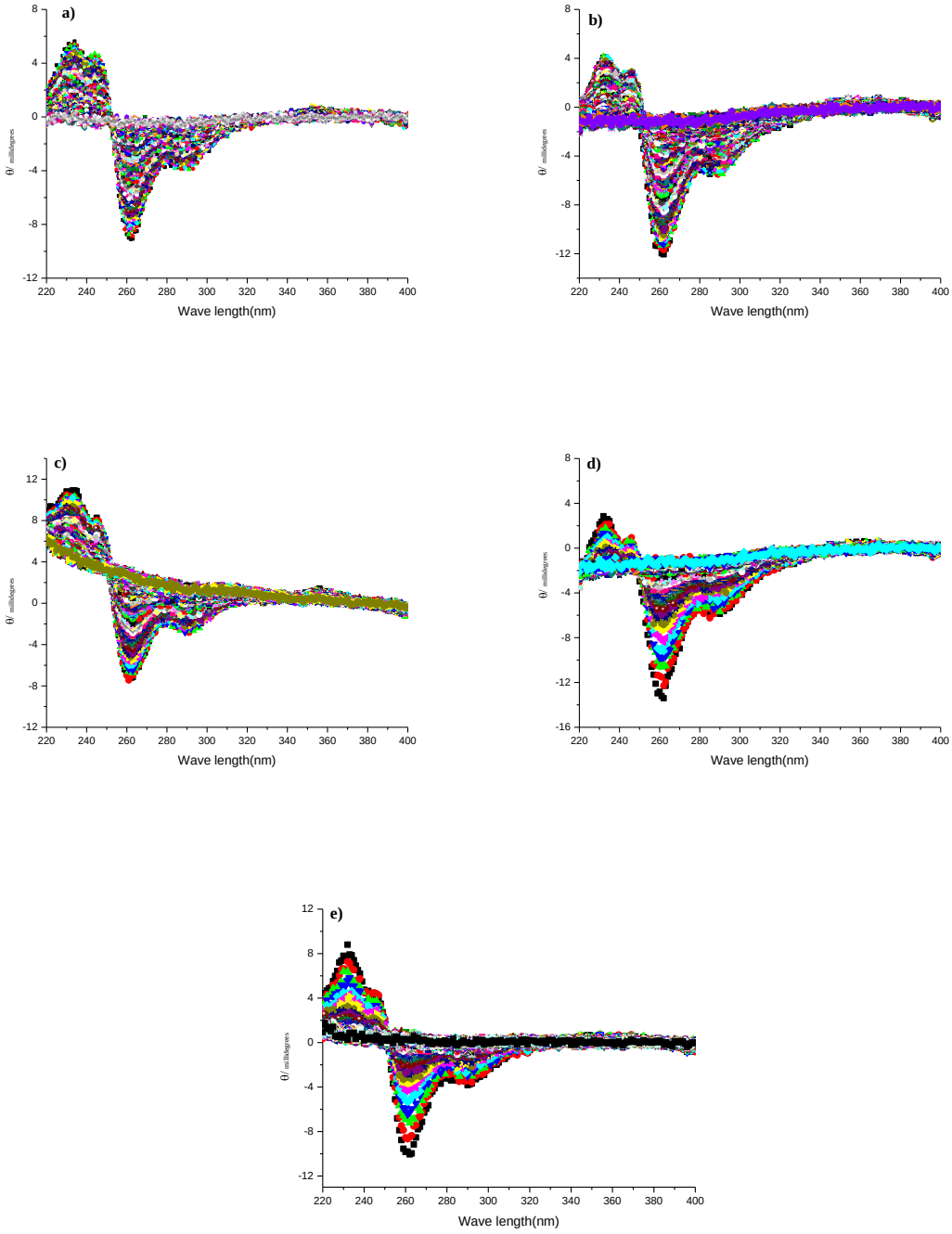

Figure a4.1: Change in ellipticity over time for solutions of **4.1** in H_2O-phosphate buffer at a) 0.045 M, b) 0.09 M, c) 0.18 M, d) 0.27 M and e) 0.36 M total phosphate with ionic strength of 0.9 M *I*, pH 7.4 at 37 °C.

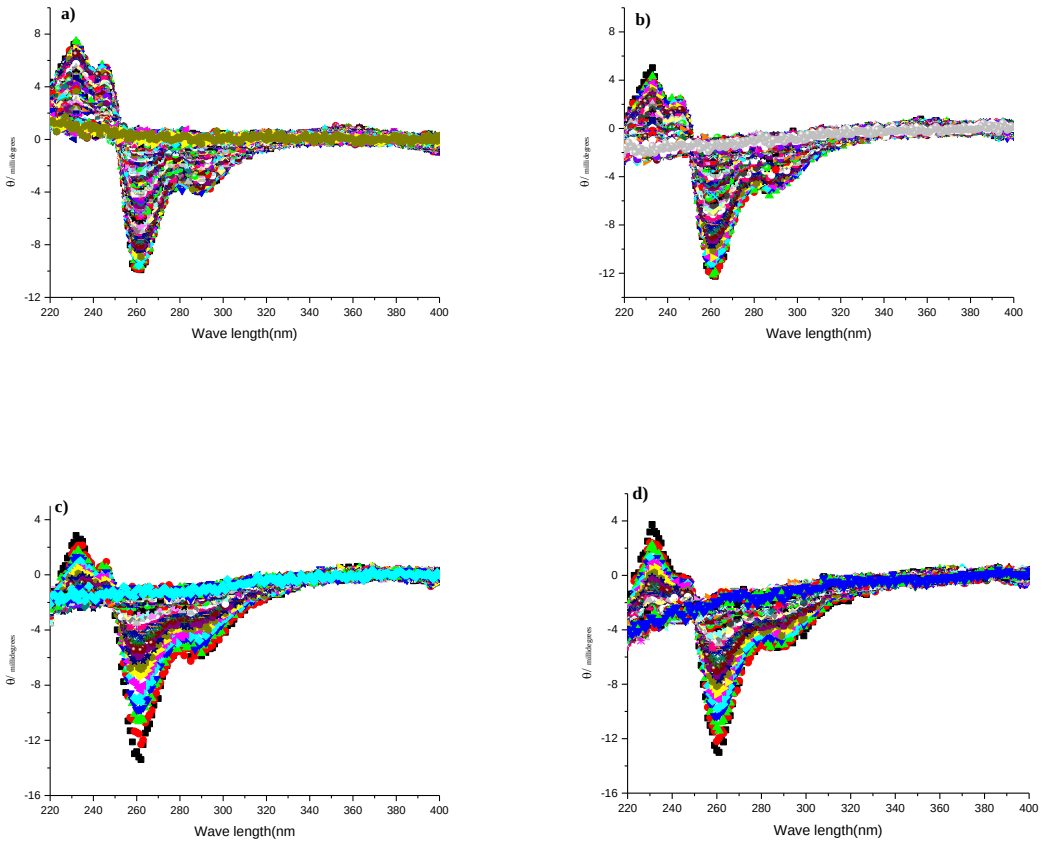

Figure a4.2: Change in ellipticity over time for solutions **4.1** in D_2O-phosphate buffer at a) 0.045 M, b) 0.09 M, c) 0.18 M, d) 0.27 M and e) 0.36 M total phosphate with ionic strength of 0.9 M *I*, pH^* 7.4 at 37 °C.

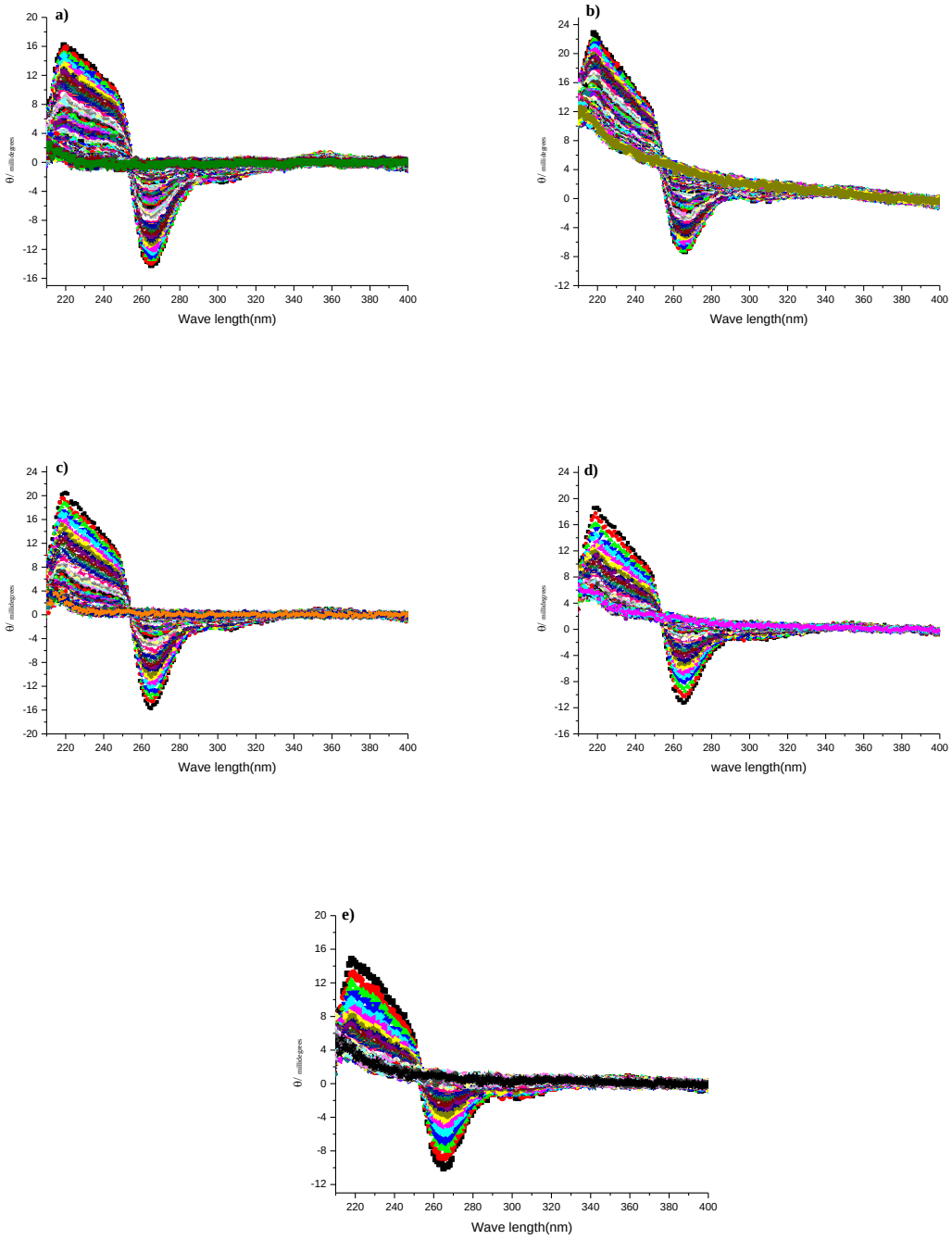

Figure a4.3: Change in ellipticity over time for solutions of **4.2** in H_2O-phosphate buffer at a) 0.045 M, b) 0.09 M, c) 0.18 M, d) 0.27 M and e) 0.36 M total phosphate with ionic strength of 0.9 M *I*, pH 7.4 at 37 °C.

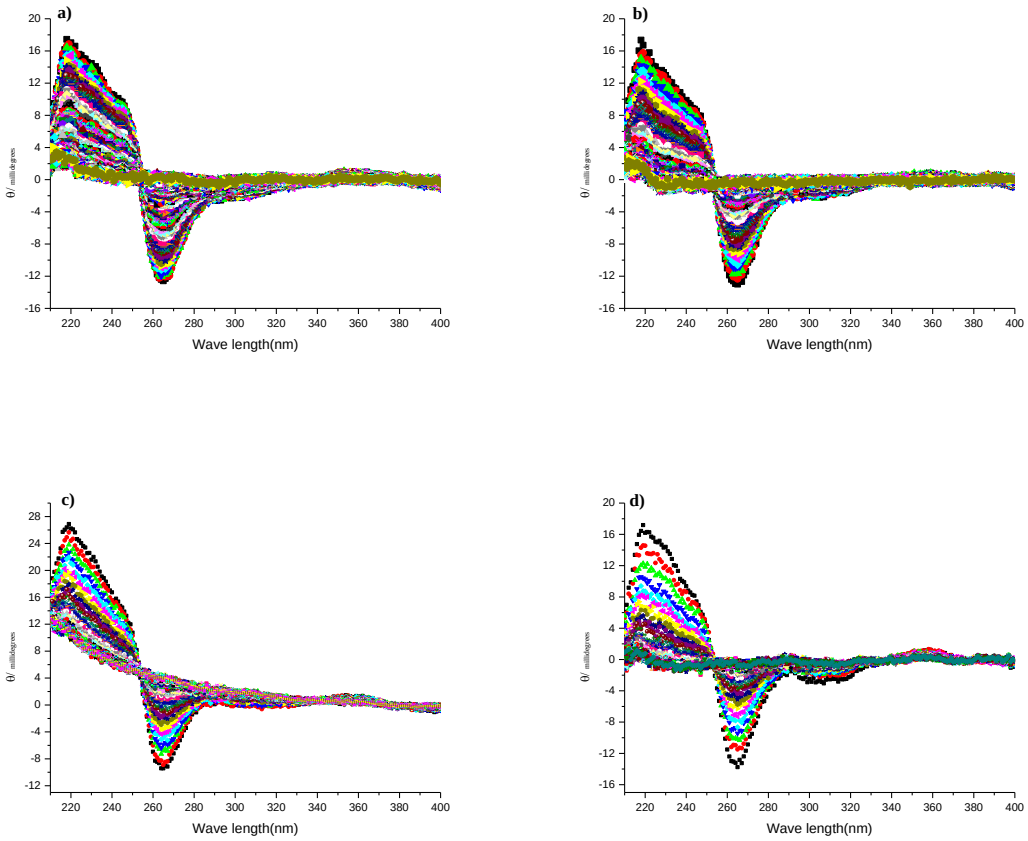

Figure a4.4: Change in ellipticity over time for solutions of **4.2** in D_2O-phosphate buffer at a) 0.045 M, b) 0.09 M, c) 0.18 M, d) 0.27 M and e) 0.36 M total phosphate with ionic strength of 0.9 M *I*, pH^* 7.4 at 37 °C.

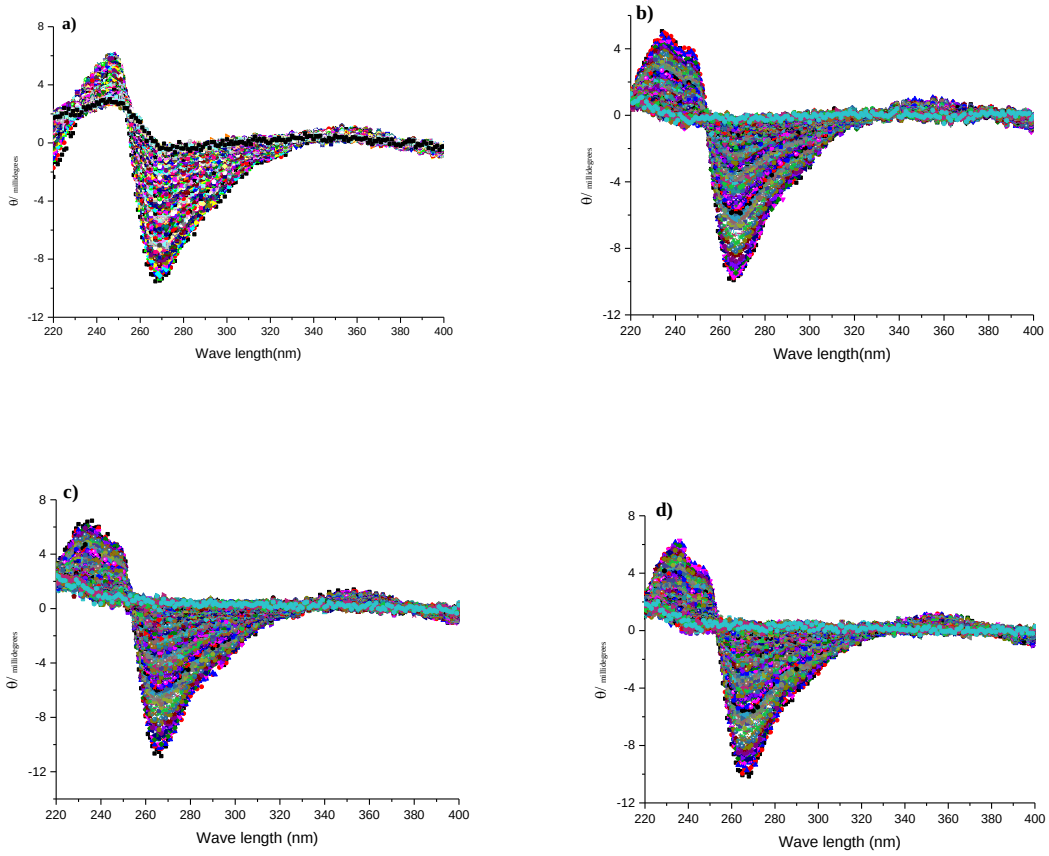

Figure a4.5: Change in ellipticity over time for solutions of **4.3** in H_2O-phosphate buffer at a) 0.045 M, b) 0.09 M, c) 0.18 M, d) 0.27 M and e) 0.36 M total phosphate with ionic strength of 0.9 M *I*, pH 7.4 at 37 °C.

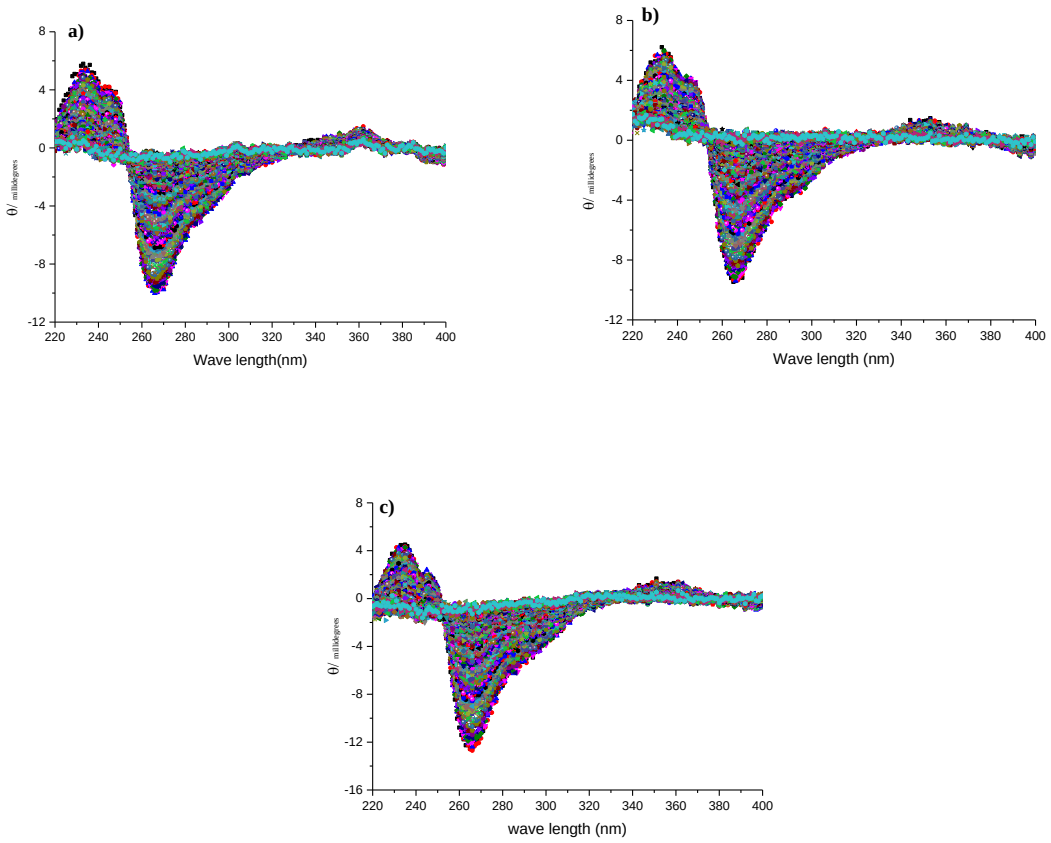

Figure a4.6: Change in ellipticity over time for solutions of **4.3** in D_2O-phosphate buffer at a) 0.045 M, b) 0.09 M, c) 0.18 M, d) 0.27 M and e) 0.36 M total phosphate with ionic strength of 0.9 M *I*, pH 7.4 at 37 °C.

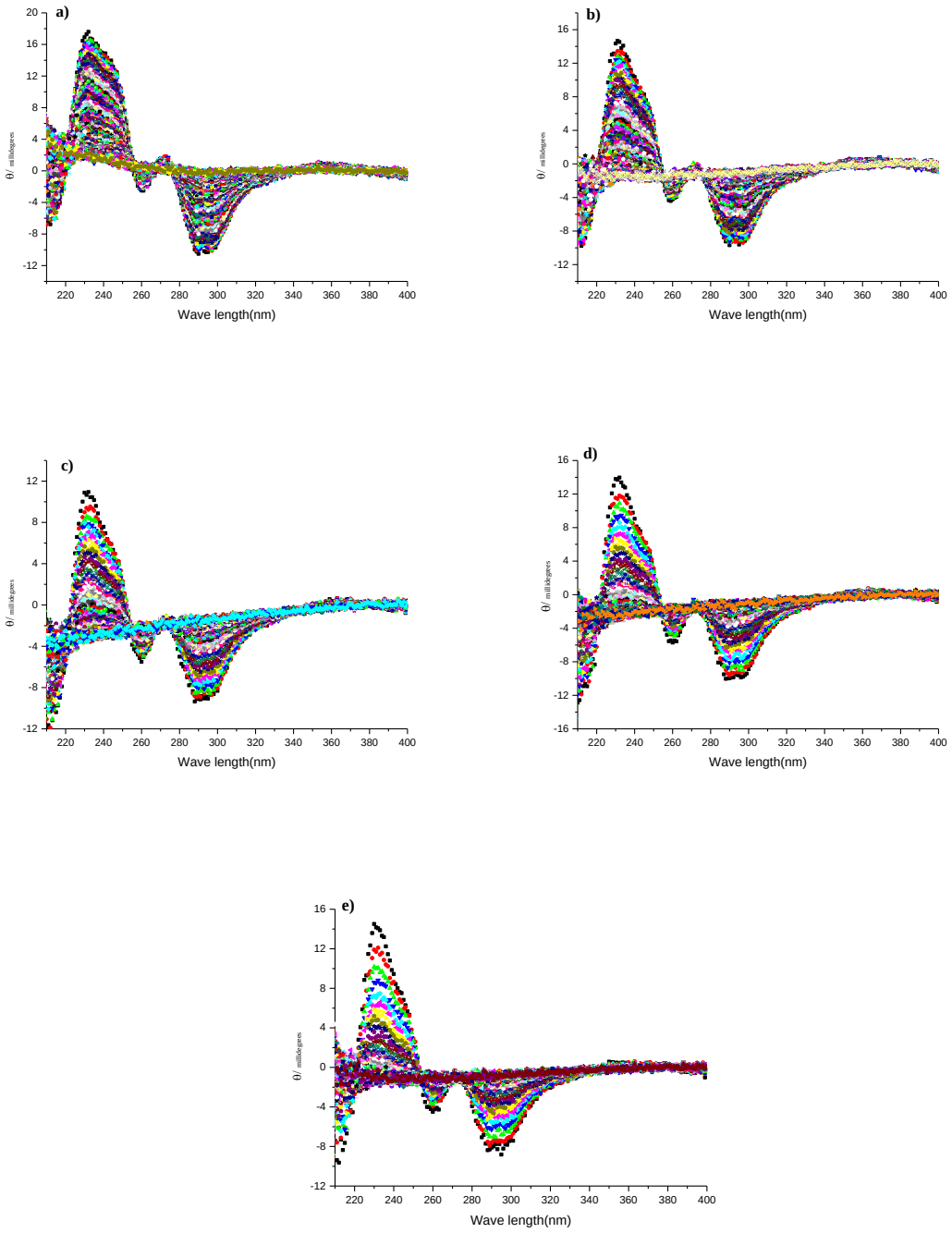

Figure a4.7: Change in ellipticity over time for solutions of **4.4** in H_2O-phosphate buffer at a) 0.045 M, b) 0.09 M, c) 0.18 M, d) 0.27 M and e) 0.36 M total phosphate with ionic strength of 0.9 M *I*, pH 7.4 at 37 °C.

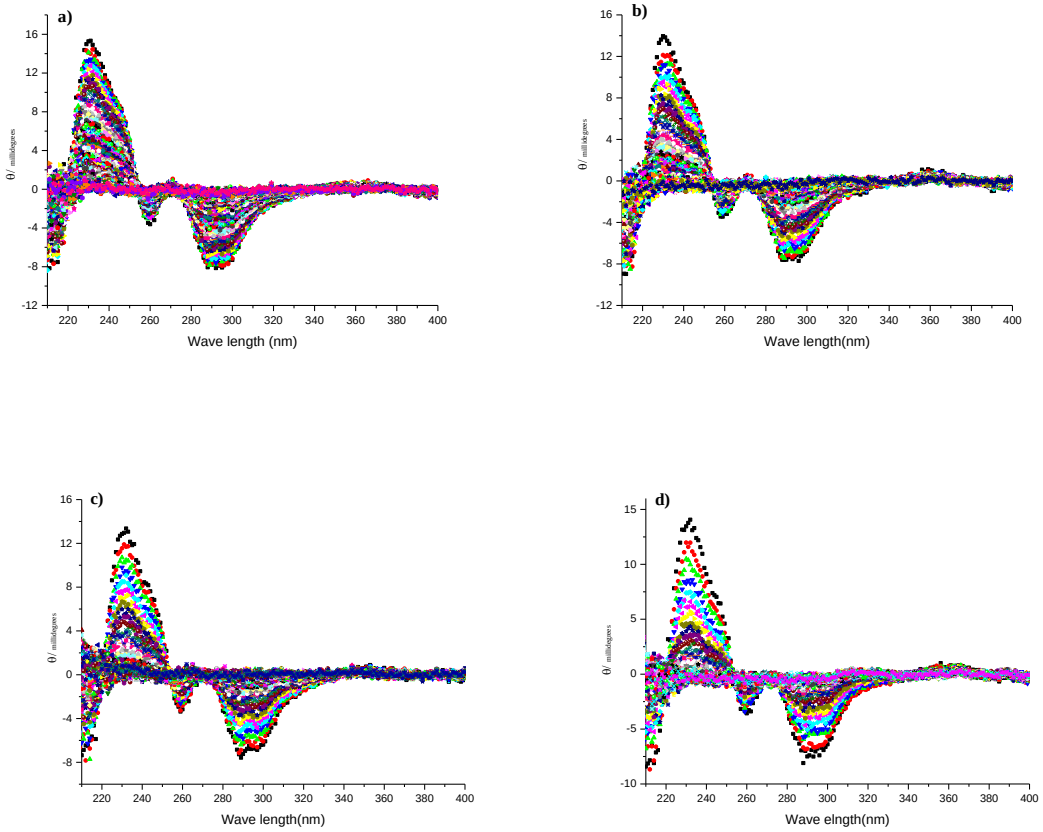

Figure a4.8: Change in ellipticity over time for solutions of **4.4** in D_2O-phosphate buffer at a) 0.045 M, b) 0.09 M, c) 0.18 M, d) 0.27 M and e) 0.36 M total phosphate with ionic strength of 0.9 M *I*, pH 7.4 at 37 °C.

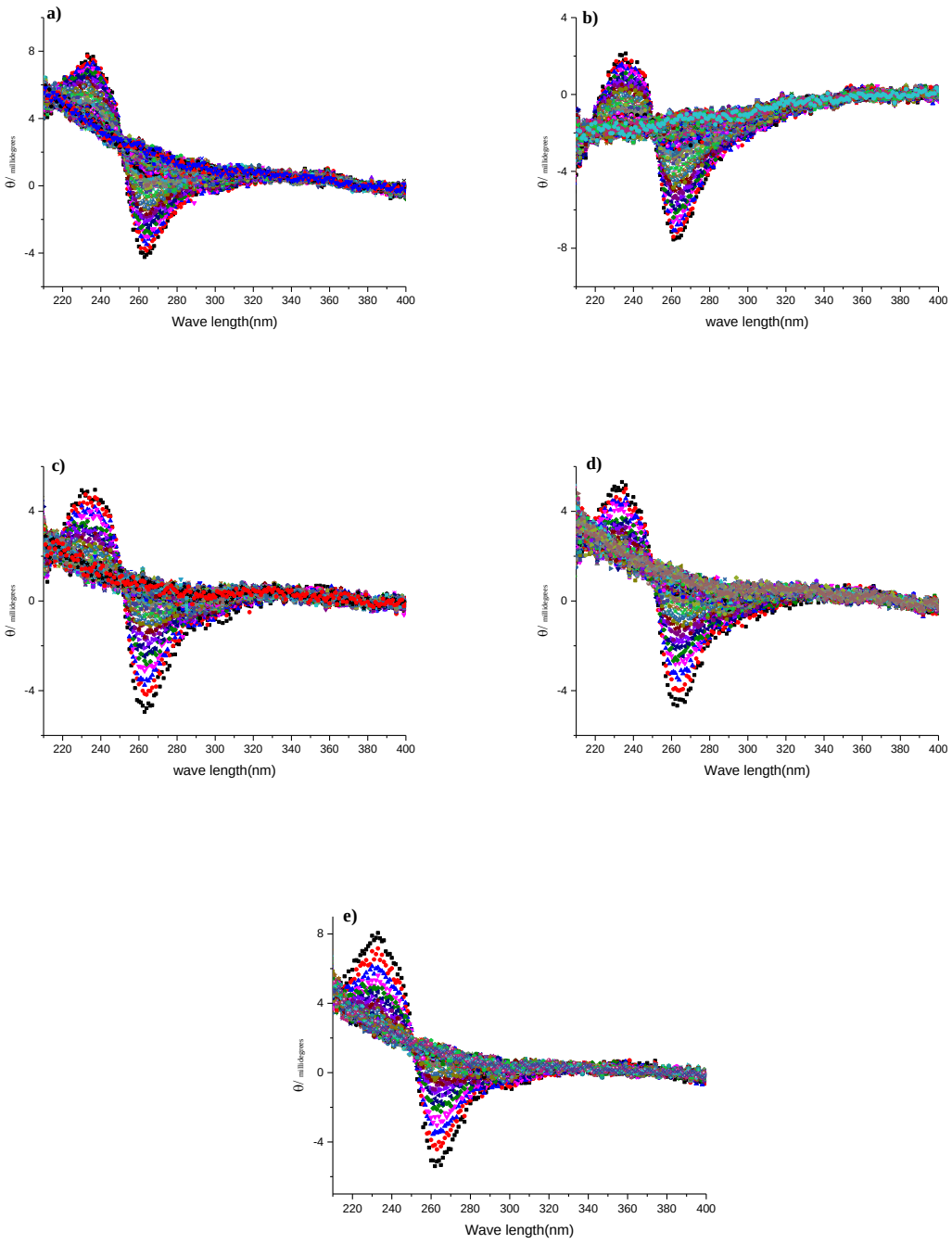

Figure a4.9: Change in ellipticity over time for solutions of **4.5** in H_2O-phosphate buffer at a) 0.045 M, b) 0.09 M, c) 0.18 M, d) 0.27 M and e) 0.36 M total phosphate with ionic strength of 0.9 M *I*, pH 7.4 at 37 °C.

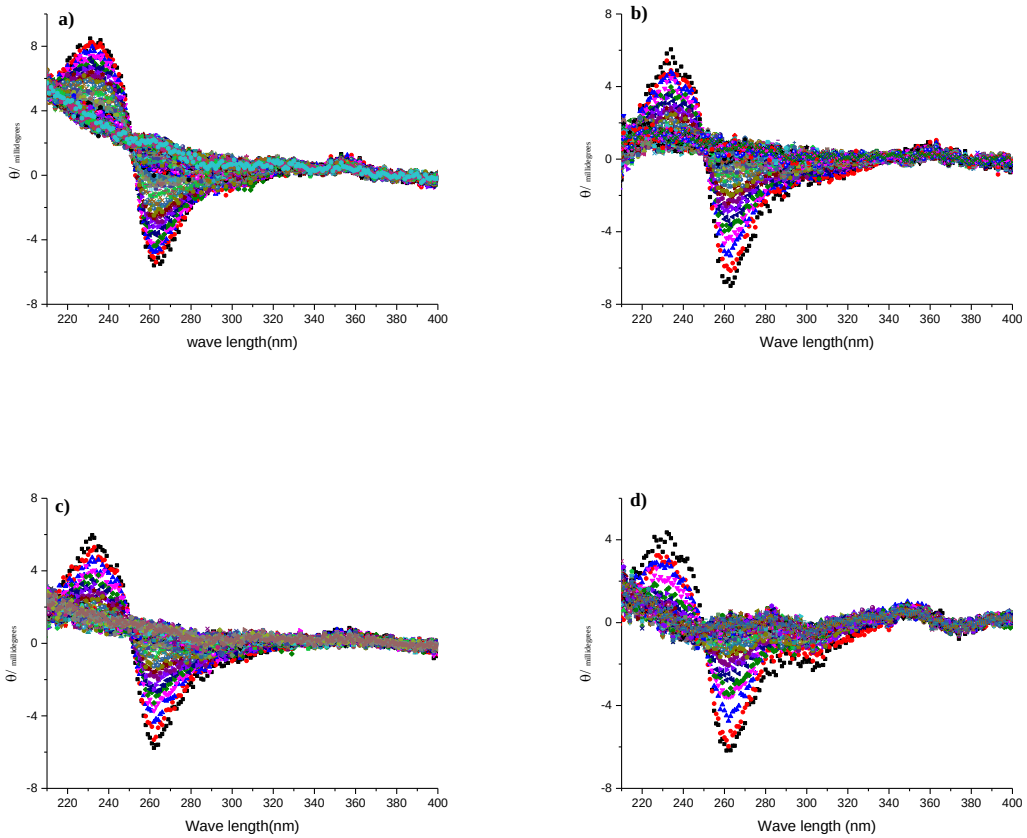

Figure a4.10: Change in ellipticity over time for solutions of **4.5** in D_2O-phosphate buffer at a) 0.045 M, b) 0.09 M, c) 0.18 M, d) 0.27 M and e) 0.36 M total phosphate with ionic strength of 0.9 M *I*, pH* 7.4 at 37 °C.

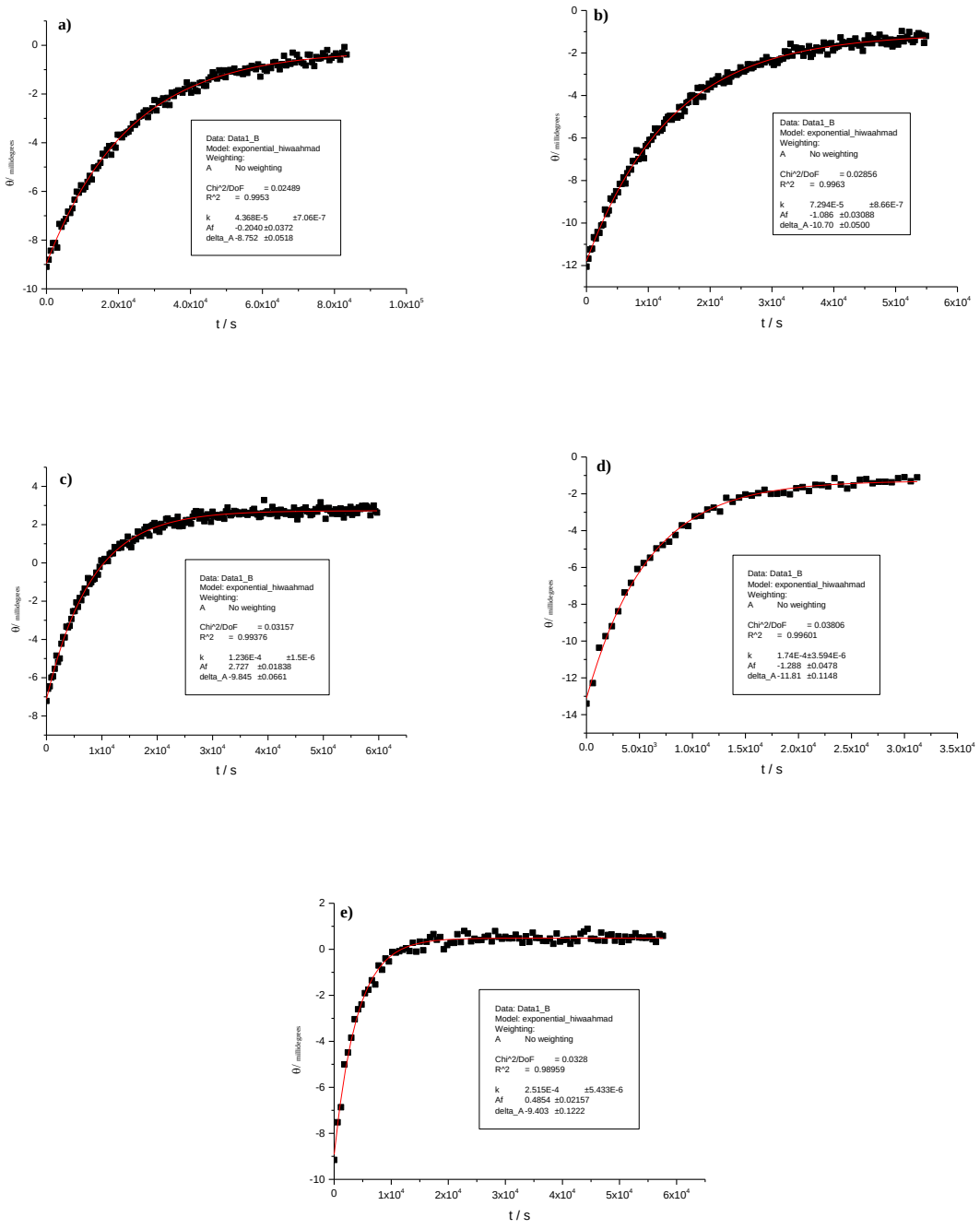

Figure a4.11: The ellipticities of **4.1** at 262 nm versus time in H_2O-phosphate buffer at a) 0.045 M, b) 0.09 M, c) 0.18 M, d) 0.27 M and e) 0.36 M total phosphate with ionic strength of 0.9 M *I*, pH 7.4 at 37 °C.

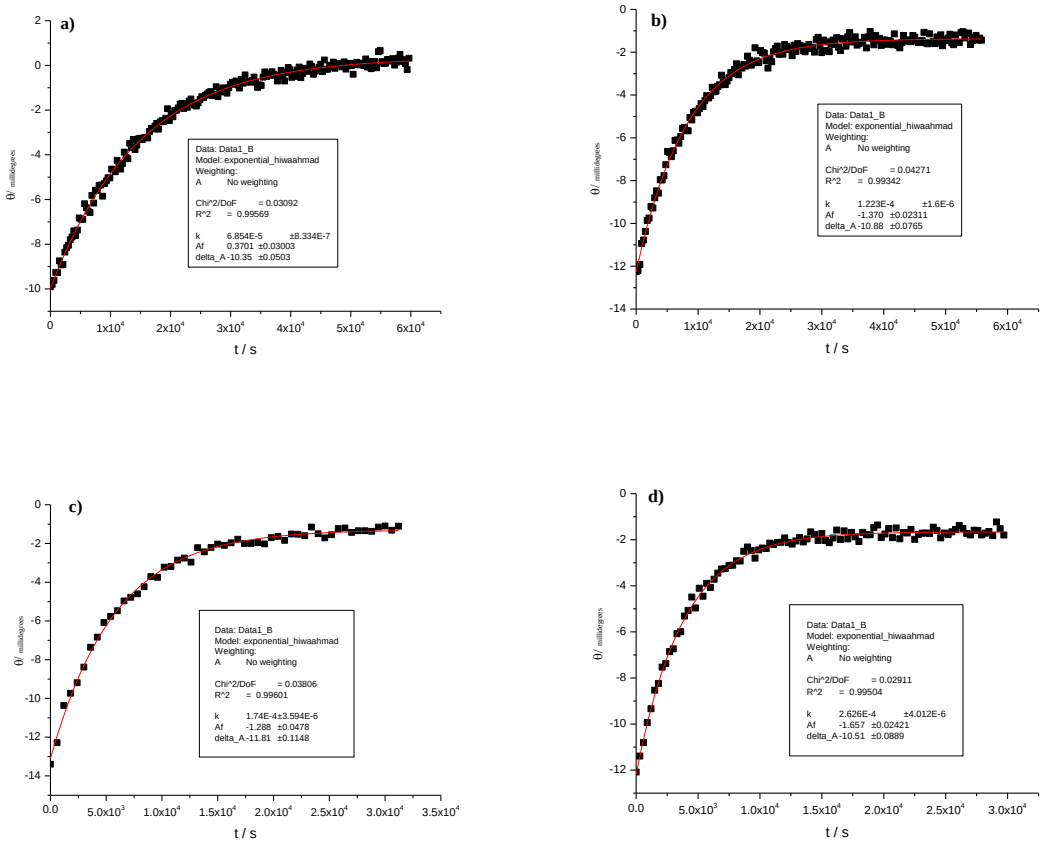

Figure a4.12: The ellipticities of **4.1** at 262 nm versus time in D_2O-phosphate buffer at a) 0.09 M, b) 0.18 M, c) 0.27 M and d) 0.36 M total phosphate with ionic strength of 0.9 M *I*, pH^* 7.4 at 37 °C.

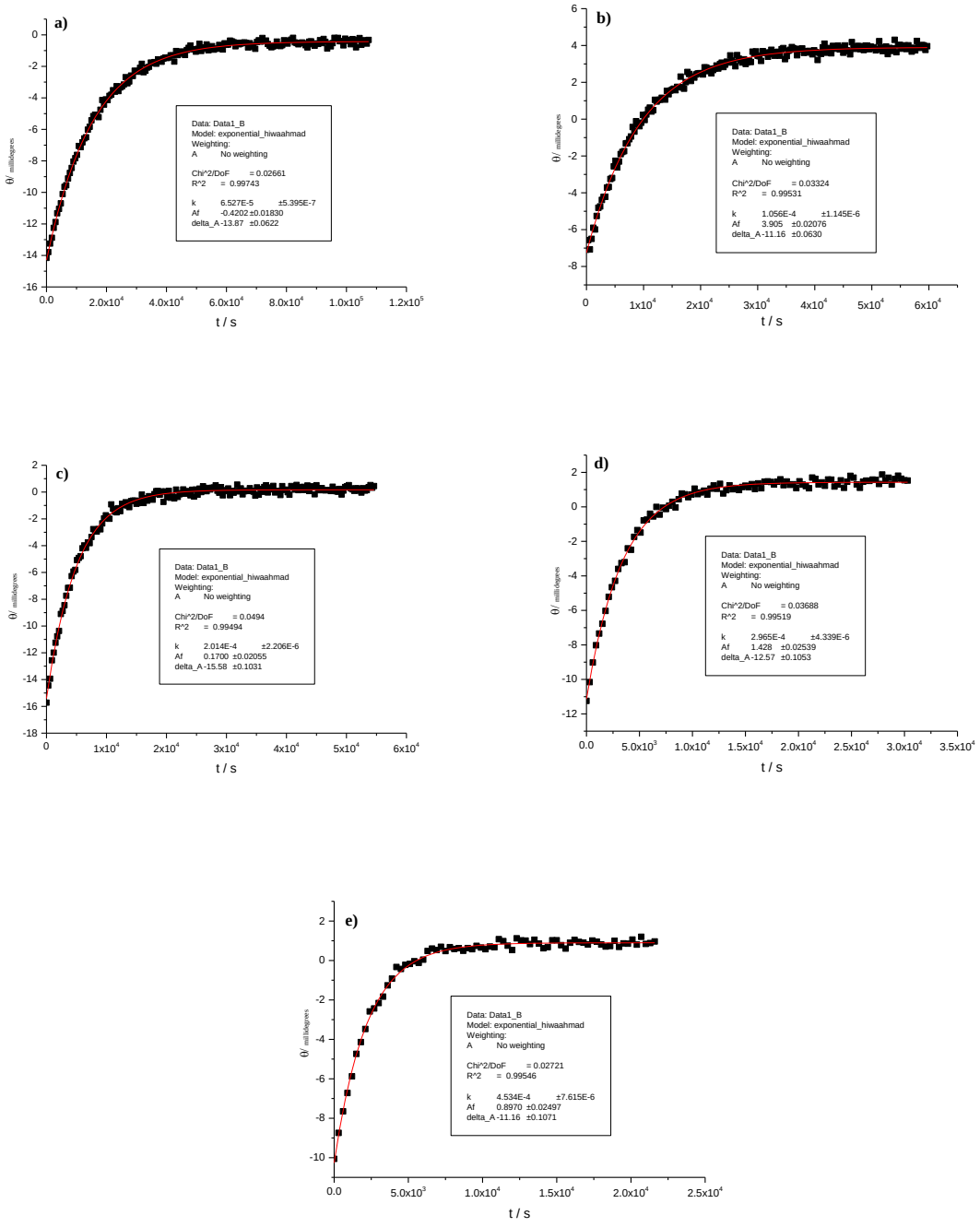

Figure a4.13: The ellipticities of **4.2** at 265 nm versus time in H_2O-phosphate buffer at a) 0.045 M, b) 0.09 M, c) 0.18 M, d) 0.27 M and e) 0.36 M total phosphate with ionic strength of 0.9 M *I*, pH 7.4 at 37 °C.

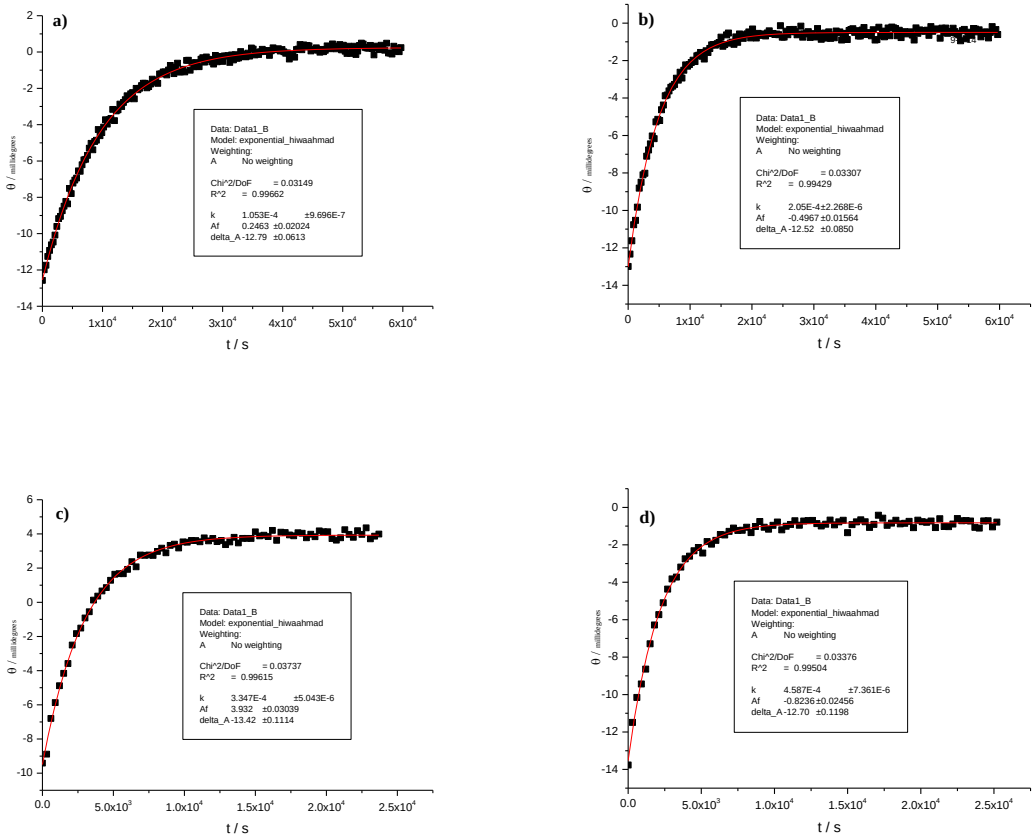

Figure a4.14: The ellipticities of **4.2** at 265 nm versus time in D_2O-phosphate buffer at a) 0.09 M, b) 0.18 M, c) 0.27 M and d) 0.36 M total phosphate with ionic strength of 0.9 M *I*, pH^* 7.4 at 37 °C.

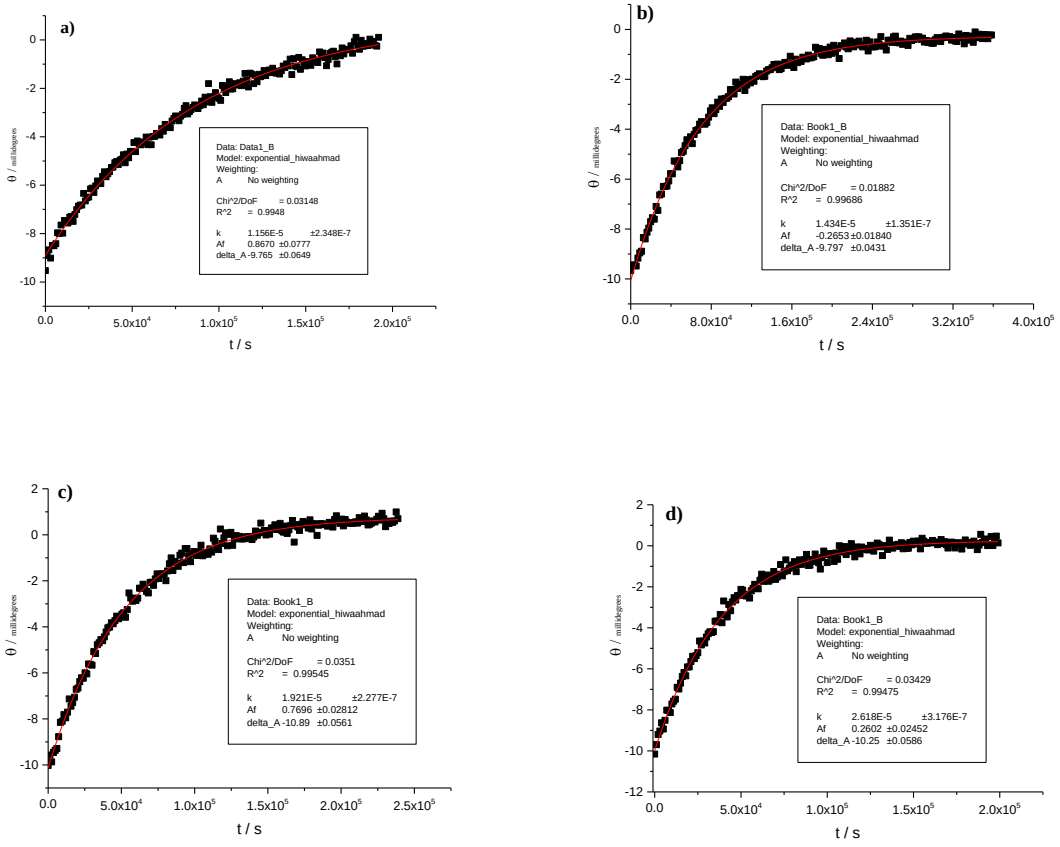

Figure a4.15: The ellipticities of **4.3** at 268 nm versus time in H_2O-phosphate buffer at a) 0.045 M, b) 0.09 M, c) 0.18 M, d) 0.27 M and e) 0.36 M total phosphate with ionic strength of 0.9 M *I*, pH 7.4 at 37 °C.

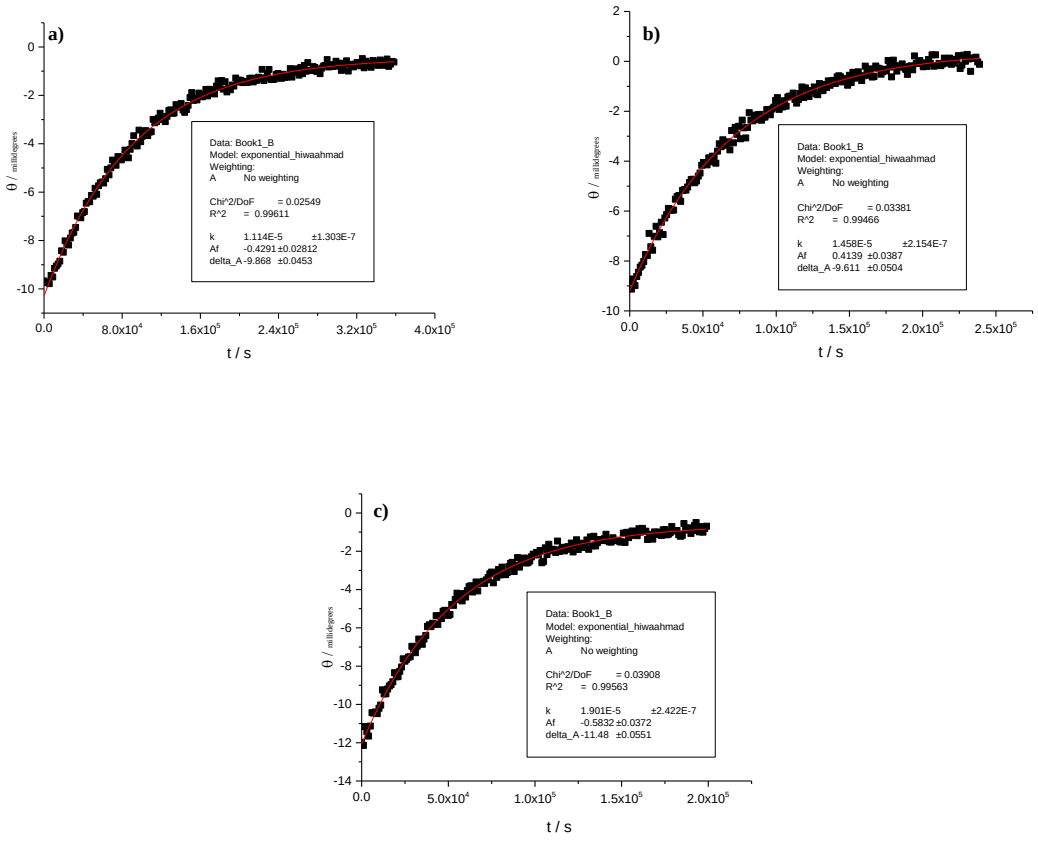

Figure a4.16: The ellipticities of **4.3** at 268 nm versus time in D_2O-phosphate buffer at a) 0.09 M, b) 0.18 M, c) 0.27 M and d) 0.36 M total phosphate with ionic strength of 0.9 M *I*, pH^* 7.4 at 37 °C.

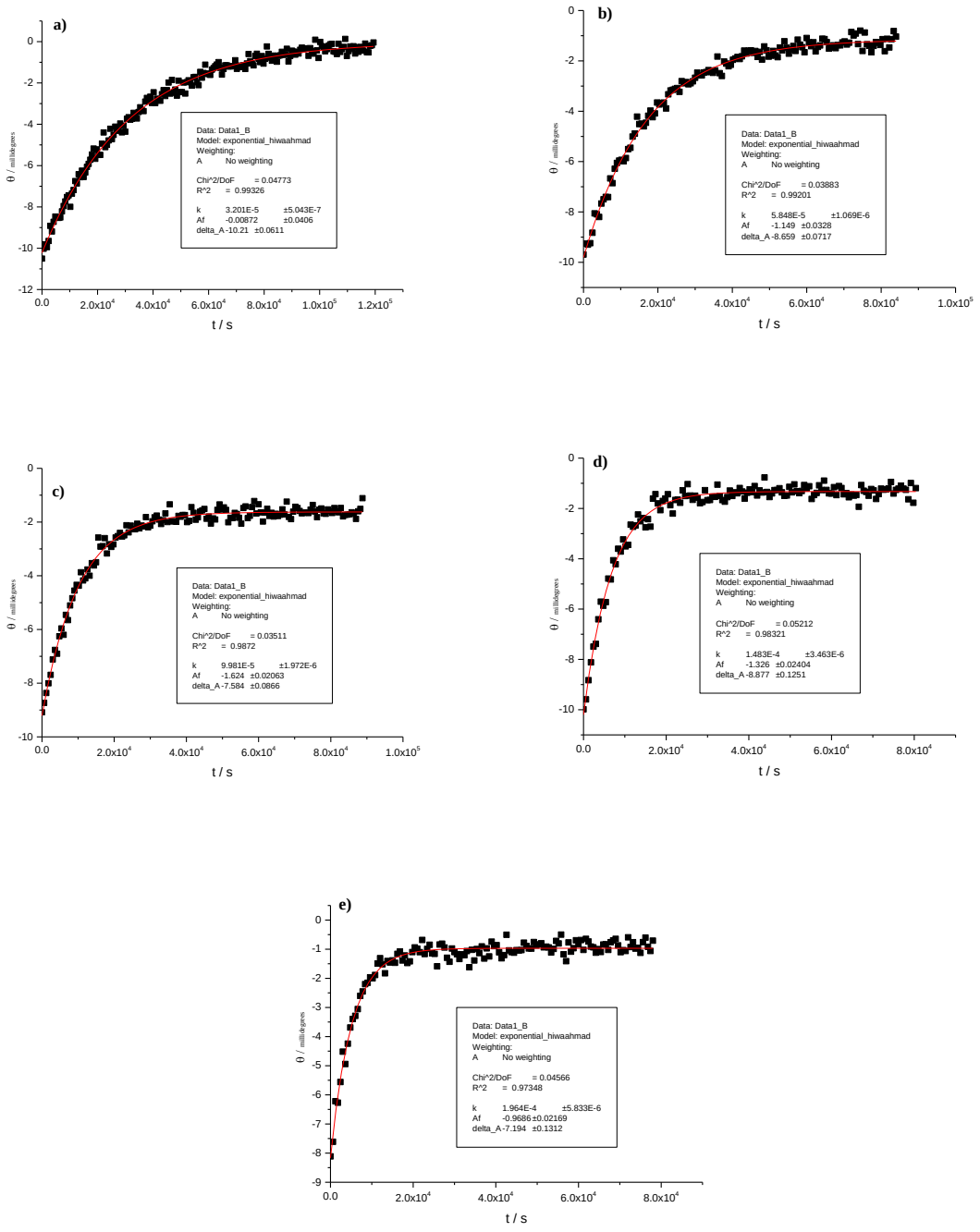

Figure a4.17: The ellipticities of **4.3** at 290 nm versus time in H_2O-phosphate buffer at a) 0.045 M, b) 0.09 M, c) 0.18 M, d) 0.27 M and e) 0.36 M total phosphate with ionic strength of 0.9 M *I*, pH 7.4 at 37 °C.

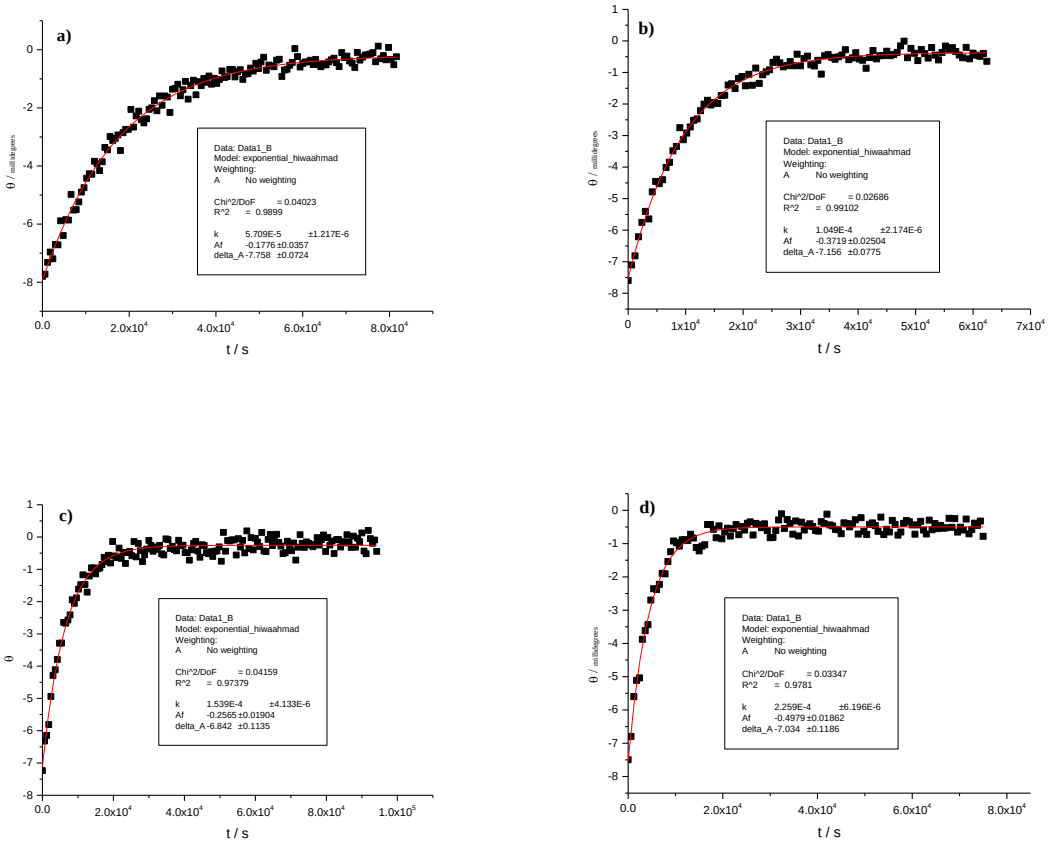

Figure a4.18: The ellipticities of **4.4** at 290 nm versus time in D_2O-phosphate buffer at a) 0.09 M, b) 0.18 M, c) 0.27 M and d) 0.36 M total phosphate with ionic strength of 0.9 M *I*, pH^* 7.4 at 37 °C.

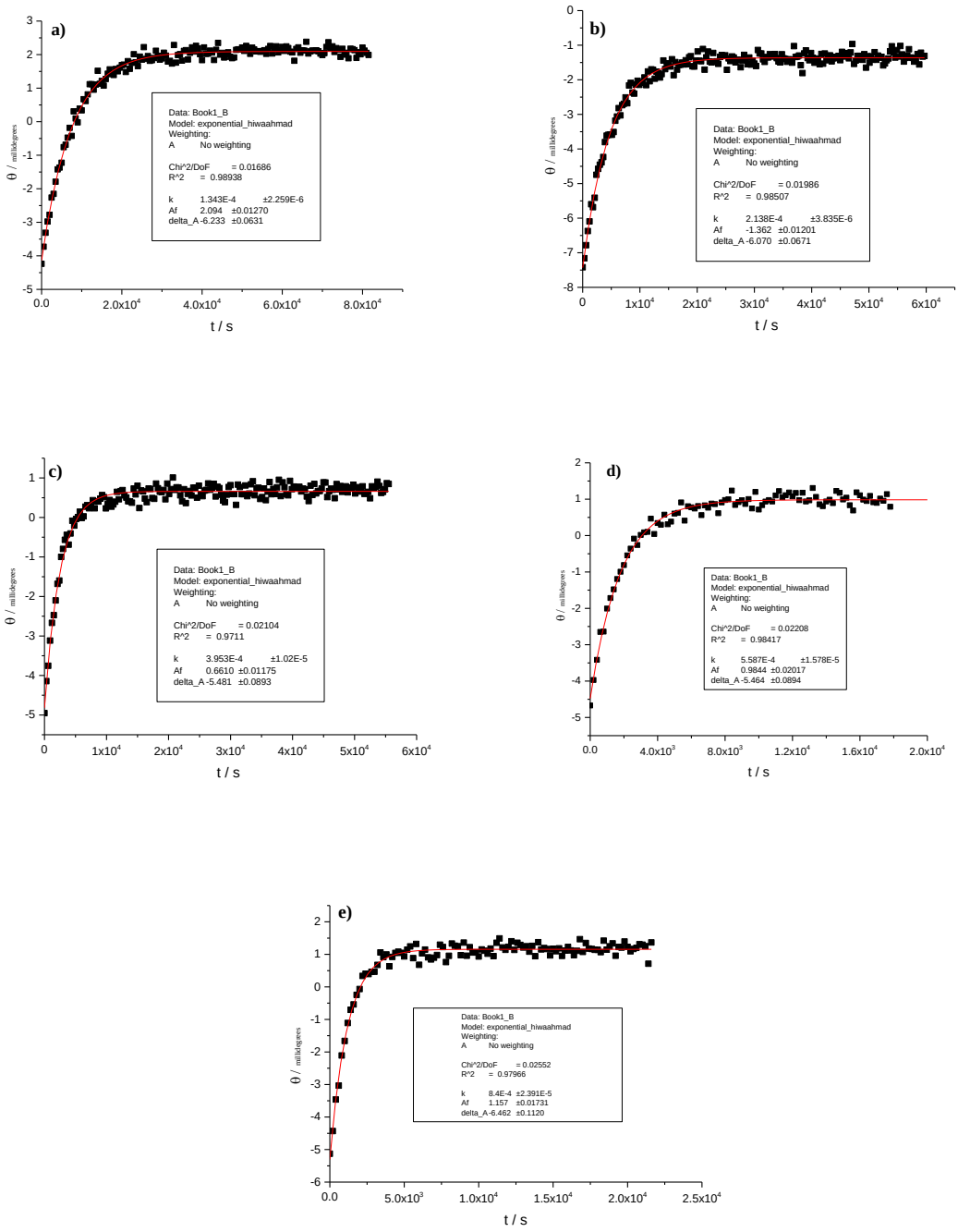

Figure a4.19: The ellipticities of **4.5** at 263 nm versus time in H_2O-phosphate buffer at a) 0.045 M, b) 0.09 M, c) 0.18 M, d) 0.27 M and e) 0.36 M total phosphate with ionic strength of 0.9 M *I*, pH 7.4 at 37 °C.

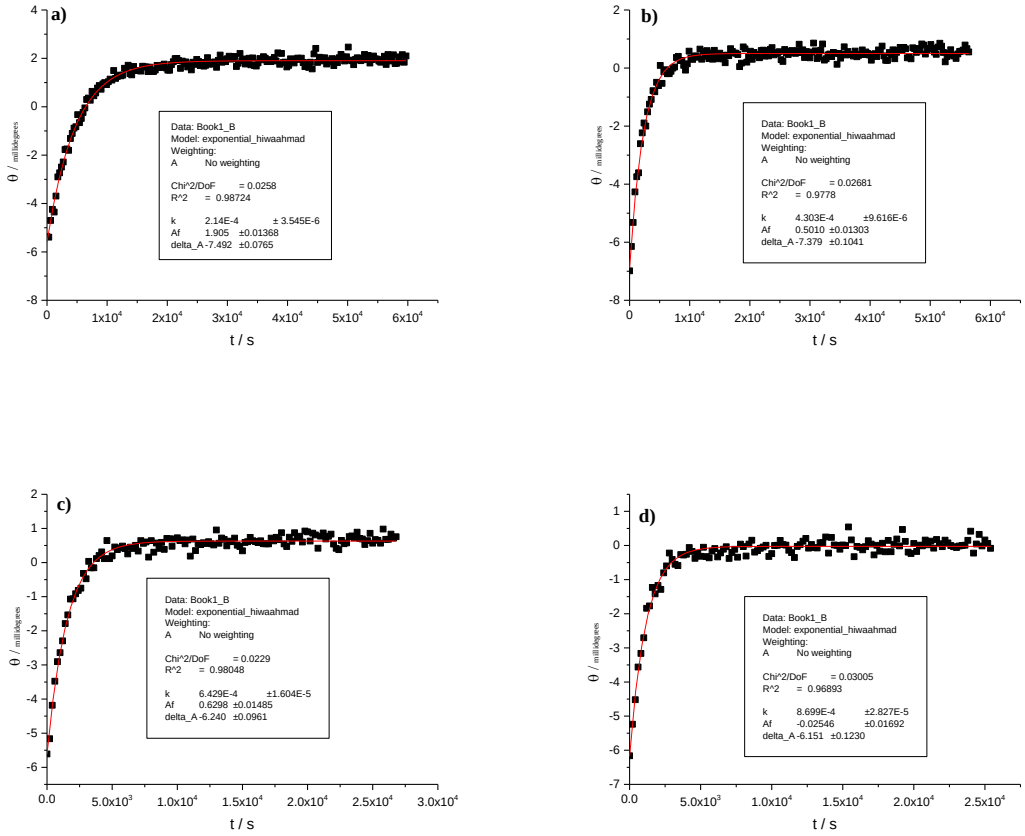

Figure a4.20: The ellipticities of **4.5** at 263 nm versus time in D_2O-phosphate buffer at a) 0.09 M, b) 0.18 M, c) 0.27 M and d) 0.36 M total phosphate with ionic strength of 0.9 M *I*, pH^* 7.4 at 37 °C.

Table a4.1: Pseudo-first-order rate constants k_Θ determined by CD spectroscopy of (*S*)-1-acetyl-5-methyl-2-thioxoimidazolidin-4-one (**4.1**) in H_2O- and D_2O-phosphate buffer at 0.36 M, 0.27 M, 0.18 M, 0.09 M and 0.045 M total phosphate and 0.29 M, 0.22 M, 0.14 M, 0.072 M and 0.036 M phosphate basic, respectively with ionic strength of 0.9 M *I*, pH and pH* 7.4 and 37 °C.

Total buffer con./M	k_Θ (H_2O)/ 10^{-6} s^{-1}	k_Θ (D_2O) / 10^{-6} s^{-1}	k_H/k_D
0.045	43.7 ± 0.9 (± 0.7)[a]		
0.09	72.9 ± 1.5 (± 0.9)[a]	68.5 ± 1.4 (± 0.8)[a]	1.06 ± 0.03
0.18	123.6 ± 2.5 (± 1.5)[a]	122.3 ± 2.5 (± 1.6)[a]	1.01 ± 0.02
0.27	174.0 ± 3.7 (± 3.6)[a]	174.0 ± 3.7 (± 3.6)[a]	1.00 ± 0.03
0.36	251.5 ± 6.2 (± 5.4)[a]	262.6 ± 5.3 (± 4.0)[a]	0.96 ± 0.02

c) Where the error from the data fit is reported as less than 2% of the rate constant, an error of 2% was assumed. Values in brackets are the errors from the data fit which are less than 2%.

Table a4.2: Pseudo-first order rate constants k_Θ determined by CD spectroscopy of (*S*)-1-acetyl-5-benzyl-2-thioxoimidazolidin-4-one (**4.2**) in H_2O- and D_2O-phosphate buffer at 0.36 M, 0.27 M, 0.18 M, 0.09 M and 0.045 M total phosphate and 0.29 M, 0.22 M, 0.14 M, 0.072 M and 0.036 M phosphate basic, respectively with ionic strength of 0.9 M *I*, pH and pH* 7.4 and 37 °C.

Total buffer con./M	k_Θ (H_2O)/ 10^{-6} s^{-1}	k_Θ (D_2O)/ 10^{-6} s^{-1}	k_H/k_D
0.045	65.3 ± 1.3 (± 0.5)[a]		
0.09	105.6 ± 2.1 (± 1.2)[a]	105.3 ± 2.1 (± 1.0)[a]	1.00 ± 0.03
0.18	201.4 ± 4.0 (± 2.2)[a]	205.0 ± 4.1 (± 2.3)[a]	0.98 ± 0.03
0.27	296.5 ± 5.9 (± 4.3)[a]	334.7 ± 6.7 (± 5.0)[a]	0.89 ± 0.03
0.36	453.4 ± 9.1 (± 7.6)[a]	458.7 ± 9.2 (± 7.4)[a]	0.99 ± 0.03

a) Where the error from the data fit is reported as less than 2% of the rate constant, an error of 2% was assumed. Values in brackets are the errors from the data fit which are less than 2%.

Table a4.3: Pseudo-first order rate constants k_θ determined by CD spectroscopy of (*S*)-1-acetyl-5-isopropyl-2-thioxoimidazolidin-4-onein (**4.3**) H_2O- and D_2O-phosphate buffer at 0.36 M, 0.27 M, 0.18 M, and 0.09 M total phosphate 0.29 M, 0.22 M, 0.14 M, 0.072 M and 0.036 M phosphate basic, respectively with ionic strength of 0.9 M *I*, pH and pH^* 7.4 and 37 °C.

Total buffer con./M	k_θ (H_2O)/ 10^{-6} s^{-1}	k_θ (D_2O)/ 10^{-6} s^{-1}	k_H/k_D
0.09	11.6 ± 0.2 (± 0.2)[a]		
0.18	14.3 ± 0.3 (± 0.1)[a]	11.1 ± 0.2 (± 0.1)[a]	1.29 ± 0.04
0.27	19.2 ± 0.4 (± 0.2)[a]	14.6 ± 0.3 (± 0.2)[a]	1.32 ± 0.04
0.36	26.2 ± 0.5 (± 0.3)[a]	19.0 ± 0.4 (± 0.2)[a]	1.38 ± 0.04

a) Where the error from the data fit is reported as less than 2% of the rate constant, an error of 2% was assumed. Values in brackets are the errors from the data fit which are less than 2%.

Table a4.4: Pseudo-first order rate constants k_θ determined by CD spectroscopy of (*S*)-5-((1H-indol-3-yl)methyl)-1-acetyl-2-thioxoimidazolidin-4-one (**4.4**) in H_2O- and D_2O-phosphate buffer at 0.36 M, 0.27 M, 0.18 M, 0.09 M and 0.045 M total phosphate 0.29, 0.22, 0.14, 0.072 and 0.036 M phosphate basic, respectively with ionic strength of 0.9 M *I*, pH and pH^* 7.4 and 37 °C.

Total buffer con./M	k_θ (H_2O)/ 10^{-6} s^{-1}	k_θ (D_2O) / 10^{-6} s^{-1}	k_H/k_D
0.045	32.0 ± 0.6 (± 0.5)[a]		
0.09	58.5 ± 1.2 (± 1.1)[a]	57.1 ± 1.2	1.02 ± 0.03
0.18	99.8 ± 2.0 (± 2.0)[a]	104.9 ± 2.2	0.95 ± 0.03
0.27	148.3 ± 3.5	153.9 ± 4.1	0.96 ± 0.04
0.36	196.4 ± 5.8	225.9 ± 6.2	0.87 ± 0.04

a) Where the error from the data fit is reported as less than 2% of the rate constant, an error of 2% was assumed. Values in brackets are the errors from the data fit which are less than 2%.

Table a4.5: Pseudo-first-order rate constants k_Θ determined by CD spectroscopy of (*S*)-1-acetyl-5-(2-(methylthio)ethyl)-2-thioxoimidazolidin-4-one (**4.5**) in H_2O- and D_2O-phosphate buffer at 0.36 M, 0.27 M, 0.18 M, 0.09 M and 0.045 M total phosphate 0.29 M, 0.22 M, 0.14 M, 0.072 M and 0.036 M phosphate basic, respectively with ionic strength of 0.9 M I, pH and pH* 7.4 and 37 °C.

Total buffer con./M	k_Θ (H_2O)/ 10^{-6} s^{-1}	k_Θ (D_2O)/ 10^{-6} s^{-1}	k_H/k_D
0.045	134.3 ± 2.7(± 2.3)[a]		
0.09	213.8 ± 4.3 (± 3.8)[a]	214.0 ± 4.3	1.00 ± 0.02
0.18	395.3 ± 10.2	430.3 ± 9.6	0.92 ± 0.02
0.27	558.7 ± 15.8	642.9 ± 16.0	0.87 ± 0.02
0.36	840.0 ± 23.9	869.9 ± 28.3	0.97 ± 0.03

a) Where the error from the data fit is reported as less than 2% of the rate constant, an error of 2% was assumed. Values in brackets are the errors from the data fit which are less than 2%.

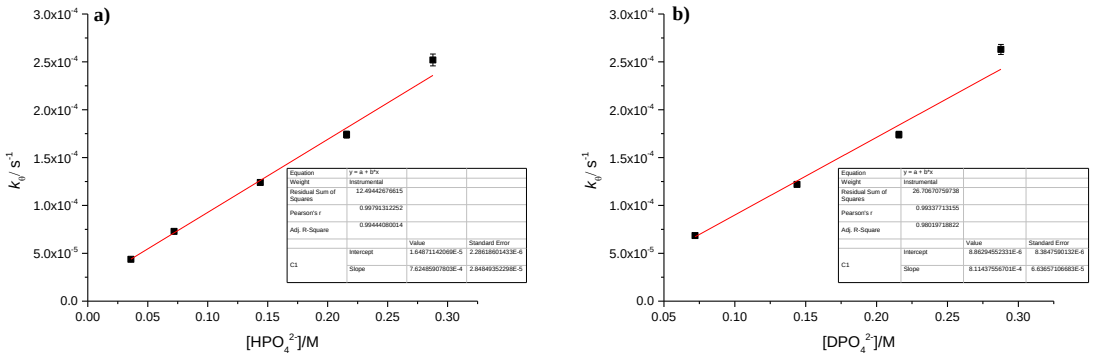

Figure a4.21: Observed rate constants k_Θ of (*S*)-1-acetyl-5-methyl-2-thioxoimidazolidin-4-one (**4.1**) as a function of the concentration of the basic components of a) (H_2O- based phosphate buffer at 37 °C, 0.9 M *I*, pH 7.4, 0.36 M, 0.27 M, 0.18 M, 0.09, and 0.045 M, and b) D_2O-based phosphate buffer at 37 °C, 0.9 M *I*, pH* 7.4, 0.36 M, 0.27 M, 0.18 M, and 0.09 M.

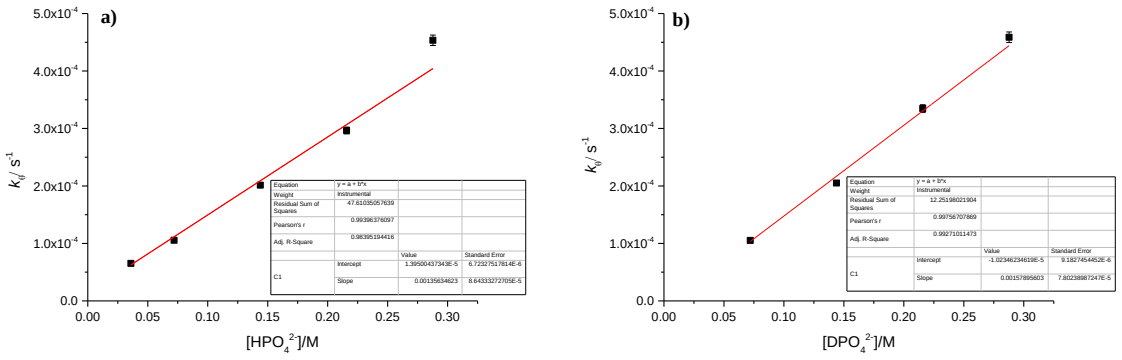

Figure a4.22: Observed rate constants $k_{ψ}$ of (*S*)-1-acetyl-5-benzyl-2-thioxoimidazolidin-4-one (**4.2**) as a function of the concentration of the basic components of a) (H_2O- based phosphate buffer at 37 °C, 0.9 M *I*, pH 7.4, 0.36 M, 0.27 M, 0.18 M, 0.09, and 0.045 M, and b) D_2O-based phosphate buffer at 37 °C, 0.9 M *I*, pH* 7.4, 0.36 M, 0.27 M, 0.18 M, and 0.09 M.

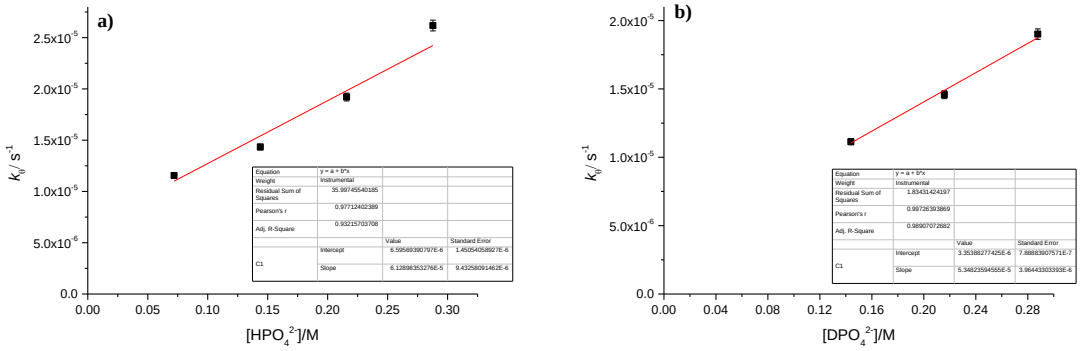

Figure a4.23: Observed rate constants $k_{ψ}$ of (S)-1-acetyl-5-isopropyl-2-thioxoimidazolidin-4-onein (**4.3**) as a function of the concentration of the basic components of a) (H_2O- based phosphate buffer at 37 °C, 0.9 M *I*, pH 7.4, 0.36 M, 0.27 M, 0.18 M, and 0.09, and b) D_2O-based phosphate buffer at 37 °C, 0.9 M *I*, pH* 7.4, 0.36 M, 0.27 M, and 0.18 M.

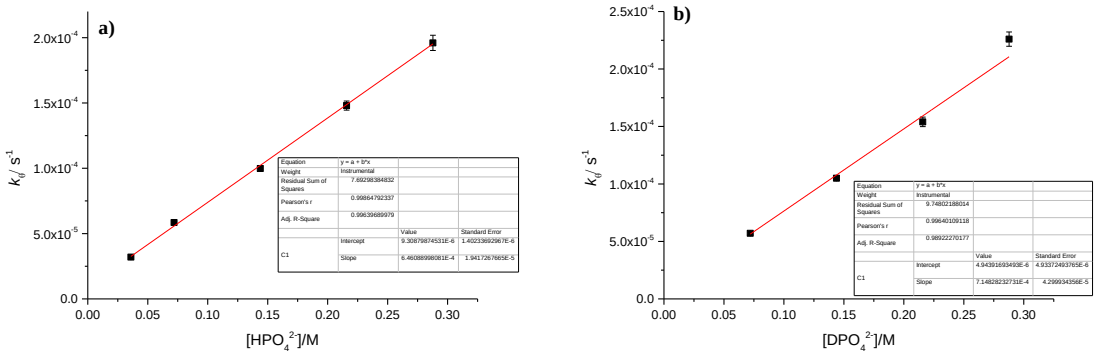

Figure a4.24: Observed rate constants k_Θ of (S)-5-((1H-indol-3-yl)methyl)-1-acetyl-2-thioxoimidazolidin-4-one (**4.4**) as a function of the concentration of the basic components of a) (H_2O- based phosphate buffer at 37 °C, 0.9 M *I*, pH 7.4, 0.36 M, 0.27 M, 0.18 M, 0.09, and 0.045 M, and b) D_2O-based phosphate buffer at 37 °C, 0.9 M *I*, pH^* 7.4, 0.36 M, 0.27 M, 0.18 M, and 0.09 M.

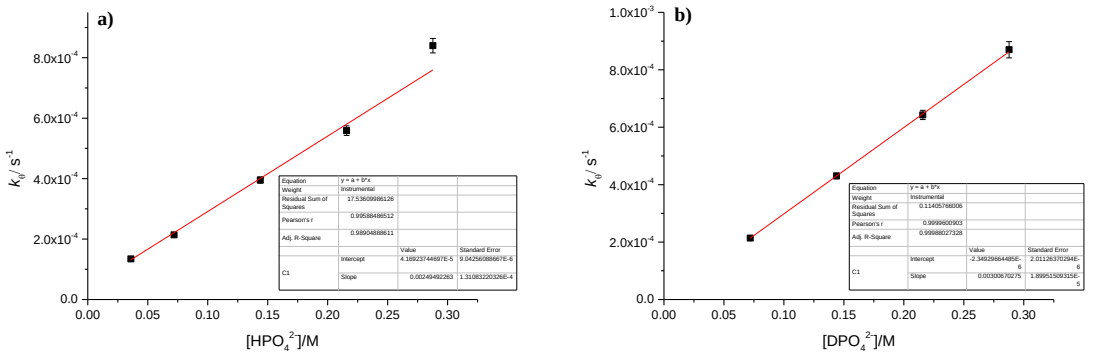

Figure a4.25: Observed rate constants k_Θ of (S)-1-acetyl-5-(2-(methylthio)ethyl)-2-thioxoimidazolidin-4-one (**4.5**) as a function of the concentration of the basic components of a) (H_2O- based phosphate buffer at 37 °C, 0.9 M *I*, pH 7.4, 0.36 M, 0.27 M, 0.18 M, 0.09, and 0.045 M, and b) D_2O-based phosphate buffer at 37 °C, 0.9 M *I*, pH^* 7.4, 0.36 M, 0.27 M, 0.18 M, and 0.09 M.

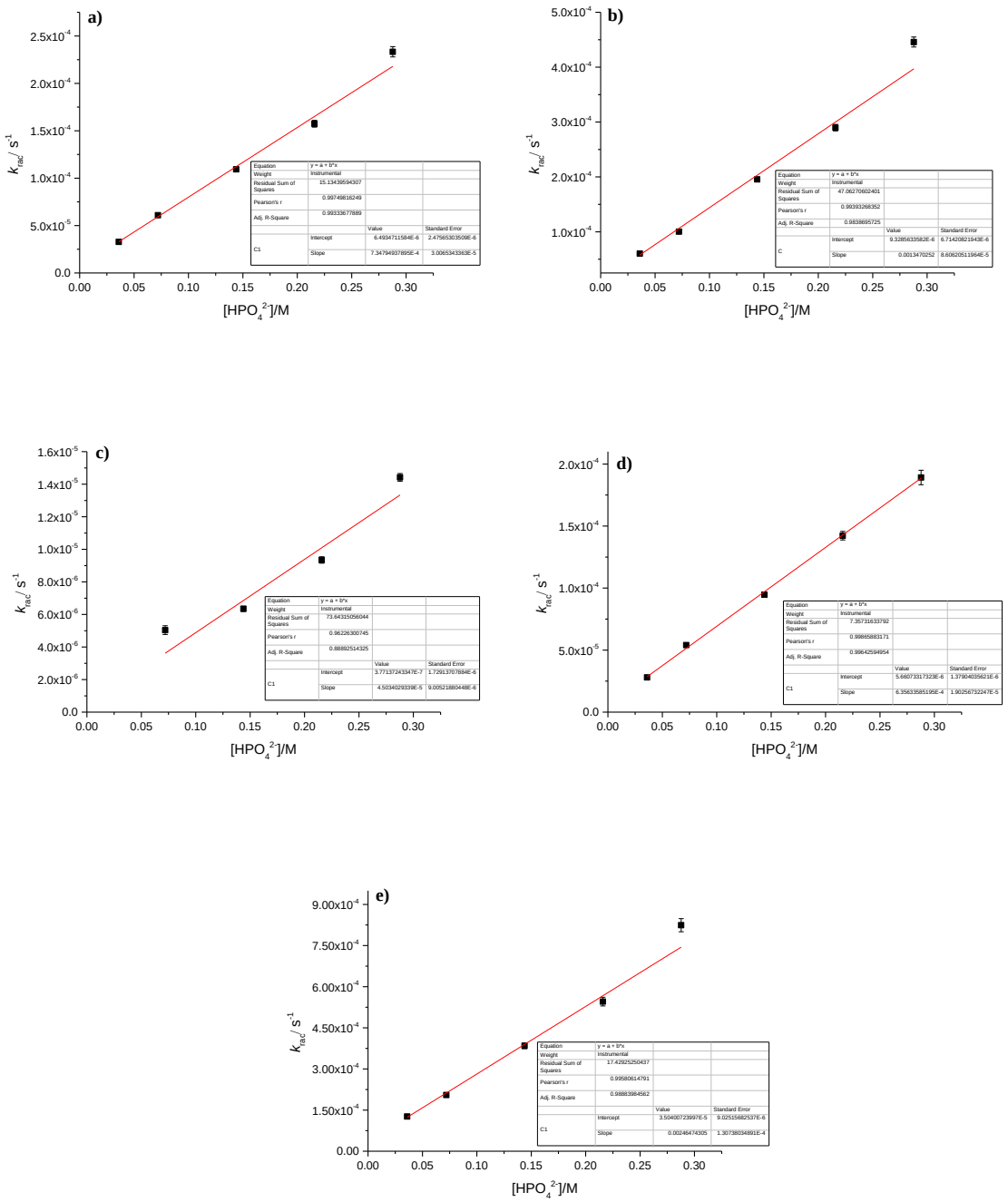

Figure a4.26: Observed rate constants of racemisation k_{rac} determined by Equation 4.5 for compounds a) **4.1**, b) **4.2**, c) **4.3**, d) **4.4** and e) **4.5** as a function of the concentration of the basic components of (H_2O-based total phosphate buffer at 37 °C, 0.9 M *I*, pH 7.4, 0.36 M, 0.27 M, 0.18 M, 0.09, and 0.045 M.

Table a4.6: Second-order rate constants for buffer-catalysed $k_{\theta,}$ determined from Figures a4.21-a4.25 and k_{rac} obtained in Figure a4.26 and the combined uncatalysed, deuteroxide-catalysed and hydronium-catalysed k_{in} observed in Figures a4.21-a4.26 for **4.1**-**4.5** in H_2O phosphate buffers, 0.9 M *I*, pH and pH 7.4 at 37 °C.

Comp.	k_{θ} / 10^{-6} s^{-1} M^{-1}	k_{in} / 10^{-6} s^{-1}	k_{rac,H_2O} / $10^{-6}M^{-1}$ s^{-1}	k_{in} / 10^{-6} s^{-1}
4.1	763 ± 29	16.5 ± 2.3	735 ± 30	6.5 ± 2.5
4.2	1356 ± 86	14 ± 6.7	1347 ± 86	9.3 ± 6.7
4.3	61.3 ± 9.4	6.6 ± 1.5	45.0 ± 9.0	0.4 ± 1.7
4.4	646 ± 19.4	9.3 ± 1.4	636 ± 19	5.7 ± 1.4
4.5	2495 ± 131	41.7 ± 9.0	2465 ± 131	35.0 ± 9.0

A4.2. Brønsted plot for proton transfer

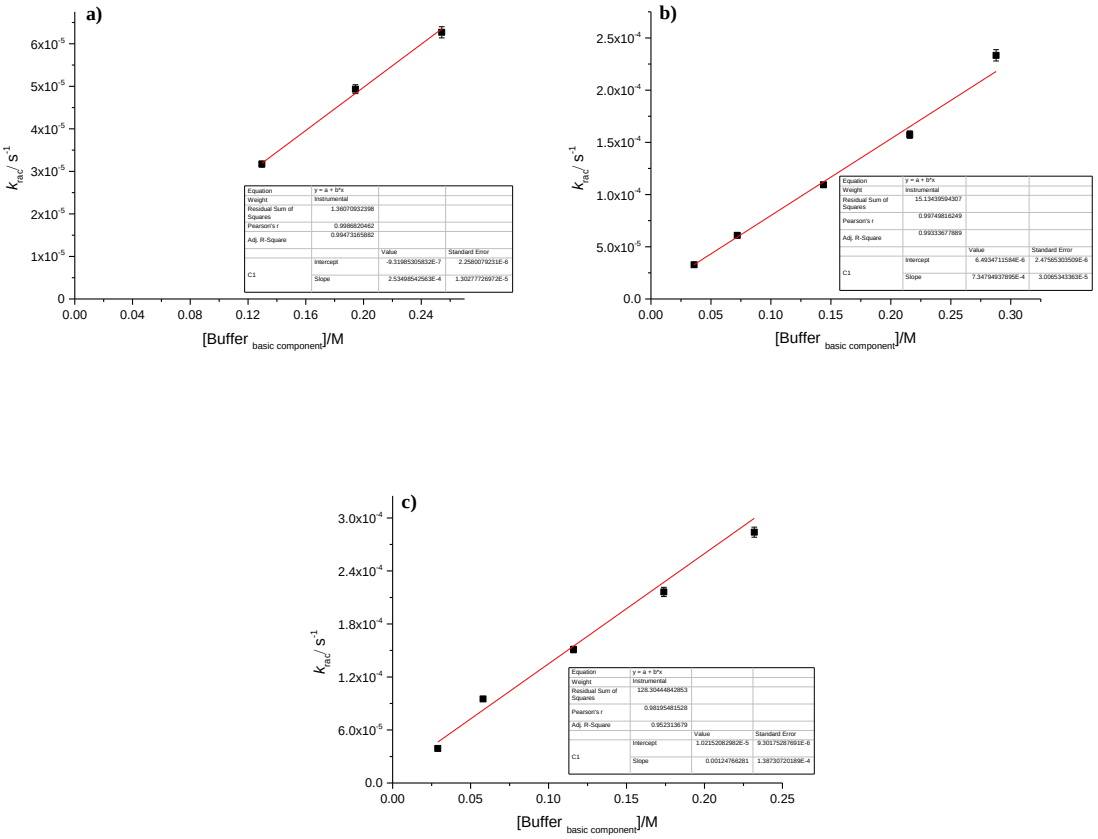

Figure a4.27: Observed rate constants of racemisation determined by Equation 4.5 for **4.1** a) acetate, b) phosphate, and c) TRIS buffer as a function of the concentration of the basic components of (H_2O-based buffer at 37 °C, 0.9 M *I*, pH 5.0, 7.4, and 8.2, respectively.

Table a4.7: The pK_a , k_{o}, and k_{rac} of **4.1** in acetate, phosphate, and TRIS buffers at 0.9 M *I*, pH 5.0, 7.4, 8.2 and 9.7, respectively.

Buffers	pK_a	k_{o} (H_2O) / 10^{-6} s^{-1} M^{-1}	k_{rac} (H_2O) / 10^{-6} s^{-1} M^{-1}
Acetate	4.59[a]	246.0 ± 18.0	253.5 ± 13.0
phosphate	6.8[b]	763 ± 28	735 ± 30
TRIS	7.88[a]	1381 ± 127	1248 ± 139

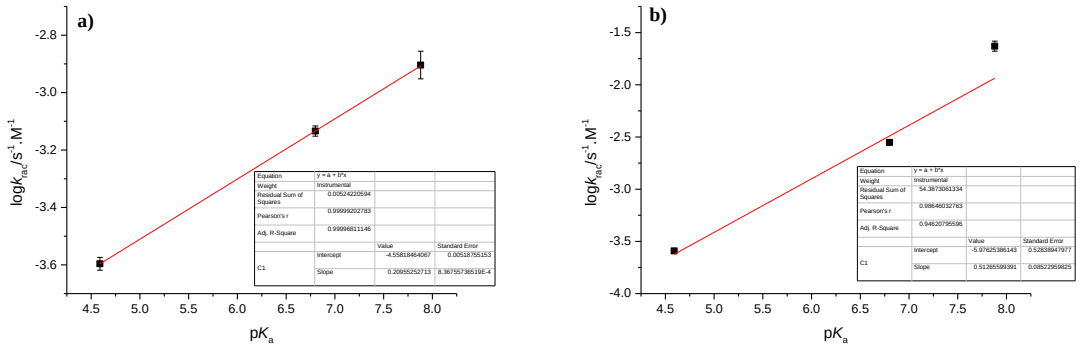

Figure a4.28: Bronsted plot for the base-catalysed racemisation of a) deprotonated **4.1** data and b) protonated **4.1** data from Table h 4.7.

A4.3. Racemisation of tri-substituted 2-thiohydantoin

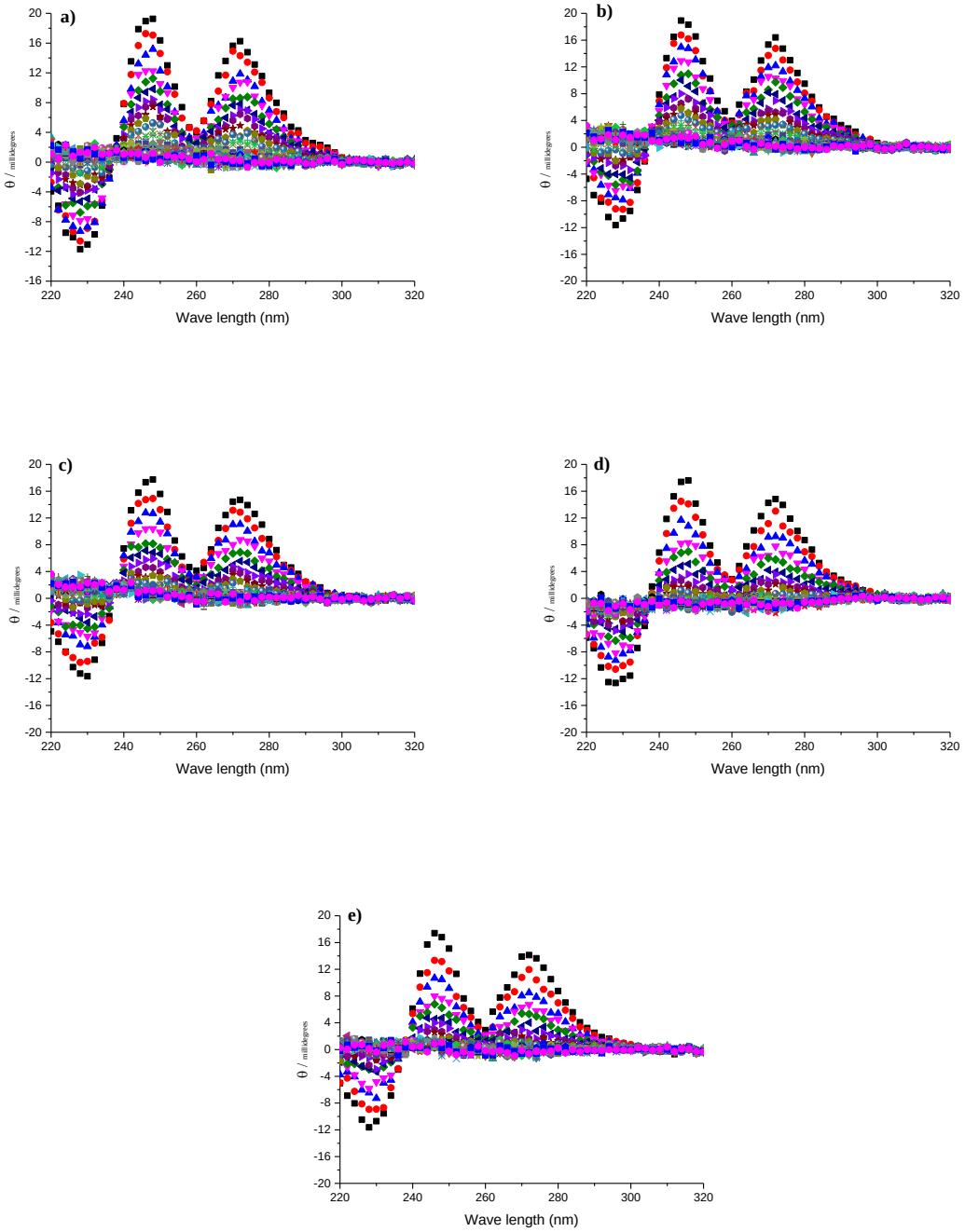

Figure a4.29: Change in ellipticity over time for solutions of **4.7** in H_2O-phosphate buffer at a) 0.009 M, b) 0.018 M, c) 0.027 M, d) 0.036 M and e) 0.045 M total phosphate with ionic strength of 0.9 M *I*, pH 7.4 at 37 °C.

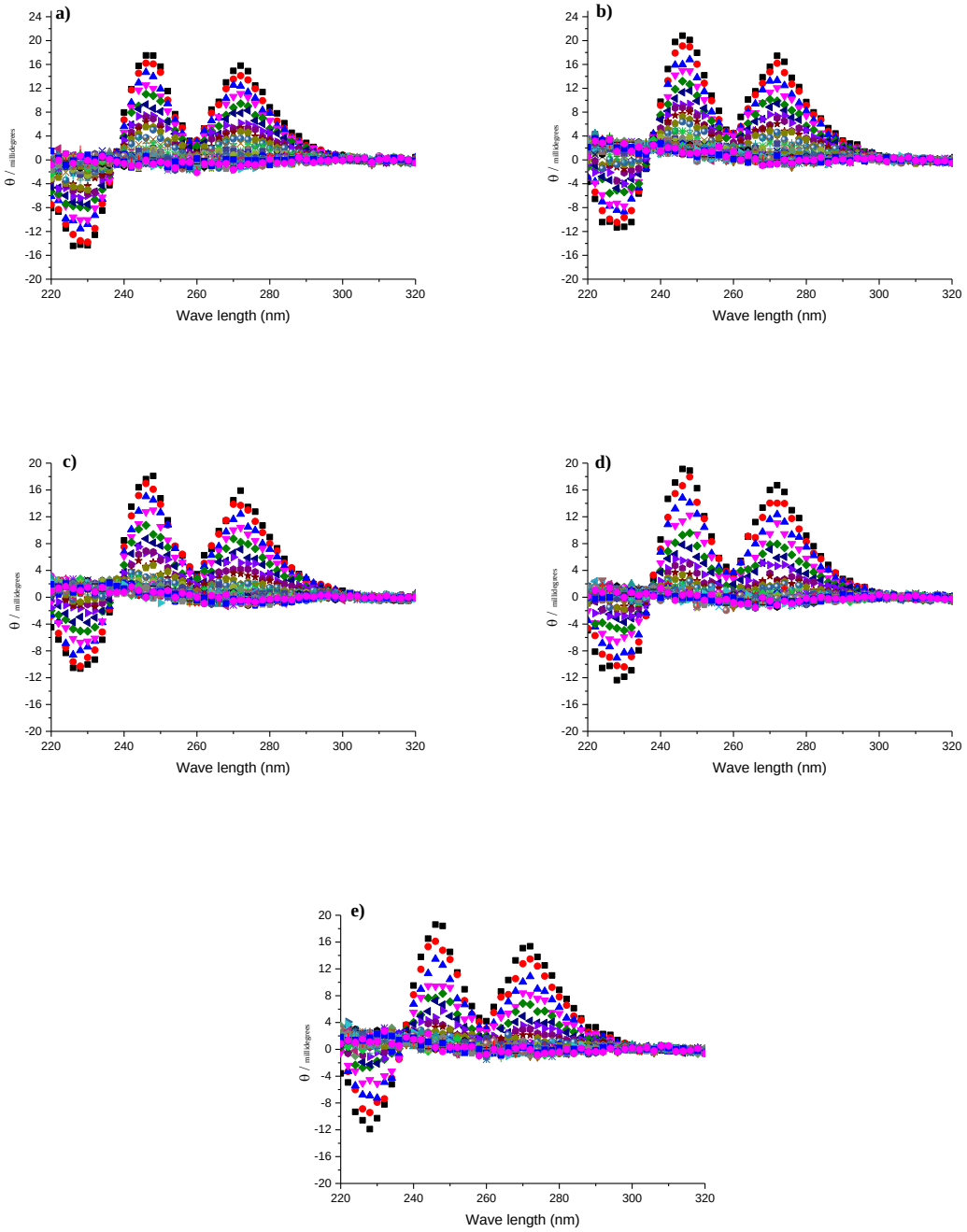

Figure a4.30: Change in ellipticity over time for solutions of **4.7** in D_2O-phosphate buffer at a) 0.009 M, b) 0.018 M, c) 0.027 M, d) 0.036 M and e) 0.045 M total phosphate with ionic strength of 0.9 M *I*, pH* 7.4 at 37 °C.

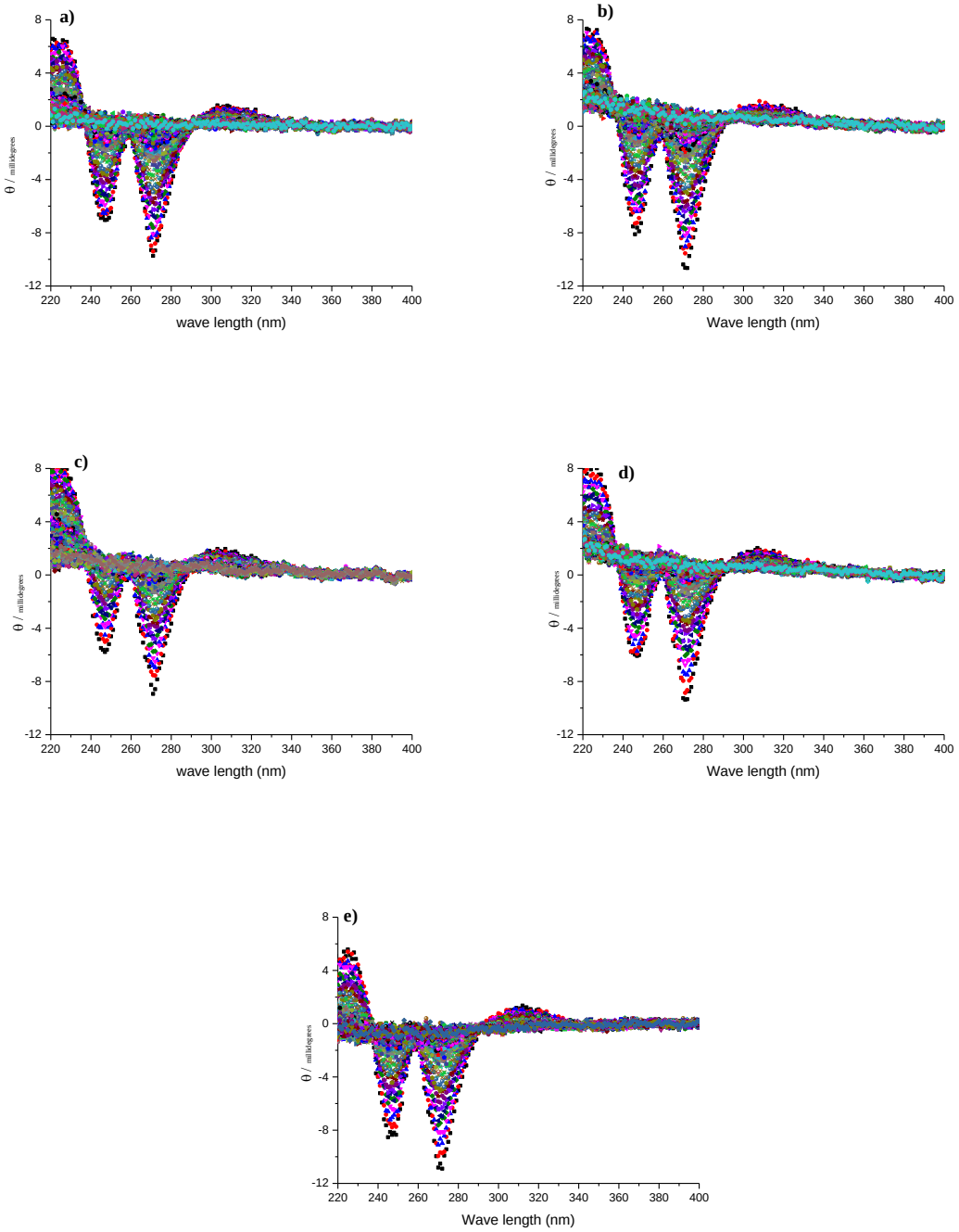

Figure a4.31: Change in ellipticity over time for solutions of **4.8** in H_2O-phosphate buffer at a) 0.009 M, b) 0.018 M, c) 0.027 M, d) 0.036 M and e) 0.045 M total phosphate with ionic strength of 0.9 M *I*, pH 7.4 at 37 °C.

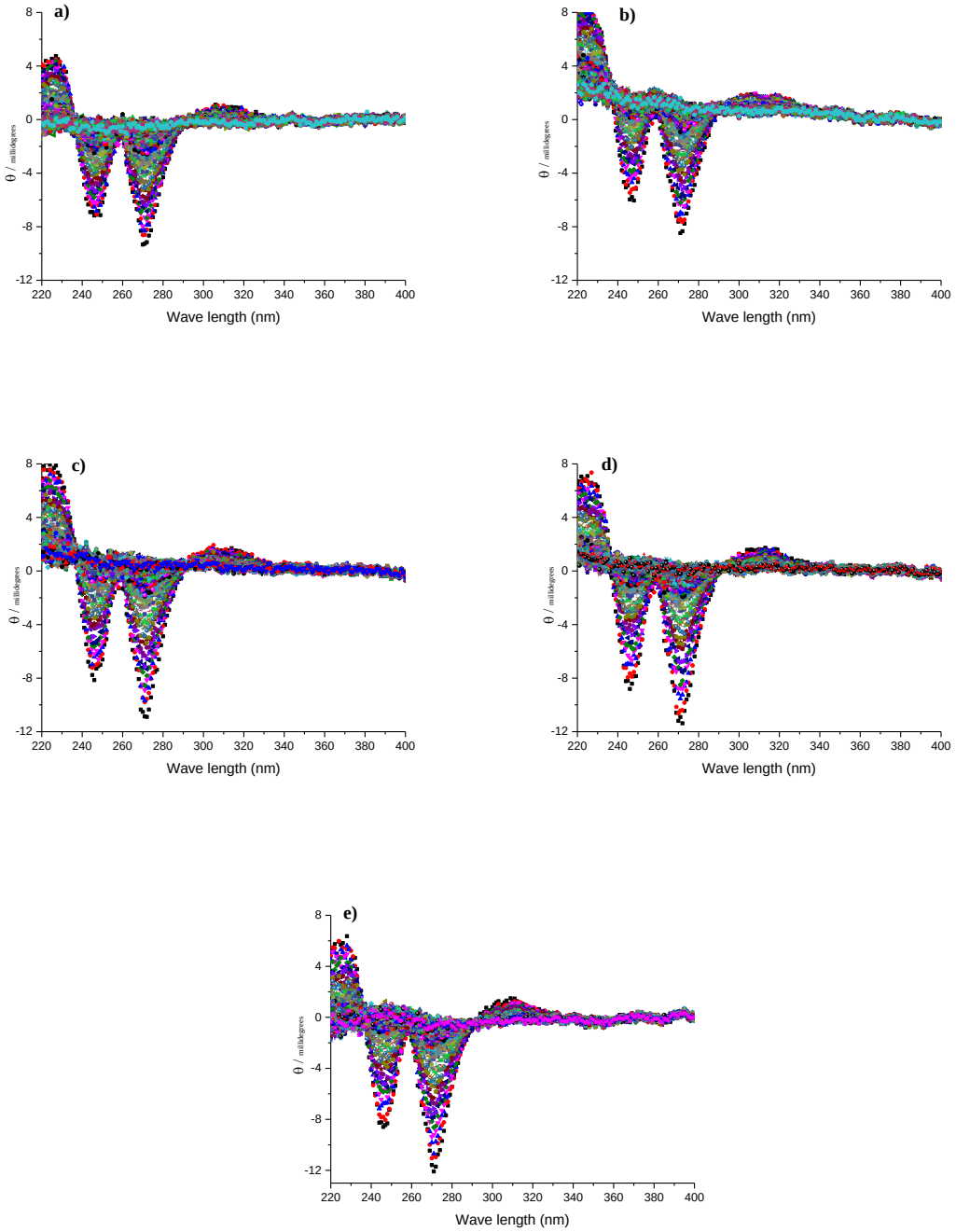

Figure a4.32: Change in ellipticity over time for solutions of **4.8** in D_2O-phosphate buffer at a) 0.009 M, b) 0.018 M, c) 0.027 M, d) 0.036 M and e) 0.045 M total phosphate with ionic strength of 0.9 M *I*, pH^* 7.4 at 37 °C.

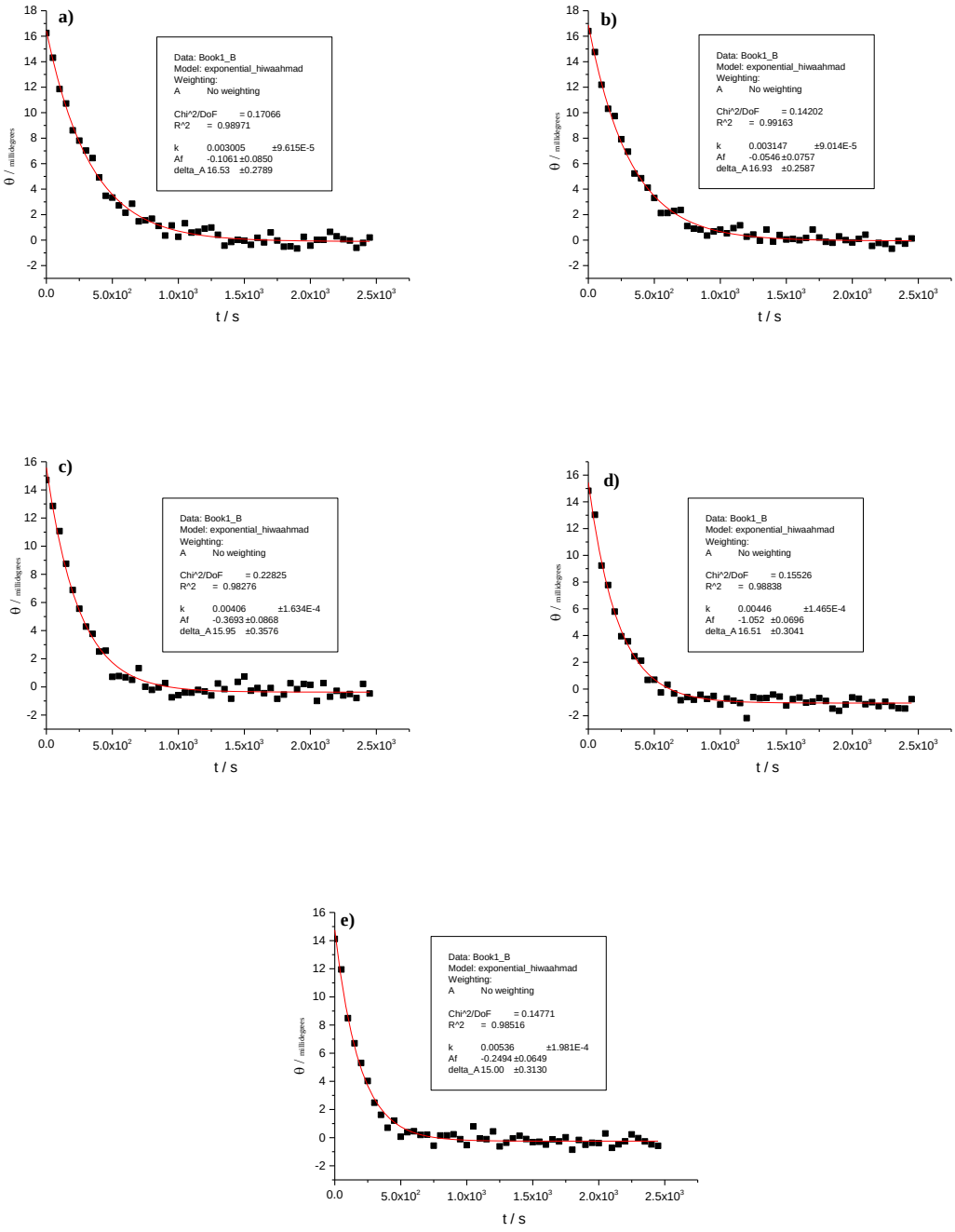

Figure a4.33: The ellipticities of **4.7** at 272 nm versus time in H_2O-phosphate buffer at a) 0.009 M, b) 0.018 M, c) 0.027 M, d) 0.036 M and e) 0.045 M total phosphate with ionic strength of 0.9 M *I*, pH 7.4 at 37 °C.

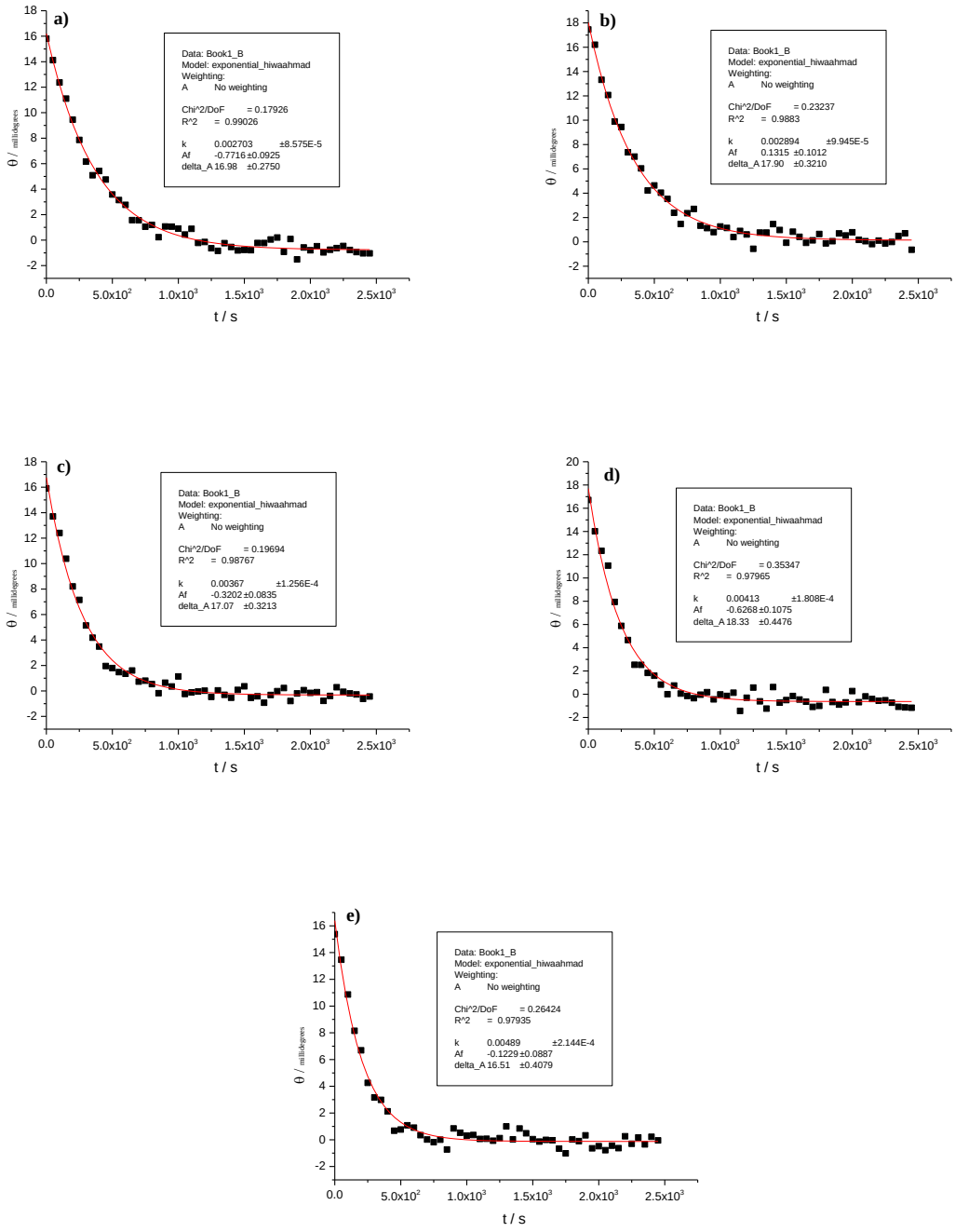

Figure a4.34: The ellipticities of **4.7** at 272 nm versus time in D_2O-phosphate buffer at a) 0.009 M, b) 0.018 M, c) 0.027 M, d) 0.036 M and e) 0.045 M total phosphate with ionic strength of 0.9 M *I*, pH* 7.4 at 37 °C.

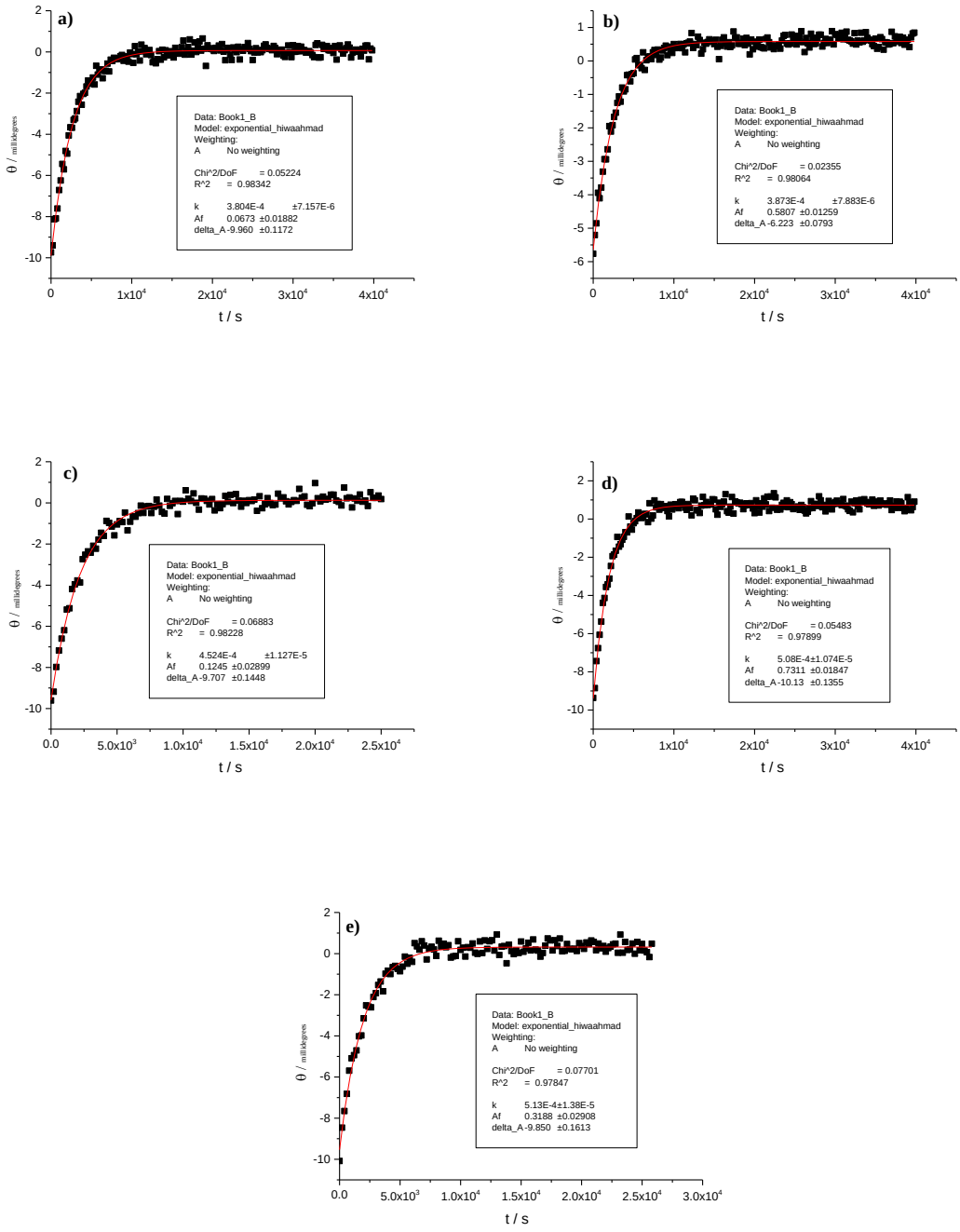

Figure a4.35: The ellipticities of **4.8** at 271 nm in H_2O-phosphate buffer at a) 0.009 M, b) 0.018 M, c) 0.027 M, d) 0.036 M and e) 0.045 M total phosphate with ionic strength of 0.9 M *I*, pH 7.4 at 37 °C.

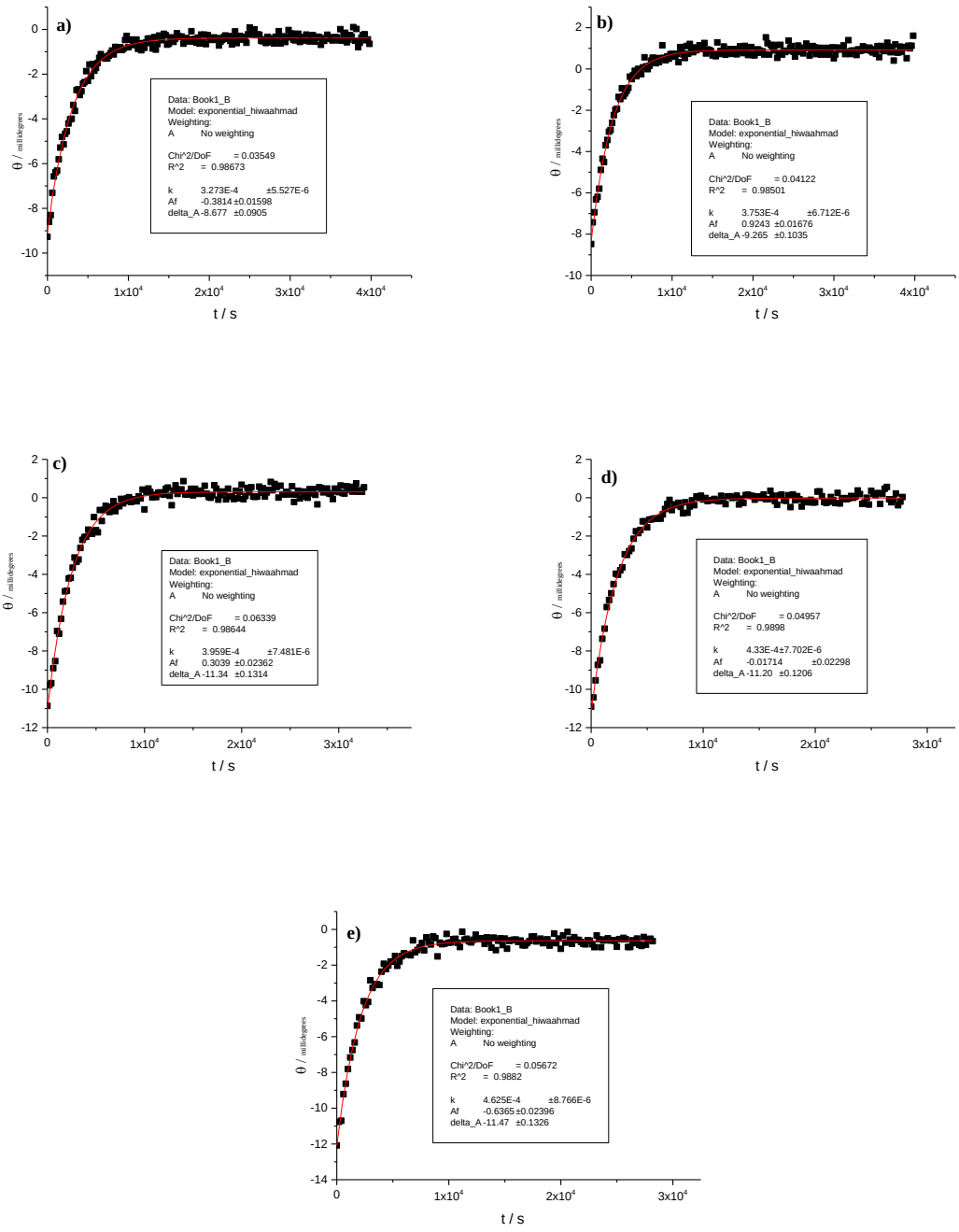

Figure a4.36: The ellipticities of **4.8** at 271 nm in D_2O-phosphate buffer at a) 0.009 M, b) 0.018 M, c) 0.027 M, d) 0.036 M and e) 0.045 M total phosphate with ionic strength of 0.9 M *I*, pH* 7.4 at 37 °C.

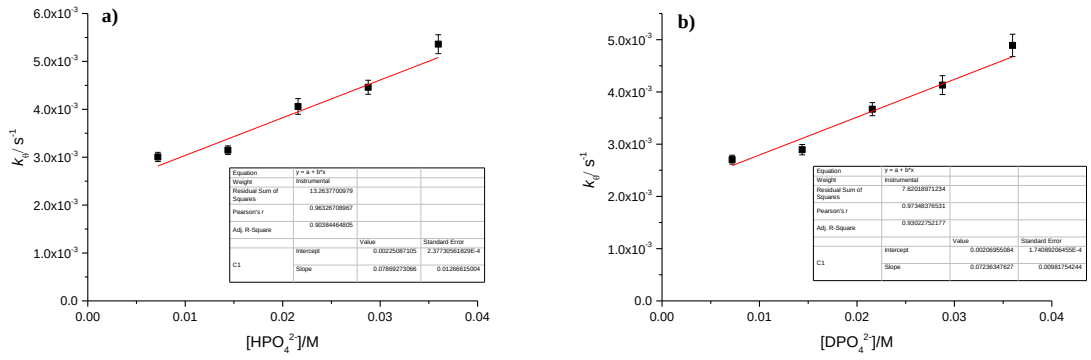

Figure a4.37: Observed rate constants of racemisation of (R)-5-benzyl-3-phenyl-1-(pyridin-2-ylmethyl)-2-thioxoimidazolidin-4-one (**4.7**) at 272 nm as a function of the concentration of the basic components of a) (H_2O- based phosphate buffer at 37 °C, 0.9 M *I*, pH 7.4, 0.045 M, 0.036 M, 0.027 M, 0.018 M, and 0.09 and b) D_2O-based phosphate buffer at 37 °C, 0.9 M *I*, pH^* 7.4, 0.045 M, 0.036 M, 0.027 M, 0.018 M, and 0.09 M.

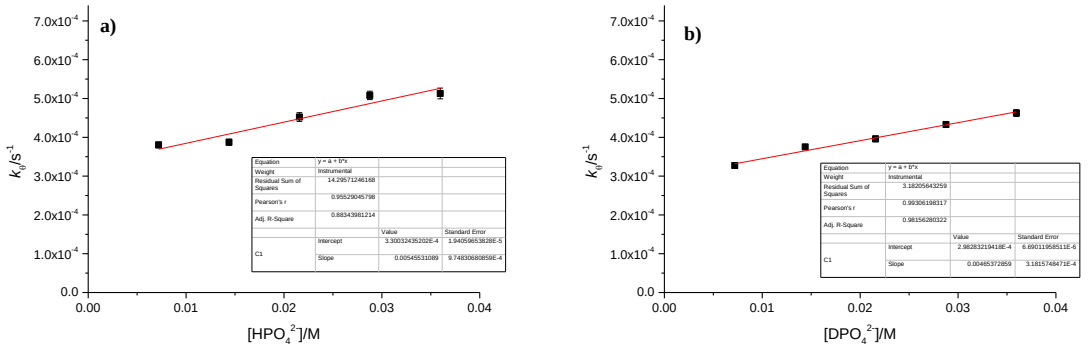

Figure a4.38: Observed rate constants of racemisation of (S)-5-isopropyl-3-phenyl-1-(pyridin-2-ylmethyl)-2-thioxoimidazolidin-4-one (**4.8**) at 271 nm as a function of the concentration of the basic components of a) (H_2O- based phosphate buffer at 37 °C, 0.9 M *I*, pH 7.4, 0.045 M, 0.036 M, 0.027 M, 0.018 M, and 0.09 M and b) D_2O-based phosphate buffer at 37 °C, 0.9 M *I*, pH^* 7.4, 0.045 M, 0.036 M, 0.027 M, 0.018 M, and 0.09 M .

Table a4.8: Pseudo-first-order rate constants k_Θ determined by CD spectroscopy of (*R*)-5-benzyl-3-phenyl-1-(pyridin-2-ylmethyl)-2-thioxoimidazolidin-4-one (**4.7**) at 272 nm in H_2O and D_2O phosphate buffer at 0.045, 0.036 M, 0.027 M, 0.018 M, and 0.09 M total phosphate and 0.036, 0.029, 0.022, 0.014 and 0.0072 M phosphate basic, respectively with ionic strength of 0.9 M *I*, pH and pH* 7.4 at 37 °C.

Comp. (**4.7**)	k_Θ (H_2O)/ 10^{-6} s^{-1}	k_Θ *(D_2O)* / 10^{-6} s^{-1}	k_H/k_D
0.009	3005 ± 96	2703 ± 86	1.11 ± 0.05
0.018	3147 ± 90	2894 ± 99	1.09 ± 0.05
0.027	4060 ± 163	3670 ± 126	1.11± 0.06
0.036	4460 ± 147	4130 ± 181	1.08 ± 0.06
0.045	5360 ± 198	4890 ± 214	1.10 ± 0.06

Table a4.9: Pseudo-first-order rate constants k_Θ determined by CD spectroscopy of (*S*)-5-isopropyl-3-phenyl-1-(pyridin-2-ylmethyl)-2-thioxoimidazolidin-4-one (**4.8**) at 271 nm in H_2O and D_2O-phosphate buffer at 0.045, 0.036 M, 0.027 M, 0.018 M, and 0.09 M total phosphate and 0.036, 0.029, 0.022, 0.014 and 0.0072 M phosphate basic, respectively with ionic strength of 0.9 M *I*, pH and pH* 7.4 at 37 °C.

Comp. (**4.8**)	k_Θ (H_2O)/ 10^{-6} s^{-1}	k_Θ *(D_2O)* / 10^{-6} s^{-1}	k_H/k_D
0.009	380.4 ± 7.2	327.3 ± 5.5	1.16 ± 0.03
0.018	387.3 ± 7.9	375.3 ± 6.7	1.03 ± 0.03
0.027	452.4 ± 11.3	395.9 ± 7.5	1.14 ± 0.04
0.036	508.0 ± 10.7	433.0 ± 7.7	1.17 ± 0.03
0.045	513.0 ± 13.8	462.5 ± 8.8	1.11 ± 0.04

A4.4. Racemisation of 5-substituted 2-thiohydantoins

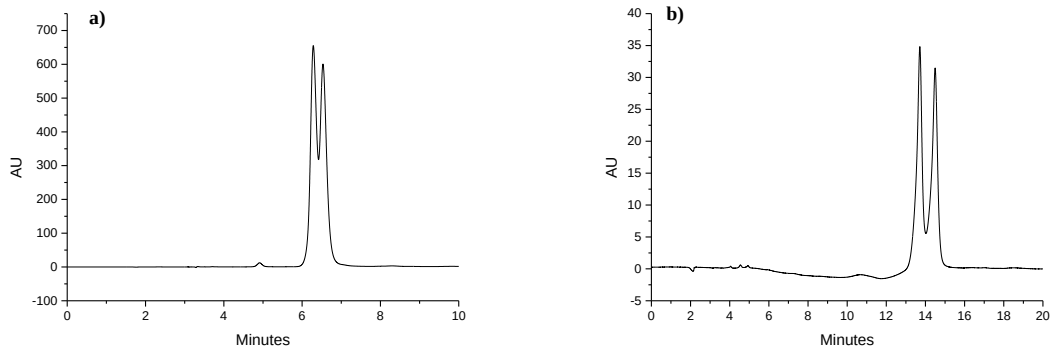

Figure a4.39: Chromatogram of compounds a) **4.15** and b) **4.16** by using 70 of Water and 30% of methanol with the flow rate of 1.0 ml/ min at room temperature. The chiral column of Astec CHIROBIOTIC T, 25 cm x 4.6 mm, 5 μm particles.

Appendix 4

for Chapter 5

Kinetics of H/D exchange and racemisation for substituted 2-thiohydantoins and related compounds

A5.1 The hydrogen/deuterium exchange of 5-substituted 1-acetyl-2-thiohydantoins

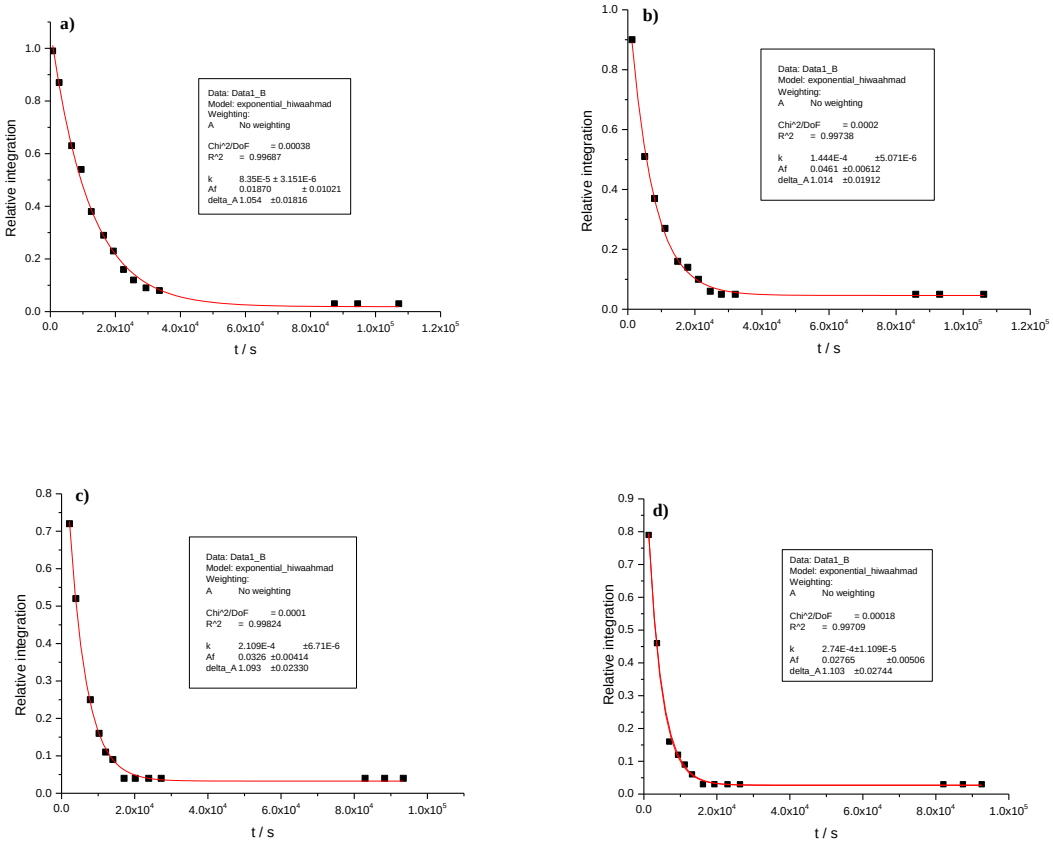

Figure a5.1: Relative integration of **5.1** in D_2O-phosphate buffer at a) 0.09 M, b) 0.18 M, c) 0.27 M and d) 0.36 M total phosphate with ionic strength of 0.9 M *I*, pH* 7.4 at 37 °C obtained by ^{1}H-NMR spectroscopy plotted versus time. The squares (■) are the experimental points, and the red solid lines are the fits to pseudo first-order kinetics.

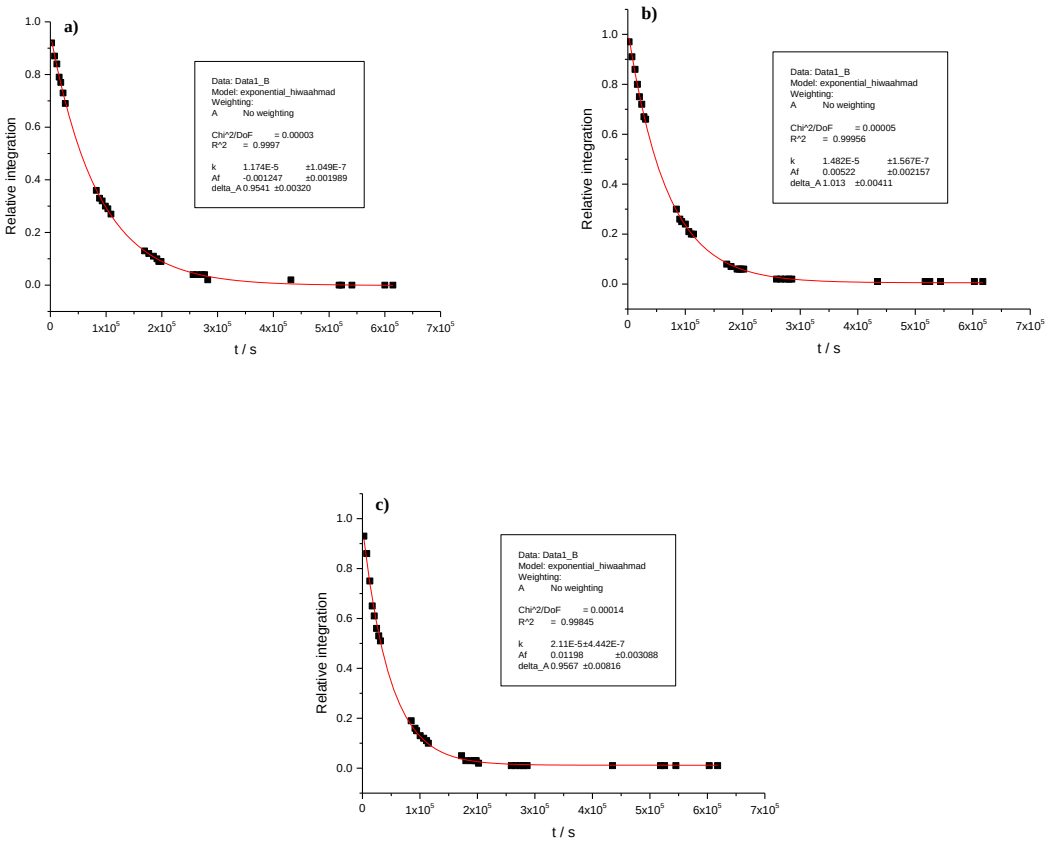

Figure a5.2: Relative integration of **5.3** in D_2O-phosphate buffer at a) 0.18 M, b) 0.27 M and c) 0.36 M total phosphate with ionic strength of 0.9 M *I*, pH* 7.4 at 37 °C obtained by ^{1}H-NMR spectroscopy plotted versus time. The squares (■) are the experimental points, and the red solid lines are the fits to pseudo-first-order kinetics.

Table a5.1:Pseudo-first-order rate constants $k_{H/D}$ determined by ^{1}H-NMR spectroscopy of (*S*)-1-acetyl-5-methyl-2-thioxoimidazolidin-4-one (**5.1**) in D_2O phosphate buffer at 0.36, 0.27, 0.18, and 0.09 total phosphate and 0.29, 0.22, 0.14, and 0.072 M basic phosphate buffer, respectively with ionic strength of 0.9 M *I*, pH* 7.4 and 37 °C.

Total phosphate	Basic phosphate	$k_{H/D}$ (D_2O)/ 10^{-6} s^{-1}
0.09	0.072	83.5 ± 3.2
0.18	0.14	144.4 ± 5.1
0.27	0.22	210.9 ± 6.7
0.36	0.29	274.0 ± 11.1

Table a5.2: Pseudo-first-order rate constants $k_{H/D}$ determined by ^{1}H-NMR spectroscopy of (*S*)-1-acetyl-5-isopropyl-2-thioxoimidazolidin-4-one (**5.3**) in D_2O-phosphate buffer at 0.36, 0.27, and 0.18, total phosphate and 0.29, 0.22, and 0.14 basic phosphate buffer, respectively with ionic strength of 0.9 M *I*, pH* 7.4 and 37 °C.

Total phosphate	Basic phosphate	$k_{H/D}$ (D_2O)/ 10^{-6} s^{-1}
0.18	0.14	11.7 ± 0.2 (± 0.1)[a]
0.27	0.22	14.8 ± 0.3 (± 0.2)[a]
0.36	0.29	21.1 ± 0.4

c) Where the error from the data fit is reported as less than 2% of the rate constant, an error of 2% was assumed. Values in brackets are the errors from the data fit which are less than 2%.

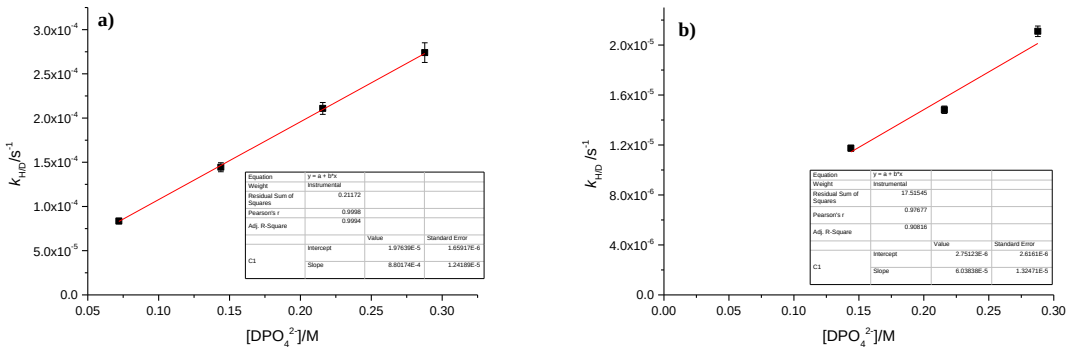

Figure a5.3: Second-order rate constants for buffer-catalysed of H/D exchange by ^{1}H-NMR spectroscopy of a) **5.1**, and b) **5.3** in D_2O-phosphate buffers, 0.9 M *I*, pH* 7.4 at 37 °C.

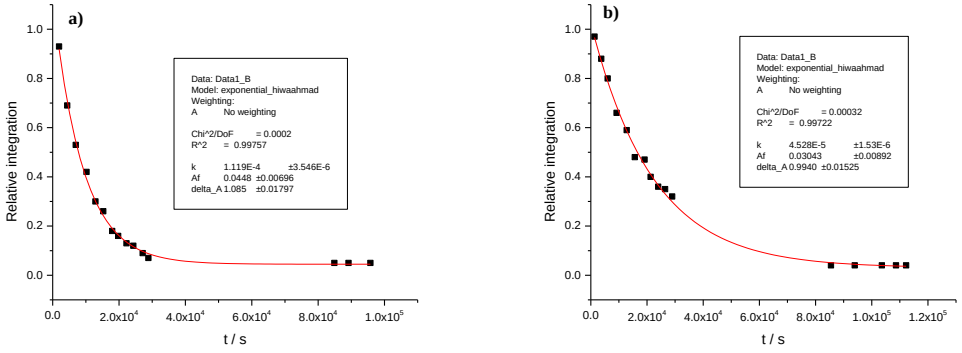

Figure a5.4: Relative integration of a) **5.2** and b**) 5.4** in D_2O-phosphate buffer at 0.09 M total phosphate with ionic strength of 0.9 M *I*, pH* 7.4 at 37 °C obtained by ^{1}H-NMR spectroscopy plotted versus time by using 10% of d_3-ACN. The squares (■) are the experimental points, and the red solid lines are the fits to pseudo-first-order kinetics.

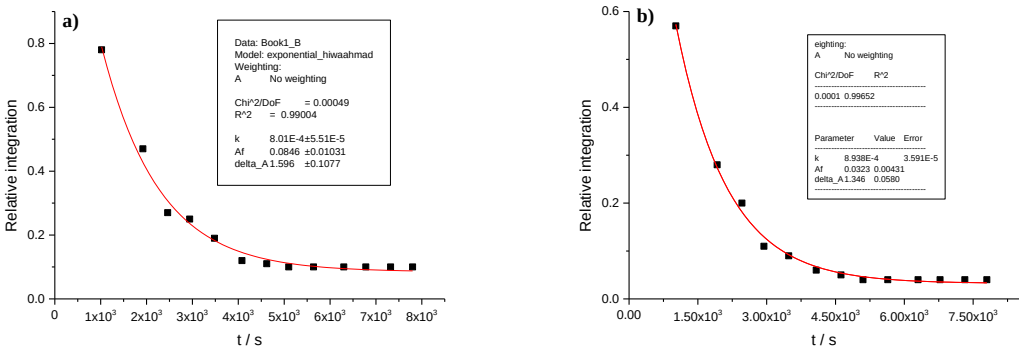

Figure a5.5: Relative integration of **5.5** with a**)** correcting phase b) without correcting the phase of base line of ^{1}H-NMR spectra by Mestrenova in D_2O-phosphate buffer at 0.09 M total phosphate with ionic strength of 0.9 M *I*, pH* 7.4 at 37 °C obtained by ^{1}H-NMR spectroscopy plotted versus time by using 10% of d_3-ACN. The squares (■) are the experimental points, and the red solid lines are the fits to pseudo-first-order kinetics. The weight average equation (See Chapter 5) for rate constant of a) and b) was used to obtained the observed rate constant of H/D exchange and reported in Table 5.3.

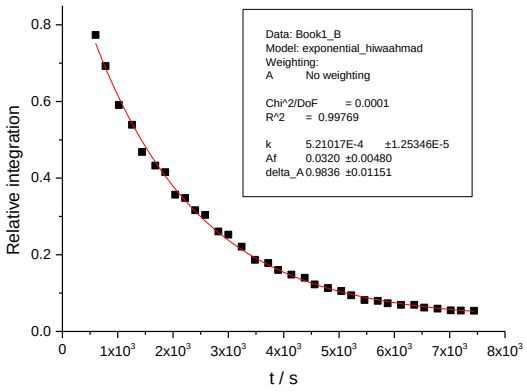

Figure a5.6: Relative integration of **5.6** in D_2O-phosphate buffer at 0.09 M total phosphate with ionic strength of 0.9 M *I*, pH* 7.4 at 37 °C obtained by ^{1}H-NMR spectroscopy plotted versus time by using 10% of d_3-ACN. The squares (■) are the experimental points, and the red solid lines are the fits to pseudo-first-order kinetics.

A5.2. The H/D exchange process of 5-substituted 2-thiohydantoins

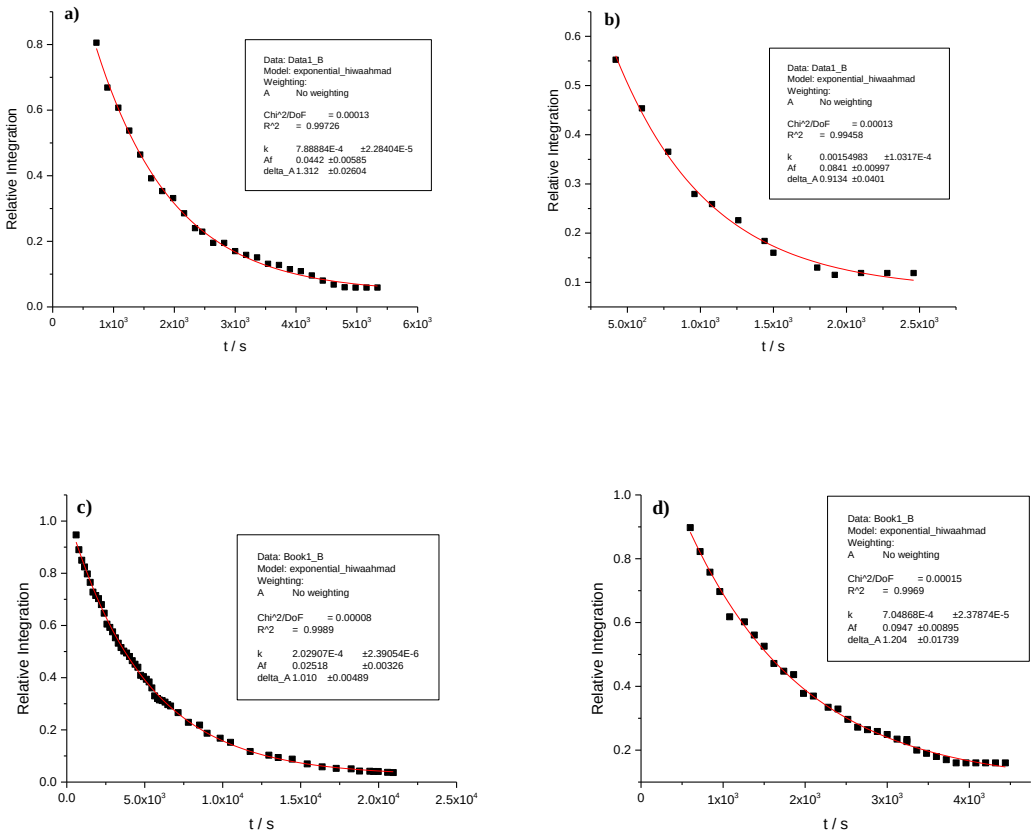

Figure a5.7: Relative integration of a) **5.7**, b) **5.8**, c) **5.9**, and d) **5.10** in D_2O-phosphate buffer at 0.009 M total phosphate with ionic strength of 0.9 M *I*, pH^* 7.4 at 37 °C obtained by ^{1}H-NMR spectroscopy plotted versus time by using 10% of d_3-ACN. The squares (■) are the experimental points, and the red solid lines are the fits to pseudo-first-order kinetics.

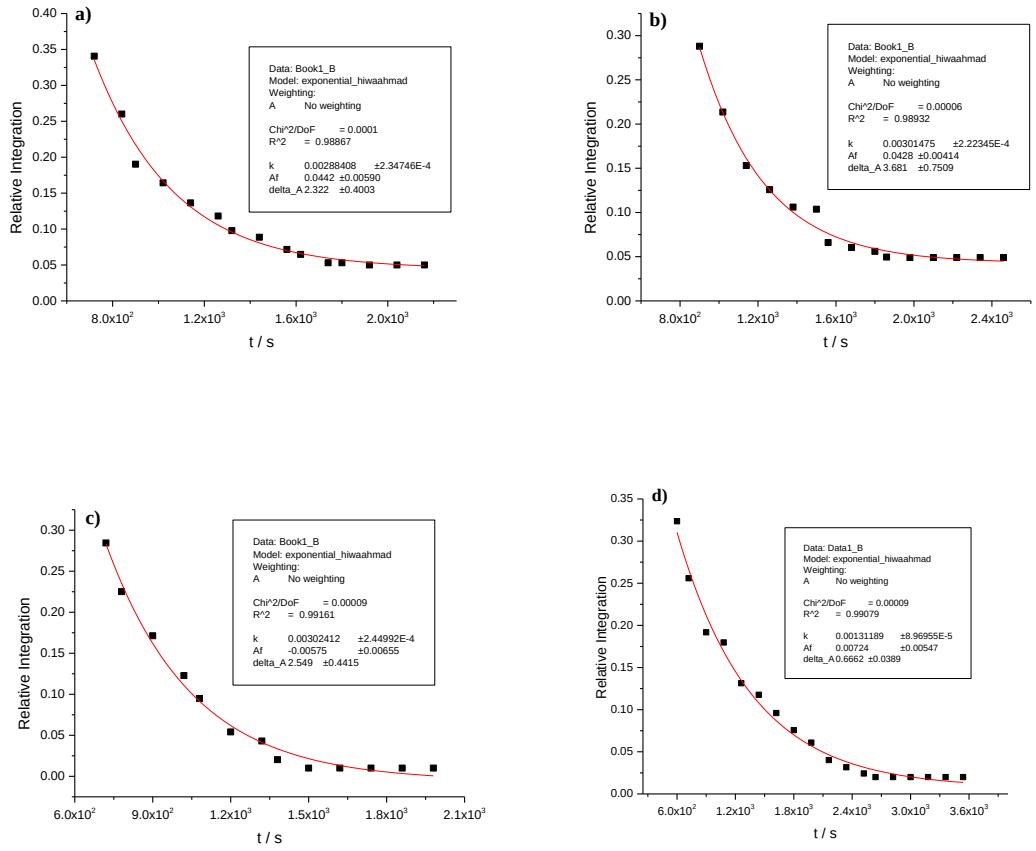

Figure a5.8: Relative integration of a) **5.11**, b) **5.12**, c) **5.13**, and d) **5.14** in D_2O-phosphate buffer at 0.009 M total phosphate with ionic strength of 0.9 M *I*, pH^* 7.4 at 37 °C obtained by ^{1}H-NMR spectroscopy plotted versus time by using 10% of d_3-ACN. The squares (■) are the experimental points, and the red solid lines are the fits to pseudo-first-order kinetics.

A5.3. The H/D exchange process of 3-phenyl-5-benzyl-2-thiohydantoin

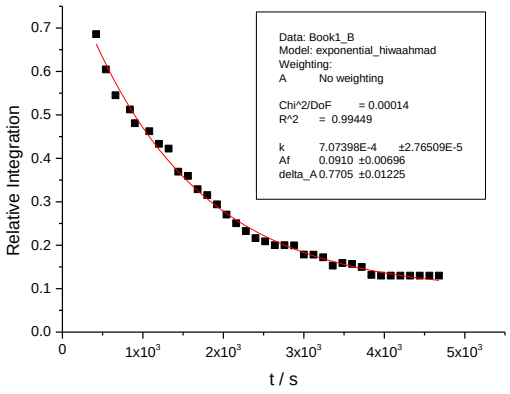

Figure a5.9: Relative integration of **5.15** in D_2O-phosphate buffer at 0.008 M total phosphate with ionic strength of 0.8 M *I*, pH* 7.4 at 37 °C obtained by ^{1}H-NMR spectroscopy plotted versus time by using 20% of d_3-ACN. The squares (■) are the experimental points, and the red solid lines are the fits to pseudo-first-order kinetics.

A5.4. The H/D exchange process of 5-substituted thiazolidine-2,4-diones

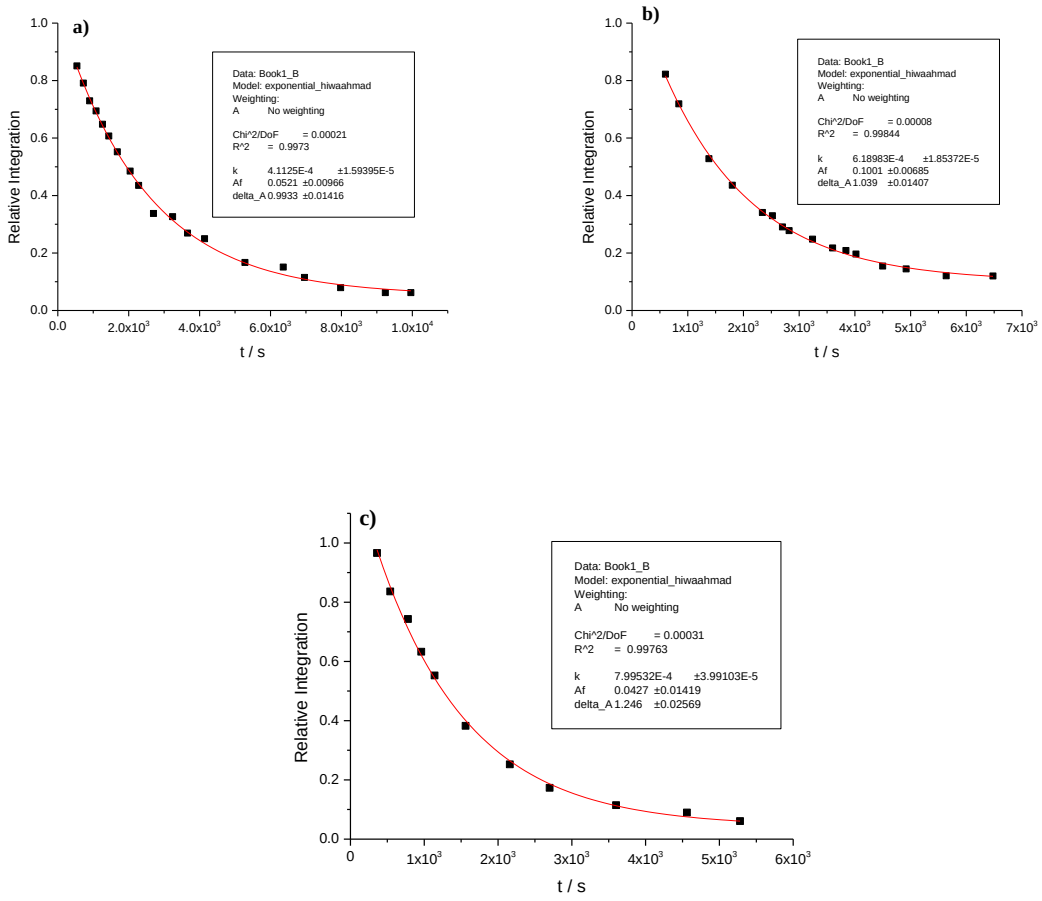

Figure a5.10: Relative integration of **5.21** in D_2O-phosphate buffer at a) 0.09 M, b) 0.18 M, and c) 0.27 M total phosphate with ionic strength of 0.9 M *I*, pH* 7.4 at 37 °C obtained by ^{1}H-NMR spectroscopy plotted versus time. The squares (■) are the experimental points, and the red solid lines are the fits to pseudo-first-order kinetics.

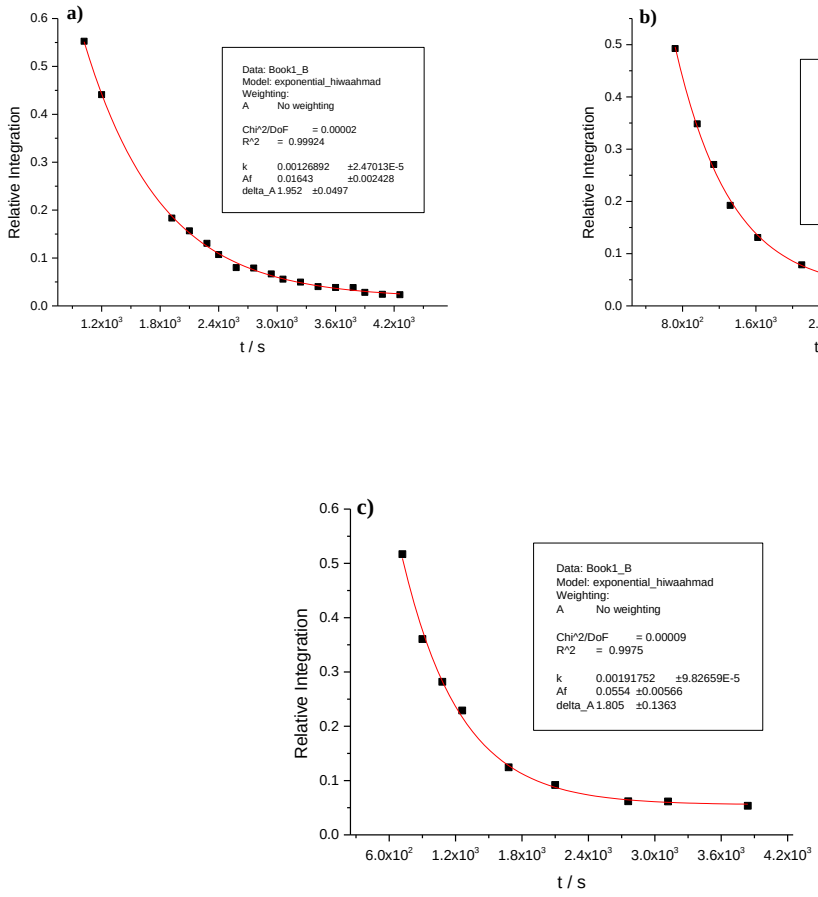

Figure a5.11: Relative integration of **5.22** in D_2O-phosphate buffer at a) 0.09 M, b) 0.18 M, and c) 0.27 M total phosphate with ionic strength of 0.9 M *I*, pH* 7.4 at 37 °C obtained by ^{1}H-NMR spectroscopy plotted versus time. The squares (■) are the experimental points, and the red solid lines are the fits to pseudo-first-order kinetics.

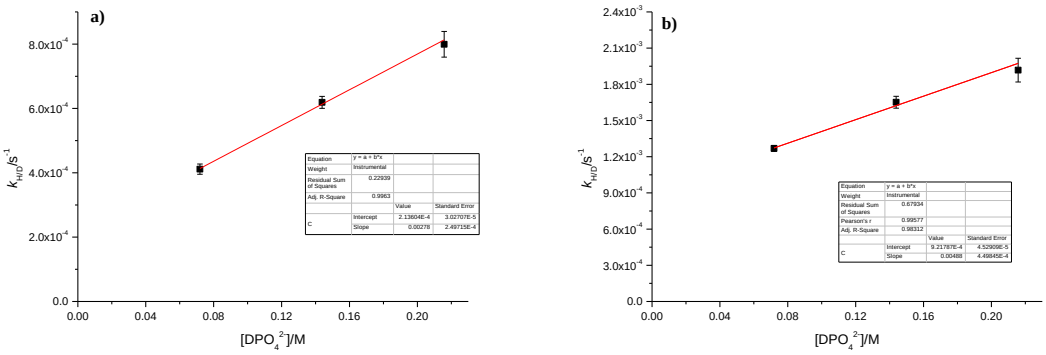

Figure a5.12: Second-order rate constants for buffer-catalysed of H/D exchange by ^{1}H-NMR spectroscopy of a) **5.21**, and b) **5.22** in D_2O-phosphate buffers, 0.9 M *I*, pH* 7.4 at 37 °C.